frontiers | Research Topics

Interactions between natural polysaccharides and gut microbiota

Edited by
Ren-You Gan, Harold Corke, Ding-Tao Wu and Riadh Hammami

Published in
Frontiers in Nutrition

ISSN 1664-8714
ISBN 978-2-83251-894-6
DOI 10.3389/978-2-83251-894-6

About Frontiers

Frontiers is more than just an open access publisher of scholarly articles: it is a pioneering approach to the world of academia, radically improving the way scholarly research is managed. The grand vision of Frontiers is a world where all people have an equal opportunity to seek, share and generate knowledge. Frontiers provides immediate and permanent online open access to all its publications, but this alone is not enough to realize our grand goals.

Frontiers journal series

The Frontiers journal series is a multi-tier and interdisciplinary set of open-access, online journals, promising a paradigm shift from the current review, selection and dissemination processes in academic publishing. All Frontiers journals are driven by researchers for researchers; therefore, they constitute a service to the scholarly community. At the same time, the *Frontiers journal series* operates on a revolutionary invention, the tiered publishing system, initially addressing specific communities of scholars, and gradually climbing up to broader public understanding, thus serving the interests of the lay society, too.

Dedication to quality

Each Frontiers article is a landmark of the highest quality, thanks to genuinely collaborative interactions between authors and review editors, who include some of the world's best academicians. Research must be certified by peers before entering a stream of knowledge that may eventually reach the public - and shape society; therefore, Frontiers only applies the most rigorous and unbiased reviews. Frontiers revolutionizes research publishing by freely delivering the most outstanding research, evaluated with no bias from both the academic and social point of view. By applying the most advanced information technologies, Frontiers is catapulting scholarly publishing into a new generation.

What are Frontiers Research Topics?

Frontiers Research Topics are very popular trademarks of the *Frontiers journals series*: they are collections of at least ten articles, all centered on a particular subject. With their unique mix of varied contributions from Original Research to Review Articles, Frontiers Research Topics unify the most influential researchers, the latest key findings and historical advances in a hot research area.

Find out more on how to host your own Frontiers Research Topic or contribute to one as an author by contacting the Frontiers editorial office: frontiersin.org/about/contact

Interactions between natural polysaccharides and gut microbiota

Topic editors

Ren-You Gan — Singapore Institute of Food and Biotechnology Innovation, Agency for Science, Technology and Research, Singapore

Harold Corke — Guangdong Technion - Israel Institute of Technology, China

Ding-Tao Wu — Chengdu University, China

Riadh Hammami — University of Ottawa, Canada

Citation

Gan, R.-Y., Corke, H., Wu, D.-T., Hammami, R., eds. (2023). *Interactions between natural polysaccharides and gut microbiota*. Lausanne: Frontiers Media SA.

doi: 10.3389/978-2-83251-894-6

Table of contents

05 The Antiviral Activity of Bacterial, Fungal, and Algal Polysaccharides as Bioactive Ingredients: Potential Uses for Enhancing Immune Systems and Preventing Viruses
Worraprat Chaisuwan, Yuthana Phimolsiripol, Thanongsak Chaiyaso, Charin Techapun, Noppol Leksawasdi, Kittisak Jantanasakulwong, Pornchai Rachtanapun, Sutee Wangtueai, Sarana Rose Sommano, SangGuan You, Joe M. Regenstein, Francisco J. Barba and Phisit Seesuriyachan

21 Changes in the Fermentation and Bacterial Community by Artificial Saliva pH in RUSITEC System
Tongqing Guo, Tao Guo, Yurong Cao, Long Guo, Fei Li, Fadi Li and Guo Yang

33 Dietary *Enteromorpha* Polysaccharide Enhances Intestinal Immune Response, Integrity, and Caecal Microbial Activity of Broiler Chickens
Teketay Wassie, Zhuang Lu, Xinyi Duan, Chunyan Xie, Kefyalew Gebeyew, Zhang Yumei, Yulong Yin and Xin Wu

47 *In vitro* Assessment of Chemical and Pre-biotic Properties of Carboxymethylated Polysaccharides From *Passiflora edulis* Peel, Xylan, and Citrus Pectin
Yongjin Sun, Yuan Guan, Hock Eng Khoo and Xia Li

59 *Cereus sinensis* Polysaccharide Alleviates Antibiotic-Associated Diarrhea Based on Modulating the Gut Microbiota in C57BL/6 Mice
Mingxiao Cui, Yu Wang, Jeevithan Elango, Junwen Wu, Kehai Liu and Yinzhe Jin

72 Dietary Resistant Starch From Potato Regulates Bone Mass by Modulating Gut Microbiota and Concomitant Short-Chain Fatty Acids Production in Meat Ducks
Huaiyong Zhang, Simeng Qin, Yao Zhu, Xiangli Zhang, Pengfei Du, Yanqun Huang, Joris Michiels, Quifeng Zeng and Wen Chen

88 Digestive Characteristics of *Hericium erinaceus* Polysaccharides and Their Positive Effects on Fecal Microbiota of Male and Female Volunteers During *in vitro* Fermentation
Baoming Tian, Yan Geng, Tianrui Xu, Xianguo Zou, Rongliang Mao, Xionge Pi, Weicheng Wu, Liangshui Huang, Kai Yang, Xiaoxiong Zeng and Peilong Sun

105 Crude Polysaccharide Extracted From *Moringa oleifera* Leaves Prevents Obesity in Association With Modulating Gut Microbiota in High-Fat Diet-Fed Mice
Lingfei Li, Li Ma, Yanlong Wen, Jing Xie, Liang Yan, Aibing Ji, Yin Zeng, Yang Tian and Jun Sheng

122 Mogroside-Rich Extract From *Siraitia grosvenorii* Fruits Ameliorates High-Fat Diet-Induced Obesity Associated With the Modulation of Gut Microbiota in Mice
Siyuan Wang, Kexin Cui, Jiahao Liu, Jiahao Hu, Ke Yan, Peng Xiao, Yangqing Lu, Xiaogan Yang and Xingwei Liang

132 *Morchella esculenta* mushroom polysaccharide attenuates diabetes and modulates intestinal permeability and gut microbiota in a type 2 diabetic mice model
Ata Ur Rehman, Nimra Zafar Siddiqui, Nabeel Ahmed Farooqui, Gulzar Alam, Aneesa Gul, Bashir Ahmad, Muhammad Asim, Asif Iqbal Khan, Yi Xin, Wang Zexu, Hyo Song Ju, Wang Xin, Sun Lei and Liang Wang

149 Polysaccharides influence human health *via* microbiota-dependent and -independent pathways
Liping Gan, Jinrong Wang and Yuming Guo

frontiers in Nutrition

REVIEW
published: 05 November 2021
doi: 10.3389/fnut.2021.772033

The Antiviral Activity of Bacterial, Fungal, and Algal Polysaccharides as Bioactive Ingredients: Potential Uses for Enhancing Immune Systems and Preventing Viruses

*Worraprat Chaisuwan[1,2], Yuthana Phimolsiripol[2,3], Thanongsak Chaiyaso[2,3], Charin Techapun[2,3], Noppol Leksawasdi[2,3], Kittisak Jantanasakulwong[2,3], Pornchai Rachtanapun[2,3], Sutee Wangtueai[3,4], Sarana Rose Sommano[3,5], SangGuan You[6], Joe M. Regenstein[7], Francisco J. Barba[8] and Phisit Seesuriyachan[2,3]**

[1] Interdisciplinary Program in Biotechnology, Graduate School, Chiang Mai University, Chiang Mai, Thailand, [2] Faculty of Agro-Industry, Chiang Mai University, Chiang Mai, Thailand, [3] Cluster of Agro Bio-Circular-Green Industry (Agro-BCG), Chiang Mai University, Chiang Mai, Thailand, [4] College of Maritime Studies and Management, Chiang Mai University, Samut Sakhon, Thailand, [5] Plant Bioactive Compound Laboratory (BAC), Department of Plant and Soil Sciences, Faculty of Agriculture, Chiang Mai University, Chiang Mai, Thailand, [6] Department of Marine Food Science and Technology, Gangneung-Wonju National University, Gangneung, South Korea, [7] Department of Food Science, College of Agriculture and Life Science, Cornell University, Ithaca, NY, United States, [8] Department of Preventive Medicine and Public Health, Food Science, Toxicology and Forensic Medicine, Faculty of Pharmacy, Universitat de València, Valencia, Spain

OPEN ACCESS

Edited by:
Ding-Tao Wu,
Chengdu University, China

Reviewed by:
Kit Leong Cheong,
Shantou University, China
Bin Du,
Hebei Normal University of Science and Technology, China

***Correspondence:**
Phisit Seesuriyachan
phisit.s@cmu.ac.th

Specialty section:
This article was submitted to Nutrition and Microbes, a section of the journal Frontiers in Nutrition

Received: *07 September 2021*
Accepted: *15 October 2021*
Published: *05 November 2021*

Citation:
Chaisuwan W, Phimolsiripol Y, Chaiyaso T, Techapun C, Leksawasdi N, Jantanasakulwong K, Rachtanapun P, Wangtueai S, Sommano SR, You S, Regenstein JM, Barba FJ and Seesuriyachan P (2021) The Antiviral Activity of Bacterial, Fungal, and Algal Polysaccharides as Bioactive Ingredients: Potential Uses for Enhancing Immune Systems and Preventing Viruses. Front. Nutr. 8:772033. doi: 10.3389/fnut.2021.772033

Viral infections may cause serious human diseases. For instance, the recent appearance of the novel virus, SARS-CoV-2, causing COVID-19, has spread globally and is a serious public health concern. The consumption of healthy, proper, functional, and nutrient-rich foods has an important role in enhancing an individual's immune system and preventing viral infections. Several polysaccharides from natural sources such as algae, bacteria, and fungi have been considered as generally recognized as safe (GRAS) by the US Food and Drug Administration. They are safe, low-toxicity, biodegradable, and have biological activities. In this review, the bioactive polysaccharides derived from various microorganisms, including bacteria, fungi, and algae were evaluated. Antiviral mechanisms of these polysaccharides were discussed. Finally, the potential use of microbial and algal polysaccharides as an antiviral and immune boosting strategy was addressed. The microbial polysaccharides exhibited several bioactivities, including antioxidant, anti-inflammatory, antimicrobial, antitumor, and immunomodulatory activities. Some microbes are able to produce sulfated polysaccharides, which are well-known to exert a board spectrum of biological activities, especially antiviral properties. Microbial polysaccharide can inhibit various viruses using different mechanisms. Furthermore, these microbial polysaccharides are also able to modulate immune responses to prevent and/or inhibit virus infections. There are many molecular factors influencing their bioactivities, e.g., functional groups, conformations, compositions, and molecular weight. At this stage of development, microbial polysaccharides will be used as adjuvants, nutrient supplements, and for drug delivery to prevent several virus infections, especially SARS-CoV-2 infection.

Keywords: sulfated polysaccharides, immunomodulation, SARS-CoV-2, COVID-19, antiviral activity

INTRODUCTION

Viruses are the most numerous living organisms on the earth and can be found in terrestrial and aquatic environments. They are infectious agents containing a genetic material within a protein coat—requiring an appropriate host cell where they can replicate (called infection) often resulting in diseases. Viruses can infect all types of organisms: prokaryotes (archaea and bacteria), eukaryotes (animals, algae, plants, and protozoa), and giant viruses namely virophages (1). Like other viruses, human viruses are able to replicate and mutate. A new virus was discovered in December 2019 and characterized as a pandemic by World Health Organization (WHO) on March 11, 2020 (2). This virus was characterized as the severe acute respiratory syndrome coronavirus 2 (SARS-CoV-2), which causes human infection called coronavirus disease 2019 (COVID-19). The disease has spread worldwide and caused over 200 million cases and 4 million deaths from its start until August 2021 (3).

Coronaviruses (CoV) are enveloped positive-sense single-stranded RNA (+ ssRNA) viruses with crown-like spikes on their spherical surface (4). Coronaviruses belong to the order *Nidovirales*, the suborder *Coronavirineae*, and the family *Caronaviridae*. The family was divided into the subfamilies of *Orthocoronavirinae* and *Letovirinae* by the International Committee on Taxonomy of Viruses (ICTV) in 2018 (5). The former sorts into 4 genera, including *Alphacoronavirus*, *Betacoronavirus*, *Gammacoronavirus*, and *Deltacoronavirus*, with α- and β-coronaviruses infect mammalian species, but γ-, and δ-coronaviruses infect avian species causing respiratory and enteric diseases both as acute and persistent infections (6, 7). The human coronavirus first emerged in patients with the common cold in the 1960s. Other human coronaviruses have emerged within the last two decades: SARS-CoV-1 (2003), Middle East respiratory syndrome (MERS-CoV, 2012), as well as SARS-CoV-2 (2019), which is the seventh human-infecting coronavirus identified (7).

SARS-CoV-2 belongs to the β-coronaviruses, which include SARS-CoV-1 and MERS-CoV. These viruses are highly pathogenic and have a high mortality rate (8). The RNA genome of SARS-CoV-2 is 25–32 kb and similar to SARS-CoV-1 (82% similarity) (4). The structural proteins of SARS-CoV-2 are the envelope (E), membrane (M), nucleocapsid (N), and spike (S) proteins (**Figure 1**). The spike of coronaviruses (S protein) is a glycoprotein associated with the pathogenesis because it is involved in virus adsorption and entry. Thus, the S protein is the virus' important virulence factor (5). The virus uses the S protein for cell binding and membrane fusion. The S protein binds to the angiotensin-converting enzyme 2 (ACE2), a host cell receptor, primed by the transmembrane protease serine protease 2 (TMPRSS2), with the interaction mediating the virus attachment and entry into a host cell (5, 6, 9). The ACE2 receptor is found in a range of human tissues and organs, including the small intestine, lungs, heart, testis, kidneys, blood vessels, muscle, adipose tissues, bladder, epithelia cells of the oral cavity, and the upper esophagus (10–12). Therefore, there are many targets for SARS-CoV-2 infection.

Four antiviral drugs were repurposed for COVID-19, including tocilizumab, remdesivir, favipiravir, and dexamethasone (13). Remdesivir, a drug approved by the US Food and Drug Administration (FDA) for COVID-19, showed a high efficacy as a COVID-19 treatment (14, 15). On the other hand, the WHO Solidarity Trial Consortium announced that remdesivir had little or no effect on hospitalized patients with COVID-19 (16). Various researchers have been evaluating and developing other antiviral agents, as well as vaccines, with high efficacy and low-toxicity (17). As of August 2021, people have been administered different Covid vaccines in many countries, but the pandemic still goes on. Nutrients in foods have an important role in stimulating human immunity and preventing viral infections. Several nutrients including polysaccharides, proteins, and lipids have been reported to have antiviral and immune-enhancing properties. In addition, micronutrients, such as vitamin A, C, D, and E, and few minerals, such as iron, selenium, and zinc have the potential to improve the immune system. Furthermore, natural extracts containing some non-nutrients, such as polyphenols, flavonoids, alkaloids, thiophenes, terpenoids, tannins, and lignins have also shown

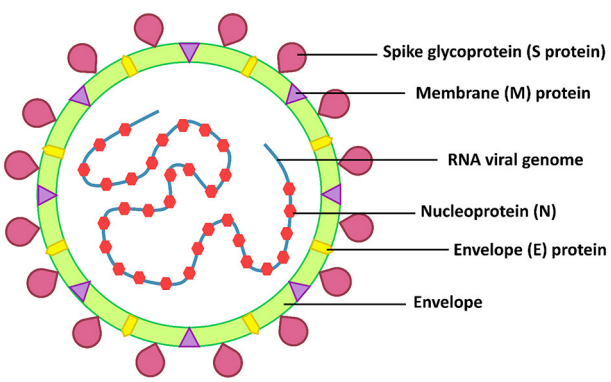

FIGURE 1 | SARS-CoV-2 structure.

Abbreviations: ACE2, Angiotensin-converting enzyme 2; ACV, Acyclovir; APS, Acidic polysaccharide; BoHV-1, Bovine herpesvirus type 1; BoHV-1, Bovine herpes virus type 1; CoV, Coronaviruses; COVID-19, Coronavirus disease 2019; Cox-B3, Coxsackie B virus type 3; CVB3, Coxsackie virus B3; CXCL10, C-X-C motif chemokine 10; ED_{50}, 50% effective dose; EMCV, Encephalomyocarditis virus; EPS, Exopolysaccharides; EV71, Enterovirus 71; FCoV, Feline coronavirus; FCV, Feline calicivirus; FDA, US Food and Drug Administration; FHV-1, Feline herpesvirus 1; FIV, Feline influenza; FPV, Feline panleukopenia; HAdV-5, Human adenovirus type 5; HAV, Hepatitis A virus; HCMV, Human cytomegalovirus; HHV-6, Human herpesvirus type 6; HIV, Human immunodeficiency virus; HSV, Herpes simplex virus; IC_{50}, 50% inhibitory concentration; ICP, Intracellular polysaccharides; ICTV, International Committee on Taxonomy of Viruses; IFN, Interferon; IHNV, Hematopoietic necrosis virus; IL, Interleukin; KHV, Koi herpesviruses; LAB, Lactic acid bacteria; MAPK, Mitogen-activated protein kinase; MERS-CoV, Middle East respiratory syndrome; MW, Molecular weight; NDV, Newcastle disease virus; NF-κB, Nuclear factor kappa B; NK, Natural killer cells; NO, Nitric oxide; PBMC, Peripheral blood mononuclear cells; PV-1, Poliovirus type 1; SARS-CoV-2, Severe acute respiratory syndrome coronavirus 2; SCFA, Short-chain fatty acids; SuHV-1, Suid herpesvirus type 1; TLR3, Toll-like receptor 3; TMPRSS2, Transmembrane protease serine protease 2; TMV, Tobacco mosaic virus; VSV, Vesicular stomatitis virus; VZV, Varicella zoster virus; WHO, World Health Organization.

biological activities (18). For instance, *Erodium glaucophyllum* extracts containing phenolic compounds such as gallic acid, quercetin 3-O-glucuronide, (+)-gallocatechin, and (+)-catechin exhibited antibacterial and antiviral activities (19). During the COVID-19 pandemic, healthy, nutrient-rich, and functional foods may be more important because their consumption may prevent and modulate the immune system (20). In addition, the development of bioactive ingredients, functional, and nutrient-rich foods that can moderate consumers' overall health will be more interested (21).

Polysaccharides are polymeric carbohydrates, defined as composed of more than 10 monomers that are linked by glycosidic linkages. Polysaccharides are grouped into 2 classes: homopolysaccharides (contain one type of monomer) and heteropolysaccharide (contain more than one type of monomer) (22). Polysaccharides from each sources have different branched chains, composition of monosaccharides, molecular weight (MW), and structural conformations (23). Polysaccharides are the most abundant biological macromolecules in nature and can be obtained from every living organisms including animals (24), plants (25), and microorganisms (26). In living cells, polysaccharides are involved in structure, storage, adhesion, and cell recognition (27). Microorganisms including archaea, bacteria, fungi, and microalgae produced diverse polysaccharides with different structures and functions. Moreover, microorganisms synthesize polysaccharides and secrete them to the outside, these are called exopolysaccharides (EPS). Their functions include cell adhesion, migration of bacteria in groundwater, protection from predators and white blood cells, protection from undesired environments (extreme environments), intercellular signal transduction, and molecular recognition (28, 29). Microbial polysaccharides are composed of not only monosaccharides, but also proteins, lipids, metal ions, extracellular DNA (eDNA), and other organic and inorganic compounds (30). Furthermore, polysaccharides derived from microorganisms, especially marine microorganisms may include sulfate groups, and are called sulfated polysaccharides (31). Sulfated polysaccharides are negatively-charged biopolymers found in the cell wall of marine algae (green, brown, and red algae). Sulfate groups are linked to the sugar structure's backbone to stabilize the structure in extreme environments, especially high salinity (32). Sulfated polysaccharides can be founded not only in marine microalgae and macroalgae, but also in marine animals, and marine bacteria (31). Microbial polysaccharides and sulfated polysaccharides show various biological activities such as immunomodulatory, antioxidant, antimicrobial, anticancer, and anti-inflammatory activities (30). In particular, the antiviral activity of microbial polysaccharides has been studied, showing in several cases an inhibitory effect against various animal, human, and plant pathogenic viruses (33–35). Many studies have reported that natural and modified polysaccharides could inhibit various virus infections (36). Some microbial polysaccharides had antiviral activity against various viruses including *Herpes simplex*, influenza, Newcastle disease (NDV), *Varicella zoster* (VZV), human immunodeficiency viruses (HIV), and human adenoviruses (37–45). According to their biological activities, the bioactive polysaccharides can be applied as a bioactive ingredients to improve the immune system and reduce the damage caused by viruses (23). Among microbial polysaccharides, EPS produced by lactic acid bacteria (LAB) have been recognized as GRAS, which allows their use in food without the need for regulatory oversight in the USA (46). Although bioactive polysaccharides have been derived from plants, many researchers have investigated the characteristics, compositions, properties, biological activities of novel polysaccharides from various microorganisms (30). There are many advantages to using microbial polysaccharides compared to other polysaccharides. For example, the microbial polysaccharide production can be done using optimized conditions indoors. Microbes grow easily and fast with a high yield of polysaccharides. The recovery process of polysaccharides is simple. Moreover, microbial growth media are simple and non-toxic. If agricultural wastes are used as microbial growth media, the cost of the production is often decreased (32, 47). Microbial polysaccharides are biocompatible and biodegradable, and have no known toxic effects (23). As mentioned above, microbial polysaccharides show antioxidant, anti-inflammatory, antiviral, and immunomodulatory activities; therefore, microbial polysaccharides are attractive as antiviral agents or bioactive ingredients to treat viral infectious diseases, especially COVID-19. This review focuses on microbial polysaccharides with antiviral and immunomodulatory activities and their antiviral mechanisms, and provides the potential approach to use microbial polysaccharides as bioactive ingredients.

MICROBIAL POLYSACCHARIDES WITH ANTIVIRAL ACTIVITY

Antiviral Polysaccharides From Algae

Algae are eukaryotic photosynthetic organisms, often microorganisms. Some algae are unicellular, but some of them are multicellular organisms lacking of specialized tissues. Both micro- and macroalgae are good sources of biomedical compounds, especially polysaccharides (48). Algal polysaccharides are nontoxic, edible, biocompatible, biodegradable, and easily available; therefore, these biopolymers have been applied in many fields such as the food, pharmaceutical, and biomedical industries (49). Algal polysaccharides have several pharmaceutical properties, including anticancer (50), antioxidant (51), antimicrobial (52), anti-inflammatory (53), and immunomodulatory activities (54). Moreover, several algae, especially marine algae, can produced sulfate polysaccharides, which have different beneficial biological activities (50, 55–58). Different algal polysaccharides possess a variety of structures, composition, and conformations, which influence their properties (55). A summary of algal polysaccharides with antiviral potential are shown in **Table 1**.

Most of the algal polysaccharides have the ability to decrease viral infections by blocking the attachment of virus particles to host cell surfaces. In this line, three polysaccharides extracted from *Sargassum trichophyllum* (a brown alga) were characterized as laminaran, alginate and fucoidan, observing that only fucoidan showed an antiviral effect against herpes simplex virus type

TABLE 1 | The microbial polysaccharides with antiviral activity.

Source	Polysaccharide	Virus	Action	References
Algae				
Coccomyxa gloeobotrydiformi	Acidic polysaccharide (CmAPS)	Human influenza A virus: A/H1N1, A/H2N2, A/H3N2 and A/H1N1	Inhibited virus adsorption and virus-induced erythrocyte hemagglutination and hemolysis	(40)
Gracilaria lemaneiformis	Sulfated polysaccharide	Human influenza virus H1-364	Prevented virus adsorption and replication	(59)
Gyrodinium impudicum	Sulfated exopolysaccharide (p-KG03)	Ecephalomyocarditis virus (EMCV)	Inhibited EMCV infection in HeLa cells	(56)
Gyrodinium impudicum	Sulfated exopolysaccharide (p-KG03)	Influenza A virus	Inhibition of influenza virus replication	(60)
Himanthalia elongata	Polysaccharide	HSV-1	N/A	(61)
Hydroclathrus clathratus	Sulfated polysaccharide HC-b1	HSV-1, including acyclovir-resistant strain and clinical strain	Inhibited virus absorption and penetration, and inhibited replication of HSV-1 in host cells	(62)
Hydroclathrus clathratus	Sulfated polysaccharide	HSV-2	N/A	(63)
Laminaria japonica	Polysaccharide	Respiratory syncytial virus (RSV)	Inhibited RSV replication and induced IFN-α secretion	(64)
Laminaria japonica	LJ04 polysaccharide	Enterovirus 71 (EV71)	Inhibited viral proliferation, viral-induced apoptosis, and increased IFN-β expression	(65)
Laminaria japonica	Fucoidan	I-type influenza virus, adenovirus and parainfluenza virus I	N/A	(66)
Navicula directa	Naviculan	HSV-1, HSV-2, and Influenza A virus (H1N1)	Inhibited viral adsorption and penetration	(67)
Padina tetrastromatica	Polysaccharide	Herpes simplex virus type 1 and 2 (HSV-1 and HSV-2)	Inhibited virus adsorption	(37)
Porphyridium cruentum	i Polysaccharide	Varicella zoster virus (VZV)	i Polysaccharide may block different phases of viral replication cycle	(43)
Porphyridium sp.	Cell-wall sulfated polysaccharide	HSV-1, HSV-2, and VZV	Inhibited virus adsorption and/or production of new virions in host cells	(38)
Porphyridium sp., *P. aerugineum*, *and Rhodella reticulata,*	Polysaccharide	Murine leukemia virus (MuLV) and murine sarcoma virus (MuSV-124)	Inhibition of virus adsorption	(68)
Saccharina japonica	Sulfated galactofucan (SJ-D-S-H) and glucuronomannan (Gn)	SARS-CoV-2	Binding SARS-Cov-2 spike glycoprotein	(69)
Sargassum fusiforme	Polysaccharide SFP	Avian leukosis virus subgroup J (ALV-J)	Inhibited on virus adsorption phase by binding to virions and showed inhibitory effects both *in vitro* and *in vivo*	(70)
Sargassum patens	Sulfated polysaccharide SP-2a	HSV-1	Inhibition of virus adsorption	(71)
Sargassum trichophyllum	Fucoidan	HSV-2	Inhibition of virus adsorption and/or virus penetration steps	(72)
Ulva lactuca	Sulfated polysaccharide	Japanese encephalitis virus (JEV)	Inhibited virus adsorption	(73)
Bacteria				
Arthrospira platensis	Spirulan-like molecules	Human cytomegalovirus, HSV-1, human herpesvirus type 6 and HIV-1	Inhibited the herpesviruses at an entry phase, but at a stage later than virus entry for HIV	(44)
Arthrospira platensis	Calcium spirulan (Ca-SP)	HSV-1, human cytomegalovirus, measles virus, mumps virus, influenza A virus, and HIV-1	Inhibited the penetration of virus into host cells	(74)
Arthrospira platensis	Exopolysaccharide	Koi herpesvirus (KHV)	Inhibited the viral replication	(75)
Bacillus licheniformis T14	Exopolysaccharide	HSV-2	Inhibited virus replication in human peripheral blood mononuclear cells (PBMC)	(76)
Lactobacillus delbrueckii OLL1073R-1	Exopolysaccharide	Intestinal viruses	Increased the expression of the antiviral factors MxA and RNase L	(77)

(Continued)

TABLE 1 | Continued

Source	Polysaccharide	Virus	Action	References
Lactobacillus plantarum strain N4(Lp)	Exopolysaccharide	Transmissible Gastroenteritis Virus (TGEV) - Coronavirus	Inhibition effect that co-incubation with TGEV "Coronavirus"	(78)
Lactobacillus spp.	Exopolysaccharide 26a	Human adenovirus type 5 (HAdV-5)	Suppressed the formation and release of HAdV-5 virions	(41)
Nostoc flagelliforme	Nostoflan	HSV-1, HSV-2,HCMV, and influenza A virus	Blocked virus adsorption and/or virus penetration steps	(79)
Pseudomonas sp. WAK-1	Extracellular glycosaminoglycan and sulfated polysaccharide	HSV-1, Influenza A virus	N/A	(80)
Fungi				
Auricularia auricula	Sulfated *Auricularia auricula* polysaccharide (AAPt)	Newcastle disease virus	Inhibit the cellular infectivity (in chicken embryo fibroblast, CEF) of NDV in three ways (pre-, post- and simultaneous-adding polysaccharide)	(42)
Fomes fomentarius	Polysaccharide BAS-F	Tobacco mosaic virus (TMV)	N/A	(34)
Inonotous obiquus	*Inonotus obliquus* polysaccharides (IOPs)	Feline calicivirus (FCV) strain F9, feline herpesvirus 1, feline influenza virus H3N2 and H5N6, feline panleukopenia virus and feline infectious peritonitis virus	Antiviral effects on virus particles through blocking viral binding/absorption	(35)
Porodaedalea pini (Brot.) Murrill (syn. *Phellinus pini*)	Polysaccharide EP-AV1 and EP-AV2	HSV-1, coxsackie virus B3 (CVB3)	N/A	(81)
Grifola frondosa	Heteropolysaccharide GFP1	Enterovirus 71	Inhibited EV71 replication and suppressed viral VP1 protein expression and genomic RNA synthesis	(82)
Lentinus edodes	Lentinan	Infectious hematopoietic necrosis virus (IHNV)	Inhibited viral replication	(83)
Cordyceps militaris	Acidic polysaccharide (APS)	Influenza A virus	Reduced virus titer the bronchoalveolar lavage fluid and the lung of mice infected with influenza A virus	(39)

N/A, Not available.

2 (HSV-2) (72). The 50% inhibitory concentration (IC_{50}) of the fucoidan was 18 $\mu g \cdot mL^{-1}$ when it was added during the viral infection, being lower than adding after the viral infection. Therefore, this polysaccharide might inhibit HSV-2 at the virus adsorption and/or penetration step(s) (72). *Sargassum henslowianum* produced antiviral fucoidans against both HSV-1 and HSV-2 (84). For instance, the authors observed how two fractions of the fucoidans (SHAP-1 and SHAP-2) could inhibit HSV-1 with IC_{50} of 0.89 and 0.82 $\mu g \cdot mL^{-1}$, respectively. Both SHAP-1 and SHAP-2 showed higher antiviral activity against HSV-2 with IC_{50} of 0.48 $\mu g \cdot mL^{-1}$. These fucoidans interfered with the virions' attachment to host cells (84). Moreover, low MW fucoidan fractions (LF1 and LF2) from *Laminaria japonica* could inhibit I-type influenza virus, adenovirus and parainfluenza virus I *in vitro*. The IC_{50} for LF1 were 0.3, 0.6, and 0.3 $mg \cdot mL^{-1}$, respectively, whereas The IC_{50} for LF2 were 0.6, 1.2, and 0.6 $mg \cdot mL^{-1}$, respectively (66). Fucoidan from *Cladosiphon okamuranus* also showed higher antiviral activity against NDV with lower cytotoxicity than Ribavirin, an antiviral drug, preventing this polysaccharide the viral infection at early steps by blocking the F protein (85). In addition, *Scytosiphon lomentaria*, a brown seaweed, also produced fucoidans with antiviral activity, in particular, they had the ability to block HSV-1 and HSV-2 infections (86). Moreover, a fucoidan with high levels of sulfate groups also showed the highest antiviral activity against HSV-1 and HSV-2 (86).

Carrageenans are sulfated linear polysaccharides extracted from some red algae, such as *Chondrus*, *Gigartina*, *Hypnea*, and *Eucheuma* spp. (49). These polysaccharides showed an antiviral activity against several viruses. For instance, González et al. (87) reported a good inhibitory effect of carrageenan against some enveloped viruses, including HSV-1, HSV-2, Semliki Forest, vaccinia, and swine fever viruses, but they did not find any impact on vesicular stomatitis and measles viruses. Moreover, these authors also showed the antiviral activity of carrageenan against encephalomyocarditis virus (EMCV), a naked virus, but they did not observe significant effects on poliovirus or adenovirus. The carrageenan interfered with the viral protein synthesis. On the other hand, λ-carrageenan and moderately cyclized μ/ℓ-carrageenan extracted from a red seaweed (*Gigartina skottsbergii*) inhibited the viral attachment of HSV-1 and HSV-2 (88). Various types of carrageenans also have shown antiviral activities against

hepatitis A virus (HAV). The 50% effective dose (ED_{50}) for ι-carrageenan, λ-carrageenan, and κ-carrageenan against HAV were >400, >222, and >10 $\mu g \cdot mL^{-1}$, respectively (89). λ-Carrageenan from *G. skottsbergii* showed an inhibitory effect on both bovine herpesvirus type 1 (BoHV-1) and Suid herpesvirus type 1 (SuHV-1). The IC_{50} of this polysaccharide was 0.52 and 10.4 $\mu g \cdot mL^{-1}$, respectively (90).

The red micro algae, *Porphyridium* spp., produce antiviral polysaccharides against many types of viruses, including HSV-1, HSV-2, and VZV. The algae inhibited viral entry and/or blocked virus replication in host cells (38, 43). In this line, the sulfated polysaccharide SP-2a obtained from a brown alga, *Sargassum patens*, exhibited strong antiviral property against different strains of HSV-1. The EC_{50} of SP-2a against the standard, acyclovir (ACV)-sensitive and -resistant strains of HSV-1 were 5.5, 1.5, and 4.1 $\mu g \cdot mL^{-1}$, respectively. The SP-2a had a weak virucidal activity against the standard and ACV-sensitive strains of HSV-1, but not the ACV-resistant strain. During virus adsorption, the SP-2a showed ≥80% inhibition of adsorption against all strains of HSV-1 (71). p-KG03 is a sulfated exopolysaccharide with an average MW of 1.87×10^7 Da extracted from a dinoflagellate, *Gyrodinium impudicum* strain KG03. The p-KG03 could inhibit EMCV in HeLa cells with an EC_{50} of 26.9 $\mu g \cdot mL^{-1}$, and influenza A at the virus adsorption step, but was ineffective against influenza B, HSV-1, HSV-2, human immunodeficiency virus type 1 (HIV-1), HIV-2, Coxsackie B virus type 3 (Cox-B3), and vesicular stomatitis virus (VSV). In addition, the p-KG03 also showed antiviral activity against influenza A virus at the virus adsorption step, but did not inhibit all influenza B virus isolates. The EC_{50} for p-KG03 against different strains of influenza A virus (H1N1: PR8 and Tw; H3N2: Se) ranged from 0.19 to 0.48 $\mu g \cdot mL^{-1}$ (56, 60). Lee et al. (67) reported that *Navicula directa*, a diatom collected from deep-sea water in Toyama Bay (Japan), produced naviculan (a sulfated polysaccharide). The naviculan is a heteropolysaccharide consisting of fucose, xylose, galactose, mannose, rhamnose, and sulfate with an average MW of ∼2.2×10^5 Da. It is a broad-spectrum antiviral against HSV-1, HSV-2, and influenza A virus with IC_{50} of 14, 7.4, and 170 $\mu g \cdot mL^{-1}$, respectively, at the virus adsorption phase. Moreover, it could also interfere with the cell-cell fusion of HIV gp160- and CD4-expressing HeLa cells. Therefore, it might prevent HIV infections.

Antiviral Polysaccharides From Bacteria

Bacteria (including cyanobacteria or blue-green algae) have the ability to synthesize polysaccharides for various purposes such as storage, cell protection, and adhesion. Polysaccharides accumulated in cells are called intracellular polysaccharides (ICP). While those outside of cell are called extracellular polysaccharides or EPS. The latter are secreted by cells or produced extracellularly using cell wall-anchored enzymes (28). Bacterial polysaccharides show biological (bioactive) activities, including anti-inflammatory, anticancer, antimicrobial, antioxidant, and immunomodulatory (91–97). They showed an inhibitory effect against various viruses, both DNA and RNA viruses. The inhibitory effect is usually associated with the viral adsorption and/or replication phases in host cells. For example, *Arthrospira platensis* (formerly *Spirulina platensis*) produced calcium spirulan, a sulfated polysaccharide, with antiviral activity against several enveloped viruses. The calcium spirulan composed of rhamnose, ribose, mannose, fructose, galactose, xylose, glucose, glucuronic acid, galacturonic acid, sulfate, and calcium. This polysaccharide showed antiviral activity against HSV-1, human cytomegalovirus (HCMV), measles, mumps, influenza A, and HIV-1 viruses by inhibiting virus penetration (74). Spirulan-like substances extracted from *A. platensis* showed strong antiviral activity against HCMV, HSV-1, human herpesvirus type 6 (HHV-6), and HIV-1. Their mechanisms depended on the type of virus. For example, in the case of herpesviruses, spirulan-like substances inhibited virus adsorption and/or penetration steps, while HIV-1 was inhibited after viral entry. For HCMV, the inhibition occurred at intracellular steps, especially the viral protein synthesis step (44). EPS from *A. platensis* also inhibited koi herpesviruses (KHV). Reichert et al. (75) reported that EPS from *A. platensis* between 18 and 36 $\mu g \cdot mL^{-1}$ suppressed KHV *in vitro* Furthermore, nostoflan, an acidic polysaccharide from *Nostoc flagelliforme* (a cyanobacterium), showed an interesting antiviral activity against enveloped viruses: HSV-1, HSV-2, HCMV, and influenza A viruses. The virus infections were blocked when nostoflan was added at the same time as viral infections. Therefore, nostoflan blocked the viruses at the virus adsorption stage. The IC_{50} values of nostoflan for HSV-1, HSV-2, HCMV, and influenza A viruses were 0.37, 2.9, 0.47, and 78 $\mu g \cdot mL^{-1}$, respectively (79). In addition, other authors also observed how an EPS derived from *Bacillus licheniformis* strain T14 can prevent HSV-2 infection at 300 and 400 $\mu g \cdot mL^{-1}$ in human peripheral blood mononuclear cells (PBMC) (76). EPS26a from *Lactobacillus* sp. could completely inhibit human adenovirus type 5 (HAdV-5) formation and release (41).

Bacterial polysaccharides also indirectly inhibited virus infections by modulation of the immune response. For instance, an EPS produced by *Lactobacillus delbrueckii* OLL1073R-1 activated the Toll-like receptor 3 (TLR3) and the expression of interferon (IFN)-α, IFN-β, MxA, and RNase L in porcine intestinal epithelial (PIE) cells, which was associated with the innate antiviral immune response (77). Mizuno et al. (98) reported that an EPS from *Streptococcus thermophilus* ST538 can activate TLR3, thus promoting the expression of IFN-β, interleukin 6 (IL-6), and C-X-C motif chemokine 10 (CXCL10). Antiviral bacterial polysaccharides are also shown in **Table 1**.

Antiviral Polysaccharides From Fungi

Fungi are unicellular-to-multicellular eukaryotic microorganisms. They can produce a plethora of biologically active compounds, especially secondary metabolites. Similar to algae and bacteria, fungal polysaccharides (primary metabolites) also showed antiviral activity. Fungal polysaccharides can be derived from culture broth, mycelial culture and/or fruiting bodies (99). Fungal polysaccharides, such as glucan, chitin, mannan, PSK or lentinan, showed antiviral potential

against animal, human, and plant viruses (100–103). Fungal polysaccharides with antiviral activity are summarized in **Table 1**. For example, BAS-F, a polysaccharide from *Fomes fomentarius*, at 2 $\mu g \cdot mL^{-1}$ can prevent tobacco mosaic virus (TMV) infection on the leaf surfaces (34). *Porodaedalea pini* (formerly known as *Phellinus pini*) produced two antiviral polysaccharides (EP-AV1 and EP-AV2) against HSV-1 and coxsackie virus B3 (CVB3) in Vero and HeLa cells, respectively. The EP-AV2 with a lower MW (∼100 kDa) showed more potent antiviral activity than EP-AV1 (∼1,010 kDa) against CVB3. It was observed how EP-AV1 and EP-AV2 polysaccharides inhibited the plaque formation caused by CVB3 in HeLa cells by 32 and 84% at 1 $mg \cdot mL^{-1}$, respectively. These polysaccharides specifically inhibited HSV-1 more than CVB3 as indicated by their EC_{50} values. The EC_{50} values of EP-AV1 and EP-AV2 for HSV-1 were 0.20 and 0.21 $\mu g \cdot mL^{-1}$, respectively, whereas CVB3 were 1 and 0.576 $mg \cdot mL^{-1}$, respectively (81). Furthermore, a polysaccharide extracted from the mycelium and fruiting body of *Lentides edodes* was able to inhibit poliovirus type 1 (PV-1) and bovine herpes virus type 1 (BoHV-1) with IC_{50} values of 0.19 and 0.1 $mg \cdot mL^{-1}$, respectively (101). In another study, *Grifola frondosa* mycelia were evaluated as a source of antiviral polysaccharides, observing that it had the antiviral polysaccharide, GFP1. This polysaccharide was a heteropolysaccharide containing glucose and fucose with a MW of ∼40.5 kDa. Zhao et al. (82) reported that GFP1 blocked enterovirus 71 (EV71) infection at the virus replication phase. The GFP1 suppressed the viral protein expression and viral RNA genome synthesis. Fungal polysaccharides also showed important antiviral properties against animal viruses. For example, a polysaccharide from *L. edodes*, called lentinan comprised of glucose, mannose, and galactose with MW of $\sim 3.79 \times 10^5$ Da showed antiviral activity against infectious hematopoietic necrosis virus (IHNV) infecting rainbow trout (*Oncorhynchus mykiss*) and several species of salmon. The LNT-I acted both direct inactivation and inhibition of viral replication with 62.3, and 82.4% inhibition, respectively (83). *Inonotus obliquus*, chaga mushroom, also produced broad-spectrum antiviral polysaccharides against feline viruses. The polysaccharides suppressed infections of feline calicivirus (FCV), feline herpesvirus 1 (FHV-1), feline panleukopenia (FPV), feline coronavirus (FCoV), and feline influenza (FIV, H3N2, and H5N6) viruses. These polysaccharides had low toxicity and blocked virus entry by affecting the virions and/or the receptor(s) on host cell surfaces (35).

Therefore, polysaccharides from different species show various biological activities with different levels of action. Sulfated polysaccharides derived from marine microalgae and seaweeds showed many different bioactive properties and were effective against viruses at low concentrations, compared to other polysaccharides. In addition, bacteria and fungi are easily grow on simple media or agricultural wastes. The production can be done using controllable conditions and they produce high amounts of polysaccharides. Therefore, it would also benificial if the bioactivities and physicochemical properties of bacterial and fungal polysaccharides could be modified. The molecular modification of polysaccharides is an alternative approach to modulate their properties.

ANTIVIRAL MECHANISMS OF MICROBIAL POLYSACCHARIDES

In viral replication, there are 6 major steps during the infection: (1) virus attachment, (2) penetration, (3) uncoating, (4) genome replication and protein synthesis, (5) viral assembly, and (6) release of new virions (104). Different microbial polysaccharides have different antiviral mechanisms depending on virus types. The polysaccharides mostly prevented the initial steps of the virus life cycle. They interacted with virus particles and/or receptors on host cells to interfere with virus adsorption and invasion. However, some microbial polysaccharides could inhibit viral replication and protein translation. While others showed immune-enhancing activity, especially antiviral immune responses, which prevent virus infections and reduce disease severity (31, 105).

Inactivating Virus Particles Directly

Microbial polysaccharides, especially sulfated polysaccharides, have a negative charge that can interact directly with the viral surfaces. The virucidal activity of microbial polysaccharides is caused by theses interactions (106). The complexes interfere with the viral infection process, reducing viral proliferation in host cells (**Figure 2**). For example, polysaccharides extracted from *Auricularia auricular*, a basidiomycete mushroom, can inhibit NDV in CEF cells. During the process of adding polysaccharides and virus simultaneously, the virus inhibitory rates were higher than pre- and post-addition of the polysaccharides. These polysaccharides might be combined with virus particles to block virus attachment to host cells (42). *Inonotus obliquus* polysaccharides also directly blocked feline virus virions (FCV, FHV-1, FPV, feline coronavirus FCoV, and FIV). These polysaccharides were mixed with the viruses for 1 h before adding to the cell lines, decreasing significantly the viral infectivity compared to untreated viruses (35).

Inhibiting Virus Adsorption and Penetration

Viruses bind to a host cell surface using electrostatic interactions. Some microbial polysaccharides mimic virus particles. Microbial polysaccharides, especially sulfated polysaccharides, are strongly anionic and bind to the positively charged host cell receptors blocking virus attachment, which prevents virus infection (**Figure 3**) (7). Additionally, some microbial polysaccharides are able to prevent the allosteric process of viral protein formation and/or virus internalization and uncoating steps (106).

Many microbial polysaccharides act at this step. For example, a polysaccharide SP-2a from *S. patens* showed ≥80% inhibition against all strains of HSV-1 when added during virus adsorption (71). Fucoidans from a brown alga, *Padina tetrastromatica* showed the highest percentage (>70%) inhibition against HSV-1 during the virus adsorption period (37). Human influenza virus H1-364 was blocked by sulfated polysaccharides from *Gracilaria lemaneiformis*, a red alga, at virus adsorption and replication on host cells. The sulfated polysaccharides inhibited against the

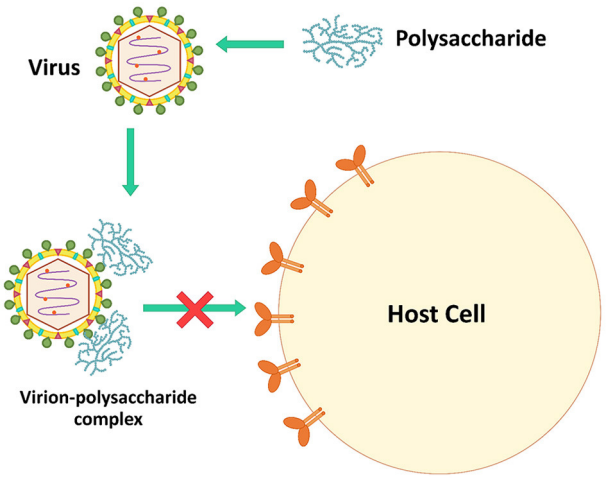

FIGURE 2 | The inhibition mechanism by directly inactivating virus.

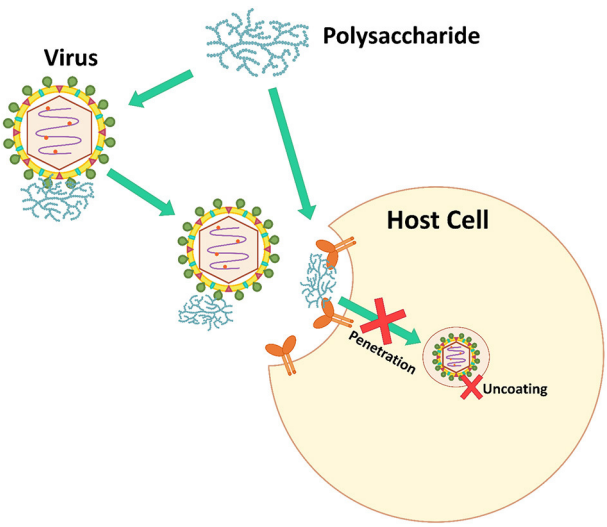

FIGURE 3 | The inhibition mechanism of inhibiting virus adsorption and penetration.

virus at ≥60% during virus adsorption and replication, while these polysaccharides were not effective at the virus release step. The polysaccharides at 62.5 $\mu g \cdot mL^{-1}$ showed 83.5 and 83.0% inhibition against human influenza virus H1-364 at the virus adsorption and replication steps, respectively (59).

Inhibiting Viral Genome Replication and Protein Synthesis

Microbial polysaccharides, especially the low MW polysaccharides, show antiviral effects on infected host cells. They interfere directly with enzymes associated with the viral replication and inhibit other intracellular targets (107) as presented in **Figure 4**. Carrageenans are sulfated polysaccharide that are available from most of red seaweeds.

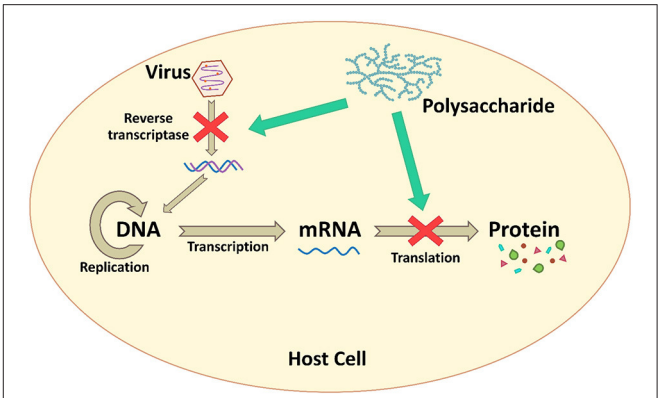

FIGURE 4 | The inhibition mechanism by interfering with viral genome replication and protein synthesis.

These polysaccharides show a broad-spectrum antiviral activity. González et al. (87) reported that carrageenan inhibited HSV-1 at viral protein synthesis. When carrageenan was added 1 h after HSV-1 infection, viral proteins were not detected, whereas when carrageenan was added immediately, viral proteins were detected. Furthermore, polysaccharide GFP1 from *G. frondosa*, which was composed of glucose and fucose with a MW of 40.5 kDa, acted on viral replication and protein synthesis against EV71. The GFP1 was effective in inhibiting EV71 when it was added before or shortly after the viral inoculation. The viral RNA synthesis and VP1 protein were suppressed in a dose-dependent manner (82).

Modulating Host Antiviral Immune Responses

During virus infection in animals, the body induces the immune responses to defend against viral infection. The responses regulate immune cells such as natural killer (NK) cells and macrophages, and increase the production of cytokines, i.e., the type I interferon system (IFN-α/β system) (36). The microbial polysaccharides interact with cell receptors on the macrophage and NK cell, and then activate the cells using the nuclear factor kappa B (NF-κB) and the mitogen-activated protein kinase (MAPK) signaling pathways. These proteins are inducible factors, which increases the gene expression of various cytokines, chemokines, enzymes, and other proteins involving both innate and adaptive immunity (27). The IFN secreted from activated immune cells triggers activation of other immune cells including NK cells, macrophages, and T-cell lymphocytes, which have important roles in the host immune system and antiviral responses. Meanwhile, microbial polysaccharides can activate NK cells that non-specifically kill virus-infected cells by secreting perforins and granzymes (**Figure 5**).

Several polysaccharides can enhance the antiviral immune responses, thus reducing the number of virus particles and the severity of diseases. For example, an EPS extracted from *S. thermophilus* ST538 was able to induce the expression of IFN-β, IL-6, and CXCL10 in response to TLR3 stimulation. These

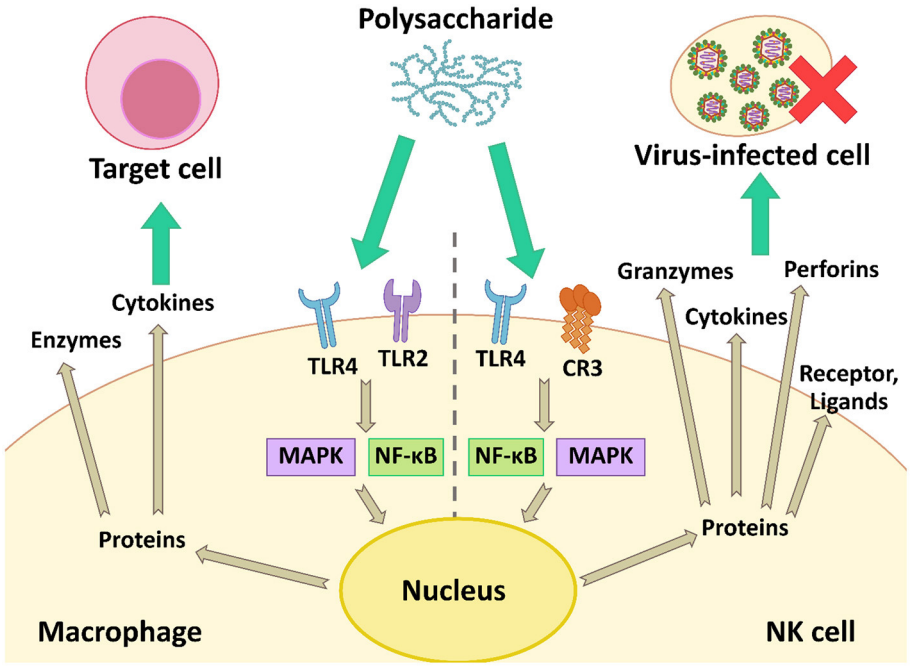

FIGURE 5 | The modulation of the antiviral immune response by activation of macrophage and NK cell using the NF-κB and MAPK signaling pathways.

immune factors are associated with antiviral immune responses, which induce the recruitment and activation of immune cells to struggle pathogens (98). Moreover, *L. delbrueckii* OLL1073R-1 produced immunomodulatory EPS. These EPS activated TLR3 and induced the expression of IFN-α, IFN-β, MxA, and RNase L. The latter two factors are known as antiviral factors (77). Polysaccharides also showed immune-enhancing activity. Ren et al. (83) reported that LNT-I from *L. edodes* mycelia could modulate the immune response by up-regulating the expression of IFN-1 and IFN-γ to prevent IHNV infection. In addition, an acidic polysaccharide (APS) from *Cordyceps militaris* enhanced TNF-α, IFN-γ, and nitric oxide (NO) production, and induced the expression of several cytokines: IL-1β, IL-6, IL-10, and TNF-α. These cytokines have the potential to prevent influenza A virus infection (39). Cao et al. (64) also reported a polysaccharide from *L. japonica* which could increase IFN-α secretion in a dose-dependent manner. The IFN-α level was 144 pg·mL^{-1} when cells were treated with 1000 μg·mL^{-1} of polysaccharide.

FACTORS INFLUENCING THE ANTIVIRAL ACTIVITY

Polysaccharides derived from different sources showed several unique characteristics, properties, and bioactivities at different levels. **Table 2** shows various microbial polysaccharides and/or polysaccharide fractions with different characteristics. Their MW, compositions, functional groups, and structural conformations including type of linkage and degree of branching associate with their biological properties, especially antiviral and immunomodulatory activities. Moreover, extraction and purification methods affect the compositions of polysaccharides; therefore, these factors also influence biological activities of the polysaccharides (110).

Sulfate Content

Several studies have reported that sulfated polysaccharides could exhibit several biological activities (antiviral, anticancer, antioxidant, and immunomodulatory activities), so the sulfate contents could be an important factor affecting antiviral and other bioactivities. Sulfation has been used for enhancing various biological activities of polysaccharides (111, 112). For example, a marine *Pseudomonas* sp. WAK-1 produces extracellular glycosaminoglycan (A1) and sulfated polysaccharide (A2) with antiviral activity. Matsuda et al. (80) modified the polysaccharides by over-sulfation using a dicyclohexyl-carbodiimide-mediated reaction. The over-sulfated polysaccharides were called A1S and A2S, respectively. These 4 compounds showed antiviral activity against influenza A virus with EC_{50} values of >100, >100, 11.0, and 2.9 μg·mL^{-1}, respectively. From the results, over-sulfated polysaccharides (A1S and A2S) showed higher antiviral activity against influenza A virus than the natural polysaccharides (A1 and A2). Moreover, a xylogalactofucan (sulfated polysaccharide) from a brown alga *Sphacelaria indica* also exhibited antiviral activity against HSV-1. The sulfate contents of the polysaccharide affected the antiviral property. The sulfate content of the purified polysaccharide was 4% (w/w). Bandyopadhyay et al. (113) chemically modified the xylogalactofucan produced derivatives with up to 7% (w/w). The IC_{50} values of natural and artificially over-sulfated polysaccharides were 1.3 and 1.5 μg·mL^{-1}, respectively, while a desulfated derivative of the polysaccharide

Table of contents

05 The Antiviral Activity of Bacterial, Fungal, and Algal Polysaccharides as Bioactive Ingredients: Potential Uses for Enhancing Immune Systems and Preventing Viruses
Worraprat Chaisuwan, Yuthana Phimolsiripol, Thanongsak Chaiyaso, Charin Techapun, Noppol Leksawasdi, Kittisak Jantanasakulwong, Pornchai Rachtanapun, Sutee Wangtueai, Sarana Rose Sommano, SangGuan You, Joe M. Regenstein, Francisco J. Barba and Phisit Seesuriyachan

21 Changes in the Fermentation and Bacterial Community by Artificial Saliva pH in RUSITEC System
Tongqing Guo, Tao Guo, Yurong Cao, Long Guo, Fei Li, Fadi Li and Guo Yang

33 Dietary *Enteromorpha* Polysaccharide Enhances Intestinal Immune Response, Integrity, and Caecal Microbial Activity of Broiler Chickens
Teketay Wassie, Zhuang Lu, Xinyi Duan, Chunyan Xie, Kefyalew Gebeyew, Zhang Yumei, Yulong Yin and Xin Wu

47 *In vitro* Assessment of Chemical and Pre-biotic Properties of Carboxymethylated Polysaccharides From *Passiflora edulis* Peel, Xylan, and Citrus Pectin
Yongjin Sun, Yuan Guan, Hock Eng Khoo and Xia Li

59 *Cereus sinensis* Polysaccharide Alleviates Antibiotic-Associated Diarrhea Based on Modulating the Gut Microbiota in C57BL/6 Mice
Mingxiao Cui, Yu Wang, Jeevithan Elango, Junwen Wu, Kehai Liu and Yinzhe Jin

72 Dietary Resistant Starch From Potato Regulates Bone Mass by Modulating Gut Microbiota and Concomitant Short-Chain Fatty Acids Production in Meat Ducks
Huaiyong Zhang, Simeng Qin, Yao Zhu, Xiangli Zhang, Pengfei Du, Yanqun Huang, Joris Michiels, Quifeng Zeng and Wen Chen

88 Digestive Characteristics of *Hericium erinaceus* Polysaccharides and Their Positive Effects on Fecal Microbiota of Male and Female Volunteers During *in vitro* Fermentation
Baoming Tian, Yan Geng, Tianrui Xu, Xianguo Zou, Rongliang Mao, Xionge Pi, Weicheng Wu, Liangshui Huang, Kai Yang, Xiaoxiong Zeng and Peilong Sun

105 Crude Polysaccharide Extracted From *Moringa oleifera* Leaves Prevents Obesity in Association With Modulating Gut Microbiota in High-Fat Diet-Fed Mice
Lingfei Li, Li Ma, Yanlong Wen, Jing Xie, Liang Yan, Aibing Ji, Yin Zeng, Yang Tian and Jun Sheng

had no effect on HSV-1. Furthermore, Ponce et al. (86) also reported that the level of sulfated esters in sulfated galactofucans extracted from a brown alga *Scytosiphon lomentaria* was an important factor influencing the antiviral activity. The whole extract (A) of *S. lomentaria* was fractionated to yield fractions A0, A5, A10, A20, A30, and A40, with different components, MW, and monosaccharide composition. A0 was soluble and the fraction A5 was an uronofucoidan. A10–A40 were galactofucans and showed antiviral activity against HSV-1 and HSV-2 with IC_{50} values in the range 0.76–10.0 $\mu g \cdot mL^{-1}$. Among the 4 galactofucan fractions, A30 (pure galactofucan) contained the highest sulfate content (29.5% SO_3Na) and the lowest uronate content (1.8%). A30 showed the strongest antiviral activity against HSV-1 and HSV-2 with IC_{50} values of 0.76 and 1.3 $\mu g \cdot mL^{-1}$, respectively. Therefore, the low content of uronic acids and the high content of sulfate was associated with the antiviral activity of these polysaccharides. In conclusion, sulfate content is an important factor influencing biological activities. Adding sulfate groups into polysaccharide structures led to enhance bioactivities, whereas desulfation decreased their bioactivities.

Molecular Weight

The MW of polysaccharides also influenced their biological properties. Polysaccharides with low MW could easily pass through target cells to act inside the cells. Moreover, the low MW polysaccharides might bind better to cell receptors to inactivate or activate the target cells (114). Some polysaccharides with lower MW showed high biological activities, but some polysaccharides with higher MW were better. For example, Surayot et al. (26) reported the effect of MW of an EPS from *Weisella confusa* on immunomodulatory activity. The EPS with low MW ($\leq 70 \times 10^3$ Da) could stimulate RAW264.7 cells to induce NO and production of various cytokines such as TNF-α, IL-1β, IL-6, and IL-10, but the native EPS (MW of $\sim 506 \times 10^6$ Da) had no immunomodulatory activity. In addition, Ponce et al. (86) reported that the galactofucan fraction A30 had the lowest MW (∼8.5 kDa) and the low MW might be another factor influencing the antiherpes activity against HSV-1 and HSV-2. On the contrary, high molecular weight carrageenans from different rea algae (*Chondrus armatus*, *Kappaphycus alvarezii*, and *Tichocarpus crinitus*) had effective antiviral activity (115). The different carrageenans with molecular weight of 250, 390, and 400 kDa, respectively show antiviral activity with 88, 85, and 77%, respectively. While low molecular weight (LMW) derivatives (1.2–3.5 kDa) were obtained from different depolymerization methods. The LMW derivatives showed low antiviral properties (28–54%) compared to the native polysaccharides. Therefore, the antiviral activity of these polysaccharides depended on their molecular weight (115).

Enhancement of Bioactivities

To enhance the biological activities, natural microbial polysaccharides need molecular modification of their structure, size, and functional groups to optimize activity (114). The MW can be reduced using external energy and/or specific enzymes to break glucoside chains. Using ultrasonic disruption and microwave exposure to reduce the MW are "physical modification," whereas the enzymatic degradation is "biological modification" (114). For instance, Surayot et al. (26) hydrolyzed an EPS from *W. confusa* TISTR 1498 using HCl and heating in hot water or in a microwave oven. The low MW products could induce production of cytokines from RAW264.7 macrophage cells. Bioactivities were also enhanced by changing the functional substituents of polysaccharides, which is "chemical modification," such as alkylation, sulfation, sulfonation, phosphorylation, carboxymethylation, and selenization (114).

THE POTENTIAL USES OF MICROBIAL POLYSACCHARIDES TO PREVENT VIRAL DISEASES

Microbial polysaccharides showed various bioactivities, while almost always having any significant side-effects, yet are biodegradable, biocompatible, and cost-effective. Microbial and algal polysaccharides may be applied as drug resistance solutions. These polysaccharides can combine with other antiviral drugs for preventing drug-resistance strains (110). In addition to the prevention of viral infections, these polysaccharides also prevent recurrence of latent viruses. For example, calcium spirulan (Ca-SP) derived from *Spirulina platensis* was developed as microalgal cream, which effectively prevented the recurrence of HSV-1 (116). Therefore, the bioactive polysaccharides may be used to prevent viral diseases and reduce the risks of diseases, especially COVID-19.

SARS-CoV-2 has an S-protein on its envelope and the protein has an important role with binding to a host cell receptor (ACE2) (8). Heparin, heparan sulfates, and other sulfated polysaccharides can bind tightly to the S-protein *in vitro* (117). The binding inhibits viral infection. Other microbial polysaccharides showed immunomodulatory properties that stimulated the immune system to prevent SARS-CoV-2 infection. Several microbes can produce sulfated polysaccharides. Beneficial sulfated polysaccharides might be produced from natural microbial polysaccharides (114). Type I IFN, including IFN-α, -β, -ε, -κ, -ω, -δ, -ζ, and -τ, are essential cytokines for antiviral immune responses. Type I IFN can induce antiviral responses within infected and neighboring cells that block the spread of virus particles. They activate both innate and adaptive immune responses that promote NK cell functions and antibody production (118, 119). Hadjadj et al. (120) reported that most severe COVID-19 patients had a low type I IFN response (No IFN-β and low IFN-α production and activity). Many microbial and algal polysaccharides induced type I IFN production *in vivo*. Thus, these polysaccharides might be applied to modulate the immune system in both patients and healthy people. In severe COVID-19 cases, aggressive inflammatory responses were found and the inflammation caused tissue damage in many organs (121). Some microbial polysaccharides showed anti-inflammatory activity. These polysaccharides inhibited the production of pro-inflammatory cytokines including TNF-α, IL-1β, IL-6, and IL-8 (122–124).

ACE2 receptors are expressed by several tissues and organs as described above, especially the respiratory and gastrointestinal

tracts. Microbial polysaccharides with antiviral activity can be used as a nasal spray, metered dose inhaler, or delivered orally to prevent the binding of SARS-CoV-2 (117). Several natural polysaccharides have been designed as nanomaterials for drug delivery systems, such as antiviral agent. These nanomaterials may be not only used to treat the virus, but also to modulate the immune responses (7).

Algal, bacterial, and fungal polysaccharides and sulfated polysaccharides showed pharmaceutical properties due to their biological activities as mentioned above. These polysaccharides could be used as bioactive supplements in foods and could enrich nutritional quality. Indeed, some of these polysaccharides have been granted as GRAS status by the US FDA, so they can consume to enhance immune response and reduce the severity of viral diseases, especially COVID-19 (117). Some microbial polysaccharides have prebiotic properties, which enhance the proliferation of beneficial intestinal microflora, especially *Bifidobacterium* spp. (125). In addition, some algal polysaccharides (alginate and laminaran) could be fermented by gut microbiota and promoted the growth of *Bacteroides*, *Bifidobacterium*, and *Lactobacillus* species (126). When microbial polysaccharides were consumed, they could enhance the host's immune response and modulate the microbial community (microflora). The microbes degrade the polysaccharides into short-chain fatty acids (SCFA) such as acetic, propionic, and butyric acids. SCFA show benefit for the maintenance intestinal cells and modulating of the immune system (27). Microbial polysaccharides have the potential to be bioactive ingredients that can be added into foods or food products to enhance the nutritional quality of foods by modulating consumers' immune response. Therefore, the biological activities of foods supplemented with these polysaccharides should be investigated. The intake of foods with bioactive polysaccharides in patients and healthy people to prevent viruses and/or reduce the adverse symptoms needs further study.

CONCLUSION

Microorganisms produce various types of polysaccharides with unique characteristics and can be produced on a large scale with controllable conditions. Several microbial/algal polysaccharides show bioactivities, especially antiviral and immunomodulatory activities. They have strong antiviral effects by interfering with the life cycle of viruses and/or modulating host immune responses, which may benefit patients infected with COVID-19. Polysaccharides and sulfated polysaccharides from different microorganism and algae species have different characteristics and levels of bioactivities. Their constituents, structural conformations, MW, and functional groups significantly influence their bioactivities. To enhance their activities, physical, chemical, or biological modifications might be beneficial. The microbial polysaccharides have potential uses as adjuvants for antiviral vaccines and micro- and/or nano-particles for drug delivery systems. Some sulfated polysaccharides obtained from microbes and algae have been approved as GRAS, which may be used as bioactive ingredients adding in food products to prevent viruses. Many microbial polysaccharides are safe, biocompatible, biodegradable, and easily available. Therefore, the intake of proper dosage of the right polysaccharides may modulate physiological functions to prevent viral diseases and decrease their damage. They may be an alternative therapy to treat COVID-19 patients. In the future, the development of polysaccharides as functional food products should be explored. For foods supplemented with bioactive polysaccharides, more pharmaceutical investigations and clinical evidence are required to analyze their antiviral and immune-enhancing effects. The mechanisms that occur in the food products against viral infections should also be further investigated.

AUTHOR CONTRIBUTIONS

PS, TC, CT, and SY contributed to conception and supervised the project. WC, NL, KJ, and SS contributed in doing literature searches and wrote the manuscript draft. YP, PR, SW, JR, FB, and PS equally revised and approved the manuscript. All authors have read and approved the final draft manuscript.

FUNDING

The authors gratefully acknowledge the financial support from the National Research Council of Thailand (NRCT) through the Royal Golden Jubilee Ph.D. Program, Thailand (grant no. PHD/0185/2560) to WC and PS. Additionally, this work was also partially financially supported along with in-kind support by the Biotechnology Program of the Graduate School of Chiang Mai University; the Cluster of Agro Bio-Circular-Green Industry (Agro BCG) Faculty of Agro-Industry; and Chiang Mai University.

REFERENCES

1. Dimmock NJ, Easton AJ, Leppard KN. *Introduction to Modern Virology*. Chichester: John Wiley & Sons (2016). 544 p.
2. World Health Organization. *Rolling Updates on Coronavirus Disease (COVID-19)* (2021). Available online at: https://www.who.int/emergencies/diseases/novel-coronavirus-2019/events-as-they-happen (accessed May 3, 2021).
3. World Health Organization. *WHO Coronavirus (COVID-19) Dashboard* (2021). Available online at: https://covid19.who.int/ (accessed August 9, 2021).
4. Mohan SV, Hemalatha M, Kopperi H, Ranjith I, Kumar AK. SARS-CoV-2 in environmental perspective: occurrence, persistence, surveillance, inactivation and challenges. *Chem Eng J.* (2021) 405:126893. doi: 10.1016/j.cej.2020.126893
5. Chen B, Tian EK, He B, Tian L, Han R, Wang S, et al. Overview of lethal human coronaviruses. *Signal Transduct Target Ther.* (2020) 5:89. doi: 10.1038/s41392-020-0190-2
6. V'Kovski P, Kratzel A, Steiner S, Stalder H, Thiel V. Coronavirus biology and replication: implications for SARS-CoV-2. *Nat Rev Microbiol.* (2020) 19:155–70. doi: 10.1038/s41579-020-00468-6

7. Chen X, Han W, Wang G, Zhao X. Application prospect of polysaccharides in the development of anti-novel coronavirus drugs and vaccines. *Int J Biol Macromol.* (2020) 164:331–43. doi: 10.1016/j.ijbiomac.2020.07.106
8. Cevik M, Kuppalli K, Kindrachuk J, Peiris M. Virology, transmission, and pathogenesis of SARS-CoV-2. *BMJ.* (2020) 371:m3862. doi: 10.1136/bmj.m3862
9. Di Nardo M, van Leeuwen G, Loreti A, Barbieri MA, Guner Y, Locatelli F, et al. A literature review of 2019 novel coronavirus (SARS-CoV2) infection in neonates and children. *Pediatr Res.* (2020) 89:1101–8. doi: 10.1038/s41390-020-1065-5
10. Jia HP, Look DC, Shi L, Hickey M, Pewe L, Netland J, et al. ACE2 receptor expression and severe acute respiratory syndrome coronavirus infection depend on differentiation of human airway epithelia. *J Virol.* (2005) 79:14614–21. doi: 10.1128/JVI.79.23.14614-14621.2005
11. Li MY, Li L, Zhang Y, Wang XS. Expression of the SARS-CoV-2 cell receptor gene ACE2 in a wide variety of human tissues. *Infect Dis Poverty.* (2020) 9:45. doi: 10.1186/s40249-020-00662-x
12. Xu H, Zhong L, Deng J, Peng J, Dan H, Zeng X, et al. High expression of ACE2 receptor of 2019-nCoV on the epithelial cells of oral mucosa. *Int J Oral Sci.* (2020) 12:8. doi: 10.1038/s41368-020-0074-x
13. Kelleni MT. Tocilizumab, remdesivir, favipiravir, and dexamethasone repurposed for COVID-19: a comprehensive clinical and pharmacovigilant reassessment. *SN Compr Clin Med.* (2021) 3:919–23. doi: 10.1007/s42399-021-00824-4
14. Beigel JH, Tomashek KM, Dodd LE, Mehta AK, Zingman BS, Kalil AC, et al. Remdesivir for the treatment of covid-19 - final report. *N Engl J Med.* (2020) 383:1813–26. doi: 10.1056/NEJMoa2007764
15. Centers for Disease Control and Prevention. *Treatments Your Healthcare Provider Might Recommend if You Are Sick* (2020). Available online at: https://www.cdc.gov/coronavirus/2019-ncov/your-health/treatments-for-severe-illness.html (accessed December 24, 2020).
16. WHO Solidarity Trial Consortium. Repurposed antiviral drugs for COVID-19—interim WHO solidarity trial results. *N Engl J Med* (2021) 384:497–511. doi: 10.1056/NEJMoa2023184
17. Centers for Disease Control and Prevention. *Different COVID-19 Vaccines* (2020). Available online at: https://www.cdc.gov/coronavirus/2019-ncov/vaccines/different-vaccines.html (accessed December 24, 2020).
18. Thirumdas R, Kothakota A, Pandiselvam R, Bahrami A, Barba FJ. Role of food nutrients and supplementation in fighting against viral infections and boosting immunity: a review. *Trends Food Sci Technol.* (2021) 110:66–77. doi: 10.1016/j.tifs.2021.01.069
19. Abdelkebir R, Alcántara C, Falcó I, Sánchez G, Garcia-Perez JV, Neffati M, et al. Effect of ultrasound technology combined with binary mixtures of ethanol and water on antibacterial and antiviral activities of *Erodium glaucophyllum* extracts. *Innov Food Sci Emerg Technol.* (2019) 52:189–96. doi: 10.1016/j.ifset.2018.12.009
20. Galanakis CM, Aldawoud TMS, Rizou M, Rowan NJ, Ibrahim SA. Food ingredients and active compounds against the coronavirus disease (COVID-19) pandemic: a comprehensive review. *Foods.* (2020) 9:1701. doi: 10.3390/foods9111701
21. Galanakis CM, Rizou M, Aldawoud TMS, Ucak I, Rowan NJ. Innovations and technology disruptions in the food sector within the COVID-19 pandemic and post-lockdown era. *Trends Food Sci Technol.* (2021) 110:193–200. doi: 10.1016/j.tifs.2021.02.002
22. El Khadem HS. Carbohydrates. In: Meyers RA, editor. *Encyclopedia of Physical Science and Technology, 3rd Edn*. Amsterdam, Netherlands: Elsevier B.V (2003). p. 369–416.
23. Barbosa JR, de Carvalho Junior RN. Polysaccharides obtained from natural edible sources and their role in modulating the immune system: biologically active potential that can be exploited against COVID-19. *Trends Food Sci Technol.* (2021) 108:223–35. doi: 10.1016/j.tifs.2020.12.026
24. Shi Y, Xiong Q, Wang X, Li X, Yu C, Wu J, et al. Characterization of a novel purified polysaccharide from the flesh of *Cipangopaludina chinensis*. *Carbohydr Polym.* (2016) 136:875–83. doi: 10.1016/j.carbpol.2015.09.062
25. Surin S, Surayot U, Seesuriyachan P, You SG, Phimolsiripol Y. Antioxidant and immunomodulatory activities of sulphated polysaccharides from purple glutinous rice bran (*Oryza sativa* L.). *Int J Food Sci.* (2018) 53:994–1004. doi: 10.1111/ijfs.13674
26. Surayot U, Wang J, Seesuriyachan P, Kuntiya A, Tabarsa M, Lee Y, et al. Exopolysaccharides from lactic acid bacteria: structural analysis, molecular weight effect on immunomodulation. *Int J Biol Macromol.* (2014) 68:233–40. doi: 10.1016/j.ijbiomac.2014.05.005
27. Chaisuwan W, Jantanasakulwong K, Wangtueai S, Phimolsiripol Y, Chaiyaso T, Techapun C, et al. Microbial exopolysaccharides for immune enhancement: fermentation, modifications and bioactivities. *Food Biosci.* (2020) 35:100564. doi: 10.1016/j.fbio.2020.100564
28. Nwodo UU, Green E, Okoh AI. Bacterial exopolysaccharides: functionality and prospects. *Int J Mol Sci.* (2012) 13:14002–15. doi: 10.3390/ijms131114002
29. Wang J, Salem DR, Sani RK. Extremophilic exopolysaccharides: a review and new perspectives on engineering strategies and applications. *Carbohydr Polym.* (2019) 205:8–26. doi: 10.1016/j.carbpol.2018.10.011
30. Rana S, Upadhyay LSB. Microbial exopolysaccharides: synthesis pathways, types and their commercial applications. *Int J Biol Macromol.* (2020) 157:577–83. doi: 10.1016/j.ijbiomac.2020.04.084
31. Andrew M, Jayaraman G. Marine sulfated polysaccharides as potential antiviral drug candidates to treat Corona Virus disease (COVID-19). *Carbohydr Res.* (2021) 505:108326. doi: 10.1016/j.carres.2021.108326
32. Muthukumar J, Chidambaram R, Sukumaran S. Sulfated polysaccharides and its commercial applications in food industries—A review. *J Food Sci Technol.* (2021) 58:2453–66. doi: 10.1007/s13197-020-04837-0
33. Ipper NS, Cho S, Lee SH, Cho JM, Hur JH, Lim CK. Antiviral activity of the exopolysaccharide produced by *Serratia* sp. strain Gsm01 against Cucumber mosaic virus. *J Microbiol Biotechnol.* (2008) 18:67–73.
34. Aoki M, Tan M, Fukushima A, Hieda T, Kubo S, Takabayashi M, et al. Antiviral substances with systemic effects produced by Basidiomycetes such as *Fomes fomentarius*. *Biosci Biotechnol Biochem.* (1993) 57:278–82. doi: 10.1271/bbb.57.278
35. Tian J, Hu X, Liu D, Wu H, Qu L. Identification of *Inonotus obliquus* polysaccharide with broad-spectrum antiviral activity against multi-feline viruses. *Int J Biol Macromol.* (2017) 95:160–7. doi: 10.1016/j.ijbiomac.2016.11.054
36. Chen L, Huang G. The antiviral activity of polysaccharides and their derivatives. *Int J Biol Macromol.* (2018) 115:77–82. doi: 10.1016/j.ijbiomac.2018.04.056
37. Karmakar P, Pujol CA, Damonte EB, Ghosh T, Ray B. Polysaccharides from *Padina tetrastromatica*: structural features, chemical modification and antiviral activity. *Carbohydr Polym.* (2010) 80:513–20. doi: 10.1016/j.carbpol.2009.12.014
38. Huleihel M, Ishanu V, Tal J, Arad SM. Antiviral effect of red microalgal polysaccharides on *Herpes simplex* and *Varicella zoster* viruses. *J Appl Phycol.* (2001) 13:127–34. doi: 10.1023/A:1011178225912
39. Ohta Y, Lee JB, Hayashi K, Fujita A, Park DK, Hayashi T. *In vivo* anti-influenza virus activity of an immunomodulatory acidic polysaccharide isolated from *Cordyceps militaris* grown on germinated soybeans. *J Agric Food Chem.* (2007) 55:10194–9. doi: 10.1021/jf0721287
40. Komatsu T, Kido N, Sugiyama T, Yokochi T. Antiviral activity of acidic polysaccharides from *Coccomyxa gloeobotrydiformi*, a green alga, against an *in vitro* human influenza A virus infection. *Immunopharmacol Immunotoxicol.* (2013) 35:1–7. doi: 10.3109/08923973.2012.710636
41. Biliavska L, Pankivska Y, Povnitsa O, Zagorodnya S. Antiviral activity of exopolysaccharides produced by lactic acid bacteria of the genera *Pediococcus*, *Leuconostoc* and *Lactobacillus* against human adenovirus type 5. *Medicina.* (2019) 55:519. doi: 10.3390/medicina55090519
42. Nguyen TL, Chen J, Hu Y, Wang D, Fan Y, Wang J, et al. *In vitro* antiviral activity of sulfated *Auricularia auricula* polysaccharides. *Carbohydr Polym.* (2012) 90:1254–8. doi: 10.1016/j.carbpol.2012.06.060
43. Abu-Galiyun E, Huleihel M, Levy-Ontman O. Antiviral bioactivity of renewable polysaccharides against *Varicella Zoster*. *Cell Cycle.* (2019) 18:3540–9. doi: 10.1080/15384101.2019.1691363
44. Rechter S, König T, Auerochs S, Thulke S, Walter H, Dörnenburg H, et al. Antiviral activity of *Arthrospira*-derived spirulan-like substances. *Antivir Res.* (2006) 72:197–206. doi: 10.1016/j.antiviral.2006.06.004

45. Stepanenko LS, Maksimov OB, Fedoreev SA, Miller GG. Polysaccharides of lichens and their sulfated derivatives: antiviral activity. *Chem Nat Compd.* (1998) 34:337–8. doi: 10.1007/BF02282419
46. Angelin J, Kavitha M. Exopolysaccharides from probiotic bacteria and their health potential. *Int J Biol Macromol.* (2020) 162:853–65. doi: 10.1016/j.ijbiomac.2020.06.190
47. Delbarre-Ladrat C SC, Lebellenger L, Zykwinska A, Colliec-Jouault S. Exopolysaccharides produced by marine bacteria and their applications as glycosaminoglycan-like molecules. *Front Chem.* (2014) 2:85. doi: 10.3389/fchem.2014.00085
48. Rosales-Mendoza S, García-Silva I, González-Ortega O, Sandoval-Vargas JM, Malla A, Vimolmangkang S. The potential of algal biotechnology to produce antiviral compounds and biopharmaceuticals. *Molecules.* (2020) 25:4049. doi: 10.3390/molecules25184049
49. Ahmadi A, Moghadamtousi SZ, Abubakar S, Zandi K. Antiviral potential of algae polysaccharides isolated from marine sources: a review. *Biomed Res Int.* (2015) 2015:825203. doi: 10.1155/2015/825203
50. Alboofetileh M, Rezaei M, Tabarsa M, You S. Bioactivities of *Nizamuddinia zanardinii* sulfated polysaccharides extracted by enzyme, ultrasound and enzyme-ultrasound methods. *J Food Sci Technol.* (2019) 56:1212–20. doi: 10.1007/s13197-019-03584-1
51. Gong G, Dang T, Deng Y, Han J, Zou Z, Jing S, et al. Physicochemical properties and biological activities of polysaccharides from *Lycium barbarum* prepared by fractional precipitation. *Int J Biol Macromol.* (2018) 109:611–8. doi: 10.1016/j.ijbiomac.2017.12.017
52. Vishwakarma J, Vavilala SL. Evaluating the antibacterial and antibiofilm potential of sulphated polysaccharides extracted from green algae *Chlamydomonas reinhardtii*. *J Appl Microbiol.* (2019) 127:1004–17. doi: 10.1111/jam.14364
53. Xu Y, Xu J, Ge K, Tian Q, Zhao P, Guo Y. Anti-inflammatory effect of low molecular weight fucoidan from *Saccharina japonica* on atherosclerosis in apoE-knockout mice. *Int J Biol Macromol.* (2018) 118:365–74. doi: 10.1016/j.ijbiomac.2018.06.054
54. Bahramzadeh S, Tabarsa M, You S, Li C, Bita S. Purification, structural analysis and mechanism of murine macrophage cell activation by sulfated polysaccharides from *Cystoseira indica*. *Carbohydr Polym.* (2019) 205:261–70. doi: 10.1016/j.carbpol.2018.10.022
55. Sanjeewa KKA, Kang N, Ahn G, Jee Y, Kim YT, Jeon YJ. Bioactive potentials of sulfated polysaccharides isolated from brown seaweed *Sargassum* spp in related to human health applications: a review. *Food Hydrocoll.* (2018) 81:200–8. doi: 10.1016/j.foodhyd.2018.02.040
56. Yim JH, Kim SJ, Ahn SH, Lee CK, Rhie KT, Lee HK. Antiviral effects of sulfated exopolysaccharide from the marine microalga *Gyrodinium impudicum* strain KG03. *Mar Biotechnol.* (2004) 6:17–25. doi: 10.1007/s10126-003-0002-z
57. Cho M, Yang C, Kim SM, You S. Molecular characterization and biological activities of watersoluble sulfated polysaccharides from *Enteromorpha prolifera*. *Food Sci Biotechnol.* (2010) 19:525–33. doi: 10.1007/s10068-010-0073-3
58. Cao RA, Lee Y, You S. Water soluble sulfated-fucans with immune-enhancing properties from *Ecklonia cava*. *Int J Biol Macromol.* (2014) 67:303–11. doi: 10.1016/j.ijbiomac.2014.03.019
59. Chen MZ, Xie HG, Yang LW, Liao ZH, Yu J. *In vitro* anti-influenza virus activities of sulfated polysaccharide fractions from *Gracilaria lemaneiformis*. *Virol Sin.* (2010) 25:341–51. doi: 10.1007/s12250-010-3137-x
60. Kim M, Yim JH, Kim SY, Kim HS, Lee WG, Kim SJ, et al. *In vitro* inhibition of influenza a virus infection by marine microalga-derived sulfated polysaccharide p-KG03. *Antivir Res.* (2012) 93:253–9. doi: 10.1016/j.antiviral.2011.12.006
61. Santoyo S, Plaza M, Jaime L, Ibañez E, Reglero G, Señorans J. Pressurized liquids as an alternative green process to extract antiviral agents from the edible seaweed *Himanthalia elongata*. *J Appl Phycol.* (2010) 23:909–17. doi: 10.1007/s10811-010-9611-x
62. Wang H, Ooi VEC, Ang PO. Anti-herpesviral property and mode of action of a polysaccharide from brown seaweed (*Hydroclathrus clathratus*). *World J Microbiol Biotechnol.* (2010) 26:1703–13. doi: 10.1007/s11274-010-0348-0
63. Wang H, Ooi EV, Ang Jr PO. Antiviral polysaccharides isolated from Hong Kong brown seaweed *Hydroclathrus clathratus*. *Sci China C Life Sci.* (2007) 50:611–8. doi: 10.1007/s11427-007-0086-1
64. Cao YG, Hao Y, Li ZH, Liu ST, Wang LX. Antiviral activity of polysaccharide extract from *Laminaria japonica* against respiratory syncytial virus. *Biomed Pharmacother.* (2016) 84:1705–10. doi: 10.1016/j.biopha.2016.10.082
65. Yue Y, Li Z, Li P, Song N, Li B, Lin W, et al. Antiviral activity of a polysaccharide from *Laminaria japonica* against enterovirus 71. *Biomed Pharmacother.* (2017) 96:256–62. doi: 10.1016/j.biopha.2017.09.117
66. Sun T, Zhang X, Miao Y, Zhou Y, Shi J, Yan M, et al. Studies on antiviral and immuno-regulation activity of low molecular weight fucoidan from *Laminaria japonica*. *J Ocean Univ China.* (2018) 17:705–11. doi: 10.1007/s11802-018-3794-1
67. Lee JB, Hayashi K, Hirata M, Kuroda E, Suzuki E, Kubo Y, et al. Antiviral sulfated polysaccharide from *Navicula directa*, a diatom collected from deep-sea water in Toyama Bay. *Biol Pharm Bull.* (2006) 29:2135–9. doi: 10.1248/bpb.29.2135
68. Talyshinsky MM, Souprun YY, Huleihel MM. Anti-viral activity of red microalgal polysaccharides against retroviruses. *Cancer Cell Int.* (2002) 2:8. doi: 10.1186/1475-2867-2-8
69. Jin W, Zhang W, Mitra D, McCandless MG, Sharma P, Tandon R, et al. The structure-activity relationship of the interactions of SARS-CoV-2 spike glycoproteins with glucuronomannan and sulfated galactofucan from *Saccharina japonica*. *Int J Biol Macromol.* (2020) 163:1649–58. doi: 10.1016/j.ijbiomac.2020.09.184
70. Sun Y, Chen X, Zhang L, Liu H, Liu S, Yu H, et al. The antiviral property of *Sargassum fusiforme* polysaccharide for avian leukosis virus subgroup J *in vitro* and *in vivo*. *Int J Biol Macromol.* (2019) 138:70–8. doi: 10.1016/j.ijbiomac.2019.07.073
71. Zhu W, Chiu LC, Ooi VE, Chan PK, Ang Jr PO. Antiviral property and mechanisms of a sulphated polysaccharide from the brown alga *Sargassum patens* against Herpes simplex virus type 1. *Phytomedicine.* (2006) 13:695–701. doi: 10.1016/j.phymed.2005.11.003
72. Lee J-B, Takeshita A, Hayashi K, Hayashi T. Structures and antiviral activities of polysaccharides from *Sargassum trichophyllum*. *Carbohydr Polym.* (2011) 86:995–9. doi: 10.1016/j.carbpol.2011.05.059
73. Chiu YH, Chan YL, Li TL, Wu CJ. Inhibition of Japanese encephalitis virus infection by the sulfated polysaccharide extracts from *Ulva lactuca*. *Mar Biotechnol.* (2012) 14:468–78. doi: 10.1007/s10126-011-9428-x
74. Hayashi T, Hayashi K. Calcium spirulan, an inhibitor of enveloped virus replication, from a blue-green alga *Spirulina platensis*. *J Nat Prod.* (1996) 59:83–7. doi: 10.1021/np960017o
75. Reichert M, Bergmann SM, Hwang J, Buchholz R, Lindenberger C. Antiviral activity of exopolysaccharides from *Arthrospira platensis* against koi herpesvirus. *J Fish Dis.* (2017) 40:1441–50. doi: 10.1111/jfd.12618
76. Gugliandolo C, Spano A, Lentini V, Arena A, Maugeri TL. Antiviral and immunomodulatory effects of a novel bacterial exopolysaccharide of shallow marine vent origin. *J Appl Microbiol.* (2014) 116:1028–34. doi: 10.1111/jam.12422
77. Kanmani P, Albarracin L, Kobayashi H, Iida H, Komatsu R, Kober AKMH, et al. Exopolysaccharides from *Lactobacillus delbrueckii* OLL1073R-1 modulate innate antiviral immune response in porcine intestinal epithelial cells. *Mol Immunol.* (2018) 98:253–65. doi: 10.1016/j.molimm.2017.07.009
78. Yang Y, Song H, Wang L, Dong W, Yang Z, Yuan P, et al. Antiviral effects of a probiotic metabolic products against transmissible gastroenteritis Coronavirus. *J Probiotics Health.* (2017) 5:3. doi: 10.4172/2329-8901.1000184
79. Kanekiyo K, Lee JB, Hayashi K, Takenaka H, Hayakawa Y, Endo S, et al. Isolation of an antiviral polysaccharide, nostoflan, from a terrestrial cyanobacterium, *Nostoc flagelliforme*. *J Nat Prod.* (2005) 68:1037–41. doi: 10.1021/np050056c
80. Matsuda M, Shigeta S, Okutani K. Antiviral activities of marine *Pseudomonas* polysaccharides and their oversulfated derivatives. *Mar Biotechnol.* (1999) 1:68–73. doi: 10.1007/PL00011753
81. Lee SM, Kim SM, Lee YH, Kim WJ, Park JK, Park YI, et al. Macromolecules isolated from *Phellinus pini* fruiting body: chemical

characterization and antiviral activity. *Macromol Res.* (2010) 18:602–9. doi: 10.1007/s13233-010-0615-9
82. Zhao C, Gao L, Wang C, Liu B, Jin Y, Xing Z. Structural characterization and antiviral activity of a novel heteropolysaccharide isolated from *Grifola frondosa* against enterovirus 71. *Carbohydr Polym.* (2016) 144:382–9. doi: 10.1016/j.carbpol.2015.12.005
83. Ren G, Xu L, Lu T, Yin J. Structural characterization and antiviral activity of lentinan from *Lentinus edodes* mycelia against infectious hematopoietic necrosis virus. *Int J Biol Macromol.* (2018) 115:1202–10. doi: 10.1016/j.ijbiomac.2018.04.132
84. Sun QL, Li Y, Ni LQ, Li YX, Cui YS, Jiang SL, et al. Structural characterization and antiviral activity of two fucoidans from the brown algae *Sargassum henslowianum*. *Carbohydr Polym.* (2020) 229:115487. doi: 10.1016/j.carbpol.2019.115487
85. Elizondo-Gonzalez R, Cruz-Suarez LE, Ricque-Marie D, Mendoza-Gamboa E, Rodriguez-Padilla C, Trejo-Avila LM. *In vitro* characterization of the antiviral activity of fucoidan from *Cladosiphon okamuranus* against Newcastle Disease Virus. *Virol J.* (2012) 9:307. doi: 10.1186/1743-422X-9-307
86. Ponce NMA, Flores ML, Pujol CA, Becerra MB, Navarro DA, Cordoba O, et al. Fucoidans from the phaeophyta *Scytosiphon lomentaria*: chemical analysis and antiviral activity of the galactofucan component. *Carbohydr Res.* (2019) 478:18–24. doi: 10.1016/j.carres.2019.04.004
87. González ME, Alarcón B, Carrasco L. Polysaccharides as antiviral agents: antiviral activity of carrageenan. *Antimicrob Agents Chemother.* (1987) 31:1388–93. doi: 10.1128/AAC.31.9.1388
88. Carlucci MJ, Pujol CA, Ciancia M, Noseda MD, Matulewicz MC, Damonte EB, et al. Antiherpetic and anticoagulant properties of carrageenans from the red seaweed *Gigartina skottsbergii* and their cyclized derivatives: correlation between structure and biological activity. *Int J Biol Macromol.* (1997) 20:97–105. doi: 10.1016/S0141-8130(96)01145-2
89. Girond S, Crance JM, Van Cuyck-Gandre H, Renaudet J, Deloince R. Antiviral activity of carrageenan on hepatitis a virus replication in cell culture. *Res Virol.* (1991) 142:261–70. doi: 10.1016/0923-2516(91)90011-Q
90. Diogo JV, Novo SG, Gonzalez MJ, Ciancia M, Bratanich AC. Antiviral activity of lambda-carrageenan prepared from red seaweed (*Gigartina skottsbergii*) against BoHV-1 and SuHV-1. *Res Vet Sci.* (2015) 98:142–4. doi: 10.1016/j.rvsc.2014.11.010
91. El-Newary SA, Ibrahim AY, Asker MS, Mahmoud MG, El Awady ME. Production, characterization and biological activities of acidic exopolysaccharide from marine *Bacillus amyloliquefaciens* 3MS 2017. *Asian Pac J Trop Med.* (2017) 10:652–62. doi: 10.1016/j.apjtm.2017.07.005
92. Farag MMS, Moghannem SAM, Shehabeldine AM, Azab MS. Antitumor effect of exopolysaccharide produced by *Bacillus mycoides*. *Microb Pathog.* (2020) 140:103947. doi: 10.1016/j.micpath.2019.103947
93. Kumar CG, Mongolla P, Pombala S. Lasiosan, a new exopolysaccharide from *Lasiodiplodia* sp. strain B2 (MTCC 6000): Structural characterization and biological evaluation. *Process Biochem.* (2018) 72:162–9. doi: 10.1016/j.procbio.2018.06.014
94. Lobo RE, Gómez MI, Font de Valdez G, Torino MI. Physicochemical and antioxidant properties of a gastroprotective exopolysaccharide produced by *Streptococcus thermophilus* CRL1190. *Food Hydrocoll.* (2019) 96:625–33. doi: 10.1016/j.foodhyd.2019.05.036
95. Sahana TG, Rekha PD. A bioactive exopolysaccharide from marine bacteria *Alteromonas* sp. PRIM-28 and its role in cell proliferation and wound healing *in vitro*. *Int J Biol Macromol.* (2019) 131:10–8. doi: 10.1016/j.ijbiomac.2019.03.048
96. Nehal F, Sahnoun M, Smaoui S, Jaouadi B, Bejar S, Mohammed S. Characterization, high production and antimicrobial activity of exopolysaccharides from *Lactococcus lactis* F-mou. *Microb Pathog.* (2019) 132:10–9. doi: 10.1016/j.micpath.2019.04.018
97. Domingos-Lopes MFP, Nagy A, Stanton C, Ross PR, Gelencsér E, Silva CCG. Immunomodulatory activity of exopolysaccharide producing *Leuconostoc citreum* strain isolated from Pico cheese. *J Funct Foods.* (2017) 33:235–43. doi: 10.1016/j.jff.2017.03.054
98. Mizuno H, Tomotsune K, Islam MA, Funabashi R, Albarracin L, Ikeda-Ohtsubo W, et al. Exopolysaccharides from *Streptococcus thermophilus* ST538 modulate the antiviral innate immune response in porcine intestinal epithaliocytes. *Front Microbiol.* (2020) 11:894. doi: 10.3389/fmicb.2020.00894
99. He X, Fang J, Guo Q, Wang M, Li Y, Meng Y, et al. Advances in antiviral polysaccharides derived from edible and medicinal plants and mushrooms. *Carbohydr Polym.* (2020) 229:115548. doi: 10.1016/j.carbpol.2019.115548
100. Cardozo FT, Camelini CM, Mascarello A, Rossi MJ, Nunes RJ, Barardi CR, et al. Antiherpetic activity of a sulfated polysaccharide from *Agaricus brasiliensis* mycelia. *Antivir Res.* (2011) 92:108–14. doi: 10.1016/j.antiviral.2011.07.009
101. Rincão VP, Yamamoto KA, Ricardo NM, Soares SA, Meirelles LD, Nozawa C, et al. Polysaccharide and extracts from *Lentinula edodes*: Structural features and antiviral activity. *Virol J.* (2012) 9:37. doi: 10.1186/1743-422X-9-37
102. Tochikura TS, Nakashima H, Hirose K, Yamamoto N. A biological response modifier, PSK, inhibits human immunodeficiency virus infection *in vitro*. *Biochem Biophys Res Commun.* (1987) 2:726–33. doi: 10.1016/0006-291X(87)90936-3
103. Tochikura TS, Nakashima H, Ohashi Y, Yamamoto N. Inhibition (*in vitro*) of replication and of the cytopathic effect of human immunodeficiency virus by an extract of the culture medium of *Lentinus edodes* mycelia. *Med Microbiol Immunol.* (1988) 177:235–44. doi: 10.1007/BF00189409
104. Ryu WS. Virus life cycle. In: Ryu WS, editor. *Molecular Virology of Human Pathogenic Viruses*. Cambridge, MA: Academic Press (2017). p. 31–45.
105. Seo DJ, Changsun C. Antiviral bioactive compounds of mushrooms and their antiviral mechanisms: a review. *Viruses.* (2021) 13:350. doi: 10.3390/v13020350
106. Wang W, Wang SX, Guan HS. The antiviral activities and mechanisms of marine polysaccharides: an overview. *Mar Drugs.* (2012) 10:2795–816. doi: 10.3390/md10122795
107. Shi Q, Wang A, Lu Z, Qin C, Hu J, Yin J. Overview on the antiviral activities and mechanisms of marine polysaccharides from seaweeds. *Carbohydr Res.* (2017) 453–454:1–9. doi: 10.1016/j.carres.2017.10.020
108. Wang J, Wu T, Fang X, Min W, Yang Z. Characterization and immunomodulatory activity of an exopolysaccharide produced by *Lactobacillus plantarum* JLK0142 isolated from fermented dairy tofu. *Int J Biol Macromol.* (2018) 115:985–93. doi: 10.1016/j.ijbiomac.2018.04.099
109. Wang N, Jia G, Wang C, Chen M, Xie F, Nepovinnykh NV, et al. Structural characterisation and immunomodulatory activity of exopolysaccharides from liquid fermentation of *Monascus purpureus* (Hong Qu). *Food Hydrocoll.* (2020) 103:105636. doi: 10.1016/j.foodhyd.2019.105636
110. Liu ZH, Niu FJ, Xie YX, Xie SM, Liu YN, Yang YY, et al. A review: natural polysaccharides from medicinal plants and microorganisms and their anti-herpetic mechanism. *Biomed Pharmacother.* (2020) 129:110469. doi: 10.1016/j.biopha.2020.110469
111. Liu C, Chen H, Chen K, Gao Y, Gao S, Liu X, et al. Sulfated modification can enhance antiviral activities of *Achyranthes bidentata* polysaccharide against porcine reproductive and respiratory syndrome virus (PRRSV) *in vitro*. *Int J Biol Macromol.* (2013) 52:21–4. doi: 10.1016/j.ijbiomac.2012.09.020
112. Sinha S, Astani A, Ghosh T, Schnitzler P, Ray B. Polysaccharides from *Sargassum tenerrimum*: structural features, chemical modification and anti-viral activity. *Phytochemistry.* (2010) 71:235–42. doi: 10.1016/j.phytochem.2009.10.014
113. Bandyopadhyay SS, Navid MH, Ghosh T, Schnitzler P, Ray B. Structural features and *in vitro* antiviral activities of sulfated polysaccharides from *Sphacelaria indica*. *Phytochemistry.* (2011) 72:276–83. doi: 10.1016/j.phytochem.2010.11.006
114. Li S, Xiong Q, Lai X, Li X, Wan M, Zhang J, et al. Molecular modification of polysaccharides and resulting bioactivities. *Compr Rev Food Sci Food Saf.* (2016) 15:237–50. doi: 10.1111/1541-4337.12161
115. Kalitnik AA, Byankina Barabanova AO, Nagorskaya VP, Reunov AV, Glazunov VP, Solov'eva TF, et al. Low molecular weight derivatives of different carrageenan types and their antiviral activity. *J Appl Phycol.* (2012) 25:65–72. doi: 10.1007/s10811-012-9839-8
116. Mader J, Gallo A, Schommartz T, Handke W, Nagel CH, Günther P, et al. Calcium spirulan derived from *Spirulina platensis* inhibits herpes simplex virus 1 attachment to human keratinocytes and protects against herpes labialis. *J Allergy Clin Immunol.* (2016) 137:197–203. doi: 10.1016/j.jaci.2015.07.027

117. Kwon PS, Oh H, Kwon SJ, Jin W, Zhang F, Fraser K, et al. Sulfated polysaccharides effectively inhibit SARS-CoV-2 *in vitro*. *Cell Discov.* (2020) 6:50. doi: 10.1038/s41421-020-00192-8
118. Lee AJ, Ashkar AA. The dual nature of type I and type II interferons. *Front Immunol.* (2018) 9:2061. doi: 10.3389/fimmu.2018.02061
119. Ivashkiv LB, Donlin LT. Regulation of type I interferon responses. *Nat Rev Immunol.* (2014) 14:36–49. doi: 10.1038/nri3581
120. Hadjadj J, Yatim N, Barnabei L, Corneau A, Boussier J, Smith N, et al. Impaired type I interferon activity and inflammatory responses in severe COVID-19 patients. *Science.* (2020) 369:718–24. doi: 10.1126/science.abc6027
121. Hu B, Guo H, Zhou P, Shi ZL. Characteristics of SARS-CoV-2 and COVID-19. *Nat Rev Microbiol.* (2021) 19:141–54. doi: 10.1038/s41579-020-00459-7
122. Cheng J-J, Chao C-H, Chang P-C, Lu M-K. Studies on anti-inflammatory activity of sulfated polysaccharides from cultivated fungi *Antrodia cinnamomea*. *Food Hydrocoll.* (2016) 53:37–45. doi: 10.1016/j.foodhyd.2014.09.035
123. Wu G-J, Shiu S-M, Hsieh M-C, Tsai G-J. Anti-inflammatory activity of a sulfated polysaccharide from the brown alga *Sargassum cristaefolium*. *Food Hydrocoll.* (2016) 53:16–23. doi: 10.1016/j.foodhyd.2015.01.019
124. Dinić M, Pecikoza U, Djokić J, Stepanović-Petrović R, Milenković M, Stevanović M, et al. Exopolysaccharide produced by probiotic strain *Lactobacillus paraplantarum* BGCG11 reduces inflammatory hyperalgesia in rats. *Front Pharmacol.* (2018) 9:1. doi: 10.3389/fphar.2018.00001
125. Kansandee W, Moonmangmee D, Moonmangmee S, Itsaranuwat P. Characterization and *Bifidobacterium* sp. growth stimulation of exopolysaccharide produced by *Enterococcus faecalis* EJRM152 isolated from human breast milk. *Carbohydr Polym.* (2019) 206:102–9. doi: 10.1016/j.carbpol.2018.10.117
126. Gotteland M, Riveros K, Gasaly N, Carcamo C, Magne F, Liabeuf G, et al. The pros and cons of using algal polysaccharides as prebiotics. *Front Nutr.* (2020) 7:163. doi: 10.3389/fnut.2020.00163

Conflict of Interest: The authors declare that the research was conducted in the absence of any commercial or financial relationships that could be construed as a potential conflict of interest.

Publisher's Note: All claims expressed in this article are solely those of the authors and do not necessarily represent those of their affiliated organizations, or those of the publisher, the editors and the reviewers. Any product that may be evaluated in this article, or claim that may be made by its manufacturer, is not guaranteed or endorsed by the publisher.

frontiers in Nutrition

ORIGINAL RESEARCH
published: 16 November 2021
doi: 10.3389/fnut.2021.760316

Changes in the Fermentation and Bacterial Community by Artificial Saliva pH in RUSITEC System

Tongqing Guo[1], Tao Guo[1], Yurong Cao[1], Long Guo[1], Fei Li[1], Fadi Li[1] and Guo Yang[2]*

[1] State Key Laboratory of Grassland Agro-Ecosystems, Key Laboratory of Grassland Livestock Industry Innovation, Ministry of Agriculture and Rural Affairs, Engineering Research Center of Grassland Industry, Ministry of Education, College of Pastoral Agriculture Science and Technology, Lanzhou University, Lanzhou, China, [2] Gaolan Ecological and Agricultural Integrated Experiment Station, Northwest Institute of Ecological Environment and Resources, Chinese Academy of Sciences, Lanzhou, China

The purpose of the study was to assess the artificial saliva (AS) pH on ruminal fermentation and rumen bacteria community in the rumen simulation technique (RUSITEC) system. The experiment was performed in two treatments (low AS pH vs. high AS pH) with four replicates. The low AS pH was sustained by altering the composition of the AS ($NaHCO_3$ from 9.8 to 1.96 g/L, Na_2HPO_4 from 9.3 to 1.86 g/L) according to McDougall's method. The diets were supplemented with 16 g basic diets with forage to the concentrate ratio of 50:50. The experiments were conducted over 13-day incubation periods, with 9 days adaption and 4 days sample collection. The results showed low AS pH decreased dry matter (DM) degradability (64.37 vs. 58.67%), organic matter (OM) degradability (64.38 vs. 59.32%), neutral detergent fiber (NDF) degradability (46.87 vs. 39.94%), acid detergent fiber (ADF) degradability (38.16 vs. 31.13%), and crude protein (CP) degradability (70.33 vs. 62.99%), respectively. Compared with the high AS pH, the low AS pH increased the proportion of butyrate ($P = 0.008$) and decreased the proportion of propionate ($P < 0.001$). At the bacteria community, the low AS pH increased the abundances of *Spirochaetes* ($P = 0.001$) and *Synergistetes* ($P = 0.004$) and decreased the *Verrucomicrobia* abundance ($P = 0.004$) in solid-associated bacteria. At the genus level, the low AS pH increased the abundance of *Lactobacillus* ($P = 0.050$) and decreased the abundance of *Schwartzia* ($P = 0.002$) in solid-associated bacteria. The abundances of *Prevotellaceae_YAB2003_group* ($P = 0.040$), *Schwartzia* ($P = 0.002$), and *Ruminobacter* ($P = 0.043$) were lower in the low AS pH group compared with the high AS pH group in liquid-associated bacteria. Low AS pH decreased the number of *Ruminococcus albus*, *Ruminococcus flavefaciens*, *Fibrobacter succinogenes* ($P < 0.001$) both in the solid- and liquid-associated bacteria, respectively. The results of the present study included three groups of bacteria communities according to the different sensitives to rumen pH: the abundances of *Lactobacillus*, *Succinivibrio*, *and Prevotella_7* are increased with decreasing AS pH; the amounts of *R. albus*, *R. flavefaciens*, *F. succinogenes* as well as the abundances of *Schwartzia* and *Ruminobacter* decreased with the reducing AS pH; the abundances of *Selenomonas_1*, *Rikenellaceae_RC9_gut_group,* and *Succiniclasticum* were not affected by the AS pH in RUSTITEC.

Keywords: artificial saliva, rumen bacteria, rumen pH, *in vitro*, ruminant

OPEN ACCESS

Edited by:
Ren-You Gan,
Institute of Urban Agriculture, Chinese Academy of Agricultural Sciences (CAAS), China

Reviewed by:
Anusorn Cherdthong,
Khon Kaen University, Thailand
Yury Tatiana Granja-Salcedo,
Colombian Corporation for Agricultural Research (AGROSAVIA), Colombia
Haitao Shi,
University of Saskatchewan, Canada

****Correspondence:***
Fei Li
lfei@lzu.edu.cn

Specialty section:
This article was submitted to Nutrition and Microbes, a section of the journal Frontiers in Nutrition

Received: *18 August 2021*
Accepted: *29 September 2021*
Published: *16 November 2021*

Citation:
Guo T, Guo T, Cao Y, Guo L, Li F, Li F and Yang G (2021) Changes in the Fermentation and Bacterial Community by Artificial Saliva pH in RUSITEC System. Front. Nutr. 8:760316. doi: 10.3389/fnut.2021.760316

INTRODUCTION

A high grain-based diet has been a common strategy to improve animal performance in ruminant production. However, the fermentable carbohydrate diets can lead to the accumulation of organic acids in the rumen, which results in the reduction of ruminal pH, and increases the risk of subacute rumen acidosis (SARA) (1, 2). SARA was described as the daily average rumen pH between 6.25 and 5.5 (3). The main SARA model was obtained by increasing the dietary proportions of grain or decreasing physically effective fiber (peNDF) content (4, 5). The SARA induction approaches have a different impact on the rumen fermentation and bacterial community because of the different substrates (6). The low dietary peNDF induced SARA usually increased the feed intake of dairy cows (7), and the increased feed intake resulted in increasing the production of volatile fatty acids (VFA) and decreased pH (8). Therefore, the low peNDF induced SARA needs to avoid the impact of different feed intake between the treatments. Decreasing the peNDF intake for ruminants could reduce the chewing time and the amount of saliva secretion (9). The *in vitro* SARA model that induced in the rumen simulation technique (RUSITEC) system usually by decreasing the buffer capacity of artificial saliva (AS) (10, 11), which could simulate the low peNDF induced SARA. In addition, the RUSITEC system was designed to ensure the identical substrate intake and rumen passage rate during the fermentation that avoids the disturbance of different feed intake and rumen content passage rate of *in vivo* when the ruminants received different dietary peNDF. Orton et al. (10) decreased the buffer capacity of AS (NaCl from 28 up to 118.5 mmol/L and $NaCO_3$ from 97.0 to 20 mmol/L) decreased pH from 7.0 to 6.0 in the RUSITEC system.

The ruminal pH plays an important role in affecting the communities of rumen bacteria. Li et al. (8) found the low-peNDF diet induced SARA increased the numbers of *Fibrobacter succinogenes* and *Ruminococcus flavefaciens* for the dairy goats. The increased feed intake and cellulolytic bacteria were due to the more substrates or particulate surfaces available for these bacteria attachment and proliferation (12). The solid-associated bacteria attached to the feed particles play a key role in fiber digestion, while the liquid-associated bacteria have significant functions in the metabolism of soluble nutrients (13, 14). There is a difference in the bacteria community between the solid and liquid fractions. The rumen bacteria are influenced by the combination of substrate, physical structure, and pH environment. Li et al. (15) demonstrated that the three groups of bacteria communities change under grain-induced SARA: pH-sensitive but substrate insensitive bacteria, pH-insensitive but substrate sensitive bacteria, and bacteria that are both pH and substrate sensitive. However, it is difficult to design and execute experiments *in vivo* to test this hypothesis. The RUSITEC system is an optional tool *in vitro* model to simulate the rumen microbial fermentation and could strictly control the effects of substrate and pH independently (10).

Therefore, we hypothesized that the low AS pH would alter the rumen bacteria community, which also lead to the variation of the rumen fermentation. The objectives of this study were to determine the effects of AS pH on the nutrients digestion, rumen fermentation, and ruminal bacteria community.

TABLE 1 | The composition of the infused buffer[a].

	High AS pH	Low AS pH
$NaHCO_3$	9.8 g/L	1.96 g/L
Na_2HPO_4	9.3 g/L	1.86 g/L
NaCl	0.47 g/L	0.47 g/L
KCl	0.57 g/L	0.57 g/L
$MgSO_4{\cdot}7H_2O$	0.12 g/L	0.12 g/L
$CaCl_2{\cdot}2H_2O$	0.045 g/L	0.045 g/L

[a] *The infused buffer was referenced to McDougall's method (17).*

MATERIALS AND METHODS

All the procedures involving animals were carried out in accordance with the Biological Studies Animal Care and Use Committee of Gansu Province, China (2005–2012).

Equipment, Animals, and Procedures

The study was conducted using RUSITEC (Sanshin, Tokyo, Japan) as described by Kajikawa et al. (16). The RUSITEC system contained eight fermenters with a volume of 800 ml each per tank. The inoculum used in the fermenters was obtained from four ruminal fistulated *Hu* lambs fed two equivalent meals at 07:00 and 19:00 daily in the form of totally mixed ration (TMR) pellets with forage to concentrate of 80:20. The rumen contents were collected through the ruminal fistula before the morning feed and separated into liquid and solid fractions by four layers of cheesecloth. The squeezed solid inoculum (70 g wet weight) was enclosed in a nylon bag (7 × 13 cm, pore size: 100 μm). On the 1st day during fermentation, 400 ml of liquid inoculum was distributed to each fermenter under CO_2 flux after mixing with an equal volume of AS, and two bags were placed in the fermenter, one with feed and the other with solid inoculum. After 24 h, the bag with the inoculum was replaced by a new bag with the feed. Subsequently, the bag that included the feed incubated 48 h was replaced by a new feed bag. A continuous infusion of AS at a rate of 600 ml/day was maintained in each fermenter. The fermenters were kept in a water bath at 39°C and slowly moved up and down by an electric motor (five times per minute).

Experimental Diets

The fermenters were randomly assigned to the two treatments with four replicates of each treatment. The treatment included high AS pH (pH 7.0) or low AS pH (pH 6.0) according to McDougall's method (17) (**Table 1**). The low AS pH was sustained by decreasing the AS buffer capacity ($NaHCO_3$ from 9.8 to 1.96 g/L and Na_2HPO_4 from 9.3 to 1.86 g/L). The pH of all the fermenters was recorded at 07:30, 15:30, and 23:30 daily throughout the experiment periods. The diets were supplemented with 16 g basic diets with forage to the concentrate ratio of 50:50 (**Table 2**). The diets were ground through a 2 mm

TABLE 2 | The dietary ingredients and nutrient composition (% dry matter [DM]).

Ingredients	Contents
Alfalfa hay, %	40.60
Corn straw, %	9.40
Corn, %	18.80
Molasses, %	2.50
Cottonseed meal, %	3.80
Soybean hull, %	4.40
Corn gluten meal, %	6.30
Corn husk, %	12.50
Expanded urea, %	0.80
NaCl, %	0.40
Expanded urea, %	0.40
Premix, %	0.30
Nutritional levels	
DM, % as fed	91.74
NDF, % as DM	42.17
ADF, % as DM	21.78
EE, % as DM	1.13
CP, % as DM	17.00

sieve. The experiment was conducted for 13-day incubation periods, with 9 days adaption and 4 days sample collection.

Date and Sample Collection

During the last 4 days of the experiment, the ice water was added around the over flow bottle to terminate fermentation. On days 10 and 11, about 10 ml of fermenter fluid were collected at 0, 3, 6, 9, and 12 h after the morning feed, the ruminal pH was immediately measured with a mobile pH meter (PHB-4, Shanghai Hongyi instrument Limited, Shanghai, China). Then, 5-ml of rumen fluid was preserved with 1 ml of metaphosphoric acid (25% wt/vol) and stored at −20°C for the determination of VFA. On day 12, about 10 ml of ruminal fluid was collected from each fermenter and immediately stored at −80°C to exact bacterial DNA. On day 13, about 20% of solid contents from each nylon bag were frozen at −80°C for the solid phase bacteria DNA extraction. The bag from each vessel on days 10, 11, and 12 was collected, washed one time with 100 ml of artificial saliva, washed with cold water until the outflow was clear, and stored to determine dry matter (DM) disappearance. The DM disappearance was calculated from the loss in weight after oven drying at 65°C for 48 h by using the following equation: DM disappearance (%) = {(g Sample DM – g Residue DM – g Bag DM)/g Sample DM} *100, and the residues were analyzed for DM, organic matter (OM), neutral detergent fiber (NDF), acid detergent fiber (ADF), and crude protein (CP).

Analytical Procedures

The content of DM, ash, and N in the feed and residues were determined according to the Association of Official Analytical Chemists (AOAC) method (18). The DM content was determined by drying at 105°C in a forced-air oven for 4 h. The ash content was determined by complete combustion in a muffle furnace (PrepASH-340, Precisa, Swizerland) at 550°C for 6 h. The N contents of the feed bag were carried out by a protein analyzer (K9840, Hanon Advanced Technology Group Co., Ltd, Jinan, China) according to the Kjeldahl method and CP was calculated as N × 6.25 (18). The NDF and ADF were determined by the method of Van Soest et al. (19).

The thawed rumen fluid samples were centrifuged at 2,500 ×g at 4°C for 5 min, and the supernatants were processed as described by Liang et al. (20). The VFA concentrations were measured with gas chromatography (GC) on a Thermo Fisher Trace 1300 GC system (TRACE 1300, Thermo Scientific, Milan, Italy) as described by Li et al. (15). The GC was fitted with a silica capillary column (DB-FFAP, 30 m × 0.32 mm × 0.25 μm, Agilent Technologies Co., Ltd, Santa Clara, CA, USA), and crotonic acid (1% wt/vol) was used as the internal standard. The injector and detector temperatures were set at 240°C. The following temperature program was used: the temperature was increased from 50 to 190°C at a rate of 25°C/min, and the temperature increased was increased to 200°C at 10°C/min for 5 min. Finally, the temperature was increased to 220°C at a rate of 10°C/min and was held for 5 min. The concentration of lactate was determined by a commercial Lactate Analysis Kit (Nanjing Jiancheng Technology Co., LTD., Nanjing, China).

Microbial DNA Extraction and Relative Quantitative Real-Time PCR

The DNA of rumen bacteria was extracted by an E.Z.N. A® Bacterial DNA Kit (Omega Bio-Tek, Inc., Norcross, GA, USA) according to the instructions from the manufacturer. The final elution volume was 80 μl, and DNA concentration and purity were measured by an ND-2000 spectrophotometer (NanoDrop Technologies, Wilmington, DE, USA). The primer design for all the rumen bacteria to amplify was selected on the basis of the published literature (**Table 3**). The quantitative real-time PCR (qPCR) protocol was described by Liang et al. (20). Each sample contained 1 μl of DNA, 10 μl of SYBR Green (TransGen Biotech, Beijing, China), 0.6 μl of each primer, and 8.6 μl of ddH_2O in a final volume of 20 μl. The amplification conditions were as follows: 95°C for 10 s; 40 cycles of 10 s at 95°C; 30 s at 60°C; 72°C for 10 s; and a final cycle at 72°C for 5 min. To obtain melting curve data, the temperature increased in 0.5°C increments from 65 to 95°C. All investigated PCR products had only single melting peaks. The relative abundance of rumen bacteria was expressed as a proportion of total rumen bacterial 16S rRNA according to the equation: relative quantification $= 2^{-(CTctarget - CTctotal\ bacteria)}$, where *CT* represents a threshold cycle (26). Before the statistical analysis, the percentage of each microbe target was calculated as $(2^{-\Delta CT}) \times 100$, then, the data were log10–scale transformed before the statistical analysis (20). The quantity of each species was expressed as the log10 copy number of 16S rRNA gene copies per milliliter of rumen fluid.

The sequence analysis and bioinformatics were conducted by SMRT Portal (version. 2.7; PacBio, CA, USA). The Lima (version. 1.7.0; PacBio, CA, USA) software was applied to export circular consensus sequencing (CCS) sequences from raw data and perform Barcode identification for the CCS sequences. Then,

TABLE 3 | The sequence of primers used to analyze the relative abundance of bacteria.

Primer name	Primer sequences (5′–3′)	References
Fibrobacter succinogenes	F: 5-GGTATGGGATGAGCTTGC-3 R: 5-GCCTGCCCCTGAACTATC-3	(21)
Butyrivibrio fibrisolvens	F: 5-GCCTCAGCGTCAGTAATCG-3 R: 5-GGAGCGTAGGCGGTTTTAC-3	(22)
Ruminococcus flavefaciens	F: 5-CGAACGGAGATAATTTGAGTTTACTTAGG-3 R: 5-CGGTCTCTGTATGTTATGAGGTATTACC-3	(22)
Prevotella brevis	F: 5-GGTTCTGAGAGGAAGGTCCCC-3 R: 5-TCCTGCACGCTACTTGGCTG-3	(23)
Selenomonas ruminantium	F: 5-CAATAAGCATTCCGCCTGGG-3 R: 5-TTCACTCAATGTCAAGCCCTGG-3	(23)
Ruminococcus albus	F: 5-CCCTAAAAGCAGTCTTAGTTCG-3 R: 5-CCTCCTTGCGGTTAGAAC-3	(24)
Total bacteria	F: 5-TCCTACGGGAGGCAGCAGT-3 R: 5-GGACTACCAGGGTATCTAATCCTGTT-3	(25)

the chimera was filtered by UCHIME (version. 4.2; Tiburon, CA, USA) software to get the Optimization-CCS (27). We cluster Optimization-CCS sequences to get operational taxonomic units (OTU) by USEARCH (version 10.0; Tiburon, CA, USA) software (28), then get the species classification according to the sequence composition of OTU. The principal coordinate analysis (PCoA) plot of samples according to the distance matrix was obtained to analyze. The Ace, Chao1, Shannon, and Simpson indexes of each sample were statistically calculated by using Mothur (version v.1.30; Mothur, Michigan, USA) to evaluate the alpha diversity at 97% similarity level (29). According to OTU analysis results, a taxonomic analysis was performed with RDP Classifier (version 2.2; RDP Classifier, Michigan, USA) at the taxonomic level of phylum and genus (30). The raw sequencing data were in the Sequence Read Archive (SRA) of NCBI and can be accessed *via* accession number: PRJNA752826.

Statistical Analysis

The nutrients degradation, fermentation parameters, and rumen bacteria abundances were analyzed by using SPSS software version 17.0 (IBM, Armonk, NY, United States). The independent sample *T*-test was used to calculate the differences in the results between the high AS pH group and the low AS pH group in this experiment. The effect of time on fermentation variables was used as a repeated measure. The model included the effects of AS pH, time, and their interaction as fixed effects, and individual fermenters as a random effect. The Kruskal–Wallis test was used to test the rumen bacteria in the solid and liquid fraction at the phylum and genus. The significant difference of data was analyzed by Kruskal–Wallis one-way ANOVA analysis. The significance was set as $P \leq 0.05$ and the tendencies were considered when $0.05 < P < 0.10$.

RESULTS

Decreasing the AS buffer capacity resulted in a reduction in average pH to 6.02 in the low AS group. The effect of AS pH on the nutrients degradabilities is presented in **Table 4**. The degradabilities of DM, OM, NDF, ADF, and CP were lower in the low AS pH group compared with the high AS pH group ($P < 0.001$).

TABLE 4 | Effect of AS pH on the nutrients degradability in the rumen simulation technique (RUSITEC).

Degradability rate, % DM	High AS pH	Low AS pH	SEM[a]	*P*-value
DM	64.37 ± 0.72	58.67 ± 1.37	0.555	<0.001
OM	64.38 ± 1.26	59.32 ± 1.34	0.669	<0.001
NDF	46.87 ± 0.83	39.94 ± 2.10	1.001	<0.001
ADF	38.16 ± 1.54	31.13 ± 2.51	1.274	<0.001
CP	70.33 ± 1.76	62.99 ± 2.83	1.239	<0.001

SEM[a], standard error of the sample means.

TABLE 5 | Effect of artificial saliva (AS) pH on pH and volatile fatty acids in the rumen simulating fermenter (RUSITEC).

	High AS pH	Low AS pH	SEM[a]	*P*-value
pH	7.03 ± 0.05	6.02 ± 0.05	0.023	< 0.001
VFA molar ratios, mol/100 mol				
Acetate	46.47 ± 0.74	45.24 ± 1.25	0.727	0.140
Propionate	35.84 ± 1.59	24.94 ± 1.88	1.232	< 0.001
Isobutyrate	0.04 ± 0.002	0.04 ± 0.003	0.002	0.161
Butyrate	8.57 ± 1.87	14.18 ± 0.32	0.951	0.008
Isovalerate	1.68 ± 0.33	5.50 ± 2.13	1.075	0.012
Valerate	7.39 ± 0.60	10.07 ± 0.41	0.363	< 0.001
Acetate:propionate	1.30 ± 0.04	1.82 ± 0.14	0.723	< 0.001
Lactate, mmol/L	0.07 ± 0.01	0.05 ± 0.02	0.010	0.209
TVFA[b], mmol/L	52.41 ± 8.77	42.66 ± 2.92	4.624	0.080

SEM[a], standard error of the sample means; TVFA[b], total volatile fatty acids.

The effect of AS pH on VFA in RUSITEC is shown in **Table 5**. The total concentration of VFA tended to be lower ($P = 0.080$) in the low AS pH group compared with the high AS pH group. The proportions of acetate, isobutyrate, and the concentration of lactate were not affected by different AS pH ($P > 0.05$). The low AS pH decreased the proportion of propionate ($P < 0.001$) and increased the proportions of butyrate ($P = 0.008$), isovalerate ($P = 0.012$), valerate ($P < 0.001$), and the ratio of acetate to propionate ($P < 0.001$).

The effect of AS pH on the fermentation parameters at 0, 3, 6, 9, and 12 h after feeding is shown in **Supplementary Table 1**. An interaction between AS pH and time affected the rumen pH ($P = 0.003$); the low AS pH had lower rumen pH than high AS pH ($P < 0.001$), and rumen pH was decreased at 0 and 9 h after feeding ($P < 0.001$). The proportion of acetate was increased at 0 h and decreased at 3 h after feeding in the high AS pH group, respectively ($P = 0.039$). The proportion of butyrate was affected by an interaction between the AS pH and time ($P = 0.037$). The low AS pH had a greater proportion of butyrate than high AS pH ($P = 0.002$), and the proportion of butyrate was decreased at 0 h and increased at 3 and 9 h between the low and high AS pH group

TABLE 6 | Effect of AS pH on the α-diversity of the rumen bacteria and community at phylum level in RUSITEC.

		High AS pH	Low AS pH	SEM[1]	*P*-value	
					AS pH	Rumen bacteria
α-diversity						
ACE	Solid	168.34 ± 25.19	190.62 ± 25.60	17.956	0.261	0.075
	Liquid	219.64 ± 12.85	179.92 ± 15.22	9.961	0.007	
Chao1	Solid	162.49 ± 25.37^{ab}	184.05 ± 16.48^{b}	16.126	0.204	0.030
	Liquid	218.33 ± 9.27^{a}	183.69 ± 24.38^{ab}	13.021	0.038	
Simpson	Solid	0.09 ± 0.22^{ab}	0.13 ± 0.04^{a}	0.227	0.126	0.009
	Liquid	0.03 ± 0.00^{b}	0.12 ± 0.08^{ab}	0.038	0.098	
Shannon	Solid	3.38 ± 0.25^{ab}	2.93 ± 0.19^{b}	0.157	0.031	0.008
	Liquid	4.22 ± 0.12^{a}	3.22 ± 0.46^{ab}	0.235	0.006	
Phylum, %						
Firmicutes	Solid	44.65 ± 2.07	47.35 ± 8.87	4.552	0.574	0.075
	Liquid	32.94 ± 1.83	31.02 ± 12.50	6.317	0.373	
Bacteroidetes	Solid	47.50 ± 2.63^{a}	39.68 ± 9.56^{ab}	4.957	0.166	0.030
	Liquid	37.60 ± 1.49^{ab}	29.74 ± 8.17^{b}	4.150	0.107	
Proteobacteria	Solid	5.26 ± 1.94^{b}	7.87 ± 4.01^{ab}	2.229	0.286	0.009
	Liquid	12.82 ± 3.43^{ab}	27.53 ± 5.72^{a}	3.335	0.005	
Planctomycetes	Solid	0.88 ± 0.80^{ab}	0.37 ± 0.48^{b}	0.465	0.313	0.008
	Liquid	10.70 ± 2.43^{a}	2.26 ± 1.07^{ab}	1.328	0.001	
Spirochaetes	Solid	0.88 ± 0.34^{ab}	3.15 ± 0.66^{a}	0.371	0.001	0.005
	Liquid	1.35 ± 0.49^{ab}	0.06 ± 0.048^{b}	0.245	0.002	
Verrucomicrobia	Solid	1.67 ± 0.72^{a}	0.06 ± 0.06^{ab}	0.023	0.004	0.082
	Liquid	0.02 ± 0.04^{b}	0.006 ± 0.01^{b}	0.361	0.510	
Actinobacteria	Solid	0.02 ± 0.03	0.95 ± 1.21	0.603	0.221	0.105
	Liquid	0.01 ± 0.02	0	0.012	0.391	
Tenericutes	Solid	0.20 ± 0.13	0.33 ± 0.23	0.132	0.386	0.364
	Liquid	0.31 ± 0.12	0.06 ± 0.07	0.071	0.012	
Lentisphaerae	Solid	0.03 ± 0.03^{ab}	0^{b}	0.016	0.190	0.040
	Liquid	0.40 ± 0.20^{a}	0.03 ± 0.02^{ab}	0.099	0.031	
Synergistetes	Solid	0.006 ± 0.01^{b}	0.05 ± 0.02^{ab}	0.010	0.004	0.060
	Liquid	0.15 ± 0.10^{ab}	0.25 ± 0.17^{a}	0.100	0.342	
Others	Solid	0.01 ± 0.02^{ab}	0^{b}	0.011	0.391	0.311
	Liquid	0.13 ± 0.12^{ab}	0.17 ± 0.08^{a}	0.073	0.586	
Unclassified	Solid	0.54 ± 0.29^{ab}	0.25 ± 0.14^{b}	0.162	0.134	0.006
	Liquid	1.92 ± 0.54^{a}	0.82 ± 0.12^{ab}	0.275	0.024	

^{a,b}Differences ($P < 0.05$) between the abundance of rumen bacteria within solid fraction and liquid fraction.
SEM[1], standard error of the sample means.

($P < 0.001$). The proportion of valerate was higher at 0, 3, 6, and 9 h than at 12 h after feeding in the low AS pH group ($P = 0.009$).

The effect of AS pH on the α diversity and phylum abundances of the ruminal bacteria are shown in **Table 6**. The sequence coverage sufficiently met a coverage >97% for all the samples. Across all the samples, a total of 102,043 CCS sequences were obtained, and an average of 6,378 CCS sequences per sample. In total, 94% of CCS sequences were classified at the phyla level and 66% at the genus level. In the solid-associated bacteria, the ACE, Chao1, and Simpson indexes were not affected by AS pH ($P > 0.05$). However, the Shannon index was greater in the high AS pH group ($P = 0.031$) compared with the low AS pH group. In the liquid-associated bacteria, the ACE, Chao1, and Shannon indexes were greater ($P < 0.05$) in the high AS pH group compared with the low AS pH group, whereas the Simpson index tended to be higher ($P = 0.098$). The ACE, Chao1, Simpson, and Shannon indexes have no difference between solid-associated bacteria and liquid-associated bacteria.

The abundance of *Firmicutes* and *Bacteroidetes* was not affected by AS pH treatment ($P > 0.05$). The low AS pH increased the abundances of *Spirochaetes* ($P = 0.001$), *Synergistetes* ($P = 0.004$), and decreased the *Verrucomicrobia* abundance ($P = 0.004$) in the solid-associated bacteria. In the liquid-associated bacteria, low AS pH increased the abundance of *Proteobacteria*

($P = 0.005$) and decreased the abundances of *Planctomycetes* ($P = 0.001$), *Spirochaetes* ($P = 0.002$), *Tenericutes* ($P = 0.012$), and *Lentisphaerae* ($P = 0.031$). At the AS pH 6.0, the abundance of *Spirochaetes* was greater in solid than a liquid fraction. For the liquid and solid fraction, the abundances of *Firmicutes*, *Bacteroidetes*, and *Proteobacteria* were similar in solid fraction compared with the liquid fraction.

The beta diversities of bacteria communities within different AS pH for each fraction were calculated and visualized through the two-dimensional PCoA analysis using the binary-Jaccard (**Figure 1**). A significant difference between the bacterial communities in the AS pH treatment was noted. Both principal components accounted for 34.79% (PC1) and 27.78% (PC2) of the explained variance.

The ruminal bacteria with abundances >1% at the genus level were presented in **Table 7**. The low AS pH increased the abundance of *Lactobacillus* ($P = 0.050$) and decreased the abundances of *Schwartzia* ($P = 0.002$) in solid-associated bacteria compared with the high AS pH group. In the solid-associated bacteria, the abundance of *Succinivibrio* tended to be greater ($P = 0.059$) in the low AS pH group compared with the high AS pH group, whereas the abundance of *Ruminobacter* tended to be lower ($P = 0.086$). In the liquid-associated bacteria, the abundances of *Prevotellaceae_YAB2003_group* ($P = 0.040$), *Schwartzia* ($P = 0.002$), and *Ruminobacter* ($P = 0.043$) were lower in the low AS pH group compared with the high AS pH group. However, the abundances of *Succinivibrio* ($P < 0.001$) and *Prevotella_1* ($P = 0.001$) were higher in the low AS pH treatment compared with the high AS pH group. At the AS pH 7.0 and 6.0, the abundance of *Prevotellaceae_YAB2003_group* was greater in a solid fraction than a liquid fraction ($P < 0.05$). The abundance of *Prevotella_1* was decreased in a solid fraction when the AS pH was 6.0 ($P = 0.008$), while the abundance of *Prevotella_7* was increased ($P = 0.007$).

The effect of AS pH on the number of rumen bacteria is presented in **Table 8**. The low AS pH decreased the number of *Ruminococcus albus*, *R. flavefaciens*, *F. succinogenes* ($P < 0.001$) both in the solid- and liquid-associated bacteria, respectively. The low AS pH tended to increase the amount of *Prevotella brevis* ($P = 0.091$) in liquid-associated bacteria. The low AS pH decreased the amounts of *Selenomonas ruminantium* in solid-associated bacteria ($P = 0.022$) and tended to decrease in liquid-associated bacteria ($P = 0.065$). The number of *S. ruminantium* was increased in solid fractions both in high AS pH and low AS pH ($P < 0.001$). At the high AS pH, the amounts of *P. brevis*, *Butyrivibrio fibrisolvens,* and *total bacteria* were increased in solid fraction compared with the liquid fraction ($P < 0.05$). The number of *F. succinogenes* was greater in solid fraction than liquid fraction at the low AS pH ($P < 0.001$).

DISCUSSION

The rumen pH is the most monitored parameter for SARA diagnosis. According to the severity of SARA, the average daily pH threshold was 5.50–6.25 (3). In the current study, decreasing the AS buffer capacity resulted in an average pH of 6.02. The ruminal pH was an important factor that affect the degradation of NDF and OM degradation in the rumen (31). In our study, low AS pH decreased the degradabilities of DM, OM, NDF, and ADF. These results are consistent with the previous reports that the digestion rates of DM and NDF were reduced with the decreasing AS pH (7.0 vs. 4.9) *in vitro* (32). The decreased digestibilties of NDF and ADF at the low AS pH are mainly attributed to the reduction of cellulolytic bacteria populations and the ability of cellulolytic bacteria to attach to the feed particles (33).

Reduction in the rumen pH lower than 6.0 has a negative impact on the amount of cellulolytic bacteria (*R. albus*, *R. R. flavefaciens*, *F. succinogenes,* and *B. fibrisolvens*) in the rumen (15, 34). As expected, the low AS pH decreased the amount of ruminal *R. albus*, *R. flavefaciens*, *F. succinogenes,* and *B. fibrisolvens* in the solid- and liquid-associated bacteria with the identical substrates chemical compositions. However, Li et al. (8) found that the ruminal cellulolytic bacteria, such as the amounts of *F. succinogenes* and *R. flavefaciens* were increased when the dairy goats experience the low-peNDF diet induced SARA. Khafipour et al. (6) found the mild grain-induced SARA increased the populations of *R. albus* and *R. flavefaciens*. The result of cellulolytic bacteria was not consistent between the low peNDF-induced SARA with the high grained-induced SARA *in vivo* (6). In the present study, we intended to stimulate the low peNDF induced SARA by decreasing the AS pH in Rustitec, which is similar to the decreased saliva secretion when the ruminants received the low peNDF diets *in vivo*. The increased cellulolytic bacteria when the cows or goats received the low peNDF diets (decreased the roughage particle size without changing the roughage to concentrate ratio) mainly attributed to the increased surface area for microbial attachment (8, 35–37). However, the particle size of feed was identical between the treatments, and the changes of cellulolytic bacteria only response to the different AS pH in the present study. Therefore, the results of the present study indicated that the low AS pH indeed decreased the number of cellulolytic bacteria when the substrate was identical in the Rustitec. The rumen bacteria abundance of the solid fraction is significantly higher than that of the liquid fraction (38). The amounts of *B. fibrisolvens* and *F. succinogenes*, *total bacteria* were enriched in a solid fraction in our study. This result was in accordance with De Mulder et al. (14), who identified that cellulolytic bacteria are prevalent in the solid fraction.

The ruminal genus of *Prevotella.app* is considered to be associated with starch degradation and growth well at low pH conditions (6, 39). In our study, the amount of *P. brevis* was not affected by AS pH in the solid-associated bacteria, but the number of *P. brevis* in the liquid-associated bacteria tended to be increased in the low AS pH group.

In the current study, the degradability of CP decreased in the low AS pH group. Several studies have indicated that the low AS pH decreased or unaffected CP degradability (32, 40). The plant proteins were integrated within non-protein polymers, such as polysaccharides, which may limit the access of proteolytic bacteria to the substrate (41). It is possible that the low AS pH decreased ruminal cellulolytic activity and led to a reduction

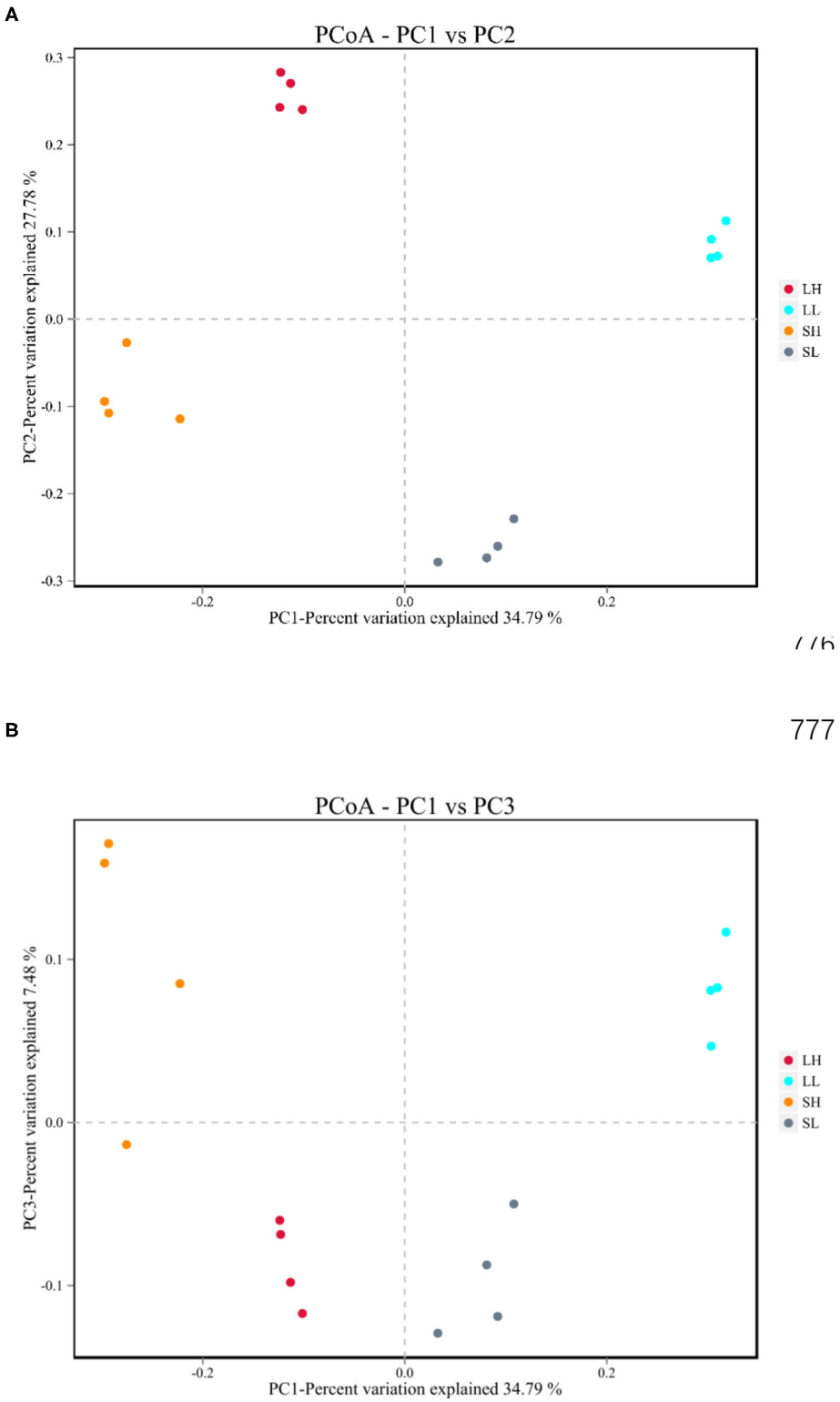

FIGURE 1 | Effects of artificial saliva (AS) pH on the β diversity in the rumen bacteria **(A,B)** in RUSITEC. LH, the high artificial saliva (AS) pH in the liquid-associated bacteria; LL, the low AS pH in the liquid-associated bacteria; SH, the high AS pH in the solid-associated bacteria; SL, the low AS pH in the solid-associated bacteria.

TABLE 7 | Effect of AS pH on the rumen bacteria at genus level in RUSITEC.

		High AS pH	Low AS pH	SEM[1]	*P*-value	
					AS pH	Rumen bacteria
Lactobacillus	Solid	17.35 ± 5.96^{ab}	29.32 ± 7.76^{a}	4.895	0.050	0.019
	Liquid	4.55 ± 1.20^{b}	19.21 ± 18.54^{ab}	9.292	0.212	
Prevotellaceae_YAB2003_group	Solid	25.91 ± 4.41^{a}	23.91 ± 11.57^{a}	6.129	0.755	0.005
	Liquid	7.51 ± 3.99^{b}	0.64 ± 0.53^{b}	2.014	0.040	
Succinivibrio	Solid	3.90 ± 1.51^{b}	7.47 ± 4.12^{ab}	2.193	0.059	0.012
	Liquid	6.28 ± 2.14^{ab}	25.59 ± 5.24^{a}	2.831	<0.001	
Selenomonas_1	Solid	6.20 ± 1.160	7.85 ± 2.18	1.234	0.206	0.481
	Liquid	7.81 ± 1.29	8.99 ± 3.84	2.025	0.592	
Prevotella_1	Solid	6.14 ± 1.45^{ab}	3.38 ± 1.42^{b}	1.017	0.340	0.008
	Liquid	3.05 ± 0.71^{b}	14.09 ± 3.61^{a}	1.841	0.001	
Rikenellaceae_RC9_gut_group	Solid	2.96 ± 1.09^{b}	3.16 ± 1.43^{ab}	0.898	0.827	0.009
	Liquid	8.68 ± 2.59^{ab}	10.92 ± 3.88^{a}	2.330	0.374	
Prevotella_7	Solid	4.30 ± 2.19^{ab}	6.89 ± 2.07^{a}	1.507	0.137	0.007
	Liquid	1.76 ± 0.90^{ab}	0.38 ± 0.12^{b}	0.454	0.053	
Schwartzia	Solid	5.20 ± 0.98^{a}	2.34 ± 0.38^{ab}	0.523	0.002	0.005
	Liquid	2.13 ± 0.25^{ab}	1.30 ± 0.39^{b}	0.229	0.011	
Ruminobacter	Solid	1.00 ± 0.78^{ab}	0.15 ± 0.02^{b}	0.390	0.086	0.005
	Liquid	4.66 ± 2.76^{a}	0.01 ± 0.01^{ab}	1.381	0.043	
Succiniclasticum	Solid	0.34 ± 0.27^{b}	0.57 ± 0.40^{ab}	0.243	0.391	0.012
	Liquid	1.70 ± 0.77^{ab}	3.01 ± 1.50^{a}	0.840	0.171	
Others	Solid	18.39 ± 4.59^{ab}	11.35 ± 2.71^{ab}	2.651	0.038	0.013
	Liquid	21.43 ± 3.36^{a}	10.18 ± 3.59^{b}	2.459	0.004	
Unclassified	Solid	8.38 ± 4.25^{b}	3.75 ± 0.86^{ab}	2.168	0.076	0.009
	Liquid	3.04 ± 3.21^{a}	5.67 ± 1.10^{ab}	1.695	<0.001	

^{a,b}*Differences ($P < 0.05$) between the abundance of rumen bacteria within the solid fraction and liquid fraction.*
SEM[1], standard error of the sample means.

TABLE 8 | Effect of AS pH on the number of ruminal bacteria in RUSITEC.

		High AS pH	Low AS pH	SEM[1]	*P*-value	
					AS pH	Rumen bacteria
Ruminococcus Flavefaciens	Solid	9.85 ± 0.89^{a}	7.24 ± 0.98^{b}	0.399	< 0.001	< 0.001
	Liquid	9.19 ± 0.21^{a}	7.05 ± 0.47^{b}	0.232	< 0.001	
Fibrobacter succinogenes	Solid	8.59 ± 0.67^{a}	7.86 ± 0.31^{a}	0.223	< 0.001	< 0.001
	Liquid	7.75 ± 0.22^{a}	6.36 ± 0.45^{b}	0.192	< 0.001	
Prevotella brevis	Solid	9.38 ± 0.24^{a}	9.32 ± 0.45^{a}	0.148	0.693	0.001
	Liquid	8.85 ± 0.42^{b}	9.09 ± 0.18^{ab}	0.132	0.091	
Ruminococcus albus	Solid	10.22 ± 0.54^{a}	8.26 ± 0.22^{b}	0.254	< 0.001	< 0.001
	Liquid	9.69 ± 0.21^{a}	7.77 ± 0.41^{b}	0.213	< 0.001	
Selenomonas ruminantium	Solid	10.78 ± 0.24^{a}	10.50 ± 0.29^{a}	0.453	0.028	< 0.001
	Liquid	10.26 ± 0.16^{b}	10.14 ± 0.13^{b}	0.121	0.065	
Butyrivibrio fibrisolvens	Solid	8.94 ± 0.40^{a}	8.54 ± 0.28^{ab}	0.145	0.081	0.011
	Liquid	8.40 ± 0.10^{b}	8.55 ± 0.18^{ab}	0.058	0.022	
Total bacteria	Solid	15.59 ± 0.49^{a}	15.55 ± 0.40^{a}	0.178	0.833	0.002
	Liquid	15.03 ± 0.18^{b}	15.34 ± 0.15^{ab}	0.072	< 0.001	

^{a,b}*Differences ($P < 0.05$) between the number of rumen bacteria within the solid fraction and liquid fraction.*
SEM[1], standard error of the sample means.

in the CP degradability due to the limitation of the access of proteases to their matrix (8).

In our experiment, the total concentration of VFA was reduced in the low AS pH treatment. This result was in accordance with Jiao et al. (42), who found that the total concentration of VFA (42.66 vs. 52.41 mmol/L) declined when pH was at 5.8 compared with the pH 6.5 *in vitro*. The declined total VFA concentration in the present study is mainly attributed to the decreased OM degradability. In our study, the proportion of acetate was increased at 0 h and decreased at 3 h after feeding in the high AS pH group. Because the fermenters are opened to supply new nylon bags with feed; this operation exposes the cellulolytic bacteria to oxygen and inhibits the activity (43). The decrease AS pH reduced the proportion of propionate in our experiment. The results were consistent with Strobel and Russell (44) found the concentration of propionate from starch fermentation (2.9 vs. 1.1 mM) decreased when the pH decreased from 6.7 to 5.8. The previous studies reported the amylolytic bacteria to produce amounts of propionate, but many cellulolytic bacteria generate a large amount of succinate, an intermediate that is eventually converted to propionate (45). The decreased proportion of propionate was because the low ruminal pH inhibited the succinate conversion to propionate. The lower molar ratio of the propionate in the low AS pH group also resulted in a higher acetate to propionate compared with the high AS pH group. These results are different from Cardozo et al. (46), who reported the ratio of acetate to propionate was lower when pH was decreased from 7.0 to 5.5 because the high-grain diets decreased the acetate production and increased the propionate production in the rumen.

In the present study, the proportion of butyrate was greater in the low AS pH group compared with the high AS pH group. The results were in accordance with Esdale and Satter (47), who reported that the butyrate production was higher at pH 5.6 compared with at pH 6.2 *in vitro*. In addition, Shriver et al. (48) found butyrate production increased as pH was decreased from 6.2 to 5.8 *in vivo*. Calsamiglia et al. (32) identified that the concentration of butyrate was only affected by the changes of pH and not affected by diet compositions *in vitro*. The results could be associated with the increasing abundance of *Prevotellaceae* (e.g., *Prevotella_1*) in the liquid-associated bacteria that resulted in the increased butyrate production *in vitro* (49). In the current study, the proportion of butyrate was decreased at 0 h and increased at 3, 6, and 9 h after feeding. At 2 h after the start of incubation, the16S rDNA copy numbers of amylolytic bacteria attached to the grain were increased (50), which may promote butyrate production at 3, 6, and 9 h after feeding.

The concentrations of isovalerate and valerate in the rumen were related to the protein degradation and fermentation of branched-chain AA (51). The isovalerate and valerate are also considered as stimulating factors that enhanced the growth of cellulolytic bacteria (52). In the current study, the low AS pH increased the proportion of isovalerate and valerate, and the proportion of valerate was higher at 0, 3, 6, and 9 h than at 12 h after feeding. It had a low pH, which inhibited the growth of cellulolytic bacteria. The RUSITEC system fermenters were opened when the bags were replaced by the new nylon bags with feed; this operation exposed cellulolytic bacteria to oxygen and inhibited the activity of cellulolytic bacteria (43). This therefore would have resulted in the accumulation of valerate and isovalerate in the fermenters and increased at 3, 6, 9, and 12 h after feeding.

Using the sequence and bioinformatics analysis, we obtained 6,378 CCS sequences on average for each sample with good coverage (>97.0%). In accordance with our hypothesis, both the microbial α-diversity and β-diversity were affected by AS pH treatment. Meanwhile, most of the alpha diversity indices (except Simpson index) decreased with the low AS pH in the liquid-associated bacteria, suggesting that the low pH significantly decreased the activity and number of ruminal bacteria. These results are in agreement with Shen et al. (53), who reported the reduction of pH decreased the bacteria alpha diversity. In addition, the PCoA analysis also showed that the bacterial communities of the high AS pH and low AS pH clustered separately, indicating their distinct bacterial compositions in the rumen. These results were similar to the founding by Li et al. (15) who found the bacterial compositions were different between the sheep with high rumen pH and low rumen pH with identical feed composition. Interestingly, the ACE, Chao1, Simpson, and Shannon indexes have no difference between solid fractions and liquid fractions in our study. Because the solid- and liquid-associated bacteria do not have differences in the taxonomic composition but can be distinguished based on the relative abundance of species (14).

In the present study, the relative abundances of ruminal *Firmicutes* and *Bacteroidetes* were not affected by AS pH. The *Firmicutes* are predominantly composed of Gram-positive bacteria in the rumen, which are metabolically capable of utilizing the fermentable carbohydrates (54). Previous studies showed that feeding high-grain diets for cattle increased the abundance of ruminal *Firmicutes* (55). However, AS pH did not affect the abundance of *Firmicutes* in our study suggests that the *Firmicutes* were pH-insensitive bacteria. The *Bacteroidetes* are the most abundant Gram-negative bacteria found in the anaerobic communities of the rumen, and low pH resulted in the death and lysis of Gram-negative bacteria (15, 54). However, the abundance of *Bacteroidetes* was not affected by AS pH in the present study. Although the *Bacteroidetes* were not different in statistics, the value of *Bacteroidetes* decreased in the low pH group (47.50 vs. 39.68% in solid-associated bacteria and 37.60 vs. 29.74% in liquid-associated bacteria). Wang et al. (56) reported that feeding high-concentrate diets decreased the ruminal pH and increased the abundance of *Proteobacteria* in the rumen for cows. Furthermore, the low AS pH increased the abundance of *Proteobacteria* in the liquid-associated bacteria in this experiment. This result suggests that the phylum of *Proteobacteria* can tolerate the low pH condition. For the liquid and solid fraction, the abundances of *Firmicutes*, *Bacteroidetes*, and *Proteobacteria* were similar in solid fraction compared with the liquid fraction in our study. It is possible that the fermenters were moved up and down by an electric motor, and promoted the exchange of rumen bacteria in solid fraction and liquid

fraction. The *Spirochaetes* commonly fermented xylan and pectin in feed (57). After 6 h fermentation, the *Spirochaetes* phyla became abundant in the forage-adherent community (58). The *Spirochaetes* was greater in low pH conditions in the solid-associated bacteria, which was also greater in high AS pH in the liquid-associated bacteria in the current study. And the abundance of *Spirochaetes* was greater in a solid fraction than a liquid fraction. These results indicated that *Spirochaetes* tend to colonize in the solid phase in the rumen.

The bacteria genus of *Lactobac*ria was suitable for growth at pH 6.0 (59). The previous studies indicated that the increased non-fiber carbohydrate for ruminant promoted the growth of amylolytic and other starch-digesting bacterial species, such as *Lactobacillus* (60–62). In the current study, the relative abundance of *Lactobacillus* was increased when the AS pH decreased. Wang et al. (63) reported that the abundance of ruminal *Lactobacillus* was increased when cows intake the SARA diet. These studies indicated that *Lactobacillus* affected not only the dietary compositions but also the magnitude of pH. The *Prevotella* species were essential to hemicellulose degradation in the rumen, and *Prevotella_1* and *Prevotellaceae_YAB2003* (*Bactenroidetes*) were identified to have the ability to degrade hemicellulose or xylan *in vivo* (64, 65). In the current study, the low AS pH increased the abundances of *Prevotella_1*, and decreased the abundances of *Prevotellaceae_YAB2003,* and *Prevotella_7* in the liquid-associated bacteria. These results indicate the sensitivity of *Prevotella* strains to AS pH was inconsistent. Similarly, the abundance of *Prevotellaceae_YAB2003_group* was greater in a solid fraction than a liquid fraction. The abundance of *Prevotella_1* was decreased in solid fractions at the low AS pH, whereas the abundance of *Prevotella_7* was increased. The *Prevotellaceae* comprises up to 40% of the community in the liquid samples, and ruminal *Prevotella* is non-cellulolytic but has a broad saccharolytic and proteolytic potential (14, 66). The abundances of *Prevotellaceae_YAB2003_group* and *Prevotella_1* were increased in liquid fraction, which primarily consumed the soluble nutrients.

The function of *Succinivibrio* produced succinate, the precursor of propionate (67). In this research, the related abundance of *Succinivibrio* was higher in the low AS pH group compared with low AS pH, whereas the proportion of propionate was decreased. It should be presumed that the conversion of succinate to propionate acid was inhibited by low pH and producing less propionate. In addition, the *Schwartzia* fermented succinate and produced propionate (68). The *Schwartzia* abundance decreased in the low AS pH group, which was coordinated with the results of propionate in this study. The low AS pH decreased the abundance of *Ruminobacter* (*Firmicutes*) in this current study. Wang et al. (69) reported that the cow intake high-forage diets increased the ruminal *Ruminobacter* abundance. Mu et al. (70) found that fed a high grain-diet induce cow SARA increased the abundance of *Ruminobacter*. These results indicated that the growth of *Ruminobacter* in the rumen was affected by the combination of pH and diet compositions.

CONCLUSIONS

The nutrients degradabilities were decreased by reducing AS pH in the present study. The reduction of AS pH increased the proportion of butyrate, valerate, and isovalerate and decreased the proportion of propionate. The results of the present study indicated the three groups of bacteria communities according to the different sensitives to rumen pH: the abundances of *Lactobacillus*, *Succinivibrio*, *Prevotella_7* are increased with decreasing AS pH; the amounts of *R. albus*, *R. flavefaciens*, *F. succinogenes* as well as the abundances of *Schwartzia* and *Ruminobacter* decreased with reducing AS pH; the abundances of *Selenomonas_1*, *Rikenellaceae_RC9_gut_group,* and *Succiniclasticum* were not affected by AS pH in Rustitec. In addition, the effect of the interaction of rumen pH and diets on the rumen bacteria community should be further investigated.

DATA AVAILABILITY STATEMENT

The data for this study can be found in the NCBI database (https://www.ncbi.nlm.nih.gov/bioproject/PRJNA752826).

ETHICS STATEMENT

The animal study was reviewed and approved by the Biological Studies Animal Care and Use Committee of Gansu Province, China (2005–12). Written informed consent was obtained from the owners for the participation of their animals in this study.

AUTHOR CONTRIBUTIONS

ToG collected the sample, analyzed the data, and drafted the manuscript. TaG, YC, LG, FaL, and GY collected the sample. FeL presented the idea of this manuscript, supported the funding, analyzed the conclusions, and revised the manuscript. All authors contributed to the article and approved the submitted version.

FUNDING

The research was financially supported by the National Natural Science Foundation of China, grant number (No. 32072754) and the Natural Science Foundation of Gansu Province (20JR5RA299), China.

ACKNOWLEDGMENTS

The author thanks GY of the Northwest Institute of Eco-Environment and Resources, Chinese Academy of Sciences, who kindly assisted on the experiment site.

SUPPLEMENTARY MATERIAL

The Supplementary Material for this article can be found online at: https://www.frontiersin.org/articles/10.3389/fnut.2021.760316/full#supplementary-material

REFERENCES

1. Kleen JL, Hooijer GA, Rehage J, Noordhuizen JP. Subacute ruminal acidosis (SARA): A review. *J Vet Med.* (2003) 50:406–14. doi: 10.1046/j.1439-0442.2003.00569.x
2. Seddik H, Xu L, Wang Y, Mao SY. A rapid shift to high-grain diet results in dynamic changes in rumen epimural microbiome in sheep. *Animal.* (2018) 13:1–9. doi: 10.1017/S1751731118003269
3. Sauvant D, Meschy F, Mertens D. Les composantes de l'acidose ruminale et les effets acidogènes des rations. *Prod Anim.* (1999) 12:49–60. doi: 10.20870/productions-animales.1999.12.1.3854
4. Kleen JL, Hooijer GA, Rehage J, Noordhuizen JP. Subacute ruminal aacidosis in Dutch dairy herds. *Vet Rec.* (2009) 164:681–3. doi: 10.1136/vr.164.22.681
5. Colman E, Khafipour E, Vlaeminck B, De Baets B, Plaizier JC, Fievez V. Grain-based versus alfalfa-based subacute ruminal acidosis induction experiments: similarities and differences between changes in milk fatty acids. *J. Dairy Sci.* (2013) 96:4100–11. doi: 10.3168/jds.2012-6109
6. Khafipour E, Li SC, Plaizier JC, Krause DO. Rumen microbiome composition determined using two nutritional models of subacute ruminal acidosis. *Appl Environ Microb.* (2009) 75:7115–24. doi: 10.1128/AEM.00739-09
7. Lechartier C, Peyraud JL. The effects of forage proportion and rapidly degradable dry matter from concentrate on ruminal digestion in dairy cows fed corn silage-based diets with fixed neutral detergent fiber and starch contents. *J Dairy Sci.* (2010) 93:666–81. doi: 10.3168/jds.2009-2349
8. Li F, Li Z, Li S, Ferguson JD, Cao Y, Yao J, et al. Effect of dietary physically effective fiber on ruminal fermentation and the fatty acid profile of milk in dairy goats. *J Dairy Sci.* (2014) 97:2281–90. doi: 10.3168/jds.2013-6895
9. Park JH, Kim KH, Park PJ, Jeon BT, Oh MR, Jang SY, et al. Effects of physically effective neutral detergent fibre content on dry-matter intake, digestibility and chewing activity in beef cattle fed total mixed ration. *Anim Prod Sci.* (2014) 55:166. doi: 10.1071/AN14241
10. Orton T, Rohn K, Breves G, Brede M. Alterations in fermentation parameters during and after induction of a subacute rumen acidosis in the rumen simulation technique. *J Anim Physiol An N.* (2020) 104:1678–89. doi: 10.1111/jpn.13412
11. Brede M, Orton T, Pinior B, Roch FF, Dzieciol M, Zwirzitz B, et al. PacBio and Illumina MiSeq amplicon sequencing confirm full recovery of the bacterial community after subacute ruminal acidosis challenge in the Rusitec system. *Front Microbiol.* (2020) 11:1813. doi: 10.3389/fmicb.2020.01813
12. Wanapat M, Cherdthong A. Use of real-time PCR technique in studying rumen cellulolytic bacteria population as affected by level of roughage in swamp buffalo. *Curr Microbiol.* (2009) 58:294–9. doi: 10.1007/s00284-008-9322-6
13. McAllister TA, Bae HD, Jones GA, Cheng KJ. Microbial attachment and feed digestion in the rumen. *J Anim Sci.* (1994) 72:3004–18. doi: 10.2527/1994.72113004x
14. De Mulder T, Goossens K, Peiren N, Vandaele L, Haegeman A, De Tender C, et al. Exploring the methanogen and bacterial communities of rumen environments: solid adherent, fluid and epimural. *Fems Microbiol Ecol.* (2016) 93:fiw251. doi: 10.1093/femsec/fiw251
15. Li F, Wang Z, Dong C, Li F, Wang W, Yuan F, et al. Rumen bacteria communities and performances of fattening lambs with a lower or greater subacute ruminal acidosis risk. *Front Microbiol.* (2017) 8:2506. doi: 10.3389/fmicb.2017.02506
16. Kajikawa H, Jin H, Terada F, Suga T. *Operation and Characteristics of Newly Improved and Marketable Artificial Rumen (Rusitec).* Japan: Memoirs of National Institute of Livestock and Grassland Science (2003).
17. McDougall EI. Studies on ruminant saliva. I. the composition and output of sheep's saliva. *Biochem J.* (1948) 43:99–109. doi: 10.1042/bj0430099
18. Association of Official Analytical Chemists (AOAC). *Official Methods of Analysis, 16th ed.* Washington, DC: AOAC International (1997).
19. Van Soest PJ, Robertson JB, Lewis BA. Methods for dietary fiber, neutral detergent fiber, and nonstarch polysaccharides in relation to animal nutrition. *J Dairy Sci.* (1991) 74:3583–97. doi: 10.3168/jds.S0022-0302(91)78551-2
20. Liang YS, Li GZ, Li XY, Lu JY, Li FD, Tang DF, et al. Growth performance, rumen fermentation, bacteria composition, and gene expressions involved in intracellular pH regulation of rumen epithelium in finishing hu lambs differing in residual feed intake phenotype. *J Anim Sci.* (2017) 95:1727–38. doi: 10.2527/jas.2016.1134
21. Tajima K, Aminov RI, Nagamine T, Matsui H, Nakamura M, Benno Y. Diet-dependent shifts in the bacterial population of the rumen revealed with real-time PCR. *Appl Environ Microbe.* (2001) 67:2766–74. doi: 10.1128/AEM.67.6.2766-2774.2001
22. Denman SE, McSweeney CS. Development of a real-time PCR assay for monitoring anaerobic fungal and cellulolytic bacterial populations within the rumen. *Fems Microbiol Ecol.* (2006) 58:572–82. doi: 10.1111/j.1574-6941.2006.00190.x
23. Stevenson DM, Weimer PJ. Dominance of Prevotella and low abundance of classical ruminal bacterial species in the bovine rumen revealed by relative quantification real-time PCR. *Appl Microbiol Biot.* (2007) 75:165–74. doi: 10.1007/s00253-006-0802-y
24. Koike S, Kobayashi Y. Development and use of competitive PCR assays for the rumen cellulolytic bacteria: Fibrobacter succinogenes, Ruminococus albus and Ruminococcus flavefaciens. *Fems Microbiol Lett.* (2001) 204:361–6. doi: 10.1111/j.1574-6968.2001.tb10911.x
25. Nadkarni MA, Martin FE, Jacques NA, Hunter N. Determination of bacterial load by real-time PCR using a broad-range (universal) probe and primers set. *Microbiology-Sgm.* (2002) 148:257–66. doi: 10.1099/00221287-148-1-257
26. Chen XL, Wang JK, Wu YM, Liu JX. Effects of chemical treatments of rice straw on rumen fermentation characteristics, fibrolytic enzyme activities and populations of liquid- and solid-associated ruminal microbes *in vitro*. *Anim Feed Sci Tech.* (2008) 141:1–14. doi: 10.1016/j.anifeedsci.2007.04.006
27. Edgar RC, Haas BJ, Clemente JC, Quince C, Knight R. UCHIME improves sensitivity and speed of chimera detection. *Bioinformatics.* (2011) 27:2194–200. doi: 10.1093/bioinformatics/btr381
28. Edgar RC. UPARSE: highly accurate OTU sequences from microbial amplicon reads. *Nat Methods.* (2013) 10:996–8. doi: 10.1038/nmeth.2604
29. Schloss PD, Westcott SL, Ryabin T, Hall JR, Hartmann M, Hollister EB, et al. Introducing MOTHUR: open-source, platform-independent, community-supported software for describing and comparing microbial communities. *Appl Environ Microb.* (2009) 75:7537–41. doi: 10.1128/AEM.01541-09
30. Wang Q, Garrity GM, Tiedje JM, Cole JR. Naive bayesian classifier for rapid assignment of rRNA sequences into the new bacterial taxonomy. *Appl Environ Microb.* (2007) 73:5261–7. doi: 10.1128/AEM.00062-07
31. Mould FL, Ørskov ER. Manipulation of rumen fluid pH and its influence on cellulolysis in sacco, dry matter degradation and the rumen microflora of sheep offered either hay or concentrate. *Anim Feed Sci Tech.* (1983) 10:1–14. doi: 10.1016/0377-8401(83)90002-0
32. Calsamiglia S, Cardozo P, Ferret WA, Bach A. Changes in rumen microbial fermentation are due to a combined effect of type of diet and pH. *J Anim Sci.* (2008) 86:702–11. doi: 10.2527/jas.2007-0146
33. Sung HG, Kobayashi Y, Chang J, Ha A, Hwang IH. Low ruminal pH reduces dietary fiber digestion via reduced microbial attachment. *Asian Austr J Anim.* (2007) 20:200–7. doi: 10.5713/ajas.2007.200
34. Nagaraja TG, Titgemeyer EC. Ruminal acidosis in beef cattle: the current microbiological and nutritional outlook. *J Dairy Sci.* (2007) 90:E17–38. doi: 10.3168/jds.2006-478
35. Miron J, Ben-Ghedalia D, Morrison M. Invited Review: adhesion mechanisms of rumen cellulolytic bacteria. *J Dairy Sci.* (2001) 84:1294–309. doi: 10.3168/jds.S0022-0302(01)70159-2
36. Bhandari SK, Ominski KH, Wittenberg KM, Plaizier JC. Effects of chop length of alfalfa and corn silage on milk production and rumen fermentation of dairy cows. *J Dairy Sci.* (2007) 90:2355–66. doi: 10.3168/jds.2006-609
37. Zebeli Q, Tafaj M, Junck B, Oelschlaeger V, Ametaj BN, Drochner W. Evaluation of the response of ruminal fermentation and activities of nonstarch polysaccharide-degrading enzymes to particle length of corn silage in dairy cows. *J Dairy Sci.* (2008) 91:2388–98. doi: 10.3168/jds.2007-0810
38. Pei C, Mao S, Cheng Y, Zhu W. Diversity, abundance and novel 16S rRNA gene sequences of methanogens in rumen liquid, solid and epithelium fractions of Jinnan cattle. *Animal.* (2010) 4:20–9. doi: 10.1017/S1751731109990681
39. Matsui H, Ogata K, Tajima K, Nakamura M, Nagamine T, Aminov RI, et al. Phenotypic characterization of polysaccharidases produced by four prevotella type strains. *Curr Microbiol.* (2000) 41:45–9. doi: 10.1007/s002840010089

40. Cerrato-Sánchez M, Calsamiglia S, Ferret A. Effects of patterns of suboptimal pH on rumen fermentation in a dual-flow continuous culture system. *J Dairy Sci.* (2007) 90:4368–77. doi: 10.3168/jds.2006-804
41. Wallace RJ, Onodera R, Cotta MA. *Metabolism of Nitrogen-Containing Compounds*. Dordrecht: Springer (1997). doi: 10.1007/978-94-009-1453-7_7
42. Jiao P, Wei C, Sun Y, Xie X, Zhang Y, Wang S, et al. Screening of live yeast and yeast derivatives for their impact of strain and dose on *in vitro* ruminal fermentation and microbial profiles with varying media pH levels in high-forage beef cattle diet. *J Sci Food Agr.* (2019) 99:6751–60. doi: 10.1002/jsfa.9957
43. Gizzi G, Zanchi R, Sciaraffia F. Comparison of microbiological and fermentation parameters obtained with an improved rumen *in vitro* technique with those obtained *in vivo*. *Anim Feed Sci Tech.* (1998) 73:291–305. doi: 10.1016/S0377-8401(98)00150-3
44. Strobel HJ, Russell JB. Effect of pH and energy spilling on bacterial protein synthesis by carbohydrate-limited cultures of mixed rumen bacteria. *J Dairy Sci.* (1986) 69:2941–7. doi: 10.3168/jds.S0022-0302(86)80750-0
45. Hungate RE. *The Rumen and Its Microbes*. New York, NY: Academy Press (1966).
46. Cardozo PW, Calsamiglia S, Ferret A, Kamel C. Screening for the effects of natural plant extracts at different pH on *in vitro* rumen microbial fermentation of a high-concentrate diet for beef cattle. *J Anim Sci.* (2005) 83:2572–9. doi: 10.2527/2005.83112572x
47. Esdale WJ, Satter LD. Manipulation of ruminal fermentation. IV. Effect of altering ruminal pH on volatile fatty acid production. *J Dairy Sci.* (1972) 55:964–70. doi: 10.3168/jds.S0022-0302(72)85603-0
48. Shriver BJ, Hoover WH, Sargent JP, Crawford RJ, Thayne WV. Fermentation of a high concentrate diet as affected by ruminal pH and digesta flow. *J Dairy Sci.* (1986) 69:413–9. doi: 10.3168/jds.S0022-0302(86)80419-2
49. Esquivel-Elizondo SR, Ilhan ZE, Garcia-Pena EI, Krajmalnik-Brown R, Beiko RG. Insights into butyrate production in a controlled fermentation system via gene predictions. *mSystems.* (2017) 2:e00051–e00017. doi: 10.1128/mSystems.00051-17
50. Kozakai K, Nakamura T, Kobayashi Y, Tanigawa T, Osaka I, Kawamoto S, et al. Effect of mechanical processing of corn silage on *in vitro* ruminal fermentation, and *in situ* bacterial colonization and dry matter degradation. *Can J Anim Sci.* (2007) 87:259–67. doi: 10.4141/A06-028
51. Martínez ME, Ranilla MJ, Tejido ML, Saro C, Carro MD. Comparison of fermentation of diets of variable composition and microbial populations in the rumen of sheep and Rusitec fermenters. II. Protozoa population and diversity of bacterial communities. *J Dairy Sci.* (2010) 93:3699–712. doi: 10.3168/jds.2009-2934
52. Hespell RB, Cotta MA. Degradation and utilization by Butyrivibrio-Fibrisolvens H17c of xylans with different chemical and physical-properties. *Appl Environ Microb.* (1995) 61:3042–50. doi: 10.1128/aem.61.8.3042-3050.1995
53. Shen H, Xu Z, Shen Z, Lu Z. The regulation of ruminal short-chain fatty acids on the functions of rumen barriers. *Front Physiol.* (2019) 10:1305. doi: 10.3389/fphys.2019.01305
54. Huo W, Zhu W, Mao S. Impact of subacute ruminal acidosis on the diversity of liquid and solid-associated bacteria in the rumen of goats. *World J Microbiol Biotechnol.* (2014) 30:669–80. doi: 10.1007/s11274-013-1489-8
55. Sato S. Pathophysiological evaluation of subacute ruminal acidosis (SARA) by continuous ruminal pH monitoring. *Anim Sci J.* (2016) 87:168–77. doi: 10.1111/asj.12415
56. Wang LJ, Zhang GN, Li Y, Zhang YG. Effects of high forage/concentrate diet on volatile fatty acid production and the microorganisms involved in VFA production in cow rumen. *Animals.* (2020) 10:12. doi: 10.3390/ani10020223
57. Paster BJ, Canale-Parola E. Physiological diversity of rumen spirochetes. *Appl Environ Microbiol.* (1982) 43:686–93. doi: 10.1128/aem.43.3.686-693.1982
58. Liu J, Zhang M, Xue C, Zhu W, Mao S. Characterization and comparison of the temporal dynamics of ruminal bacterial microbiota colonizing rice straw and alfalfa hay within ruminants. *J Dairy Sci.* (2016) 99:9668–81. doi: 10.3168/jds.2016-11398
59. Mackie RI, Gilchrist FM. Changes in lactate-producing and lactate-utilizing bacteria in relation to pH in the rumen of sheep during stepwise adaptation to a high-concentrate diet. *Appl Environ Microbiol.* (1979) 38:422–30. doi: 10.1128/aem.38.3.422-430.1979
60. Goad DW, Goad CL, Nagaraja TG. Ruminal microbial and fermentative changes associated with experimentally induced subacute acidosis in steers. *J Anim Sci.* (1998) 76:234–41. doi: 10.2527/1998.761234x
61. Metzler-Zebeli BU, Schmitz-Esser S, Klevenhusen F, Podstatzky-Lichtenstein L, Wagner M, Zebeli Q. Grain-rich diets differently alter ruminal and colonic abundance of microbial populations and lipopolysaccharide in goats. *Anaerobe.* (2013) 20:65–73. doi: 10.1016/j.anaerobe.2013.02.005
62. Mickdam E, Khiaosa-ard R, Metzler-Zebeli BU, Klevenhusen F, Chizzola R, Zebeli Q. Rumen microbial abundance and fermentation profile during severe subacute ruminal acidosis and its modulation by plant derived alkaloids *in vitro*. *Anaerobe.* (2016) 39:4–13. doi: 10.1016/j.anaerobe.2016.02.002
63. Wang H, Pan X, Wang C, Wang M, Yu L. Effects of different dietary concentrate to forage ratio and thiamine supplementation on the rumen fermentation and ruminal bacterial community in dairy cows. *Anim Prod Sci.* (2015) 55:189–93. doi: 10.1071/AN14523
64. Emerson EL, Weimer PJ. Fermentation of model hemicelluloses by Prevotella Strains and B. *Fibrisolvens* in pure culture and in ruminal enrichment cultures. *Appl Microbiol Biot.* (2017) 101:4269–78. doi: 10.1007/s00253-017-8150-7
65. Wang B, Ma PM, Diao QY, Tu Y. Saponin-induced shifts in the rumen microbiome and metabolome of young cattle. *Front Microbio.* (2019) 10:356. doi: 10.3389/fmicb.2019.00356
66. Avgustin G, Wallace RJ, Flint HJ. Phenotypic diversity among ruminal isolates of Prevotella ruminicola: proposal of *P. brevis sp. nov., Prevotella bryantii sp. nov.,* and *Prevotella albensis sp. nov*. and redefinition of *Prevotella ruminicola*. *Int J Syst Bacteriol.* (1997) 47:284–8. doi: 10.1099/00207713-47-2-284
67. Elolimy AA, Arroyo JM, Batistel F, Iakiviak MA, Loor JJ. Association of residual feed intake with abundance of ruminal bacteria and biopolymer hydrolyzing enzyme activities during the periportal period and early lactation in Holstein dairy cows. *J Anim Sci.* (2018) 9:43. doi: 10.1186/s40104-018-0258-9
68. Vangylswyk NO, Hippe H, Rainey FA. Schwartzia Succinivorans Gen. Nov., Sp. Nov., another ruminal bacterium utilizing succinate as the sole energy source. *Int J Syst Bacteriol.* (1997) 47:155–9. doi: 10.1099/00207713-47-1-155
69. Wang L, Li Y, Zhang Y, Wang L. The effects of different concentrate-to-forage ratio diets on rumen bacterial microbiota and the structures of Holstein cows during the feeding cycle. *Animals.* (2020) 10:957. doi: 10.3390/ani10060957
70. Mu YY, Qi WP, Zhang T, Zhang JY, Mao. S. Y. Gene function adjustment for carbohydrate metabolism and enrichment of rumen microbiota with antibiotic resistance genes during subacute rumen acidosis induced by a high-grain diet in lactating dairy cows. *J Dairy Sci.* (2021) 104:2087–105. doi: 10.3168/jds.2020-19118

Conflict of Interest: The authors declare that the research was conducted in the absence of any commercial or financial relationships that could be construed as a potential conflict of interest.

Publisher's Note: All claims expressed in this article are solely those of the authors and do not necessarily represent those of their affiliated organizations, or those of the publisher, the editors and the reviewers. Any product that may be evaluated in this article, or claim that may be made by its manufacturer, is not guaranteed or endorsed by the publisher.

frontiers in Nutrition

ORIGINAL RESEARCH
published: 29 November 2021
doi: 10.3389/fnut.2021.783819

Dietary *Enteromorpha* Polysaccharide Enhances Intestinal Immune Response, Integrity, and Caecal Microbial Activity of Broiler Chickens

Teketay Wassie[1], *Zhuang Lu*[1], *Xinyi Duan*[1,2], *Chunyan Xie*[2], *Kefyalew Gebeyew*[1], *Zhang Yumei*[1,2], *Yulong Yin*[1,3] *and Xin Wu*[1,3]*

[1] *Key Laboratory of Agro-ecological Processes in Subtropical Region, National Engineering Laboratory for Pollution Control and Waste Utilization in Livestock and Poultry Production, Hunan Provincial Engineering Research Center for Healthy Livestock and Poultry Production, Institute of Subtropical Agriculture, Chinese Academy of Sciences, Changsha, China,* [2] *College of Resources and Environment, Hunan Agricultural University, Changsha, China,* [3] *Tianjin Institute of Industrial Biotechnology, Chinese Academy of Sciences, Tianjin, China*

OPEN ACCESS

Edited by:
Ren-You Gan,
Institute of Urban Agriculture, Chinese Academy of Agricultural Sciences (CAAS), China

Reviewed by:
Wen-Chao Liu,
Guangdong Ocean University, China
Shuangshuang Guo,
Wuhan Polytechnic University, China
Kyung-Woo Lee,
Konkuk University, South Korea

***Correspondence:**
Xin Wu
wuxin@isa.ac.cn

Specialty section:
This article was submitted to Nutrition and Microbes, a section of the journal Frontiers in Nutrition

Received: *27 September 2021*
Accepted: *25 October 2021*
Published: *29 November 2021*

Citation:
Wassie T, Lu Z, Duan X, Xie C, Gebeyew K, Yumei Z, Yin Y and Wu X (2021) Dietary Enteromorpha Polysaccharide Enhances Intestinal Immune Response, Integrity, and Caecal Microbial Activity of Broiler Chickens. Front. Nutr. 8:783819. doi: 10.3389/fnut.2021.783819

Marine algae polysaccharides have been shown to regulate various biological activities, such as immune modulation, antioxidant, antidiabetic, and hypolipidemic. However, litter is known about the interaction of these polysaccharides with the gut microbiota. This study aimed to evaluate the effects of marine algae *Enteromorpha (Ulva) prolifera* polysaccharide (EP) supplementation on growth performance, immune response, and caecal microbiota of broiler chickens. A total of 200 1-day-old Ross-308 broiler chickens were randomly divided into two treatment groups with ten replications of ten chickens in each replication. The dietary treatments consisted of the control group (fed basal diet), and EP group (received diet supplemented with 400 mg EP/kg diet). Results showed that chickens fed EP exhibited significantly higher ($P < 0.05$) body weight and average daily gain than the chicken-fed basal diet. In addition, significantly longer villus height, shorter crypt depth, and higher villus height to crypt depth ratio were observed in the jejunal and ileal tissues of chickens fed EP. EP supplementation upregulated the mRNA expression of NF-κB, TLR4, MyD88, IL-2, IFN-α, and IL-1β in the ileal and jejunal tissues ($P < 0.05$). Besides, we observed significantly higher ($P < 0.05$) short-chain volatile fatty acids (SCFAs) levels in the caecal contents of the EP group than in the control group. Furthermore, 16S-rRNA analysis revealed that EP supplementation altered gut microbiota and caused an abundance shift at the phylum and genus level in broiler chicken. Interestingly, we observed an association between microbiota and SCFAs production. Overall, this study demonstrated that supplementation of diet with EP promotes growth performance, improves intestinal immune response and integrity, and modulates the caecal microbiota of broiler chickens. This study highlighted the application of marine algae polysaccharides as an antibiotic alternative for chickens. Furthermore, it provides insight to develop marine algae polysaccharide-based functional food and therapeutic agent.

Keywords: chicken, *Enteromorpha* polysaccharide, immunity, intestinal integrity, marine algae, microbiota

INTRODUCTION

In the poultry industry, antibiotics have been used for long years as a feed additive to promote growth and control disease. However, recently, its use has been banned due to the risk of antibiotic-resistant microbes, residues in animal products, and environmental pollution (1). Therefore, there is an urgent need for antibiotic substitutes that can replace its functions while surmounting its shortcomings. In this regard, dietary fibers such as polysaccharides are known to improve health and homeostasis by enhancing the intestinal immune response and gastrointestinal barrier function (2). However, human and animal enzymes are unable to digest dietary fibers and are subject to fermentation by the gut microbiota (3). The gut microbiota lives in a symbiotic relationship with the host, in which the host provides habitat and nutrients for their growth, while the microbiota provides essential nutrients via the fermentation of fibers. Therefore, the dynamic diet-microbiota interactions shape the health and immune response of the host (4).

In chicken, caecum is the main organ that harbors a vast diversity of microbes responsible for the fermentation of fiber (5). These microbes possess polysaccharide-degrading enzyme-encoding genes and pathways involved in the production of short-chain volatile fatty acids (SCFAs), which are beneficial to the host physiology and energy homeostasis (6). The microbiota-derived SCFAs play an important role in maintaining an intestinal immune response, barrier function, and immune metabolism via the activation of metabolite-sensing G-protein coupled receptors (GPCRs) (7). Apart from metabolites production, gut microbiota plays a decisive role in maintaining the homeostasis and health of the host via direct involvement in gut structure and morphology, regulating immune responses, and protection from luminal pathogens (8). Therefore, changes in the type of polysaccharides consumed are expected to alter the composition and function of the microbiota, thereby altering the host immune system. Thus, understanding how a given microbial population responds to polysaccharides diet, and the role and association of this microbiota and its metabolites with immune response of the host play crucial roles to develop polysaccharide-based functional foods to prevent and treat gut microbiota-related diseases.

Enteromorpha prolifera (*E. prolifera*) is a seaweed green alga with a long history of use as food and traditional medicine. A sulfated polysaccharide is one of the main biologically active substances in *E. prolifera,* which is responsible for the immunomodulating, hypolipidemic, antitumor, anti-aging, antibacterial, anticoagulant, antiviral, and anticancer activities of these algae (9–12). *E. prolifera* polysaccharides (EP) are made up of α- and β-(1, 4)- linked monosaccharides (rhamnose, xylose, and glucuronic acid) (13), where the sulfate group is attached at the C-3 position of rhamnose (14). Recent studies indicated increased production performance, breast muscle yield, egg quality, antioxidant capacity, and intestinal morphology of chickens fed seaweed polysaccharides (15–18). In addition, EP supplementation increased the weight and differentially regulates the gene expression at the transcriptome level in the bursa of Fabricius of Arbor Acres chickens (19). Similarly, EP supplementation has been shown to improve the growth performance, non-specific immunity, and intestinal function of banana shrimp *F. merguiensis* fish (20). Furthermore, administration of EP was found to regulate intestinal microbiota in mice (21) and fecal microbiota in humans (22). Our recent study showed that supplementation of diet with EP- zinc complex could reduce diarrhea rate and improved intestinal barrier function in piglets (23). Although the biological activities of EP have been well-established so far, their interactions with gut microbiota in broiler chickens are largely unknown.

Considering the above information and the fact that polysaccharides are digested by the intestinal microbiota, we designed this study to investigate the effects of EP supplementation on growth performance, immune response, intestinal integrity, and gut microbiota in broiler chickens.

MATERIALS AND METHODS

Source of *Enteromorpha* Polysaccharide

The EP was extracted from the marine algae *E. prolifera* and provided by Qingdao Seawin Biotechnology Group Co., Ltd. (Qingdao, China). The content of EP was not <45%, and the molecular weight was 4,431 Da. The water-soluble sulfated polysaccharides of EP were extracted from the *E. prolifera* by an enzymatic method according to the procedure previously described (13, 24). Briefly, the algae were washed with distilled water and dried at 60°C, then minced to get homogenate powder. The algal powders were soaked in water, and then the water extracts algae were subjected to stepwise enzymatic treatment with pectinase, cellulase, and papain at 50°C for 1.5 h. The enzyme reaction was inactivated by heating the reaction at 90–100°C for 10 min, and then immediately cooled on an ice bath, centrifugal concentrated, ethanol precipitation, and finally spray drying to obtain the polysaccharide products (25). The monosaccharide composition was determined using high-performance liquid chromatography (HPLC) according to the procedures previously described (14). Based on the HPLC analysis results, the monosaccharide composition of the EP used in this study was composed of rhamnose (Rha), glucuronic acid (GlcA), xylose (Xyl), glucose (Glc), and galactose (Gal) with the molar percentage of 40.6, 38.2, 9.3, 5.6, and 6.3%, respectively.

Bird Management

The experimental design and procedures used in this study were reviewed and approved by the Animal Care and Use Committee of the Institute of Subtropical Agriculture, Chinese Academy of Sciences. The animal experiments and sample collection strictly followed the relevant guidelines. For this experiment, 200 healthy 1-day-old male Ross-308 broiler chickens were used. The chickens were kept in a room with 23-h of light and 1-h darkness. The room temperature was kept at about 32°C for 3 d and gradually reduced by 1°C every other day until the temperature reached 24°C, and then maintaining this temperature. The experimental chickens had access to *ad libitum* feed and water. All nutrients in experimental diets were formulated to meet or exceed the recommendations for Ross broiler chickens (26). The

TABLE 1 | Ingredient composition and nutrient contents of basal diets.

Ingredients, %	1 ~ 21 d	22 ~ 42 d
Corn	56.41	56.64
Soybean meal (CP, 43%)	29.85	28.30
Corn gluten meal	5.00	5.00
Soybean oil	3.90	5.30
Limestone	1.30	1.30
Dicalcium phosphate	1.80	1.75
$_{L}$-Lysine	0.32	0.30
$_{DL}$-Methionine	0.12	0.11
Premix[a]	1.00	1.00
Salt	0.30	0.30
Total	100	100
Nutrient levels, %		
Metabolizable energy, MJ/kg	12.86	13.20
Crude protein	21.12	19.40
Calcium	1.02	0.93
Available phosphorus	0.47	0.43
Lysine	1.20	1.06
Methionine	0.50	0.43
Methionine + cysteine	0.85	0.77
Arginine	1.35	1.33
Threonine	0.80	0.74

[a]*The premix provided per kilogram of diet: vitamin A, 15,600 IU; vitamin D3, 4,480 IU; vitamin E, 31 IU; vitamin B1, 2.4 mg; vitamin B2, 7.2 mg; vitamin B6, 6.3 mg; vitamin B12, 0.32 mg; niacin, 47 mg; pantothenic acid, 16.2 mg; folic acid, 1.6 mg; biotin, 0.26 mg; Cu, 10.4 mg; Zn, 83.2 Fe, 75 mg; Mn, 83.1 mg; Se, 0.5 mg; I, 0.5 mg.*

dietary composition and nutrient levels of the basal diet are presented in **Table 1**.

Diet and Experimental Design

For this experiment, 200-1-day-old male broiler chickens were randomly divided into two treatment groups with ten replications of ten chickens per replication. The first group was fed a basal diet (control group) and the treatment group received a basal diet supplemented with 400 mg EP/kg diet (EP group), according to the dose recommended (15). The experiment lasted for 42 days.

Sample Collection

The feed offers, leftover, and body weight were recorded to calculate the average daily feed intake (ADFI) and average daily gain (ADG). Feed conversion ratio (FCR) was calculated as ADFI/ADG. At the end of the experiment (day 42), blood samples were collected from one chicken from each replication ($n = 10$/treatment). The sera were separated by centrifuging at 3,000 rpm for 15 min at 4°C and stored at −20°C for subsequent analysis. Thereafter, one chicken from each replication ($n = 10$/treatment) close to the average body weight of the group was humanely euthanized by cervical dislocation for tissue samples collection.

Small intestinal tissues (jejunum and ileum) were isolated. The middle sections of small intestinal tissues were then fixed in 4% formaldehyde for morphological analysis. The other half of the small intestinal tissues were immediately frozen in liquid nitrogen and stored at −80°C for gene expression analysis. Caecal contents were collected and frozen for microbiota and volatile fatty acids analysis.

Serum Cytokine Analysis

Serum concentrations of interleukin-1β (IL-1β), IL-2, IL-6, IL-10, tumor necrosis alpha (TNF-α), and interferon-gamma (INF-γ) were measured using commercial chicken-specific ELISA kits (Shanghai Kexin Biotech Co., Ltd, Shanghai, China), following the kit instruction.

Morphological Analysis of Small Intestinal Tissues

The paraformaldehyde-fixed segment of the jejunum and ileum tissues were embedded in paraffin, sectioned (5 μm), and stained with hematoxylin and eosin as previously described (27). Villus height was then measured from the tip of the villus to the top of the lamina propria, and crypt depth was measured from the villus-crypt axis to the tip of the muscular mucosa. The villus height to crypt depth ratio was then calculated.

mRNA Expression Analysis of Immune-Related Genes and Tight Junction Molecules

Quantitative real-time polymerase chain reaction (RT-qPCR) was used to investigate the effects of EP supplementation on immunity and intestinal integrity-related genes expression. Briefly, total RNA was isolated from the frozen intestinal tissues using a trizol reagent (Invitrogen Co., CA, USA) and then treated with DNase I (Invitrogen, Carlsbad, CA, USA) according to the manufacturer instructions. The integrity was detected by 1% agarose gel electrophoresis, and the quality and quantity were assessed using Nanodrop 2000 (Thermo Fisher Scientific, Waltham, MA, USA). The cDNA was then synthesized using EvoM-MLV RT kit (Accurate Biotechnology, Hunan, China) according to the kit instructions. The RT-qPCR was performed on Roche LightCycler® 480II (Roche, Basel, Switzerland) using SYBR Green mix (Takara, Tokyo, Japan) with targets and β-actin (housekeeping) genes primers (**Table 2**). Thermal cycling conditions were initial denaturation of 95°C for 30 s, followed by 40 amplification cycles of 95°C for 15 s, 60°C for 30 s, and 72°C for 60 s. The gene expression levels were recorded as the threshold cycle (CT) values that corresponded to the number of cycles at which fluorescence signals can be detected. The relative mRNA expression of genes was calculated using the $2^{-\Delta\Delta Ct}$ methods described previously (28).

Microbiota Profiling

Microbial DNA was isolated from the caecal content of six chickens in each group using the E.Z.N.A. Stool DNA Kit (D4015, Omega, Norcross GA, USA) according to the manufacturer's instructions. Following the extraction, the quality and quantity of DNA were assessed using NanoDrop 2000 spectrophotometer (Thermo Scientific, Waltham, MA, USA) and integrity was checked using 1% agarose gel electrophoresis. Then, the V3–V4

TABLE 2 | Primers used for quantitative polymerase chain reaction.

Gene name	Accession no	Primer 5′-3′
IL-2	AF000631	F: TCTGGGACCACTGTATGCTCT
		R: ACACCAGTGGGAAACAGTATCA
IL-10	AJ621614	F: CGGGAGCTGAGGGTGAA
		R: GTGAAGAAGCGGTGACAGC
IL-1β	Y15006	F: GTGAGGCTCAACATTGCGCTGTA
		R: TGTCCAGGCGGTAGAAGATGAAG
TNF-α	AY765397	F: TGCTGTTCTATGACCGCC
		R: CTTTCAGAGCATCAACGCA
IFN-γ	NM_205149.1	F: TGAGCCAGATTGTTTCGA
		R: ACGCCATCAGGAAGGTTG
TLR-2	AB046119.2	F: GGGGCTCACAGGCAAAATC
		R: AGCAGGGTTCTCAGGTTCACA
TLR4	AY064697	F: AGTCTGAAATTGCTGAGCTCAAAT
		R: GCGACGTTAAGCCATGGAAG
MyD88	EF011109	F: TGATGCCTTCATCTGCTACTG
		R: TCCCTCCGACACCTTCTTTCTA
NF-kB	NM_205129	F: TCCCTCCCGACGAATTTTGG
		R: CTGACACTGCACCAAACGTG
Occludin 1	NM_205128.1	F: ACGGCAGCACCTACCTCAA
		R: GGGCGAAGAAGCAGATGAG
Claudin 1	NM_001013611.2	F: CATACTCCTGGGTCTGGTTGGT
		R: GACAGCCATCCGCATCTTCT
ZO2	NM_204918.1	F: GGATACAATTCAGCAACAGCAAGG
		R: ACATGCGATCATCTGCGTCATCT
Mucin 2	XM_421035	F: AGGTAATTGTCTGGCCGTGG
		R: GTGGTTGTACCTTCGGTGCT
β-actin	NM 205518.1	F: ACCGGACTGTTACCAACACC
		R: CCTGAGTCAAGCGCCAAAAG

region of the bacterial 16S-rRNA gene was amplified by PCR using the primers (F: 5′-ACTCCTACGGGAGGCAGCAG-3′; R: 5′-GGACTACHVGGGTWTCTAAT-3′). The PCR product was run on 2% agarose gel, and then excised and purified using the AxyPrep DNA Gel Extraction Kit (Axygen Biosciences, Union City, CA, USA) and quantified using Quantus™ Fluorometer (Promega, Madison, USA). DNA libraries were constructed using the TruSeq® DNA PCR-Free Sample Preparation Kit (Illumina, San Diego, USA). The sequencing library was evaluated on the Qubit® 2.0 Fluorometer and Agilent Bioanalyzer system (Thermo Fisher Scientific, Waltham, MA, USA) and then subjected to paired-end sequencing on an Illumina HiSeq platform at Novogene Bioinformatics Technology Co., Ltd. (Beijing, China). Paired-end reads from the original DNA fragments were merged by FLASH and resulting labels were assigned to the Operational Taxonomic Units (OTUs) with a threshold value of 97% using UPARSE (http://drive5.com/uparse). The species diversity (α-diversity) Chao, Shannon, and Simpson indices were estimated using QIIME2. Linear discriminant analysis (LDA) effect size (LEfSe) was performed to reveal the difference in the bacterial communities across the treatments using the non-parametric factorial Kruskal-Wallis test with an alpha value of 0.05 and LDA score of 2.5. In addition, the relative abundance of dominant bacteria at the phylum and genus levels was also analyzed. Spearman correlation was used to investigate the association between gut microbiota and SCFAs production.

TABLE 3 | The effects of EP supplementation on growth performance of broiler chickens.

Parameters	Treatment groups		*P-Value*
	Control	EP	
Initial BW, g	41.14 ± 0.25	41.03 ± 0.22	0.94
Final BW, g	2,145.14 ± 32.01[b]	2,243.11 ± 30.27[a]	0.038
ADG, g/day	50.10 ± 0.76[b]	52.43 ± 0.72[a]	0.039
FI, g/day	86.61 ± 1.94	87.40 ± 0.63	0.57
FCR	1.73 ± 0.02	1.67 ± 0.03	0.39

BW, body weight; ADG, average daily gain; FI, feed intake; FCR, feed conversion ratio. Data are presented mean ± SEM; n = 10. Means across a row with different superscript letter denotes significant different at P < 0.05.

Short-Chain Fatty Acids Analysis

The short-chain volatile fatty acids (acetate, butyrate, propionate, iso-butyrate, valerate, and iso-valerate) were determined from caecal digesta samples using the Agilent 6,890 gas chromatography (Agilent Technologies, Inc, Palo Alto, CA) according to the previous study (29).

Data Analysis

All data except the 16S-rRNA were analyzed using the statically analytical software (SAS 9.1 Institute, Inc., Cary, NC, USA). The growth performances, cytokines, mRNA expression, and caecal SCFAs content data were checked for normality and homoscedasticity of the data variance using the Shapiro-Wilk test and Levene's test, respectively, and then subjected to an independent *t*-test. The data are presented as the mean ± standard error of the mean (SEM) and statistically significant was considered when $P < 0.05$.

RESULTS

Growth Performance

The effects of EP supplementation on the growth performances of chickens are shown in **Table 3**. Results showed that chickens fed a diet supplemented with EP exhibited significantly higher ($P < 0.05$) body weight and average daily gain compared with the control group. There were no significant differences in feed intake (FI) and feed conversion ratio (FCR) between the treatment groups ($P > 0.05$).

Dietary EP Supplementation Regulates Serum Cytokine Levels

To better understand the effects of EP supplementation on immune response, we measured six common cytokines in sera obtained from experimental chickens (**Figure 1**). Compared with

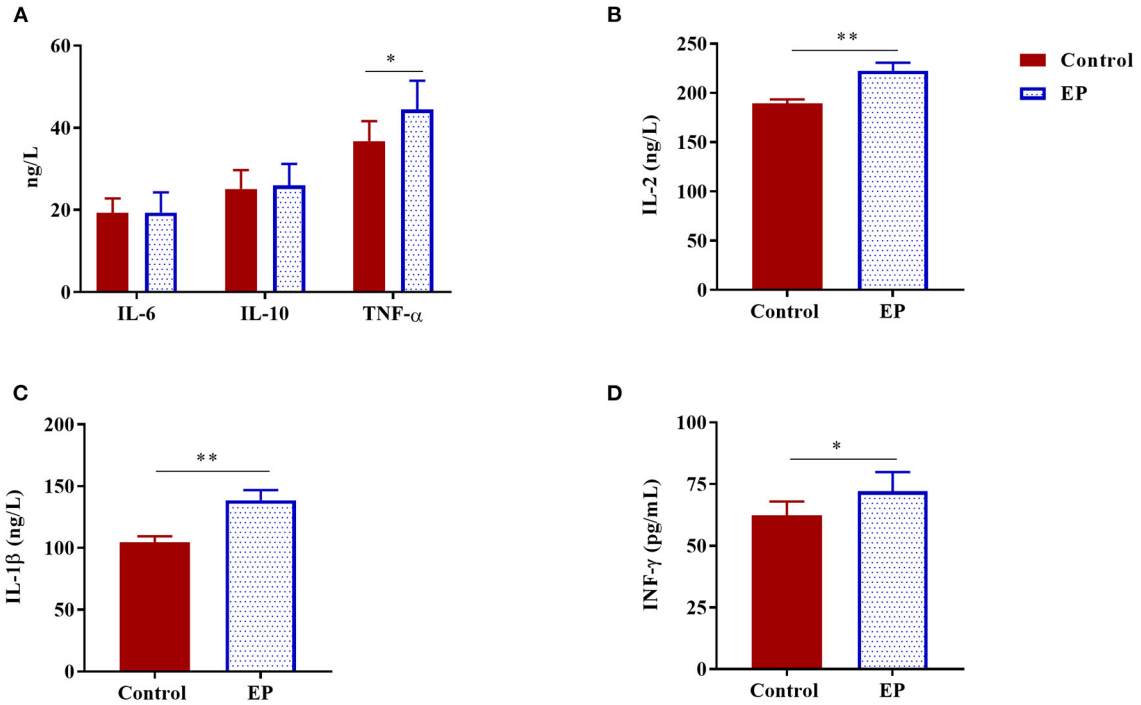

FIGURE 1 | The effects of dietary EP supplementation on serum cytokine levels of broiler chickens. Data are presented as mean ± SEM, $n = 10$. $^{*}P < 0.05$ and $^{**}P < 0.01$, respectively. **(A)** IL-6, Interleukin 6; IL-10, Interleukin 10; TNF-α, Tumor necrosis factor-alpha; **(B)** IL-2, Interleukin 2; **(C)** IL-1β, Interleukin 1 beta; **(D)** IFN-γ, Interferon-gamma.

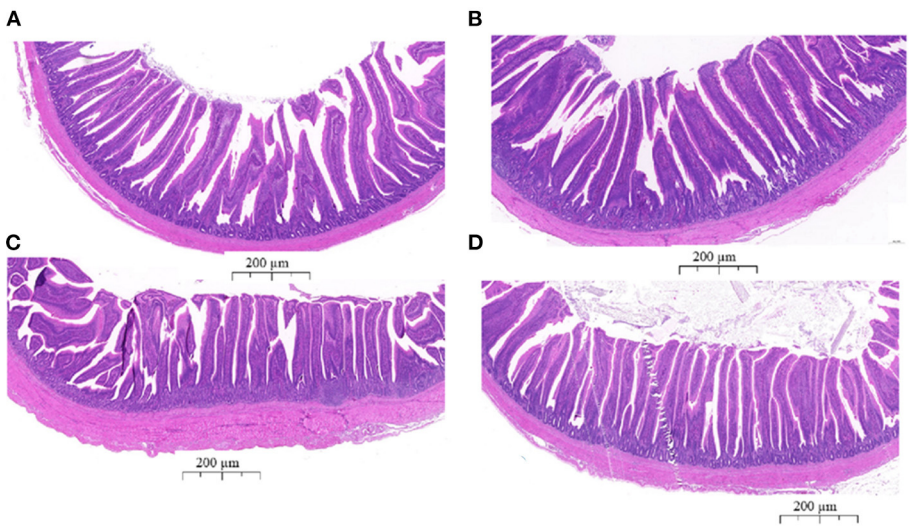

FIGURE 2 | The histological analyses of the jejunum and ileum tissues from the control group **(A,C)** and EP supplemented **(B,D)** broiler chickens stained with hematoxylin and eosin. **(A)** Jejunum tissue from the control group; **(B)** jejunum tissue from the EP group; **(C)** Ileum tissue from the control group; **(D)** Ileum tissue from the EP group. The scale bar represents 200 μm.

the control chickens, a significant increase in serum levels of IL-1β, IL-2, TNF-α, and IFN-γ ($P < 0.05$) were observed in chickens fed the basal diet supplemented with EP. In this study, EP supplementation did not affect the serum IL-6 and IL-10 levels in broiler chickens.

Intestinal Morphology Analysis

To determine the effects of EP supplementation on intestinal morphology, jejunal and ileal tissues were fixed using hemotoxin and eosin (**Figure 2**). In the jejunum, longer villus height and shorter crypt depth ratio were observed in the EP supplemented

TABLE 4 | Effects of EP polysaccharide supplementation on the intestinal morphology of broiler chickens.

Parameters	Treatment groups		*P*-Value
	Control	EP	
Villus height (μm)			
Jejunum	1,094.61 ± 29.13[b]	1,207.51 ± 65.47[a]	0.017
Ileum	855.93 ± 45.98[b]	1,038.91 ± 46.96[a]	0.008
Crypt depth(μm)			
Jejunum	238.08 ± 7.83[a]	201.23 ± 7.51[b]	0.03
Ileum	210.43 ± 16.83[a]	172.28 ± 12.13[b]	0.013
VH/CD			
Jejunum	4.6 ± 0.20	6.0 ± 0.44	0.063
Ileum	4.11 ± 0.24[b]	6.20 ± 0.43[a]	0.020

VH/CD, villus height: crypt depth ratio; n = 10 for each group. Means with a different superscript letter in the same raw indicate a significant difference at P < 0.05.

group ($P < 0.05$; **Table 4**). Similarly in the ileum, villus height and villus height: crypt depth ratio were significantly ($P < 0.05$) increased, while crept depth was markedly reduced ($P < 0.05$) in the EP supplemented group than in the control group (**Table 4**). However, a significant difference in the villus height: crypt depth ratio between treatment groups was not observed ($P = 0.064$) in the jejunal tissue.

Effects of EP Supplementation on Immune-Related Gene Expression

To determine the effects of EP supplementation on intestinal immune response, we detected the mRNA expression of immune-related genes from the jejunal and ileal tissues. In the jejunum, compared with the control group, EP supplementation upregulated ($P < 0.05$) the mRNA expression of IL-1β, TNF-α, TLR4, MyD88, and NF-κB (**Figures 3A,B**). However, dietary EP inclusion did not significantly alter the mRNA expression of IL-2, IFN-γ, IL-10, and TLR2 in the jejunal tissue (**Figures 3A,B**; $P > 0.05$).

In the ileum, the mRNA expressions of IL-1β, IL2, and TNFα were upregulated ($P < 0.05$) in the EP group than in the control group (**Figure 3C**). In addition, the expressions of Toll-like receptor (TLR-2), TLR4, myeloid differentiation (MyD88), and nuclear factor-kappa B (NF-κB) in the ileum tissue were significantly increased ($P < 0.05$) in the supplemented group (**Figure 3D**). However, EP supplementation did not affect ($P > 0.05$) the mRNA expression of IFN-γ and IL-10.

Effects of EP Supplementation on Mucin-2 and Tight Junctions Gene Expression

The effects of EP supplementation on mRNA expression of mucin-2 and tight junction in the jejunum and ileum tissues are presented in **Figure 4**. In the jejunum, the addition of EP to diet upregulated ($P < 0.05$) the mRNA expression of mucin-2, claudin-1, and occludin-1. In the ileum, birds fed EP had a significantly higher expression of mucin-2 and occludin-1 ($P < 0.05$) than the control group. However, no differences ($P > 0.05$) were observed between the treatments in ZO2 expression in the jejunum, and claudin-1 and ZO2 in the ileum.

Effects of EP Supplementation on Microbiota Dynamics

To assess the caecal microbial composition in response to EP supplementation, the caecal contents of 10 experimental broiler chickens were collected and subjected to metagenomic sequencing. We retrieved 60,537.45 and 6,053.75 Mbp total raw and average raw reads, respectively. After quality control, we obtained 58,156.5 and 5,815.65 Mbp total and average clean data, respectively. To explore the differences in species diversity and richness between EP supplemented and control groups, we calculated the alpha diversity indexes at the phylum level. The results showed that there were no significant differences in observed species, Chao, Shannon, and Simpson indexes between treatment groups [Mann–Whitney *U* (MWU) (**Figures 5A–D**; $P > 0.05$].

The gut microbiota is composed of different bacterial species and is classified according to genus, family, order, and phyla. Therefore, analyzing their composition helps to identify specific microorganisms involved in different processes and the associated metabolic pathways. Thus, we analyzed the microbial abundance from taxonomic phylum to genus levels in different groups. We found that *Firmicutes* and *Bacteroidetes* are the two most predominant phyla, which accounted for more than 75% of the microbes observed (**Figure 5E**). The results further demonstrated that EP supplementation reduced the relative abundance of *Firmicutes* and decreased *Bacteroidetes* microbes. Furthermore, an increase in the relative abundance of *Bacteroides* and decreased *Faecalibacterium* were observed at the genus level (**Figure 5F**). The difference in bacterial abundance between treatment groups was estimated using linear discriminant analysis (LDA), which could be used as a biomarker. In total, 38 phylotypes from phylum to species were identified as high-dimensional biomarkers with LDA scores >2.5 (**Figure 6**) Remarkably, the species *Bacillus_licheniformis, Auraticoccus_monumenti,* and *Alkalibacillus_haloalkaliphilus* were biomarkers in the EP group, while *uncultured_Butyricicoccus_sp*, *Agathobaculum_desmolans*, and *Clostridium_sp_M62_1* were predominant in the control group.

Effects of EP Supplementation on the SCFAs and Correlation Analyses Between SCFAs and Gut Microbiota

To determine the effects of EP supplementation on SCFAs production, we measured the concentrations of SCFAs from caecal content (**Figure 7**). Compared with the control group, chickens fed a diet supplemented with EP had significantly higher ($P < 0.05$) acetate, butyrate, and propionate levels in the caecal content. However, a significant treatment effect ($P > 0.05$) on the valerate, iso-butyrate, and iso-valerate content was not observed.

To gain insight into whether the altered gut microbiota had an association with the SCFAs, we carried out Spearman

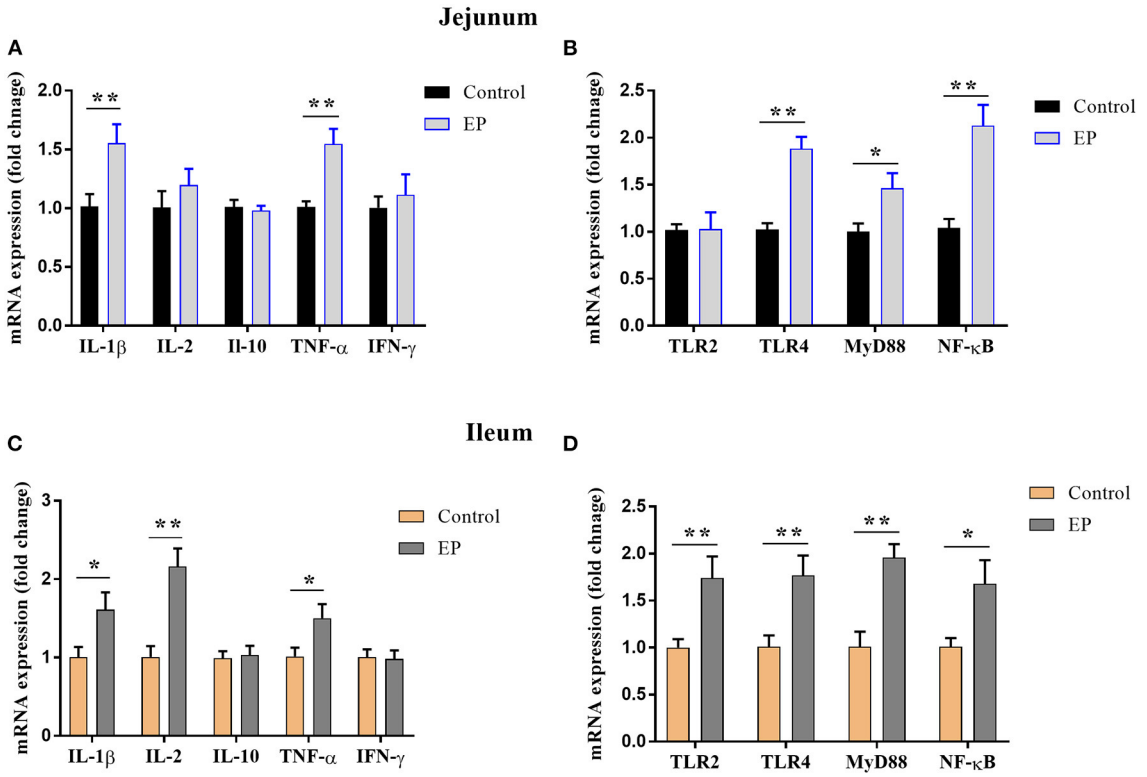

FIGURE 3 | Effects of EP supplementation on the expression of immune factor-related genes **(A,C)** and inflammatory signaling pathway genes **(B,D)** in the jejunum tissues **(A,B)** and ileum **(C,D)** of broiler chickens. Data are presented as mean ± SEM, $n = 10$. $^{*}P < 0.05$ and $^{**}P < 0.01$, respectively. IL-1β, Interleukin 1 beta; IL-2, Interleukin 2; IL-10, Interleukin 10; TNF-α, Tumor necrosis factor-alpha; IFN-γ, Interferon-gamma; TLR, Toll-like receptor; MyD88, myeloid differentiation 88; NF-κB, Nuclear factor-kappa B.

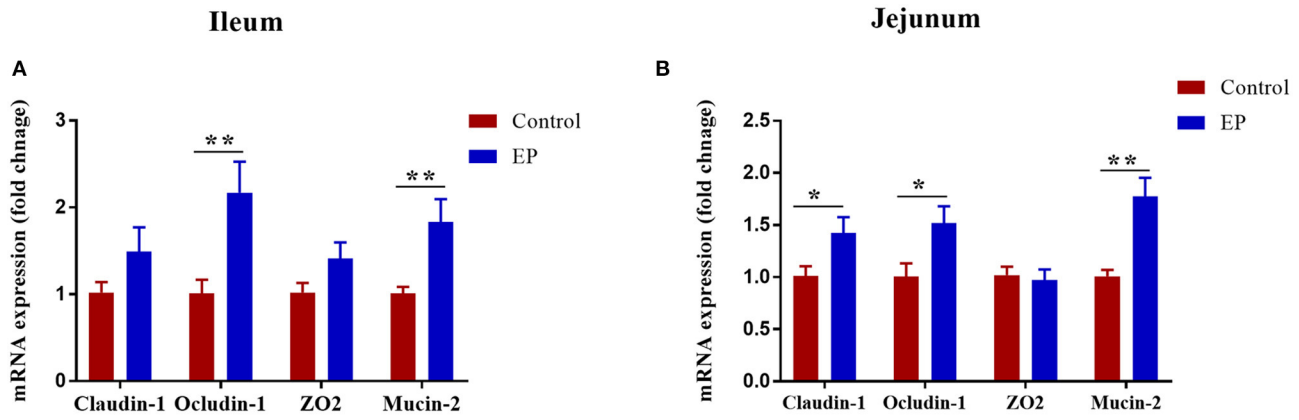

FIGURE 4 | Effects of EP supplementation on Mucin-2 and tight junction gene expression in the ileum **(A)** and jejunum **(B)** tissues of broiler chickens. Data are presented as mean ± SEM, $n = 10$. $^{*}P < 0.05$ and $^{**}P < 0.01$, respectively.

correlation analyses. The relationships of the altered gut microbiota and cecal SCFAs in response to EP treatment based on the Spearman correlation coefficients are shown in **Figure 8**. Notably, the relative abundance of the *Bacteroides, Prevotella, Ruminiclostridium, Butyricicoccus,* and *Faecalibacterium* had a significant positive association with propionate, acetate, butyrate, isobutyrate, and isovalerate production, respectively ($P < 0.05$). In addition, *Prevotella* had also a positive association with valerate ($P < 0.05$). In contrast, the abundance of *Chlamydia* had a negative association with propionate, and

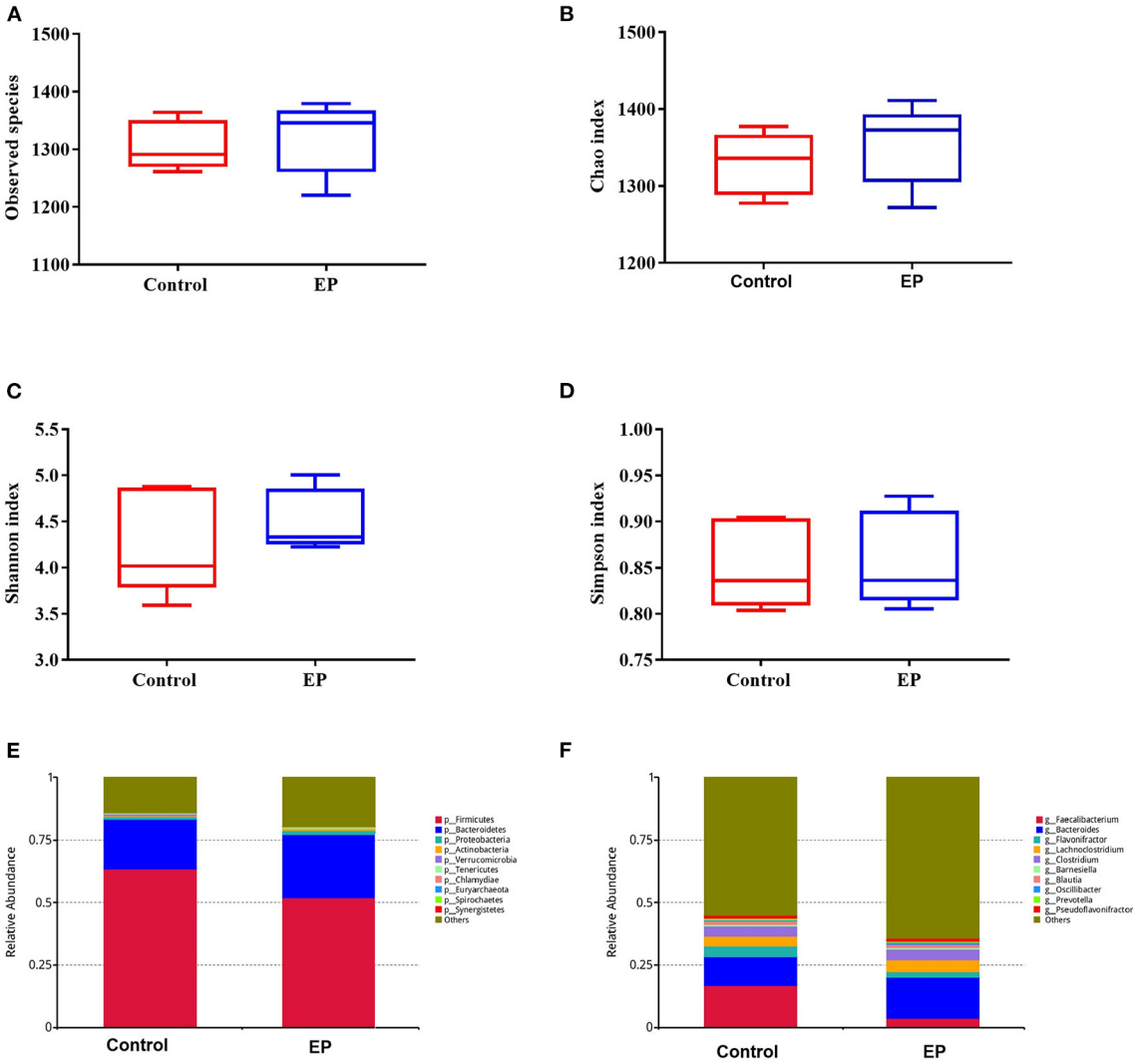

FIGURE 5 | The alpha diversity and the relative abundances of caecal microbiota from the EP and control groups broiler chickens. The number of observed species **(A)**, Chao index **(B)**; Shannon index **(C)**; Simpson index **(D)**; the relative abundance of major bacterial phyla **(E)**; and major bacterial genus **(F)** between the EP and control groups. EP, *Enteromorpha prolifera* polysaccharide.

Enterococcus and *Mycoplasma* had a negative association with isovalerate ($P < 0.05$).

DISCUSSION

Apart from its use as a food and traditional medicine, recent studies have shown that sulfated polysaccharides from marine algae exerted various biological activities, such as immunomodulation, antioxidant, antidiabetic, and hypolipidemic. In the present study, we supplemented the broiler diet with polysaccharides isolated from marine algae EP to evaluate its effect on growth performance, immune response, intestinal barrier function, and caecal microbiota.

Herein, chickens fed EP exhibited higher body weight and average daily gain than chickens fed only basal diet, suggesting that EP supplementation to broiler diet could improve growth performance. Similar conclusions were made by Liu et al. (16) and Li et al. (30), reported that algae-derived polysaccharide could enhance growth performance in chicken. Likewise, dietary supplementation of EP was found to improve growth performance in mice (31) and crucian carp (32). The growth-promoting effect of EP may be associated with its enhancement of nutrient absorption by improving intestinal function and morphology (31).

Research evidence has shown that polysaccharide from *E. prolifera* has an immunomodulatory activity (33). Cytokine profiling is a valuable tool for monitoring immune responses associated with inflammation and immunity. In this study, supplementation of diet with EP induced a profound change in the serum cytokine contents of broilers as evidenced by

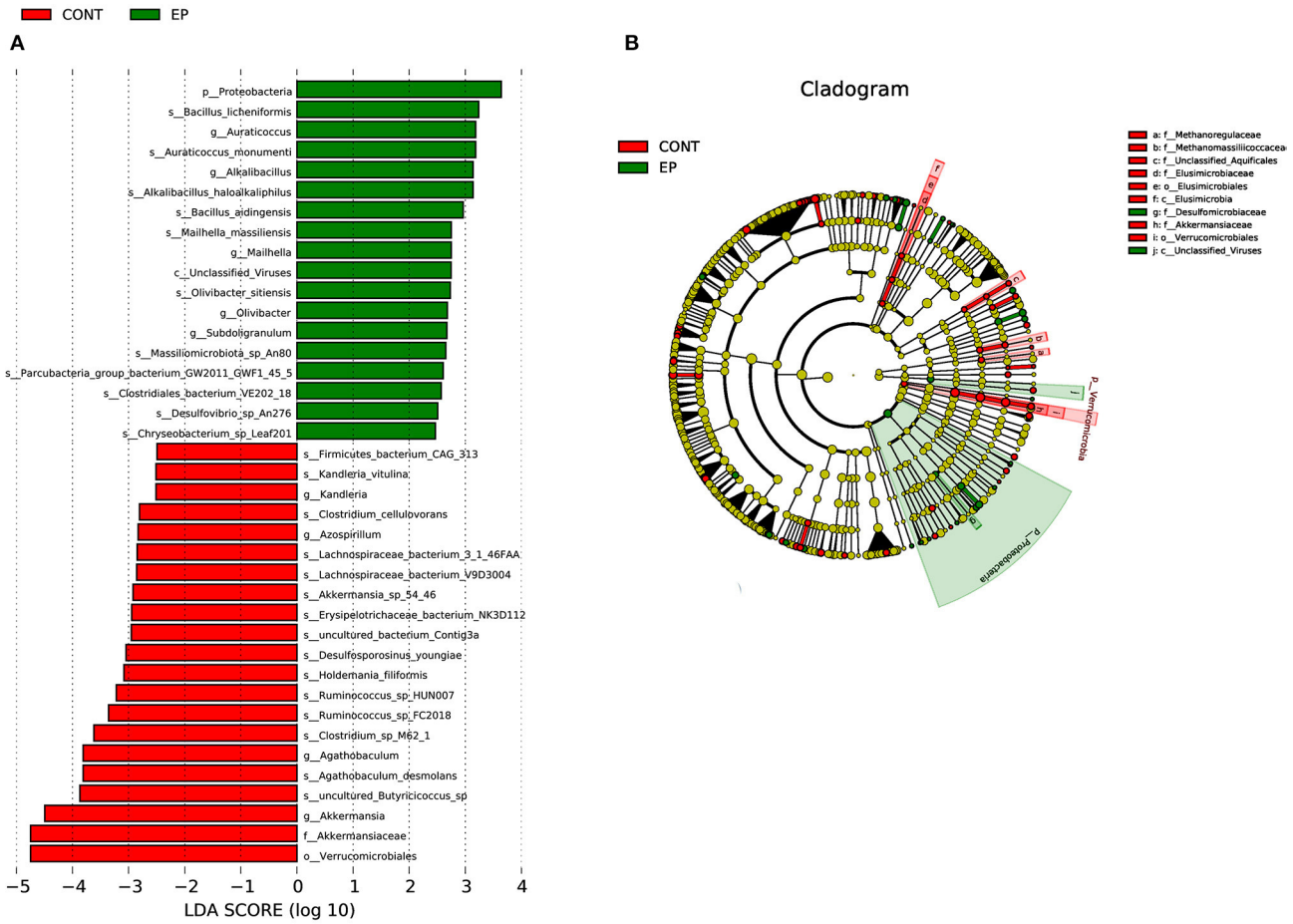

FIGURE 6 | Linear discriminant analysis (LDA) effect size (LEFSe) analysis identified microbial taxa between EP (green) and (control (red) groups. **(A)** histogram plot from LEfSe analysis that presents the LDA scores of microbial taxa whose abundance showed significant differences between EP supplemented and control group broiler chickens (LDA score > 2.5). The length of the bar column represents the LDA score. **(B)** The cladogram, circles radiating from inner side to outer side represents the differences in the relative abundance of taxa from phylum to genus level between EP and control group. The red and green dots indicate a significant difference in the relative abundance between EP and the control group.

significantly higher IL-1β, IL-2, IFNα-, and IFN-γ levels in the supplemented group. This study is consistent with the previous study that reported EP could stimulate proinflammatory cytokine production in mice (34). The results of the present study also support the idea that EP has an immunomodulatory activity by stimulating proinflammatory cytokines.

To better understand whether the changes in cytokine levels were accompanied by changes in the expression of inflammatory factor genes, we detected mRNA expression in the jejunum and ileum tissues. We found upregulated mRNA expression levels of IL-1β and TNF-α in the ileum and jejunum, and IL-2 in the ileum in the EP group compared with the control group. In contrast, Liu et al. (35) reported that algae-derived polysaccharides down-regulated the mRNA expression of TNF-α, and IL-6 in the bursa of Fabricius of heat stress chicken. The discrepancy of our study with the previous study could attribute to the difference in immune status and stress condition of chicken.

More importantly, the pro-inflammatory pathway is transcriptionally regulated by NF-κB, and the up-regulation of NF-κB activates the immune response and cytokine production. The TLR4/MyD88 signaling pathway is the upstream gatekeeper of NF-κB (36). The present data showed that the expression of TLR4, MyD88, and NF-κB in ileum and jejunum were significantly higher in chicken-fed EP than in chicken-fed only basal diet. TLR4 is a family of pathogen recognition receptors (PRRs) that orchestrate the host immune system through MyD88 to induce pro-inflammatory cytokines via NF-κB (37, 38). As the downstream of the TLR4 and interleukin-1 (IL-1) receptor, MyD88 activates NF-κB, and thereby the inflammatory signaling pathways (39). Therefore, the present study indicated that EP supplementation activates the TLR4/MyD88/NF-κB signaling pathway, thereby induces an immune response. This observation further supported the viewpoint that EP has immunomodulatory activity. Similarly, Wei et al. (33) reported upregulation of

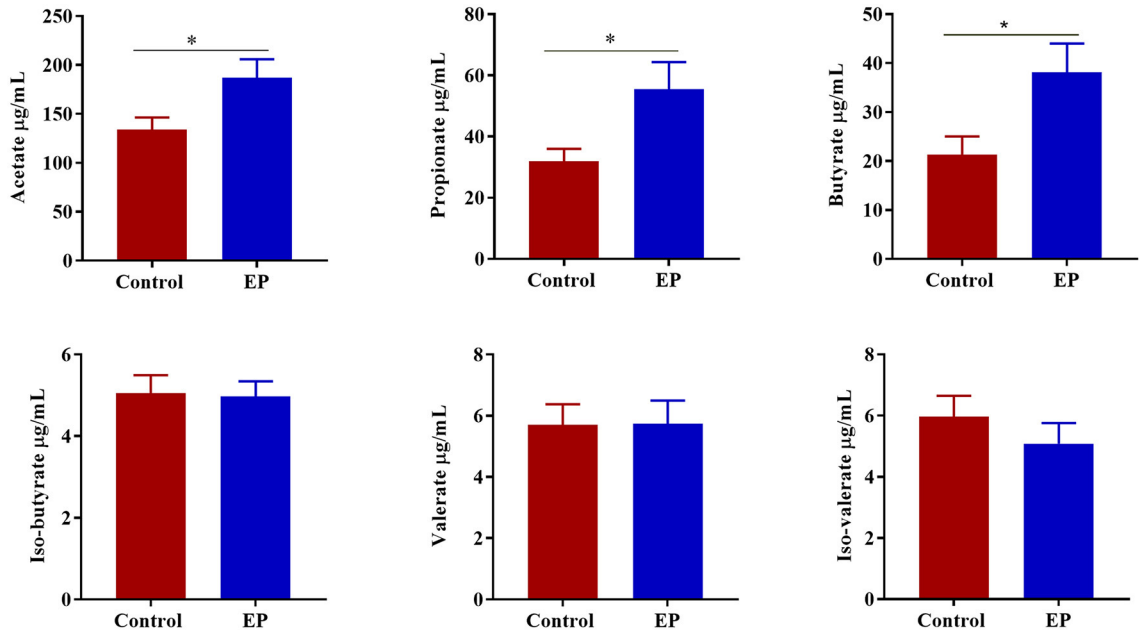

FIGURE 7 | The effects of EP supplementation on the short chain volatile fatty acid concentration from caecal content of broiler chickens. *$P < 0.05$.

NF-κB transcription factors in mice that received EP. In contrast, a study on oxygen-glucose deprivation-induced human cardiac microvascular endothelial cells showed that EP inhibits proinflammatory factors expression through the up-regulation of HIF-1α and inactivation of the NF-κB pathway (40). This may be due to EP might play both immunomodulatory and anti-inflammatory roles depending on the physiological condition of experimental animals or cells.

Intestinal morphology affects nutrient absorption in the body. The longer intestinal villi and lower crypt depth are an indicator of higher nutrient absorption (41). The present study demonstrated that EP supplementation increased villus height and reduced crypt depth in the ileum and jejunum of supplemented chicken. The longer villus height and higher villus height: crypt depth ratio is associated with active cell mitosis, improved nutrient digestibility, and absorption in chickens (42, 43). Thus, the present study suggests the beneficial effects of EP supplementation on improving intestinal morphology. These results are in agreement with the study by Liu et al. (16), who reported villus height and villus height: crypt depth was higher in chickens fed algae-derived polysaccharides. Similar results were obtained by Guo et al. (15), who showed that marine-derived polysaccharide enhanced jejunal villus height and villus height/crypt depth ratio in layer chickens.

The mucus layer of the epithelial cells is an essential first line of defense that forms a barrier to prevent the penetration of the epithelium by gut microorganisms (44, 45). In addition, epithelial barrier integrity is maintained by the tight junction proteins, including occludin, claudins, and zonula occludens. Herein, we examined the effects of EP supplementation on intestinal barrier function by measuring the mRNA expression of mucin-2 and tight junction proteins. Our data demonstrated that the mRNA expressions of mucin-2 and occludin 1 in the ileum and jejunum were upregulated in the EP supplemented chickens. mucin-2 plays an important role in the secretion of mucus, which is a layer that protects the epithelial cells from exposure to the microbiome (46). Occludin provides structural integrity and assembly of tight junction and knockdown of occludin induces an increase in paracellular permeability to macromolecules (47). Claudins are also playing an essential role in barrier formation and paracellular permeable selectivity (48). Therefore, an increase in the expression of mucin-2, occludin 1, and claudin 1 in the intestinal segments in this study, indicates EP supplementation improved intestinal integrity in broiler chickens via regulating mucin-2 and tight junction protein. This is partly explained by the fact that *Enteromorpha* polysaccharides may be directly recognized by the pattern recognition receptors of intestinal epithelial cells (31, 49), leading to the activation of mucin-2 and tight junction proteins, thereby improving intestinal integrity. This idea is reinforced by the mRNA expression results of TLR4 and TLR2 in jejunum and ileum. In addition, EP was fermented by caecal microtia and produced SCFA, which could stimulate intestinal goblet cells to secrete mucin-2 through their action on NOD-like receptor family pyrin domain containing 6 (NLRP6) and G protein-coupled receptors (GPCRs) (50).

In broiler chickens, TLR2 is the principal receptor for peptidoglycan from gram-negative and gram-positive bacteria (51). Toll-like receptor 2 signaling has been implicated in preserving intestinal barrier integrity and is considered to be a crucial target for therapeutic intervention of metabolic and inflammatory conditions (52). In the present study, we found a

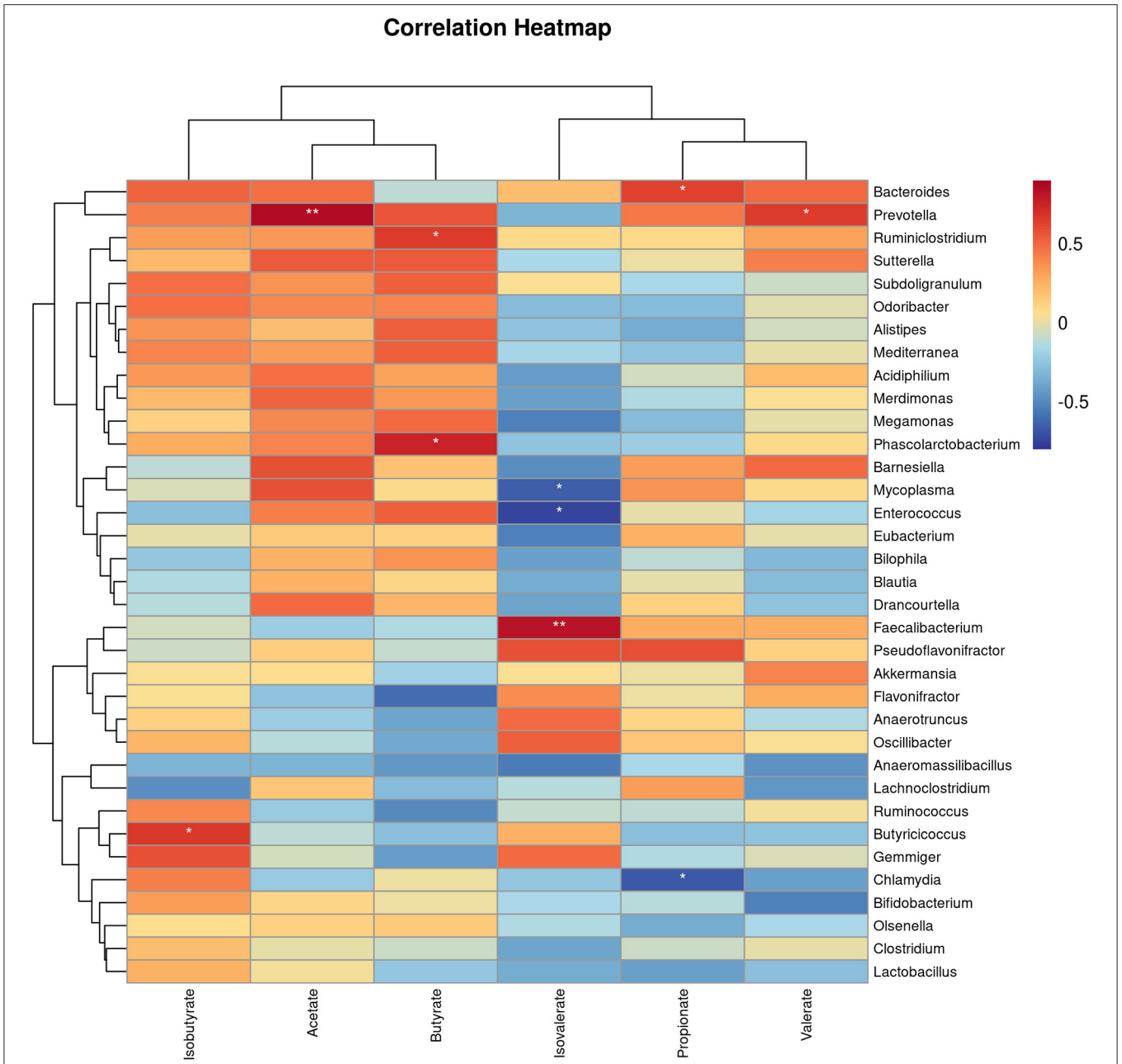

FIGURE 8 | The heat map represents the correlation between caecal SCFAs and caecal microbiota in EP and control group broiler chickens. *$P < 0.05$ and **$P < 0.01$, respectively.

significant increment in the mRNA expression of TLR2 in the ileum tissue of chicken fed EP. This result indicates that apart from the mucin-2 and tight junction protein, TLR2 might also be involved in the improvement of intestinal integrity observed in this study.

The fermentation of fiber diet by gut microbiota produced metabolites such as short-chain volatile fatty acids. These microbiota-derived short-chain fatty acids play important roles in maintaining an intestinal immune response, barrier function, and immune metabolism either by modulating gene transcription or via the activation of metabolite sensing GPCRs (53). In the current study, we found that the SCFAs particularly acetate, butyrate, and propionate increased in the caecal content of EP supplemented chickens, suggesting that EP enhanced the ability of the microbiota to induce SCFAs. Furthermore, we found significant correlations of differentially abundant gut microbes with acetate, propionate, and butyrate production, which further confirmed that the increase of SCFA observed in this study was

due to the microbiota compositional shift. In agreement with the current study, mice fed EP showed an increase in SCFAs production in the colon (21). The SCFAs, particularly butyrate and propionate, provide energy for the immune cell by activating intestinal gluconeogenesis, thereby improving inflammatory and effector cytokines production and antigen presentation (54, 55). Furthermore, microbial-derived butyrate was found to promote mucosal barrier integrity by stimulating the production of mucin-2, tight junction proteins, and antimicrobial peptides (56). Therefore, the immune-modulatory role of EP in the current study might be via enhancing the gut microbiota-derived SCFA that contribute to intestinal immune response and gut barrier function.

A growing body of evidence suggests that gut microbiota is involved in the digestion and utilization of fibers such as polysaccharides, which otherwise cannot be utilized by the host. It is well-established that diet and nutritional factors have a direct effect on the microbial colonization of the gut (57–59). In this study, we conducted 16S-RNA sequencing from the caecal content of chickens fed EP to investigate microbiota dysbiosis. We found that the abundances of phylum *Bacteroidetes* and genera *Bacteroides* were increased, whereas phylum *Firmicutes* and genus *Faecalibacterium* were decreased in chickens fed EP, suggesting that *Bacteroides* might involve in the digestion of *E. prolifera* polysaccharides. This may be explained by the fact that *Bacteroides* possess genes encoding carbohydrate-active enzymes (CAZymes) within their polysaccharide utilization loci (PUL) (60, 61), which could confer them with the strong ability to ferment diverse types of dietary polysaccharides (62). Apart from polysaccharide fermentation, *Bacteroides* can also affect host immune system development (63), and maintenance of gut microbial balance (64). The present study is concurrent with the previous study that showed *E. prolifera* polysaccharides supplementation caused microbiota dysbiosis in mice (21) and rabbitfish *S. oramin* (65). These findings suggest that EP supplementation shifts microbiota composition, particularly *Bacteroides*, which produce SCFA that involve in immune response and gut barrier function. Notably, the species *Bacillus_licheniformis, Auraticoccus_monumenti,* and *Alkalibacillus_haloalkaliphilus* were biomarkers in the EP group. Previous studies reported that *B. licheniformis* isolated from a human fecal sample can be used for manufacturing biochemicals, enzymes, antibiotics, and aminopeptidase (66, 67). *Alkalibacillus_haloalkaliphilus* is used in enzyme synthesis, organic acid, food biotechnology, biodegradation, and antibiotics (68) and can convert carbohydrates to organic acids such as acetic acid (69). However, further study is needed to confirm their specific roles in the fermentation of polysaccharides in the intestine.

CONCLUSION

We concluded that EP inclusion in chickens' diet improves growth performance, enhances intestinal immune response and integrity, and modulates the caecal microbiota of broilers. This study suggests the application of EP as an alternative to antibiotics in chicken and also provides insight to develop marine algae polysaccharide-based functional food and therapeutic agent.

DATA AVAILABILITY STATEMENT

The original contributions presented in the study are publicly available. This data can be found here: https://www.ncbi.nlm.nih.gov/bioproject/765947.

ETHICS STATEMENT

The animal study was reviewed and approved by Animal Care and Use Committee of the Institute of Subtropical Agriculture, Chinese Academy of Sciences, Hunan, China.

AUTHOR CONTRIBUTIONS

TW: conceptualization, investigation, data generation, curation, and original draft preparation. XD, KG, and ZY: data generation and curation and editing. ZL: methodology, investigation, data generation, curation, and reviewing. YY, CX, and XW: conceptualization, supervision, validation, reviewing, and editing. All authors contributed to the article and approved the submitted version.

FUNDING

We would like to acknowledge the earmarked fund for National Natural Science Foundation of China (31902196), China Agriculture Research System (CARS-35), China Postdoctoral Science Foundation-funded project (2021M693383 and 2019M662273), and Taishan industry leading talent blue talent project for their financial support.

REFERENCES

1. Dibner J, Richards J. Antibiotic growth promoters in agriculture: history and mode of action. *Poult Sci.* (2005) 84:634–43. doi: 10.1093/ps/84.4.634
2. Fardet A. New hypotheses for the health-protective mechanisms of whole-grain cereals: what is beyond fibre? *Nutr Res Rev.* (2010) 23:65–134. doi: 10.1017/S0954422410000041
3. Nicholson JK, Holmes E, Kinross J, Burcelin R, Gibson G, Jia W, et al. Host-gut microbiota metabolic interactions. *Science.* (2012) 336:1262–7. doi: 10.1126/science.1223813
4. Jeffery IB, O'Toole PW. Diet-microbiota interactions and their implications for healthy living. *Nutrients.* (2013) 5:234–52. doi: 10.3390/nu5010234
5. Stanley D, Hughes RJ, Moore RJ. Microbiota of the chicken gastrointestinal tract: influence on health, productivity and disease. *Appl Microbiol Biotechnol.* (2014) 98:4301–10. doi: 10.1007/s00253-014-5646-2
6. Sergeant MJ, Constantinidou C, Cogan TA, Bedford MR, Penn CW, Pallen MJ. Extensive microbial and functional diversity within the chicken cecal microbiome. *PLoS ONE.* (2014) 9:e91941. doi: 10.1371/journal.pone.0091941
7. Mishra SP, Karunakar P, Taraphder S, Yadav H. Free fatty acid receptors 2 and 3 as microbial metabolite sensors to shape host health: pharmacophysiological

view. *Biomedicines.* (2020) 8:154. doi: 10.3390/biomedicines 8060154
8. Berg D, Clemente JC, Colombel JF. Can inflammatory bowel disease be permanently treated with short-term interventions on the microbiome? *Expert Rev Gastroenterol Hepatol.* (2015) 9:781–95. doi: 10.1586/17474124.2015.1013031
9. Zhang Y, Duan X, Wassie T, Wang H, Li T, Xie C, et al. Enteromorpha prolifera polysaccharide-zinc complex modulates the immune response and alleviates LPS-induced intestinal inflammation via inhibiting the TLR4/NF-κB signaling pathway. *Food Funct.* (2021). doi: 10.1039/d1fo02171k. [Epub ahead of print].
10. Jiao L, Jiang P, Zhang L, Wu M. Antitumor and immunomodulating activity of polysaccharides from *Enteromorpha intestinalis*. *Biotechnol Bioproc Eng.* (2010) 15:421–8. doi: 10.1007/s12257-008-0269-z
11. Wijesekara I, Pangestuti R, Kim SK. Biological activities and potential health benefits of sulfated polysaccharides derived from marine algae. *Carbohydr Polym.* (2011) 84:14–21. doi: 10.1016/j.carbpol.2010.10.062
12. Wassie T, Niu K, Xie C, Wang H, Wu X. Extraction techniques, biological activities and health benefits of marine algae *Enteromorpha prolifera* polysaccharide. *Front Nutr.* (2021) 8:747928. doi: 10.3389/fnut.2021.747928
13. Chi Y, Li Y, Zhang G, Gao Y, Ye H, Gao J, et al. Effect of extraction techniques on properties of polysaccharides from *Enteromorpha prolifera* and their applicability in iron chelation. *Carbohydr Polym.* (2018) 181:616–23. doi: 10.1016/j.carbpol.2017.11.104
14. Yu Y, Li Y, Du C, Mou H, Wang P. Compositional and structural characteristics of sulfated polysaccharide from *Enteromorpha prolifera*. *Carbohydr Polym.* (2017) 165:221–8. doi: 10.1016/j.carbpol.2017.02.011
15. Guo Y, Zhao ZH, Pan ZY, An LL, Balasubramanian B, Liu WC. New insights into the role of dietary marine-derived polysaccharides on productive performance, egg quality, antioxidant capacity, and jejunal morphology in late-phase laying hens. *Poult Sci.* (2020) 99:2100–7. doi: 10.1016/j.psj.2019.12.032
16. Liu WC, Guo Y, Zhihui Z, Jha R, Balasubramanian B. Algae-derived polysaccharides promote growth performance by improving antioxidant capacity and intestinal barrier function in broiler chickens. *Front Vet Sci.* (2020) 7:990. doi: 10.3389/fvets.2020.601336
17. Zhao Y, Balasubramanian B, Guo Y, Qiu SJ, Jha R, Liu WC. Dietary *Enteromorpha* polysaccharides supplementation improves breast muscle yield and is associated with modification of mRNA transcriptome in broiler chickens. *Front Vet Sci.* (2021) 8:337. doi: 10.3389/fvets.2021.663988
18. Liu WC, Zhu YR, Zhao ZH, Jiang P, Yin FQ. Effects of dietary supplementation of algae-derived polysaccharides on morphology, tight junctions, antioxidant capacity and immune response of duodenum in broilers under heat stress. *Animals.* (2021) 11:2279. doi: 10.3390/ani11082279
19. Qiu SJ, Zhang R, Guo Y, Zhao Y, Zhao ZH, Liu WC. Transcriptome analysis reveals potential mechanisms of the effects of dietary *Enteromorpha* polysaccharides on bursa of fabricius in broilers. *Vet Med Sci.* (2021) 7:1881–9. doi: 10.1002/vms3.573
20. Liu WC, Zhou SH, Balasubramanian B, Zeng F-Y, Sun CB, Pang HY. Dietary seaweed (*Enteromorpha*) polysaccharides improve growth performance involved in the regulation of immune responses, intestinal morphology and microbial community in banana shrimp *Fenneropenaeus merguiensis*. *Fish Shellfish Immunol.* (2020) 104:202–12. doi: 10.1016/j.fsi.2020.05.079
21. Zhang Z, Wang X, Han S, Liu C, Liu F. Effect of two seaweed polysaccharides on intestinal microbiota in mice evaluated by illumina PE250 sequencing. *Int J Biol Macromol.* (2018) 112:796–802. doi: 10.1016/j.ijbiomac.2018.01.192
22. Kong Q, Dong S, Gao J, Jiang C. In vitro fermentation of sulfated polysaccharides from *E. prolifera* and *L. japonica* by human fecal microbiota. *Int J Biol Macromol.* (2016) 91:867–71. doi: 10.1016/j.ijbiomac.2016.06.036
23. Xie C, Zhang Y, Niu K, Liang X, Wang H, Shan J, et al. *Enteromorpha* polysaccharide-Zinc replacing prophylactic antibiotics contributes to improving gut health of weaned piglets. *Anim Nutr.* (2021) 7:641–9. doi: 10.1016/j.aninu.2021.01.008
24. Guo Y, Balasubramanian B, Zhao ZH, Liu WC. Marine algal polysaccharides alleviate aflatoxin B1-induced bursa of fabricius injury by regulating redox and apoptotic signaling pathway in broilers. *Poult Sci.* (2021) 100:844–57. doi: 10.1016/j.psj.2020.10.050
25. Lv H, Xiao B, Gao Y. Study on the extraction, purification and structural characterization of polysaccharide from *Enteromorpha*. *Food Res Dev.* (2013) 34:33–6.
26. Aviagen R. *Ross Broiler Management Manual, 2009*. (2014). Available online at: http://ptaviagen.com/assets/Tech_Center/Ross_broiler/Ross_broiler_manual_
27. Shang HM, Song H, Xing YL, Niu SL, Ding GD, Jiang YY, et al. Effects of dietary fermentation concentrate of *Hericium caput-medusae* (bull: Fr.) Pers. on growth performance, digestibility, and intestinal microbiology and morphology in broiler chickens. *J Sci Food Agric.* (2016) 96:215–22. doi: 10.1002/jsfa.7084
28. Livak KJ, Schmittgen TD. Analysis of relative gene expression data using real-time quantitative PCR and the $2^{-\Delta\Delta CT}$ method. *Methods.* (2001) 25:402–8. doi: 10.1006/meth.2001.1262
29. Saarinen MT, Kärkkäinen O, Hanhineva K, Tiihonen K, Hibberd A, Mäkelä KA, et al. Metabolomics analysis of plasma and adipose tissue samples from mice orally administered with polydextrose and correlations with cecal microbiota. *Sci Rep.* (2020) 10:21577. doi: 10.1038/s41598-020-78484-y
30. Yang S, Shan C, Ma X, Qin Y, Ju A, Duan A, et al. Immunomodulatory effect of Acanthopanax senticosus polysaccharide on immunosuppressed chickens. *Poult Sci.* (2021) 100:623–30. doi: 10.1016/j.psj.2020.11.059
31. Liu Y, Wu X, Jin W, Guo Y. Immunomodulatory effects of a low-molecular-weight polysaccharide from *Enteromorpha prolifera* on RAW 264.7 macrophages and cyclophosphamide-induced immunosuppression mouse models. *Mar Drugs.* (2020) 18:340. doi: 10.3390/md18070340
32. Zhou Z, Pan S, Wu S. Modulation of the growth performance, body composition and nonspecific immunity of crucian carp *Carassius auratus* upon *Enteromorpha prolifera* polysaccharide. *Int J Biol Macromol.* (2020) 147:29–33. doi: 10.1016/j.ijbiomac.2020.01.065
33. Wei J, Wang S, Liu G, Pei D, Liu Y, Liu Y, et al. Polysaccharides from *Enteromorpha prolifera* enhance the immunity of normal mice. *Int J Biol Macromol.* (2014) 64:1–5. doi: 10.1016/j.ijbiomac.2013.11.013
34. Kim J-K, Cho ML, Karnjanapratum S, Shin I-S, You SG. In vitro and in vivo immunomodulatory activity of sulfated polysaccharides from *Enteromorpha prolifera*. *Int J Biol Macromol.* (2011) 49:1051–8. doi: 10.1016/j.ijbiomac.2011.08.032
35. Liu WC, Ou BH, Liang ZL, Zhang R, Zhao ZH. Algae-derived polysaccharides supplementation ameliorates heat stress-induced impairment of bursa of fabricius via modulating NF-κB signaling pathway in broilers. *Poult Sci.* (2021) 100:101139. doi: 10.1016/j.psj.2021.101139
36. Burns K, Martinon F, Esslinger C, Pahl H, Schneider P, Bodmer JL, et al. MyD88, an adapter protein involved in interleukin-1 signaling. *J Biol Chem.* (1998) 273:12203–9. doi: 10.1074/jbc.273.20.12203
37. Janssens S, Burns K, Vercammen E, Tschopp J, Beyaert R. MyD88S, a splice variant of MyD88, differentially modulates NF-κB-and AP-1-dependent gene expression. *FEBS Lett.* (2003) 548:103–7. doi: 10.1016/S0014-5793(03)00747-6
38. Yamamoto M, Sato S, Hemmi H, Hoshino K, Kaisho T, Sanjo H, et al. Role of adaptor TRIF in the MyD88-independent toll-like receptor signaling pathway. *Science.* (2003) 301:640–3. doi: 10.1126/science.1087262
39. Deguine J, Barton GM. MyD88: a central player in innate immune signaling. *F1000Prime Rep.* (2014) 6:97. doi: 10.12703/P6-97
40. Wang Z, Zhang Z, Zhao J, Yong C, Mao Y. Polysaccharides from *Enteromorpha prolifera* ameliorate acute myocardial infarction *in vitro* and *in vivo* via up-regulating HIF-1α. *Int Heart J.* (2019) 60:964–73. doi: 10.1536/ihj.18-519
41. Caspary WF. Physiology and pathophysiology of intestinal absorption. *Am J Clin Nutr.* (1992) 55:299S−308S. doi: 10.1093/ajcn/55.1.299s
42. Onderci M, Sahin N, Sahin K, Cikim G, Aydin A, Ozercan I, et al. Efficacy of supplementation of α-amylase-producing bacterial culture on the performance, nutrient use, and gut morphology of broiler chickens fed a corn-based diet. *Poult Sci.* (2006) 85:505–10. doi: 10.1093/ps/85.3.505
43. Silva MAd, Pessotti BMdS, Zanini SF, Colnago GL, Rodrigues MRA, Nunes LdC, et al. Intestinal mucosa structure of broiler chickens infected experimentally with *Eimeria tenella* and treated with essential oil of oregano. *Ciencia Rural.* (2009) 39:1471–7. doi: 10.1590/S0103-84782009005000135

44. Ma N, Tian Y, Wu Y, Ma X. Contributions of the interaction between dietary protein and gut microbiota to intestinal health. *Curr Protein Peptide Sci.* (2017) 18:795–808. doi: 10.2174/1389203718666170216153505
45. Liu T, Li J, Liu Y, Xiao N, Suo H, Xie K, et al. Short-chain fatty acids suppress lipopolysaccharide-induced production of nitric oxide and proinflammatory cytokines through inhibition of NF-κB pathway in RAW264. 7 cells. *Inflammation.* (2012) 35:1676–84. doi: 10.1007/s10753-012-9484-z
46. Yu Y, Sitaraman S, Gewirtz AT. Intestinal epithelial cell regulation of mucosal inflammation. *Immunol Res.* (2004) 29:55–67. doi: 10.1385/IR:29:1-3:055
47. Al-Sadi R, Khatib K, Guo S, Ye D, Youssef M, Ma T. Occludin regulates macromolecule flux across the intestinal epithelial tight junction barrier. *Am J Physiol Gastrointest Liver Physiol.* (2011) 300:G1054–64. doi: 10.1152/ajpgi.00055.2011
48. Fujibe M, Chiba H, Kojima T, Soma T, Wada T, Yamashita T, et al. Thr203 of claudin-1, a putative phosphorylation site for MAP kinase, is required to promote the barrier function of tight junctions. *Exp Cell Res.* (2004) 295:36–47. doi: 10.1016/j.yexcr.2003.12.014
49. Erturk-Hasdemir D, Oh SF, Okan NA, Stefanetti G, Gazzaniga FS, Seeberger PH, et al. Symbionts exploit complex signaling to educate the immune system. *Proc Natl Acad Sci USA.* (2019) 116:26157–66. doi: 10.1073/pnas.1915978116
50. Birchenough GM, Nyström EE, Johansson ME, Hansson GC. A sentinel goblet cell guards the colonic crypt by triggering Nlrp6-dependent Muc2 secretion. *Science.* (2016) 352:1535–42. doi: 10.1126/science.aaf7419
51. Higuchi M, Matsuo A, Shingai M, Shida K, Ishii A, Funami K, et al. Combinational recognition of bacterial lipoproteins and peptidoglycan by chicken Toll-like receptor 2 subfamily. *Dev Comparat Immunol.* (2008) 32:147–55. doi: 10.1016/j.dci.2007.05.003
52. Chen JQ, Szodoray P, Zeher M. Toll-like receptor pathways in autoimmune diseases. *Clin Rev Allergy Immunol.* (2016) 50:1–17. doi: 10.1007/s12016-015-8473-z
53. Tan J, McKenzie C, Potamitis M, Thorburn AN, Mackay CR, Macia L. The role of short-chain fatty acids in health and disease. *Adv Immunol.* (2014) 121:91–119. doi: 10.1016/B978-0-12-800100-4.00003-9
54. Shi LZ, Wang R, Huang G, Vogel P, Neale G, Green DR, et al. HIF1α-dependent glycolytic pathway orchestrates a metabolic checkpoint for the differentiation of TH17 and Treg cells. *J Exp Med.* (2011) 208:1367–76. doi: 10.1084/jem.20110278
55. Everts B, Amiel E, Huang SCC, Smith AM, Chang CH, Lam WY, et al. TLR-driven early glycolytic reprogramming via the kinases TBK1-IKKε supports the anabolic demands of dendritic cell activation. *Nat Immunol.* (2014) 15:323–32. doi: 10.1038/ni.2833
56. Zhang W, Zhang X, Zou K, Xie J, Zhao S, Liu J, et al. Seabuckthorn berry polysaccharide protects against carbon tetrachloride-induced hepatotoxicity in mice via anti-oxidative and anti-inflammatory activities. *Food Funct.* (2017) 8:3130–8. doi: 10.1039/C7FO00399D
57. Gobet A, Mest L, Perennou M, Dittami SM, Caralp C, Coulombet C, et al. Seasonal and algal diet-driven patterns of the digestive microbiota of the European abalone *Haliotis tuberculata*, a generalist marine herbivore. *Microbiome.* (2018) 6:60. doi: 10.1186/s40168-018-0430-7
58. Hills RD, Pontefract BA, Mishcon HR, Black CA, Sutton SC, Theberge CR. Gut microbiome: profound implications for diet and disease. *Nutrients.* (2019) 11:1613. doi: 10.3390/nu11071613
59. Kartzinel TR, Hsing JC, Musili PM, Brown BR, Pringle RM. Covariation of diet and gut microbiome in African megafauna. *Proc Natl Acad Sci USA.* (2019) 116:23588–93. doi: 10.1073/pnas.1905666116
60. Bäckhed F, Ding H, Wang T, Hooper LV, Koh GY, Nagy A, et al. The gut microbiota as an environmental factor that regulates fat storage. *PNAS.* (2004) 101:15718–23. doi: 10.1073/pnas.0407076101
61. Flint HJ, Scott KP, Duncan SH, Louis P, Forano E. Microbial degradation of complex carbohydrates in the gut. *Gut Microbes.* (2012) 3:289–306. doi: 10.4161/gmic.19897
62. Xu J, Mahowald MA, Ley RE, Lozupone CA, Hamady M, Martens EC, et al. Evolution of symbiotic bacteria in the distal human intestine. *PLoS Biol.* (2007) 5:e156. doi: 10.1371/journal.pbio.0050156
63. Hooper LV. Bacterial contributions to mammalian gut development. *Trends Microbiol.* (2004) 12:129–34. doi: 10.1016/j.tim.2004.01.001
64. Sears CL. A dynamic partnership: celebrating our gut flora. *Anaerobe.* (2005) 11:247–51. doi: 10.1016/j.anaerobe.2005.05.001
65. Xu Y, Li J, Han X, Zhang Z, Zhong M, Hu Z. *Enteromorpha prolifera* diet drives intestinal microbiome composition in *Siganus oramin*. *Curr Microbiol.* (2020) 78:229–37. doi: 10.1007/s00284-020-02218-6
66. Rey MW, Ramaiya P, Nelson BA, Brody KSD, Zaretsky EJ, Tang M, et al. Complete genome sequence of the industrial bacterium *Bacillus licheniformis* and comparisons with closely related bacillus species. *Genome Biol.* (2004) 5:R77. doi: 10.1186/gb-2004-5-10-r77
67. Lee C, Kim JY, Song HS, Kim YB, Choi YE, Yoon C, et al. Genomic analysis of *Bacillus licheniformis* CBA7126 isolated from a human fecal sample. *Front Pharmacol.* (2017) 8:724. doi: 10.3389/fphar.2017.00724
68. Shameer S. Haloalkaliphilic Bacillus species from solar salterns: an ideal prokaryote for bioprospecting studies. *Ann Microbiol.* (2016) 66:1315–27. doi: 10.1007/s13213-016-1221-7
69. Paavilainen S, Helistö P, Korpela T. Conversion of carbohydrates to organic acids by *Alkaliphilic bacilli*. *J Ferment Bioeng.* (1994) 78:217–22. doi: 10.1016/0922-338X(94)90293-3

Conflict of Interest: The authors declare that the research was conducted in the absence of any commercial or financial relationships that could be construed as a potential conflict of interest.

Publisher's Note: All claims expressed in this article are solely those of the authors and do not necessarily represent those of their affiliated organizations, or those of the publisher, the editors and the reviewers. Any product that may be evaluated in this article, or claim that may be made by its manufacturer, is not guaranteed or endorsed by the publisher.

frontiers in Nutrition

ORIGINAL RESEARCH
published: 03 December 2021
doi: 10.3389/fnut.2021.778563

In vitro Assessment of Chemical and Pre-biotic Properties of Carboxymethylated Polysaccharides From *Passiflora edulis* Peel, Xylan, and Citrus Pectin

Yongjin Sun[1], *Yuan Guan*[1,2], *Hock Eng Khoo*[1]* *and Xia Li*[1,2]*

[1] *Department of Bioengineering, College of Chemistry and Bioengineering, Bioengineering Program, Guilin University of Technology, Guilin, China,* [2] *Guangxi Key Laboratory of Electrochemical and Magnetochemical Functional Materials, College of Chemistry and Bioengineering, Bioengineering Program, Guilin University of Technology, Guilin, China*

OPEN ACCESS

Edited by:
Ren-You Gan, Institute of Urban Agriculture, Chinese Academy of Agricultural Sciences (CAAS), China

Reviewed by:
Libo Liu, Northeast Agricultural University, China
Nditange Shigwedha, Independent Researcher, Vevey, Switzerland

***Correspondence:**
Xia Li
biology754@163.com
Hock Eng Khoo
2020153@glut.edu.cn

Specialty section:
This article was submitted to Nutrition and Microbes, a section of the journal Frontiers in Nutrition

Received: *17 September 2021*
Accepted: *09 November 2021*
Published: *03 December 2021*

Citation:
Sun Y, Guan Y, Khoo HE and Li X (2021) In vitro Assessment of Chemical and Pre-biotic Properties of Carboxymethylated Polysaccharides From Passiflora edulis Peel, Xylan, and Citrus Pectin. Front. Nutr. 8:778563. doi: 10.3389/fnut.2021.778563

This study aimed to determine the carboxymethylation effect of crude water-soluble polysaccharides of *Passiflora edulis* peel (WPEP), xylan (XY), and citrus pectin (CP). Their chemical and pre-biotic properties were also determined. The polysaccharides were carboxymethylated by reacting with chloroacetic acid and sodium hydroxide. The carboxymethylated and non-carboxymethylated polysaccharides were also used as pre-biotics to study the growth pattern of selected intestinal microflora. These polysaccharides substituted the glucose solution in culture media for culturing *Lactobacillus brevis* GIM1.773, *Lactobacillus plantarum* GIM1.19, *Lactobacillus delbrueckii* subsp. *bulgaricus* GIM1.155, and *Streptococcus thermophilus* GIM1.540. The results showed that the carboxymethylated polysaccharides c-XY, c-CP, and c-WPEP, had substitution degrees of 0.682, 0.437, and 0.439, respectively. The polysaccharides demonstrated resistance to digestion in the simulated human digestive models. The resistance to digestion was enhanced by carboxymethylation, especially the carboxymethylated CP and WPEP. The results also showed that the pre-biotic activities of the polysaccharides increased after carboxymethylation. The c-XY had a better pre-biotic effect than XY and the other carbohydrate samples. The findings suggested that carboxymethylated polysaccharides may be developed into novel pre-biotics and nutraceuticals that could promote growth of the probiotic strains.

Keywords: chemical modification, growth curve, passion fruit, probiotic, functional group

INTRODUCTION

Pre-biotics are defined as substrates that could selectively promote growth and activity of the host microorganisms. They are non-digestible oligosaccharides that have a beneficial effect on the human gut. The substrates also maintain the balance of intestinal microecology (1, 2). These oligosaccharides are food for gut microflora, such as lactobacilli or bifidobacteria. These bacteria inhabit the human intestinal tract, and they are responsible for regulating fat storage and biosynthesis of essential vitamins (3). Pre-biotics are metabolized into lactic acid and short-chain fatty acids in the large intestine. These substances promote the growth of intestinal bacteria

and improve the physiological health of the host. Regular consumption of pre-biotics is essential for maintaining good health and regulating intestinal microflora (4). Studies have shown that the experimental mice fed pre-biotics had improved intestinal microflora. Pre-biotics not only help to treat obesity but also improve the host's immune system and prevent the development of diseases like type 2 diabetes mellitus, irritable bowel syndrome, and colorectal cancer. These oligosaccharides can also indirectly regulate cardiovascular diseases (5).

Polysaccharides are potent sources of pre-biotics. They have antiviral, immuno-enhancing, hypoglycemic, antioxidation, and antitumor effects in addition to the pre-biotic properties (6–8). The substances also effectively promote the growth of intestinal microflora and increase short-chain fatty acid levels (9, 10). Literature showed that the polysaccharides extracted from the citrus peel (11), bamboo shoots (12), *Ganoderma lucidum*, and *Poria cocos* (13) exhibited pre-biotic potential. However, the pre-biotic activities of carboxymethylated polysaccharides were yet unknown. The consumption of sulfated polysaccharides from marine seaweeds as pre-biotics showed anti-inflammatory effects and prevented peptic-ulcer disease and gastrointestinal disorders (14). The disease-prevention mechanism is related to the blocking of the leucocyte adhered to the epithelium of blood vessels. The polysaccharides also prevented the migration of these cells to the inflammation sites. However, the biological activities of these polysaccharides are limited by their low solubility. Many scholars have also attempted to chemically modify the structures of polysaccharides to improve their physicochemical properties and bioactivities (2, 15).

The chemical modification of polysaccharides, especially carboxymethylation, has recently drawn wide attention. The carboxymethylation technique has been used to improve the physicochemical properties and bioactivity of plant polysaccharides. The carboxymethylated polysaccharides exhibited immunoregulatory, oxidation, and antitumor effects (16–19). A study on characterization of carboxymethylated xylan has been done previously, and the structural information has been obtained using ^{13}C nuclear magnetic resonance (20). The structural characteristics of carboxymethylated pectin had also been studied using Fourier-transform infrared spectroscopy (FTIR), X-ray diffraction, and thermogravimetric analysis (21). Moreover, physicochemical characteristics of polysaccharides extracted from passion fruit peel had been performed (22). As no previous study has been done on carboxymethylation of polysaccharides extracted from passion fruit peel, this study is, therefore, aimed to fill such a gap.

Currently, the valorization of natural resources and utilization of renewable energy resources leads to universal sustainability. The by-products of food processing are the new sources of sustainable food that are renewable and eco-friendly (23). Fruit peels or pericarps are some of the polysaccharide-rich wastes. Polysaccharides have been extracted from citrus and passion fruit peels. The use of polysaccharides from fruit peel provides a new idea for waste utilization. These polysaccharides are potent functional foods. Functional food is one of the most promising and fastest developing health foods in the food industry. Pre-biotics have been widely studied and commercially explored. The data on pre-biotic effects of carboxymethylated polysaccharides are also limited. Therefore, these polysaccharides have great application potential in the functional food and medical industries.

MATERIALS AND METHODS

Chemicals and Reagents

Fructooligosaccharide (FOS) was purchased from Guangdong Guanghua Chemical Factory Co., Ltd (Guangdong, China); trypsin, pancreatin solution, bile salt, and α-amylase were purchased from Qingdao Hi-tech Park Haibo Biological Technology Co., Ltd. (China). All other chemicals and reagents were obtained from Xilong Chemical Co., Ltd. (Guangdong, China). All chemicals and reagents used in this study were of analytical grade.

Sample Preparation

The analytical grade of xylan (XY) was obtained from the Guangxi Institute of Botany (Guilin, China). The XY sample was prepared according to the method described by Miao et al. (24). Citrus pectin (PC) was purchased from the Shanghai Yuanye Biotechnology Co., Ltd. (Shanghai, China), and the WPEP sample was prepared according to the method described by Guan et al. (22). *Lactobacillus brevis* GIM1.773, *L. plantarum* GIM1.19, *L. delbrueckii* subsp. *bulgaricus* GIM1.155, and *Streptococcus thermophilus* GIM1.540 were obtained from the Guangdong Institute of Microbiology (Guangzhou, China).

Preparation of Carboxymethylated Polysaccharides

The chloroacetic acid–sodium hydroxide reaction procedure was adapted from the method described by Wang et al. (25). An exact 240 mg of XY, CP, and WPEP was separately dissolved in 20 mL of 20% sodium hydroxide (NaOH) solution and 50 mL isopropanol and stirred for 3 h in an ice-water bath to obtain a uniform suspension. Next, 6.0 g chloroacetic acid was mixed with 50 mL of isopropanol until complete dissolution was achieved. Then, 20 mL of 20% NaOH solution was added to the mixture and heated for 3 h in a water bath of 60°C. The conical flask was cooled to room temperature, and the solution pH was adjusted to 7 by adding 1 M hydrochloric acid (HCl). Finally, the mixture was dialyzed for 24 h with tap water, concentrated, and freeze-dried to obtain carboxymethylated polysaccharides. The carboxymethylated XY, CP, and WPEP were named c-XY, c-CP, and c-WPEP, respectively.

Determination of Chemical Composition

The phenol-sulfuric acid method was used to determine the total sugar content of the polysaccharide samples (26). Briefly, 1 mL of 0.1 mg/mL sample was added with 0.5 mL of 6% phenol reagent and 2.5 mL of concentrated sulfuric acid. The reacting solution was placed into a HH-W420 water bath (Shanghai Fangrui Instrument Co., Ltd., Shanghai, China) at 100°C for 10 min and then cooled to room temperature. The changes in absorbances at 490 nm were determined, and the total sugar content was calculated based on the glucose standard curve (0–1.0 mg/mL).

The m-hydroxydiphenyl method was used to determine the galacturonic acid content of the polysaccharide samples (27). In brief, 400 μL sample solution (0.1 mg/mL) was added with sulfamic acid (0.39 mg/mL), homogenized, and then added with 2.5 mL of concentrated sulfuric acid. The mixture was placed in boiling water for 20 min. After cooling to room temperature, 40 μL of m-hydroxydiphenyl reagent was added to the solution mixture and kept at room temperature for 15 min. The absorbance was measured at 595 nm. The standard curve was plotted based on different concentrations of galacturonic acid (0–400 mg/mL).

Bradford method was used to determine the total protein content of the polysaccharide samples (28). Briefly, 1.0 mL of the sample solution (0.1 mg/mL) was added with 4 mL of Coomasie Blue reagent and then placed at room temperature for 5 min. Bovine serum albumin (0–1.0 mg/mL) was used as the protein standard. The absorbance was measured at 595 nm.

Fourier-Transform Infrared Spectroscopy

Exactly 1.0 mg of the freeze-dried sample was mixed with 100 mg potassium bromide, pulverized, and then pressed into disks. The Nicolet iS10 FTIR spectrometer (Thermo Scientific, Waltham, USA) was used to obtain the absorption spectra of compounds. The wavelengths used ranged from 4,000 to 400 cm^{-1}.

Scanning Electron Microscopy

The polysaccharide samples (1 mg/mL) were dissolved in deionized water and freeze-dried to produce sample specimens. A SU5000 field emission scanning electron microscope (SEM) (Hitachi, Tokyo, Japan) was performed to observe the morphology of the polysaccharide samples at 20°C with an acceleration voltage of 5 kV and magnification of 300×.

Determination of Degree of Substitution

The degree of substitution (DS) was determined by the neutralization titration (29). Briefly, 10 mg polysaccharide was diluted with 3 mL 70% methanol, then 10 mL distilled water and 5 mL 0.5 mol/L sodium hydroxide were added, and finally titrated with 0.1 M HCl until the color of phenolphthalein in the mixture faded. The carboxymethylation degree (A) of the polysaccharide samples was determined as follows:

$$\mathrm{A} = \frac{V_0 M_0 - (V_2 - V_1)M}{W} \quad (1)$$

where V_0 is the amount of NaOH (mL) added, V_1 is the volume of HCl used to titrate the sample (mL), V_2 is the amount of HCl (mL) used, M_0 is the increase in the concentration of sodium hydroxide (0.5 mol/L), M is the concentration of HCl used to titrate the sample (0.1 mol/L), and W is the mass of the sample (g). The degree of substitution (DS) was calculated as follows:

$$DS = \frac{0.162A}{1 - 0.058A} \quad (2)$$

Hydrolysis Degree of Polysaccharides

Simulated Saliva Digestion

The digestion reagent of the simulated saliva was prepared by adding 0.764 g sodium chloride, 1.491 g potassium chloride, and 0.133 g of calcium chloride into distilled water. The total volume was increased to 1,000 mL, and the solution was adjusted to pH 6.9 with 1 M sodium bicarbonate. An exact 0.345 g α-amylase was then dissolved with 400 mL of the digestion reagent, magnetically stirred for 20 min, and finally filtered. The filtered was added with another 400 mL of the digestion reagent before adding 1 mg/mL sample solution at a ratio (1:1) and then placed in the water bath of 37°C to imitate the oral environment. The digesting samples were collected at 0 h and 0.5 h and then boiled for 5 min to inactivate the enzyme. The 3,5-dinitrosalicylic acid method and phenol-sulfuric acid were used to determine the reducing sugar and total sugar content. The degree of hydrolysis was calculated based on the formula as follows:

$$\text{Hydrolysis degree (\%)} = \frac{\text{Hydrolyzed reducing sugar}}{\text{Total sugar} - \text{Non hydrolyzed reducing sugar}} \times 100 \quad (3)$$

Simulated Gastric Digestion

The experimental method was slightly modified from the method described previously (30–32). The buffer solution was prepared by adding 8.25 g disodium hydrogen phosphate monohydrate, 14.35 g monosodium phosphate, 8.0 g sodium chloride, 0.2 g potassium chloride, 0.1 g calcium chloride, and 0.18 g magnesium chloride hexahydrate with distilled water and diluted to 1,000 mL. The pH of the buffer solution was adjusted to 1, 2, or 3 with 1 M HCl solution. The sample weighing 100 mg was added to 10.0 mL of the buffer solution and placed in a water bath at 37°C for 6 h. An exact 1.0 mL of the sample solution was obtained at 4 and 6 h during the simulated gastric digestion to determine reducing sugar and total sugar content. The degree of hydrolysis was calculated using Equation (3).

Simulated Small Intestinal Digestion

The simulated small intestinal digestion was performed according to the method described previously (2, 31). The simulated small-intestinal juice was prepared by adding 5.40 g sodium chloride, 0.65 g potassium chloride, and 0.33 g calcium chloride into a conical flask, dissolved with distilled water, and diluted to 1,000 mL. Next, 13 mg trypsin, 100 mL of pancreatin solution (7%, w/w), 200 mL of bile salt (4%, w/w), and the juice solution were mixed before the pH was adjusted to 7 with 1 M sodium bicarbonate. Then, 1 mg/mL sample solution was mixed with the simulated small-intestinal juice at a ratio of 1:1. During the digestion, 1.0 mL of the digesting sample was separately collected at 4 and 6 h and then boiled for 5 min to inactivate the enzymes. The reducing sugar and total sugar content were determined. The degree of hydrolysis was calculated according to Equation (3).

Preparation of Culture Media

The basal medium for culturing *S. thermophilus* was prepared by mixing peptone (5.0 g), yeast extract powder (10.0 g), calcium carbonate (1.0 g), dipotassium phosphate (2.0 g), glucose (15.0 g/L), cysteine (0.50 g), and Tween-80 (1.0 mL) in a beaker, and the mixture was heated until dissolution. The medium was topped

up with distilled water to 1 L. The pH was adjusted to 6.5, and the solution was sterilized for 20 min at 121°C. The basal medium for the other strains was prepared by mixing tryptone (10 g/L), beef extract powder (10.0 g), yeast extract powder (5.0 g), ammonium citrate (2.0 g), dipotassium phosphate (2.0 g), manganese sulfate monohydrate (0.30 g), Tween-80 (1 ml/L), urea (15 g/L), and sodium acetate (5 g/L), and then heated until dissolution. The distilled water was then added to the mixture to obtain a total volume of 1 L. The pH was adjusted to 6.5, and the solution was sterilized. The experimental media were prepared by replacing glucose solution in the basal medium with XY, CP, WPEP, and the carboxymethylated polysaccharide samples.

Pre-biotic Effect of the Carboxymethylated Polysaccharides

The pre-biotic effect of the polysaccharide samples was determined based on the microbial growth assay. The polysaccharide samples were added to the culture media as the only carbon source. The four probiotic strains used were *L. brevis*, *L. plantarum*, *L. delbrueckii subsp. bulgaricus*, and *S. thermophilus*. Different concentrations of the polysaccharide samples were first used to screen for the microbial growth-promoting effect. In brief, a 100 μL of probiotic solution (2×10^8 CFU/mL) was pipetted to the culture medium and then cultured for 48 h at 37°C. The optical density (OD) values were determined by measuring the absorbance at a wavelength of 600 nm. The OD value denotes the optimal concentration of polysaccharides used for the growth of the probiotic strains. The microbials were then cultured at different incubation times (0, 4, 8, 12, 24, and 36 h) by applying the optimized polysaccharide concentration. The OD values of the cultures were measured, and the results were expressed as log CFU/mL. A linear regression equation was obtained for each probiotic strain. The optimal polysaccharide concentration of 3% (w/v) was chosen as the only carbon source, and FOS was used for comparison. The growth curves of the four probiotic strains cultured using the culture media containing different polysaccharide samples were plotted.

Statistical Analysis

All data were expressed as mean ± standard error of the mean (n = 3). The statistically significant differences were determined between the different groups based on the analysis of variance coupled with Duncan's multiple range test and student's *t*-test. The statistical analysis was performed using SPSS 26.0 software. $P < 0.05$ was considered a statistically significant difference.

RESULTS AND DISCUSSION

Chemical Composition Analysis

Three polysaccharides were used in carboxymethylation. They were XY, CP, and WPEP. The degrees of substitution for c-XY, c-CP, and c-WPEP were 0.68, 0.44, and 0.44, respectively (**Table 1**). XY had the highest degree of saturation in comparison with CP and WPEP. The results also showed that the carboxymethylated polysaccharide samples had a significantly lower total sugar content than the non-carboxymethylated samples ($P < 0.05$). Although the carboxymethylated polysaccharides had total protein content lesser than the non-carboxymethylated forms, no significant differences were found between the polysaccharide samples ($P > 0.05$). WPEP also had a significantly lower galacturonic acid content besides the total sugar and protein content. On the contrary, the c-XY and c-CP had a significantly higher galacturonic acid content than the non-carboxymethylated forms ($P < 0.05$).

The XY was a fine light-yellow powder, CP was a white powder, and WPEP was a golden particle (**Figure 1**). The colors and appearances of XY, CP, and WPEP were remarkably changed after carboxymethylation. These changes indicated that the internal structure of the polysaccharides could have been modified chemically. Carboxymethylation of polysaccharides extracted from *Cyclocarya paliurus* showed a lower protein content than the non-carboxymethylated samples (33). Besides, the solubility of the polysaccharides increased after carboxymethylation (34). Moreover, the bioactivity of the c-XY improved (35).

The IR spectra of the c-XY and XY are shown in **Figure 1A**. The result showed that the broad peak at 3,480 cm^{-1} could be attributed to the stretching vibrations of the OH group. The IR peak at 2,930 cm^{-1} could also be attributed to the stretching vibration of the CH group. The result revealed C–O–C stretching vibrations at 1,330 cm^{-1}. The peak spectra of c-XY close to 1,609 and 1,405 cm^{-1} also showed the characteristic absorption peaks of C=O and CO, respectively.

The IR spectra of the c-CP and CP are shown in **Figure 1B**. The broad peak at 3,420 cm^{-1} could be attributed to the stretching vibrations of the OH group. The IR peak at 2,926 cm^{-1} was due to the stretching vibration of the CH group in c-XY, and the peak at 1,330 cm^{-1} revealed C–O–C stretching vibrations of the carboxymethylated structure. The peak spectra of c-XY close to 1,616 and 1,419 cm^{-1} also showed the characteristic absorption peaks of C=O and CO, respectively.

The IR spectra of the c-WPEP and WPEP are shown in **Figure 1C**. The broad spectrum peak at 3,420 cm^{-1} could be attributed to the stretching vibrations of the OH group. Similar to c-XY and c-CP, the CH, C–O–C, C=O, and CO stretching vibrations were found for the c-WPEP. Also, the spectra of XY, CP, WPEP, c-XY, c-CP, and c-WPEP indicated typical characteristic absorption peaks of the polysaccharides at wavelengths of 1,100 and 3,500 cm^{-1}.

The carboxymethylated polysaccharides had a lower peak height (broad peak) than the non-carboxymethylated forms. There was a sharp band at 900 cm^{-1}, where it arose from the C1 group frequency or ring frequency. It was the characteristic of β-glucosidic linkages between the sugar units. The peak spectra of c-XY, c-CP, and c-WPEP close to 1,600 and 1,425 cm^{-1} also revealed the characteristic absorption peaks of C=O and CO, respectively. The findings indicated the successful carboxymethylation of the polysaccharide samples.

The carboxymethylation was performed using both aqueous and organic media. The use of organic medium has many advantages, including high reaction stability and degree of substitution. The substitution degree of XY was higher than CP and WPEP because the purity of XY was higher than these substances. CP and WPEP had the same substitution

TABLE 1 | Chemical compositions of polysaccharide samples.

Samples	Total sugar (%)	Total protein (%)	Galactoronic acid (%)	DS
WPEP	54.23 ± 1.62^{e}	2.98 ± 0.43^{a}	39.43 ± 2.33^{a}	
XY	94.43 ± 4.77^{a}	1.49 ± 0.22^{c}	4.32 ± 1.74^{f}	
CP	87.25 ± 3.76^{b}	1.33 ± 0.92^{c}	6.72 ± 2.25^{e}	
c-WPEP	39.46 ± 1.25^{f}	2.48 ± 0.57^{b}	33.23 ± 1.92^{b}	0.44 ± 0.06^{b}
c-XY	79.12 ± 3.62^{d}	1.42 ± 0.14^{c}	9.43 ± 1.43^{c}	0.68 ± 0.02^{a}
c-CP	79.63 ± 1.89^{c}	1.12 ± 0.91^{d}	7.66 ± 1.47^{d}	0.44 ± 0.04^{b}

Data are presented as mean ± standard error of the mean of three replicates. Different lowercase superscript letters in the same column denote significant differences ($P < 0.05$).

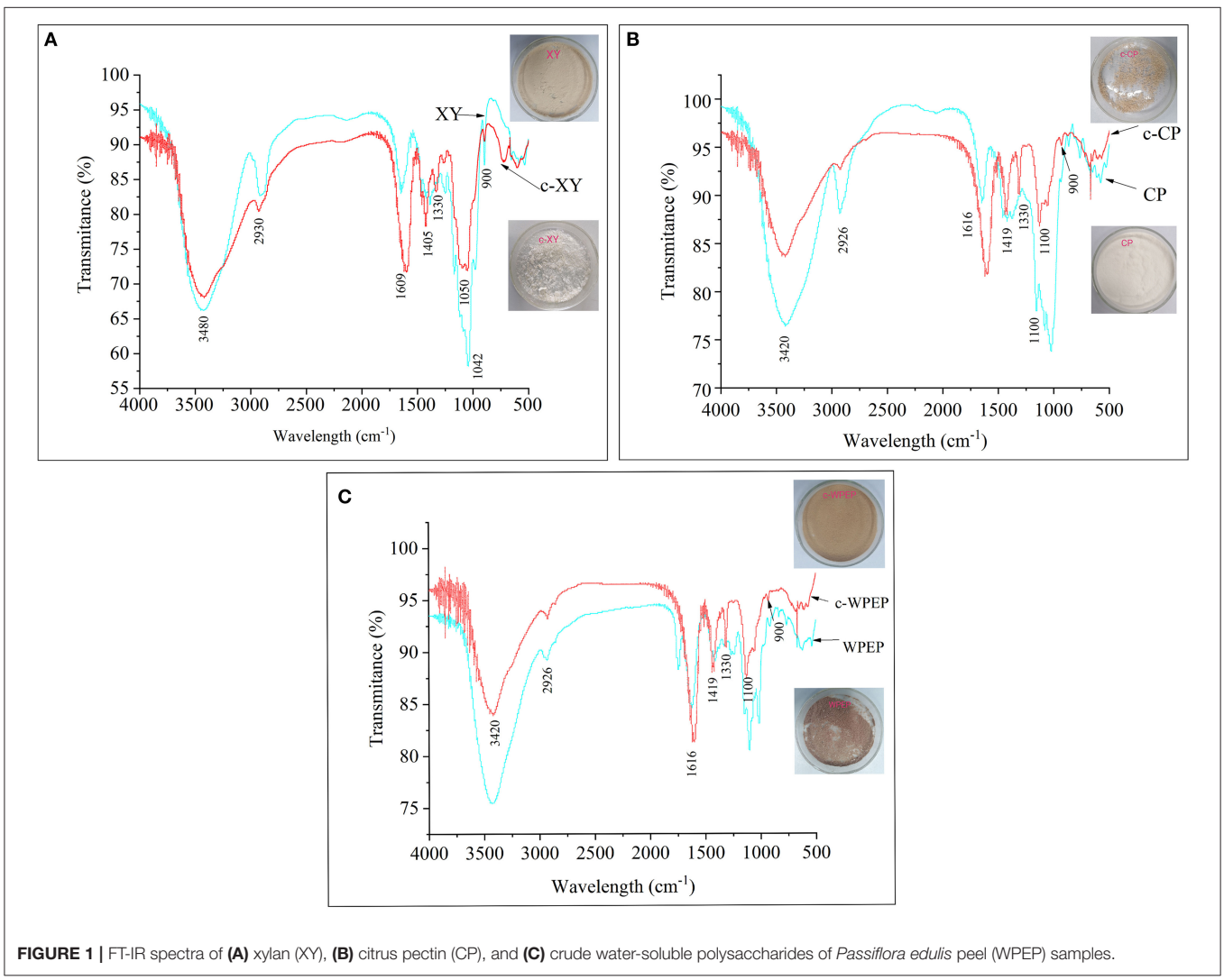

FIGURE 1 | FT-IR spectra of **(A)** xylan (XY), **(B)** citrus pectin (CP), and **(C)** crude water-soluble polysaccharides of *Passiflora edulis* peel (WPEP) samples.

degree because the main polysaccharide in WPEP was pectin. Literature shows that the purple passion fruit peel has as high as 12.6% of pectin. The major monosaccharides of pectin were rhamnose, arabinose, and galactose (36). These monosaccharides had been confirmed as the major components of the water-soluble polysaccharides of passion fruit peel (37).

The biological activity of polysaccharides is greatly affected by the functional groups that exist in the molecular structures. The presence of functional groups in a polysaccharide determines the size and bioactivity of the polysaccharide. Also, the chemical modification of a polysaccharide introduces new functional groups to its molecular structure. The spatial structure influences

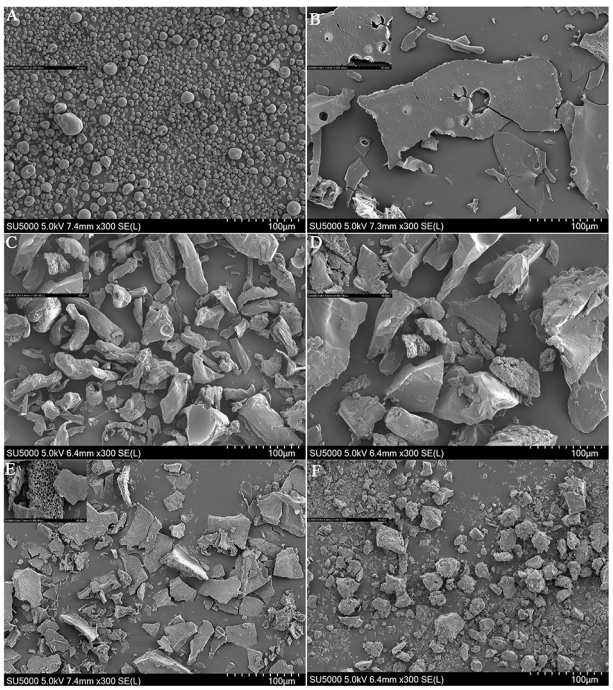

FIGURE 2 | SEM micrographs of **(A)** xylan (XY), **(B)** carboxymethylated xylan (c-XY), **(C)** citrus pectin (CP), **(D)** carboxymethylated citrus pectin (c-CP), **(E)** crude water soluble polysaccharides of Passiflora edulis peel (WPEP) samples, **(F)** carboxymethylated crude water soluble polysaccharides oPfassiflora edulis peel (c-WPEP) samples; magnification factor: 300×.

bioactivity of the polysaccharide. The polysaccharide structure with flexural waves has higher bioactivity than the others, whereas the polysaccharide with wrinkle-shaped or stretchable ribbons has low bioactivity (38).

The sweetness of a polysaccharide is derived from the monosaccharide molecules. The high number of hydroxyl groups (–OH) of a polysaccharide denotes a high polysaccharide solubility in water and bioactivity (39). The sweetness of a polysaccharide is also attributed to the OH group. The carboxymethylation increased the intensity of stretching vibrations of the OH group. Therefore, the carboxymethylated polysaccharide could be sweeter than the non-carboxymethylated form.

Scanning Electron Microscopy Analysis

The surface structures of the polysaccharides were observed by SEM (**Figure 2**). The result showed that the surface structure of WPEP was multiporous, mildly rough, and unbounded. The surface structure of CP was less flaky, mild fibrous look, and some were rod-like structure; the XY had a granular shape. The changes in the surface structures of the polysaccharide samples were observed after the carboxymethylation, especially the surface of XY became flaky. The WPEP became lumpy after the carboxymethylation. The size of the flaky structure of c-WPEP was also reduced. The rod-like shape was not seen in the c-CP. The findings confirm that the structural surface of these polysaccharides had been modified by carboxymethylation.

The surface structural differences between the polysaccharide samples were due to the variation in molecular structures and bondings (40). The WPEP could contain other glycans besides pectin. The CP used in this study had 65% purity. The pectin in the purified extract might be bound together with glycans like xylan, xyloglucan, and glucuronoxylan (41). However, carboxymethylation increased the roughness and irregularity of the surface structure of xylan, with hollows and embossment (42). Also, CP prepared from manosonication assisted extraction formed an amorphous, rough, and hard surface with surface cracking and particles stuck to the surface.

Hydrolysis Degree of Polysaccharides

The study of resistance of the polysaccharide digestion was performed based on assays mimicking the human digestive tract. The digestion resistance was explored using simulated saliva, gastric juice, and small intestinal juice methods. The digestion resistance rate was determined based on the hydrolysis degree. The minimal differences among the polysaccharides and FOS in terms of the degree of hydrolysis are shown in **Table 2**. The results showed that most polysaccharide samples had a moderate degree of resistance to digestion. The hydrolysis degrees of c-WPEP assessed by the simulated saliva, gastric juice, and small intestinal juice methods were lower than the WPEP ($P < 0.05$). It showed that the carboxymethylation of WPEP increased digestion resistance in the human digestive tract. The hydrolysis degrees of c-XY and c-CP were not significantly improved ($P > 0.05$). The hydrolysis degrees of XY and CP after 4 h of hydrolysis using the simulated small intestinal juice test were significantly higher than the carboxymethylated samples ($P < 0.05$).

The minimal changes in hydrolysis degrees of the polysaccharide samples following digestion by saliva and gastric juice between 4 and 6 h indicated that the polysaccharide samples have a good resistance against digestion. Literature shows that pH values of gastric juice in a healthy individual ranged from 1.3 to 2.5. The pH values increase to 4.5–5.8 after eating. The ingested polysaccharides remain in the stomach for 4–6 h, and the undigested substances enter the large intestine. The undigested polysaccharides are pre-biotics in the large intestine (37). The FTIR analysis showed that the molecular structures of the polysaccharide samples had a β-D glycosidic bond. The hydrolytic actions of human digestive enzymes on carbohydrates are mainly involved in the cleavage of α-glycosidic bonds (43). Therefore, the polysaccharide samples were digestion resistant. In the simulated human digestive system, the degrees of hydrolysis of all polysaccharides were lower than 10%. The polysaccharides also have relatively stable main structures. They are hydrolysis resistant, and they are potent pre-biotics (44).

Bile salts are the functional components of bile. They are biological surfactants involved in the digestion and absorption of lipids in the small intestine. The concentrations of bile salts in the small intestine also ranged between 4 and 20 mM. The values may fall to as low as 2.6 mM in the fasted state or rise to over 15 mM in the fed state (45, 46). The effects of different bile salts on the absorption of fluid, electrolytes, and monosaccharides

TABLE 2 | Hydrolysis degrees (%) of polysaccharides in simulated salivary, gastric, and intestinal conditions.

Samples	Simulated saliva	Simulated gastric						Simulated intestinal	
	0.5 h	4 h			6 h			4 h	6 h
		pH 1	pH 2	pH 3	pH 1	pH 2	pH 3		
XY	8.49 ± 0.025^{c}	2.00 ± 0.014^{e}	1.23 ± 0.022^{e}	0.66 ± 0.003^{g}	4.07 ± 0.004^{d}	2.98 ± 0.002^{d}	3.53 ± 0.002^{a}	3.15 ± 0.004^{c}	3.5 ± 0.026^{d}
CP	3.36 ± 0.020^{f}	2.13 ± 0.030^{c}	1.74 ± 0.041^{c}	2.15 ± 0.069^{c}	5.53 ± 0.042^{b}	3.51 ± 0.041^{c}	2.92 ± 0.028^{c}	3.36 ± 0.02^{b}	3.77 ± 0.008^{c}
WPEP	10.30 ± 0.023^{a}	2.86 ± 0.023^{b}	3.89 ± 0.045^{a}	3.93 ± 0.045^{a}	2.34 ± 0.025^{f}	3.67 ± 0.025^{b}	1.87 ± 0.010^{e}	4.30 ± 0.025^{a}	4.70 ± 0.020^{b}
c-XY	8.86 ± 0.020^{b}	1.49 ± 0.005^{f}	1.22 ± 0.002^{e}	1.04 ± 0.033^{e}	4.16 ± 0.003^{c}	2.38 ± 0.001^{f}	3.27 ± 0.002^{b}	0.88 ± 0.006^{g}	5.28 ± 0.038^{a}
c-CP	2.61 ± 0.017^{g}	2.04 ± 0.004^{d}	1.73 ± 0.031^{c}	2.58 ± 0.02^{b}	5.62 ± 0.006^{a}	4.11 ± 0.032^{a}	2.76 ± 0.006^{d}	1.09 ± 0.009^{f}	1.78 ± 0.013^{g}
c-WPEP	7.70 ± 0.024^{d}	0.54 ± 0.025^{g}	1.31 ± 0.023^{d}	1.15 ± 0.015^{d}	1.14 ± 0.025^{g}	1.30 ± 0.025^{g}	1.22 ± 0.0025^{f}	1.50 ± 0.004^{d}	2.40 ± 0.010^{f}
FOS	5.20 ± 0.015^{e}	2.98 ± 0.056^{a}	2.64 ± 0.073^{b}	0.82 ± 0.005^{f}	3.10 ± 0.008^{e}	2.50 ± 0.002^{e}	0.70 ± 0.001^{g}	1.30 ± 0.002^{e}	2.82 ± 0.012^{e}

Data are presented as mean ± standard error of the mean of three replicates. Different lowercase superscript letters in the same column denote significant differences ($P < 0.05$).

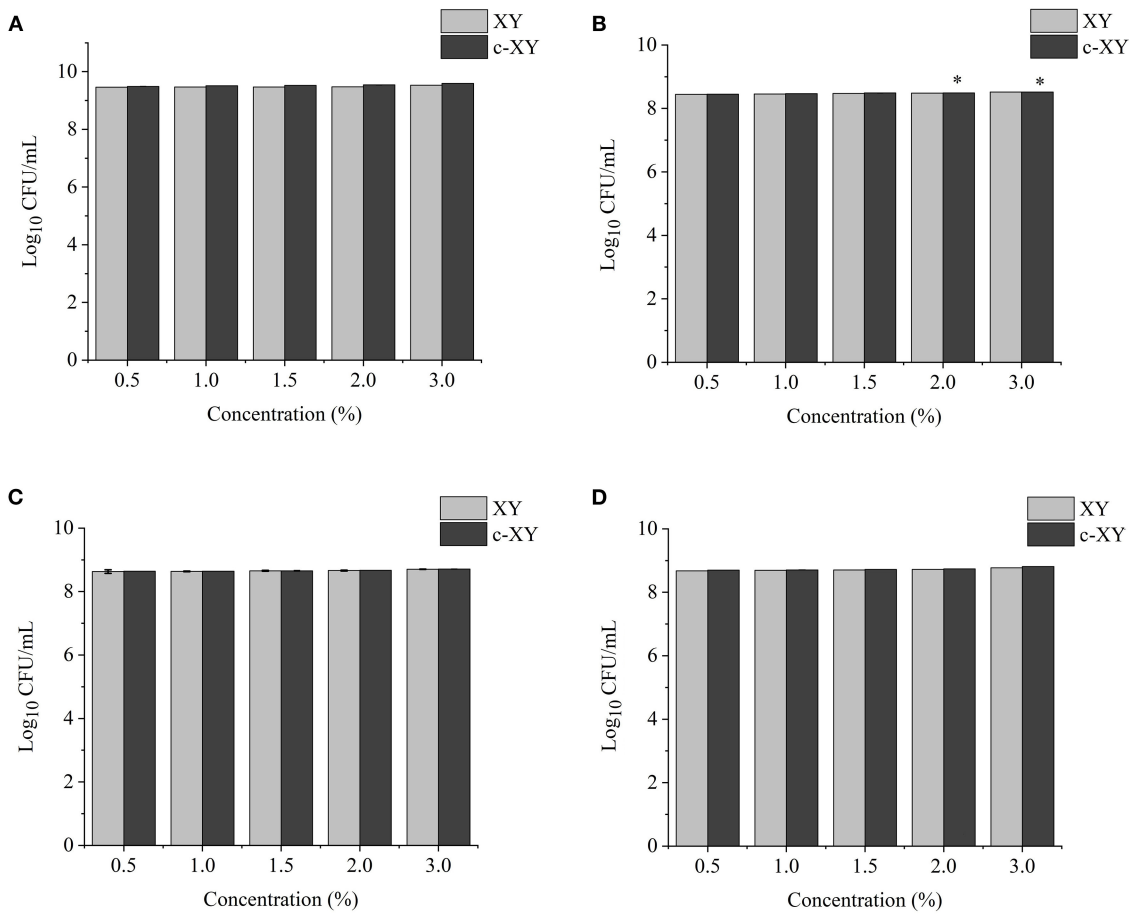

FIGURE 3 | Effects of different concentrations of carboxymethylated xylan (c-XY) sample on the growth of probiotics **(A)** *L. brevis*, **(B)** *L. plantarum*, **(C)** *L. delbrueckii* subsp. *bulgaricus*, and **(D)** *S. thermophilus*. *$P < 0.05$.

have been investigated in the small intestine of the experimental rats (47). The deoxycholate (1 mM) impaired absorption of water and potassium in the jejunum, but not of sodium or glucose. At higher concentrations (2.5 and 5 mM), the secretion of fluid and electrolytes occurred, and glucose and fructose absorption was impaired (48).

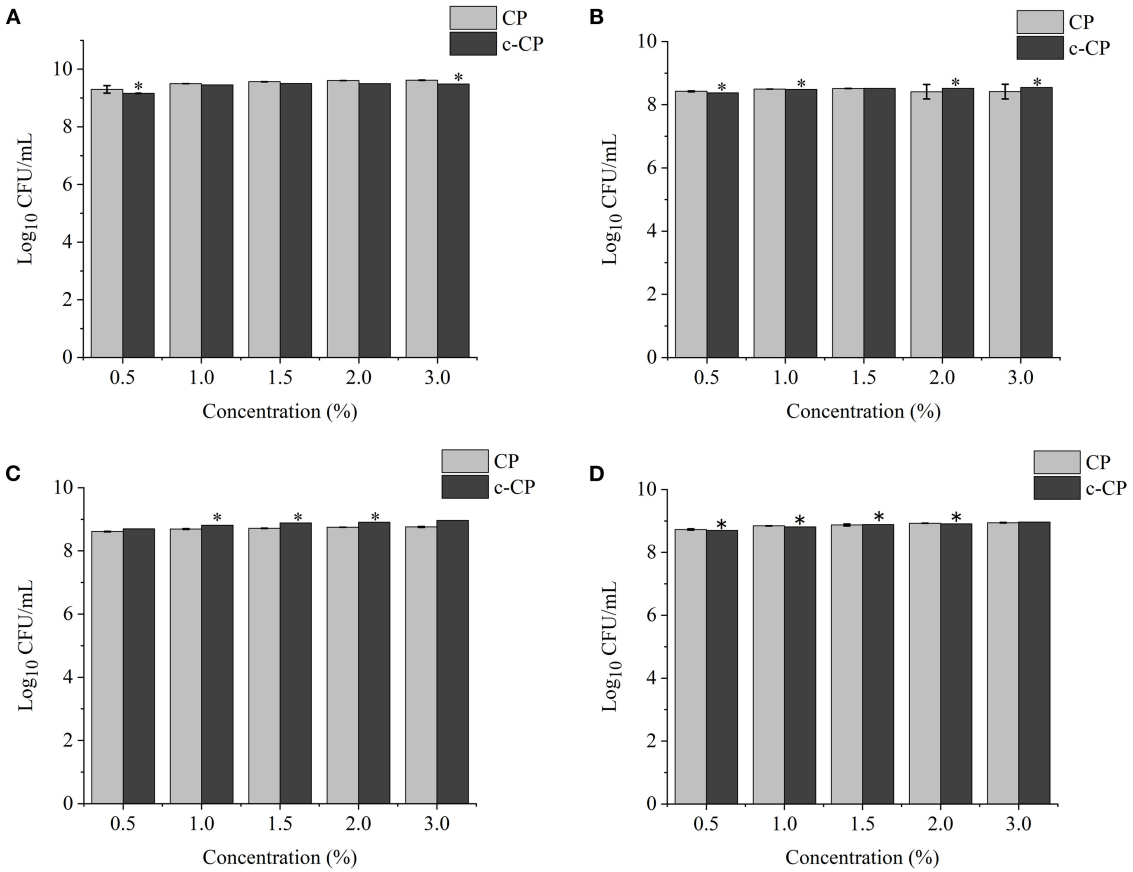

FIGURE 4 | Effects of different concentrations of carboxymethylated citrus pectin (c-CP) sample on the growth of **(A)** *L. brevis*, **(B)** *L. plantarum*, **(C)** *L. delbrueckii* subsp. *bulgaricus*, and **(D)** *S. thermophilus*. *$P < 0.05$.

Effects of Different Concentrations of Polysaccharides on Probiotic Growth

The effects of different concentrations of XY, CP, WPEP, c-XY, c-CP, and c-WPEP on the growth of the probiotic strains were determined (**Figures 3**–**5**). The OD values reflected the microbial counts in the fermentation broth. The changes in the values represented the growth rate of the intestinal microflora. The growth of the probiotic strains could be more accurately expressed as CFU/mL (49). The regression equations of the standard curves for *L. brevis*, *L. plantarum*, *L. delbrueckii* subsp. *bulgaricus*, and *S. thermophilus* were $y = 4^{-10}x + 0.007$ ($R^2 = 0.9995$), $y = 8^{-9}x - 1.1215$ ($R^2 = 0.9948$), $y = 4^{-9}x - 0.5944$ ($R^2 = 0.9926$), and $y = 2^{-9}x - 0.26$ ($R^2 = 0.9958$), respectively. The results showed that c-XY and c-CP promoted the growth of the probiotic strains (**Figures 3**, **4**), especially *L. plantarum* and *L. delbrueckii* subsp. *bulgaricus*. Hence, the c-WPEP inhibited the microbial growth (**Figure 5**).

The finding of this study revealed that c-XY was the most effective pre-biotic in promoting the growth of *L. brevis*. It is because c-CP and c-WPEP significantly inhibited the growth of *L. brevis* and *S. thermophilus*. In this study, the polysaccharide samples promoted the growth of the *Lactobacillus* strains except for c-WPEP. The 3% c-XY had the best effect in promoting the proliferation of the probiotic strains. As shown in **Figures 3**, **4**, c-XY and c-CP at concentrations of up to 3% effectively increased the growth of *L. plantarum* ($P < 0.05$). On the contrary, some polysaccharides were not positively correlated with the growth of the probiotic strains.

Literature demonstrated that the effect of polysaccharides isolated from the dried root of *Atractylodis macrocephalae* (42) and Fu Brick tea (37) on the growth of probiotics was not concentration-dependent. When a higher concentration of the polysaccharides was used, the growth-promoting effect weakened. It could be due to the high sugar concentration causing an increase in the osmotic pressure and accumulation of metabolites, thus limiting the proliferation of bifidobacteria.

Effect of Optimal Concentrations of Polysaccharides on Growth Curve of Probiotics

The growth curves of the probiotic strains supplemented with the optimal concentrations of polysaccharide samples are presented in **Figure 6**. The addition of polysaccharide samples to the

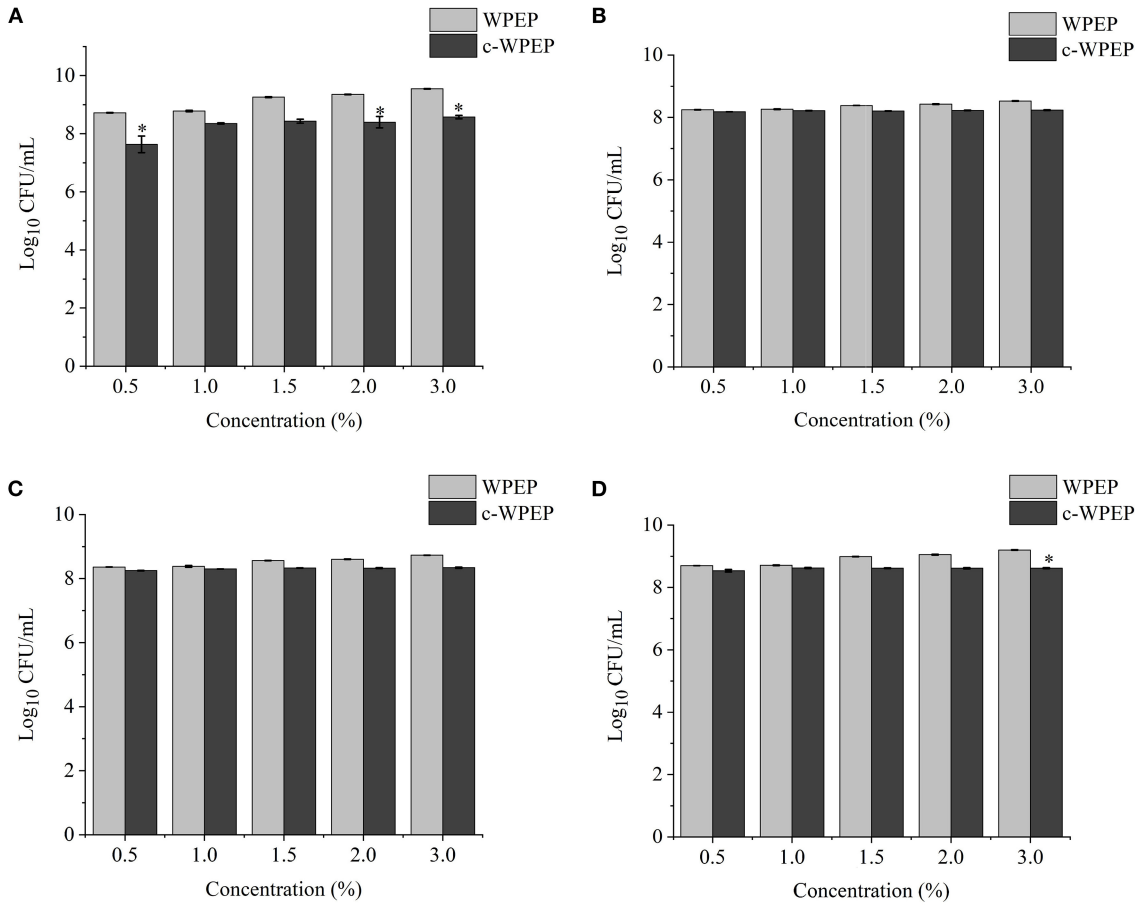

FIGURE 5 | Effects of different concentrations of the carboxymethylated crude water-soluble polysaccharides of *Passiflora edulis* peel (c-WPEP) sample on the growth of **(A)** *L. brevis*, **(B)** *L. plantarum*, **(C)** *L. delbrueckii* subsp. *bulgaricus*, and **(D)** *S. thermophilus*. *$P < 0.05$.

basal medium as sole carbon sources promoted microbial growth. The growth rate remained consistent for about 10 h, and the growth rate increased rapidly and reached a maximum growth rate at 24 h. After 24 h, the growth rate started to drop gradually until the end of the experiment at 48 h. The treatment with FOS showed the highest growth rates for all four probiotic strains.

The carboxymethylated polysaccharides significantly improved the growth performance of the probiotics compared with the non-carboxymethylated samples, especially for *L. brevis*. As shown in **Figure 4**, c-XY and c-CP had better growth-promoting effects than c-WPEP. Besides, the probiotics exposed to the carboxymethylated polysaccharides had a slightly stable growth phase after 24 h of incubation. Among the polysaccharides tested, c-XY was the most effective pre-biotic.

FOS is low molecular weight and low polymerization degree substance, and it has a better pre-biotic effect than the other polysaccharides. When FOS is added to the fermentation broth as the only energy source, it promotes the growth of the intestinal microflora. Literature also showed that FOS was the best carbon source for the proliferation of probiotics (12). Moreover, the ketone-rich FOS relieved allergic dermatitis by regulating the intestinal microflora, and it played an essential role in regulating the growth of these microorganisms (50).

The c-XY and FOS showed a similar growth performance of the four probiotics. This finding demonstrated that c-XY is a more effective pre-biotic for promoting growth of the intestinal microflora than c-CP and c-WPEP. It could be because the carboxymethylation of XY changed in its surface structure and structural bonds. Previous studies showed that the characteristics of fructose-oligosaccharides, including structural units and degree of polymerization, had a fundamental influence on its probiotic activity; c-XY and FOS might also have similar chemical information.

The growth curves of the probiotics could be divided into different phases, such as the stagnation phase, logarithmic growth phase, stationary phase, and decline phase (51). *S. thermophilus* and *L. brevis* cultivated with most polysaccharide samples had a 4 h stagnation phase, whereas *L. plantarum*

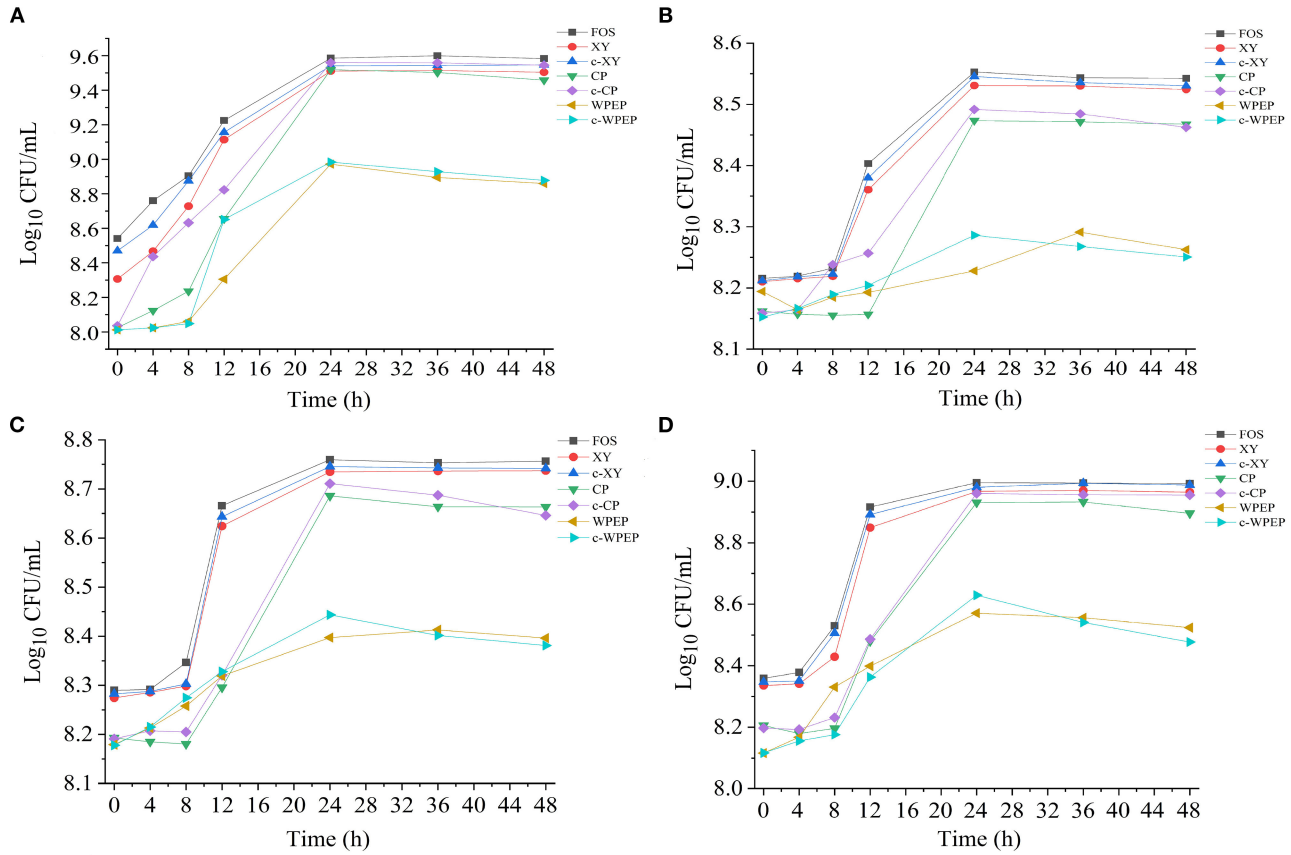

FIGURE 6 | Effects of polysaccharide samples on the growth of **(A)** *L. brevis*, **(B)** *L. plantarum*, **(C)** *L. delbrueckii* subsp. *bulgaricus*, and **(D)** *S. thermophilus*.

and *L. delbrueckii* subsp. *bulgaricus* showed a long hour of stagnation phase before entering the logarithmic growth phase. The declining growth curves were also observed if the probiotics were kept at a prolonged period, especially after 36 h.

Studies have shown that the intestinal microflora mainly obtained nutrients from carbohydrate sources by digesting the complex polysaccharides (52). The c-WPEP showed a moderate effect in promoting the growth of the probiotics, but the result was less significant than the c-XY and c-CP. Among the three carboxymethylated polysaccharides, c-WPEP had the lowest sugar content. It indicated that c-WPEP did not provide enough energy for the growth of probiotics. Therefore, appropriate sources of pre-biotics are needed for the optimal growth of intestinal microflora (53). Also, the solubility of the c-XY and c-CP increased after carboxymethylation. The intestinal microflora could have fully utilized these carboxymethylated polysaccharides for their growth. As carboxymethylated polysaccharides have shorter chains than the non-carboxymethylated forms, the polysaccharides are easier to decompose and use by the intestinal microflora (54). Therefore, the carboxymethylated polysaccharides had a better pre-biotic effect.

CONCLUSION

The carboxymethylation of XY, CP, and WPEP was successfully performed using a combination of chloroacetic acid and NaOH reactions. The successful carboxymethylation of these polysaccharides was shown by the FTIR spectra. The carboxymethylated polysaccharides had total protein content lesser than the non-carboxymethylated forms, and no significant differences were found between the polysaccharide samples. The three carboxymethylated polysaccharides resisted hydrolysis based on the assays mimicking the human digestive tract, where c-WPEP had the best resistance to digestion. The hydrolysis degrees of c-WPEP accessed by the simulated saliva, gastric juice, and small intestinal juice methods were lower than the WPEP. It showed that the carboxymethylation of WPEP increased digestion resistance in the human digestive tract. The uses of c-XY, c-CP, and c-WPEP as sole carbon sources demonstrated a variation in the effects on the growth of *L. brevis*, *L. plantarum*, *L. delbrueckii* subsp. *bulgaricus*, and *S. thermophilus*. These probiotic strains had different abilities to decompose and utilize the polysaccharides. The carboxymethylated polysaccharide samples also demonstrated better pre-biotic effects than the non-carboxymethylated samples, and c-XY had a better pre-biotic-promoting effect than c-CP and c-WPEP. The findings

collectively suggested that c-XY, c-CP, and c-WPEP are potent pre-biotics that should be developed into dietary supplements for regulating *Lactobacillus* and *Streptococcus* in the human gut.

DATA AVAILABILITY STATEMENT

The original contributions presented in the study are included in the article/**Supplementary Material**, further inquiries can be directed to the corresponding author.

AUTHOR CONTRIBUTIONS

YS: conceptualization, investigation, methodology, software, and writing—original draft. HEK: supervision, formal analysis, writing—review, and editing. YG: methodology, project administration, and funding acquisition. XL: supervision, project administration, funding acquisition, writing—review, and editing. All authors contributed to the article and approved the submitted version.

FUNDING

This study was supported by the National Natural Science Foundation of China (31860251), the Guangxi Science & Technology Program (AD20297088), and the Guangxi Key Laboratory of Electrochemical and Magnetochemical Functional Materials (EMFM20211104 and EMFM20211102).

ACKNOWLEDGMENTS

All authors would like to thank Guozhu Zhang and Miao Zhang for helping in part of this research work.

SUPPLEMENTARY MATERIAL

The Supplementary Material for this article can be found online at: https://www.frontiersin.org/articles/10.3389/fnut.2021.778563/full#supplementary-material

REFERENCES

1. Gibson GR, Hutkins R, Sanders ME, Prescott SL, Reimer RA, Salminen SJ, et al. The International Scientific Association for Probiotics and Prebiotics (ISAPP) consensus statement on the definition and scope of prebiotics. *Nat Rev Gastroenterol Hepatol*. (2017) 14:491–502. doi: 10.1038/nrgastro.2017.75
2. Li F, Sun X, Yu W, Shi C, Zhang X, Yu H, et al. Enhanced konjac glucomannan hydrolysis by lytic polysaccharide monooxygenases and generating prebiotic oligosaccharides. *Carbohydr Polym*. (2021) 253:117241. doi: 10.1016/j.carbpol.2020.117241
3. Gurpilhares DD, Cinelli LP, Simas NK, Pessoa A, Sette LD. Marine prebiotics: polysaccharides and oligosaccharides obtained by using microbial enzymes. *Food Chem*. (2019) 280:175–86. doi: 10.1016/j.foodchem.2018.12.023
4. Hill C, Guarner F, Reid G, Gibson GR, Merenstein DJ, Pot B, et al. The International Scientific Association for Probiotics and Prebiotics consensus statement on the scope and appropriate use of the term probiotic. *Nat Rev Gastroenterol Hepatol*. (2014) 11:506–14. doi: 10.1038/nrgastro.2014.66
5. Moludi J, Maleki V, Jafari-Vayghyan H, Vaghef-Mehrabany E, Alizadeh M. Metabolic endotoxemia and cardiovascular disease: a systematic review about potential roles of prebiotics and probiotics. *Clin Exp Pharmacol Physiol*. (2020) 47:927–39. doi: 10.1111/1440-1681.13250
6. Huang C, Zhu Z, Cao X, Chen X, Fu Y, Chen Z, et al. A pectic polysaccharide from Sijunzi decoction promotes the antioxidant defenses of SW480 cells. *Molecules*. (2017) 22:1341. doi: 10.3390/molecules22081341
7. Kong X, Duan W, Li D, Tang X, Duan Z. Effects of polysaccharides from *Auricularia auricula* on the immuno-timulatory activity and gut microbiota in immunosuppressed mice induced by cyclophosphamide. *Front Immunol*. (2020) 11:595700. doi: 10.3389/fimmu.2020.595700
8. Tong C, Chen Z, Liu F, Qiao Y, Chen T, Wang X. Antiviral activities of *Radix isatidis* polysaccharide against pseudorabies virus in swine testicle cells. *BMC Complement Med Ther*. (2020) 20:48. doi: 10.1186/s12906-020-2838-4
9. Kim M, Qie YQ, Park J, Kim CH. Gut microbial metabolites fuel host antibody responses. *Cell Host Microbe*. (2016) 20:202–14. doi: 10.1016/j.chom.2016.07.001
10. Xu J, Wang R, Zhang H, Wu J, Zhu L, Zhan X. *In vitro* assessment of prebiotic properties of oligosaccharides derived from four microbial polysaccharides. *LWT-Food Sci Technol*. (2021) 147:111544. doi: 10.1016/j.lwt.2021.111544
11. Zhang S, Hu H, Wang L, Liu F, Pan S. Preparation and prebiotic potential of pectin oligosaccharides obtained from citrus peel pectin. *Food Chem*. (2018) 244:232–7. doi: 10.1016/j.foodchem.2017.10.071
12. He S, Wang X, Zhang Y, Wang J, Sun H, Wang J, et al. Isolation and prebiotic activity of water-soluble polysaccharides fractions from the bamboo shoots (*Phyllostachys praecox*). *Carbohydr Polym*. (2016) 151:295–304. doi: 10.1016/j.carbpol.2016.05.072
13. Khan I, Huang G, Li X, Leong W, Xia W, Hsiao WLW. Mushroom polysaccharides from *Ganoderma lucidum* and *Poria cocos* reveal prebiotic functions. *J Funct Foods*. (2018) 41:191–201. doi: 10.1016/j.jff.2017.12.046
14. Zaporozhets TS, Besednova NN, Kuznetsova TA, Zvyagintseva TN, Makarenkova ID, Kryzhanovsky SP, et al. The prebiotic potential of polysaccharides and extracts of seaweeds. *Russ J Mar Biol*. (2014) 40:1–9. doi: 10.1134/S1063074014010106
15. Huang G, Chen X, Huang H. Chemical modifications and biological activities of polysaccharides. *Curr Drug Targets*. (2016) 17:1799–803. doi: 10.2174/1389450117666160502151004
16. Chen F, Huang G. Preparation and immunological activity of polysaccharides and their derivatives. *Int J Biol Macromol*. (2018) 112:211–6. doi: 10.1016/j.ijbiomac.2018.01.169
17. Li XL, Tu XF, Thakur K, Zhang YS, Zhu DY, Zhang JG, et al. Effects of different chemical modifications on the antioxidant activities of polysaccharides sequentially extracted from peony seed dreg. *Int J Biol Macromol*. (2018) 112:675–85. doi: 10.1016/j.ijbiomac.2018.01.216
18. Liu Y, You Y, Li Y, Zhang L, Yin L, Shen Y, et al. The characterization, selenylation and antidiabetic activity of mycelial polysaccharides from *Catathelasma ventricosum*. *Carbohydr Polym*. (2017) 174:72–81. doi: 10.1016/j.carbpol.2017.06.050
19. Ming K, Chen Y, Shi J, Yang J, Yao F, Du H, et al. Effects of *Chrysanthemum indicum* polysaccharide and its phosphate on anti-duck hepatitis a virus and alleviating hepatic injury. *Int J Biol Macromol*. (2017) 102:813–21. doi: 10.1016/j.ijbiomac.2017.04.093
20. Wang L, Qin X, Miao X, Chen H, Zhou Y, Cai A. Synthesis and nondestructive detailed structure characterization of carboxymethyl xylan from bagasse. *J Carbohydr Chem*. (2020) 39:131–44. doi: 10.1080/07328303.2020.1748643
21. Muthukumaran C, Kanmani BR, Sharmila G, Kumar NM, Shanmugaprakash M. Carboxymethylation of pectin: optimization, characterization and *in-vitro* drug release studies. *Carbohydr Polym*. (2018) 194:311–8. doi: 10.1016/j.carbpol.2018.04.042
22. Guan Y, Sun H, Chen H, Li P, Shan Y, Li X. Physicochemical characterization and the hypoglycemia effects of polysaccharide isolated from *Passiflora edulis* Sims peel. *Food Funct*. (2021) 12:4221–30. doi: 10.1039/D0FO02965C
23. Saratale GD, Bhosale R, Shobana S, Banu JR, Pugazhendhi A, Mahmoud E, et al. A review on valorization of spent coffee grounds (SCG)

towards biopolymers and biocatalysts production. *Bioresour Technol*. (2020) 314:123800. doi: 10.1016/j.biortech.2020.123800
24. Miao L, Zhou YH, Zhang HD, Hao ZB. Comparison of analytical methods for the quantitation of xylan in sugarcane bagasse. *Food Sci*. (2016) 37:162–7. doi: 10.7506/spkx1002-6630-201616026
25. Wang X, Zhang Z, Zhao M. Carboxymethylation of polysaccharides from *Tremella fuciformis* for antioxidant and moisture-preserving activities. *Int J Biol Macromol*. (2015) 72:526–30. doi: 10.1016/j.ijbiomac.2014.08.045
26. Dubois M, Gilles KA, Hamilton JK, Colorimetric method for determination of sugars and related substances. *Anal Chem*. (1956) 28:350–6. doi: 10.1021/ac60111a017
27. Kintner PK, Van Buren JP. Carbohydrate interference and its correction in pectin analysis using the m-hydroxydiphenyl method. *Food Sci*. (1982) 47:756–9. doi: 10.1111/j.1365-2621.1982.tb12708.x
28. MM B. A rapid and sensitive method for the quantitation of microgram quantities of protein utilizing the principle of protein-dye binding. *Anal Biochem*. (1976) 72:248–54. doi: 10.1016/0003-2697(76)90527-3
29. Li J, Shang WT, Si X, Bu DD, Strappe P, Zhou ZK, et al. Carboxymethylation of corn bran polysaccharide and its bioactive property. *Int J Food Sci Technol*. (2017) 52:1176–84. doi: 10.1111/ijfs.13382
30. Hur SJ, Lim BO, Decker EA, McClements DJ. *In vitro* human digestion models for food applications. *Food Chem*. (2011) 125:1–12. doi: 10.1016/j.foodchem.2010.08.036
31. Minekus M, Alminger M, Alvito P, Ballance S, Bohn T, Bourlieu C, et al. A standardised static *in vitro* digestion method suitable for food - an international consensus. *Food Funct*. (2014) 5:1113–24. doi: 10.1039/C3FO60702J
32. Zhao L, Qin Y, Guan R, Zheng W, Liu J, Zhao J. Digestibility of fucosylated glycosaminoglycan from sea cucumber and its effects on digestive enzymes under simulated salivary and gastrointestinal conditions. *Carbohydr Polym*. (2018) 186:217–25. doi: 10.1016/j.carbpol.2018.01.029
33. Wang Z-J, Xie J-H, Shen M-Y, Tang W, Wang H, Nie S-P, et al. Carboxymethylation of polysaccharide from *Cyclocarya paliurus* and their characterization and antioxidant properties evaluation. *Carbohydr Polym*. (2016) 136:988–94. doi: 10.1016/j.carbpol.2015.10.017
34. Geng WH, Venditti RA, Pawlak JJ, Chang HM, Pal L, Ford E. Carboxymethylation of hemicellulose isolated from poplar (*Populus grandidentata*) and its potential in water-soluble oxygen barrier films. *Cellulose*. (2020) 27:3359–77. doi: 10.1007/s10570-020-02993-2
35. Chen T, Liu H, Liu J, Li J, An Y, Zhu M, et al. Carboxymethylation of polysaccharide isolated from Alkaline Peroxide Mechanical Pulping (APMP) waste liquor and its bioactivity. *Int J Biol Macromol*. (2021) 181:211–20. doi: 10.1016/j.ijbiomac.2021.03.125
36. Cheng XQ, Li K, Chen XM, Jiang XN, Gai Y. Comparison of pectin structural monosaccharides in cell wall of dicotyledon and monocotyledon. *J Beijing For Univ*. (2012) 34:44–9. doi: 10.1007/s11783-011-0280-z
37. Kong F, Singh RP. Disintegration of solid foods in human stomach. *J Food Sci*. (2008) 73:R67–80. doi: 10.1111/j.1750-3841.2008.00766.x
38. Ohno N, Miura NN, Chiba N, Adachi Y, Yadomae T. Comparison of the immunopharmacological activities of triple and single-helical schizophyllan in mice. *Biol Pharm Bull*. (1995) 18:1242–7. doi: 10.1248/bpb.18.1242
39. Huang S, Chen F, Cheng H, Huang G. Modification and application of polysaccharide from traditional Chinese medicine such as *Dendrobium officinale*. *Int J Biol Macromol*. (2020) 157:385–93. doi: 10.1016/j.ijbiomac.2020.04.141
40. Qi X, Su T, Zhang M, Tong X, Pan W, Zeng Q, et al. Sustainable, flexible and biocompatible hydrogels derived from microbial polysaccharides with tailorable structures for tissue engineering. *Carbohydr Polym*. (2020) 237:116160. doi: 10.1016/j.carbpol.2020.116160
41. Shakhmatov EG, Toukach PV, Makarova EN. Structural studies of the pectic polysaccharide from fruits of *Punica granatum*. *Carbohydr Polym*. (2020) 235:115978. doi: 10.1016/j.carbpol.2020.115978
42. Velkova N, Doliska A, Zemljic LF, Vesel A, Saake B, Strnad S. Influence of carboxymethylation on the surface physical-chemical properties of glucuronoxylan and arabinoxylan films. *Polym Eng Sci*. (2015) 55:2706–13. doi: 10.1002/pen.24059
43. Martinez-Gonzalez AI, Diaz-Sanchez AG, de la Rosa LA, Vargas-Requena CL, Bustos-Jaimes I, Alvarez-Parrilla E. Polyphenolic compounds and digestive enzymes: *in vitro* non-covalent interactions. *Molecules*. (2017) 22:669. doi: 10.3390/molecules22040669
44. Liang L, Liu G, Zhang F, Li Q, Linhardt RJ. Digestibility of squash polysaccharide under simulated salivary, gastric and intestinal conditions and its impact on short-chain fatty acid production in type-2 diabetic rats. *Carbohydr Polym*. (2020) 235:115904. doi: 10.1016/j.carbpol.2020.115904
45. Kalantzi L, Goumas K, Kalioras V, Abrahamsson B, Dressman JB, Reppas C. Characterization of the human upper gastrointestinal contents under conditions simulating bioavailability/bioequivalence studies. *Pharm Res*. (2006) 23:165–76. doi: 10.1007/s11095-005-8476-1
46. Maldonado-Valderrama J, Wilde P, Macierzanka A, Mackie A. The role of bile salts in digestion. *Adv Colloid and Interface Sci*. (2011) 165:36–46. doi: 10.1016/j.cis.2010.12.002
47. Bauer E, Jakob S, Mosenthin R. Principles of physiology of lipid digestion. *Asian-Australas J Anim Sci*. (2005) 18:282–95. doi: 10.5713/ajas.2005.282
48. Harries JT, Sladen GJ. The effects of different bile salts on the absorption of fluid, electrolytes, and monosaccharides in the small intestine of the rat *in vivo*. *Gut*. (1972) 13:596–603. doi: 10.1136/gut.13.8.596
49. Ji NQ, Chen XD, Wang H, Ren C, Bao ZJ. Resistant mechanism of polymyxin resistant-*Klebsiella pneumoniae*. *Chin J Antibiot*. (2018) 43:1443–8. doi: 10.13461/j.cnki.cja.006438
50. Kim JH, Baek J, Sa S, Park J, Kih M, Kim W. Kestose-enriched fructo-oligosaccharide alleviates atopic dermatitis by modulating the gut microbiome and immune response. *J Funct Foods*. (2021) 85:104650. doi: 10.1016/j.jff.2021.104650
51. Rolfe MD, Rice CJ, Lucchini S, Pin C, Thompson A, Cameron ADS, et al. Lag phase is a distinct growth phase that prepares bacteria for exponential growth and involves transient metal accumulation. *J Bacteriol*. (2012) 194:686–701. doi: 10.1128/JB.06112-11
52. Cockburn DW, Koropatkin NM. Polysaccharide degradation by the intestinal microbiota and its influence on human health and disease. *J Mol Biol*. (2016) 428:3230–52. doi: 10.1016/j.jmb.2016.06.021
53. Bello B, Mustafa S, Tan JS, Ibrahim TAT, Tam YJ, Ariff AB, et al. Evaluation of the effect of soluble polysaccharides of palm kernel cake as a potential prebiotic on the growth of probiotics. *3 Biotech*. (2018) 8:346. doi: 10.1007/s13205-018-1362-4
54. Feng R, Kou J, Chen S, Wang N, Wang W, Wang L, et al. Preparation optimization, characterization, and antioxidant and prebiotic activities of carboxymethylated polysaccharides from jujube. *J Food Qual*. (2021) 2021:3268149. doi: 10.1155/2021/3268149

Conflict of Interest: The authors declare that the research was conducted in the absence of any commercial or financial relationships that could be construed as a potential conflict of interest.

Publisher's Note: All claims expressed in this article are solely those of the authors and do not necessarily represent those of their affiliated organizations, or those of the publisher, the editors and the reviewers. Any product that may be evaluated in this article, or claim that may be made by its manufacturer, is not guaranteed or endorsed by the publisher.

frontiers in Nutrition

ORIGINAL RESEARCH
published: 13 December 2021
doi: 10.3389/fnut.2021.751992

Cereus sinensis Polysaccharide Alleviates Antibiotic-Associated Diarrhea Based on Modulating the Gut Microbiota in C57BL/6 Mice

Mingxiao Cui[1], *Yu Wang*[1], *Jeevithan Elango*[1], *Junwen Wu*[1], *Kehai Liu*[1,2]* *and Yinzhe Jin*[1,2]*

[1] *Department of Biopharmaceutics, College of Food Science and Technology, Shanghai Ocean University, Shanghai, China,*
[2] *National R&D Branch Center for Freshwater Aquatic Products Processing Technology (Shanghai), Shanghai, China*

The present study investigated whether the purified polysaccharide from *Cereus sinensis* (CSP-1) had beneficial effects on mice with antibiotic-associated diarrhea (AAD). The effects of CSP-1 on gut microbiota were evaluated by 16S rRNA high-throughput sequencing. Results showed that CSP-1 increased the diversity and richness of gut microbiota. CSP-1 enriched *Phasecolarctobacterium*, *Bifidobacterium* and reduced the abundance of *Parabacteroides*, *Sutterella*, *Coprobacillus* to near normal levels, modifying the gut microbial community. Microbial metabolites were further analyzed by gas chromatography-mass spectrometry (GC-MS). Results indicated CSP-1 promoted the production of various short-chain fatty acids (SCFAs) and significantly improved intestinal microflora dysfunction in AAD mice. In addition, enzyme linked immunosorbent assay and hematoxylin-eosin staining were used to assess the effects of CSP-1 on cytokine levels and intestinal tissue in AAD mice. Results demonstrated that CSP-1 inhibited the secretion of interleukin-2 (IL-2), interleukin-1β (IL-1β) and tumor necrosis factor-α (TNF-α) and improved the intestinal barrier. Correspondingly, the daily records also showed that CSP-1 promoted recovery of diarrhea status score, water intake and body weight in mice with AAD. In short, CSP-1 helped alleviate AAD by regulating the inflammatory cytokines, altering the composition and richness of intestinal flora, promoting the production of SCFAs, improving the intestinal barrier as well as reversing the dysregulated microbiota function.

Keywords: ***Cereus sinensis*, polysaccharide, antibiotic-associated diarrhea, gut microbiota, short chain fatty acid**

OPEN ACCESS

Edited by:
Riadh Hammami,
University of Ottawa, Canada

Reviewed by:
Kit Leong Cheong,
Shantou University, China
Bin Du,
Hebei Normal University of Science and Technology, China

***Correspondence:**
Kehai Liu
khliu@shou.edu.cn
Yinzhe Jin
yzjin@shou.edu.cn

Specialty section:
This article was submitted to Nutrition and Microbes, a section of the journal Frontiers in Nutrition

Received: *02 August 2021*
Accepted: *19 November 2021*
Published: *13 December 2021*

Citation:
Cui M, Wang Y, Elango J, Wu J, Liu K and Jin Y (2021) Cereus sinensis Polysaccharide Alleviates Antibiotic-Associated Diarrhea Based on Modulating the Gut Microbiota in C57BL/6 Mice. Front. Nutr. 8:751992. doi: 10.3389/fnut.2021.751992

INTRODUCTION

Antibiotics are highly effective in treating numerous bacterial or pathogenic infections (1). Nevertheless, the misuse or inappropriate use of antibiotics may alter the structure of the gut microbiota, disrupt the microbial balance, and thereby cause potential clinical complications in the host (2). As a common intestinal complication due to the use of antibiotics, AAD may manifest as symptoms, such as mild diarrhea, colitis and toxic megacolon. Many reports have shown that long-term probiotic therapy can significantly improve intestinal flora, promote the recovery of intestinal tissue architecture, and alleviate systemic inflammation, suggesting that probiotics are beneficial to the recovery of AAD mice (3). At present, probiotic therapy is the principal method to alleviate

AAD disease. However, probiotics were easily inactivated. Therefore, it was still a hot topic to find effective alternatives with long-term stable storage.

Prebiotics have also been reported to have a good effect on restoring intestinal balance and have a long storage period (4). Some natural polysaccharides with few adverse effects and particular biological activities are important prebiotics (5, 6). It has also been confirmed that certain polysaccharides have shown efficacy in alleviating or treating certain diseases, involving colitis, diabetes and AAD, by upregulating the healthful bacteria and suppressing the maleficent bacteria to regulate the intestinal flora (7, 8). For instance, polysaccharides derived from inulin and yam were reported to up-regulate the abundance of bacteria producing lactic acid and SCFAs, reduce the abundance of *Bacteroides*, *Proteobacteria* and sulfate-reducing bacteria, modulate the gut microbiota composition and function and ultimately ameliorate colitis of rats (9). Furthermore, polysaccharides isolated from *Schisandra chinensis* reduced intestinal mucosal damage based on beneficial regulation of intestinal flora, thereby helping to alleviate AAD (10). Therefore, certain natural polysaccharides may be potential prebiotic agents to effectively alleviate AAD disease based on their beneficial effects on the intestinal flora.

Cereus sinensis belonging to Actiniaria, *HormathiidaeCarlgren*, *CalliactisVerrill* grown mainly along the Pacific coast (11). At present, many substances with toxic or important functions, such as anti-cancer, antibacterial, anticoagulant, and anti-inflammatory, have been found and extracted from sea anemones (12–14). Moreover, the research on sea anemone mainly focused on the field of proteins, polypeptides, the toxins structure and biological activities (15–18). Nevertheless, there were few reports about sea anemone polysaccharide. In our previous research, a novel *Cereus sinensis* polysaccharide (CSP-1) was obtained and further analyzed (19). Its monosaccharide composition mainly includes Fucose, Mannose, and Glucose (14.9: 1.2: 1.0), and its mean molecular weight is 56,335 Da. The glycosidic linkage of CSP-1 was inferred as 1→ 2, 1→ 4, 1→ 2, 6, and 1→ 4, 6. The beneficial effects of CSP-1 on the body are still unclear, which also limits its development and utilization. Currently, probiotics are commonly used to treat antibiotic-associated diarrhea. However, they are easily inactivated in the gastrointestinal environment and require high storage conditions. As a prebiotic, polysaccharides have good stability in the gastrointestinal environment and room temperature, and may also positively regulate the intestinal microbiota and have beneficial effects on intestinal diseases. Thus, we decided to evaluate the unexplored polysaccharide CSP-1's regulatory effects on the disordered intestinal flora and its beneficial effects on AAD, providing a candidate effective ingredient for the treatment of AAD. This could provide a theoretical basis for CSP-1 as a stable and effective prebiotic for AAD therapy, and at the same time provide the applied basis for the development of CSP-1 as a functional food ingredient or additive to alleviate AAD. AAD has been reported to be closely bound up with changes in the structure and function of intestinal flora, physiological performance, intestinal barrier, serum cytokine secretion and SCFAs production in mice (20). Based on the above indicators, the beneficial effects of CSP-1 were further explored.

MATERIALS AND METHODS

Samples and Materials

Lincomycin hydrochloride (LH) was purchased from Anhui Shuanghe Pharmaceutical Co., Ltd. (Anhui, China). ELISA kits were purchased from Shanghai MLBIO Biotechnology Co., Ltd. QIAamp DNA stool mini kit was manufactured by TIANGEN (Germany). Other reagents were purchased from Sinopharm Chemical Reagent Co., Ltd. (Shanghai, China).

According to our previous methods, CSP-1 was isolated from *Cereus sinensis* (19, 21). After being soaked in NaCl solution (2%) to remove impurities, fresh *Cereus sinensis* was crushed and mixed with an equal volume of acetone for 12 h. The solution was filtered and freeze-dried to obtain degreased *Cereus sinensis* powder. The powder was mixed with distilled water at 72°C for 3 h and then precipitated with 3 times the volume of ethanol for 2 days. The above solution was centrifuged to obtain the precipitate, which was the crude polysaccharides. 50 mg/mL crude polysaccharide solution was mixed with 3% trichloroacetic acid for 12 h to remove protein. The solution was centrifuged, concentrated, dialyzed (3500D MWCO), and lyophilized. 5 mL of 20 mg/mL polysaccharide solution were further purified by column chromatography, involving DEAE-52 ion-exchange column and Sephadex G-100 column. 0.3 mol/L NaCl solution was used as eluate. The solution containing polysaccharides was collected, concentrated, dialyzed, and lyophilized to obtain CSP-1.

Ultraviolet (UV) and Fourier Transform Infrared (FT-IR) Spectral Analysis of CSP-1

A UV-752 spectrophotometer (Qingdao Lubo Jianye Environmental Protection Technology Co., Ltd., Qingdao, China) was used to record the UV spectra of CSP-1 (scanning range 200–400 nm). FT-IR spectrometer (Tianjin Gangdong Technology Co., Ltd., Tianjin, China) was used to measure the FT-IR spectra of CSP-1 (scanning range 4,000–400 cm-1). The polysaccharide sample was mixed with dried KBr and then pressed into a thick pellet for FT-IR determination. The FT-IR and UV spectra of CSP-1 were shown in **Supplementary Figure S1**.

Animals and Experimental Design

All experimental procedures were approved by the Committee for Animal Research of Shanghai Ocean University, China (SCXK (HU) 2007-0003). At the same time, animal experiments were carried out strictly following the Guidelines for the Care and Use of Laboratory Animals. Efforts were made to maximize the well-being of mice and minimize their suffering.

C57BL/6 male mice, 6–8 weeks, were obtained from the Shanghai Jiesijie Experimental Animal Co., Ltd and raised in a standard environment (12 h light-dark cycle, 22 ± 0.5°C, RH: 50 ± 5%) for 1 week. And then mice were randomly distributed into 6 groups with 3 mice per group. It was reported that short-term high-dose of LH will cause diarrhea in mice, which is mainly

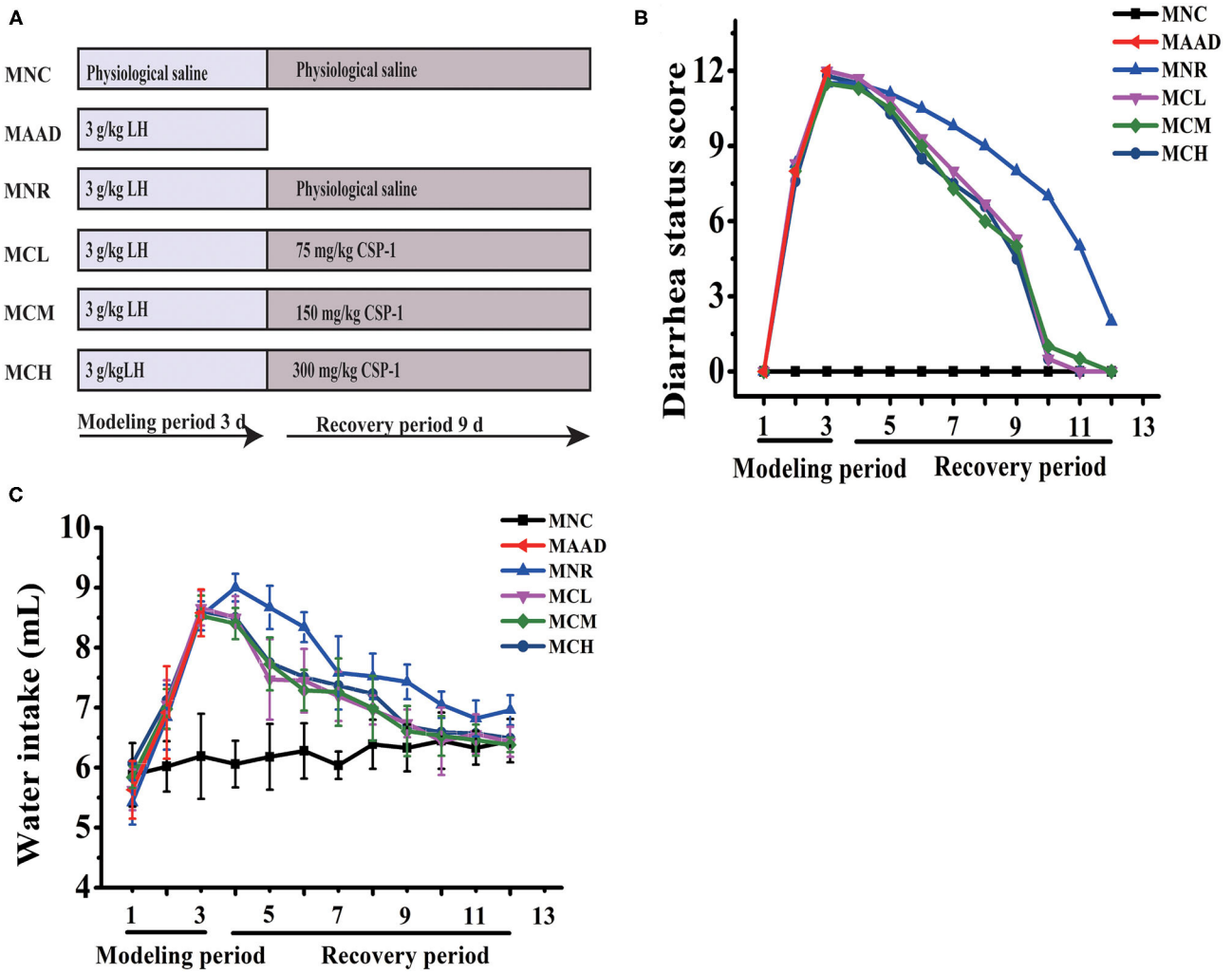

FIGURE 1 | Schematic diagram in the experiment **(A)**; Changes of diarrhea status score and water intake **(B,C)**. Values are shown as means ± SD.

due to the disturbance of intestinal flora and inflammation of the intestinal tissues caused by LH (22). Therefore, LH is often used in the establishment of AAD models. Mice in the antibiotic-associated diarrhea group (MAAD) were gavaged with LH for only 3 days. Mice in the natural recovery group (MNR) were gavaged with LH for 3 days and then gavaged with physiological saline for the next 9 days. Mice in the Low- (MCL), medium- (MCM), and high- (MCH) dosage CSP-1 groups were gavaged with LH for 3 days and then gavaged with CSP-1 (MCL, MCM and MCH groups were 75, 150 and 300 mg/kg, respectively) for the next 9 days. Mice in the normal control group (MNC) were gavaged with physiological saline for 12 days. The dosage of LH in this experiment was 3 g/kg. Mice were gavaged twice a day during the experimental period. The experimental design was shown in **Figure 1A**.

The state of all mice was recorded daily, such as body weight, water intake, and diarrhea status. Diarrhea status was evaluated as previously reported (**Table 1**) (20). At the end of the experiment, mice were euthanized. The caecal specimens were temporarily immersed in formalin solution (10%) for histological observation. The caecal contents were collected and next stored at −80°C.

TABLE 1 | Diarrhea status scoring methods.

Scores	Diarrhea status
0	Normal mental state and stools
1	General mental state, loose and nonstic perianal stools
2	Bad mental state, adhesion stool at anus, inappetence, weight reduction

Histological Examination

After overnight fixation, the samples of each group were embedded, sectioned and stained by Shanghai Viao

Biotechnology Co., Ltd. Briefly, caecal specimens were prepared by ethanol dehydrating and paraffin embedding (23). The sliced (thickness of 5 μm) specimens were stained with hematoxylin and eosin. The sections were observed under a light microscope (40×) and images were obtained.

Determination of Serum Cytokine Secretion and SCFAs Production

The blood was collected and then centrifuged at 2,000 rpm for 10 min. The serum was obtained by collecting the supernatants. The secretion of TNF-α, IL-1β, and IL-2 was measured using ELISA kits according to the corresponding instructions.

Pretreatment of caecal content was carried out as previously reported (24). 100 mg cecal contents were mixed with 0.4 mL of distilled water and centrifuged at 5,000 rpm for 20 min. The supernatant was mixed with 50% H_2SO_4 (0.2 mL) and 50 μg mL^{-1} (1 mL) solution containing diethyl ether and 2-methylvaleric acid. The above solution was centrifuged at 12,000 rpm for 10 min and then placed at 4°C for 30 min. The upper liquid was used for the determination of SCFAs. Furthermore, standard solutions of SCFAs (acetate, propionate, isobutyrate, butyrate, 2-methylbutyrate, valerate and hexanoate) at different concentrations (5 μg mL^{-1}, 10 μg mL^{-1}, 50 μg mL^{-1},100 μg mL^{-1}, 200 μg mL^{-1}, 400 μg mL^{-1}, 1,000 μg mL^{-1}) were prepared in ether. 2-methylpentanoic acid was mixed with diethyl ether as an internal standard solution. The SCFAs were detected using Agilent 7890A-5975C GC-MS System (Agilent, USA). The conditions were as follows: injection volume: 1 μL; carrier gas helium at a flow rate of 1 mL/min; the split ratio was 5: 1; injector temperature: 250°C. column temperature program: 100°C (maintained for 5 min) to 160 °C at 5°C/min; next increased to 240°C (maintained for 10 min) at 40°C/min.

16S rRNA High-Throughput Sequencing and Bioinformatics Analysis

DNA from the intestinal flora was obtained from the cecal contents using the DNA stool kit. PCR amplification of the V3-V4 region of bacterial 16S rRNA gene was carried out using forward primer (5′-ACTCCTACGGGAGGCAGCA-3′) and reverse primer (5′-GGACTACHVGGGTWTCTAAT-3′). Data can be obtained at NCBI with accession no. SUB9203775. The next procedures were the collection, purification, fluorescence quantification of amplification products and preparation of sequencing library. Sequencing of PCR products was performed by the Illumina MiSeq (Illumina, United States) sequencing platform at Personal Biotechnology Co., Ltd (Shanghai, China). The paired-end sequence was filtered using the sliding window method, then paired and connected using the FLASH software (v1.2.7), identified and further assigned to the corresponding sample to obtain the valid sequence for each sample (25). USEARCH (v5.2.236) was applied to filter the sequences obtained above and to cluster the superior reads into operational taxonomic units with a 97% similarity threshold. Using QIIME (v1.8.0) (26). Gut microbiota was analyzed by Illumina MiSeq sequencing based on QIIME analysis (27).

Statistical Analysis

The data was presented as mean ± standard deviation (SD). A significant difference between groups was performed by one-way analysis of variance (ANOVA) followed by Duncan's multiple range tests using SPSS statistics 17.0 (IBM, USA). Differences were considered significant at $P < 0.05$.

RESULTS

Effects of CSP-1 on Diarrhea Status Scores, Water Intake, Bodyweight

During LH intragastric administration, the mice showed a gradual increase in diarrhea status score and drinking water (**Figures 1B,C**). After 3 days, these mice exhibited 100% diarrhea. From the 4th day, the diarrhea status scores and water consumption of the MCL, MCM and MCH groups began to drop. As for the MNR group, the diarrhea status scores began to drop from the 4th day, while water intake began to decrease from the 5th day. On the 12th day, in terms of diarrhea status score and water consumption, the MNR group was obviously higher than the MNC group, while the MCL, MCM and MCH groups were similar to the MNC group. The bodyweight of the mice treated with the LH significantly decreased (**Table 2**). During the recovery period, the bodyweight of each group was gradually increasing. At the end of the experiments, the bodyweight of the mice in the MCL, MCM and MCH groups was higher than their starting weight, while the bodyweight of the mice in the MNR group was still lower than their starting weight.

Effects of CSP-1 on Histological Changes

The cecal tissue in MAAD group exhibited serious histopathological changes, including edema, massive inflammatory cell infiltration, as well as villus shortening, sparse and irregular arrangement (**Figure 2**). Compared with the MNR group, CSP-1 significantly reduced the inflammatory cell infiltration and edema of the cecal tissue. Moreover, the cecal villi of the MCL, MCM and MCH groups were longer, thinner and relatively regular arrangement. There were no obvious differences among the MCL, MCM and MCH groups.

Effects of CSP-1 on Inflammatory Cytokines Production

LH treatment significantly stimulated the secretion of IL-2, IL-1β, and TNF-α in the serum of mice (**Figure 3**). Low, medium and high doses of CSP-1 significantly down-regulated levels of IL-2, TNF-α and high dosage of CSP-1 significantly decreased the level of IL-1β compared with the MNR group. No significant differences were observed among the MCL, MCM MCH, and MNC groups in the secretion of IL-2, IL-1β and TNF-α.

Effects of CSP-1 on SCFAs Production

Mice treated with low, medium and high dosage CSP-1 showed significant enhancements in acetate and total SCFAs production, compared with mice of the MNR group (**Figure 4**). Furthermore, mice treated with medium and high dosage CSP-1 also showed significant enhancements in propionate and butyrate production. CSP-1 treatment and MNC groups had no significant difference

TABLE 2 | Effects of CSP-1 on the body weight of mice.

Groups	Bodyweight (g)		
	Day 0	Day 3	Day 12
MNC	23.65 ± 0.47	23.80 ± 0.46	24.81 ± 0.60
MAAD	23.96 ± 0.37	19.83 ± 0.60	-
MNR	23.45 ± 0.53	20.23 ± 1.13	22.94 ± 0.71
MCL	23.90 ± 0.76	20.39 ± 0.67	24.73 ± 0.69
MCM	23.14 ± 0.72	19.55 ± 0.82	23.74 ± 0.65
MCH	24.07 ± 0.74	21.53 ± 0.75	24.24 ± 0.51

Values are shown as means ± SD.

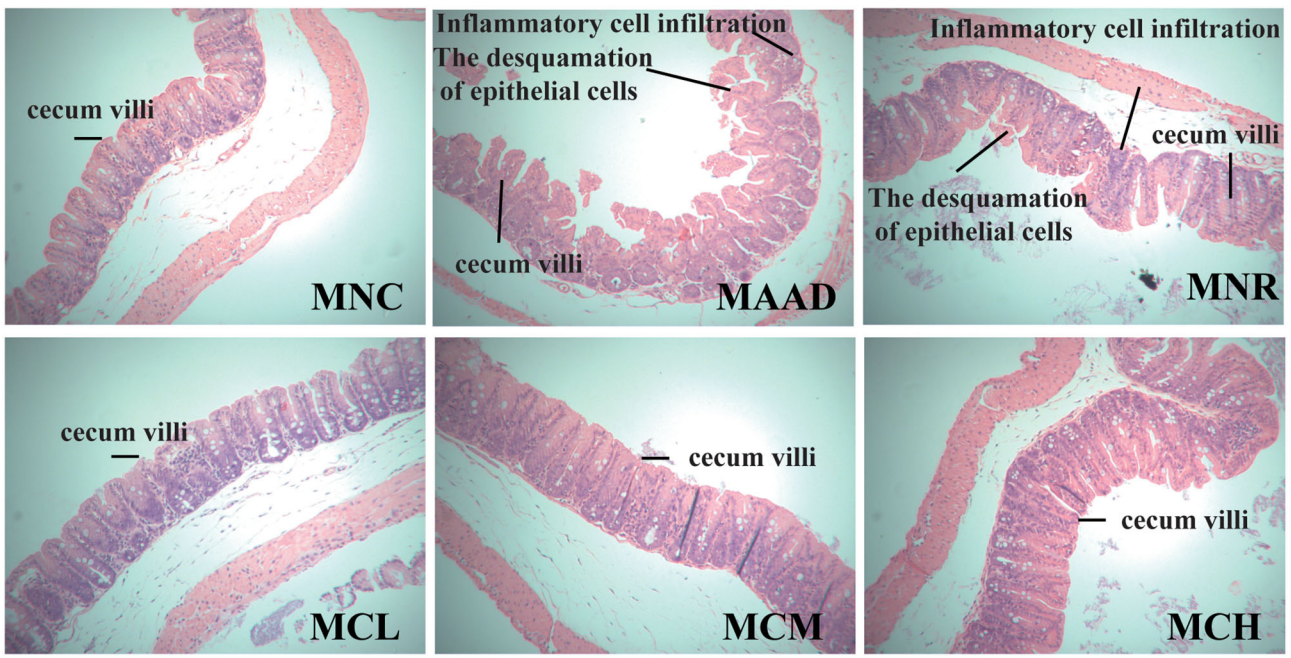

FIGURE 2 | Histological changes of the cecum. Values are shown as means ± SD.

in terms of the production of acetate, propionate, butyrate and total SCFAs.

Effects of CSP-1 on the Gut Microbiota

Shannon and Chao 1 indexes were used to evaluate the diversity and richness of intestinal flora, respectively (**Figures 5A,B**). In terms of Shannon and Chao 1 indices, MNR, MCL, MCM and MCH groups were significantly higher than the MAAD group, while MCL, MCM and MCH groups were closer to the MNC group compared to the MNR group. In terms of Chao 1 index, MNC group was significantly higher than MNR group, while there was no significant difference among MCL, MCM and MNC group.

β diversity analysis (**Figures 5C,D**) showed that the MCL and MCM groups were closer to the MNC group than the MNR group. Meanwhile, the MNR group is closer to the MAAD group than the MCL, MCM, and MCH groups. PLS-DA analysis also demonstrated the structural changes of intestinal flora among the groups (**Figure 5E**). The significant separation between the MAAD and MNC groups indicated the successful establishment of the AAD model. **Figure 5E** also revealed that the MCL, MCM and MCH groups were closer to the MNC group than the MNR group.

The main components of each group included *Firmicutes*, *Bacteroidetes*, *Proteobacteria*, *Actinobacteria* at the phylum level (**Figure 6A**). However, their abundance was different. The MAAD group had significantly higher *Firmicutes* and lower *Bacteroidetes* and *Proteobacteria* than the MNC group. Compared with the MNR group, *Bacteroides* was enriched, while *Proteobacteria* and *Firmicutes* were down-regulated in the MCL, MCM and MCH groups. MNC, MCL, MCM and MCH groups in *Firmicutes* had no significant difference. **Figure 6B** showed the genera with the highest abundance in the MAAD group were *Coprococcus*. Compared to the MAAD group, CSP-1 significantly reduced *Coprococcus* and increased other bacterial communities in the MCL, MCM and MCH groups.

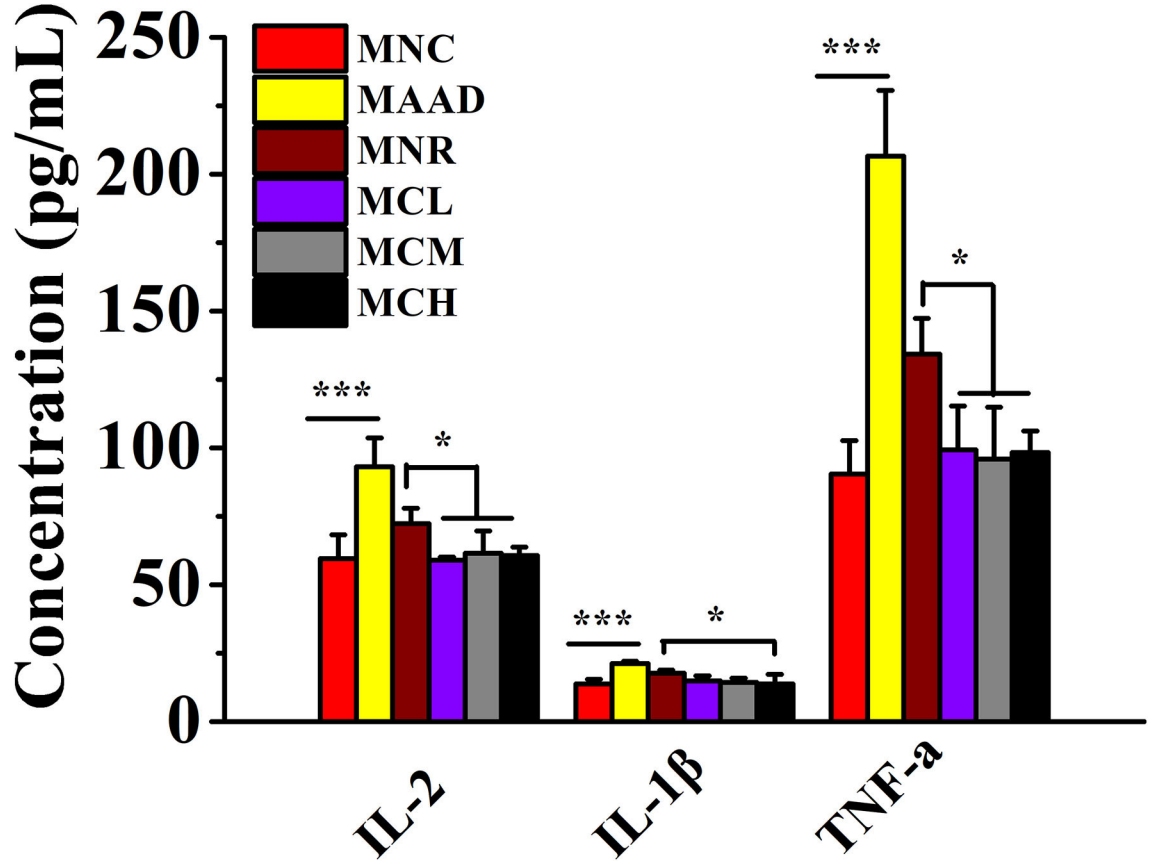

FIGURE 3 | Changes in the secretion of inflammatory factors. Values are shown as means ± SD. *$p < 0.05$, ***$p < 0.001$.

Compared with MNR group, MCL, MCM and MCH groups had lower abundance of *Bacteroides*, *Parabacteroides*, *Sutterella*, *Coprobacillus* and higher abundance of *Phasecolarctobacterium* and *Bifidobacterium* (**Figures 6C–H**).

Prediction of Metabolic Function of the Gut Communities

LH disrupted normal microbial metabolic pathways in the gut community of mice, like mice in the AAD group (**Figure 7**). Compared to the MNR group, amino acid metabolism, nervous system, translation, metabolic diseases were obviously enhanced and transcription, membrane transport was significantly weakened in three CSP-1 treated groups. At the same time, mice treated with a medium and high dosage of CSP-1 showed significant enhancements in transport and catabolism, glycan biosynthesis and metabolism. In addition, mice treated with a medium dosage of CSP-1 also showed significant enhancement in digestive system. Moreover, three CSP-1 treated groups and the MNC group did not show significant differences in transport and catabolism, transcription, membrane transport, digestive system, glycan biosynthesis and metabolism. Furthermore, CSP-1 also had good effects on regulating amino acid metabolism, cell motility and translation.

DISCUSSIONS AND CONCLUSIONS

AAD was closely connected with gut microbiota dysbiosis, intestinal structural changes, inflammation, SCFAs production (28). Compared to normal mice, mice with AAD manifested an imbalanced gut microbial environment, increased serum inflammatory cytokine levels, decreased SCFAs production, a destroyed gut structure. These were consistent with mice of the MAAD group. At present, it has been reported that natural polysaccharides as prebiotics helped the resistance of AAD by modulating the intestinal flora. For instance, a polysaccharide from Chinese yam alleviated AAD disease by upregulating the abundance of probiotics, suppressing the growth of potential pathogen, repairing the intestinal microbiota disorder, and up-regulating the concentration of SCFAs (9). These provided a reliable basis for natural polysaccharides as potential prebiotic agents to play a beneficial role by regulating intestinal flora.

Gut microbiota was closely associated with inflammation, gut mucosal dysfunction, SCFAs and certain diseases such as AAD and colitis. It is reported that certain gut bacteria and their metabolites can activate the mucosal immune system, which leads to inflammation and gut mucosal dysfunction (29). In addition, a significant reduction of SCFA-producing bacteria, such as *Bacteroidetes* and *Clostridium*, led to a decrease in SCFAs

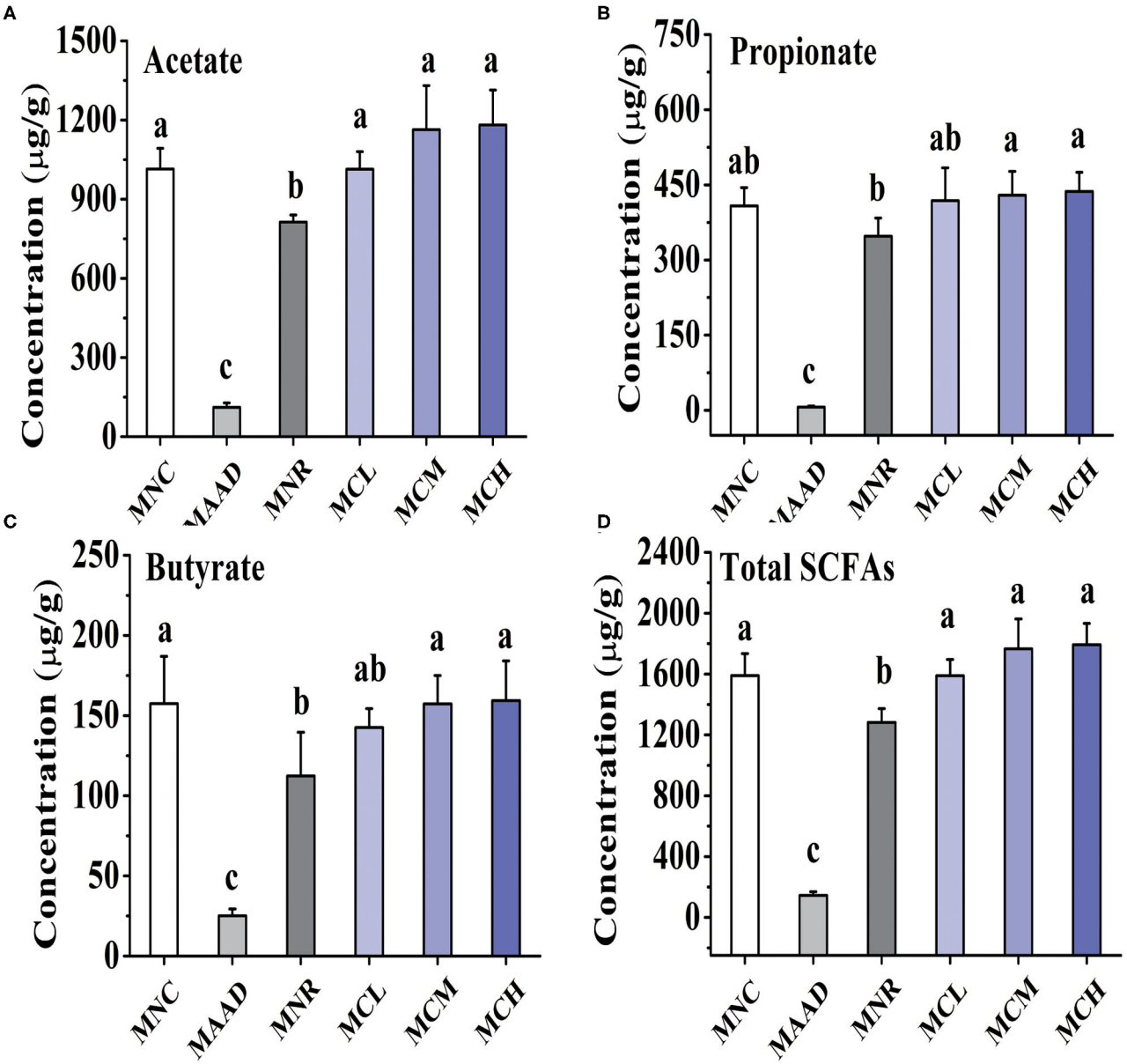

FIGURE 4 | Changes in concentrations of acetate **(A)**, propionate **(B)**, butyrate **(C)** and total SCFAs **(D)**. Values are shown as means ± SD. Different letters are significant differences ($p < 0.05$).

production. The composition and structure of gut microbiota were properly regulated, which can contribute to the restoration of health (30). For instance, some herbal medicines changed the composition and structure of the gut microbial community to achieve anti-inflammatory and immunomodulatory effects, thereby contributing to alleviating ulcerative colitis (31, 32). Moreover, the compound polysaccharides containing yam and inulin polysaccharides ameliorated the experimental colitis of rats by decreasing the abundance of harmful bacteria and increasing the abundance of beneficial bacteria, such as SCFAs-producing bacteria lactic acid-producing bacteria, to reverse the dysregulated microbiota function (33).

Mice with AAD showing decrease diversity and abundance of intestinal flora and abnormal composition and functions of gut microbiota has been reported. Natural polysaccharides have shown a good effect in restoring the balance of the gut microbiota. *Panax ginseng* polysaccharides have been reported to significantly alter the composition and diversity of the gut microbiota by increasing the relative abundance of *Lactobacillus* and balanced metabolic processes by reversing carbohydrate, amino acid, and energy metabolism to normal levels (34). This research showed that CSP-1 regulated the gut microbial community of AAD mice by enriching *Phasecolarctobacterium*, *Bifidobacterium*, and reducing the abundance of *Parabacteroides*,

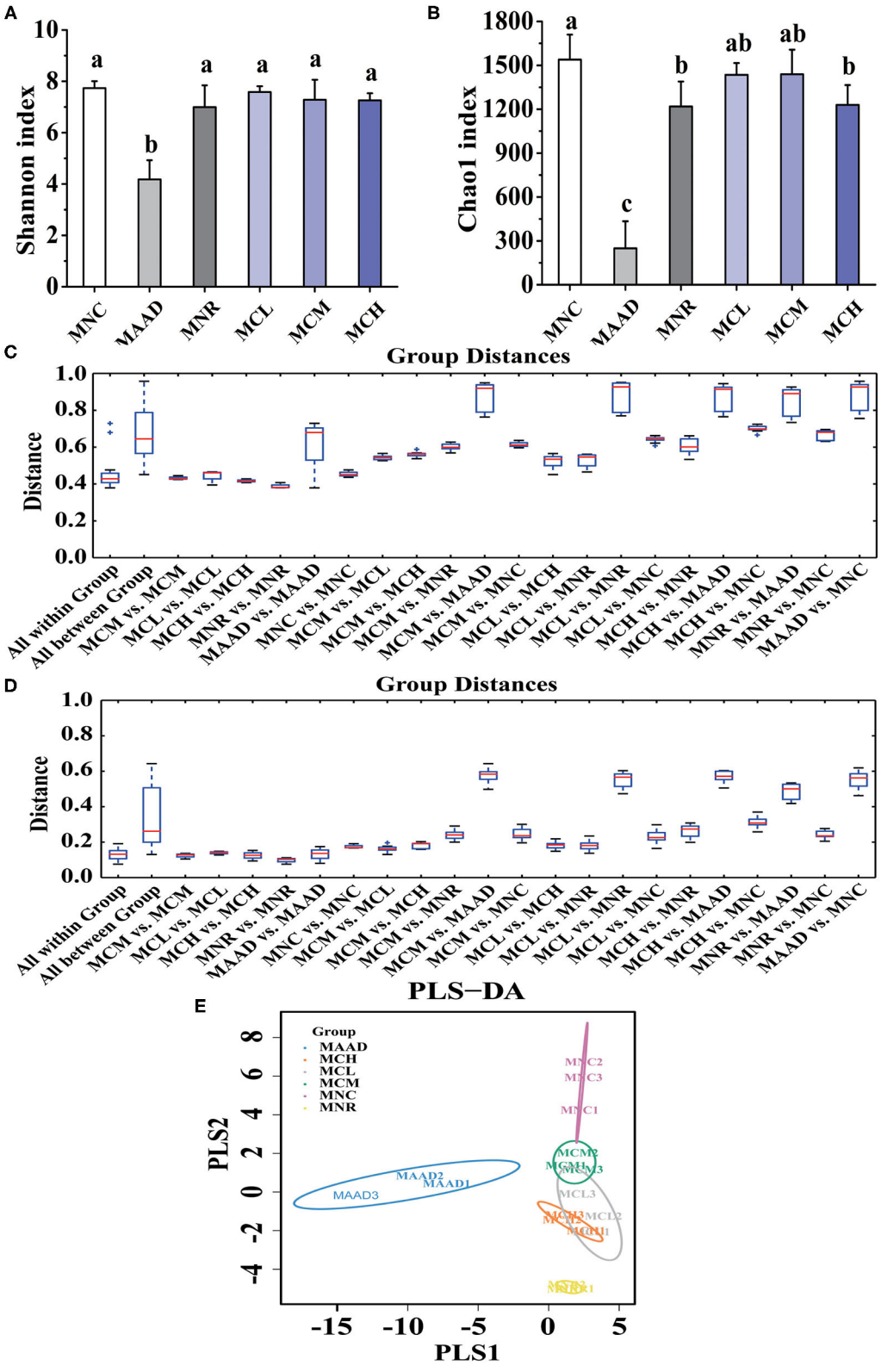

FIGURE 5 | α diversity analysis, **(A,B)** Shannon and Chao 1 indices, and β diversity analysis, **(C,D)** Unweighted and Weighted UniFrac-distance box-line graph, **(E)** PLS-DA analysis, of the gut microbiota. Values are shown as means ± standard deviation (SD). Different letters are significant differences ($p < 0.05$).

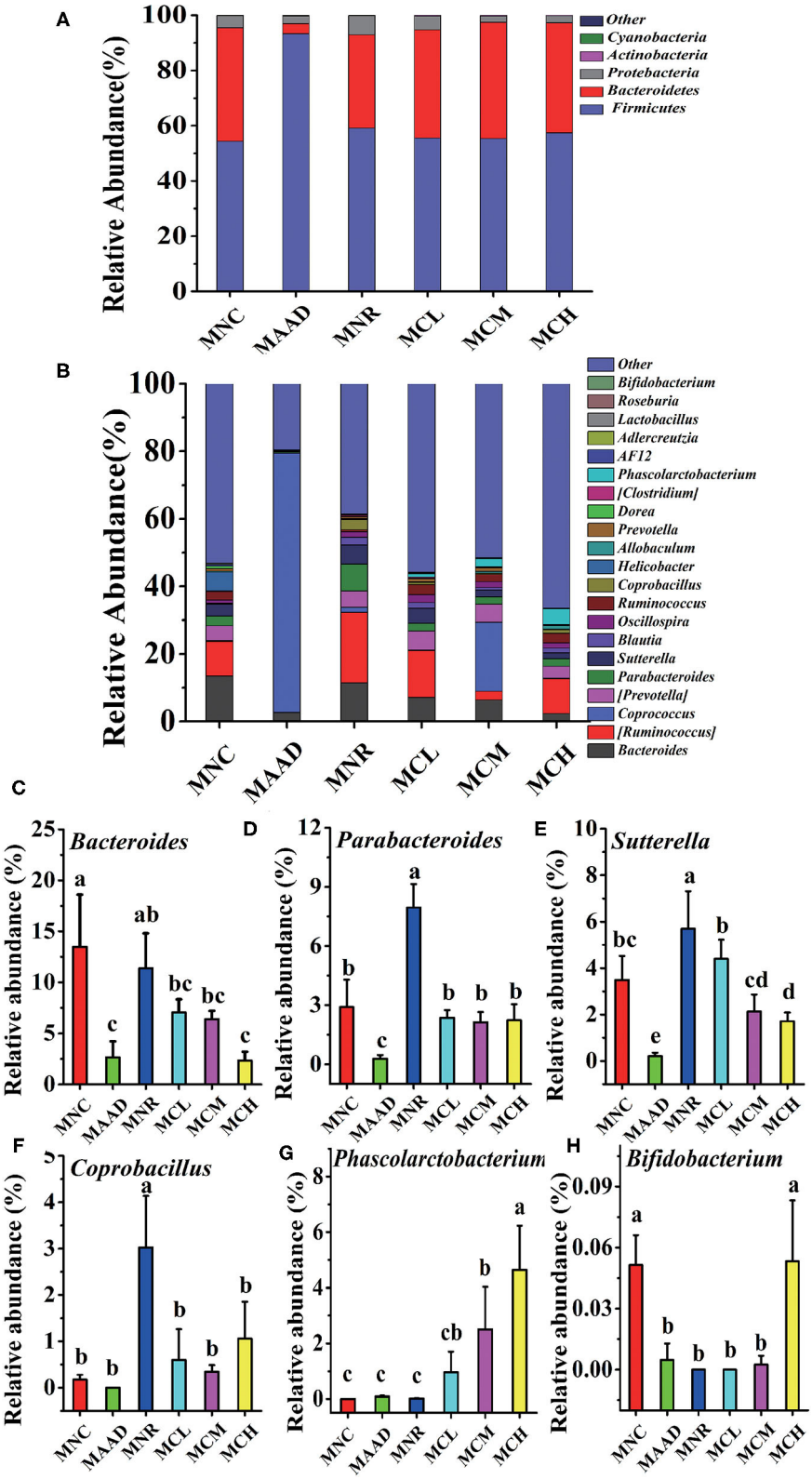

FIGURE 6 | Changes of microbial communities at different levels. **(A,B)** Phylum and Genus levels. **(C–H)** Comparison of intestinal flora with major differences at the genus level. Values are shown as means ± SD.

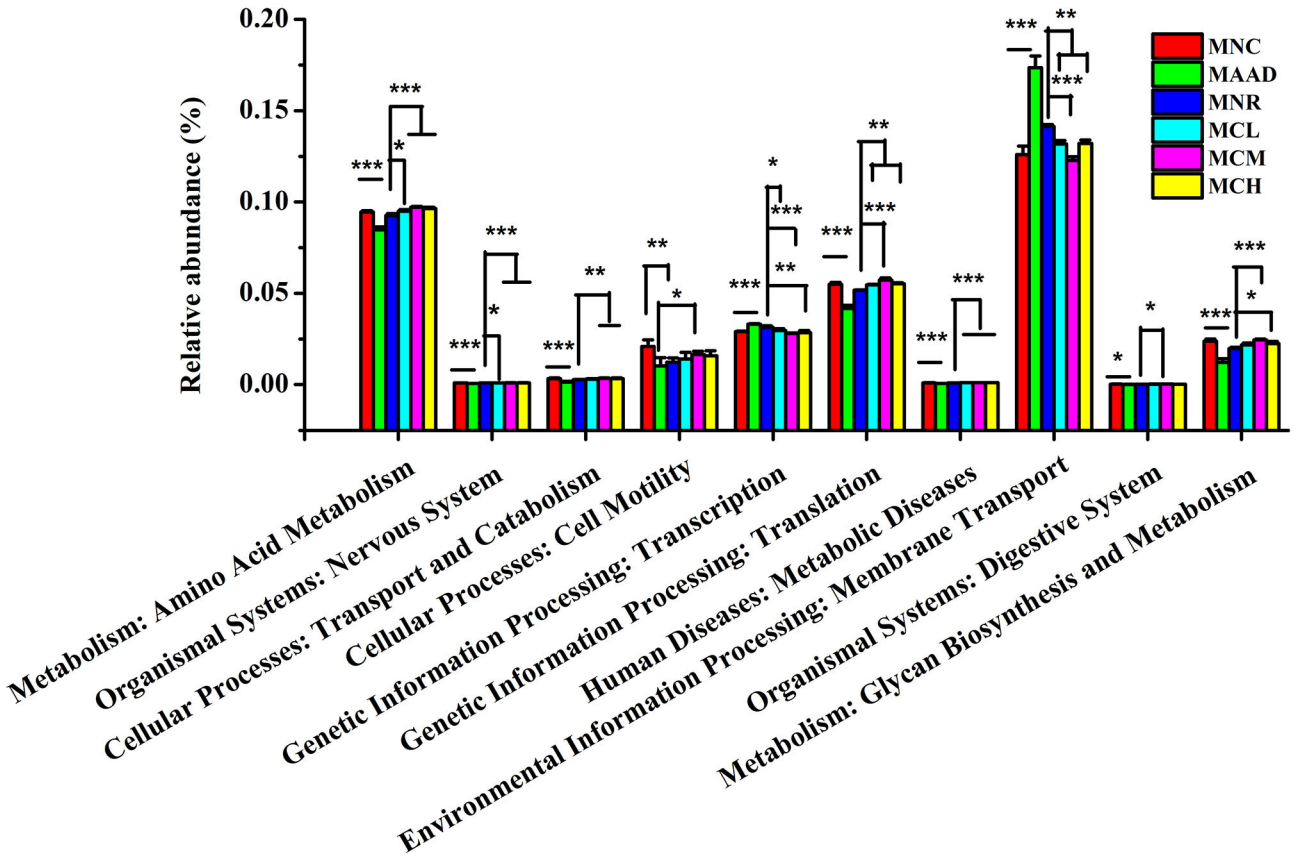

FIGURE 7 | Prediction of metabolic function by PICRUSt analysis. Values are shown as means ± SD. Different letters are significant differences. $^{*}p < 0.05$, $^{**}p < 0.01$, $^{***}p < 0.001$.

Sutterella, *Coprobacillus* to near normal levels. Furthermore, CSP-1 also up-regulated the richness of intestinal flora. Probiotic bacteria in the intestinal flora have many beneficial effects on the host, which may greatly promote the recovery of mice with AAD. For instance, acetic acid and lactic acid which developed by the fermentation of *Bifidobacteria* can alter the acidity of the microbial ecosystem, thereby inhibiting the colonization of harmful intestinal flora (35). Furthermore, *Bifidobacteria* has also been reported to enhance immunity, resist pathogenic bacterial infection and exhibit anti-inflammatory activity (36). As SCFAs-producing bacteria, the increased abundance of *Phascolarctobacterium* exhibited positive effects on restoring the health of the host. The abundance of *Paracteroides* and *Coprobacillus* in MCL, MCM and MCH groups also returned to normal levels due to the effective regulation of CPS-1. Even for beneficial microorganisms, abnormal up-regulation of their relative abundance may not be beneficial to the host. *Sutterella wadsworthensis* reportedly may be a symbiotic, innocuous microbe in certain populations, such as those suffering from diarrhea-related intestinal diseases (20). The specific reasons for the reduced abundance of *Bacteroidetes* remained to be further studied.

It has been reported that the concentration of normal fecal anaerobic bacteria in mice with AAD was dramatically reduced due to the use of antibiotics, which leads to a decrease in carbohydrate metabolism and SCFAs (37). Fortunately, this research showed that three doses of CSP-1 promoted the production of SCFAs in AAD mice. This may be because CSP-1 is a prebiotic that cannot be digested by the stomach, and is successfully fermented by anaerobic microorganisms in the large intestine, thereby promoting the production of propionate butyrate acetate, etc. The increased production of SCFAs not only provides energy for intestinal cells helping maintain normal intestinal function, but also promotes intestinal water absorption improving dehydration in AAD mice (38). In addition, acetate and butyrate contributed to anti-inflammatory effects by activating GPR41 and GPR43 and inhibiting histone deacetylase (29). Thus, CSP-1 promoted the growth of SCFAs-associated bacteria, increased SCFAs production, inhibited inflammation, contributing to relieve antibiotic-related diarrhea in mice.

Antibiotics had a significant negative effect on the metabolism of amino acids in the body (39). It has been reported that the level of free amino acids in the stool may increase tenfold

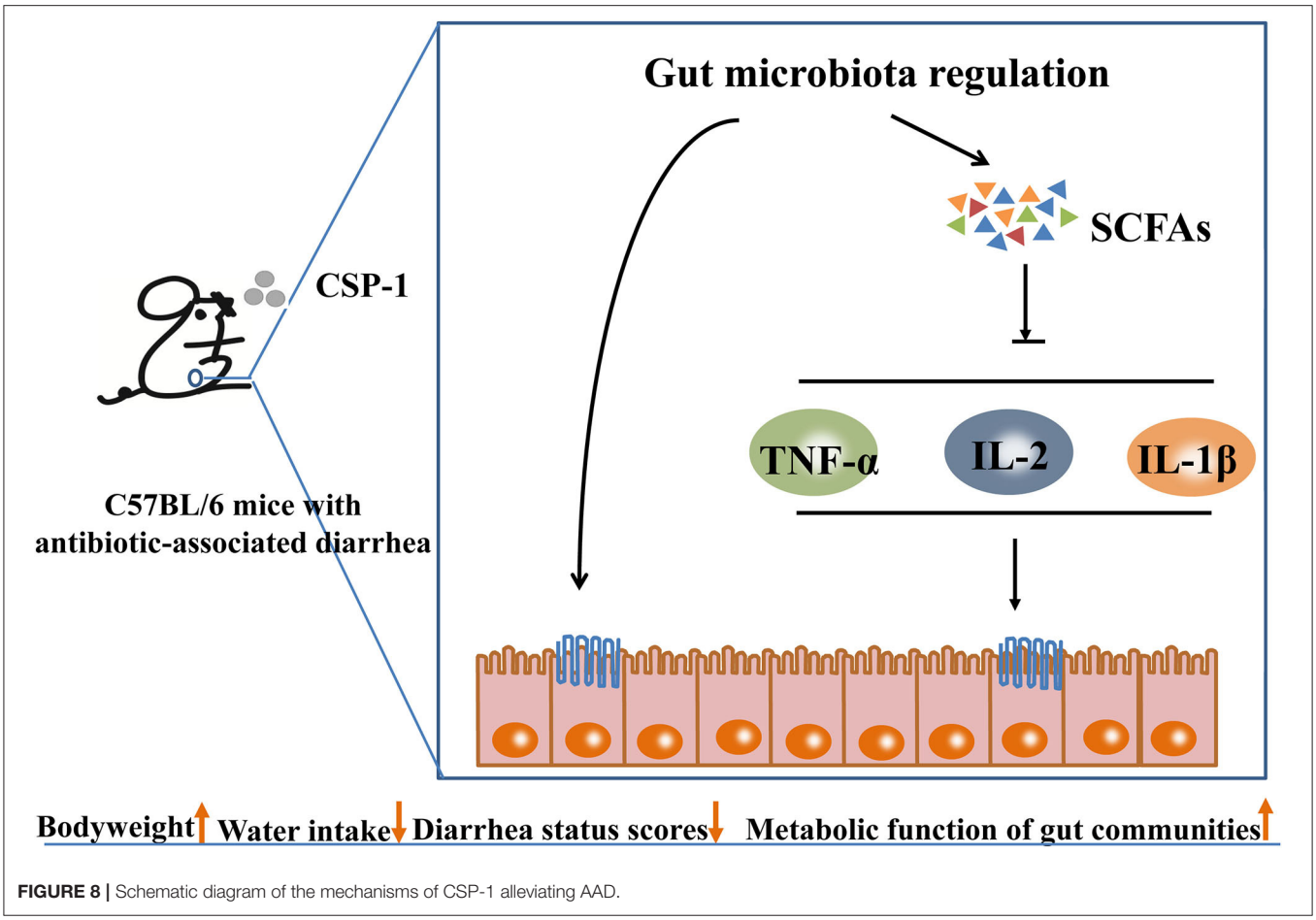

FIGURE 8 | Schematic diagram of the mechanisms of CSP-1 alleviating AAD.

during diarrhea (40). LH inhibited the metabolism of amino acids in mice, which may lead to the accumulation of free amino acids. Fortunately, CSP-1 can significantly enhance the metabolism of amino acids in the body. Amino acids can enhance cell metabolism, increase protein synthesis by regulating protein translation, and increase mitochondrial content in skeletal muscle and adipocytes (41). The enhancement of amino acid metabolism by CSP-1 may also positively affect the translation process. Glycan biosynthesis and metabolism were closely related to many physiological and biochemical processes in the body, and its recovery was crucial for the maintenance of normal physiological homeostasis (42). Furthermore, CSP-1 also improved other metabolic functions of the gut microbiota in mice with AAD, involving digestive system, nervous system, translation, metabolic diseases, membrane transport, cell motility, transport and catabolism. Their mechanisms still need further studying.

The schematic diagram of the mechanisms of CSP-1 alleviating AAD is shown in **Figure 8**. Overall, CSP-1 improved the intestinal barrier and regulated the gut microbiota and their metabolites as well as microbial metabolic function. On the basis of improving the composition and structure of intestinal flora, CSP-1 exhibited beneficial effects helping the recovery of AAD mice, which provided a basis for finding effective prebiotics for AAD.

DATA AVAILABILITY STATEMENT

The datasets presented in this study can be found in online repositories. The names of the repository/repositories and accession number(s) can be found at: https://www.ncbi.nlm.nih.gov/, SUB9203775.

ETHICS STATEMENT

The animal study was reviewed and approved by Shanghai Ocean University.

AUTHOR CONTRIBUTIONS

KL and YJ conceived and designed research. MC, YW, and JW performed experiments. MC and YW analyzed data. JE contributed new reagents or analytical tools. MC wrote the manuscript. KL and JE revised the manuscript.

All authors contributed to the article and approved the submitted version.

FUNDING

The research was supported by the International Academic Cooperation of Science and Technology Committee of Shanghai, China (18430721100) and the National Natural Science Foundation of China (81572989).

SUPPLEMENTARY MATERIAL

The Supplementary Material for this article can be found online at: https://www.frontiersin.org/articles/10.3389/fnut.2021.751992/full#supplementary-material

REFERENCES

1. Moser C, Lerche CJ, Thomsen K, Hartvig T, Schierbeck J, Jensen PO, et al. Antibiotic therapy as personalized medicine - general considerations and complicating factors. *APMIS.* (2019) 127:361–71. doi: 10.1111/apm.12951
2. Hayes SR, Vargas AJ. Probiotics for the prevention of pediatric antibiotic-associated diarrhea. *Explore (NY).* (2016) 12:463–6. doi: 10.1016/j.explore.2016.08.015
3. Bergogne-Brzin E. Treatment and prevention of antibiotic associated diarrhea. *Int J Antimicrob Agents.* (2000) 16:521–6.
4. Nicolucci AC, Reimer RA. Prebiotics as a modulator of gut microbiota in paediatric obesity. *Pediatr Obes.* (2017) 12:265–73. doi: 10.1111/ijpo.12140
5. Liu J, Willför S, Xu C. A review of bioactive plant polysaccharides: Biological activities, functionalization, and biomedical applications. *Bioact Carbohydr Diet Fibre.* (2015) 5:31–61. doi: 10.1016/j.bcdf.2014.12.001
6. Xu Y, Wu YJ, Sun PL, Zhang FM, Linhardt RJ, Zhang AQ. Chemically modified polysaccharides: Synthesis, characterization, structure activity relationships of action. *Int J Biol Macromol.* (2019) 132:970–7. doi: 10.1016/j.ijbiomac.2019.03.213
7. Ai C, Duan M, Ma N, Sun X, Yang J, Wen C, et al. Sulfated polysaccharides from pacific abalone reduce diet-induced obesity by modulating the gut microbiota. *J Funct Foods.* (2018) 47:211–9. doi: 10.1016/j.jff.2018.05.061
8. Ren Y, Geng Y, Du Y, Li W, Lu ZM, Xu HY, et al. Polysaccharide of *Hericium erinaceus* attenuates colitis in C57BL/6 mice via regulation of oxidative stress, inflammation-related signaling pathways and modulating the composition of the gut microbiota. *J Nutr Biochem.* (2018) 57:67–76. doi: 10.1016/j.jnutbio.2018.03.005
9. Zhang N, Liang T, Jin Q, Shen C, Zhang Y. Jing P. Chinese yam (Dioscorea opposita Thunb) alleviates antibiotic-associated diarrhea, modifies intestinal microbiota, and increases the level of short-chain fatty acids in mice. *Food Res Int.* (2019) 122:191–8. doi: 10.1016/j.foodres.2019.04.016
10. Qi Y, Chen L, Gao K, Shao Z, Huo X, Hua M, et al. Effects of *Schisandra chinensis* polysaccharides on rats with antibiotic-associated diarrhea. *Int J Biol Macromol.* (2019) 124:627–34. doi: 10.1016/j.ijbiomac.2018.11.250
11. Li Y. Species composition and faunastic characteristics of the order Actiniaria (Cnidaria: Anthozoa) in Chinese waters. Shandong Province, China: Institute of Oceanology, Chinese Academy of Sciences, Qingdao, Shandong Province, China. (2013).
12. Hutton D, Smith VJ. Antibacterial properties of isolated amoebocytes from the sea anemone *Actinia equina*. *Biological bulletin.* (1996) 191:441–51. doi: 10.2307/1543017
13. Sintsova OV, Monastyrnaya MM, Pislyagin EA, Menchinskaya ES, Leychenko EV, Aminin DL, et al. Anti-Inflammatory activity of the polypeptide of the sea anemone, *Heteractis crispa. Bioorg Khim.* (2015) 41:657–63. doi: 10.1134/s106816201506014x
14. Thangaraj S, Bragadeeswaran S, Gokula V. Bioactive compounds of sea anemones: A review. *Int J Pept Res Ther.* (2018) 25:1405–16. doi: 10.1007/s10989-018-9786-6
15. Gendeh GS, Jeyaseelan K, Chung MCM. Structure-function studies of sea anemone peptide toxins. *Toxicon.* (1995) 33:1399. doi: 10.1016/0041-0101(95)98356-z
16. Khiralla A, Spina R, Saliba S, Laurain-Mattar D. Diversity of natural products of the genera *Curvularia* and *Bipolaris*. *Fungal Biol Rev.* (2019) 33:101–22. doi: 10.1016/j.fbr.2018.09.002
17. Knight K. Sea anemone proteins repair damaged mouse cochlear hair cells. *Journal of Experimental Biology.* (2016) 219:2229–30. doi: 10.1242/jeb.135459
18. Mikov AN, Kozlov SA. Structural features of cysteine-stabilized polypeptides from sea anemones venoms. *Bioorg Khim.* (2015) 41:511–23. doi: 10.1134/s1068162015050088
19. Wu J, Zhou X, Zhang M, Yao Y, Han J, Liu K. *Cereus sinensis* polysaccharide and its immunomodulatory properties in human monocytic cells. *Mar Drugs.* (2017) 15:140. doi: 10.3390/md15050140
20. Cui M, Wu J, Wang S, Shu H, Zhang M, Liu K, et al. Characterization and anti-inflammatory effects of sulfated polysaccharide from the red seaweed *Gelidium pacificum Okamura*. *Int J Biol Macromol.* (2019) 129:377–85. doi: 10.1016/j.ijbiomac.2019.02.043
21. Cui M, Zhang M, Wu J, Han P, Lv M, Dong L. Liu K. Marine polysaccharides from Gelidium pacificum Okamura and Cereus sinensis reveal prebiotic functions. *Int J Biol Macromol.* (2020) 164:4381–90. doi: 10.1016/j.ijbiomac.2020.08.255
22. Kuang Z, Gao Z, Zhang R, Song S, Tan J, Li J. The effect of lincomycin hydrochloride on the intestinal flora of mice. *Jilin Medicine.* (2009) 30:1230−1. doi: CNKI:SUN:JLYX.0.2009-13-009
23. Xie SZ, Liu B, Ye HY Li QM, Pan LH, Zha XQ, et al. *Dendrobium huoshanense* polysaccharide regionally regulates intestinal mucosal barrier function and intestinal microbiota in mice. *Carbohydr Polym.* (2019) 206:149–62. doi: 10.1016/j.carbpol.2018.11.002
24. Cui M, Zhou R, Wang Y, Zhang M, Liu K, Ma C. Beneficial effects of sulfated polysaccharides from the red seaweed *Gelidium pacificum Okamura* on mice with antibiotic-associated diarrhea. *Food Funct.* (2020) 11:4625–37. doi: 10.1039/d0fo00598c
25. Ding Y, Yan Y, Chen D, Ran L, Mi J, Lu L, et al. Modulating effects of polysaccharides from the fruits of *Lycium barbarum* on the immune response and gut microbiota in cyclophosphamide-treated mice. *Food Funct.* (2019) 10:3671–83. doi: 10.1039/c9fo00638a
26. Zhao R, Cheng N, Nakata PA, Zhao L, Hu Q. Consumption of polysaccharides from *Auricularia auricular* modulates the intestinal microbiota in mice. *Food Res Int.* (2019) 123:383–92. doi: 10.1016/j.foodres.2019.04.070
27. Li P, Niu Q, Wei Q, Zhang Y, Ma X, Kim SW, et al. Microbial shifts in the porcine distal gut in response to diets supplemented with *Enterococcus Faecalis* as alternatives to antibiotics. *Sci Rep.* (2017) 7:41395. doi: 10.1038/srep41395
28. Ling Z, Liu X, Cheng Y, Luo Y, Yuan L, Li L, et al. *Clostridium butyricum* combined with Bifidobacterium infantis probiotic mixture restores fecal microbiota and attenuates systemic inflammation in mice with antibiotic-associated diarrhea. *Biomed Res Int*. (2015) 582048. doi: 10.1155/2015/582048
29. Chen WX, Ren LH, Shi RH. Enteric microbiota leads to new therapeutic strategies for ulcerative colitis. *World J Gastroenterol.* (2014) 20:15657–63. doi: 10.3748/wjg.v20.i42.15657
30. Shao S, Wang D, Zheng W, Li X, Zhang H, Zhao D, et al. unique polysaccharide from *Hericium erinaceus* mycelium ameliorates acetic acid-induced ulcerative colitis rats by modulating the composition of the gut microbiota, short chain fatty acids levels and GPR41/43 respectors. *Int Immunopharmacol.* (2019) 71:411–22. doi: 10.1016/j.intimp.2019.02.038
31. Guo M, Ding S, Zhao C, Gu X, He X, Huang K, et al. Red ginseng and semen coicis can improve the structure of gut microbiota and relieve the symptoms of ulcerative colitis. *J Ethnopharmacol.* (2015) 62:7–13. doi: 10.1016/j.jep.2014.12.029
32. Liu L, Yuan S, Long Y, Guo Z, Sun Y, Li Y, et al. Immunomodulation of *Rheum tanguticum* polysaccharide (RTP) on the immunosuppressive effects of dexamethasone (DEX) on the treatment of colitis in rats induced by

2,4,6-trinitrobenzene sulfonic acid. *Int Immunopharmacol.* (2009) 9:1568–77. doi: 10.1016/j.intimp.2009.09.013
33. Cai Y, Liu W, Lin Y, Zhang S, Zou B, Xiao D, et al. Compound polysaccharides ameliorate experimental colitis by modulating gut microbiota composition and function. *J Gastroenterol Hepatol.* (2019) 34:1554–62. doi: 10.1111/jgh.14583
34. Sun Y, Liu Y, Ai C, Song S, Chen X. *Caulerpa lentillifera* polysaccharides enhance the immunostimulatory activity in immunosuppressed mice in correlation with modulating gut microbiota. *Food Funct.* (2019) 10:4315–29. doi: 10.1039/c9fo00713j
35. Cui D, Zuo L, Chen A, Long S, Zhong Z. The therapeutic effect of Ganoderma spore powder and *bifidobacteria* on intestinal microflora imbalance of mice. *Guiyang Yixueyuan Xuebao.* (2009) 33:363–70. doi: 10.19367/j.cnki.1000-2707.2008.04.012
36. Zhu G, Ma F, Wang G, Wang Y, Zhao J, Zhang H, et al. *Bifidobacteria* attenuate the development of metabolic disorders, with inter- and intra-species differences. *Food Funct.* (2018) 9:3509–22. doi: 10.1039/c8fo00100f
37. Gustafsson A, Berstad A, Lund-Tnnesen S, Midtvedt T, Norin E. The effect of faecal enema on five microflora-associated characteristics. *Scand J Gastroenterol.* (1999) 34:580–6. doi: 10.1080/003655299750026038
38. Canani RB, Terrin G, Cirillo P, Castaldo G, Salvatore F, Cardillo G, et al. Butyrate as an effective treatment of congenital chloride diarrhea. *Gastroenterology.* (2004) 127:630–4. doi: 10.1053/j.gastro.2004.03.071
39. Du R, Bei H, Jia L, Huang C, Chen Q, Tao C, et al. Danggui Buxue Tang restores antibiotic-induced metabolic disorders by remodeling the gut microbiota. *J Ethnopharmacol.* (2020) 259:112953. doi: 10.1016/j.jep.2020.112953
40. Ghadimi H, Kumar S, Abaci F. Amino acid loss and its significance in infantile diarrhea. *Pediat Res.* (1973) 7:161–8. doi: 10.1203/00006450-197303000-00008
41. Bifari F, Nisoli E. Branched-chain amino acids differently modulate catabolic and anabolic states in mammals: a pharmacological point of view. *Br J Pharmacol.* (2017) 174:1366–77. doi: 10.1111/bph.13624
42. Harada Y, Nakajima K, Li S, Suzuki T, Taniguchi N. Protocol for analyzing the biosynthesis and degradation of N-glycan precursors in mammalian cells. *STAR Protoc.* (2021) 2:100316. doi: 10.1016/j.xpro.2021.100316

Conflict of Interest: The authors declare that the research was conducted in the absence of any commercial or financial relationships that could be construed as a potential conflict of interest.

Publisher's Note: All claims expressed in this article are solely those of the authors and do not necessarily represent those of their affiliated organizations, or those of the publisher, the editors and the reviewers. Any product that may be evaluated in this article, or claim that may be made by its manufacturer, is not guaranteed or endorsed by the publisher.

frontiers in Nutrition

ORIGINAL RESEARCH
published: 17 March 2022
doi: 10.3389/fnut.2022.860086

Dietary Resistant Starch From Potato Regulates Bone Mass by Modulating Gut Microbiota and Concomitant Short-Chain Fatty Acids Production in Meat Ducks

Huaiyong Zhang[1,2†], *Simeng Qin*[3†], *Yao Zhu*[1†], *Xiangli Zhang*[1], *Pengfei Du*[1], *Yanqun Huang*[1], *Joris Michiels*[2], *Quifeng Zeng*[3*] and *Wen Chen*[1*]

[1] *Key Laboratory of Animal Biochemistry and Nutrition, College of Animal Science and Technology, Ministry of Agriculture, Henan Agricultural University, Zhengzhou, China,* [2] *Laboratory for Animal Nutrition and Animal Product Quality, Department of Animal Sciences and Aquatic Ecology, Ghent University, Ghent, Belgium,* [3] *Key Laboratory for Animal Disease-Resistance Nutrition of China, Institute of Animal Nutrition, Ministry of Education, Sichuan Agricultural University, Chengdu, China*

OPEN ACCESS

Edited by:
Ding-Tao Wu,
Chengdu University, China

Reviewed by:
Shiping Bai,
Sichuan Agricultural University, China
Chengjun Hu,
Chinese Academy of Tropical Agricultural Sciences, China
Vidal Delgado Rizo,
University of Guadalajara, Mexico

***Correspondence:**
Quifeng Zeng
keying@sicau.edu.cn
Wen Chen
zqf@sicau.edu.cn

[†] *These authors have contributed equally to this work*

Specialty section:
This article was submitted to Nutrition and Microbes, a section of the journal Frontiers in Nutrition

Received: *22 January 2022*
Accepted: *15 February 2022*
Published: *17 March 2022*

Citation:
Zhang H, Qin S, Zhu Y, Zhang X, Du P, Huang Y, Michiels J, Zeng Q and Chen W (2022) Dietary Resistant Starch From Potato Regulates Bone Mass by Modulating Gut Microbiota and Concomitant Short-Chain Fatty Acids Production in Meat Ducks. Front. Nutr. 9:860086. doi: 10.3389/fnut.2022.860086

Gut microbiota interfered with using prebiotics may improve bone mass and alleviate the onset of bone problems. This study aimed to investigate the beneficial effect of resistant starch from raw potato starch (RPS) on bone health in meat ducks. Response to the dietary graded level of RPS supplementation, both tibia strength and ash were taken out linear and quadratic increase and positively correlated with increased propionate and butyrate levels in cecal content. Moreover, further outcomes of gut microbiota and micro-CT analysis showed the beneficial effect of RPS on bone mass might be associated with higher Firmicutes proportion and the production of short-chain fatty acids (SCFAs) in the cecum. Consistent with improving bone mass, SCFAs promoted phosphorus absorption, decreased the digestive tract pH, and enhanced intestinal integrity, which decreased the expression of pro-inflammatory genes in both gut and bone marrow, and consequently depressed osteoclastic bone resorption mediated by inflammatory cytokines. These findings highlight the importance of the "gut-bone" axis and provide new insight into the effect of prebiotics on bone health.

Keywords: resistant starch, gut microbiota, SCFAs, bone mass, meat ducks

INTRODUCTION

Gait problem in livestock is a welfare issue with a prevalence of about 14–21% in commercial meat ducks, which affects mainly modified behavior and pain (1). Birds with leg weakness are difficult to access to the food and water, and thus the gait problems might compromise growth performance. In response to this, a complex interplay between pathological and nutritional factors contributes to the etiopathogenesis of leg abnormalities (2). Of note, gut microbiome dysbiosis has been observed in both osteoporosis patients and experimentally ovariectomized rodent models (3). Manipulating microbiota (e.g., establishing germ-free, oral antibiotics, probiotics, etc.) could interfere with bone remodeling and bone quality through acting on the immune system, endocrine system, and calcium (Ca) absorption (4, 5). For instance, comparing germ-free mice with conventionally raised mice showed that the presence of microbiota led to lower trabecular and cortical bone mass (6), which companies with reduced number of osteoclasts and lower level of interleukin (IL)-6,

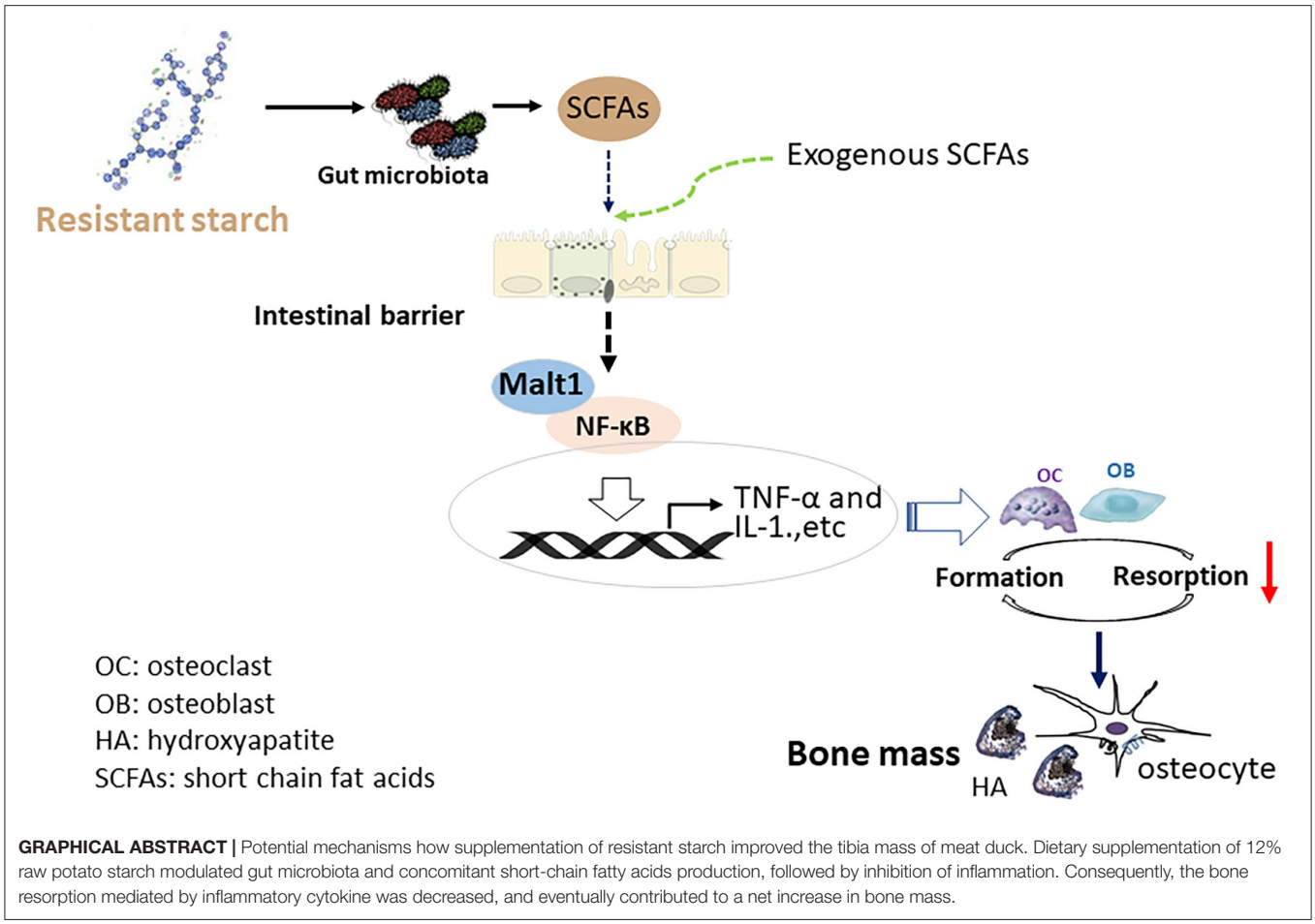

GRAPHICAL ABSTRACT | Potential mechanisms how supplementation of resistant starch improved the tibia mass of meat duck. Dietary supplementation of 12% raw potato starch modulated gut microbiota and concomitant short-chain fatty acids production, followed by inhibition of inflammation. Consequently, the bone resorption mediated by inflammatory cytokine was decreased, and eventually contributed to a net increase in bone mass.

receptor activator of nuclear factor-κ B ligand (RANKL), tumor necrosis factor-alpha (TNF-α), and $CD4^+$T cells in bone (7, 8).

Diet and microbial metabolism were noticed to interact with the intestinal barrier and mucosal immune system to affect the immune responses and inflammation (9), which is possible to modify bone mass (4). Reports from our recent studies have demonstrated that impaired intestinal barrier and increased expression of inflammatory cytokines in ileum and bone marrow resulted in inferior tibia material properties and bone mass, and these features were further reversed by dietary 25-hydroxycholecalciferol treatment (10). The addition of propionate, a kind of short-chain fatty acid (SCFA), significantly relieved bone erosion and improved bone quality in the right knees from collagen-induced arthritis mice (11). In this context, as a subgroup of dietary fiber, resistant starch (RS) has been receiving great attention due to its health benefits on disease processes prevention, including arthritis (11) and bone loss (12). In addition to altering the composition of the gut microbiota, as evidenced by increasing the proportion of Bifidobacterium, Lactobacillus, and Firmicutes (13), RS could be also used as substrates by bacterial species that reside in the hindgut to generate important metabolites, including SCFAs (14). Ongoing research has provided important evidence for the positive role of RS on gut epithelial integrity and anti-inflammatory functions (9). Especially, we noticed that dietary supplements with 12% raw potato starch (RPS) as the resource of type 2 RS can thicken the mucosal layer, tighten the gut barrier, and decreased intestinal inflammation in meat ducks (14, 15). Pieces of evidence from the estrogen deficiency model have described significant remission in bone loss of mice given by 12% RS by regulating the intestinal microbiota and bone-marrow inflammation (12, 16, 17). Nevertheless, it is unclear how the bone characteristics and gut microbiota can be precisely modified by dietary graded RS supplementation in meat ducks. In this study, therefore, the responses of bone metabolism, inflammation, and the composition of intestinal microbiota to different levels of dietary RS were evaluated in meat ducks. Additionally, the key molecular factors and potential mechanism that determined how RS improved the bone quality was also explored.

MATERIALS AND METHODS

Animals and Management

All experimental protocols were approved by the Animal Care and Use Committee of Henan Agricultural University and the animals were maintained in accordance with office guidelines for the care and use of laboratory animals. The 1-d-old Cherry Valley male ducks were purchased from Sichuan Mianying Breeding

Duck Co. Ltd. and were housed (0.16 m^2/bird) in a 12:12-h light-dark cycle room at 32°C for the 1–7 d, following which the temperature was decreased to 25°C at d 7 and 14. During the experiments, body weight, feed intake, and mortality were recorded, gain and feed conversion as the feed-to-gain ratio was calculated on a per-cage basis.

Trial Design

Experiment 1. To investigate the dose-dependent effect of RS on bone characteristics and intestinal integrity, ducklings were fed the same basal diets with 0, 6, 12, or 24% RPS for 14 days. Each group had 6 replicate pens with 15 ducks per pen. Four isonitrogenous and isocaloric diets were formulated under a digestible amino acid basis to meet the nutrient requirements of duck suggested in the National Nutrition Council (18) and our previous studies (14) (**Table 1**). RPS was purchased from AVEBE Ltd. and contains 54.72% RS content (dry matter basis). RS was analyzed and confirmed proper preparation of experimental diets.

Experiment 2. To define the relationship between SCFAs and bone turnover, birds at the day 1 were assigned to one of 3 trial groups (6 replicate pens; 15 ducks/pen) for 14 d as follows: (1) Birds were given 133.4 mM sodium chloride in drinking water and fed 0% RPS diets (salt-matched control, Ctrl); (2) Ducks consumed 133.4 mM sodium chloride in drinking water and 12% RPS diets; (3) Birds received SCFAs (67.5 mM sodium acetate, 38.8 mM sodium propionate, 22.8 mM sodium butyrate) in drinking water and fed 0% RPS diets. The proportion of SCFAs used in this study was based on previously reported (19) and kept the same ratio of acetate, propionate, and butyrate in the cecal content of meat duck fed 12% RPS diet in Experiment 1.

Data Collection and Sampling

On day 14, ducks were weighed after 8 h feed withdrawal. Two birds per pen with body weight close to the pen average were selected. One was anesthetized for blood sampling through the jugular vein. Then, the animals were sacrificed by cervical dislocation, and the length and weight of the full ileum were measured, the pH of the ileal content was registered using an automated pH probe (pH-STAR, SFK-Technology, Denmark). Digesta samples of cecum were randomly divided into 2 parts. One portion was stored at −20°C for SCFAs determination and the other was kept in liquid N_2 for 16S rDNA amplicon sequencing. In addition, the left tibia (the proximal end), bone marrow, duodenal and ileal mucosa were gained and stored at −80°C until further analysis. The right tibia was collected for tibia characteristics. Another was killed by cervical dislocation, and the left tibia (the proximal end) was gained for histological determination. Right tibias were removed for a Micro-CT scan after the removal of soft tissues.

Determination of Gut Permeability

Fluorescein isothiocyanate-dextran (FITC-d) was used as an indicator of gut permeability in this study. In detail, 15 days old birds were received orally FITC-d (4.16 mg/kg body weight), and blood was harvested after 2 h. Serum fluorescence was analyzed at an excitation/emission wavelength of 485/530 nm using a Gemini XPS Microplate Reader (Molecular Devices, LLC. Sunnyvale, CA, USA). The content of serum FITC-d was calculated from the standard curves generated by the serial dilution of FITC-d.

Analysis of Dietary RS

The RS content of diets was evaluated in accordance with AACC method 32-40.01 (20) using an assay kit (Megazyme International, Bray, Ireland). Briefly, non-resistant starch is solubilized and hydrolyzed to glucose by the combined action of pancreatic α-amylase and amyloglucosidase for 16 h at 37°C. The reaction is terminated by the addition of ethanol or industrial methylated spirits and RS is recovered as a pellet by centrifugation. RS in the pellet is dissolved in 2 mol/L KOH by vigorously stirring in an ice-water bath. This solution is neutralized with acetate buffer and the starch is quantitatively hydrolyzed to glucose with amyloglucosidase. Glucose is measured with glucose oxidase-peroxidase reagent, which is a measure of RS content.

Measurement of the Serum Indicator

The concentrations of cytokines including TNF-α, IL-1β, and IL-10 were determined using available ELISA kits (Meimian Biotechnology Co., Ltd, Jiangsu, China). The concentration of secretory immunoglobulin A (IgA) in the ileum was assayed using Chicken ELISA Quantitation Kits (Bethyl Laboratories Inc., Montgomery, USA). Serum Ca and phosphorus (P) concentrations were measured with Biochemistry Analyzer (Yellow Springs Instrument Co. Inc., Yellow Springs, OH). The circulation of bone turnover markers including alkaline phosphatase (ALP) activity, procollagen type I N-terminal propeptide (P1NP) level, tartrate-resistant acid phosphatase (TRAP) activity, and C-terminal cross-linked telopeptide of type I collagen (CTx) content were assayed by ELISA assay (Nanjing Jiancheng Bioengineering Institute, Nanjing, China) following the manufacturer's instructions. All samples were tested in triplicate within each assay.

Biochemical Indices of Mucosal Growth

Cell size and metabolic activity of ileal cells were estimated through measurements of mucosal protein, DNA, and RNA and the ratios between the 3 factors. The assay for these indices was performed using commercial kits (Nanjing Jiancheng Bioengineering Institute, Nanjing, China) according to the manufacturer's instructions.

16S RDNA Amplicon Sequencing of Cecal Microbiota

The total DNA in cecal content was extracted using a DNA stool mini kit (Qiagen, Valencia, United States) and was subjected to assess the integrity and size of DNA. Primers 515 F (5′-GTGYCAGCMGCCGCGGTAA-3′) and 806 R (5′-GGACTACHVGGGTWTCTAAT-3′) were used to amplify the hypervariable V3-V4 regions of the 16S rDNA gene. Then, the resulting PCR products were sequenced on an Illumina PE250 platform (BGI, Shenzhen, China). The obtained sequences were processed using FLASH (v1.2.11) and USEARCH (v7.0.1090) for alignment and clustering. All effective reads were clustered into

TABLE 1 | Dietary formulation and composition (as fed basis).

Item	Raw potato starch, % of diet weight			
	0	6	12	24
Ingredients, %				
Corn	59.82	52.33	44.85	29.88
Raw potato starch	0	6.00	12.00	24.00
Soybean meal	33.21	34.57	35.91	38.61
Soybean oil	0.50	1.00	1.50	2.50
Calcium carbonate	1.10	1.07	1.04	0.98
Dicalcium phosphate	1.74	1.78	1.82	1.89
L-Lysine-HCL	0.11	0.09	0.07	0.04
DL-Methionine	0.16	0.16	0.16	0.17
Threonine	0.02	0.01	0.01	0.01
Bentonite	2.36	2.01	1.66	0.94
Sodium chloride	0.30	0.30	0.30	0.30
Choline chloride	0.15	0.15	0.15	0.15
Vitamin premix1	0.03	0.03	0.03	0.03
Mineral premix2	0.50	0.50	0.50	0.50
Total	100.0	100.0	100.0	100.0
Calculated nutrient level, %				
Apparent metabolism energy, MJ/kg	11.71	11.69	11.72	11.74
Crude protein	19.45	19.51	19.49	19.55
Calcium	0.91	0.89	0.92	0.9
Non-phytate phosphorus	0.43	0.41	0.42	0.39
Digestibility lysine	1.03	0.92	0.97	0.99
Digestibility methionine	0.41	0.43	0.42	0.42
Analyzed nutrient level, %				
Resistant starch	2.76	4.84	7.51	18.16

[1] *Provided per kilogram of diet: Cu ($CuSO_4 \cdot 5H_2O$), 8 mg; Fe ($FeSO_4 \cdot 7H_2O$), 80 mg; Zn ($ZnSO_4 \cdot 7H_2O$), 90 mg; Mn ($MnSO_4 \cdot H_2O$), 70 mg; Se ($NaSeO_3$), 0.3 mg; I (KI), 0.4 mg.* [2] *Provided per kilogram of diet: retinol, 2.06 mg; cholecalciferol, 0.04 mg; vitamin E, 30.01 mg; thiamine, 1 mg; riboflavin, 3.9 mg; pyridoxine, 3.375 mg; vitamin B_{12}, 0.01 mg; calcium pantothenate, 8.85 mg; folate, 0.5 mg; biotin, 0.1 mg; niacin, 49.25 mg.*

operational taxonomic units (OTUs) with a similarity threshold of 97%. The representative sequence of each OTU was aligned against the Greengene database for taxonomy analysis. As for data analysis, alpha- and beta-diversity metrics were calculated using QIIME software and the R Vegan package. In detail, the alpha diversity was evaluated with MOTHUR at the genus level by calculating the Chao1 richness index (richness), reciprocal Simpson biodiversity index (diversity), and Simpson evenness index (evenness). Beta-diversity at the genus level was estimated by calculating Bray-Curtis dissimilarity and visualized with principal coordinates analysis (PCoA).

Determination of SCFAs Concentrations in Cecal Content

According to previously described (14), the cecal content (approximately 0.5 g) was diluted with 2 ml of ultrapure water mixed, deposited for 30 min, and centrifuged at 3,000*g* for 15 min, followed by 1 ml supernatants were mixed with 0.2 ml ice-cold 25% (w/v) metaphosphoric acid solution and incubated at 4°C for 30 min. After centrifuging at 11,000*g* for 10 min, the SCFAs contents including acetate, propionate, and butyrate were separated and determined by gas chromatograph (Varian CP-3800, USA).

Assessment of Tibia Microstructure Using Micro-CT

The microstructure of tibia metaphysis was measured using a GE Explore Locus Micro-CT (GE Healthcare, Piscataway, NJ, USA) at 90 kV with instrument settings optimized for calcified tissue visualization. The trabecular bone in the tibia metaphysis was performed starting from 9 mm below the surface of the condyles and extending 4 mm distally. Bone volume/total volume (BV/TV) and thickness (Tb.Th) of trabecular bone were calculated. The average thickness of the structures was measured using the thickness plugin from Bone J as our previous method following our recent methods (10).

Detection of Tibia Mass and Strength

The breaking force test was determined with a 3-point bending test using the texture analyzer (TA. XT Plus; Stable Microsystems) with a constant 50 kg load cell. The tibia sample was placed on 2 vertically parallel supports. Loading proceeded at a constant rate (5 mm/min) until a fracture occurred, and

the maximum load of the tibia was directly read from the peak value. Hereafter, fat-free weight was determined after extraction using ethyl ether for 48 h. Subsequently, the dry-defatted tibia was ashed in a muffle furnace at 550°C for 24 h and the ash was measured based on the percentage of dry-defatted weight.

TRAP Staining

The fixed proximal end of the tibia was decalcified in ethylene diamine tetraacetic acid solution, embedded, and sliced. The decalcified section was de-paraffinized, rehydrated, and subsequently incubated for 1 h at 37°C with TRAP staining solution, according to the manufacturer's protocol (Sigma-Aldrich, Inc., St. Louis, MO, USA). Histopathological images were collected using a microscope with image analysis software (Nikon Corporation, Tokyo, Japan). The numbers of osteoclast/number of bone surface (N.Oc/BS) with multinucleated cells (≥3 nuclei) were identified as TRAP-positive and were determined in 5 consecutive microscopic fields. At least 5 serial vertical sections were evaluated for each animal per analysis. The slides were counted by 2 examiners, who were blinded to group status.

Gene Expression Assays

RNA from ileal, duodenum, tibia, and bone marrow was extracted using Trizol (Invitrogen). After examining the integrity and concentration, the 200 ng of total RNA was reversely transcribed into cDNA. Quantitative real-time PCR was performed on the ABI 7900HT detection system (Applied Biosystems, CA, USA). Relative gene expression was quantified by normalizing the expression of *β-actin* and glyceraldehyde-3-phosphate dehydrogenase (*GAPDH*). The primer sequences for the target genes were designed using Primer 3 (**Table 2**).

Statistical Analysis

Statistical analyses were performed using SAS statistical software (version 9.2, SAS Institute, Cary, NC). After checking for normal distribution and equal variance using the Shapiro–Wilk and Levene's tests, respectively. The ANOVA followed by Tukey's *post-hoc* test was conducted to examine statistical significance. Polynomial contrasts of growth performance, ileal physiochemical parameter, SCFAs level, and bone characterizing the response to dietary RPS level were examined using linear and quadratic regression. Spearman's rank correlation coefficient test was used for assessing the association between the SCFAs content, tibia strength, and ash. Broken-line regression analysis was used to estimate the recommended level of dietary RPS supplementation using the non-linear regression (NLIN) procedure of SAS (SAS Institute). Data were expressed as mean and standard deviation (SD). The *p*-values less than 0.05 were considered significant.

RESULTS

Effects of Dietary Graded RPS on Growth Performance and Intestinal Physiochemical Environment

As shown in **Table 3**, dietary graded levels of RPS supplementation quadratically affected the body weight on day 14 ($p = 0.069$) and the feed conversion ratio expressed as feed to gain ratio during 1–14 days ($p < 0.001$). Notable changes in feed intake and mortality during all experimental periods were not observed among all groups. Therewith, the intestinal physiochemical environment was inferred from the ileal length, weight, relative weight, and pH, as well as cecal SCFAs (**Table 4**). The relative weight of ileum remarkably increased as supplemented dietary RPS level ($p = 0.023$). However, the administration of dietary RPS failed to change the length and absolute weight of ileum. The pH of ileal content showed a decreased trend in the 6, 12, and 24% RPS groups when compared with the 0% RPS diet. Regarding cecal SCFAs level, dietary RPS supplementation had no effect on acetate contents in the cecal digesta, whereas the contents of both propionate and butyrate in the cecum were taken out linear and quadratically increased response to the dietary graded concentration of RPS. When compared to the 0% RPS group, the diet with 12 and 24% RPS significantly increased the level of propionate and butyrate in the cecum ($p < 0.05$), implying that diet with 12 and 24% RPS promoted propionate and butyrate production in the cecum and tended to decrease the pH of the digestive tract.

Tibia Growth, Strength, and Ash Response to Dietary RPS Supplementation

Tibia growth was assessed through bone length, diameter, and fat-free weight, and there was no significant difference in the aforementioned parameters among all groups ($p > 0.05$; **Table 5**). As dietary supplemental RPS levels increased, tibia strength and ash content increased linearly and quadratically (**Table 5**). Furthermore, to understand the connections between SCFAs change and bone characteristics, the Broken-line regression analysis between dietary graded RPS levels and tibia mass was performed and showed that both tibia strength and ash were increased with dietary RPS intervention, where the recommended level of dietary RPS was 12.81 and 11.16% based on tibia strength and tibia ash, respectively (**Figures 1A,B**). Meanwhile, Pearson's correlation analysis among significantly changed propionate, butyrate, tibia strength, and ash was also conducted. As shown in **Figures 1C,D**, the tibia strength was positively correlated with an increasing level of propionate ($r = 0.391$, $p = 0.048$) and butyrate ($r = 0.463$, $p = 0.023$). In addition, the tibia ash content was also positively associated with the levels of butyrate ($r = 0.467$, $p = 0.021$), but not propionate ($p > 0.05$). Collectively, the dietary supplementation with 12% RPS could improve tibia quality in 14 days-old meat ducks, which might be associated with SCFAs production.

Dietary 12% RPS and Drinking SCFAs Improve Tibia Quality Associated With Inhibited Bone Resorption and Increased P Absorption

To further determine whether SCFAs produced by RPS-associated gut bacteria are the pivotal factors contributing to the improvement of tibia mass in meat ducks, the exogenous addition of SCFAs in drinking water was used and showed that the experimental treatments did not apparently change the daily water consumption, body weight on the day 14, feed intake

TABLE 2 | The primers for quantitative real-time PCR.

Gene	Gene ID	Primer	Sequence (5′-3′)	Size (bp)
OPG	XM_005017709.3	Reverse	gcctaactggctgaacttgc	106
		Forward	gaaggtctgctcttgcgaac	
RANKL	XM_021276016.1	Reverse	gccttttgcccatctcatta	100
		Forward	taagtttgcctggcctttgt	
ZO-1	XM_013104939.1	Reverse	tacgcctgtgaagaatgcag	86
		Forward	ggagtggtggtgtttgcttt	
Occludin	XM_013109403.1	Reverse	caggatgtggcagaggaatacaa	160
		Forward	ccttgtcgtagtcgctcaccat	
Claudin 1	XM_013108556.1	Reverse	tcatggtatggcaacagagtgg	179
		Forward	cgggtgggtggataggaagt	
Malt1	XM_027446455.2	Reverse	ccatggaaaccgtacttgct	118
		Forward	ttgtgcaggggattggtaat	
NF-κB	XM_027455993.1	Reverse	gagcgttttcaagaggttgc	123
		Forward	agggatcttctcctgccatt	
TNF-α	EU375296.1	Reverse	agatgggaagggaatgaacc	51
		Forward	gttggcataggctgtcctgt	
IL-1β	DQ393268.1	Reverse	gcatcaagggctacaagctc	131
		Forward	caggcggtagaagatgaagc	
IL-6	AB191038.1	Reverse	atctggcaacgacgataagg	87
		Forward	ttgtgaggagggatttctgg	
IL-17	EU366165.1	Reverse	atgcctgacccaaaaagatg	145
		Forward	gtggtcctcatcgatcctgt	
IL-18	XM_027444356.2	Reverse	ctgatgacgatgagctggaa	120
		Forward	caaaagctgccatgttcaga	
GPR41	KJ523111.1	Reverse	actgacgtcctcctcctcaa	160
		Forward	tggtgaggtagatgctggtg	
GPR43	KJ523110.1	Reverse	agcagctgagctttgtcctc	129
		Forward	gtggaatattaggccgagca	
NaPi-IIb	NM_204474.3	Reverse	gctccagcacttcttcatcc	95
		Forward	aatgtttgccccataatga	
Calbindin 1	XM_027452451.2	Reverse	cagggtgtcaaaatgtgtgc	109
		Forward	gatccttcagcagtgcatca	
β-actin	NM_001310408.1	Reverse	ccagccatctttcttgggta	105
		Forward	gtgttggcgtacaggtcctt	
GAPDH	XM_005016745.3	Reverse	tttttaaccgtggctccttg	94
		Forward	actgggcatggaagaacatc	

OPG, osteoprotegerin; RANKL, receptor activator of nuclear Factor-κ B ligand; ZO-1, zonula occludens; Malt1, mucosa-associated lymphoid tissue lymphoma translocation protein 1; NF-κB, nuclear factor kappa B; TNF-α, tumor necrosis factor alpha; IL, interleukin; GPR, G protein-coupled receptor; NaPi-IIb, sodium-dependent phosphorus transport protein IIb; GAPDH, glyceraldehyde-3-phosphate dehydrogenase.

TABLE 3 | Effect of dietary raw potato starch (RPS) supplementation on growth performance for meat ducks.

Item	RPS, % of diet weight				*P*-value		
	0	6	12	24	ANOVA	Linear	Quadratic
Body weight at 14 d, g/bird	552.51 ± 27.94	592.1 ± 16.46	596.89 ± 20.86	578.86 ± 28.35	0.056	0.236	0.069
Feed intake during 1–14 d, g/bird	654.81 ± 3.24	655.78 ± 2.89	656.18 ± 2.94	654.57 ± 3.22	0.773	0.801	0.565
Feed intake: gain during 1–14 d, g/g	1.19 ± 0.06	1.11 ± 0.04	1.10 ± 0.04	1.22 ± 0.06	0.063	0.229	<0.001
Mortality during 1–14 d, %	3.33 ± 5.58	2.22 ± 3.44	1.11 ± 2.72	2.22 ± 3.44	0.813	0.635	0.626

TABLE 4 | Effect of dietary raw potato starch (RPS) supplementation on the ileal physiochemical environment and cecal short chain fat acids (SCFAs) level in 14 day-old meat ducks.

Item	RPS, % of diet weight				*P*-value		
	0	6	12	24	ANOVA	Linear	Quadratic
Ileum							
Length, cm	62.43 ± 1.54	65.34 ± 1.52	65.30 ± 3.08	64.71 ± 3.44	0.191	0.265	0.118
Weight, g	7.81 ± 0.47	7.92 ± 0.33	8.27 ± 0.47	8.38 ± 0.63	0.165	0.031	0.091
Relative weight, % body weight	1.43 ± 0.13^{b}	1.35 ± 0.09^{b}	1.39 ± 0.06^{ab}	1.56 ± 0.17^{a}	0.025	0.029	0.009
pH	6.82 ± 0.23	6.58 ± 0.35	6.43 ± 0.31	6.34 ± 0.35	0.068	0.012	0.026
Cecal SCFAs, μmol/g							
Acetate	55.55 ± 6.21	57.25 ± 7.28	58.44 ± 5.82	60.4 ± 5.72	0.602	0.166	0.386
Propionate	27.23 ± 3.65^{b}	30.6 ± 3.16^{ab}	33.55 ± 2.67^{a}	32.77 ± 3.73^{a}	0.017	0.013	0.006
Butyrate	13.80 ± 2.83^{b}	16.53 ± 4.18^{ab}	19.69 ± 2.52^{a}	19.65 ± 2.35^{a}	<0.001	0.003	0.029

^{a,b}*Mean values with different letters are significantly different by one-way analysis of variance followed by Tukey's post-hoc test ($p < 0.05$).*

TABLE 5 | Effect of dietary RPS supplementation on the tibia characterizes of 14 day-old meat ducks.

Item	RPS, % of diet weight				*P*-value		
	0	6	12	24	ANOVA	Linear	Quadratic
Tibia growth							
Length, mm	72.63 ± 2.46	72.62 ± 2.35	73.08 ± 2.58	73.01 ± 2.81	0.983	0.640	0.734
Diameter, mm	5.51 ± 0.27	5.57 ± 0.35	5.65 ± 0.20	5.59 ± 0.33	0.887	0.745	0.941
Fat-free weight, g	1.50 ± 0.16	1.57 ± 0.35	1.67 ± 0.17	1.76 ± 0.27	0.305	0.056	0.159
Tibia quality							
Strength, *N*	173.08 ± 16.37^{b}	166.01 ± 12.34^{b}	193.52 ± 9.27^{a}	191.17 ± 15.75^{a}	0.015	0.012	0.040
Ash, g/g fat-free weight	0.52 ± 0.03	0.56 ± 0.05	0.58 ± 0.02	0.59 ± 0.06	0.053	0.021	0.020

^{a,b}*Mean values with different letters are significantly different by one-way analysis of variance followed by Tukey's post-hoc test ($p < 0.05$).*

during 1–14 days, and tibia length and diameter at the day 14 (**Figures 2A–C**). As expected, as compared with the Ctrl group, both dietary 12% RPS and drinking SCFAs notably increased tibia strength and BV/TV of the proximal tibia ($p < 0.05$). Similarly, dietary 12% RPS supplementation and drinking SCFAs treatment increased tibia ash to varying degrees, although Tb.Th trabecular among these groups did not differ (**Figures 2D–G**), suggesting that dietary 12% RPS addition improved the bone mass of meat ducks might be involved in SCFAs production.

Effects of dietary 12% RPS and drinking SCFAs administration on bone resorption were assessed histologically and biochemically. TRAP-positive cells were distinctly observed in Ctrl birds (**Figure 3A**). N.Oc/BS was reduced by approximately 32 and 35% by the dietary 12% RPS and drinking SCFAs intervention, respectively (**Figure 3B**). Circulating bone resorption markers, TRAP and CTx, were decreased by dietary 12% RPS and drinking SCFAs treatment (**Figures 3C,D**). We then examined the mRNA expression of osteoclastogenesis-related factors in bone, the experimental treatments did not significantly alter the mRNA level of osteoprogerin (*OPG*), whereas both dietary 12% RPS and drinking SCFAs addition decreased the expression of *RANKL* mRNA to varying degrees ($p < 0.05$), thereby decreased the *RANKL*/*OPG* ratio (**Figure 3E**). Additionally, bone formation was also assessed by serum biochemical parameters. The serum ALP activity was numerically increased by dietary 12% RPS and drinking SCFAs ($p > 0.05$; **Figure 3F**). No appreciable changes in the P1NP concentrations were observed among the 3 groups (**Figure 3G**). Moreover, the effects of drinking SCFAs and dietary 12% RPS on Ca and P absorption were shown in **Figure 3H**. Serum P concentration tends to increase due to dietary 12% RPS treatment and was notably elevated by drinking SCFAs, whereas serum Ca concentration was unaffected ($p > 0.05$). No difference was observed in terms of the mRNA expressions of *calbindin-1* and sodium-dependent phosphorus transport protein IIb (*NaPi-IIb*) in the duodenum. However, dietary 12% RPS and drinking SCFAs treatment resulted in a remarkable increase in the transcription of *NaPi-IIb* in jejunum when compared with the Ctrl group ($p < 0.05$; **Figure 3I**). Taken together, these results suggest that feeding the 12% RPS diet improves tibia quality associated with inhibited bone resorption and increased P absorption.

Dietary 12% RPS and Drinking SCFAs Treatment Increase the Abundance of Firmicutes and Promote Concomitant SCFAs Production

Concerning the effects of the RPS and exogenous SCFAs administration on the caecal microbiome, the alpha diversity was significantly increased by experimental treatment, indicated by higher Shannon and Simpson indexes in both RPS- and

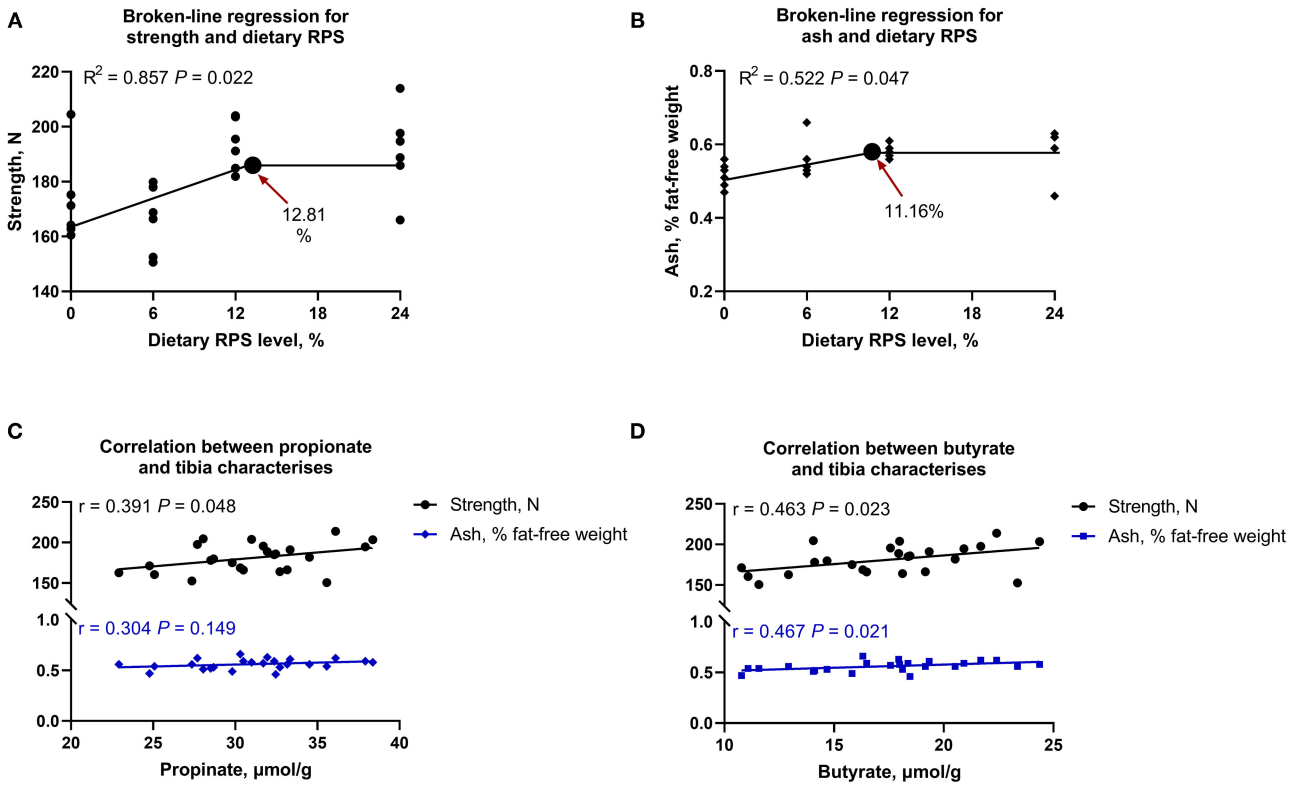

FIGURE 1 | The recommended level of dietary raw potato starch (RPS) based on broken-line analysis of **(A)** tibia strength and **(B)** ash content, as well as Pearson's correlation **(C)** between tibia strength and ash and propionate level in cecal content, and **(D)** between tibia strength and ash and butyrate level in cecal chyme.

SCFAs-treated ducks than it in the Ctrl birds, although with comparable Chao index among three groups (**Figures 4A–C**). Diversity metrics that utilize species richness and evenness (Bray-Curtis) showed a statistically apparent separation between the dietary 12% RPS and Ctrl groups, and the profile of group dietary 12% RPS was partly overlapped with that of the drinking SCFAs group (**Figure 4D**). In addition, remarkable differences in microbial composition were also demonstrated in the phylum-level distribution patterns (**Figure 4E**). Compared with the Ctrl group, dietary 12% RPS and drinking SCFAs intervention notably promoted the abundance of Firmicutes and meanwhile decreased the content of Bacteroidetes (**Figures 4F,G**). Besides, the outcomes from quantifying SCFAs in cecal content showed that the administration of dietary 12% RPS and drinking SCFAs failed to change the proportion of acetate, whereas they increased the concentration of propionate and butyrate at different levels (**Figure 4H**). Reflecting the mRNA expressions of SCFA receptors including *GPR41* and *GPR43* in the ileum and bone marrow, which were significantly upregulated by dietary 12% RPS and drinking SCFAs treatment in the ileum but not bone marrow as compared with the Ctrl groups (**Figure 4H**).

Effect on Intestinal Barrier and Biochemical Indices of Mucosal Growth

A direct comparison of the concentration of FITC-d suggests that supplementation of dietary 12% RPS and drinking SCFAs significantly decreased intestinal permeability, evidenced by lower serum FITC-d concentration than it in the Ctrl group (**Figure 5A**). Further examination of tight junction proteins (TJPs) confirmed that the expressions of *occludin*, zonula occludens-1 (*ZO-1*), and *claudin-1* were numerically upregulated by the administration of dietary 12% RPS and drinking SCFAs as compared to Ctrl birds (**Figure 5B**). As far as mucosal growth of ileum is concerned, when compared with the Ctrl birds, higher DNA content and protein/RNA ratio, as well as a lower protein/RNA ratio of the ileal mucosal homogenate were observed in ducks that received a 12% RPS diet and drinking SCFAs addition (**Figures 5C–E**). Together, these data suggest that supplementation with a 12% RPS diet and drinking SCFAs enhanced intestinal barrier function.

Dietary 12% RPS and Drinking SCFAs Addition Alleviated Inflammatory Reaction in Both Gut and Bone Marrow

Analyses of ileum pro- and anti-inflammatory cytokine expression revealed that the manipulation of dietary 12% RPS and drinking SCFAs notably decrease the *TNF-α*/*IL-10* ratio in the ileum ($p < 0.05$; **Figure 6A**), whereas these treatments did not obvious change the ileal sIgA level as compared with Ctrl group (**Figure 6B**). With comparable *IL-1β* and *IL-10* content, the ducks that were given a 12% RPS diet and drinking SCFAs

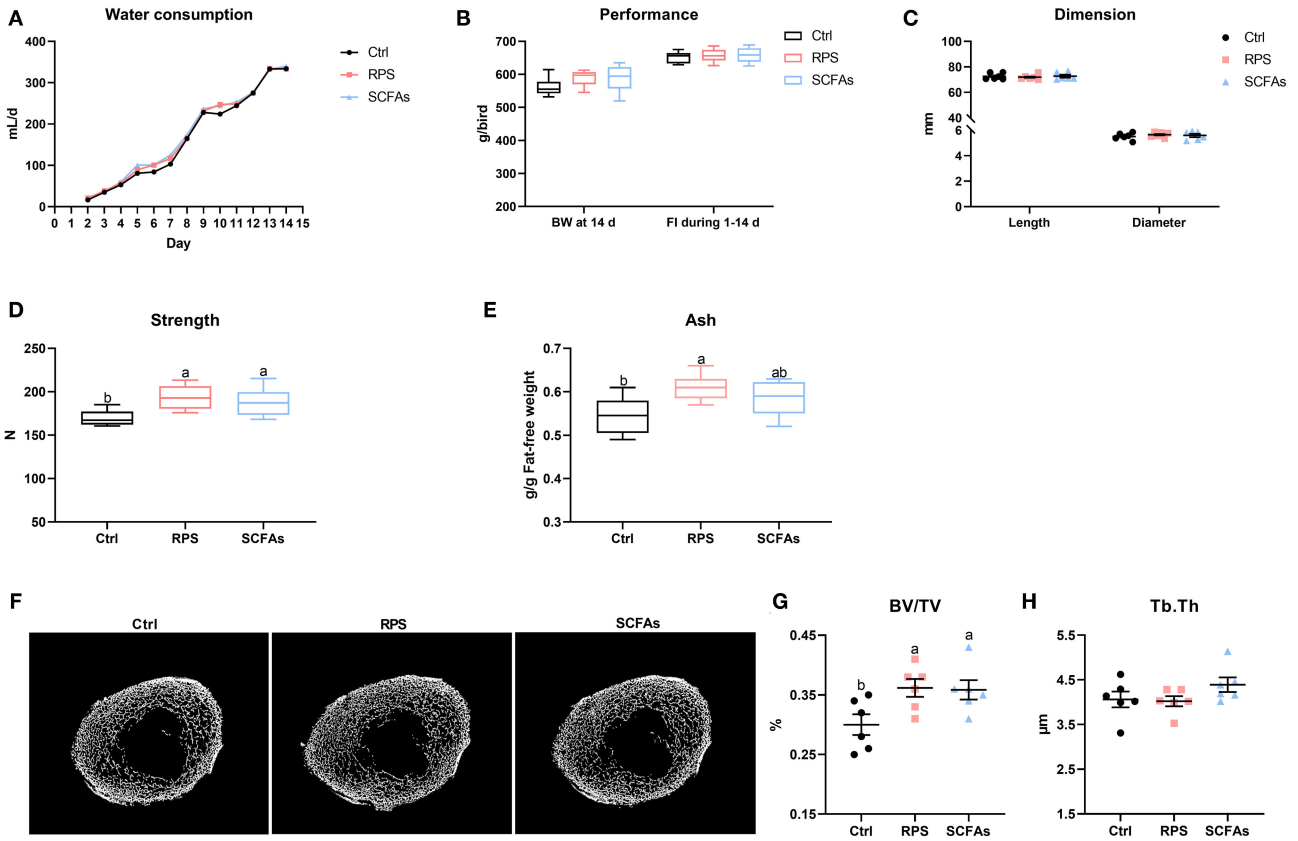

FIGURE 2 | Dietary RPS and drinking short chain fatty acids (SCFAs) addition improve tibia mass in meat ducks. **(A)** Water consumption, **(B)** performance including body weight at 14 day and feed intake during 1–14 days, and **(C)** tibia length and diameter were determined. The bone quality was indicated by **(D)** tibia strength and **(E)** ash. **(F)** Representative micro CT images and the quantification of **(G)** bone volume/total volume (BV/TV) and **(H)** trabecular thickness (Tb.Th) of the proximal tibia. Data are expressed as mean and standard deviation. [a,b] Mean values with different letters are significantly different by one-way analysis of variance followed by Tukey's *post-hoc* test ($p < 0.05$).

exhibited lower serum TNF-α content relative to Ctrl birds (**Figure 6C**). In the bone marrow, the higher mRNA levels of *TNF-α*, *IL-1β*, nuclear factor-κB (*NF-κB*), and mucosa-associated lymphoid tissue lymphoma translocation protein 1 (*Malt1*) in Ctrl birds were decreased by the 12% RPS diet and drinking SCFAs addition. In contrast, the mRNA expressions of *IL-17* and *IL-10* were similar among all groups (**Figure 6D**). Thus, these data suggest that manipulation of dietary 12% RPS and drinking SCFAs was accompanied by a notably decreased inflammation in the gut and bone marrow.

DISCUSSION

Increasing numbers of studies demonstrate a role for the gut microbiota, as well as its composition in the regulation of bone health (21). Here, using 16S rDNA sequencing and micro-CT techniques, this research characterized the gut microbial alteration in response to dietary RS supplementation from RPS and explored a potential connection between prebiotic intervention and bone mass. Our finding showed that the intake of dietary 12% RPS improves tibia quality in meat ducks by modulating gut microbiota and promotes concomitant propionate and butyrate production.

Previous reports in mice have evidenced the protective effects of dietary RS against bone loss induced by estrogen deficiency (12) and collagen-induced arthritis (11). It is, therefore, plausible that appropriate dietary RS supplementation might alleviate the gait problems for meat ducks, in which the prevalence of gait abnormalities is about 14–21% in commercial duck populations (1). With this aim, the different levels of dietary RPS were assessed and showed that both tibia strength and tibia ash were increased with dietary RPS intervention, where the recommended level of dietary RPS was 12.81 and 11.16% for optimizing tibia strength and ash based on broken-line regression analysis, respectively. One of the potential mechanisms underlying the beneficial role on bone quality may attribute to the intestinal microbiota and concomitant SCFAs production (4, 11). In fact, as a subgroup of dietary fiber, RS can be used as substrates by bacterial species to produce some fermented products such as SCFAs (14). Several studies have characterized the capacity of RS to induce alterations in the composition of the gut microbiota, including the increases in Bifidobacterium, Lactobacillus, and

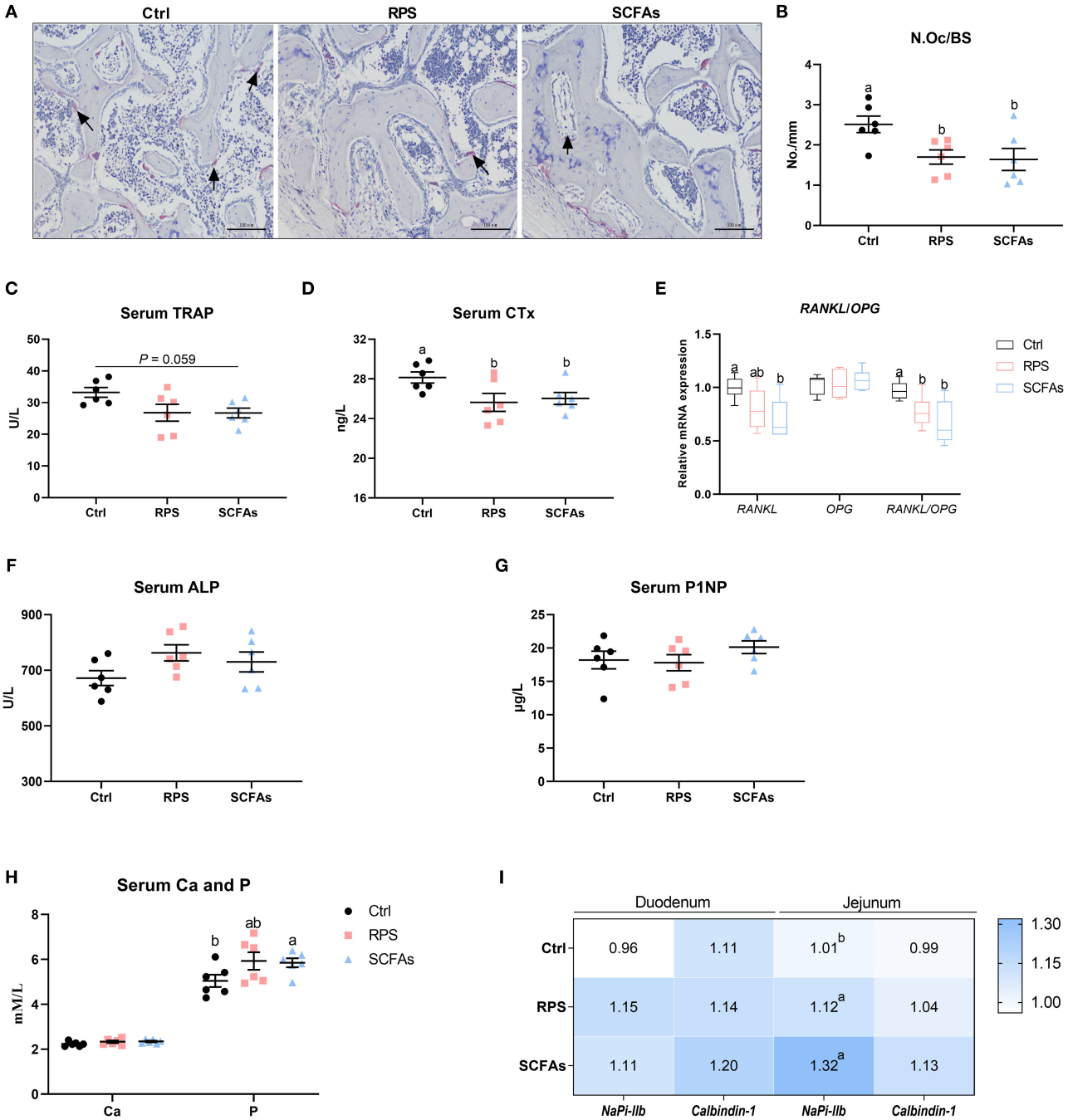

FIGURE 3 | Dietary RPS and drinking SCFAs administration suppressed osteoclastic bone resorption and induced phosphorus (P) absorption in meat ducks. **(A)** Tartrate resistant acid phosphatase (TRAP) staining of tibial sections. Bar = 100 μm. **(B)** The number of osteoclast (N.Oc/BS) in proximal tibias was determined by histomorphometry. Circulating **(C)** TRAP activity and **(D)** C-terminal cross-linked telopeptide of type I collagen (CTx) concentrations. **(E)** Real-time (RT)-PCR analysis for mRNA expression of receptor activator for nuclear factor-κB ligand (*RANKL*) and osteoprogerin (*OPG*) in the proximal end, and the ratio of *RANKL*/*OPG* was calculated. Serum bone formation including **(F)** procollagen type I N-terminal propeptide (P1NP) and **(G)** alkaline phosphatase (ALP) level, as well as **(H)** serum calcium (Ca) and phosphorus (P) concentration were evaluated. **(I)** The mRNA abundance of RT-PCR analysis for mRNA expression of sodium-dependent phosphorus transport protein II (*NaPi-IIb*) and *calbindin-1* in duodenum and ileum. Data are expressed as mean and SD. [a,b] Mean values with different letters are significantly different by one-way analysis of variance followed by Tukey's *post-hoc* test ($p < 0.05$).

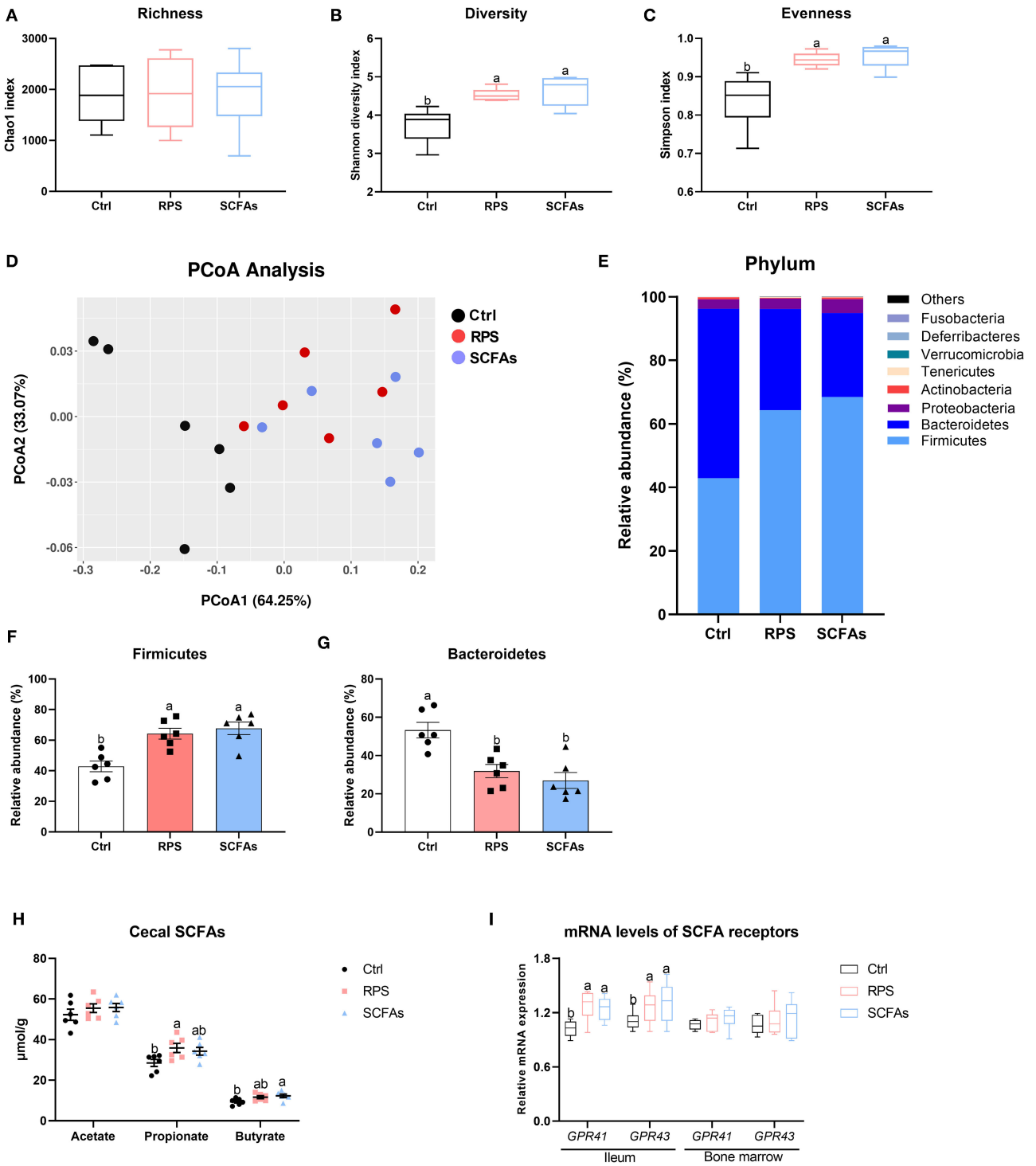

FIGURE 4 | Dietary RPS and drinking SCFAs change the microbiota composition and promote concomitant SCFAs production in the cecum of meat ducks. **(A–C)** Chao1, Shannon, and Simpson indexes were used to assess diversity and evenness of gut microbiota. **(D)** Principle coordinate analyses (PCoA) of beta diversity based on Bray-Curtis dissimilarities of bacterial operational taxonomic units. **(E)** Relative phylum level abundance of gut bacteria. The proportion of **(F)** Firmicutes and **(G)** Bacteroidetes. **(H)** SCFAs production and **(I)** SCFA receptor gene expression including G protein-coupled receptors 41 (*GPR41*) and *GPR43* in the ileum and bone marrow. Data are expressed as mean and standard deviation. ^{a,b} Mean values with different letters are significantly different by one-way analysis of variance followed by Tukey's *post-hoc* test ($p < 0.05$).

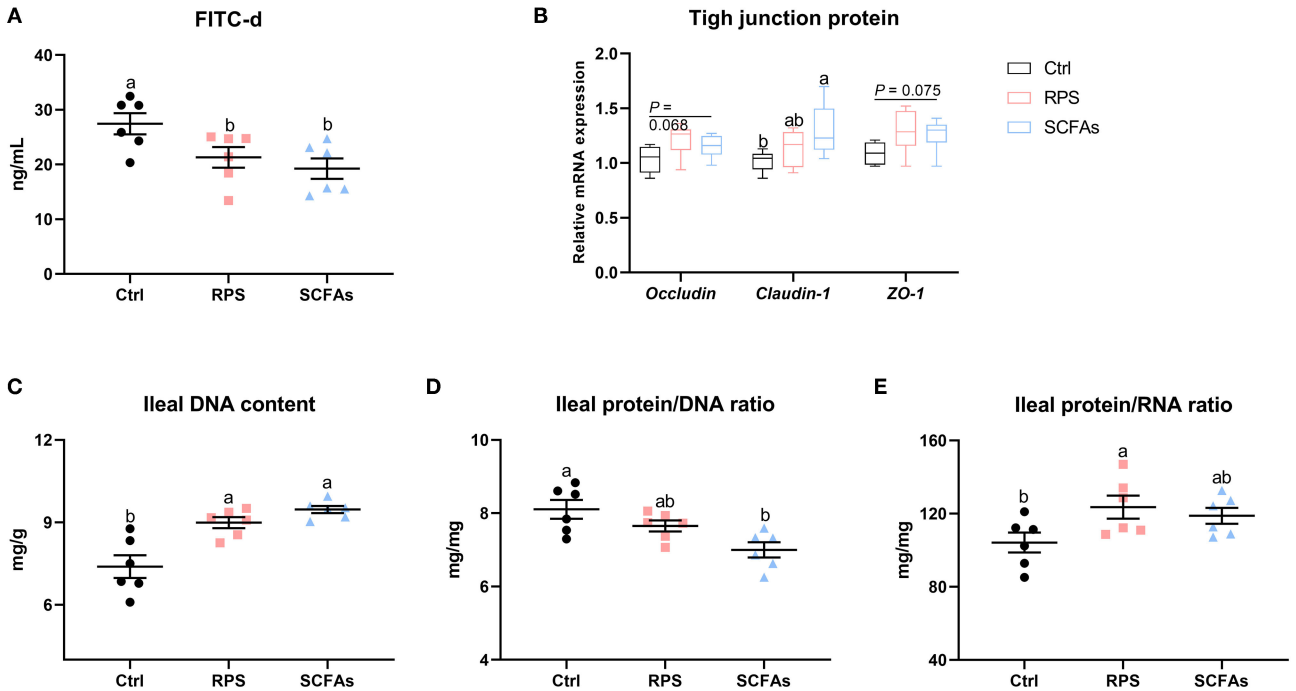

FIGURE 5 | Dietary RPS and drinking SCFAs enhance intestinal barrier and biochemical indices of mucosal growth. Intestinal integrity was assessed by **(A)** direct measurement using fluorescein isothiocyanate dextran (FITC-d) and **(B)** the mRNA level of tight junction proteins including *occluding*, *caudin-1*, and zona occludens-1 (*ZO-1*). Biochemical indices of mucosal growth including **(C)** DNA content, **(D)** protein/RNA ratio, and **(E)** protein/RNA ratio of the ileal mucosal homogenate were assessed. Data are expressed as mean and standard deviation. ^{a,b} Mean values with different letters are significantly different by one-way analysis of variance followed by Tukey's *post-hoc* test ($p < 0.05$).

Bacteroides (13). More importantly, it has been suggested that SCFAs generated from prebiotics could regulate the intestinal and systemic inflammation reaction, thereby alleviating bone metabolism (22), which was further supported by our data. In the present study, the dietary graded level of RPS supplementation linearly and quadratically increased the contents of propionate and butyrate in the cecum digest and positively correlated with tibia strength and ash to varying degrees, respectively.

How do alterations in gut microbiota and concomitant SCFAs production induced by dietary RS promote bone mass? It was established that dysbiosis has been associated with bone loss in patients and experimentally ovariectomized rodent models (3) and manipulating intestinal microbiota *via* oral antibiotics and production germ-free mice could apparently affect bone quality in rodent models (6, 23). In this study, along with the improvement of tibia strength, ash, and BV/TV of proximal bone, the dietary 12% RPS treatment significantly affected the microbial composition demonstrated by the higher proportion of Firmicutes and the lower the abundance of Bacteroidetes, which multiplied proven by our team previous studies (14). In this regard, published literature pointed out that reduced Firmicutes/Bacteroidetes ratio was linked with declined bone loss of mice (24). An increase in the proportion of Firmicutes and a decrease in Bacteroidetes due to dietary RS intervention was critical correlations with the aggravation in disease manifestations in collagen-induced arthritis mice (11). These discrepancies might interpret into that the regulation of gut microbiota on bone is not only attributed to the ratio of Firmicutes and Bacteroidetes, but also the generation of fermentation, especially SCFAs. Indeed, Firmicutes bacteria produce high amounts of butyrate and propionate, such as *Faecalibacterium prausnitzii*, *Roseburia sp.*, and *Eubacterium rectale*, whereas Bacteroidetes bacteria produce high levels of acetate and propionate (25, 26). Accordingly, in the current study, the elevated content of Firmicutes resulted in a higher concentration of propionate and butyrate in cecal chyme that is consistent with our previous observations (14). Therefore, it is possible that the SCFAs but not the Firmicutes/Bacteroidetes ratio might act as the primary mediators to promote tibia property in meat ducks.

To further determine whether SCFAs produced by dietary RS-associated gut bacteria are the pivotal factors contributing to the improvement of tibia quality in meat ducks, the direct addition of SCFAs into drinking water was used in the present study. Analogous to dietary 12% RPS-treated birds, SCFAs-treated ducks had higher tibia strength, ash, and BV/TV compared to Ctrl ducks. The addition of propionate was also observed to significantly restore bone erosion and bone loss in the right knees from collagen-induced arthritis mice (11). Considering the role of SCFAs in promoting gut development through stimulating the secretion of glucagon-like peptide (GLP)-1 and GLP-2 from

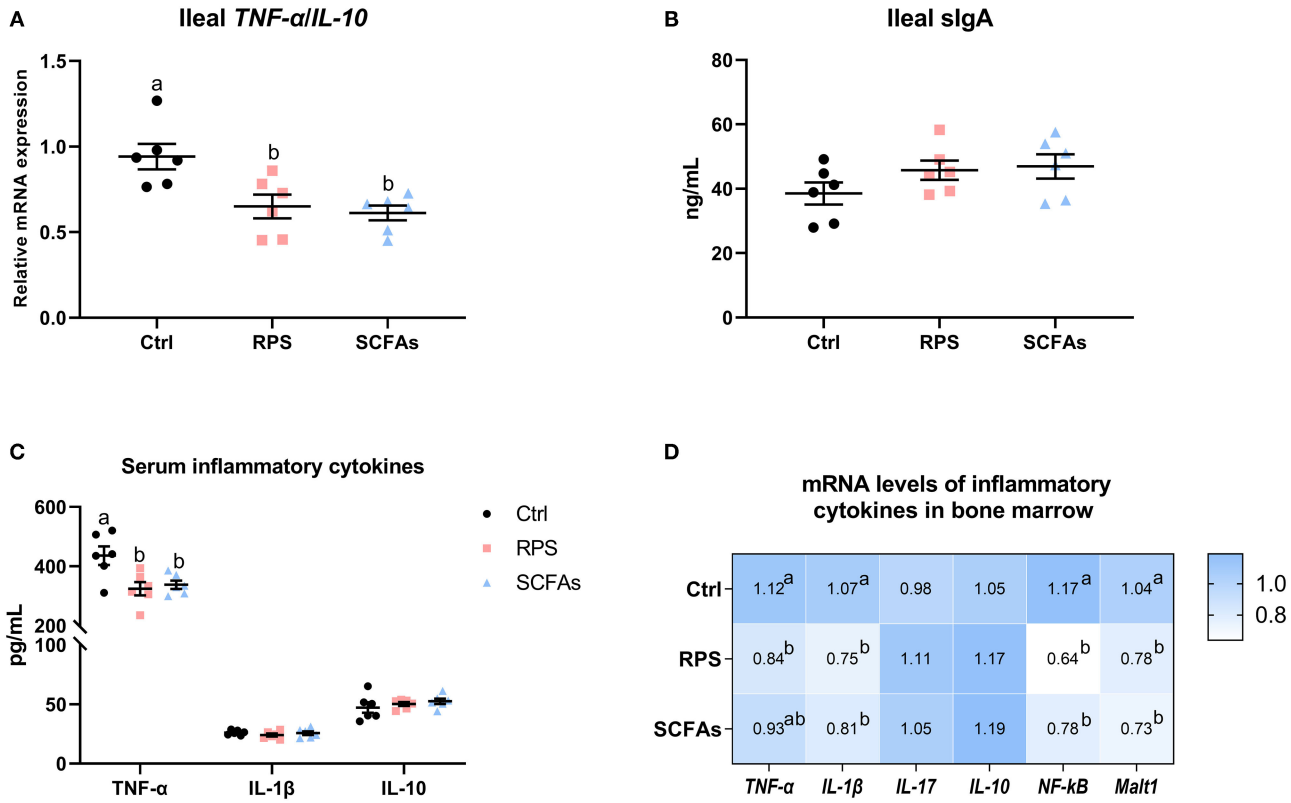

FIGURE 6 | Dietary RPS and drinking SCFAs are associated with alleviative inflammatory reactions. **(A)** The ratio of tumor necrosis factor alpha (*TNF-α*) and interleukin (*IL*)-*10*, and **(B)** the content of secretory immunoglobulin A (IgA) in the ileum. **(C)** The levels of TNF-α, IL-1β, and IL-10 in serum from different groups. **(D)** The mRNA expression of inflammatory cytokines in bone marrow including *TNF-α*, *IL-1β*, *IL-17*, *IL-10*, nuclear factor-κB (*NF-κB*), and mucosa-associated lymphoid tissue lymphoma translocation protein 1 (*Malt1*). Data are expressed as mean and standard deviation. ^{a,b} Mean values with different letters are significantly different by one-way analysis of variance followed by Tukey's *post-hoc* test ($p < 0.05$).

enteroendocrine L cells (27, 28), enhancing barrier function to suppress bone resorption mediated by inflammation probably is a critical contributor for dietary 12% RPS diets promoting bone strength and mass. As expected, in response to the increased levels of butyrate and propionate, SCFAs receptors *GPR41* and *GPR43* in ileum were notably upregulated by dietary 12% RPS like the effects of drinking SCFAs in this study. Subsequently, the biochemical indices of mucosal growth were estimated through measurements of mucosal protein, DNA, and RNA and the ratios between the three factors. In detail, changes in DNA reflect variations in cell population because the DNA content of diploid cells remains unchanged after cell formation. The ratio of protein/DNA is an indicator of cell size, while the ratio between protein and RNA measures the rate of protein synthesis (29). In the present study, higher DNA content and protein/RNA ratio, and lower protein/RNA ratio of the ileal mucosal homogenate implies that the administration with a 12% RPS diet and drinking SCFAs promoted the proliferation and activity of intestinal cells. As a result, we noticed that the addition of dietary 12% RPS enhanced the intestinal barrier of meat ducks, evidenced by lower serum FITC-d concentration and upregulated mRNA level of TJPs.

Alterations of intestinal permeability have been associated with bone loss in diseases such as inflammatory bowel disease (30). Under the condition of impairing gut integrity, bacteria and their factors probably translocate across the intestinal barrier to induce systemic inflammatory responses (31). Our recent studies have also demonstrated that impaired intestinal barrier and increased expression of inflammatory cytokines in ileum and bone marrow resulted in inferior tibia material properties and bone mass, which were further reversed by dietary 25-hydroxycholecalciferol treatment (10). In the present study, using the ileum TNF-α/IL-10 ratio as a marker of the balance between a pro- vs. anti-inflammatory state found that dietary 12% PRS and drinking SCFAs addition decreased the ileal inflammation, which accompanied with lower serum TNF-α level. Of note, dietary 12% RPS treatment also downregulated the mRNA expression of *Malt1*, *NF-κB*, *TNF-α*, and *IL-1β* in the bone marrow. The production of proinflammatory cytokines is governed by NF-κB signaling that dependent on the involvement of Malt1. Malt1 plays a key role in innate and adaptive immunity as a scaffold to activate the NF-κB signaling or exert a proteolytic activity to fine-tune gene expression in myeloid cells and non-immune cells (32). Inhibiting Malt1 could prevent the activation of NF-κB signaling

thus reducing IL-1β and IL-18 secretion in mice (33). Therefore, these results suggest that dietary 12% RPS supplementation decreased the secretion of the pro-inflammatory cytokine which might be due to the inactivation in Malt1/NF-κB signaling. In particular, receptors to SCFAs are highly expressed on innate immune cells, especially neutrophils, and function as an "anti-inflammatory chemoattractant receptor" (34), implying that the alteration in microbiota composition that allows for SCFAs production function may modulate neutrophil recruitment during inflammatory responses. The linking of inflammation and bone metabolism has been well defined (35). For instance, mice with TNF-α induced arthritis and possessed increased osteoclast precursors in serum, and subsequently was reversed by anti-TNF-α therapy and correlated with systemically increased TNF-α concentrations (36). The germ-free mice with higher trabecular and cortical bone mass were also characterized by a reduced number of osteoclasts and lower level of IL-6, RANKL, TNF-α, and CD4+ T cells in bone marrow when compared with conventionally raised mice (7, 8). Meanwhile, in the current study, while increasing bone ash and strength, we also found that dietary 12% RPS inclusion reduced N.Oc/BS, circulating TRAP, and CTx level, as well as the *RANKL* mRNA level and the *RANKL*/*OPG* ratio. Of note, RANKL binds to RANK that is expressed on the surface of osteoclast to induce osteoclast differentiation, whereas OPG acts as a decoy receptor by blocking the interaction of RANKL with its functional receptor RANK (37). The downregulated *RANKL* expression and thereby declined *RANK*/*OPG* ratio in dietary 12% RPS fed-birds probably explained the reduced osteoclast number in the tibia. In accordance with previous research saying that dietary RS could attenuate the bone loss in ovariectomized mice (12, 16, 17), this study also further confirmed that dietary 12% RPS supplementation inhibited the bone resorption and improved tibia mass and strength in meat ducks.

Another potential mechanism by which dietary 12% RPS enhanced bone quality might be related to P absorption. Increased SCFAs concentration produced by RPS fermentations tends to acidify the intestinal environment and facilitate mineral retention such as Ca and total P. In the present study, Ca content in serum did not influence by experimental treatments, whereas serum P concentration was increased due to dietary 12% RPS and drinking SCFAs administration, which was probably attributed to the upregulated transcription of *NaPi-IIb*, a regulator of P transport in the intestine (38). Studies in broiler chicken also confirmed that declining the pH of the gastrointestinal tract produced better ileal nutrient digestibility and improved P absorption (39). Analogous to SCFAs, the organic acid supplementation together with the developing desirable gut microflora was deemed to contribute to mineral retention and bone mineralization through increased digestibility and availability of nutrients (40). Accordingly, remarkably higher Ca and P blood concentrations were observed in chicks fed a diet supplemented with organic acids such as acetic, citric, and lactic acid, and further demonstrated that the beneficial effects of organic acids were caused by the lowering of gut pH and the increase in the absorption of these macro-elements (41). By contrast, manipulation with a 3% inclusion of citric acid in diet did not change blood Ca and P concentrations in broiler chickens (42). These variations or comparable serum Ca content in this study might be regarded to feed ingredients or/and the endocrine regulation for maintaining the homeostasis of Ca and P (43).

There are three new questions that need to be further elucidated in the following research. The first is the effect of dietary RS and age on bone formation. Our previous works concluded that the tibia of meat duck exhibits rapid bone growth and mineralization from 1 to 35 days (44). Theoretically, therefore, the supplementation of dietary RPS and its fermentation by gut microbiota could affect the rate of bone formation, which is inconsistent with the current study saying that serum bone formation markers such as ALP and P1NP abundance failed to be changed by dietary 12% RPS or drinking SCFAs treatment. Further studies are necessary to draw a precise conclusion on the mechanisms of observed interactions between the prebiotics and bone formation. The second is the direct role of SCFAs on bone-related cells. Undifferentiated GPR41 and GPR43 transcription of bone marrow in this study suggested that SCFAs may not directly act on the bone to interact with bone turnover. Previous studies also deemed that a direct effect of SCFAs on bone resorption *in vivo* is unlikely to interfere with the differentiation of bone cells (21). Nevertheless, more accurate knowledge of the interactions between SCFAs and bone-related cells is still required. The third is the methodology; there are only methods available to measure RNA but not protein in this study, especially for some proteins related to the Malt1/NF-κB inflammasome. Therefore, we admit the possibility that some of our conclusion may include overestimation or underestimation of roles of dietary RPS in inflammation and subsequent bone resorption. Further experiments using Western blotting would be essential to elaborate on this possibility.

CONCLUSION

In the present study, dietary 12% RPS supplementation beneficially affected tibia mass in 14 day-old meat ducks through modifying gut microbiota and bone resorption. Results of gut microbiota showed that dietary 12% RPS intervention notably changed the relevant abundance of bacteria, which was associated with higher production of cecal propionate and butyrate. In addition to regulating the physiochemical environment to stimulate P absorption *via* decreasing the digestive tract pH, SCFAs enhanced intestinal integrity and depressed osteoclastic bone resorption mediated by inflammatory cytokines, and consequently improved tibial quality. These findings are of preliminary nature that highlights the importance of the "gut-bone" axis in bone health, provides ideas for further investigations into the precise mechanisms, and gives a new perspective for nutritional application of dietary fermentable fibbers-related products.

DATA AVAILABILITY STATEMENT

The datasets presented in this study can be found in online repositories. The names of the repository/repositories and

accession number(s) can be found below: https://www.ncbi.nlm.nih.gov/genbank/, SRR7370079.

ETHICS STATEMENT

The animal study was reviewed and approved by Institutional Animal Care and Use Committee at the Henan Agricultural University.

AUTHOR CONTRIBUTIONS

HZ, QZ, and WC: experimental design. QZ, WC, and JM: supervision and reviewing. HZ, SQ, and YZ: conducted the experimental and sample collection. HZ, SQ, XZ, PD, YZ, and YH: data analysis and wrote-original draft. All authors reviewed and approved the final manuscript.

FUNDING

This study was supported by grants from the National Natural Science Foundation of China (31772622), the National Natural Science Foundation of China (32072748), and a Doctoral Fellowship from Henan Agricultural University (0501182).

ACKNOWLEDGMENTS

We thank all the volunteers for their help in collecting samples of animal tissues.

REFERENCES

1. Jones TA, Dawkins MS. Environment and management factors affecting Pekin duck production and welfare on commercial farms in the UK. *Br Poult Sci.* (2010) 51:12–21. doi: 10.1080/00071660903421159
2. Rath NC, Huff GR, Huff WE, Balog JM. Factors regulating bone maturity and strength in poultry. *Poult Sci.* (2000) 79:1024–32. doi: 10.1093/ps/79.7.1024
3. Seely KD, Kotelko CA, Douglas H, Bealer B, Brooks AE. The human gut microbiota: a key mediator of osteoporosis and osteogenesis. *Int J Mol Sci.* (2021) 22. doi: 10.3390/ijms22179452
4. D'Amelio P, Sassi F. Gut microbiota, immune system, and bone. *Calcif Tissue Int.* (2018) 102:415–25. doi: 10.1007/s00223-017-0331-y
5. Chen YC, Greenbaum J, Shen H, Deng HW. Association between gut microbiota and bone health: potential mechanisms and prospective. *J Clin Endocrinol Metab.* (2017) 102:3635–46. doi: 10.1210/jc.2017-00513
6. Schwarzer M, Makki K, Storelli G, Machuca-Gayet I, Srutkova D, Hermanova P, et al. Lactobacillus plantarum strain maintains growth of infant mice during chronic undernutrition. *Science.* (2016) 351:854–7. doi: 10.1126/science.aad8588
7. Ohlsson C, Nigro G, Boneca IG, Backhed F, Sansonetti P, Sjogren K. Regulation of bone mass by the gut microbiota is dependent on NOD1 and NOD2 signaling. *Cell Immunol.* (2017) 317:55–8. doi: 10.1016/j.cellimm.2017.05.003
8. Sjogren K, Engdahl C, Henning P, Lerner UH, Tremaroli V, Lagerquist MK, et al. The gut microbiota regulates bone mass in mice. *J Bone Miner Res.* (2012) 27:1357–67. doi: 10.1002/jbmr.1588
9. Koh A, De Vadder F, Kovatcheva-Datchary P, Bäckhed F. From dietary fiber to host physiology: short-chain fatty acids as key bacterial metabolites. *Cell.* (2016) 165:1332–45. doi: 10.1016/j.cell.2016.05.041
10. Zhang H, Majdeddin M, Gaublomme D, Taminiau B, Boone M, Elewaut D, et al. 25-hydroxycholecalciferol reverses heat induced alterations in bone quality in finisher broilers associated with effects on intestinal integrity and inflammation. *J Anim Sci Biotechno.* (2021) 12:1–21. doi: 10.1186/s40104-021-00627-6
11. Bai Y, Li Y, Marion T, Tong Y, Zaiss MM, Tang Z, et al. Resistant starch intake alleviates collagen-induced arthritis in mice by modulating gut microbiota and promoting concomitant propionate production. *J Autoimmun.* (2021) 116:102564. doi: 10.1016/j.jaut.2020.102564
12. Tousen Y, Matsumoto Y, Nagahata Y, Kobayashi I, Inoue M, Ishimi Y. Resistant starch attenuates bone loss in ovariectomised mice by regulating the intestinal microbiota and bone-marrow inflammation. *Nutrients.* (2019) 11. doi: 10.3390/nu11020297
13. Zhang Y, Wang Y, Zheng B, Lu X, Zhuang W. The in vitro effects of retrograded starch (resistant starch type 3) from lotus seed starch on the proliferation of Bifidobacterium adolescentis. *Food Funct.* (2013) 4:1609–16. doi: 10.1039/c3fo60206k
14. Qin S, Zhang K, Applegate TJ, Ding X, Bai S, Luo Y, et al. Dietary administration of resistant starch improved caecal barrier function by enhancing intestinal morphology and modulating microbiota composition in meat duck. *Br J Nutr.* (2020) 123:172–81. doi: 10.1017/S0007114519002319
15. Qin SM, Zhang KY, Ding XM, Bai SP, Wang JP, Zeng QF. Effect of dietary graded resistant potato starch levels on growth performance, plasma cytokines concentration, and intestinal health in meat ducks. *Poult Sci.* (2019) 98:3523–32. doi: 10.3382/ps/pez186
16. Tousen Y, Abe F, Ishida T, Uehara M, Ishimi Y. Resistant starch promotes equol production and inhibits tibial bone loss in ovariectomized mice treated with daidzein. *Metabolism.* (2011) 60:1425–32. doi: 10.1016/j.metabol.2011.02.009
17. Tousen Y, Matsumoto Y, Matsumoto C, Nishide Y, Nagahata Y, Kobayashi I, et al. The combined effects of soya isoflavones and resistant starch on equol production and trabecular bone loss in ovariectomised mice. *Br J Nutr.* (2016) 116:247–57. doi: 10.1017/S0007114516001537
18. National Research Council. Nutrient Requirements of Poultry: *Ninth Revised Edition, 1994.* Washington, DC: The National Academies Press (1994). doi: 10.17226/2114
19. Sadler R, Cramer JV, Heindl S, Kostidis S, Betz D, Zuurbier KR, et al. Short-chain fatty acids improve poststroke recovery via immunological mechanisms. *J Neurosci.* (2020) 40:1162–73. doi: 10.1523/JNEUROSCI.1359-19.2019
20. McCleary BV, McNally M, Rossiter P. Measurement of resistant starch by enzymatic digestion in starch and selected plant materials: collaborative study. *J AOAC Int.* (2002) 85:1103–11. doi: 10.1093/jaoac/85.3.665
21. Yan J, Takakura A, Zandi-Nejad K, Charles JF. Mechanisms of gut microbiota-mediated bone remodeling. *Gut Microbes.* (2018) 9:84–92. doi: 10.1080/19490976.2017.1371893
22. Zaiss MM, Jones RM, Schett G, Pacifici R. The gut-bone axis: how bacterial metabolites bridge the distance. *J Clin Invest.* (2019) 129:3018–28. doi: 10.1172/JCI128521
23. Yan J, Charles JF. Gut microbiome and bone: to build, destroy, or both? *Curr Osteoporos Rep.* (2017) 15:376–84. doi: 10.1007/s11914-017-0382-z
24. Schepper JD, Collins FL, Rios-Arce ND, Raehtz S, Schaefer L, Gardinier JD, et al. Probiotic lactobacillus reuteri prevents postantibiotic bone loss by reducing intestinal dysbiosis and preventing barrier disruption. *J Bone Miner Res.* (2019) 34:681–98. doi: 10.1002/jbmr.3635
25. Louis P, Flint HJ. Formation of propionate and butyrate by the human colonic microbiota. *Environ Microbiol.* (2017) 19:29–41. doi: 10.1111/1462-2920.13589
26. Godínez-Méndez LA, Gurrola-Díaz CM, Zepeda-Nuño JS, Vega-Magaña N, Lopez-Roa RI, Íñiguez-Gutiérrez L, et al. In vivo healthy benefits of galacto-oligosaccharides from lupinus albus (la-gos) in butyrate production through intestinal microbiota. *Biomolec.* (2021) 11. doi: 10.3390/biom11111658
27. Liu P, Wang Y, Yang G, Zhang Q, Meng L, Xin Y, et al. The role of short-chain fatty acids in intestinal barrier function, inflammation, oxidative stress, and colonic carcinogenesis. *Pharmacol Res.* (2021) 165:105420. doi: 10.1016/j.phrs.2021.105420

28. Drucker DJ, Yusta B. Physiology and pharmacology of the enteroendocrine hormone glucagon-like peptide-2. *Annu Rev Physiol.* (2014) 76:561–83. doi: 10.1146/annurev-physiol-021113-170317
29. lji PA, Saki AA, Tivey DR. Intestinal structure and function of broiler chickens on diets supplemented with a mannan oligosaccharide. *J Sci Food Agric.* (2001) 81:1186–92. doi: 10.1002/jsfa.925
30. Irwin R, Lee T, Young VB, Parameswaran N, McCabe LR. Colitis-induced bone loss is gender dependent and associated with increased inflammation. *Inflamm Bowel Dis.* (2013) 19:1586–97. doi: 10.1097/MIB.0b013e318289e17b
31. Bianchi ML. Inflammatory bowel diseases, celiac disease, and bone. *Arch Biochem Biophys.* (2010) 503:54–65. doi: 10.1016/j.abb.2010.06.026
32. Afonina IS, Elton L, Carpentier I, Beyaert R. MALT1–a universal soldier: multiple strategies to ensure NF-κB activation and target gene expression. *FEBS J.* (2015) 282:3286–97. doi: 10.1111/febs.13325
33. Liu W, Guo W, Hang N, Yang Y, Wu X, Shen Y, et al. MALT1 inhibitors prevent the development of DSS-induced experimental colitis in mice via inhibiting NF-κB and NLRP3 inflammasome activation. *Oncotarget.* (2016) 7:30536–49. doi: 10.18632/oncotarget.8867
34. Kamp ME, Shim R, Nicholls AJ, Oliveira AC, Mason LJ, Binge L, et al. G protein-coupled receptor 43 modulates neutrophil recruitment during acute inflammation. *PLoS ONE.* (2016) 11:e0163750. doi: 10.1371/journal.pone.0163750
35. Epsley S, Tadros S, Farid A, Kargilis D, Mehta S, Rajapakse CS. The effect of inflammation on bone. *Front Physiol.* (2020) 11:511799. doi: 10.3389/fphys.2020.511799
36. Li P, Schwarz EM, O'Keefe RJ, Ma L, Looney RJ, Ritchlin CT, et al. Systemic tumor necrosis factor alpha mediates an increase in peripheral CD11bhigh osteoclast precursors in tumor necrosis factor alpha-transgenic mice. *Arthritis Rheum.* (2004) 50:265–76. doi: 10.1002/art.11419
37. Yamamoto Y, Udagawa N, Matsuura S, Nakamichi Y, Horiuchi H, Hosoya A, et al. Osteoblasts provide a suitable microenvironment for the action of receptor activator of nuclear factor-kappaB ligand. *Endocrinology.* (2006) 147:3366–74. doi: 10.1210/en.2006-0216
38. Murer H, Forster I, Biber J. The sodium phosphate cotransporter family SLC34. *Pflugers Archiv.* (2004) 447:763–7. doi: 10.1007/s00424-003-1072-5
39. Nourmohammadi R, Hosseini SM, Farhangfar H, Bashtani M. Effect of citric acid and microbial phytase enzyme on ileal digestibility of some nutrients in broiler chicks fed corn-soybean meal diets. *Ital J Anim Sci.* (2012) 11:e7. doi: 10.4081/2326
40. Ziaie H, Bashtani M, Torshizi MK, Naeeimipour H, Farhangfar H, Zeinali A. Effect of antibiotic and its alternatives on morphometric characteristics, mineral content and bone strength of tibia in Ross broiler chickens. *Global Veterinaria.* (2011) 7:315–22. Available online at: http://www.idos.org/gv/GV(4)11/1
41. Abdel-Fattah SA E-SM, El-Mednay NM, Abdel-Azeem, F. Thyroid activity, some blood constituents, organs morphology and performance of broiler chicks fed supplemental organic acids. *Int J Poult Sci.* (2008) 7:215–22. doi: 10.3923/ijps.2008.215.222
42. Nourmohammadi R, Hosseini SM, Farhangfar H. Effect of dietary acidification on some blood parameters and weekly performance of broiler chickens. *J Animal Veter Adv.* (2010) 9:3092–7. doi: 10.3923/javaa.2010.3092.3097
43. Islam K. Use of citric acid in broiler diets. *World's Poultry Sci J.* (2012) 68:104–18. doi: 10.1017/S0043933912000116
44. Zhang HY, Zeng QF, Bai SP, Wang JP, Ding XM, Xuan Y, et al. Study on the morphology and mineralization of the tibia in meat ducks from 1 to 56 d. *Poult Sci.* (2019) 98:3355–64. doi: 10.3382/ps/pez121

Conflict of Interest: The authors declare that the research was conducted in the absence of any commercial or financial relationships that could be construed as a potential conflict of interest.

The reviewer (SB) declared a shared affiliation with the authors to the handling editor at the time of review.

Publisher's Note: All claims expressed in this article are solely those of the authors and do not necessarily represent those of their affiliated organizations, or those of the publisher, the editors and the reviewers. Any product that may be evaluated in this article, or claim that may be made by its manufacturer, is not guaranteed or endorsed by the publisher.

frontiers in Nutrition

ORIGINAL RESEARCH
published: 31 March 2022
doi: 10.3389/fnut.2022.858585

Digestive Characteristics of *Hericium erinaceus* Polysaccharides and Their Positive Effects on Fecal Microbiota of Male and Female Volunteers During *in vitro* Fermentation

Baoming Tian[1], Yan Geng[1], Tianrui Xu[1], Xianguo Zou[1], Rongliang Mao[2], Xionge Pi[3], Weicheng Wu[3], Liangshui Huang[4], Kai Yang[1], Xiaoxiong Zeng[5] and Peilong Sun[1]*

[1] College of Food Science and Technology, Zhejiang University of Technology, Hangzhou, China, [2] Changshan Haofeng Agricultural Development Co., Ltd., Quzhou, China, [3] Zhejiang Academy of Agricultural Sciences, Hangzhou, China, [4] Research Institute of Changshan Tianle Edible Fungus, Quzhou, China, [5] College of Food Science and Technology, Nanjing Agricultural University, Nanjing, China

Hericium erinaceus polysaccharides (HEPs) have attracted widespread attention in regulating gut microbiota (GM). To investigate digestibility and fermentation of HEPs and their effects on GM composition, three polysaccharide fractions, namely, HEP-30, HEP-50, and HEP-70, were fractionally precipitated with 30%, 50%, and 70% ethanol concentrations (v/v) from hot water-soluble extracts of *Hericium erinaceus*, respectively. Three kinds of prepared HEPs were structurally characterized and simulated gastrointestinal digestion, and their effects on human fecal microbiota fermentations of male and female and short-chain fatty acid (SCFA) production *in vitro* were clarified. Under digestive conditions simulating saliva, stomach, and small intestine, HEPs were not significantly influenced and safely reached the distal intestine. After 24 h of *in vitro* fermentation, the content of SCFAs was significantly enhanced ($p < 0.05$), and the retention rates of total and reducing sugars and pH value were significantly decreased ($p < 0.05$). Thus, HEPs could be utilized by GM, especially HEP-50, and enhanced the relative abundance of SCFA-producing bacteria, e.g., *Bifidobacterium*, *Faecalibacterium*, *Blautia*, *Butyricicoccus*, and *Lactobacillus*. Furthermore, HEPs reduced the relative abundances of opportunistic pathogenic bacteria, e.g., *Escherichia-Shigella*, *Klebsiella,* and *Enterobacter*. This study suggests that gradual ethanol precipitation is available for the preparation of polysaccharides from *Hericium erinaceus,* and the extracted polysaccharide could be developed as functional foods with great development value.

Keywords: gut microbiota, short-chain fatty acids, *Hericium erinaceus* polysaccharides, *in vitro* digestion, digestive characteristics

OPEN ACCESS

Edited by:
Ding-Tao Wu,
Chengdu University, China

Reviewed by:
Chao Li,
South China University of Technology, China
Sergio Perez-Burillo,
University of Granada, Spain

****Correspondence:***
Kai Yang
yangkai@zjut.edu.cn

Specialty section:
This article was submitted to Nutrition and Microbes, a section of the journal Frontiers in Nutrition

Received: *20 January 2022*
Accepted: *15 February 2022*
Published: *31 March 2022*

Citation:
Tian B, Geng Y, Xu T, Zou X, Mao R, Pi X, Wu W, Huang L, Yang K, Zeng X and Sun P (2022) Digestive Characteristics of Hericium erinaceus Polysaccharides and Their Positive Effects on Fecal Microbiota of Male and Female Volunteers During in vitro Fermentation. Front. Nutr. 9:858585. doi: 10.3389/fnut.2022.858585

INTRODUCTION

The potential contribution of gut microbiota (GM) to human health has attracted widespread attention over the last decade (1). Studies have shown that some beneficial microbiota in the intestinal tract and its metabolites (e.g., short-chain fatty acids, SCFAs) can regulate intestinal discomfort and promote human health. Bioactive polysaccharides have also been attracted much

attention due to their lack of cytotoxicity and various physiological effects (e.g., anti-oxidation, anti-tumor, and immunoregulation) (2). Despite most of the bioactive polysaccharides cannot be utilized by the upper gastrointestinal tract and safely reach into the large intestine, those polysaccharides are decomposed and utilized by the microorganisms (3). Then, the degraded polysaccharides could change the structure of the GM, promote the beneficial metabolites, e.g., SCFA, and lead to improving intestinal health function (4). GM and their fermentative products, such as SCFAs, are considered as metabolic regulators and regulatory agents of complex dietary carbohydrate function and gut health (5). As a major player in the interactions among diet, GM, and the functions of the stomach and intestines, SCFAs have also been reported to contribute to intestinal homeostasis and regulation of energy metabolism. Furthermore, SCFAs regulate intestinal epithelial cell proliferation, maintain epithelial barrier function, modulate immune responses, and help to explain the relationship between GM changes and human metabolic diseases (6). Accordingly, potential strategies or candidates for the use of polysaccharides have been proposed and evaluated by an increasing number of scholars with the aim of regulating the GM and promoting gut health.

Hericium erinaceus (*H. erinaceus*) is a large edible fungus cultivated on a large scale, usually taken as a functional food or dietary supplement (7). This fungus is widely used in Asia (used in traditional Chinese medicine). *H. erinaceus* is rich in a variety of active ingredients such as polysaccharides, ketones, sinapine, glycoprotein, and alkaloids (8) and has been demonstrated to possess multiple bioactivities including anti-tumor, gastric ulcer, diabetes, hyperlipidemia, and liver injury (9, 10). The polysaccharides in mushrooms play a prebiotic role, e.g., regulating the GM, metabolizing into SCFAs to increase glucagon-like peptide-1 secretion, and inhibiting gastric emptying function to reduce appetite (11). *H. erinaceus* polysaccharides (HEPs) have been widely reported as the main bioactive compounds, and more than 35 polysaccharides have been isolated and identified (7). Some of them have the activities of anti-oxidation (12), anti-fatigue (13), neuroprotection (14), and immunoregulation (15). HEPs in the fruiting body of *H. erinaceus* could promote the growth of the relative abundance of beneficial GM, e.g., *Lachnospiraceae* and *Akkermansiaceae*, and reduce the abundance of *Rikenellaceae* and *Bacteroids*, which could be used to develop functional food components to accelerate gut health (16). Shao et al. explored how the mycelium of HEPs could adjust the GM of mice with colitis (17). Ren et al. discovered that HEPs alleviated the symptoms of C57BL/6 colitis in mice, which may be attributed to the regulation of oxidative stress, inhibition of inflammation-related signaling pathways, and changes in GM composition (18). *H. erinaceus* extracts (containing polysaccharides) could promote the growth of beneficial gut bacteria and improve the host immunity *in vivo* in the inflammatory bowel disease (IBD) model (19). In a pilot study of population surveys, daily *H. erinaceus* supplementation increased the Alpha diversity within the GM community, upregulated the relative abundance of some SCFA-producing bacteria, and downregulated some pathobionts (20). The *in vitro* intestinal fermentation model is a powerful tool for the study of probiotics and prebiotics on GM, which can simulate different segments of the intestine and sample in real time (21). Simulated *in vitro* digestion and fecal fermentation of polysaccharides can investigate the changes of intestinal microbial environment. It has excellent experimental performance, simple operation, good repeatability, and is not subject to the constraints of human morality. Purification of HEPs is traditionally done by various chromatographic methods including anion chromatography and gel permeation chromatography (GPC) (7). However, these methods usually consume extensive resources and time, which is not ideal in the large-scale purification of polysaccharide. Even though some previous research reported that HEPs could regulate the GM in mice, to date, little information on the digestion and fecal fermentation properties of male and female volunteers is available for different HEP fractions. Therefore, in this study, the *H. erinaceus* was used to grade HEPs by a water extraction-alcohol precipitation process. The changes of total carbohydrate, reducing sugars in simulated digestive system, SCFAs, pH value, and GM communities by high-throughput sequencing *in vitro* fecal fermentation were investigated to explore the prebiotic activity of HEPs.

MATERIALS AND METHODS

Materials and Reagents

The fruiting body of dried *H. erinaceus* was kindly provided by Haofeng Agricultural Development Co., Ltd. (Changshan, Quzhou, China). Ninety-five percent food-grade ethanol was obtained from Changqing Chemical Co., Ltd. (Hangzhou, China). Dialysis tubes (Molecular weight cut-off, 3 kDa) were purchased from Yuanye Biotechnology Co., Ltd. (Shanghai, China). Bile salt, lipase, trypsin, and pepsin were purchased from Macklin Biotechnology Co., Ltd. (Shanghai, China). The basic components of the medium were purchased from Ling Feng Chemical Reagent Co., Ltd. (Shanghai, China). Lastly, other reagents and solvents were purchased from China National Pharmaceutical Industry Co., Ltd. (Shanghai).

Fresh fecal samples were taken from healthy volunteers who did not have history of digestive diseases or any treatment of antibiotics, probiotics, or prebiotics for at least 3 months (five men and five women, all aged between 22 and 25 years old). The volunteers had all been living in Hangzhou, Zhejiang province, and had a traditional Chinese diet. Further, all the volunteers were familiar with the content of the experiment and signed the consent letter in person. The study was approved by the relevant departments of the Ethics Committee of Hangzhou center for disease control and prevention.

Preparation of the Graded *Hericium erinaceus* Polysaccharides

The HEP preparation refers to the previously reported method with minor modifications (16). Three polysaccharide components were prepared with the same fruiting bodies of *H. erinaceus*. Briefly, the fruiting body of *H. erinaceus* was crushed by high-speed grinders and treated with 95% ethanol

for 12 h to remove the pigment, polyphenols, and so on. After filtration and removal of ethanol, it was naturally dried and twice extracted with distilled water (1:15, w/v) at 95°C for 3 h. The combined extracts were centrifuged at 8,000 *g* for 15 min and concentrated by rotary evaporation before 95% ethanol was added gradually in proportion to make the final concentration of 30% ethanol. This was then left to stand at room temperature for 12 h. Next, the precipitate was obtained by centrifugation at 8,000 *g* for 15 min and redissolved in distilled water before protein was removed by the Sevage method (4). Then, the precipitate was dialyzed in a 3 kDa dialysis tube for 3 days, concentrated, and freeze-dried to obtain a crude polysaccharide precipitated with 30% ethanol called HEP-30. After which, a certain amount of 95% ethanol was added to supernatants in proportion to obtain the final ethanol concentration of 50%, and the above experiment was repeated to obtain a crude polysaccharide with 50% ethanol called HEP-50. The preparation of crude polysaccharide, called HEP-70, was obtained by the similar procedure by precipitation with 70% ethanol.

Determination of Major Components and Structural Characterization of the Graded *Hericium erinaceus* Polysaccharides

The concentrations of total sugar, reducing sugar, uronic acid, and protein were quantified by phenol-sulfuric acid method (16), dinitrosalicylic acid method (DNS) (16), m-hydroxybiphenyl method (16), and coomassie brilliant blue method (22), respectively. The monosaccharide composition of HEPs was analyzed according to the a previously reported method (23), and molecular weight was determined by GPC (23). Compared with the Agilent 1260 Parallax detector, the GPC system (Waters, Milford, MA, United States) consisted of three Waters Ultra-hydrogels, namely, 120, 200 and 500 (7.8 × 300 mm) columns in series. A small amount of samples were completely dissolved in deionized water and then filtrated with a 0.22 μm water phase membrane. The column was eluted with pure water at a flow rate of 1.0 ml/min, and the injection volume of the sample was 40 μl. Fourier Transform Infrared Spectroscopy (FT-IR) analysis of HEPs was scanned on a Nicolet 6700 FT-IR spectrometer (Madison, WI, United States) with potassium bromide (KBr) pellets in a range of 4,000–400 cm^{-1} (24). To compare the microstructure of different HEPs, the apparent morphology of HEPs was observed by a scanning electron microscope (SEM) (Hitachi SU8010, Hitachi Ltd., Japan). In the SEM analysis, a certain amount of dry sample powder was put on the sample plate to spray gold with a vacuum plating apparatus and was observed in a vacuum environment (25).

Simulation of Saliva Digestion

Saliva was collected from two healthy volunteers (from volunteers who provided fecal samples) before breakfast, centrifuged at 4,500 *g* for 10 min to obtain supernatant, and then mixed with the same volume of HEP solution (8 mg/ml) in a sealed test tube before being kept in a 37°C water bath oscillator. During digestion (0, 5 and 20 min), 1.0 ml of the mixture was removed from the tube and was immediately immersed in boiling water for 5 min to deactivate the enzyme. After the supernatant was obtained by centrifugation, the contents of total and reducing sugar were determined (26).

Simulation of Gastric Digestion

Based on a previous method (26) 0.05 g $CaCl_2$, 0.22 g KCl, 0.62 g NaCl, and 0.12 g $NaHCO_3$ were dissolved in 200 ml of distilled water, and pH was adjusted to 3.0 with HCl, i.e., gastric electrolyte solution. Then, 1.0 ml CH3COONa (1 M, pH 5), 37.5 mg gastric lipase, and 35.4 mg pepsin were added into 150 g of gastric electrolyte solution and adjusted pH to 3.0 with HCl, i.e., simulated gastric solution. An equal volume of simulated gastric solution and HEP solution (8 mg/ml) were mixed and kept at 37°C and pH 3.0 in a water bath oscillator. At 0, 2, and 4 h of digestion time, 1.0 ml of the digested sample was immediately immersed in a boiling water bath for 5 min to deactivate the enzyme. After centrifugation, the contents of total sugar and reducing sugar were determined.

Simulation of Small Intestine Digestion

According to a previous method (4, 26, 27), 0.065 g KCl, 0.033 g $CaCl_2$, and 0.54 g NaCl were dissolved in 100 ml distilled water. pH was adjusted to 7.0 with 0.1 M NaOH solution to obtain small intestine medium. Fifty grams of trypsin solution (7%, w/w), 200 g of bile salt (4%, w/w), and 6.5 mg of trypsin were added into the 50 g intestinal medium, in which its pH was adjusted to 7.5 with 0.1 M NaOH solution before being stirred evenly to obtain a simulated intestinal solution. The simulated small intestinal solution and the digested simulated gastric solution were mixed in proportion (3:10). For the simulated small intestinal digestion, the mixtures of 9.0 ml of simulated small intestinal fluid with 30.0 ml of digested simulated gastric solution, 9.0 ml of distilled water with 30.0 ml of digested simulated gastric solution (control group), and 9.0 ml of simulated small intestinal fluid with 30.0 ml of distilled water (control group) were prepared and maintained at 37°C in a water bath oscillator. The digestion samples at 0, 2, and 6 h after simulated intestinal digestion were immediately immersed in a boiling water bath for 5 min to inactivate the enzyme. After centrifugation, the supernatant was taken to measure the concentrations of total and reducing sugar.

Configuration of Fermentation Medium *in vitro*

One gram of L-cysteine, 2.0 ml of heme, 10 g of tryptone, 2.5 g of yeast extract, 0.9 g of NaCl, 0.0604 g of $CaCl_2{\cdot}6H_2O$, 0.45 g of K_2HPO_4, 0.45 g of KH_2PO_4, 200 μl of vitamin I solution (biotin 0.05 g/L, cobalamin 0. 05 g/L, *p*-amino-benzoic acid 0.15 g/L, folic acid 0.25 g/L, and pyridoxamine 0.75 g/L), and 1.0 ml (1 mg/ml) of resazurin were accurately weighed/measured and dissolved in 1 L of deionized water. Vitamins and L-cysteine were filtered and sterilized, and the rest were boiled and sterilized at 121°C for 15 min. HEP-30, HEP-50, and HEP-70 were used individually as the carbon sources were added into the medium and as an equal weight of fecal diluent were added to the control vessels. Under anaerobic conditions, each bottle was filled 5 ml

of fermentation medium and then sterilized. Ten fecal samples from the ten donors were stored separately and grouped by sex in equal amounts (0.8 g) and diluted with pre-reduced anaerobic carbonate-phosphate buffer (feces/buffer 1:10 w/v), followed by filtration through four cheesecloth layers to obtain the fecal slurry. Zero-point-five milliliters of each fecal suspension were inoculated into fermentation media group (HEP-30, HEP-50, HEP-70), respectively. Zero-point-five milliliters (5 parallel tests) of buffer without feces were also treated as the control group. Each fermentation was conducted in triplicate on each of five fecal donors (five men and five women). Finally, all of the fermentation media was maintained at 37°C for 24 h. Next, liquid samples were aliquoted and centrifuged. During the fermentation, 1.0 ml of fermentation broth was taken at 0 and 24 h to determine corresponding parameters. Supernatants were used to determine SCFA production, and the pellets were stored at −80°C for DNA extraction.

DNA Extraction and High-Throughput Sequencing of Gut Microbiota and Bioinformatic Analysis

The fermentation broth of human feces was centrifuged at 10,000 *g* at 4°C for 5 min to obtain precipitated sample. Total bacterial DNA from fermentation samples of each feces was immediately extracted by the QIAamp DNA Stool Mini Kit (QIAGEN, Valencia, CA, United States) in accordance with the manufacturer's protocols. DNA concentration and integrity were measured by a NanoDrop 2,000 spectrophotometer (Thermo Fisher Scientific, Waltham, MA, United States) and agarose gel electrophoresis, respectively. The variable regions V3-V4 of the bacterial 16S rRNA genes were performed using the broadly conserved PCR forward primers 338F (5 – ACTCCTACGGGAGGCAGCAG – 3) and reverse primer 806R (5 – GGACTACHVGGGTWTCTAAT – 3) (28). All PCR reactions were carried out in 30 μl reactions with 15 μl of the Phusion® High-Fidelity PCR Master Mix (New England Biolabs), 0.2 μM of forward and reverse primers, and about 10 ng template DNA. Thermal cycling consisted of initial denaturation at 98°C for 1 min, followed by 30 cycles of denaturation at 98°C for 10 s, annealing at 50°C for 30 s, elongation at 72°C for 60 s, and, finally, 72°C for 5 min.

After qualified inspection, fluorescence quantification, and library preparation, specific sequencing ligands and PCR amplified products were combined and tested on the Illumina Miseq PE250 high-throughput sequencing platform. The obtained data were further analyzed for corresponding bioinformatic analysis [Mingke Biotechnology (Hangzhou) Co., Ltd., Hangzhou, China] (28). We processed the raw sequence data using QIIME1.9. The function search was used to detect chimerism and remove low-quality sequences. The operational taxonomic unit (OTU, or the sequences with >97% identity) was classified by annotation against the SILVA132 database. We picked representative sequences for each OTU and use the UCLUST to annotate taxonomic information for each representative sequence. In order to compute Alpha Diversity, we rarify the OTU table and calculate three metrics: Chao1 which estimates the species abundance, Observed Species which estimates the amount of unique OTUs found in each sample, and Shannon index. Rarefaction curves were generated based on these three metrics. Graphical representation of the relative abundance of bacterial diversity from phylum to species can be visualized using Krona chart. Principal coordinates analysis (PCoA) of the weighted Unifrac distances was performed using R packages (version 4.1.1) to visualize the compositional differences between the microbial communities of different groups.

Determination of pH and Air Pressure

The pH value and air pressure of the fermentation samples were quantified with a pH meter (Mettler-Toledo Instruments, China) and a barometer (HT-1895, Dongguan Hongtai Instrument Technology Co., Ltd.), respectively.

Determination of Short-Chain Fatty Acids

The samples before and after fermentation were centrifuged to obtain the supernatant before being acidified with crotonic acid-metaphosphoric acid mixed solution for 24 h. After acidification, the supernatant was centrifuged and filtered with a 0.22 μm aqueous microporous membrane. The total amount of SCFAs and the content of each component were measured by gas chromatography (GC2010, Shimadzu, Japan) (29).

Statistical Analysis

Results were shown as mean (3 independent experiments × 3 replication) ± standard deviations (SD). High-throughput sequencing of GM included 5 independent experiments. Origin V.8.5.1 and GraphPad Prism 7 software were used to analyze the data and draw the graph. SPSS V.20.0 was used to conduct analysis of variance (ANOVA) followed by a multiple-comparison test (Duncan test) for the data and difference significance analysis. The level of significance was set at $p < 0.05$.

RESULTS

The Component Analysis and Monosaccharide Identification of *Hericium erinaceus* Polysaccharides

The yield and main components of HEPs fractionally precipitated by different concentrations of ethanol are shown in **Table 1**. With the increase of ethanol concentration, the yield decreased, but there was no significant difference ($p > 0.05$). The content of polysaccharides in HEP-30, HEP-50, and HEP-70 was 46.57% ± 1.70%, 65.01% ± 1.50%, and 58.55% ± 1.40%, respectively. All three groups of HEPs contained a small amount of protein (1.00–1.47%), indicating that the protein was largely removed by the Sevage method.

The molecular weights of HEPs are shown in **Figure 1**. HEP-30 was mainly composed of three components. The polysaccharide with average molecular weight of 823.07 ± 2.30 kDa (54.36%) had the highest content, followed by 15.019 ± 1.59 kDa. HEP-50 was composed of a main peak and a shoulder peak, with a main molecular weight of 16.723 ± 2.11 kDa (71.68% of the

TABLE 1 | The main component content of different grades of *Hericium erinaceus* polysaccharides (HEPs).

Group	Yield (%)	Content (%)			
		Crude polysaccharides	Reducing sugar	Protein	Uronic acid
HEP-30	2.03 ± 0.21[a]	46.57 ± 1.70[a]	0.61 ± 0.07[a]	1.00 ± 0.07[a]	1.10 ± 0.20[a]
HEP-50	1.87 ± 0.11[a]	65.01 ± 1.50[c]	0.67 ± 0.08[a]	1.40 ± 0.02[a]	2.40 ± 0.30[b]
HEP-70	1.69 ± 0.15[a]	58.55 ± 1.40[b]	1.63 ± 0.15[a]	1.47 ± 0.05[a]	2.34 ± 0.30[b]

Data are means ± SD (3 independent experiments × 3 replication). [a,b,c] *Different lowercase letters in the same column indicate a different significance between treatments ($p < 0.05$).*

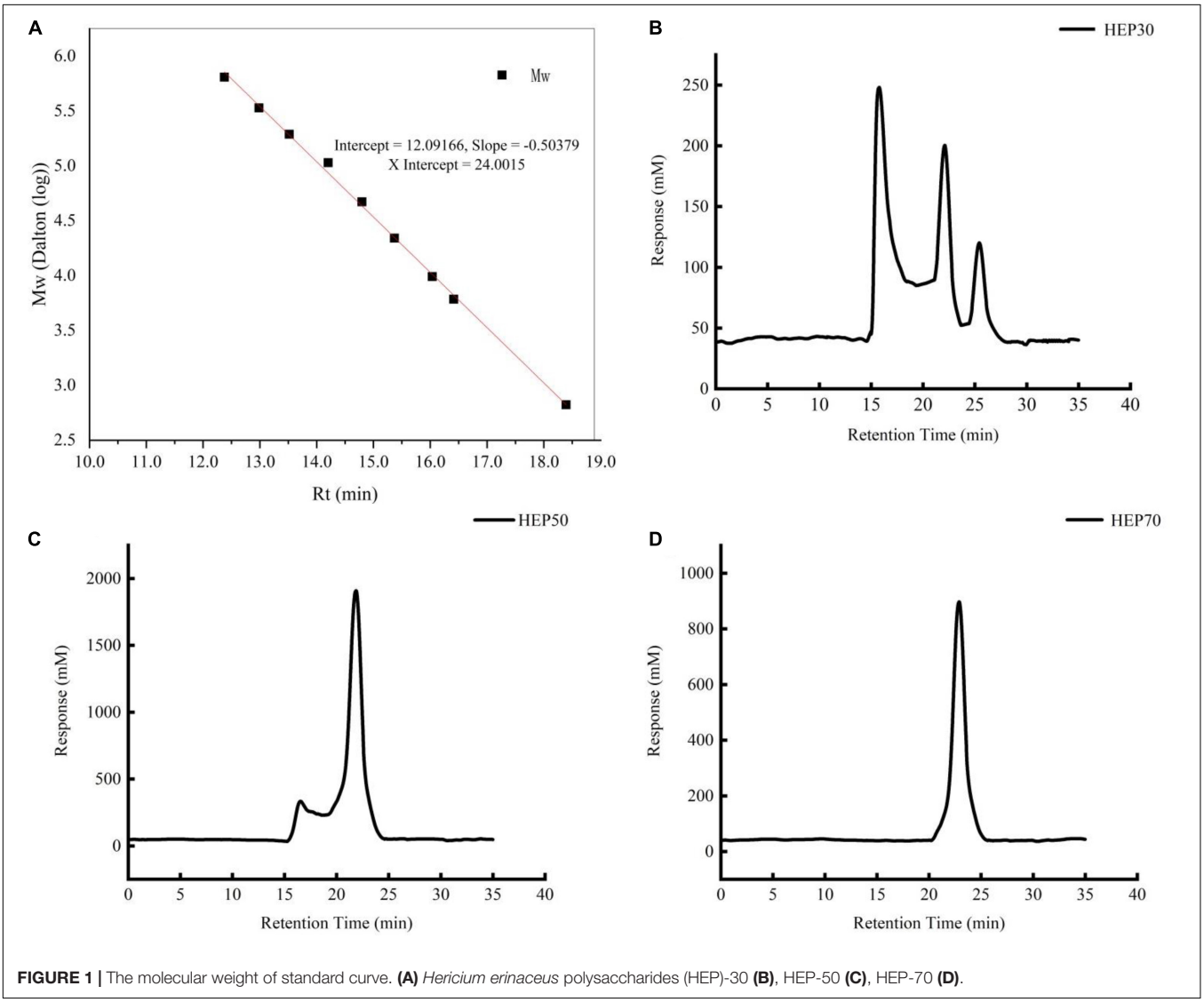

FIGURE 1 | The molecular weight of standard curve. **(A)** *Hericium erinaceus* polysaccharides (HEP)-30 **(B)**, HEP-50 **(C)**, HEP-70 **(D)**.

molecular weight segment). Lastly, HEP-70 was relatively pure, with a molecular weight of 4.771 ± 0.21 kDa (95.18% of the total molecular weight). The monosaccharide composition of HEPs is shown in **Table 2**. All the three grades of HEPs were composed of similar monosaccharide composition in a slightly different molar ratio. The monosaccharide composition of HEP-30 is in the molar ratio of fructose: mannose: glucose: galactose = 0.3: 1.3: 9.8: 0.3; HEP-50 is 1.7: 0.5: 10.6: 10.4; and HEP-70 is 1.2: 1.3: 23.7: 0.3.

Spectroscopic and Microstructure Analysis of *Hericium erinaceus* Polysaccharides

The FT-IR spectra for HEPs are presented in **Supplementary Figure 1**. HEP-30, HEP-50, and HEP-70 showed strong absorption peaks generated by the stretching vibration of polysaccharide hydroxyl groups near 3,400 cm^{-1}, suggesting that

TABLE 2 | Monosaccharide composition of different grades of HEPs.

Group	Monosaccharide (mole ratio)			
	Fucose	Mannose	Glucose	Galactose
HEP-30	0.3	1.3	9.8	0.3
HEP-50	1.7	0.5	10.6	10.4
HEP-70	1.2	1.3	23.7	0.3

polysaccharides contain a large number of hydroxyl groups in their internal structure and a large number of intermolecular and intramolecular hydrogen bonds (30). The weak absorption peak at 2,900 cm^{-1} is the characteristic absorption caused by the C-H stretching vibration of the methyl in the polysaccharide. The absorption peak at 1,653 cm^{-1} indicates that C = O groups or C = C groups are existing in the structure (31). The weak absorption peak near 1,400 cm^{-1} is caused by the variable angle vibration of C = H, while the asymmetric tensile band at 1653 cm^{-1} and the weaker symmetrical tensile band at 14,00 cm^{-1} are the two bands generated by the carboxylic acid radical groups (32, 33). Absorbance peak at 1,148, 1,096, 1,080, and 1,046 cm^{-1} was classified as pyranose type sugar, and the absorption peak in the range of 1,200–1,000 cm^{-1} was caused by the overlap of the glycoside bond vibration of the sugar ring, C-O-C glycoside bond vibration, and the stretching vibration of the C-OH side group, indicating the presence of pyran glycoside bond in the structure of polysaccharides (34). The absorption peak at 568 cm^{-1} is associated with the sugar cycle (31). The SEM image of HEP is provided in **Supplementary Figure 2**. The three kinds of polysaccharides are mainly flaky, layered, and smooth with some wrinkles on the surface, while the surface morphologies of the three HEPs presented significant differences in shape and size. In addition, the flaky structure of HEP-30 is a little larger and sparser than the other two polysaccharides, following by HEP-50, which may be attributed to their molecular weight.

Effects of *Hericium erinaceus* Polysaccharides on Total Sugar and Reducing Sugar Contents

The changes of total sugar and reducing sugar contents during *in vitro* digestion and fermentation are shown in **Figures 2**, **3**, respectively. According to the data of total sugar retention rate in **Figure 2**, the retention rates of HEP-30, HEP-50, and HEP-70 in the simulation system of oral cavity, gastric solution, and intestinal solution showed no significant change ($p > 0.05$). However, the total sugar retention rates of the three kinds of polysaccharides were all significantly reduced ($p < 0.05$) after *in vitro* fecal fermentation for 24 h, indicating that HEPs were not easily decomposed by the saliva, gastric juice, and small intestinal juice and could successfully be transported to the distal intestine for microbial fermentation and degradation. After the digestion or fermentation, among the three polysaccharides, HEP-50 had the lowest total sugar retention rate (51.99% ± 4.00%), followed by HEP-70 (58.57% ± 3.99%). The highest retention rate was HEP-30 (76.11% ± 3.60%). It was manifested that HEP-50 might be better degraded and utilized by the GM. According to the retention of reducing sugar in **Figure 3**, the different grades groups of HEPs showed that there were no significant changes in the simulated digestive solution system ($p > 0.05$). After *in vitro* fermentation for 24 h, there were significant changes ($p < 0.05$) in the retention rates of HEP-30, HEP-50, and HEP-70 (62.53% ± 2.40%, 39.17% ± 2.70% and 60.06% ± 2.60%, respectively), preliminarily concluding that the reducing sugar was absorbed and utilized by GM rather than being digested in the mouth, stomach, or small intestine.

Effects of *Hericium erinaceus* Polysaccharides *in vitro* Fermentation on Short-Chain Fatty Acids Production, pH and Air Pressure

As shown in **Figure 4A**, the total SCFAs content in feces of male volunteers was significantly increased compared with that of female volunteers (9.40 ± 1.8 mmol/L *vs.* 6.48 ± 1.7 mmol/L, $p < 0.05$). SCFAs in the fermentation broth of the four groups of media (control group, HEP-30, HEP-50, and HEP-70) after fermentation for 24 h were significantly higher than the samples before fermentation ($p < 0.05$), indicating that SCFAs were metabolized by the GM during fermentation. The content of total SCFAs in the fermentation broth after using HEPs as the carbon source was significantly enhanced compared with the control group, suggesting that HEPs could promote the production of SCFAs by modulating the GM. Hence, the HEP-50 medium had the highest total SCFAs. As shown in **Figures 4B–G**, after 24 h of fermentation, acetic acid and propionic acid in fecal fermentation broth in male and female volunteers and butyric acid in male volunteers were significantly increased ($p < 0.05$), while the butyric acid in female volunteers, valeric acid, isobutyric acid, and isovaleric acid in female and male volunteers showed no significant changes ($p > 0.05$). Acetic acid and propionic acid are the main metabolites in SCFAs. As per the results, the content of acetic acid is the highest, which is consistent with other relevant reports (17). The HEP treatment significantly increased the contents of acetic acid, propionic acid, and valeric acid compared with the control group after 24 h fermentation ($p < 0.05$).

As shown in **Figure 5A**, the initial medium pH was 7.28, and after 24 h anaerobic fermentation, except for the control group, the pH values were significantly reduced in the three HEP-treated groups ($p < 0.05$). The pH difference of the fermentation medium is related to different acids produced by microbes, among them SCFA. The GM can produce SCFAs using polysaccharides, so the difference of SCFA may be associated with the different utilization levels of the three polysaccharides by fecal microbiota. In addition, the pH of HEP-50 group decreased maximally (5.33 ± 0.09 for male and 5.41 ± 0.07 for female). After 24 h of fecal fermentation, the barometer was inserted into the penicillin bottle and the pressure was measured. The results in **Figure 5B** showed that compared to the control group, the air pressure in the polysaccharides fermentation broth of HEP-30, HEP-50, and HEP-70 groups were not significant changes ($p > 0.05$). It was implied that HEP-30, HEP-50, and HEP-70 groups did not cause

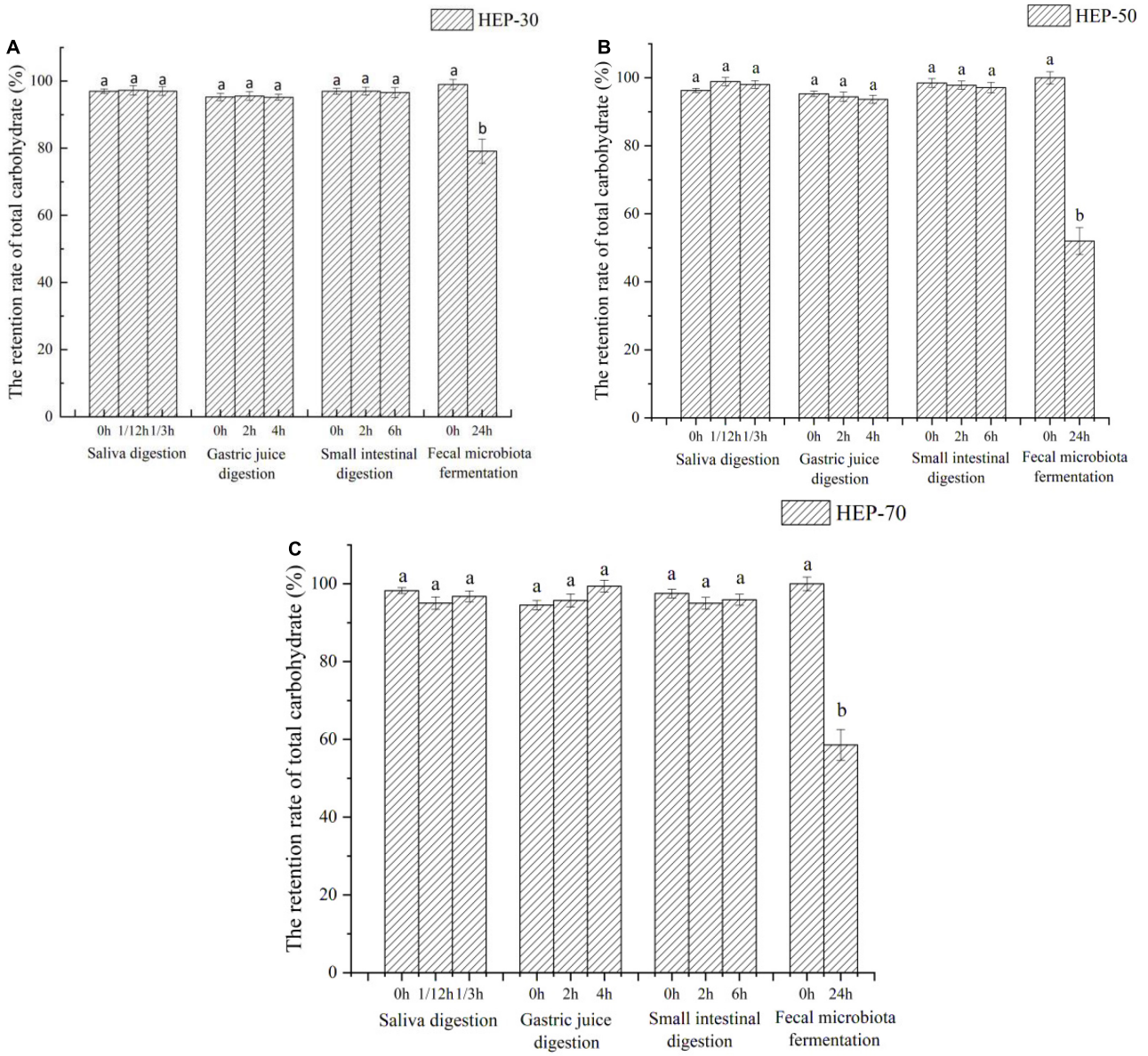

FIGURE 2 | The retention rate of total carbohydrate of HEP-30 **(A)**, HEP-50 **(B)**, and HEP-70 **(C)** during the reaction. The retention rate of total carbohydrate% = (the content of total carbohydrate during the reaction/the content of total carbohydrate before the reaction) × 100%; Data are means ± SD (3 independent experiments × 3 replication). ^{a,b}Different lowercase letters indicate significant differences ($p < 0.05$) between fermentation 0 and 24 h.

abdominal distension, and there was no significant difference between male and female samples ($p > 0.05$).

Effects of *Hericium erinaceus* Polysaccharides on α and β Diversity of the Fecal Microbiota *in vitro* Fermentation

High-throughput sequencing analysis was performed on 40 samples to explore the effects of HEPs on GM composition. As shown in **Supplementary Figure 3A**, with the increase of sample sequence number, the slope of the sample curve gradually decreased and finally became flat. This trend reflected that the sequencing depth was reasonable and large enough. **Supplementary Figure 3B** showed the Shannon-Wiener curve. In the case of this sequencing depth, the sample curves tended to flatten out, indicating that the sequencing data was large enough to evaluate the diversity of microbial species, which explained that the data met the experimental requirements. As shown in **Supplementary Figure 3C** (Rank abundance curves), there were significant differences in richness and evenness among the communities. The species accumulation curve can be used to judge whether the sample size is sufficient or not. As displayed in **Supplementary Figure 3D**, the data reflected

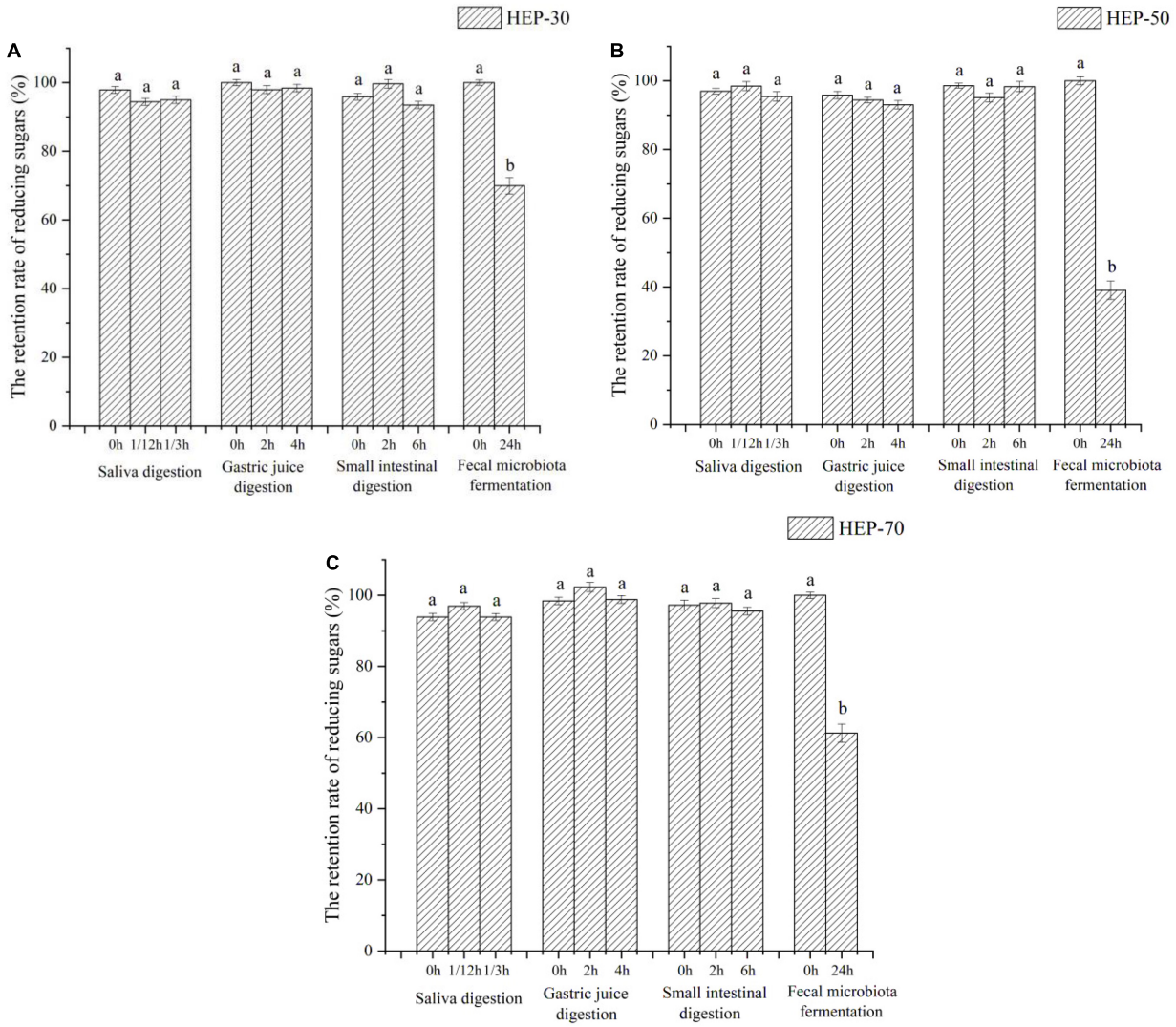

FIGURE 3 | The retention rate of reducing sugars of HEP-30 **(A)**, HEP-50 **(B)**, and HEP-70 **(C)** during the reaction. The retention rate of total carbohydrate = (the content of reducing sugars during the reaction/the content of reducing sugars before the reaction) × 100%; ^{a,b}Data are means ± SD (3 independent experiments × 3 replication). Different lowercase letters indicate significant differences ($p < 0.05$) between fermentation 0 and 24 h.

that the occurrence rate of new OTU (new species) under continuous sampling decreased and the species accumulation curve flattened with the sequencing process, indicating that the sequencing library was large enough to basically cover most bacterial diversity in all samples.

The intestinal community identification of HEP fermentation broth showed that the α diversity and β diversity indexes were significantly different after HEP addition. **Figures 6A,B** and **Supplementary Figure 4** depicted the α diversity of the GM. Compared with the control group, the number of OTUs, Chao1, and Shannon indexes were significantly increased in the fecal fermentation broth of the male volunteers treated with HEPs ($p < 0.05$). In addition, the Simpson index was significantly reduced ($p < 0.05$) (**Figure 6A**). The fecal fermentation broth of female volunteers treated with HEPs showed a similar trend, with a significant increase in Shannon index ($p < 0.05$) and a significant decrease in Simpson index ($p < 0.05$), but no significant difference was found in the number of OTUs and Chao1 index (**Figure 6B**). Moreover, as appeared in **Supplementary Figure 4**, the fecal sample fermentation of the control group for 24 h, the number of OTUs, Chao1, and Shannon indexes of female fecal fermentation broth were significantly ($p < 0.05$) increased compared with those of male fecal fermentation broth, and the Simpson index of female was significantly lower than that in male volunteers ($p < 0.05$). After HEP treatment, the differences of OTU numbers and Chao1 indexes between male and female volunteers disappeared ($p > 0.05$), while the effects of the three polysaccharides on Shannon index and Simpson index between male and female volunteers were different

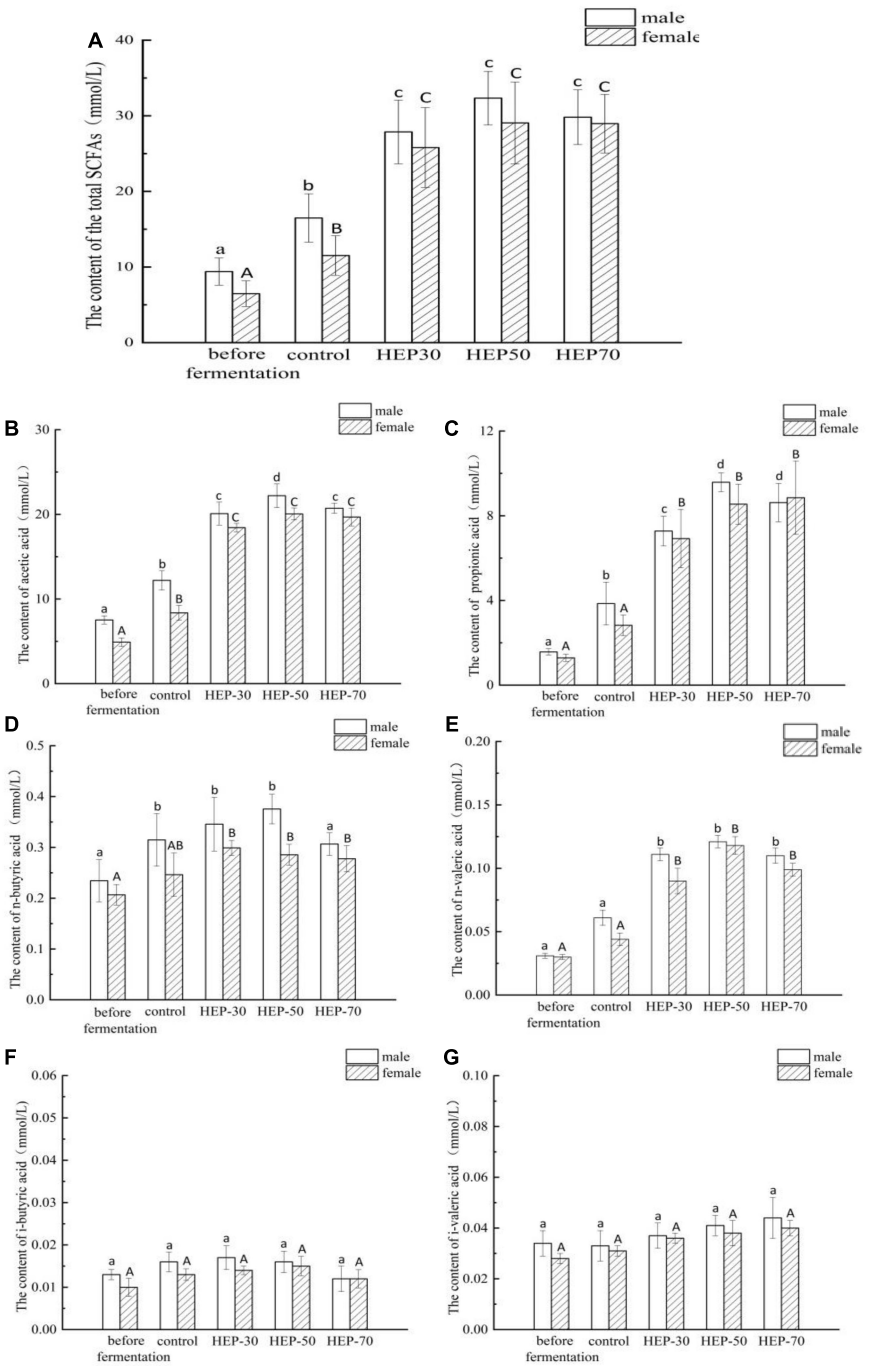

FIGURE 4 | The short-chain fatty acid (SCFA) concentrations of different groups in the feces before or after fermentation. **(A)** total SCFAs; **(B)** acetic acid; **(C)** propionic acid; **(D)** n-butyric acid; **(E)** n-valeric acid; **(F)** i-butyric acid; **(G)** i-valeric acid. Data are means ± SD (3 independent experiments × 3 replication). Different letters (without a common letter) indicated a significant difference between the two experimental groups ($p < 0.05$). ^{a,b,c,d}Lowercase and ^{A,B}uppercase letters indicate the significance of HEPs on fecal microbiota fermentation of male and female volunteers, respectively.

($p < 0.05$). HEP-30 and HEP-70 did not change the effect on diversity (Shannon index and Simpson index), while HEP-50 eliminated the difference of Shannon index and Simpson index between male and female fecal fermentation broth. As shown in **Figure 6C**, PCoA analysis showed that HEP had differences in the structure of GM in the feces fermentation broth of male volunteers. The same phenomenon was also observed in the feces of female volunteers, indicating that HEP treatment changed the microbial composition of feces of human volunteers.

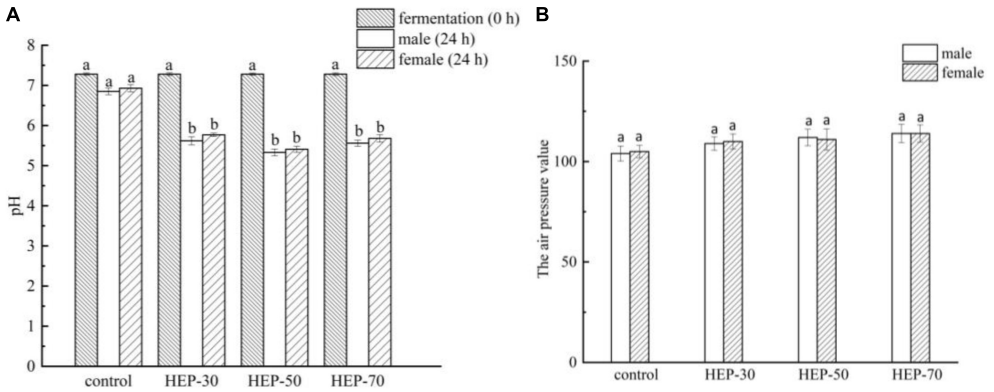

FIGURE 5 | The pH value **(A)** and air pressure **(B)** changed in different groups during *in vitro* fermentation of human feces. Different letters indicated a significant difference between the two groups ($p < 0.05$). Data are means ± SD (3 independent experiments × 3 replication). [a,b]Different lowercase letters indicate significant differences ($p < 0.05$) between fermentation 0 and 24 h.

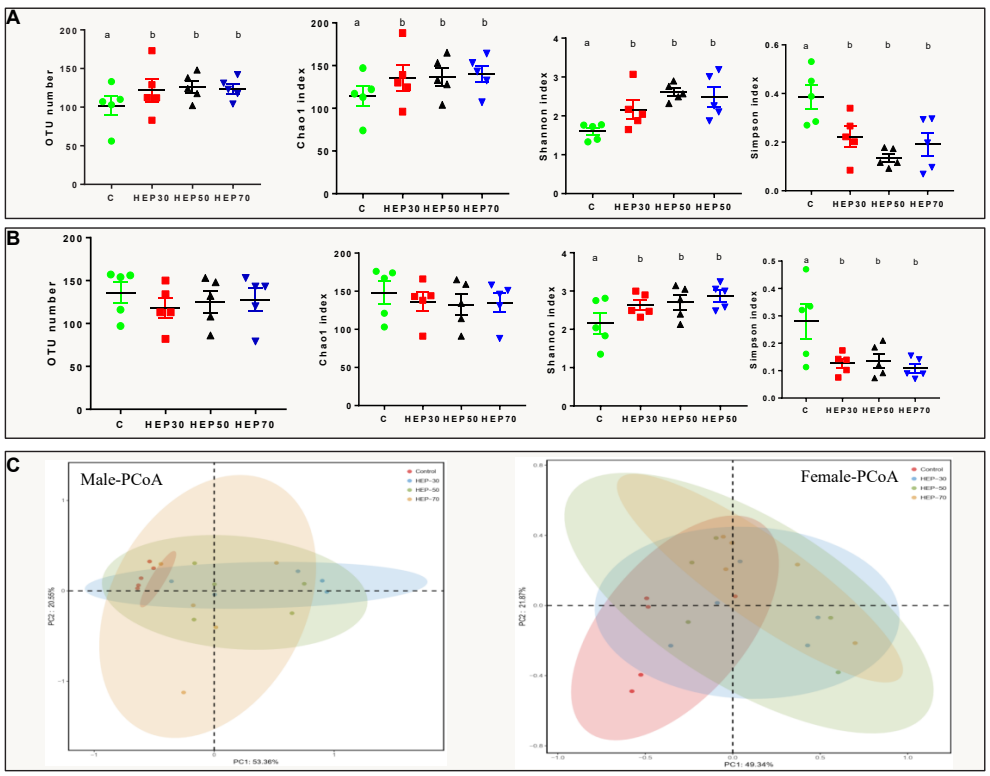

FIGURE 6 | Effects of HEPs on α and β diversity of the fecal microbiota *in vitro* fermentation. α diversity of fecal fermentation broth of male **(A)** and female **(B)** volunteers; **(C)** Principal coordinates analysis (PCoA) of microbiota of fecal fermentation broth *in vitro*. Data are means ± SD (5 independent experiments). [a,b]Different letters indicated a significant difference between the two groups ($p < 0.05$).

Effects of *Hericium erinaceus* Polysaccharides on the Fecal Microbial Taxonomic Profiles *in vitro* Fermentation

Figures 7A,B and **Supplementary Figure 5** are shown the relative abundance at the phylum level of GM (A: male; B: female). As observed from the figures, Firmicutes, Proteobacteria, Bacteroidetes, and Actinobacteria are the main microbial phyla in the fermentation broth of the four media. Actinobacteria was significantly higher in the HEP-30 and HEP-50 groups compared to the control group ($p < 0.05$), and Firmicutes and Bacteroidetes in the fermentation broth of the three groups, except for the HEP-30 group in males, was significantly increased compared with the control group ($p < 0.05$). Meanwhile Proteobacteria

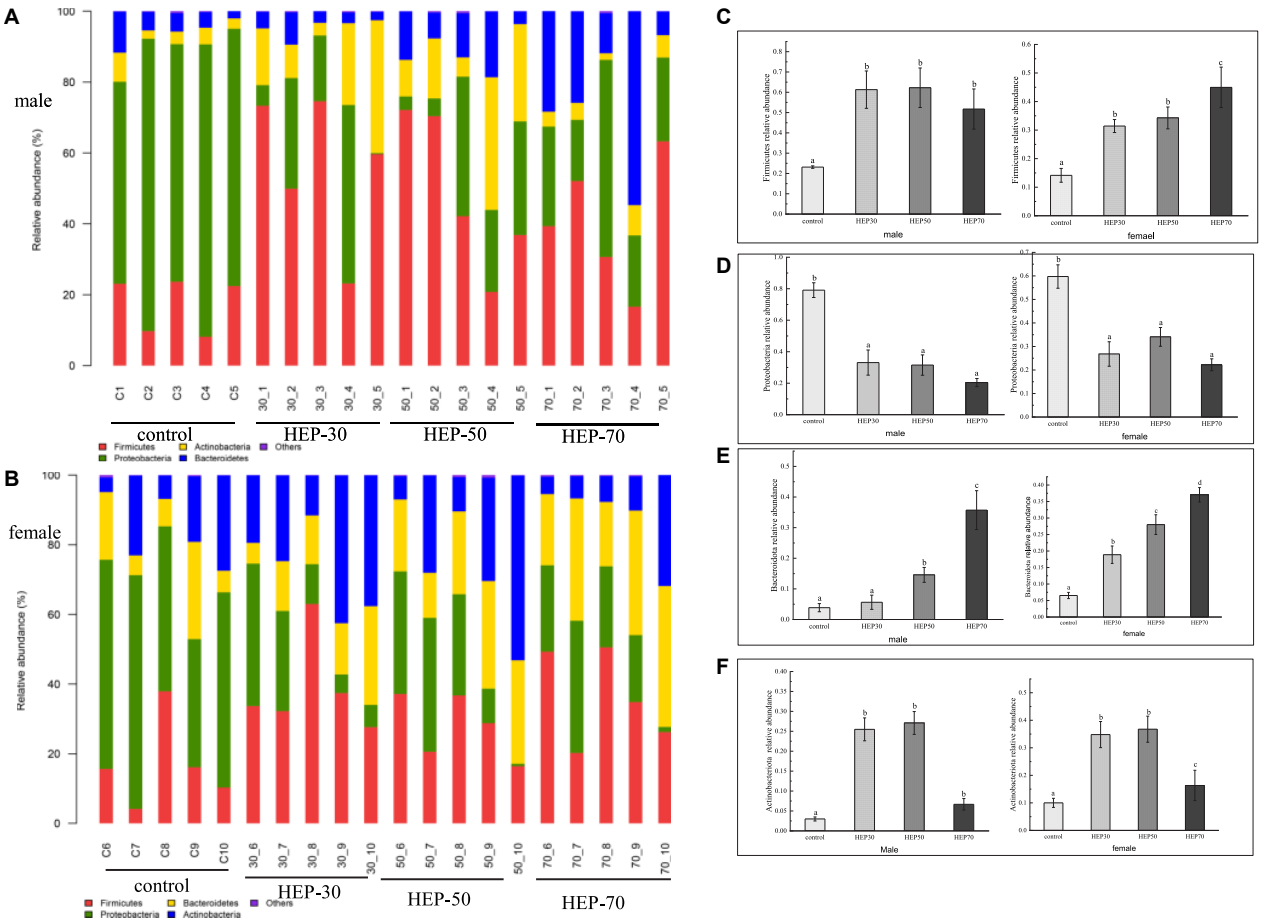

FIGURE 7 | The relative abundance of gut microbiota community at the phylum level *in vitro* fermentation. **(A)**, male; **(B)**, female; **(C)**, Firmicutes; **(D)**, Proteobacteria; **(E)**, Bacteroidetes; **(F)**, Actinobacteria. Data are means ± SD (5 independent experiments). ^{a,b,c}Different letters indicated a significant difference between the two groups ($p < 0.05$).

was significantly reduced compared with the control group ($P < 0.05$).

Figure 8, **Supplementary Figure 6**, and **Supplementary Table 1** show the relative abundance of GM at the genus level (A: male; B: female). As seen from the figures, although the GM species of male and female were different, *Bifidobacterium*, *Lactobacillus*, *Faecalibacterium,* and *Prevotella* were increased in both male and female media of the three HEP groups. Moreover, the relative abundance of *Escherichia-Shigella* was decreased compared with the control group. Excluding the HEP-70-treated female volunteers ($p > 0.05$), the overrepresentation of opportunistic pathogenic bacteria, e.g., *Escherichia-Shigella*, *Klebsiella* and, and *Enterobacter* (35), was significantly reduced in the fermentation broth after HEP treatment ($p < 0.05$). Additionally, *Acidaminococcus*, *Bacteroides*, *Dialister* ($p < 0.05$), *Dorea* ($p < 0.05$), *Prevotella 9* ($p < 0.05$), and *Megamonas* ($p < 0.05$) increased in abundance after treatment with HEPs, whereas relative abundances of *Alistipes*, *Collinsella*, *Parabacteroides,* and *Enterobacter* were lower in the HEP-treated group than those in the control group (**Supplementary Table 1**). It is worth noting that there were gender differences in the influence of HEP on some bacteria, and the influence of HEP fraction on bacteria abundance was also different, but the overall trend of HEP influence on bacteria was the same.

DISCUSSION

Through the method of hot water extraction and gradual alcohol precipitation, three different grades of HEPs were obtained. All the grades of HEP contained uronic acid, and these data support a previous study (36), but the reason which led to the different contents may be related to the selective type of extraction method, the use of extraction solvent, and the growth environment of the raw materials. The results of molecular weight distribution range of graded HEP was similar to the previous literature (22). Moreover, three graded components were used to study their activity, and Wang et al. also investigated the overall activity of crude polysaccharides (22). The reason for the difference in the molecular weight of the three polysaccharide components should be related to the different concentrations of ethanol precipitation. The lower the concentration of ethanol,

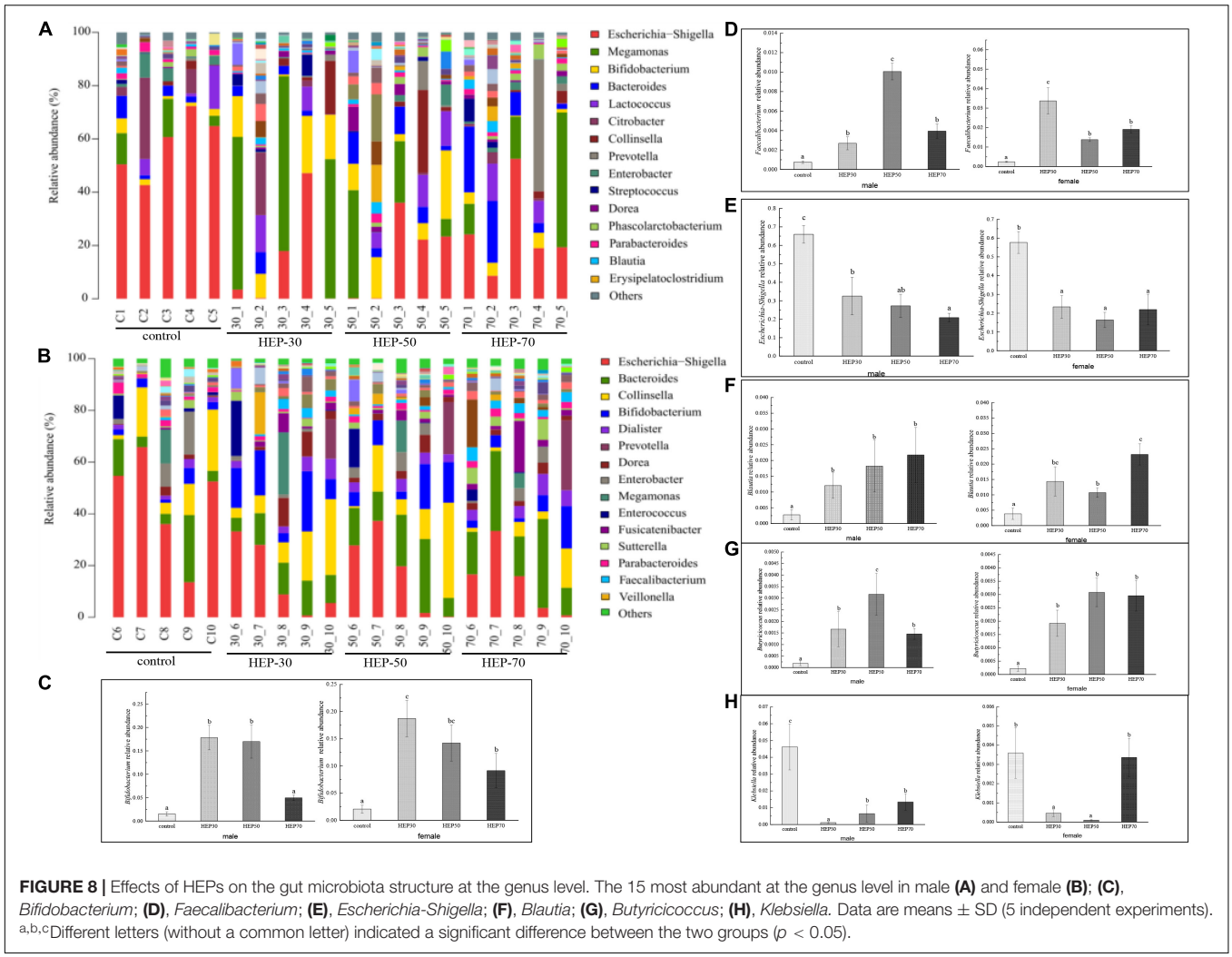

FIGURE 8 | Effects of HEPs on the gut microbiota structure at the genus level. The 15 most abundant at the genus level in male **(A)** and female **(B)**; **(C)**, *Bifidobacterium*; **(D)**, *Faecalibacterium*; **(E)**, *Escherichia-Shigella*; **(F)**, *Blautia*; **(G)**, *Butyricicoccus*; **(H)**, *Klebsiella*. Data are means ± SD (5 independent experiments). ^{a,b,c}Different letters (without a common letter) indicated a significant difference between the two groups ($p < 0.05$).

the larger molecular weight of polysaccharides that will be precipitated. The monosaccharide composition of HEP, which included fucose, glucose and galactose, was generally consistent with relevant researches (22, 37). However, a small amount of mannose component was also detected in our work, which might be attributed to the different growth environments and preparation methods of *H. erinaceus*. The microstructure of HEP appeared to curl, fold, form irregular aggregates, and can form thin film structures, consistent with other studies in the literature (36). Moreover, the intermolecular crosslinks between HEPs were very tight, which was also characteristic of most plant polysaccharides (38).

The physicochemical and structural properties of polysaccharides change during gastrointestinal digestion. Generally, food digested and absorbed by the host needs to pass through different digestive systems. Furthermore, the retention time of food in the oral cavity is 10 s–2 min, in the stomach is 15 min–3 h, in the small intestine is 2–5 h, and in the large intestine is 12–24 h (39). According to the reference, the simulated digestion time was formulated. In order to explore whether HEPs could safely reach the distal intestine, the simulated digestion ability of HEPs was studied. Some studies have shown that the GM can secrete carbohydrate hydrolase, dramatically decreasing the total sugar content (40). Therefore, the changes in total sugar content are often used as an indicator of the degree of fermentation. Results of the total sugar retention rate were similar to the data of reducing sugar and are also consistent with other relevant reports (4, 27, 41). The reason for the different retention rates of reducing sugar in the three HEP treatment groups may be due to the polysaccharides having produced reducing sugar or oligosaccharides by *in vitro* fermentation. Hence, the different fermentation rates led to different reducing sugar production rates. In addition, fecal microbiota also metabolized reducing sugar. However, the reducing sugar of the fermentation broth treated with HEPs was absorbed and utilized by the GM, which was consistent with the retention result of total sugar content mentioned above, and is also consistent with other related reports (4, 27, 41). The results of HEP in small intestinal digestion were similar to those for saliva and gastric digestion. In a word, all the results suggested that HEPs could pass through the digestive system without being broken down by saliva and simulated

gastric and small intestinal digestion and safely reach the large intestine. Thus, it was expected that the GM could metabolize it. However, considering that some oligosaccharides that are usually formed during HEP digestion do not have reductive properties, the use of this standard may underestimate the degree of HEP digestion. This subject is particularly pertinent since the structure and type of glycosidic bonds present in HEP fractions is not known. Therefore, it is difficult to predict the type of oligosaccharide or disaccharide resulting from digestion. It is necessary to further study these contents in the future. The difference of HEP utilization was also related to the structural composition of polysaccharides, e.g., side chain distribution, spatial conformation, degree of polymerization, and monosaccharide composition, or to the physicochemical properties of polysaccharides, e.g., solubility and viscosity (40). Due to its small molecular weight distribution, HEP-70 was easily decomposed, while HEP-50 was not as highly utilized by GM, which may be due to the differences in structure and composition of HEP-70 and the fewer sites of exposed microbial utilization values. Different microbes in the intestinal tract contained different enzymes, regulation, and transport mechanisms, thus specifically breaking down different polysaccharides (42). However, the high retention rate of HEP-30 may be attributed to its relatively large molecular weight, tightly clustered molecular structure, and large molecular volume, which lead to its poor water solubility and difficulty in hydrolysis (43). Current data support that too large or too small molecular weight of HEPs was not conducive to the utilization of GM.

Short-chain fatty acids (SCFAs) are the main metabolites produced by the GM after fermentation of non-degradable carbohydrates which can reduce the gut pH value. Therefore, the intestinal acid environment can suppress the growth of undesirable bacteria and pathogens and affect the enzyme activity of microorganisms. SCFAs can also prevent colorectal cancer degeneration and contribute to maintain gut homeostasis and health (44). Therefore, in this research, the contents of SCFAs were quantified to assess the effect of HEPs on the regulation of the intestinal microenvironment and to further understand the degree of GM decomposition and utilization of HEPs. The present SCFA data also support the results of previous studies *in vivo* (22). These results indicate that the GM can better decompose and utilize HEP-50. Moreover, the results are consistent with the above-mentioned results of carbohydrate utilization. pH is an important indicator that reflects the ability of GM to utilize carbohydrates by fermentation. The pH was consistent with the above SCFA results, indicating that the GM could better utilize HEP-50 components by fermentation.

The structure of GM is crucial for maintaining health. Understanding and exploring the relationship between HEPs and the structure of GM can help to improve human health and prevent some intestinal diseases. The data of α diversity indicate that HEPs can increase the bacterial richness and diversity of male fecal fermentation broth and increase the bacterial diversity of female fecal fermentation broth. This is consistent with population studies which state that daily *H. erinaceus* supplementation increases the Alpha diversity within the GM community (20). According to the previous research data of the population, the richness of the bacterial community is closely linked to obesity, e.g., obese individuals had lower bacterial abundance and gained more weight over time (45). Thus, HEPs showed a beneficial effect in increasing the diversity of GM.

Next, we further analyzed the influence of HEPs on the fecal microbial taxonomic profiles. At the phylum level, HEP treatment increased the relative abundance of Firmicutes, Bacteroidetes, and Actinobacteria to varying degrees, while reducing the relative abundance of Proteobacteria (**Figure 7**). Bacteroidetes could degrade polysaccharides, increasing their relative abundance (46), possibly indicating that HEP was degraded. In terms of Firmicutes species, many studies have found that the ratio of Firmicutes/Bacteroidetes (F/B) has been related to obesity, but due to the complex relationship of the GM, there is still no clear proportion relationship. Ismail et al. discovered that the F/B value of obese people was higher than that of the normal people (47), while Schwiertz et al. reached the opposite conclusion (48). Therefore, the increase in relative abundance of Firmicutes in this paper was not necessarily related to the obesity phenotype. Moreover, it has been reported that Firmicutes can improve the utilization rate of polysaccharides by participating in glycan degradation through the glycan degradation system (49). Moreover, Proteobacteria is a common pathogenic bacterium that could be harmful to human health (50). Proteobacteria is present at low levels in healthy populations, and its load is considered a potential diagnostic criterion for bacterial dysregulation and disease (50). Many common pathogenic bacteria, e.g., *Escherichia coli*, *Salmonella*, and *Helicobacter pylori*, belong to this phylum (51).

At the genus level, the results of the present study are consistent with *in vivo* studies in animals and human studies that *H. erinaceus* extracts or daily *H. erinaceus* supplementation could promote relative abundances of beneficial GM, e.g., *Bifidobacterium*, *Lactobacillus, Faecalibacterium,* and some SCFA-producing bacteria, and downregulated some pathobionts (19, 20). *Bifidobacterium* is a key symbiotic bacterium that plays a dominant role in human intestines. It can occupy the host soon after birth and is closely related to human health. There have been many studies on the increased abundance of *Bifidobacterium* induced by polysaccharides. In addition, the genome of *Bifidobacterium* contains lots of genes associated with carbohydrate metabolism and shows species-specific adaptability in polysaccharide-rich environments (52). Dietary fiber was conducive to reshaping intestinal microbial ecology, improving ecological imbalance, and enriching the proliferation of SCFA-producing bacteria, e.g., *Prevotella and Bifidobacterium*, thereby increasing the content of SCFAs in feces and systemic circulation. This partially explained the increase of SCFAs in fermentation broth (53). At the same time, *Bifidobacterium* could enhance intestinal barrier function, stimulate the host immune system and probiotic effects on gut function, and weaken the proinflammatory response (54). *Faecalibacterium* was more abundant in the GM of females over males, as butyrate-producing bacteria, and reduced intestinal permeability and inflammation (55). *Faecalibaculum* regulates the metabolic function of the host.

Moreover, the present study supported previous research that showed that a high fat and sugar diet reduced the abundance of *Faecalibaculum* and that mannan oligosaccharides increase the abundance of this bacterium (56). Moreover, a 6-month randomized controlled population trial found that low fat diets can increase the α diversity of the GM and the abundance of *Faecalibacterium* (the genus is known to contain butyrate-producing bacteria), whereas the high-fat diet was associated with increased *Bacteroides* and decreased *Faecalibacterium* (57). *Bifidobacterium* and *Lactobacillus* were typical anaerobic probiotics which could degrade macromolecular polysaccharides and have anti-inflammatory and anti-tumorigenic properties (58). Thus, polysaccharides can enhance the proliferation of potential probiotics (*Lactobacillus* and *Bifidobacterium*) in the intestine, reduce the relative abundance of pathogenic bacteria, produce SCFAs, and strengthen immune system of the body (59). In addition, the present data supported that HEP treatment enriched *Blautia* and *Butyricicoccus*, which is consistent with an increase in SCFA levels in feces. *Blautia* is a genus of anaerobic bacteria with probiotic characteristics that widely exists in mammalian feces and intestines and promotes the production of SCFAs and other activities to maintain intestinal homeostasis (51, 60). Moreover, *Butyricicoccus* produce butyrate as energy for gut normal cells, enhance mucosal barrier function, and reduce inflammation levels (51). HEP treatment increased the relative abundance of *Megamonas, Bacteroides*, and *Prevotella* but decreased the abundance of *Alistipes* (**Supplementary Table 1**). *Megamonas* has not been reported as a dominant genus in intestinal microbiology studies in European and American subjects, but it has been found in studies in China, suggesting that it may be a feature of East Asian populations (61). *Megamonas* genus was found to be positively correlated with the frequency of consumption of beans and serum bilirubin level, suggesting that the genus might be a beneficial microorganism (62). High-fat and low-carbohydrate diet was positively correlated with high risk of cardiac metabolic diseases, and contributed to the growth of *Bacteroides* and *Alistipes*, the reduction of *Faecalibacterium*, the increase of palmitic acid and stearic acid, and the decrease of butyric acid in human feces (63). Previous studies have shown that low-fat diets are associated with an increase in α diversity, *Blautia*, and *Faecalibacterium*, while high-fat diets are linked with an increase in *Alistipes* and *Bacteroides* and a decrease in *Faecalibacterium* (57). In addition, obesity is associated with a reduction in the abundance of intestinal *Bacteroides*, which may be beneficial to health (64). Thus, the abundance of *Bacteroides* should be at a normal level to maintain a healthy intestinal tract. As a dominant genus of bacteria in the human intestine, the *Prevotella spp.* coexist with certain individuals, particularly those with a plant-based diet, and show diversity in the use of a variety of complex carbohydrates (65). More and more people have studied *Prevotella* and regarded it as the beneficial GM (27). Microbial diversity figures reveal that the HEPs can increase the growth of these beneficial bacteria, promoted the growth of probiotics, inhibited the growth of harmful bacteria, improved the GM structure, and adjusted the host health. Physiological impacts of HEPs, both of which pass through the small intestine nearly intact and can be fermented by GM in the large intestine, are similar to each other. They exert a wide range of beneficial effects including anti-inflammation, gut epithelial barrier protection, and immune modulation through both microbiota-dependent and -independent mechanisms (5). Considering these observations, further studies on HEPs will be important for bowel health.

According to our current data analysis, HEPs had basically the same regulation effect on fecal microbiota of male and female volunteers, while the abundance and structure of fecal microbiota are different before fermentation. Therefore, the range of regulation is not completely the same. The effect of HEPs on the sex of volunteers showed a consistent trend. HEPs increased SCFAs and decreased pH value in fecal fermentation broth. The influence of HEP on the Alpha diversity of fecal fermentation broth of different genders was different to some extent, which may be attributed to the difference of Alpha diversity of fecal microbiota before fermentation. For example (**Supplementary Figure 4**), OTU number, Chao1 index, and Shannon index of female fecal samples before fermentation were significantly higher than those fecal samples of males ($p < 0.05$), while Simpson index was significantly lower than that of males ($p < 0.05$). At the phylum level, the influence trend (increase or decrease) of HEP on the abundance changes of Firmicutes, Proteobacteria, Bacteroidetes, and Actinobacteria was basically the same (**Figure 7**). At genus level (**Figure 8**), *Bifidobacterium*, *Faecalibacterium*, *Escherichia-Shigella*, *Blautia*, *Butyricicoccus*, *Klebsiella*, and other sequenced genera (**Supplementary Table 1**), but there were differences in the amplitude of increase or decrease in the abundance of different genera, which may be attributed to differences in the abundance and structure of the GM before fermentation. Compared with other HEPs, the effect of HEP-50 was relatively effective, but there was no significant difference in multiple indicators. As shown in **Table 1**, the crude polysaccharide content of HEP-50 was significantly higher than that of the other two HEPs ($p < 0.05$), and there was no significant difference in yield and reducing sugar content ($P > 0.05$), but the content of uronic acid was higher than that of HEP-30 ($p < 0.05$). The composition, structure, and external structure of HEP-50 monosaccharide are also different from those of the other two HEPs, which may be the reason for the difference in effect. Under the digestive conditions simulating saliva, stomach, and small intestine, all three kinds of HEPs were not significantly affected and safely reached the distal intestine. Compared with the other two HEPs, HEP-50 had the lowest retention rate of total sugar and low reducing sugar content in fermentation broth after fecal samples were treated for 24 h, indicating that HEP-50 was more thoroughly utilized and had a better effect on the regulation of fecal microbiota (**Figures 2**, **3**). After HEP-50 fermentation, the total SCFAs and other types of SCFAs (excluding i-valeric acid) were higher than the other two HEPs, indicating that fecal microbes could better decompose and utilize HEP-50. The results were consistent with the aforementioned results of carbohydrate utilization. The effect on pH of fecal fermentation fluid was consistent with SCFA results (**Figure 5**). In addition, the pH of HEP-50 treatment group was the lowest, but there was no significant difference among groups ($p > 0.05$). For the fecal

samples of male volunteers, HEP-50 had a better regulation effect on OTU number, Shannon index, and Simpson index compared to the other two HEPs. Moreover, HEP-50 had a better regulation effect on Chao1 index of fecal samples from female volunteers. However, there was no statistical significance in the regulation of α diversity ($p > 0.05$). At the phylum level, HEP-50 treatment had a better tendency to increase the abundance of Actinobacteria than the other two HEPs in both male and female fecal samples. At the genus level, HEP-50 had significantly better effects on *Faecalibacterium* and *Butyricicoccus* than other HEPs in male fecal samples ($p < 0.05$). In the fermentation broth of female fecal samples treated with HEP-50, *Butyricicoccus* has the highest abundance, while *Klebsiella* and *Escherichia-Shigella* have the lowest abundance.

CONCLUSION

The prepared polysaccharide contents of HEPs were 46.57–65.01%, and HEP-50 had the highest total sugar content. HEPs were not digested and utilized in simulated saliva, gastric juice, and small intestinal juice, but it can safely reach the large intestine and be degraded by GM. The effect of HEPs on fecal fermentation broth was basically the same, and there were differences for certain bacteria. After *in vitro* fermentation for 24 h, SCFA concentration was significantly increased, and pH value was decreased in the feces of male and female volunteers treated with HEPs. The phenomenon could be attributed to an increase in SCFA-producing bacteria and beneficial bacteria, such as *Bifidobacterium*, *Faecalibacterium*, *Blautia*, *Butyricicoccus*, and *Lactobacillus*. Furthermore, HEPs reduced the relative abundances of opportunistic pathogenic bacteria, e.g., *Escherichia-Shigella*, *Klebsiella*, and *Enterobacter*. In summary, the above results have shown that HEPs regulate the GM and may be developed as promising prebiotics, which may be conducive to the further development of HEPs in dietary supplement products and health food additives.

DATA AVAILABILITY STATEMENT

The datasets presented in this study can be found in online repositories. The names of the repository/repositories and accession number(s) can be found below: SRA database, accession number PRJNA806452.

ETHICS STATEMENT

The studies involving human participants were reviewed and approved by the Ethics Committee of the Hangzhou center for diesease control and prevention Approval Code: 202047. The patients/participants provided their written informed consent to participate in this study. Written informed consent was obtained from the individual(s) for the publication of any potentially identifiable images or data included in this article.

AUTHOR CONTRIBUTIONS

BT: data curation, writing – original draft, visualization, investigation, and formal analysis. YG and LH: conceptualization. TX: conceptualization, methodology, software, visualization, and investigation. XZ: visualization and methodology. RM: resources. XP: software. WW: validation. KY: project administration, funding acquisition, and writing – review and editing. PS, supervision. All authors contributed to the article and approved the submitted version.

FUNDING

This research was supported by grants from the key research and development projects of Zhejiang Province (2019C02040) and Hangzhou Agricultural and Society Development Project (202004A20).

SUPPLEMENTARY MATERIAL

The Supplementary Material for this article can be found online at: https://www.frontiersin.org/articles/10.3389/fnut.2022.858585/full#supplementary-material

REFERENCES

1. Vandeputte D, Kathagen G, D'Hoe K, Vieira-Silva S, Valles-Colomer M, Sabino J, et al. Quantitative microbiome profiling links gut community variation to microbial load. *Nature.* (2017) 551:507–11. doi: 10.1038/nature24460
2. Xie JH, Jin ML, Morris GA, Zha XQ, Chen HQ, Yi Y, et al. Advances on bioactive polysaccharides from medicinal plants. *Crit Rev Food Sci Nutr.* (2016) 56:S60–84. doi: 10.1080/10408398.2015.1069255
3. Lovegrove A, Edwards CH, De Noni I, Patel H, El SN, Grassby T, et al. Role of polysaccharides in food, digestion, and health. *Crit Rev Food Sci Nutr.* (2017) 57:237–53. doi: 10.1080/10408398.2014.939263
4. Su A, Ma G, Xie M, Ji Y, Li X, Zhao L, et al. Characteristic of polysaccharides from *Flammulina velutipes* in vitro digestion under salivary, simulated gastric and small intestinal conditions and fermentation by human gut microbiota. *Int J Food Sci Technol.* (2019) 54:2277–87. doi: 10.1111/ijfs.14142
5. Ho Do M, Seo YS, Park HY. Polysaccharides: bowel health and gut microbiota. *Crit Rev Food Sci Nutr.* (2021) 61:1212–24. doi: 10.1080/10408398.2020.1755949
6. Hee B, Wells J. Microbial regulation of host physiology by short–chain fatty acids. *Trends Microbiol.* (2021) 29:700–12. doi: 10.1016/j.tim.2021.02.001
7. He X, Wang X, Fang J, Chang Y, Ning N, Guo H, et al. Structures, biological activities, and industrial applications of the polysaccharides from *Hericium erinaceus* (Lion's Mane) mushroom: a review. *Int J Biol Macromol.* (2017) 97:228–37. doi: 10.1016/j.ijbiomac.2017.01.040
8. Friedman M. Chemistry, nutrition, and health–promoting properties of *Hericium erinaceus* (Lion's Mane) mushroom fruiting bodies and mycelia and their bioactive compounds. *J Agric Food Chem.* (2015) 63:7108–23. doi: 10.1021/acs.jafc.5b02914
9. Chaiyasut C, Sivamaruthi BS. Anti–hyperglycemic property of *Hencium erinaceus* – a mini review. *Asian Pac J Trop Biomed.* (2017) 7:1036–40. doi: 10.1016/j.apjtb.2017.09.024

10. Zhang Z, Lv G, Pan H, Pandey A, He W, Fan L. Antioxidant and hepatoprotective potential of endo–polysaccharides from *Hericium erinaceus* grown on tofu whey. *Int J Biol Macromol.* (2012) 51:1140–6. doi: 10.1016/j.ijbiomac.2012.09.002
11. Khursheed R, Singh SK, Wadhwa S, Gulati M, Awasthi A. Therapeutic potential of mushrooms in diabetes mellitus: role of polysaccharides. *Int J Biol Macromol.* (2020) 164:1194–205. doi: 10.1016/j.ijbiomac.2020.07.145
12. Han ZH, Ye JM, Wang GF. Evaluation of in vivo antioxidant activity of *Hericium erinaceus* polysaccharides. *Int J Biol Macromol.* (2013) 52:66–71. doi: 10.1016/j.ijbiomac.2012.09.009
13. Liu J, Du C, Wang Y, Yu Z. Anti–fatigue activities of polysaccharides extracted from *Hericium erinaceus*. *Exp Ther Med.* (2015) 9:483–7. doi: 10.3892/etm.2014.2139
14. Wong KH, Kanagasabapathy G, Bakar R, Phan CW, Sabaratnam V. Restoration of sensory dysfunction following peripheral nerve injury by the polysaccharide from culinary and medicinal mushroom, *Hericium erinaceus* (Bull.: Fr.) Pers. Through its neuroregenerative action. *Food Sci Technol.* (2015) 35:712–21. doi: 10.1590/1678-457x.6838
15. Wu F, Huang H. Surface morphology and protective effect of *Hericium erinaceus* polysaccharide on cyclophosphamide–induced immunosuppression in mice. *Carbohydr Polym.* (2021) 251:116930. doi: 10.1016/j.carbpol.2020.116930
16. Yang Y, Ye H, Zhao C, Ren L, Wang C, Georgiev MI, et al. Value added immunoregulatory polysaccharides of *Hericium erinaceus* and their effect on the gut microbiota. *Carbohydr Polym.* (2021) 262:117668. doi: 10.1016/j.carbpol.2021.117668
17. Shao S, Wang D, Zheng W, Li X, Zhang H, Zhao D, et al. A unique polysaccharide from *Hericium erinaceus* mycelium ameliorates acetic acid–induced ulcerative colitis rats by modulating the composition of the gut microbiota, short chain fatty acids levels and GPR41/43 respectors. *Int Immunopharmacol.* (2019) 71:411–22. doi: 10.1016/j.intimp.2019.02.038
18. Ren Y, Geng Y, Du Y, Li W, Lu ZM, Xu HY, et al. Polysaccharide of *Hericium erinaceus* attenuates colitis in C57BL/6 mice via regulation of oxidative stress, inflammation–related signaling pathways and modulating the composition of the gut microbiota. *J Nutr Biochem.* (2018) 57:67–76. doi: 10.1016/j.jnutbio.2018.03.005
19. Diling C, Xin Y, Chaoqun Z, Jian Y, Xiaocui T, Jun C, et al. Extracts from *Hericium erinaceus* relieve inflammatory bowel disease by regulating immunity and gut microbiota. *Oncotarget.* (2017) 8:85838–57. doi: 10.18632/oncotarget.20689
20. Xie XQ, Geng Y, Guan Q, Ren Y, Guo L, Lv Q, et al. Influence of short–term consumption of *Hericium erinaceus* on serum biochemical markers and the changes of the gut microbiota: a pilot study. *Nutrients.* (2021) 13:1008. doi: 10.3390/nu13031008
21. Pham VT, Mohajeri MH. The application of in vitro human intestinal models on the screening and development of pre– and probiotics. *Benef Microbes.* (2018) 9:725–42. doi: 10.3920/BM2017.0164
22. Wang XY, Yin JY, Nie SP, Xie MY. Isolation, purification and physicochemical properties of polysaccharide from fruiting body of *Hericium erinaceus* and its effect on colonic health of mice. *Int J Biol Macromol.* (2018) 107:1310–9. doi: 10.1016/j.ijbiomac.2017.09.112
23. Cai M, Xing H, Tian B, Xu J, Li Z, Zhu H, et al. Characteristics and antifatigue activity of graded polysaccharides from *Ganoderma lucidum* separated by cascade membrane technology. *Carbohydr Polym.* (2021) 269:118329. doi: 10.1016/j.carbpol.2021.118329
24. Yang K, Jin Y, Cai M, He P, Tian B, Guan R, et al. Separation, characterization and hypoglycemic activity in vitro evaluation of a low molecular weight heteropolysaccharide from the fruiting body of *Phellinus pini* dagger. *Food Funct.* (2021) 12:3493–503. doi: 10.1039/d1fo00297j
25. Yang K, Xu TR, Fu YH, Cai M, Xia QL, Guan RF, et al. Effects of ultrasonic pre–treatment on physicochemical properties of proteins extracted from cold–pressed sesame cake. *Food Res Int.* (2021) 139:109907. doi: 10.1016/j.foodres.2020.109907
26. Hu JL, Nie SP, Min FF, Xie MY. Artificial simulated saliva, gastric and intestinal digestion of polysaccharide from the seeds of *Plantago asiatica* L. *Carbohydr Polym.* (2013) 92:1143–50. doi: 10.1016/j.carbpol.2012.10.072
27. Chen G, Xie M, Wan P, Chen D, Ye H, Chen L, et al. Digestion under saliva, simulated gastric and small intestinal conditions and fermentation in vitro by human intestinal microbiota of polysaccharides from Fuzhuan brick tea. *Food Chem.* (2018) 244:331–9. doi: 10.1016/j.foodchem.2017.10.074
28. Wu DT, Yuan Q, Guo H, Fu Y, Li F, Wang SP, et al. Dynamic changes of structural characteristics of snow chrysanthemum polysaccharides during in vitro digestion and fecal fermentation and related impacts on gut microbiota. *Food Res Int.* (2021) 141:109888. doi: 10.1016/j.foodres.2020.109888
29. Bai S, Chen H, Zhu L, Liu W, Yu HD, Wang X, et al. Comparative study on the in vitro effects of *Pseudomonas aeruginosa* and seaweed alginates on human gut microbiota. *PLoS One.* (2017) 12:e0171576. doi: 10.1371/journal.pone.0171576
30. Tang W, Lin L, Xie J, Wang Z, Wang H, Dong Y, et al. Effect of ultrasonic treatment on the physicochemical properties and antioxidant activities of polysaccharide from *Cyclocarya paliurus*. *Carbohydr Polym.* (2016) 151:305–12. doi: 10.1016/j.carbpol.2016.05.078
31. Sorourian R, Khajehrahimi AE, Tadayoni M, Azizi MH, Hojjati M. Ultrasound–assisted extraction of polysaccharides from *Typha domingensis*: structural characterization and functional properties. *Int J Biol Macromol.* (2020) 160:758–68. doi: 10.1016/j.ijbiomac.2020.05.226
32. Zhou R, Cui M, Wang Y, Zhang M, Li F, Liu K. Isolation, structure identification and anti–inflammatory activity of a polysaccharide from *Phragmites rhizoma*. *Int J Biol Macromol.* (2020) 161:810–7. doi: 10.1016/j.ijbiomac.2020.06.124
33. Wang W, Wang X, Ye H, Hu B, Zhou L, Jabbar S, et al. Optimization of extraction, characterization and antioxidant activity of polysaccharides from *Brassica rapa* L. *Int J Biol Macromol.* (2016) 82:979–88. doi: 10.1016/j.ijbiomac.2015.10.051
34. Farhadi N. Structural elucidation of a water–soluble polysaccharide isolated from Balangu shirazi (*Lallemantia royleana*) seeds. *Food Hydrocoll.* (2017) 72:263–70. doi: 10.1016/j.foodhyd.2017.05.028
35. Gorrie CL, Mirčeta M, Wick RR, Edwards DJ, Thomson NR, Strugnell RA, et al. Gastrointestinal carriage is a major reservoir of *Klebsiella pneumoniae* infection in intensive care patients. *Clin Infect Dis.* (2017) 65:208–15. doi: 10.1093/cid/cix270
36. Yan JK, Ding ZC, Gao X, Wang YY, Yang Y, Wu D, et al. Comparative study of physicochemical properties and bioactivity of *Hericium erinaceus* polysaccharides at different solvent extractions. *Carbohydr Polym.* (2018) 193:373–82. doi: 10.1016/j.carbpol.2018.04.019
37. Wang ZJ, Luo DH, Liang ZY. Structure of polysaccharides from the fruiting body of *Hericium erinaceus* Pers. *Carbohydr Polym.* (2004) 57:241–7. doi: 10.1016/j.carbpol.2004.04.018
38. Qin T, Liu X, Luo Y, Yu R, Chen S, Zhang J, et al. Characterization of polysaccharides isolated from *Hericium erinaceus* and their protective effects on the DON-induced oxidative stress. *Int J Biol Macromol.* (2020) 152:1265–73. doi: 10.1016/j.ijbiomac.2019.10.223
39. Gong L, Cao W, Wang J, Sun B. Advances in dynamic,multi–compartmental gastrointestinal tract models and its food applications. *J Chin Inst Food Sci Technol.* (2018) 18:258–68. doi: 10.1016/j.cis.2018.11.007
40. Min FF, Hu JL, Nie SP, Xie JH, Xie MY. In vitro fermentation of the polysaccharides from *Cyclocarya paliurus* leaves by human fecal inoculums. *Carbohydr Polym.* (2014) 112:563–8. doi: 10.1016/j.carbpol.2014.06.027
41. Chen L, Liu J, Ge X, Xu W, Chen Y, Li F, et al. Simulated digestion and fermentation in vitro by human gut microbiota of polysaccharides from *Helicteres angustifolia* L. *Int J Biol Macromol.* (2019) 141:1065–71. doi: 10.1016/j.ijbiomac.2019.09.073
42. Li S, Hu J, Yao H, Geng F, Nie S. Interaction between four galactans with different structural characteristics and gut microbiota. *Crit Rev Food Sci Nutr.* (2021) 61:1–11. doi: 10.1080/10408398.2021.1992605
43. Xu Z, Li X, Feng S, Liu J, Zhou L, Yuan M, et al. Characteristics and bioactivities of different molecular weight polysaccharides from camellia seed cake. *Int J Biol Macromol.* (2016) 91:1025–32. doi: 10.1016/j.ijbiomac.2016.06.067
44. Fu X, Cao C, Ren B, Zhang B, Huang Q, Li C. Structural characterization and in vitro fermentation of a novel polysaccharide from *Sargassum thunbergii* and its impact on gut microbiota. *Carbohydr Polym.* (2018) 183:230–9. doi: 10.1016/j.carbpol.2017.12.048

45. Le Chatelier E, Nielsen T, Qin J, Prifti E, Hildebrand F, Falony G, et al. Richness of human gut microbiome correlates with metabolic markers. *Nature.* (2013) 500:541–6. doi: 10.1038/nature12506
46. Tamura K, Hemsworth GR, DeJean G, Rogers TE, Pudlo NA, Urs K, et al. Molecular mechanism by which prominent human gut bacteroidetes utilize mixed–linkage beta–glucans, major health–promoting cereal polysaccharides. *Cell Rep.* (2017) 21:417–30. doi: 10.1016/j.celrep.2017.09.049
47. Ismail NA, Ragab SH, Abd ElBaky A, Shoeib ARS, Alhosary Y, Fekry D. Frequency of firmicutes and bacteroidetes in gut microbiota in obese and normal weight Egyptian children and adults. *Arch Med Sci.* (2011) 7:501–7. doi: 10.5114/aoms.2011.23418
48. Schwiertz A, Taras D, Schaefer K, Beijer S, Bos NA, Donus C, et al. Microbiota and SCFA in lean and overweight healthy subjects. *Obesity.* (2010) 18:190–5. doi: 10.1038/oby.2009.167
49. Ndeh D, Gilbert HJ. Biochemistry of complex glycan depolymerisation by the human gut microbiota. *FEMS Microbiol Rev.* (2018) 42:146–64. doi: 10.1093/femsre/fuy002
50. Shin NR, Whon TW, Bae JW. Proteobacteria: microbial signature of dysbiosis in gut microbiota. *Trends Biotechnol.* (2015) 33:496–503. doi: 10.1016/j.tibtech.2015.06.011
51. Shi H, Chang Y, Gao Y, Wang X, Chen X, Wang Y, et al. Dietary fucoidan of *Acaudina molpadioides* alters gut microbiota and mitigates intestinal mucosal injury induced by cyclophosphamide. *Food Funct.* (2017) 8:3383–93. doi: 10.1039/C7FO00932A
52. Turroni F, Milani C, Duranti S, Mahony J, van Sinderen D, Ventura M. Glycan utilization and cross–feeding activities by bifidobacteria. *Trends Microbiol.* (2018) 26:339–50. doi: 10.1016/j.tim.2017.10.001
53. Li YJ, Chen X, Kwan TK, Loh YW, Singer J, Liu Y, et al. Dietary fiber protects against diabetic nephropathy through short-chain fatty acid–mediated activation of g protein–coupled receptors GPR43 and GPR109A. *J Am Soc Nephrol.* (2020) 31:1267–81. doi: 10.1681/asn.2019101029
54. Ding Y, Yan Y, Peng Y, Chen D, Mi J, Lu L, et al. In vitro digestion under simulated saliva, gastric and small intestinal conditions and fermentation by human gut microbiota of polysaccharides from the fruits of *Lycium barbarum*. *Int J Biol Macromol.* (2019) 125:751–60. doi: 10.1016/j.ijbiomac.2018.12.081
55. Mörkl S, Lackner S, Meinitzer A, Mangge H, Lehofer M, Halwachs B, et al. Gut microbiota, dietary intakes and intestinal permeability reflected by serum zonulin in women. *Eur J Nutr.* (2018) 57:2985–97. doi: 10.1007/s00394-018-1784-0
56. Yan S, Shi R, Li L, Ma S, Zhang H, Ye J, et al. Mannan oligosaccharide suppresses lipid accumulation and appetite in Western-diet-induced obese mice via reshaping gut microbiome and enhancing short–chain fatty acids production. *Mol Nutr Food Res.* (2019) 63:1900521. doi: 10.1002/mnfr.201900521
57. Wan Y, Wang F, Yuan J, Li J, Jiang D, Zhang J, et al. Effects of dietary fat on gut microbiota and faecal metabolites, and their relationship with cardiometabolic risk factors: a 6-month randomised controlled-feeding trial. *Gut.* (2019) 68:1417. doi: 10.1136/gutjnl-2018-317609
58. Ji X, Hou C, Gao Y, Xue Y, Yan Y, Guo X. Metagenomic analysis of gut microbiota modulatory effects of jujube (*Ziziphus jujuba* Mill.) polysaccharides in a colorectal cancer mouse model. *Food Funct.* (2020) 11:163–73. doi: 10.1039/C9FO02171J
59. Praveen MA, Parvathy KRK, Balasubramanian P, Jayabalan R. An overview of extraction and purification techniques of seaweed dietary fibers for immunomodulation on gut microbiota. *Trends Food Sci Technol.* (2019) 92:46–64. doi: 10.1016/j.tifs.2019.08.011
60. Liu X, Mao B, Gu J, Wu J, Cui S, Wang G, et al. Blautia–a new functional genus with potential probiotic properties? *Gut Microbes.* (2021) 13:1–21. doi: 10.1080/19490976.2021.1875796
61. Yachida S, Mizutani S, Shiroma H, Shiba S, Nakajima T, Sakamoto T, et al. Metagenomic and metabolomic analyses reveal distinct stage-specific phenotypes of the gut microbiota in colorectal cancer. *Nat Med.* (2019) 25:968–76. doi: 10.1038/s41591-019-0458-7
62. Liao M, Xie Y, Mao Y, Lu Z, Tan A, Wu C, et al. Comparative analyses of fecal microbiota in Chinese isolated Yao population, minority Zhuang and rural Han by 16sRNA sequencing. *Sci Rep.* (2018) 8:1142. doi: 10.1038/s41598-017-17851-8
63. Wan Y, Tang J, Li J, Li J, Yuan J, Wang F, et al. Contribution of diet to gut microbiota and related host cardiometabolic health: diet-gut interaction in human health. *Gut Microbes.* (2020) 11:603–9. doi: 10.1080/19490976.2019.1697149
64. Tian B, Zhao J, Zhang M, Chen Z, Ma Q, Liu H, et al. *Lycium ruthenicum* anthocyanins attenuate high-fat diet-induced colonic barrier dysfunction and inflammation in mice by modulating the gut microbiota. *Mol Nutr Food Res.* (2021) 65:2000745. doi: 10.1002/mnfr.202000745
65. Gálvez EJC, Iljazovic A, Amend L, Lesker TR, Renault T, Thiemann S, et al. Distinct polysaccharide utilization determines interspecies competition between intestinal *Prevotella* spp. *Cell Host Microbe.* (2020) 28:838–852.e6. doi: 10.1016/j.chom.2020.09.012

Conflict of Interest: RM is employed by Changshan Haofeng Agricultural Development Co., Ltd.

The remaining authors declare that the research was conducted in the absence of any commercial or financial relationships that could be construed as a potential conflict of interest.

Publisher's Note: All claims expressed in this article are solely those of the authors and do not necessarily represent those of their affiliated organizations, or those of the publisher, the editors and the reviewers. Any product that may be evaluated in this article, or claim that may be made by its manufacturer, is not guaranteed or endorsed by the publisher.

frontiers | Frontiers in Nutrition

ORIGINAL RESEARCH
published: 25 April 2022
doi: 10.3389/fnut.2022.861588

Crude Polysaccharide Extracted From *Moringa oleifera* Leaves Prevents Obesity in Association With Modulating Gut Microbiota in High-Fat Diet-Fed Mice

Lingfei Li[1,2†], *Li Ma*[1,3,4†], *Yanlong Wen*[1,2], *Jing Xie*[1,2], *Liang Yan*[3,4], *Aibing Ji*[3,4], *Yin Zeng*[3,4], *Yang Tian*[1,2*] *and Jun Sheng*[5*]

[1] College of Food Science and Technology, Yunnan Agricultural University, Kunming, China, [2] Engineering Research Center of Development and Utilization of Food and Drug Homologous Resources, Ministry of Education, Yunnan Agricultural University, Kunming, China, [3] Pu'er Institute of Pu-erh Tea, Pu'er, China, [4] College of Tea (Pu'er), West Yunnan University of Applied Sciences, Pu'er, China, [5] Key Laboratory of Pu-er Tea Science, Ministry of Education, Yunnan Agricultural University, Kunming, China

Moringa oleifera is a commonly used plant with high nutritional and medicinal values. *M. oleifera* leaves are considered a new food resource in China. However, the biological activities of *M. oleifera* polysaccharides (MOP) in regulating gut microbiota and alleviating obesity remain obscure. In the present study, we prepared the MOP and evaluated its effects on obesity and gut microbiota in high-fat diet (HFD)-induced C57BL/6J mice. The experimental mice were supplemented with a normal chow diet (NCD group), a high-fat diet (HFD group), and HFD along with MOP at a different dose of 100, 200, and 400 mg/kg/d, respectively. Physiological, histological, biochemical parameters, genes related to lipid metabolism, and gut microbiota composition were compared among five experimental groups. The results showed that MOP supplementation effectively prevented weight gain and lipid accumulation induced by HFD, ameliorated blood lipid levels and insulin resistance, alleviated the secretion of pro-inflammatory cytokines, and regulated the expression of genes related to lipid metabolism and bile acid metabolism. In addition, MOP positively reshaped the gut microbiota composition, significantly increasing the abundance of *Bacteroides*, norank_f_Ruminococcaceae, and *Oscillibacter*, while decreasing the relative abundance of *Blautia*, *Alistipes*, and *Tyzzerella*, which are closely associated with obesity. These results demonstrated that MOP supplementation has a protective effect against HFD-induced obesity in mice, which was associated with reshaping the gut microbiota. To the best of our knowledge, this is the first report on the potential of MOP to prevent obesity and modulating gut microbiota, which suggests that MOP can be used as a potential prebiotic.

Keywords: polysaccharide, *Moringa oleifera* leaves, gut microbiota, obesity, high-fat diet

OPEN ACCESS

Edited by:
Ding-Tao Wu,
Chengdu University, China

Reviewed by:
Houkai Li,
Shanghai University of Traditional Chinese Medicine, China
Qiu Li,
Qingdao Agricultural University, China
Hongli Cui,
Shanxi Agricultural University, China
Bin Wei,
Zhejiang University of Technology, China
Yilin Pang,
Hunan Agricultural University, China

***Correspondence:**
Yang Tian
tianyang1208@163.com
Jun Sheng
shengjun_ynau@163.com

†These authors have contributed equally to this work

Specialty section:
This article was submitted to Nutrition and Microbes, a section of the journal Frontiers in Nutrition

Received: *24 January 2022*
Accepted: *14 March 2022*
Published: *25 April 2022*

Citation:
Li L, Ma L, Wen Y, Xie J, Yan L, Ji A, Zeng Y, Tian Y and Sheng J (2022) Crude Polysaccharide Extracted From Moringa oleifera Leaves Prevents Obesity in Association With Modulating Gut Microbiota in High-Fat Diet-Fed Mice. Front. Nutr. 9:861588. doi: 10.3389/fnut.2022.861588

INTRODUCTION

In recent years, the prevalence of obesity has increased dramatically and has become a severe health problem worldwide. In 2016, 39% (more than 1.9 billion) of adults were overweight, and 13% were obese (1). The worldwide prevalence of obesity nearly tripled between 1975 and 2016 (2). It has been estimated that by 2030, the obesity rate will reach up to 20% of the adult population. Approximately 500 million people are obese, and 1.4 billion are overweight globally (3). The main characteristics of obesity are excessive weight gain and fat accumulation due to various factors, such as genetic predisposition, high-calorie energy intake, and sedentary lifestyle (4). Obesity can cause chronic low-grade inflammation, hyperglycemia, hyperlipidemia, and insulin resistance (5, 6). Accumulating evidence suggests that obesity is associated with various metabolic disorders, such as cardiovascular disease, type II diabetes, non-alcoholic fatty liver disease, and various kinds of cancers (3). With the recognition that obesity is responsible for a growing prevalence of chronic diseases, obesity has been recognized as "the greatest threat to global public health in this century" (7). Reducing and curbing obesity is one of the most important health challenges in the modern world. Depending on the severity of the disease, there are several ways to intervene or treat obesity, including lifestyle changes, pharmacotherapy, and bariatric surgery (8). However, the use of drugs or bariatric surgery has been shown to be associated with significant side effects, some of which could increase the risk of developing chronic diseases (6, 9). Therefore, the search for natural compounds to treat obesity and its related diseases has attracted much research interest.

Despite significant research efforts to combat obesity-induced metabolic syndrome in the last decade, there has been slow progress in understanding the causes and mechanisms that regulate its development. In recent years, accumulating evidence suggests that gut microbiota dysbiosis is strongly associated with host metabolism and obesity development (10–12). Studies have shown that the high-fat diet can change the structure of gut microbiota, disrupt the intestinal microenvironment, and lead to dysbiosis of gut microbiota (13, 14). Conversely, it has been shown that gut microbiota play an important role in the dynamic balance of metabolism by regulating intestinal endothelial barrier function, glucose metabolism, and chronic inflammation associated with obesity. Therefore, it has been proposed that altering the composition of gut microbiota by dietary or other means can confer beneficial effects, restoring the integrity of intestinal function and reversing the characteristics of obesity (15).

In recent years, polysaccharides have attracted attention for their role in weight loss. Polysaccharides are macromolecular polymers composed of at least ten monosaccharides linked by glycosidic bonds (16), and they are natural macromolecular active substances widely found in animals, plants, algae, and microbial cells (17). Polysaccharides are well-known for their health benefits, such as immunomodulatory (18), anti-tumor (19), anti-inflammatory (20), anti-oxidant (21), and hypolipidemic effects (22). Previous studies have suggested that polysaccharides from plants, such as *Angelica sinensis* (23), *Schisandra* (24), and *Ophiopogon* (25), show great lipid-lowering effects. Polysaccharides can reduce body weight, leaky gut, and low-grade inflammation in various tissues by physicochemical properties, such as water retention, and/or by probiotic activity, such as altering gut microbiota and production of microbiota-derived metabolites (26). A study showed that *Polygonatum odoratum* polysaccharides modulated gut microbiota and mitigated obesity induced by a high-fat diet (HFD) in rats (27). It has also been shown that the phylum Firmicutes was 40% higher than the phylum Bacteroidetes in HFD-fed mice, and supplementation with *Ophiopogon* polysaccharides increased Bacteroidetes by 28% and decreased Firmicutes by 15% (25). Thus, dietary polysaccharides are considered one of the effective regulators of gut microbiota, which may help the host regulate metabolism.

Moringa oleifera Lam. is a perennial plant of the Moringaceae family, also known as the "drumstick tree," "miracle tree," or "tree of life" (28). *M. oleifera* is rich in nutrients, including protein, vitamins, essential amino acids, minerals, dietary fiber, and bioactive compounds (29). In 2011, the Ministry of Health of the People's Republic of China issued a notice to consider *M. oleifera l*eaves as a new food resource. It has been demonstrated that *M. oleifera* has many biological functions such as anti-microbial, anti-oxidant, anti-inflammatory, anti-cancer, hepatoprotective, hypoglycemic, hypolipidemic, and other effects (30–32). However, the biological activities of *M. oleifera* polysaccharides (MOP) in regulating gut microbiota and alleviating obesity have not yet been reported. We hypothesized that MOP could positively modulate the gut microbiota and attenuate HFD-induced obesity. Therefore, to verify this hypothesis, we investigated the effects of MOP on body weight, fat accumulation, blood lipid levels, insulin resistance, chronic inflammation, and gut microbiota in a HFD-induced obese mice, and further investigated the correlation of gut bacteria with obesity-related parameters including host obesity phenotype, blood lipids, glucose homeostasis, and pro-inflammatory cytokines.

MATERIALS AND METHODS

Preparation of Crude Polysaccharides From *M. oleifera* Leaves (MOP)

M. oleifera leaf powder was purchased from Yunnan Tianyou Technology Development Co. (Dehong, China). The crude polysaccharide was extracted according to the methods described in previous studies (33). In brief, *M. oleifera* leaf powder was extracted three times with deionized water at a ratio of 1:10 (w/v) at 70°C for 90 min, followed by centrifuging at 4,000 rpm for 20 min. The supernatants were combined and concentrated by rotary evaporation. The concentrates were added to anhydrous ethanol to obtain a final ethanol concentration of 80% (v/v), and kept at 4°C overnight. The resulting precipitates were gained after centrifugation, washed with 95% ethanol, dissolved in deionized water, then loaded into dialysis bags (molecular weight cutoff: 3,500 Da) and

TABLE 1 | Chemical and monosaccharides compositions of MOP.

Chemical composition	Value
Total sugar (%)	38.90
Total dietary fiber (g/100 g)	48.70
Protein (g/100 g)	3.88
Mannose (g/kg)	10.81
Ribose (g/kg)	1.01
Rhamnose (g/kg)	22.42
Glucuronic acid (g/kg)	2.14
Galacturonic acid (g/kg)	34.25
Glucose (g/kg)	47.60
Galactose (g/kg)	252.72
Xylose (g/kg)	7.29
Arabinose (g/kg)	111.16
Fucose (g/kg)	2.53

dialyzed for 2 days at 4°C, and the deionized water was changed every 4 h. The dialyzed solution was vacuum freeze-dried to obtain the crude polysaccharide of *M. oleifera* (MOP). The polysaccharide content of MOP was measured by the phenol-sulfuric acid method (34). Total protein content was quantified by the Bradford method (35). Dietary fiber concentrations were determined according to the method of Prosky et al. (36). The monosaccharide composition was analyzed by the high-performance liquid chromatography (HPLC) technique (37). Chemical and monosaccharide compositions of MOP are shown in **Table 1** and **Supplementary Figure 1**.

Animals and Diets

Seven-week-old male C57BL/6J mice were purchased from Kunming Medical University Laboratory Animal Center (Kunming, China). All mice were maintained in controlled environmental conditions (a 12/12 h light/dark cycle, 25 ± 1°C, and 55% humidity) with free access to food and water. After acclimation for 1 week, the mice were randomly divided into five groups ($n = 8$, each group) to be fed the following diets for 12 weeks: (1) NCD (normal chow diet, TP23302, 10% calories from fat, Trophic Animal Feed High-tech Co., Ltd, Nantong, China), which was daily gavaged with distilled water only, as control; (2) HFD (high-fat diet, TP23300, 60% calories from fat, Trophic Animal Feed High-tech Co., Ltd, Nantong, China), which was daily gavaged with distilled water only, as control; (3) HFD + MOP100 (gavaged with 100 mg/kg/d MOP); (4) HFD + MOP200 (gavaged with 200 mg/kg/d MOP); (5) HFD + MOP400 (gavaged with 400 mg/kg/d MOP). The animal protocol used in this study was approved by the Animal Care and Use Committee of Yunnan Agricultural University.

Blood and Tissue Sample Collection

At the end of the experiment, the mice were anesthetized with 3% pentobarbital sodium after 12 h of fasting. The blood samples were collected from the retro-orbital sinus and centrifuged at 12,000 rpm for 10 min at 4°C to obtain serum. Perirenal fat, mesenteric fat, and liver from each mouse were collected and weighted. A portion of the liver and perirenal adipose tissues were immersion-fixed in 10% neutral formalin. The remaining tissues and cecum contents were snap-frozen in liquid nitrogen within 10 min postmortem, then preserved at −80°C.

Histopathological Examination

Formalin-fixed liver and perirenal adipose tissues were embedded in paraffin, cut into 5-μm sections, stained with hematoxylin and eosin (H & E), and visualized under a microscope (Olympus CX43, Japan). Adipocyte size was measured using ImageJ software.

Biochemical Analysis

Serum total cholesterol (T-CHO), triacylglycerol (TG), low-density lipoprotein cholesterol (LDL-C), and high-density lipoprotein cholesterol (HDL-C) were measured with commercial assay kits (Nanjing Jiancheng Bioengineering Institute, China), respectively. Fasting blood glucose was determined by the glucose oxidase method using the Glucose GOD-PAD kit (Rongsheng Biotech Co. Ltd, Shanghai, China). Serum insulin levels were measured using the mouse insulin ELISA kit (Beijing Solarbio Science & Technology Co., China). Serum TNF-α and IL-1β were measured using ELISA kits (Beijing 4A Biotech Co., China). All protocols were performed according to the manufacturers' instructions. The homeostasis model assessment of insulin resistance (HOMA-IR) index was calculated using the formula (HOMA-IR = fasting insulin (mU/l) × fasting glucose (mmol/l)/22.5 (38).

Quantitative PCR Analysis of Gene Expression

Total RNA was extracted from liver tissue using Trizol reagent (Takara, Dalian, China), and quantified using a NanoDrop 2000 Spectrophotometer (Thermo Fisher, USA). Complementary DNA was synthesized using the PrimeScript^{TM} RT reagent kit with a genomic DNA Eraser (Takara, Dalian, China) in accordance with the manufacturer's protocol. Real-time quantitative polymerase chain reaction (RT-qPCR) was performed with SYBR Premix Ex Taq^{TM}II (Takara, Dalian, China) in the Bio-Rad CFX96 Thermocycler (Bio-Rad, USA). All the primers are listed in **Supplementary Table 1**.

Gut Microbiota Analysis

Bacterial genomic DNA was extracted from cecal contents using the QIAamp-DNA Stool Mini Kit (Qiagen, Hilden, Germany) according to the manufacturer's instructions. DNA samples were sent to Majorbio Biotechnology Co., Ltd. (Shanghai, China) under dry ice conditions for 16S rRNA gene sequencing. The V3–V4 hypervariable regions of the 16S rRNA gene were amplified with primers 338F (5′-ACTCCTACGGGAGGCAGCAG-3′) and 806R (5′-GGACTACHVGGGTWTCTAAT-3′) using a thermocycler PCR system (GeneAmp 9700; ABI, USA). The raw reads were deposited into the NCBI Sequence Read Archive database (Accession: PRJNA759102).

Subsequent bioinformatics analysis was performed through the free online Majorbio I-Sanger Cloud Platform (www.i-sanger.com). Operational taxonomic units (OTUs)

were picked with a 97% similarity threshold. In the analysis, alpha-diversity metrics were used, including Sobs (the actually observed richness), Chao (Chao index of species richness), ACE (the ACE index of species richness), and Shannon diversity index. Beta-diversity of gut microbiota, including hierarchical clustering tree and Principal Coordinate Analysis (PCoA), was performed based on the unweighted UniFrac distance. Moreover, the analysis of similarity (ANOSIM) test was used to test the significant differences between sample groupings. The linear discriminant analysis (LDA) effect size (LEfSe) was used to identify which bacterial taxa drove changes in the microbiota community, and the LDA threshold was >3.0). The two-factor correlation network analysis was performed to determine the correlations between specific gut bacteria and obesity-related biomarkers.

Statistical Analysis

Statistical analysis was performed with SPSS statistics 19.0. Data sets involving more than two groups were analyzed using one-way ANOVA, followed by Duncan's multiple range tests. A value of $p < 0.05$ was considered to be statistically significant.

RESULTS

MOP Attenuates Body Weight Gain Induced by HFD

As shown in **Figure 1A**, the mean initial body weight of the mice in the 5 groups ranged from 22.85 to 23.73 g. One-way ANOVA showed no statistical difference in mouse body weight between all diet groups at the beginning of the experiment ($F = 0.8950$, $p = 0.4749$). As expected, the mice fed with HFD gained significantly more weight than the NCD mice after 12 weeks ($p < 0.01$) (**Figures 1A,B**). Supplementation with MOP effectively attenuated the body weight gain in HFD-fed mice, although there was no significant difference between the different MOP dose groups (100, 200, and 400 mg/kg/d). Daily food intake and caloric intake were measured to determine whether MOP functions by modulating food or energy intake in mice. The data showed that the daily food intake and caloric intake of MOP-treated groups were not statistically different from those of the HFD group (**Figures 1C,D**), but their body weight gain was lower than that of mice fed HFD ($p < 0.05$) (**Figure 1B**), suggesting that the protective effect of MOP against HFD-induced weight gain was not through suppression of food or energy intake. Additionally, the food efficiency ratio (FER) in the HFD group was significantly higher than in the NCD group ($p < 0.01$), while supplementation with MOP significantly decreased the FER (**Figure 1E**). Lee's index can comprehensively reflect the proportional relationship between body weight and body length, which can be used as an indicator to evaluate the degree of obesity in obese model mice. In the present study, HFD significantly increased the Lee's index in mice, while MOP supplementation decreased the Lee's index (**Figure 1F**). These results suggest that MOP intervention is effective in attenuating body weight gain induced by HFD in mice.

MOP Inhibits Adipose Hypertrophy and Liver Steatosis Induced by HFD

The effects of MOP on the adipose tissues were also examined after 12 weeks of treatment. Perirenal fat weight and mesenteric fat weight were induced by HFD and significantly reversed by MOP supplementation (**Figures 2A,B**). H & E staining showed an 84.12% increase in the adipocyte size of the HFD group. The average adipocyte size of the MOP-treated groups (especially at high-dose) was significantly reduced, which was similar to that of the normal diet group (**Figures 2C,D**), indicating that MOP could prevent HFD-induced adipose hypertrophy.

Fat accumulation in the liver is another important indicator of metabolic dysregulation induced by HFD. Therefore, the gross weight and histology of the liver from the different experimental groups were examined. Compared to the NCD group, the liver weights of HFD-fed mice were significantly increased. MOP supplementation remarkably reduced the liver index induced by HFD feeding, although there was no significant difference between the different MOP dose groups (**Figure 2E**). H & E staining of the liver revealed histological abnormalities of hepatocytes with larger fat vacuoles in the HFD group, indicating that the mice had suffered a higher degree of hepatic steatosis induced by HFD feding. MOP markedly reduced the size of the fat vacuoles in the liver induced by HFD (**Figure 2F**), suggesting that MOP exerted a liver protective effect by reducing fatty degeneration.

MOP Ameliorates Blood Lipid Levels and Insulin Resistance

As excessive fat accumulation in obese individuals leads to dyslipidemia, lipid concentrations in serum were measured in the present study. Levels of total cholesterol (T-CHO), triglycerides (TG), high-density lipoprotein cholesterol (HDL-C), and low-density lipoprotein cholesterol (LDL-C) in serum were significantly higher in the HFD group, compared with those of the NCD group. In addition, MOP supplementation in HFD-fed mice significantly decreased the levels of T-CHO, TG, and LDL-C in a dose-dependent manner (**Figures 3A–C**). Notably, MOP supplementation significantly increased HDL-C concentrations (**Figure 3D**). These data suggest the protective effect of MOP against HFD-induced hypercholesterolemia and hyperlipidemia.

Obesity is closely correlated with impaired insulin signaling and is a major cause of the development of insulin resistance (39). Fasting glucose and fasting serum insulin were measured, and HOMA-IR was calculated in the present study. Fasting glucose and insulin levels were significantly elevated in HFD-fed mice, along with an increase in HOMA-IR values, and they were significantly reversed by MOP supplementation (**Figures 3E–G**). Apparently, MOP supplementation significantly decreased the insulin resistance induced by HFD.

MOP Alleviates HFD-Induced Secretion of Pro-inflammatory Cytokines

Chronic low-grade inflammation is one of the most important characteristics of obesity (40). To evaluate the anti-inflammatory

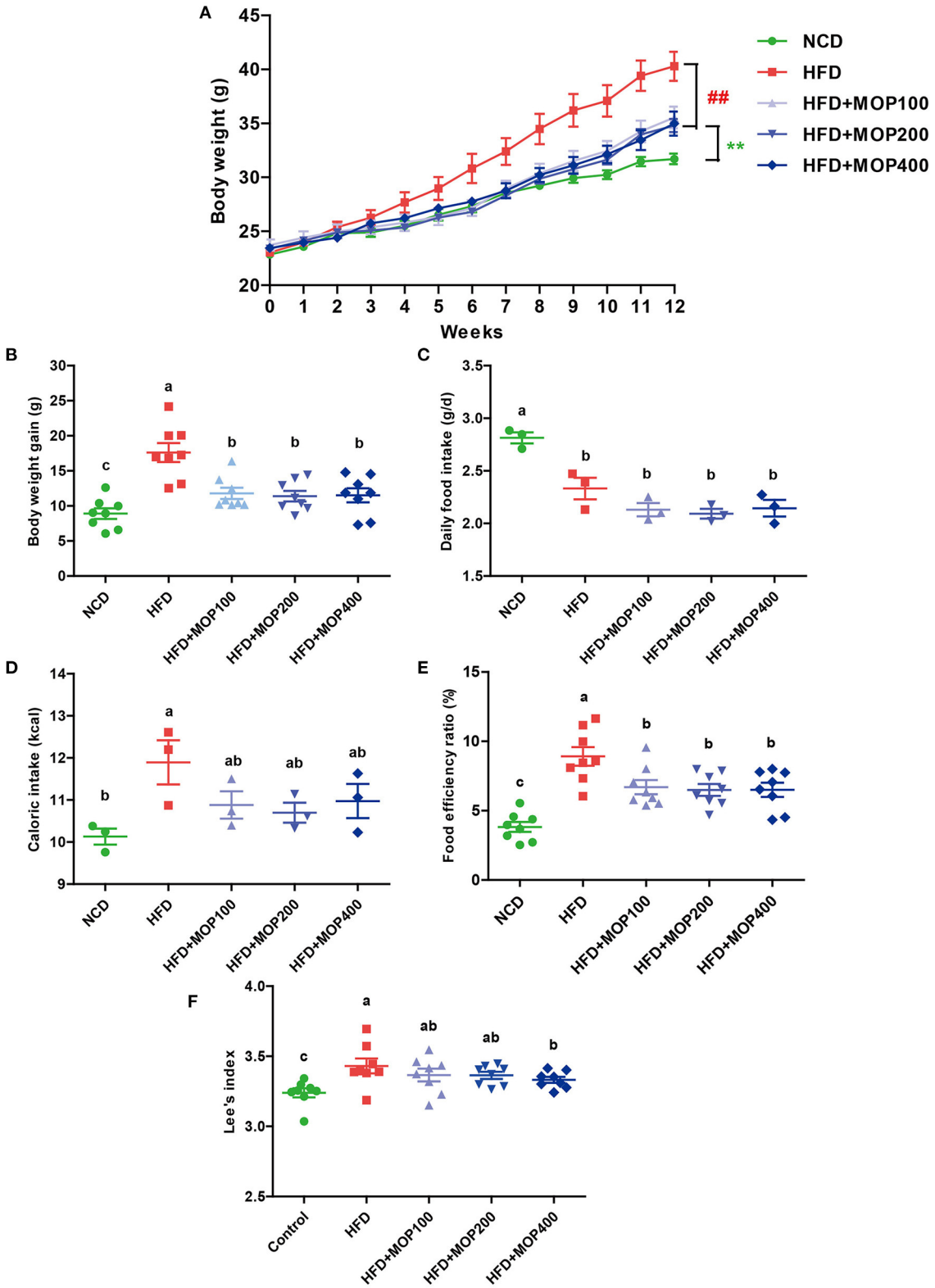

FIGURE 1 | MOP reduces body weight in HFD-fed mice. **(A)** The change in body weight of the mice during the experiment ($n = 8$ mice/group); **(B)** body weight gain ($n = 8$); **(C)** daily food intake ($n = 3$ cages/group); **(D)** caloric intake ($n = 3$); **(E)** food efficiency ratio (EFR), food efficiency ratio (%) = total body weight gain/total food intake ×100 ($n = 8$); **(F)** Lee's index, Lee's index = body weight (g)∧(1/3) × 1,000/body length (cm) ($n = 8$). Data are shown as means ± SEM. Bars marked with different superscript letters (a–c) indicate significant differences at $p < 0.05$ based on one-way ANOVA with Duncan's *post-hoc* test.

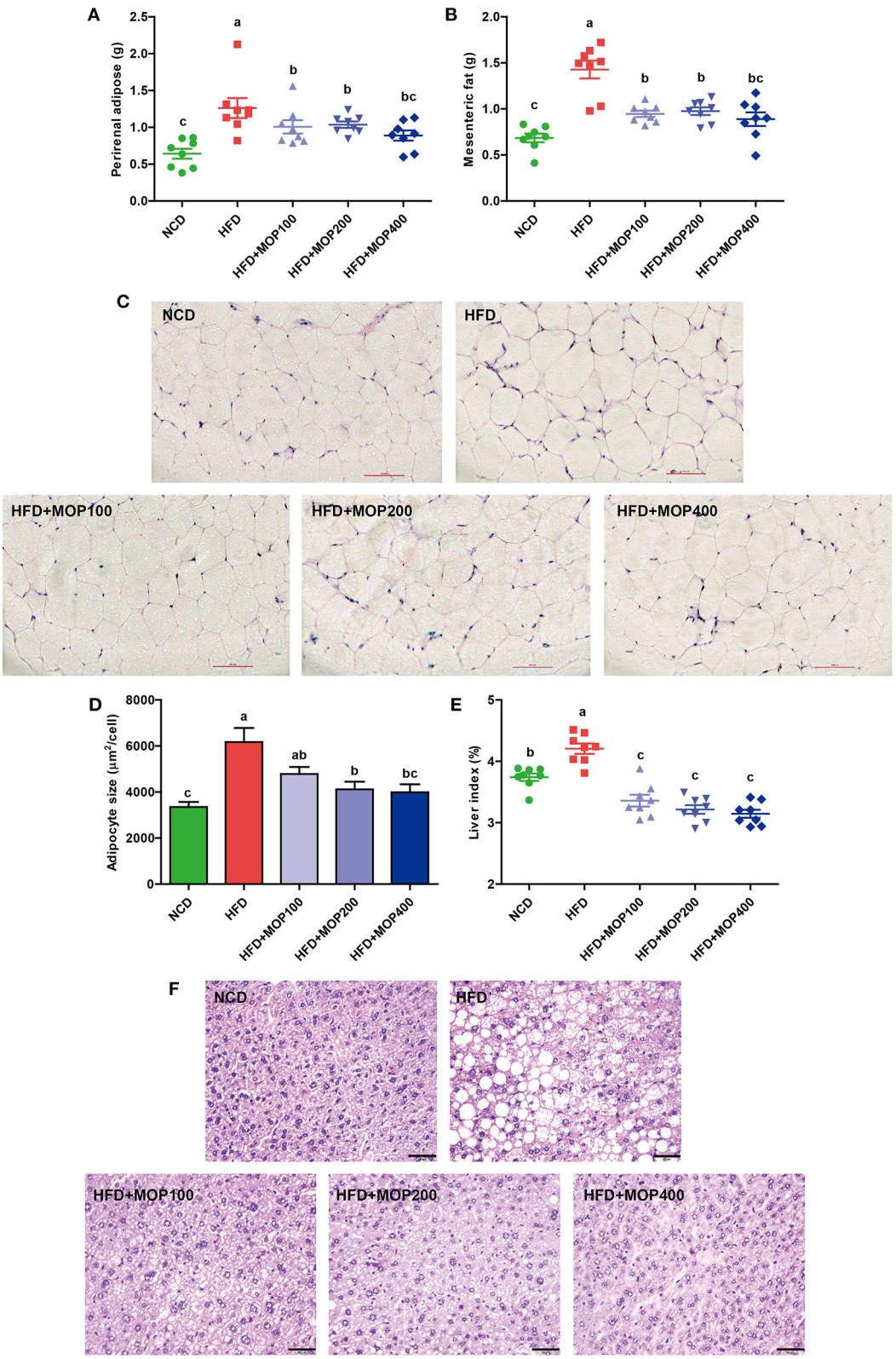

FIGURE 2 | Preventive effects of MOP on fat accumulation in HFD-fed mice ($n = 8$ mice/group). **(A)** Perirenal fat weight, **(B)** Mesenteric fat weight, **(C)** Histological examination of perirenal fat by H & E staining, scale bar = 100 μm, **(D)** Adipocyte size was monitored in mesenteric fat tissue, **(E)** Liver index, **(F)** Representative liver histology by H & E staining, scale bar = 50 μm. Data are shown as means ± SEM. Bars marked with different superscript letters (a–c) indicate significant differences at $p < 0.05$ based on one-way ANOVA with Duncan's *post-hoc* test.

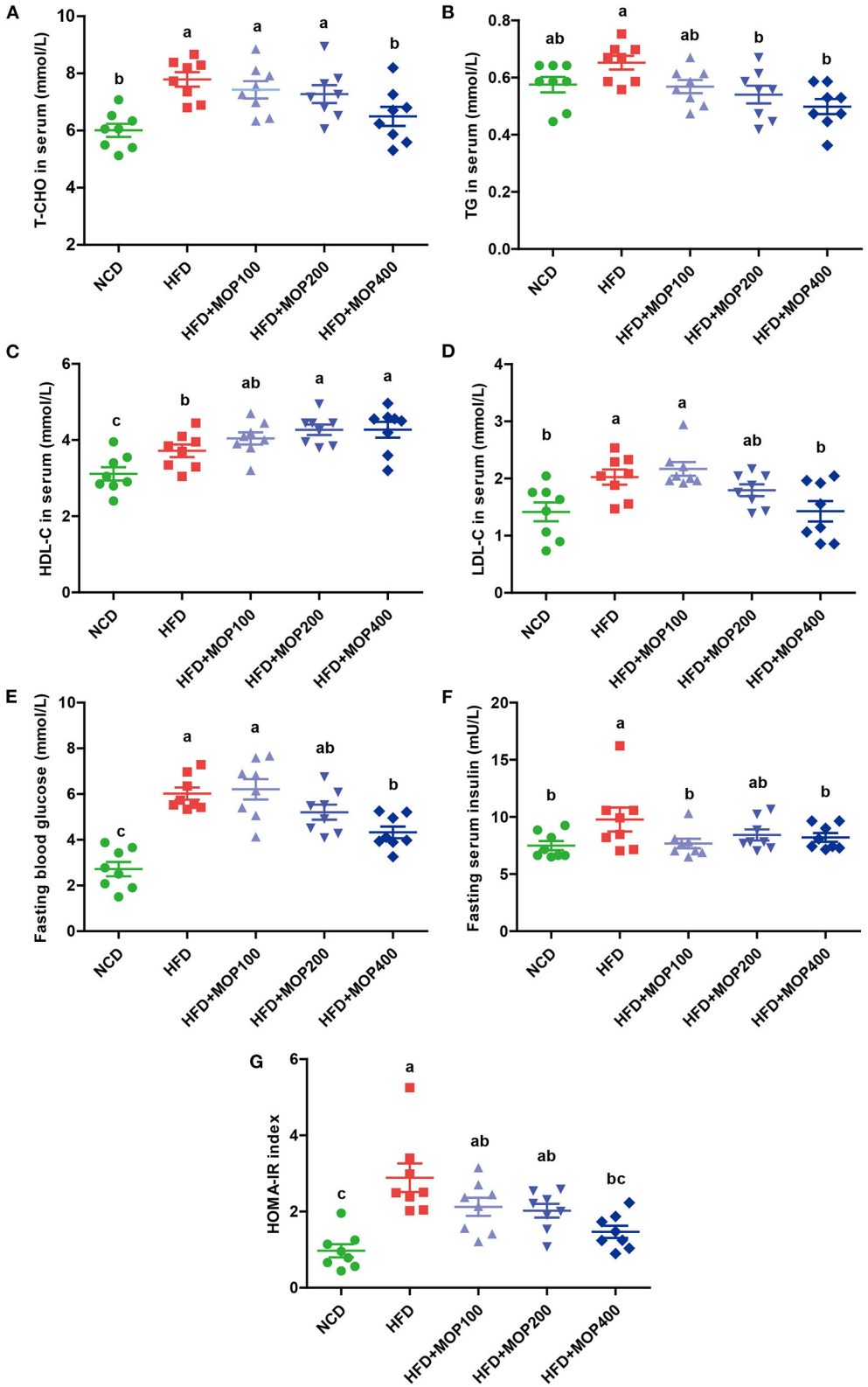

FIGURE 3 | MOP ameliorates blood lipid levels and insulin resistance in HFD-fed mice ($n = 8$ mice/group). Serum levels of **(A)** total cholesterol (T-CHO), **(B)** triglycerides (TG), **(C)** high-density lipoprotein cholesterol (HDL-C), **(D)** low-density lipoprotein cholesterol (LDL-C), **(E)** Fasting blood glucose, **(F)** fasting serum insulin, **(G)** homeostasis model assessment of insulin resistance (HOMA-IR) index. Data are shown as means ± SEM. Bars marked with different superscript letters (a-c) indicate significant differences at $p < 0.05$ based on one-way ANOVA with Duncan's *post-hoc* test.

effects of MOP, levels of representative pro-inflammatory cytokines including TNF-α and IL-1β were examined in mouse serum. Compared to the HFD group alone, MOP supplementation significantly restored serum concentrations of TNF-α and IL-1β back to normal (**Figure 4A**). Moreover, HFD significantly increased the mRNA expression of TNF-α, IL-1β, IL-6, and MCP-1 in the liver (**Figure 4B**). The expression of these pro-inflammatory cytokines was significantly reduced by MOP supplementation in a dose-dependent manner (**Figure 4B**). These results indicate that MOP supplementation can reduce HFD-induced systemic and liver inflammation.

MOP Regulates the mRNA Expression Levels of Genes Involved in Lipid Metabolism and Bile Acid Synthesis in the Liver

Previous studies have shown that synthesis and oxidation of the hepatic fatty acids might be regulated by gene expression after HFD treatment (41). Therefore, the effects of MOP on the expression levels of six genes related to fat metabolism in the liver, including PPARα, PPARγ, SREBP-1c, Fiaf, Cidea, and Cidec, were investigated. The results showed significantly higher expression of PPARγ, SREBP-1c, Cidea, and Cidec genes and lower expression of PPARα and Fiaf genes in the HFD group. The MOP intervention reversed the expression of these genes (**Figure 5A**). Moreover, bile acids play an important role in lipid metabolism and obesity. Also, Cyp7a1 and Cyp7b1 genes associated with bile acid metabolism were examined in this study. The expression levels of Cyp7a1 and Cyp7b1 genes were significantly reduced in HFD-fed mice, and the MOP intervention significantly increased the expression of Cyp7a1 and Cyp7b1 genes and was similar to the level of the NCD group (**Figure 5B**). These results suggest that MOP supplementation regulates the mRNA expression levels of genes involved in lipid metabolism and bile acid synthesis-related genes in the liver.

MOP Reshapes the HFD-Induced Change in Gut Microbiota Profile

To evaluate the effect of MOP on the gut microbiota of HFD mice, the V3–V4 regions of the 16S rRNA gene were sequenced. A total of 1,830,065 raw sequences were obtained from 32 caecal content samples, each with more than 33,820 sequences for further analysis. These reads were clustered into 704 OTUs at a 97% sequence similarity level. The α-diversity analysis reflected the richness and diversity of the microbial community. In the present study, the community richness indices, including Sobs, Chao, and Ace indices, were all significantly lower in the HFD group than in the NCD group. To a certain extent, the high concentration of MOP (400 mg/kg/d) reversed the HFD-induced changes in these indices (**Figures 6A–C**). In addition, the Shannon index was higher in the two MOP-supplement groups than in the NCD group, indicating that MOP could increase the species diversity of the gut microbial profile (**Figure 6D**). The shared and specific OTUs among different groups are represented by Venn diagrams in **Figure 6E**. A total of 431 of 704 OTUs were shared among the four groups, with the NCD group having the largest number of unique OTUs (sixty-four). This was consistent with the results of the Sobs, Chao, and Ace indices, which showed that the NCD group had the highest values. An overview of the heatmap (**Figure 6F**) suggested a significant impact of MOP on gut microbiota profile. Furthermore, β-diversity parameters were analyzed to measure the distance between each sample and the similarities between the four experimental groups. Both the hierarchical clustering tree and principal coordinate analysis (PCoA) based on the unweighted UniFrac distance revealed that all four groups presented distinctive microbiota profiles, and a more similar structure was observed for the HFD-fed groups (**Figures 6G,H**). The analysis of similarity (ANOSIM) test using unweighted UniFrac distance showed that the observed clustering patterns were significant ($R = 0.7697$, $p = 0.001$) (**Figure 6I**).

A closer look at the microbial community revealed a considerable positive influence of MOP at both the phylum and family levels (**Figures 7A,B**). At the phylum level, MOP showed a tendency to reduce the abundance of the Firmicutes, but a statistical significance difference was not achieved (**Figure 7C**). MOP treatment, however, significantly increased the abundance of Bacteroidetes (**Figure 7D**). Previous studies have shown an increase in the Firmicutes/Bacteroidetes (F/B) ratio in obese patients and in HFD-induced obese mice (42). Consistent with these studies, we also observed an increase in the F/B ratio in the HFD alone group compared to the NCD control group. It is noteworthy that MOP treatment apparently resorted the F/B ratio back to the NCD control group (**Figure 7E**), indicating a modulating effect on the gut microbiota. At the genus level, 12 of the top 30 genera in terms of abundance varied significantly between the four groups (**Figure 7F**). In particular, HFD significantly decreased the relative abundance of *Bacteroides*, norank_f_Ruminococcaceae, and *Oscillibacter*, while significantly increasing the relative abundance of *Blautia*, *Alistipes*, *Tyzzerella*, and *Faecalibaculum*. However, the intervention of MOP reversed the abundance of these bacteria.

To identify the key phylotypes that were significantly altered in response to MOP supplementation, all sequences of the four experimental groups were analyzed using the linear discriminant analysis effect size (LEfSe) method. At a threshold of 3.0 on the logarithmic LDA score, the LEfSe analysis revealed that highly enriched gut microbial taxa differed significantly between the 4 groups, with a total of 73 taxa differing significantly in abundance (see **Supplementary Figure 1**). Further LEfSe analysis revealed that HFD significantly affected 20 bacterial genera, of which the abundance of 5 genera was decreased, and the abundance of 15 genera was increased as compared to the NCD group (**Figure 7G**). The top 5 genera enriched by HFD feeding were *Blautia*, *Alistipes*, *Parabacteroides*, *Faecalibaculum*, and Rikenellaceae_RC9_gut_group. A 12-week MOP intervention also significantly affected 20 bacterial genera, of which the abundance of 8 genera was increased, and the abundance of 12 genera was decreased (**Figure 7H**). Among these species, the enrichment of *Bacteroides* and *Ruminiclostridium*, and the inhibition of *Helicobacter*, *Faecalibaculum*, *Dubosiella*, and *Romboutsia* were notable.

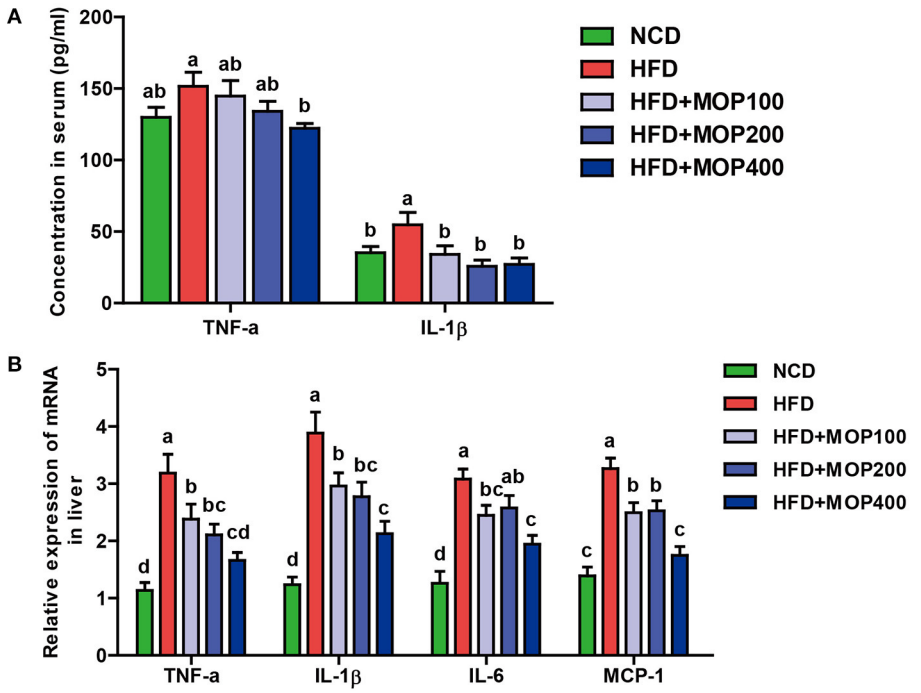

FIGURE 4 | MOP alleviates the production of pro-inflammatory cytokines in HFD-fed mice. **(A)** Serum protein levels of TNF-α and IL-1β were determined by ELISA ($n = 8$ mice/group); **(B)** Relative mRNA expression levels of TNF-α, IL-1β, IL-6, and monocyte chemotactic protein-1 (MCP-1) in the liver as determined by qRT-PCR ($n = 6$). Bars marked with different superscript letters (a-d) indicate significant differences at $p < 0.05$ based on one-way ANOVA with Duncan's *post-hoc* test.

Potential Relations Between Gut Microbiota and Obesity-Related Biomarkers

Based on the significant improvement of obesity-related symptoms and gut microbiota in HFD mice by MOP, the two-factor correlation network analysis was used to establish the relations between gut microbiota and obesity-related parameters (**Figures 8A–D**). As shown in **Figure 8A**, the correlations between 28 specific gut bacterial genera and 4 weight parameters (body weight, mesenteric fat, perirenal fat, and liver weight) were clearly visible. *Tyzzerella* was the only genus that was significantly positively correlated with all four weight parameters. *Blautia*, *Ruminiclostridium*_9, *Alistipes*, and *Parabacteroides* were positively correlated with three of the weight parameters. However, *Harryflintia* was significantly negatively correlated with all four weight parameters, while *Alloprevotella*, norank_o_Gastranaerophilales, and norank_f__Lachnospiraceae were negatively correlated with three of the weight parameters.

The correlations between specific gut bacterial genera and lipid-related parameters are shown in **Figure 8B**. The unclassified GCA-900066575 was the only genus with significant positive correlations for TG, T-CHO, and HDL-C. *Tyzzerella*, *Acetatifactor*, *Blautia*, and Ruminococcaceae_UCG-009 were significantly positively correlated with two of the lipid parameters. However, *Ileibacterium* and norank_o_WCHB1-41 were significantly negatively correlated with T-CHO and HDL-C. Notably, those taxa significantly correlated with LDL-C were not correlated with TG, T-CHO, and HDL-C.

Some specific genera of gut bacteria were closely associated with glucose homeostasis (**Figure 8C**). Six genera such as *Erysipelatoclostridium*, *Tyzzerella*, and *Blautia* were significantly positively associated with blood glucose and HOMA-IR. *Mucispirillum* and *Alistipes* were significantly negatively associated with insulin and HOMA-IR. Notably, *Elusimicrobium*, norank_o_Gastranaerophilales, g_ASF356, and norank_o__WCHB1-41 showed significant negative correlations with all three glucose homeostatic parameters.

The correlations between specific gut bacteria and pro-inflammatory cytokines are shown in **Figure 8D**. *Tyzzerella*, *Alistipes*, norank_f_Erysipelotrichaceae, and unclassified_o_Bacteroidales were significantly positively correlated with TNF-α and IL-1β. In contrast, *Harryflintia*, *Elusimicrobium*, *Alloprevotella*, and norank_f_Lachnospiraceae were significantly negatively correlated with these two pro-inflammatory cytokines. These correlations suggested that gut microbiota could influence not only host phenotypes, but also serum lipid-related parameters, glucose metabolism, and inflammatory markers.

DISCUSSION

The prevalence of overweight and obesity is an increasing chronic disease worldwide, and has become a growing global

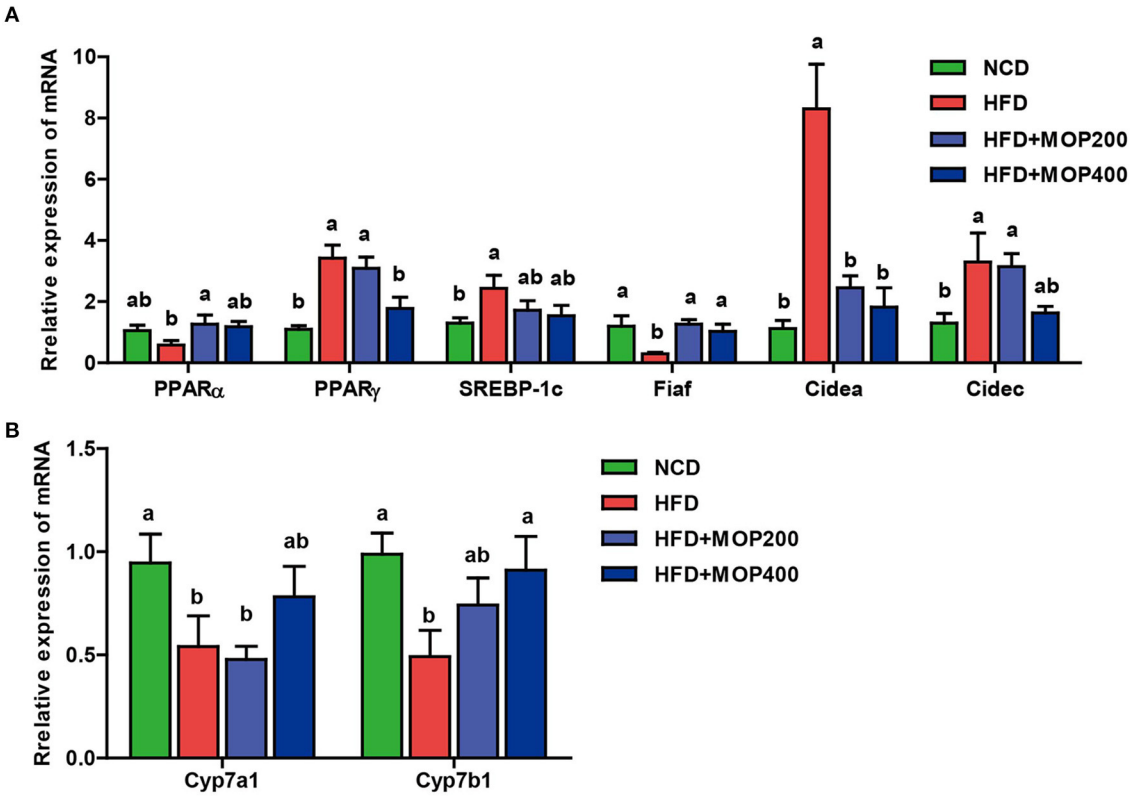

FIGURE 5 | MOP regulates the mRNA expression levels of genes involved in lipid metabolism and bile acid synthesis in the liver. **(A)** Relative mRNA expression levels of genes involved in lipid synthesis; **(B)** Relative mRNA expression levels of genes involved in bile acids metabolism. The data are expressed as means ± SEM ($n = 6$). Bars marked with different superscript letters (a-c) indicate significant differences at $p < 0.05$ based on one-way ANOVA with Duncan's *post-hoc* test.

health problem. In recent years, some studies have shown that extracts from *M. oliefera* leaves could regulate lipid metabolism. For example, Syamsunarno et al. (43) explored the effects of ethanol extract from *M. oleifera* leaves on modulating brown adipose tissue differentiation in mice fed an HFD. Mabrouki et al. (44) evaluated the effect of the methanolic extract of *M. oleifera* leaves on HFD-induced obesity and cardiac damage in rats. Sha et al. (45) investigated the efficacy and mechanism of new resource medicinal material *M. oleifera* leaves against hyperlipidemia. Our team has also investigated *M. oleifera* leaf petroleum ether extract inhibits lipogenesis (46). In these studies, the main components of *M. oleifera* leaf extracts were phenolic compounds (44) and flavonoid glycosides (46), without even elucidating their main components (43, 45). Therefore, the activity of MOP in regulating lipid metabolism is currently unclear. Furthermore, there has been growing evidence that the occurrence of obesity is closely related to alteration in the gut microbiota. Thus, growing interests have been aimed to modulate gut microbiota as a therapeutic strategy against obesity and its related diseases (11, 12). Many studies have shown that bioactive components of plants, including kale (47), *Ganoderma lucidum* (42), *Lobelia chinensis* (48), and *Dictyophora indusiata* (3), can inhibit the development of obesity in experimental animals by regulating gut microbiota. However, the biological activities of MOP in modulating gut microbiota is also unclear. The present study demonstrated that crude polysaccharides extracted from *M. oleifera* leaves could effectively prevent weight gain, fat accumulation, lipid increase, and chronic inflammation in HFD-induced obese mice, which were associated with modulation of the gut microbiota. This is the first report to assess the activity of MOP for obesity prevention, and to investigate the regulation of the gut microbial community by MOP. These findings suggested that easily available MOP could be served as an alternative strategy for preventing obesity and obesity-related metabolic diseases.

Our study found that MOP supplementation significantly reduced fat weight and adipocyte size in HFD-induced obese mice (**Figures 2A–D**). Meanwhile, the size of fat vacuoles in the liver gradually decreased with the increase of MOP dose, suggesting that MOP helped reduce fat accumulation to protect the liver (**Figure 2F**). Previous studies have shown that the feeling of satiety is increased due to the swelling effect of natural polysaccharides, and thus reduced feeding occurs during the ingestion of undigested polysaccharides (49). Our results showed that MOP supplementation did not reduce daily food intake or caloric intake in mice (**Figures 1C,D**), suggesting that the protective effect of MOP on HFD-induced weight gain was not achieved by suppressing food or energy intake. Abnormal

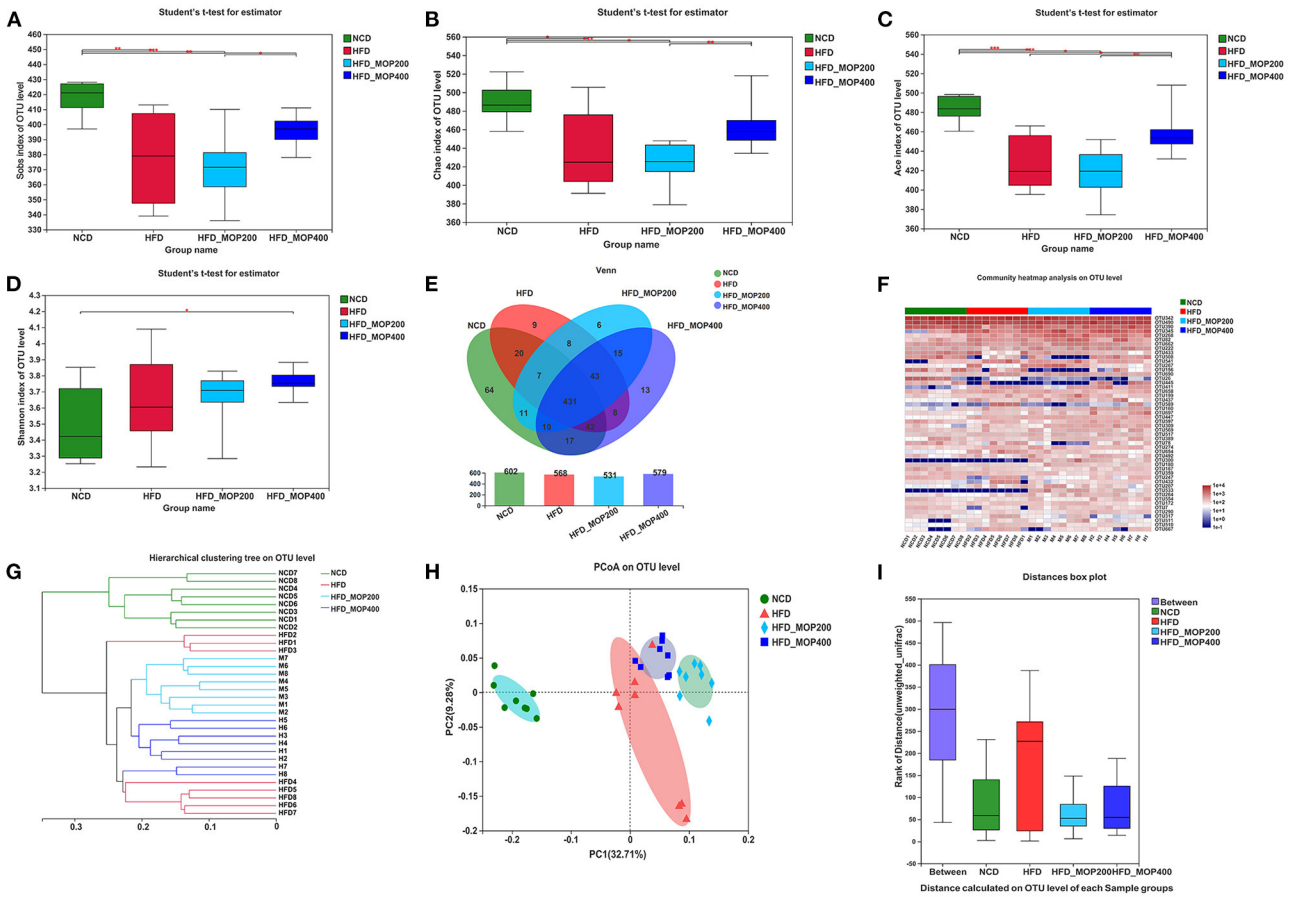

FIGURE 6 | MOP alters the diversity and composition of the gut microbiota in HFD-fed mice ($n = 8$ mice/group). **(A–D)** Sobs index, Chao index, ACE index, and Shannon index, respectively; **(E)** Venn diagrams that illustrated the observed overlap of OTUs; **(F)** Heatmap of top 50 OTUs; **(G)** Hierarchical clustering dendrograms of all samples based on unweighted UniFrac distance; **(H)** PCoA plot of unweighted UniFrac distance; **(I)** Analysis of similarity (ANOSIM) using bray-curtis distance at OTU level. The data are expressed as mean ± SD. Bars marked with different superscript letters (a-c) indicate significant differences at $p < 0.05$ based on one-way ANOVA with Duncan's *post-hoc* test.

lipid metabolism is one of the most common characteristics of obesity and related chronic diseases. Our study found that MOP significantly reduced serum TG, T-CHO, and LDL-C concentrations, and increased HDL-C concentrations in a dose-dependent manner, compared to HFD-fed mice (**Figures 3A–D**). This is consistent with the results of previous studies (50, 51). These results suggest that MOP probably plays an influential role in reducing obesity-induced abnormal lipid metabolism and dyslipidemia.

Obesity is a major cause of impaired insulin signaling and, therefore, insulin resistance development (52). Insulin resistance leads to impaired glycogen synthesis and proteolytic metabolism in skeletal muscle, and inhibits lipoprotein lipase activity in adipocytes, resulting in the release of free fatty acids and inflammatory cytokines. In addition, insulin resistance could lead to impaired glucose output and fatty acid metabolism, resulting in increased triglyceride levels and hepatic VLDL secretion (53). Hyperglycemia is a hallmark of insulin resistance (54). In this study, MOP supplementation reduced fasting blood glucose and fasting serum insulin in HFD-fed mice (**Figures 3E–G**), indicating a positive effect of MOP on improving insulin resistance.

Previous studies have shown that obesity is associated with inflammation. Obesity is regarded as a chronic low-grade inflammatory state (55). To assess the anti-inflammatory effects of MOP, the levels of representative pro-inflammatory cytokines including TNF-α and IL-1β in serum, and the mRNA expression of TNF-α, IL-1β, IL-6, and MCP-1 in the liver were examined. The results showed that these pro-inflammatory cytokines were significantly reduced by MOP intervention in a dose-dependent manner (**Figure 4**), indicating that MOP supplementation could reduce HFD-induced systemic inflammation and liver inflammation. This is similar to the findings of Sang et al. (42), who found that *Ganoderma lucidum* polysaccharides significantly inhibited HFD-induced inflammatory response, manifested in the reduction of inflammatory factors (TNF-α, IL-1β, and MCP-1) in serum and adipose tissue, and reduced macrophage infiltration in adipose tissue.

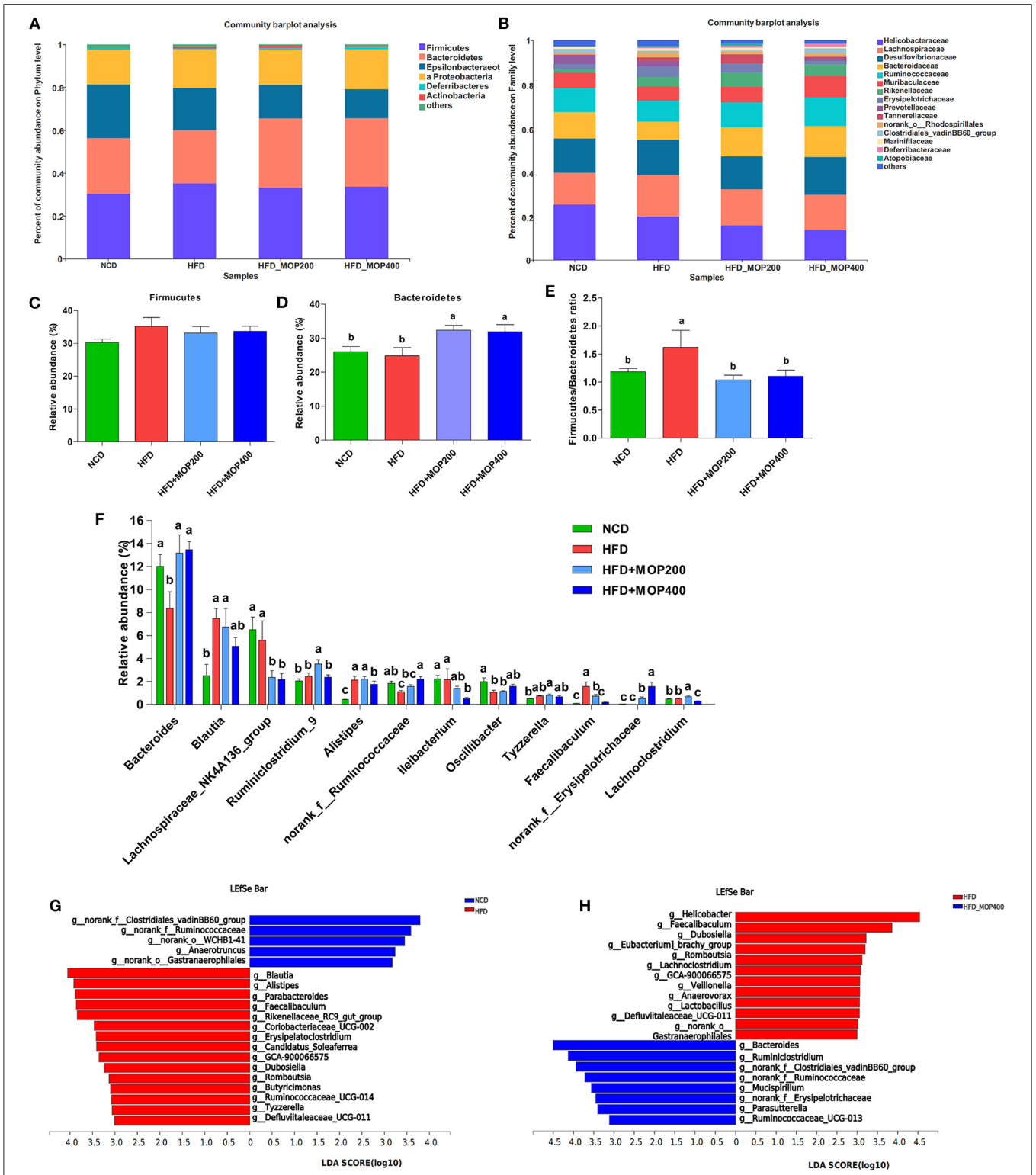

FIGURE 7 | MOP affects the relative abundance of gut microbiota at the phylum and family level in HFD-fed mice (n = 8 mice/group). Bacterial taxonomic profiling at the phylum **(A)** and family **(B)** levels from different experimental groups. The relative abundance of Firmicutes **(C)** and Bacteroidetes **(D)**; **(E)** The Firmicutes to Bacteroidetes (F/B) ratio in different groups; **(F)** Comparisons of relative abundance of the bacterial genera. The LEfSe analysis of the gut microbiota differed between NCD and HFD groups **(G)**, and between HFD and HFD+MOP 400 groups **(H)**. The histogram showed the lineages with LDA values of 3.0 or higher as determined by LEfSe.

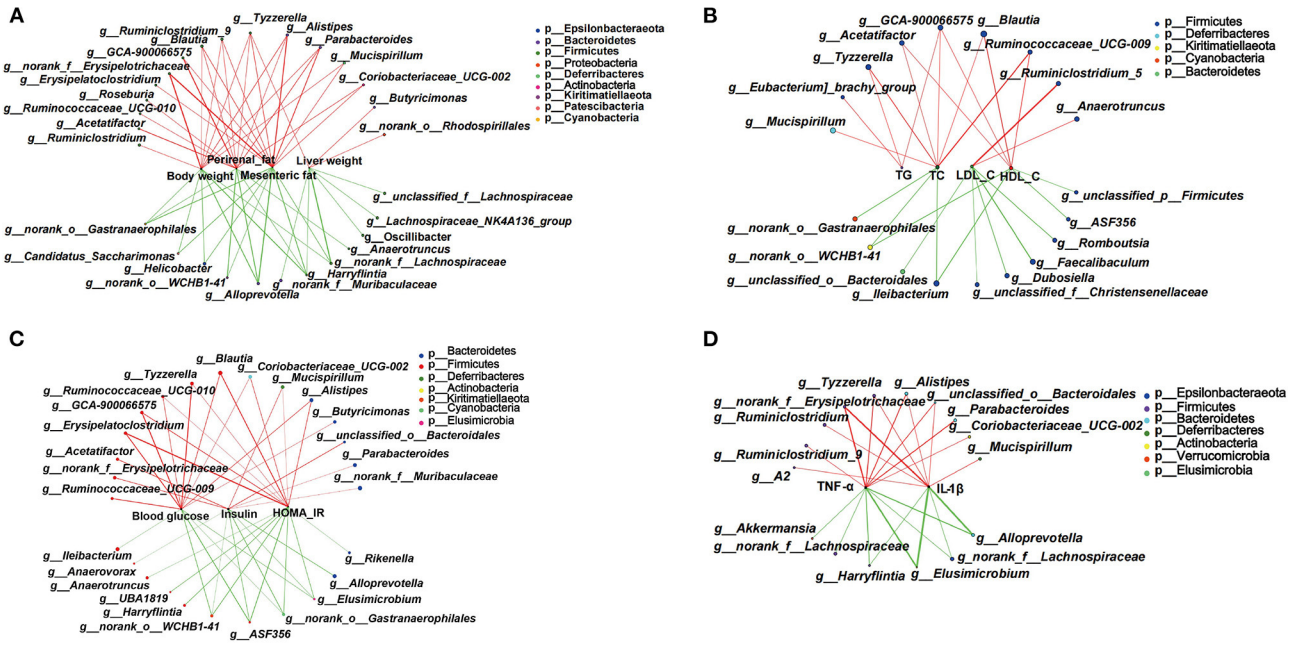

FIGURE 8 | Two-factor correlation network analysis showing correlations between specific gut microbiota and obesity-related biomarkers ($n = 8$ mice/group). **(A)** Correlations between gut bacteria and weight parameters, including body weight, mesenteric fat, perirenal fat, and liver weight. **(B)** Correlation between gut bacteria and blood lipid profile of TG, T-CHO, LDL-C, and HDL-C in serum. **(C)** Correlations between gut bacteria and glucose hemostasis, including fasting blood glucose, insulin, and the HOMA-IR index. **(D)** Correlations between gut bacteria and pro-inflammatory cytokines including TNF-α and IL-1β in serum. Spearman's r coefficient, $|r|$ of ≥ 0.5, $p < 0.05$. Red lines represent $r \geq 0.5$, and green lines represent $r \leq -0.5$.

As previously reported, HFD can promote obesity by altering the expression of lipid-related genes in the liver (56). Peroxisome proliferator-activated receptors (PPARs) are ligand-activated transcription factors that belong to the nuclear receptor superfamily (57). PPARs have been considered potential therapeutic targets for treating several metabolic syndromes (58). PPARs, including PPARα, PPARγ, and other subtypes, could regulate the expression of many genes, involved in lipid metabolism, adipogenesis, inflammation, apoptosis, immune response, oxidative stress, and adipocyte differentiation (59). PPARα is highly expressed in tissues associated with increased fatty acid oxidation (e.g., liver, skeletal muscle, and heart), and its activation leads to lower lipid levels and the elimination of TG in plasma, resulting in high levels of HDL-C (60). In contrast, PPARγ is a transcription factor involved in adipocyte differentiation and adipogenesis, which includes the processes of preadipocyte recruitment, differentiation, and TG synthesis (50). In the present study, we found by RT-qPCR analysis that MOP treatment resulted in increased expression of PPARα and decreased expression of PPARγ in the liver, compared to the HFD group (**Figure 5A**). SREBP-1c could regulate the expression of fatty acid synthase, participate in hepatic adipose differentiation and adipogenesis (61, 62). In this study, MOP supplementation decreased the expression of the SREBP-1c gene (**Figure 5A**). Fasting-induced adipose factor (Fiaf) is a multifunctional protein involved in plasma triglyceride (TG) metabolism, energy metabolism, cancer metastasis, angiogenesis, wound healing, inflammation, and nephrotic syndrome (63). Increased levels of Fiaf have been shown to be protective against diet-induced obesity (64). In the present study, MOP treatment significantly decreased the gene expression of Fiaf compared to HFD (**Figure 5A**). The Cide (cell death-inducing DFF45-like effector) family of proteins has been shown to play a critical role in lipid metabolism and energy metabolism, including lipolysis, lipid oxidation, and lipid droplet formation (65). The expression levels of Cidea and Cidec genes were examined in this study, and it was found that MOP treatment decreased their expression levels (**Figure 5A**). Bile acids are critical to lipid digestion, cholesterol metabolism, and other lipid-related pathways (66). Increased primary bile acid biosynthesis has been shown to be associated with obesity (67). Cyp7a1 is a rate-limiting enzyme for cholesterol catabolism and bile acid synthesis (68). Cyp7b1 is a microsomal enzyme involved in various physiological functions, including bile acid biosynthesis (69). Several studies have confirmed that an HFD significantly reduces the gene expression of Cyp7a1 and Cpy7b1 in the liver (70). In this study, MOP supplementation increased Cyp7a1 and Cyp7b1 expression in the liver compared to the HFD group, suggesting that MOP may prevent obesity by regulating bile acid metabolism (**Figure 5B**). This is consistent with the results of a previous study (71), in which a significant increase was found in the mRNA expression levels of Cpy7a1 and Cyp7b1 in the liver after theabrownin treatment. In conclusion, our findings suggested that MOP regulated the expression levels of genes

related to hepatic fatty acid synthesis and lipid metabolism, thereby preventing obesity.

The gut microbiota depends heavily on plant-derived dietary fiber and polysaccharides as energy sources. Besides, dietary polysaccharides significantly impact the host's gut microbial ecology and health (42). Some studies have shown that the gut microbiota is an environmental factor associated with obesity (72, 73). There is growing evidence that dysbiosis of the gut microbiota is associated with the development of obesity. However, emerging evidence supports the benefits of gut microbiota in weight management (74). Many natural products, including plant foods and phytochemicals, have been found to be effective in weight management by modulating gut microbiota (75). Several studies have also found that the prevention of obesity by plant polysaccharides is related to the regulation of gut microbiota (3, 42, 76). The decrease in microbial diversity and abundance is one of the main features of human obesity-related gut malnutrition (77). The present study showed that HFD reduced the diversity indices of gut microbiota, including Sobs, Chao, and Ace, while high concentrations of MOP (400 mg/kg/d) reversed the HFD-induced changes in these indices to some extent. Moreover, MOP supplementation increased the species diversity of the gut microbiota (**Figures 6A–D**). It is probably explained that dietary polysaccharides, which are usually indigestible in the stomach and small intestine, reach the large intestine, where they are available for fermentation, thereby enhancing the growth of beneficial bacteria and improving gut microbial diversity.

The human gut microbiota is dominated by two phyla, Firmicutes and Bacteroidetes, which account for more than 90% of all bacterial species in the gut (78). These two bacteria contribute to the host's energy absorption and metabolism associated with gut microbiota. The F/B ratio was confirmed to be higher in obese individuals compared with the healthy population (56). Although many studies point toward a relative increase in the F/B ratio as a characteristic of the "obese microbiome," the findings are inconsistent. For example, some studies reported that polyphenols or herbal extracts with anti-obesity bioactivity could downregulate the F/B ratio (9), whereas the protective effect of berberine against HFD-induced obesity was not associated with any significant change in the F/B ratio (79). In the current study, MOP supplementation did not significantly reduce the abundance of Firmicutes, but significantly increased the abundance of Bacteroidetes and the F/B ratio (**Figures 7C–E**). The results of this study showed that MOP treatment helped maintain the F/B ratio at a level similar to that of the NCD group, thereby helping to control energy absorption and body weight in the HFD mice.

Our results showed that MOP treatment altered the abundance of some bacterial genera (**Figure 7F**). For instance, the abundance of *Bacteroides* and *Oscillibacter* was increased. *Bacteroides* is a major genus in the human microbiota with a broad ability to use various types of dietary polysaccharides (42). Kaoutari et al. reported that members of the Bacteroidetes encode a proportionally higher number of carbohydrate-active enzymes (CAZymes) that are key enzymes for digesting polysaccharides than bacteria of other phyla (80). *Oscillibacter* is considered a potentially beneficial bacterium (81). Studies have shown that *Oscillibacter* is a valeric acid producer that enhances the differentiation of interleukin 10 (IL-10)-producing Tregs *in vivo* (82). Kim et al. (83) investigated the effect of *Ephedra sinica* on gut microbiota composition, and found that *Oscillibacter* in Firmicutes was negatively correlated with body weight and body mass index (BMI). These studies support our findings that MOP treatment increased the abundance of *Bacteriodes* and *Oscillibacter*. Furthermore, our results showed that MOP treatment reduced the relative abundance of *Blautia* compared to HFD (**Figure 7F**). *Blautia* is a commonly present genus in the gut microbiota. However, the results of studies on the relationship between *Blautia* and obesity are inconsistent. In a Japanese weight loss study, the genus *Blautia* was observed as the only gut microbe that was inversely associated with visceral fat, independent of sex (84). In contrast, some studies have suggested that *Blautia* is a harmful bacterium (85). In the current study, the results of LFSE analysis showed that *Blautia* was an important factor in distinguishing HFD and NCD groups (**Figure 7G**). Moreover, our findings showed that *Blautia* was positively associated with most obesity markers, including body weight, perirenal fat, mesenteric fat, T-CHO, HDL-C, blood glucose, and HOMA-IR (**Figures 8A–C**). Our findings are consistent with those of Goffredo et al., who reported a positive correlation between the abundance of *Blautia* and obesity in American youth and verified that the level of acetate, which is the product by *Blautia*, was associated with body fat partitioning and hepatic lipogenesis (86). *Alistipes* is considered to be an obesity-associated bacterium. Previous studies showed that HFD significantly increased the abundance of *Alistipes* in feces (87). In this study, MOP treatment reduced the abundance of *Alistipes* (**Figure 7F**). This is consistent with the previous study, in which the probiotic-fermented blueberry juice treated mice showed relatively low abundances of obese-related gut bacteria (*Oscillibacter* and *Alistipes*) (88). In a randomized controlled trial, overweight and obese adults consuming avocado daily for 12 weeks were enriched in the relative abundance of *Alistipes* compared to the control group (89). *Tyzzerella* is considered a pathogenic bacteria in the intestine (90). Huang et al. investigated the protective effects of sodium alginate on the gut microbiota, immunity, and intestinal mucosal barrier function in cyclophosphamide-induced immunosuppressed BALB/c mice, and found that sodium alginate significantly decreased the pathogenic bacteria *Tyzzerella* in the intestine (90). However, few studies have reported the correlation between *Tyzzerella* and obesity. The current study showed that MOP treatment reduced the relative abundance of *Tyzzerella* (**Figure 7F**). Furthermore, *Tyzzerella* was positively correlated with the majority of the obesity indicators, including body weight, liver weight, perirenal fat, mesenteric fat, TG, T-CHO, blood glucose, HOMA-IR, TNF-α, and IL-1β (**Figure 8**). These results suggested that *Tyzzerella* is a "harmful indicator" closely related to obesity.

In conclusion, this study demonstrated that MOP could effectively prevent HFD-induced weight gain and lipid accumulation, ameliorate blood lipid levels and insulin resistance, and reduce the secretion of inflammatory cytokines in mice. In addition, MOP supplementation also

modulated gut microbiota composition, increasing the abundance of some beneficial bacteria and decreasing the abundance of some harmful bacteria. These results might be attributed to the change in gut microbial composition and regulation of lipid metabolism induced by the prebiotic ability of polysaccharides. This study suggests that MOP possesses great potential to be utilized as a dietary supplement for obesity management. In future, it would be important to confirm the composition of polysaccharides in *M. oleifera* leaves and to identify specific ones with anti-obesity properties.

DATA AVAILABILITY STATEMENT

The original contributions presented in the study are publicly available. This data can be found here: NCBI, PRJNA759102.

ETHICS STATEMENT

The animal study was reviewed and approved by the Animal Care and Use Committee of Yunnan Agricultural University.

AUTHOR CONTRIBUTIONS

JS, YT, and LM conceived and designed the experiments. LL, LM, YW, JX, LY, AJ, and YZ performed the experiments. YT, LL, and LM analyzed the data. LL and LM wrote the paper. All authors contributed to the article and approved the submitted version.

FUNDING

This work was supported by Major Project of Science and Technology Department of Yunnan Province (2018ZI001 and 202002AA100005), YEFICRC Project of Yunnan Provincial Key Programs (2019ZG009), and Yunnan Province Young and Middle-Aged Academic and Technical Leaders Reserve Talents Project (2018HB040).

SUPPLEMENTARY MATERIAL

The Supplementary Material for this article can be found online at: https://www.frontiersin.org/articles/10.3389/fnut.2022.861588/full#supplementary-material

REFERENCES

1. Bray GA, Kim KK, Wilding JPH. Obesity: a chronic relapsing progressive disease process. A position statement of the world obesity federation. *Obes Rev.* (2017) 18:715–23. doi: 10.1111/obr.12551
2. Miah L, Strafford H, Fonferko-Shadrach B, Hollinghurst J, Sawhney IM, Hadjikoutis S, et al. Incidence, prevalence and healthcare outcomes in idiopathic intracranial hypertension: a population study. *Neurology.* (2021) 96:1251–61. doi: 10.1212/WNL.0000000000011463
3. Kanwal S, Aliya S, Xin Y. Anti-obesity effect of *Dictyophora indusiata* mushroom polysaccharide (DIP) in high fat diet-induced obesity via regulating inflammatory cascades and intestinal microbiome. *Front Endocrinol.* (2020) 11:558874. doi: 10.3389/fendo.2020.558874
4. Barazzoni R, Bischoff SC, Boirie Y, Busetto L, Cederholm T, Dicker D, et al. Sarcopenic obesity: time to meet the challenge. *Clin Nutr.* (2018) 37:1787–93. doi: 10.1016/j.clnu.2018.04.018
5. Alkhudhayri DA, Osman MA, Alshammari GM, Al Maiman SA, Yahya MA. *Moringa peregrina* leaf extracts produce anti-obesity, hypoglycemic, anti-hyperlipidemic, and hepatoprotective effects on high-fat diet fed rats. *Saudi J Biol Sci.* (2021) 28:3333–42. doi: 10.1016/j.sjbs.2021.02.078
6. Heymsfield SB, Wadden TA. Mechanisms, pathophysiology, and management of obesity. *N Engl J Med.* (2017) 376:254–66. doi: 10.1056/NEJMra1514009
7. Leidy HJ, Gwin JA, Roenfeldt CA, Zino AZ, Shafer RS. Evaluating the intervention-based evidence surrounding the causal role of breakfast on markers of weight management, with specific focus on breakfast composition and size. *Adv Nutr.* (2016) 7:563–75. doi: 10.3945/an.115.010223
8. Bomberg EM, Ryder JR, Brundage RC, Straka RJ, Fox CK, Gross AC, et al. Precision medicine in adult and pediatric obesity: a clinical perspective. *Ther Adv Endocrinol Metab.* (2019) 10:2042018819863022. doi: 10.1177/2042018819863022
9. Guo B, Liu B, Wei H, Cheng KW, Chen F. Extract of the microalga *Nitzschia laevis* prevents high-fat-diet-induced obesity in mice by modulating the composition of gut microbiota. *Mol Nutr Food Res.* (2019) 63:e1800808. doi: 10.1002/mnfr.201800808
10. Zhao L. The gut microbiota and obesity: from correlation to causality. *Nat Rev Microbiol.* (2013) 11:639–47. doi: 10.1038/nrmicro3089
11. Lai Z-L, Tseng C-H, Ho HJ, Cheung CKY, Lin J-Y, Chen Y-J, et al. Fecal microbiota transplantation confers beneficial metabolic effects of diet and exercise on diet-induced obese mice. *Sci Rep.* (2018) 8:15625. doi: 10.1038/s41598-018-33893-y
12. Gomes AC, Hoffmann C, Mota JF. The human gut microbiota: metabolism and perspective in obesity. *Gut Microbes.* (2018) 9:308–25. doi: 10.1080/19490976.2018.1465157
13. Zhang W-J, Su W-W, Li P-B, Rao H-Y, Lin Q-W, Zeng X, et al. Naoxintong capsule inhibits the development of cardiovascular pathological changes in Bama minipig through improving gut microbiota. *Front Pharmacol.* (2019) 10:1128. doi: 10.3389/fphar.2019.01128
14. Murphy EA, Velazquez KT, Herbert KM. Influence of high-fat diet on gut microbiota: a driving force for chronic disease risk. *Curr Opin Clin Nutr Metab Care.* (2015) 18:515–20. doi: 10.1097/MCO.0000000000000209
15. Chen J, Liu J, Yan C, Zhang C, Pan W, Zhang W, et al. *Sarcodon aspratus* polysaccharides ameliorated obesity-induced metabolic disorders and modulated gut microbiota dysbiosis in mice fed a high-fat diet. *Food Funct.* (2020) 11:2588–602. doi: 10.1039/C9FO00963A
16. Tan M, Chang S, Liu J, Li H, Xu P, Wang P, et al. Physicochemical properties, antioxidant and antidiabetic activities of polysaccharides from quinoa (*Chenopodium quinoa* Willd.) seeds. *Molecules.* (2020) 25:3840. doi: 10.3390/molecules25173840
17. Zhang Z-P, Shen C-C, Gao F-L, Wei H, Ren D-F, Lu J. Isolation, purification and structural characterization of two novel water-soluble polysaccharides from *Anredera cordifolia*. *Molecules.* (2017) 22:1276. doi: 10.3390/molecules22081276
18. Hwang J, Yadav D, Lee PC, Jin JO. Immunomodulatory effects of polysaccharides from marine algae for treating cancer, infectious disease, and inflammation. *Phytother Res.* (2021) 36:761–77. doi: 10.1002/ptr.7348
19. Zhong C, Liu Z, Zhang X, Pu Y, Yang Z, Bao Y. Physicochemical properties of polysaccharides from *Ligusticum chuanxiong* and analysis of their anti-tumor potential through immunoregulation. *Food Funct.* (2021) 12:1719–31. doi: 10.1039/D0FO02978E
20. Alliouche Kerboua K, Benosmane L, Namoune S, Ouled-Diaf K, Ghaliaoui N, Bendjeddou D. Anti-inflammatory and antioxidant activity of the hot water-soluble polysaccharides from *Anacyclus pyrethrum* (L.) Lag. *roots*. *J Ethnopharmacol.* (2021) 281:114491. doi: 10.1016/j.jep.2021.114491
21. Jiao R, Liu Y, Gao H, Xiao J, So KF. The anti-oxidant and antitumor properties of plant polysaccharides. *Am J Chin Med.* (2016) 44:463–88. doi: 10.1142/S0192415X16500269

22. Mirzadeh M, Keshavarz Lelekami A, Khedmat L. Plant/algal polysaccharides extracted by microwave: a review on hypoglycemic, hypolipidemic, prebiotic, and immune-stimulatory effect. *Carbohydr Polym.* (2021) 266:118134. doi: 10.1016/j.carbpol.2021.118134
23. Wang K, Cao P, Wang H, Tang Z, Wang N, Wang J, et al. Chronic administration of *Angelica sinensis* polysaccharide effectively improves fatty liver and glucose homeostasis in high-fat diet-fed mice. *Sci Rep.* (2016) 6:26229. doi: 10.1038/srep26229
24. Wang CM, Yuan RS, Zhuang WY, Sun JH, Wu JY, Li H, et al. Schisandra polysaccharide inhibits hepatic lipid accumulation by downregulating expression of SREBPs in NAFLD mice. *Lipids Health Dis.* (2016) 15:195. doi: 10.1186/s12944-016-0358-5
25. Shi L, Wang J, Wang Y, Feng Y. MDG-1, an Ophiopogon polysaccharide, alleviates hyperlipidemia in mice based on metabolic profile of bile acids. *Carbohydr Polym.* (2016) 150:74–81. doi: 10.1016/j.carbpol.2016.05.008
26. Do MH, Lee HB, Oh MJ, Jhun H, Choi SY, Park HY. Polysaccharide fraction from greens of *Raphanus sativus* alleviates high fat diet-induced obesity. *Food Chem.* (2021) 343:128395. doi: 10.1016/j.foodchem.2020.128395
27. Wang Y, Fei Y, Liu L, Xiao Y, Pang Y, Kang J, et al. *Polygonatum odoratum* polysaccharides modulate gut microbiota and mitigate experimentally induced obesity in rats. *Int J Mol Sci.* (2018) 19:3587. doi: 10.3390/ijms19113587
28. Starzak K, Creaven B, Matwijczuk A, Matwijczuk A, Karcz D. Anti-hypochlorite and catalytic activity of commercially available *Moringa oleifera* diet supplement. *Molecules.* (2019) 24:3330. doi: 10.3390/molecules24183330
29. Rocchetti G, Rizzi C, Pasini G, Lucini L, Giuberti G, Simonato B. Effect of *Moringa oleifera* L. leaf powder addition on the phenolic bioaccessibility and on *in vitro* starch digestibility of durum wheat fresh pasta. *Foods.* (2020) 9:628. doi: 10.3390/foods9050628
30. Grosshagauer S, Pirkwieser P, Kraemer K, Somoza V. The future of *Moringa* foods: a food chemistry perspective. *Front Nutr.* (2021) 8:751076. doi: 10.3389/fnut.2021.751076
31. Hassan MA, Xu T, Tian Y, Zhong Y, Ali FAZ, Yang X, et al. Health benefits and phenolic compounds of *Moringa oleifera* leaves: a comprehensive review. *Phytomedicine.* (2021) 93:153771. doi: 10.1016/j.phymed.2021.153771
32. Arora S, Arora S. Nutritional significance and therapeutic potential of *Moringa oleifera*: the wonder plant. *J Food Biochem.* (2021) 45:e13933. doi: 10.1111/jfbc.13933
33. Xu Y, Zhang M, Wu T, Dai S, Xu J, Zhou Z. The anti-obesity effect of green tea polysaccharides, polyphenols and caffeine in rats fed with a high-fat diet. *Food Funct.* (2015) 6:297–304. doi: 10.1039/C4FO00970C
34. Le B, Golokhvast KS, Yang SH, Sun S. Optimization of microwave-assisted extraction of polysaccharides from *Ulva pertusa* and evaluation of their antioxidant activity. *Antioxidants.* (2019). 8:129. doi: 10.3390/antiox8050129
35. Bradford MM. A rapid and sensitive method for the quantitation of microgram quantities of protein utilizing the principle of protein-dye binding. *Anal Biochem.* (1976) 72:248–54. doi: 10.1016/0003-2697(76)90527-3
36. Prosky L, Asp NG, Schweizer TF, DeVries JW, Furda I, Lee SC. Determination of soluble dietary fiber in foods and food products: collaborative study. *J AOAC Int.* (1994) 77:690–4. doi: 10.1093/jaoac/77.3.690
37. Hao L, Sheng Z, Lu J, Tao R, Jia S. Characterization and antioxidant activities of extracellular and intracellular polysaccharides from Fomitopsis pinicola. *Carbohydr Polym.* (2016) 141:54–9. doi: 10.1016/j.carbpol.2015.11.048
38. Atteia HH, Alzahrani S, El-Sherbeeny NA, Youssef AM, Farag NE, Mehanna ET, et al. *Evening primrose* oil ameliorates hyperleptinemia and reproductive hormone disturbances in obese female rats: Impact on estrus cyclicity. *Front Endocrinol.* (2020) 10:942. doi: 10.3389/fendo.2019.00942
39. Kim GR, Choi D-W, Nam CM, Jang S-I, Park E-C. Synergistic association of high-sensitivity C-reactive protein and body mass index with insulin resistance in non-diabetic adults. *Sci Rep.* (2020) 10:18417. doi: 10.1038/s41598-020-75390-1
40. Minaya DM, Turlej A, Joshi A, Nagy T, Weinstein N, DiLorenzo P, et al. Consumption of a high energy density diet triggers microbiota dysbiosis, hepatic lipidosis, and microglia activation in the nucleus of the solitary tract in rats. *Nutr Diabetes.* (2020) 10:20. doi: 10.1038/s41387-020-0119-4
41. Chen G, Xie M, Wan P, Chen D, Dai Z, Ye H, et al. Fuzhuan brick tea polysaccharides attenuate metabolic syndrome in high-fat diet induced mice in association with modulation in the gut microbiota. *J Agric Food Chem.* (2018) 66:2783–95. doi: 10.1021/acs.jafc.8b00296
42. Sang T, Guo C, Guo D, Wu J, Wang Y, Wang Y, et al. Suppression of obesity and inflammation by polysaccharide from sporoderm-broken spore of *Ganoderma lucidum* via gut microbiota regulation. *Carbohydr Polym.* (2021) 256:117594. doi: 10.1016/j.carbpol.2020.117594
43. Syamsunarno M, Alia F, Anggraeni N, Sumirat VA, Praptama S, Atik N. Ethanol extract from Moringa oleifera leaves modulates brown adipose tissue and bone morphogenetic protein 7 in high-fat diet mice. *Vet World.* (2021) 14:1234–40. doi: 10.14202/vetworld.2021.1234-1240
44. Mabrouki L, Rjeibi I, Taleb J, Zourgui L. Cardiac Ameliorative effect of *Moringa oleifera* Leaf extract in high-fat diet-induced obesity in rat model. *Biomed Res Int.* (2020) 2020:6583603. doi: 10.1155/2020/6583603
45. Sha ZJ, Li CF, Tang SH, Yang HJ, Zhang Y, Li ZY, et al. [Efficacy and mechanism of new resource medicinal materia *Moringa oleifera* leaves against hyperlipidemia]. *Zhongguo Zhong Yao Za Zhi.* (2021) 46:3465–77. doi: 10.19540/j.cnki.cjcmm.20210309.401
46. Xie J, Wang Y, Jiang WW, Luo XF, Dai TY, Peng L, et al. *Moringa oleifera* leaf petroleum ether extract inhibits lipogenesis by activating the AMPK signaling pathway. *Front Pharmacol.* (2018) 9:1447. doi: 10.3389/fphar.2018.01447
47. Shahinozzaman M, Raychaudhuri S, Fan S, Obanda DN. Kale attenuates inflammation and modulates gut microbial composition and function in C57BL/6J mice with diet-induced obesity. *Microorganisms.* (2021) 9:238. doi: 10.3390/microorganisms9020238
48. Zhang X, Hu P, Zhang X, Li X. Chemical structure elucidation of an inulin-type fructan isolated from *Lobelia chinensis* lour with anti-obesity activity on diet-induced mice. *Carbohydr Polym.* (2020) 240:116357. doi: 10.1016/j.carbpol.2020.116357
49. Zhang T, Yang Y, Liang Y, Jiao X, Zhao C. Beneficial effect of intestinal fermentation of natural polysaccharides. *Nutrients.* (2018) 10:1055. doi: 10.3390/nu10081055
50. Nie Y, Luo F, Wang L, Yang T, Shi L, Li X, et al. Anti-hyperlipidemic effect of rice bran polysaccharide and its potential mechanism in high-fat diet mice. *Food Funct.* (2017) 8:4028–41. doi: 10.1039/C7FO00654C
51. Kim MJ, Jeon J, Lee JS. Fucoidan prevents high-fat diet-induced obesity in animals by suppression of fat accumulation. *Phytother Res.* (2014) 28:137–43. doi: 10.1002/ptr.4965
52. Lee BC, Lee J. Cellular and molecular players in adipose tissue inflammation in the development of obesity-induced insulin resistance. *Biochim Biophys Acta.* (2014) 1842:446–62. doi: 10.1016/j.bbadis.2013.05.017
53. Ormazabal V, Nair S, Elfeky O, Aguayo C, Salomon C, Zuñiga FA. Association between insulin resistance and the development of cardiovascular disease. *Cardiovasc Diabetol.* (2018) 17:122. doi: 10.1186/s12933-018-0762-4
54. Thompson LH, Kim HT, Ma Y, Kokorina NA, Messina JL. Acute, muscle-type specific insulin resistance following injury. *Mol Med.* (2008) 14:715–23. doi: 10.2119/2008-00081.Thompson
55. Cao Y, Song Y, Ning P, Zhang L, Wu S, Quan J, et al. Association between tumor necrosis factor alpha and obstructive sleep apnea in adults: a meta-analysis update. *BMC Pulm Med.* (2020) 20:215. doi: 10.1186/s12890-020-01253-0
56. Ji Y, Ma N, Zhang J, Wang H, Tao T, Pei F, et al. Dietary intake of mixture coarse cereals prevents obesity by altering the gut microbiota in high-fat diet fed mice. *Food Chem Toxicol.* (2021) 147:111901. doi: 10.1016/j.fct.2020.111901
57. Park C, Ji H-M, Kim S-J, Kil S-H, Lee JN, Kwak S, et al. Fenofibrate exerts protective effects against gentamicin-induced toxicity in cochlear hair cells by activating antioxidant enzymes. *Int J Mol Med.* (2017) 39:960–8. doi: 10.3892/ijmm.2017.2916
58. Carrillo-Venzor MA, Erives-Anchondo NR, Moreno-González JG, Moreno-Brito V, Licón-Trillo A, González-Rodríguez E, et al. Pro12Ala PPAR-γ2 and +294T/C PPAR-δ polymorphisms and association with metabolic traits in teenagers from Northern Mexico. *Genes.* (2020) 11:776. doi: 10.3390/genes11070776
59. Gao L-N, Zhou X, Lu Y-R, Li K, Gao S, Yu C-Q, et al. Danlou prescription inhibits foam cellf formation induced by ox-LDL via the TLR4/NF-κB and PPARγ signaling pathways. *Front Physiol.* (2018) 9:590. doi: 10.3389/fphys.2018.00590

60. Mirza AZ, Althagafi, II, Shamshad H. Role of PPAR receptor in different diseases and their ligands: physiological importance and clinical implications. *Eur J Med Chem.* (2019) 166:502–13. doi: 10.1016/j.ejmech.2019.01.067
61. Mesquita I, Ferreira C, Moreira D, Kluck GEG, Barbosa AM, Torrado E, et al. The absence of HIF-1α increases susceptibility to *Leishmania donovani* infection via activation of BNIP3/mTOR/SREBP-1c axis. *Cell Rep.* (2020) 30:4052–64. doi: 10.1016/j.celrep.2020.02.098
62. Sun Q, Yu X, Peng C, Liu N, Chen W, Xu H, et al. Activation of SREBP-1c alters lipogenesis and promotes tumor growth and metastasis in gastric cancer. *Biomed Pharmacother.* (2020) 128:110274. doi: 10.1016/j.biopha.2020.110274
63. Robciuc MR, Naukkarinen J, Ortega-Alonso A, Tyynismaa H, Raivio T, Rissanen A, et al. Serum angiopoietin-like 4 protein levels and expression in adipose tissue are inversely correlated with obesity in monozygotic twins. *J Lipid Res.* (2011) 52:1575–82. doi: 10.1194/jlr.P015867
64. Roopchand DE, Carmody RN, Kuhn P, Moskal K, Rojas-Silva P, Turnbaugh PJ, et al. Dietary polyphenols promote growth of the gut bacterium *Akkermansia muciniphila* and attenuate high-fat diet-induced metabolic syndrome. *Diabetes.* (2015) 64:2847–58. doi: 10.2337/db14-1916
65. Nishimoto Y, Tamori Y. CIDE family-mediated unique lipid droplet morphology in white adipose tissue and brown adipose tissue determines the adipocyte energy metabolism. *J Atheroscler Thromb.* (2017) 24:989–98. doi: 10.5551/jat.RV17011
66. Xie S, Liu Y, Tian L, Niu J, Tan B. Low dietary fish meal induced endoplasmic reticulum stress and impaired phospholipids metabolism in juvenile pacific white shrimp, *Litopenaeus vannamei*. *Front Physiol.* (2020) 11:1024. doi: 10.3389/fphys.2020.01024
67. Ejtahed H-S, Angoorani P, Soroush A-R, Hasani-Ranjbar S, Siadat S-D, Larijani B. Gut microbiota-derived metabolites in obesity: a systematic review. *Biosci Microbiota Food Health.* (2020) 39:65–76. doi: 10.12938/bmfh.2019-026
68. Kim SK, Yim S-V, Lee B-C. Association between cytochrome P450 promoter polymorphisms and ischemic stroke. *Exp Ther Med.* (2012) 3:261–8. doi: 10.3892/etm.2011.388
69. Yantsevich AV, Dichenko YV, Mackenzie F, Mukha DV, Baranovsky AV, Gilep AA, et al. Human steroid and oxysterol 7α-hydroxylase CYP7B1: substrate specificity, azole binding and misfolding of clinically relevant mutants. *FEBS J.* (2014) 281:1700–13. doi: 10.1111/febs.12733
70. Wang S, Xiaoling G, Pingting L, Shuqiang L, Yuaner Z. Chronic unpredictable mild stress combined with a high-fat diets aggravates atherosclerosis in rats. *Lipids Health Dis.* (2014) 13:77. doi: 10.1186/1476-511X-13-77
71. Huang F, Zheng X, Ma X, Jiang R, Zhou W, Zhou S, et al. Theabrownin from Pu-erh tea attenuates hypercholesterolemia via modulation of gut microbiota and bile acid metabolism. *Nat Commun.* (2019) 10:4971. doi: 10.1038/s41467-019-12896-x
72. Rabot S, Membrez M, Bruneau A, Gérard P, Harach T, Moser M, et al. Germ-free C57BL/6J mice are resistant to high-fat-diet-induced insulin resistance and have altered cholesterol metabolism. *Faseb J.* (2010) 24:4948–59. doi: 10.1096/fj.10.164921
73. Nakahara D, Nan C, Mori K, Hanayama M, Kikuchi H, Hirai S, et al. Effect of mushroom polysaccharides from *Pleurotus eryngii* on obesity and gut microbiota in mice fed a high-fat diet. *Eur J Nutr.* (2020) 59:3231–44. doi: 10.1007/s00394-019-02162-7
74. Liu BN, Liu XT, Liang ZH, Wang JH. Gut microbiota in obesity. *World J Gastroenterol.* (2021) 27:3837–50. doi: 10.3748/wjg.v27.i25.3837
75. Weng G, Duan Y, Zhong Y, Song B, Zheng J, Zhang S, et al. Plant extracts in obesity: a role of gut microbiota. *Front Nutr.* (2021) 8:727951. doi: 10.3389/fnut.2021.727951
76. Anhê FF, Nachbar RT, Varin TV, Trottier J, Dudonné S, Le Barz M, et al. Treatment with camu camu (*Myrciaria dubia*) prevents obesity by altering the gut microbiota and increasing energy expenditure in diet-induced obese mice. *Gut.* (2019) 68:453–64. doi: 10.1136/gutjnl-2017-315565
77. Porras D, Nistal E, Martínez-Flórez S, González-Gallego J, García-Mediavilla MV, Sánchez-Campos S. Intestinal microbiota modulation in obesity-related non-alcoholic fatty liver disease. *Front Physiol.* (2018) 9:1813. doi: 10.3389/fphys.2018.01813
78. Healey GR, Murphy R, Brough L, Butts CA, Coad J. Interindividual variability in gut microbiota and host response to dietary interventions. *Nutr Rev.* (2017) 75:1059–80. doi: 10.1093/nutrit/nux062
79. Zhang X, Zhao Y, Zhang M, Pang X, Xu J, Kang C, et al. Structural changes of gut microbiota during berberine-mediated prevention of obesity and insulin resistance in high-fat diet-fed rats. *PloS ONE.* (2012) 7:e42529. doi: 10.1371/journal.pone.0042529
80. El Kaoutari A, Armougom F, Gordon JI, Raoult D, Henrissat B. The abundance and variety of carbohydrate-active enzymes in the human gut microbiota. *Nat Rev Microbiol.* (2013) 11:497–504. doi: 10.1038/nrmicro3050
81. Xue C, Lv H, Li Y, Dong N, Wang Y, Zhou J, et al. Oleanolic acid reshapes the gut microbiota and alters immune-related gene expression of intestinal epithelial cells. *J Sci Food Agric.* (2022) 102:764–73. doi: 10.1002/jsfa.11410
82. Arpaia N, Campbell C, Fan X, Dikiy S, van der Veeken J, deRoos P, et al. Metabolites produced by commensal bacteria promote peripheral regulatory T-cell generation. *Nature.* (2013) 504:451–5. doi: 10.1038/nature12726
83. Kim BS, Song MY, Kim H. The anti-obesity effect of *Ephedra sinica* through modulation of gut microbiota in obese Korean women. *J Ethnopharmacol.* (2014) 152:532–9. doi: 10.1016/j.jep.2014.01.038
84. Ozato N, Saito S, Yamaguchi T, Katashima M, Tokuda I, Sawada K, et al. Blautia genus associated with visceral fat accumulation in adults 20-76 years of age. *NPJ Biofilms Microbiomes.* (2019) 5:28. doi: 10.1038/s41522-019-0101-x
85. Wei D, Ma P, Fan Q, Yu H, Peng Y, Li X. Yanning syrup ameliorates the lipopolysaccharide-induced inflammation: adjusting the gut microbiota, short-chain fatty acids, and the CD4(+) T cell balance. *J Ethnopharmacol.* (2022) 283:114729. doi: 10.1016/j.jep.2021.114729
86. Goffredo M, Mass K, Parks EJ, Wagner DA, McClure EA, Graf J, et al. Role of gut microbiota and short chain fatty acids in modulating energy harvest and fat partitioning in youth. *J Clin Endocrinol Metab.* (2016) 101:4367–76. doi: 10.1210/jc.2016-1797
87. Wan Y, Wang F, Yuan J, Li J, Jiang D, Zhang J, et al. Effects of dietary fat on gut microbiota and faecal metabolites, and their relationship with cardiometabolic risk factors: a 6-month randomized controlled-feeding trial. *Gut.* (2019) 68:1417–29. doi: 10.1136/gutjnl-2018-317609
88. Zhong H, Abdullah, Deng L, Zhao M, Tang J, Liu T, et al. Probiotic-fermented blueberry juice prevents obesity and hyperglycemia in high fat diet-fed mice in association with modulating the gut microbiota. *Food Funct.* (2020) 11:9192–207. doi: 10.1039/D0FO00334D
89. Thompson SV, Bailey MA, Taylor AM, Kaczmarek JL, Mysonhimer AR, Edwards CG, et al. Avocado consumption alters gastrointestinal bacteria abundance and microbial metabolite concentrations among adults with overweight or obesity: a randomized controlled trial. *J Nutr.* (2021) 151:753–62. doi: 10.1093/jn/nxaa219
90. Huang J, Huang J, Li Y, Wang Y, Wang F, Qiu X, et al. Sodium alginate modulates immunity, intestinal mucosal barrier function, and gut microbiota in cyclophosphamide-induced immunosuppressed BALB/c mice. *J Agric Food Chem.* (2021) 69:7064–73. doi: 10.1021/acs.jafc.1c02294

Conflict of Interest: The authors declare that the research was conducted in the absence of any commercial or financial relationships that could be construed as a potential conflict of interest.

frontiers | Frontiers in Nutrition

ORIGINAL RESEARCH
published: 13 June 2022
doi: 10.3389/fnut.2022.870394

Mogroside-Rich Extract From *Siraitia grosvenorii* Fruits Ameliorates High-Fat Diet-Induced Obesity Associated With the Modulation of Gut Microbiota in Mice

Siyuan Wang[1,2†], Kexin Cui[1,2†], Jiahao Liu[1,2], Jiahao Hu[1,2], Ke Yan[1,2], Peng Xiao[1,2], Yangqing Lu[1,2], Xiaogan Yang[1,2] and Xingwei Liang[1,2*]*

[1] State Key Laboratory for Conservation and Utilization of Subtropical Agro-Bioresources, Guangxi University, Nanning, China, [2] College of Animal Science and Technology, Guangxi University, Nanning, China

OPEN ACCESS

Edited by:
Riadh Hammami, University of Ottawa, Canada

Reviewed by:
Francesco Suriano, University of Gothenburg, Sweden
Yi-Chen Lo, National Taiwan Ocean University, Taiwan

***Correspondence:**
Xingwei Liang
xwliang@gxu.edu.cn
Xiaogan Yang
xgyang@gxu.edu.cn

[†] *These authors have contributed equally to this work*

Specialty section:
This article was submitted to Nutrition and Microbes, a section of the journal Frontiers in Nutrition

Received: *06 February 2022*
Accepted: *05 May 2022*
Published: *13 June 2022*

Citation:
Wang S, Cui K, Liu J, Hu J, Yan K, Xiao P, Lu Y, Yang X and Liang X (2022) Mogroside-Rich Extract From Siraitia grosvenorii Fruits Ameliorates High-Fat Diet-Induced Obesity Associated With the Modulation of Gut Microbiota in Mice. Front. Nutr. 9:870394. doi: 10.3389/fnut.2022.870394

Siraitia grosvenorii is a kind of medicinal food plant. The mogroside-rich extract (MGE) of its fruits can effectively ameliorate obesity, but the underlying mechanisms remain underexplored. In this study, we aimed to determine whether MGE can ameliorate obesity by protecting against the divergences of gut microbiota. Mice were challenged with a high-fat diet (HFD) and treated with MGE by oral gavage. Then, the characteristics of the gut microbiota were determined by 16S rDNA analysis. Our findings showed that MGE could significantly reduce body weight gain and fat tissue weight of the mice fed with HFD. Moreover, MGE markedly attenuated fatty liver, and improved glucose tolerance and insulin sensitivity. We further found that the gut microbiota structures were disturbed by HFD feeding. In particular, the abundance of *Firmicutes* was increased and the abundance of *Bacteroidetes* was decreased, resulting in an increased proportion of *Firmicutes* to *Bacteroidetes* (F/B), which contributes to obesity. Interestingly, the abnormal proportion of F/B of HFD feeding mice was restored to the level of control mice by MGE treatment. Additionally, the abundances of obesogenic microbiota, such as *Ruminiclostridium* and *Oscillibacter* were also decreased after MGE treatment. In summary, our findings demonstrate that MGE can modulate gut microbiota in obese mice and shed new light on how it alleviates obesity.

Keywords: *Siraitia grosvenorii*, mogroside, obesity, high fat diet, gut microbiota

INTRODUCTION

Obesity is a worldwide pandemic in modern society. It increases the risk of various health problems and has become a leading contributor to diabetes mellitus, cardiovascular diseases, and cancers (1). Given the detrimental effects of obesity on human health, diverse strategies, including surgical operation (2), medicines (3), Chinese medicine conditioning, acupuncture (4, 5), exercise and diet, have been developed to control body weight gain or alleviate obesity (6). Among them, plant

extracts with medical and edible properties are receiving increasing attention because they are characterized by effectiveness, safety, and pleasant properties (7, 8).

Siraitia grosvenorii (Luo han guo) is a kind of medicinal food plant primarily grown in South China (9, 10). Mogrosides (MGs), the major bioactive components of *S. grosvenorii* fruit, have rich medicinal efficiency, namely, anti-inflammation (11, 12), anti-oxidative stress (13, 14), anticancer (15), neuroprotective (16), and promoting reproduction (17–19). For protecting against obesity, *in vitro* studies have shown that mogrol inhibited adipogenesis in the 3T3L cell line by activating AMP-activated protein kinase (AMPK) activity (20). *In vivo* studies have shown that MGs can reduce body weight gain and attenuate non-alcoholic fatty liver disease (NAFLD) by enhancing the phosphorylation levels of AMPK in the livers of mice challenged with a high-fat diet (HFD) (21). Similarly, Liu et al. reported that mogroside-rich extract (MGE) can alleviate hyperglycemic and hyperlipidemic syndromes in HFD/streptozotocin-induced diabetic mice, in part due to the improvement of insulin sensitivity and activation of hepatic AMPK signaling (22). Although the effects of MGE on attenuating obesity were widely explored, the underlying mechanisms still have not been sufficiently elucidated.

Microbes settle in the gut and play fundamental roles in maintaining host health. In contrast, intestinal dysbacteriosis is closely linked to a variety of health problems, particularly the pathophysiology of obesity (23). It has been revealed that not only between genetically obese mice and their lean littermates but also between obese and lean human volunteers, gut microbial diversity and gut microbiota compositions are changed, especially the relative abundance of *Bacteroidetes* and *Firmicutes,* which are decreased and increased, respectively, in obese individuals (24, 25). Conversely, shaping gut microbiota by colonizing "lean microbiota" or eating certain food can alleviate obesity and metabolic disorders (26–29).

In this study, we speculated that MGs might alleviate obesity associated with the modulation of gut microbiota. To test this hypothesis, male mice were challenged with an HFD to establish a diet-induced obese (DIO) animal model, concomitantly orally administered MGE to determine the effects on alleviating obese phenotypes. Additionally, gut microbial diversities and compositions were characterized to determine how MGE modulates gut microbiota. This study can help us to extend the current understanding of how MGs alleviate obesity.

MATERIALS AND METHODS

Ethical Approval and Animals

The animal experiments were approved by the Institutional Animal Care and Use Committee (IACUC) of Guangxi University and were conducted in accordance with the animal welfare and ethical rules. Three-week-old male C57BL/6 mice were purchased from Beijing Vital River Laboratory Animal Technology Company (Beijing, China). Mice were maintained in individually ventilated cages (IVCs) under 12 h light/12 h dark cycles at an ambient temperature of $22 \pm 2^{\circ}$. Mice were *ad libitum* accessed to food and water.

Treatments

After acclimating for one week, the mice were randomly divided into four groups with eight mice each in group (control, HFD, HFD + MGE300, and HFD + MGE600). The control mice were fed with a chow diet (10% energy from fat, D12450, Research Diets, New Brunswick, NJ) and the other mice were challenged with an HFD (60% energy from fat, D12492, Research Diets). Mice in the control and HFD groups were given orally 100 μl water at 9:00 a.m., while the HFD + MGE300 and HFD + MGE600 mice were orally administered 300 mg/kg or 600 mg/kg body weight MGE, respectively. During treatment for 18 weeks, the body weight and food intake were recorded weekly during treatment.

TheMGE was provided by Layn Biotech, Inc. (Guilin, China). Its main constituents were described in our previous publication (14).

Body Fat Percentage Measurement

The body fat percentage of mice was assayed by using Small Animal Body Composition Analysis and Imaging System NMR Analyzer (MesoQMR23-060H, Niumag Corporation, Shanghai, China).

Glucose Tolerance Test and Insulin Tolerance Test

Mice were subjected to Glucose Tolerance Test (GTT) (at 19 weeks of age) and Insulin Tolerance Test (ITT) (at 20 weeks of age) as previously described (30). Briefly, mice were fasted for 12 h or 6 h and then intraperitoneally injected with 2 g/kg body weight D-glucose or 1 IU/kg body weight insulin for GTT and ITT, respectively. Blood was collected from the tail tip at 0, 15, 30, 60, and 120 min post-injection. Glucose concentration was measured using an Accu-Chek Performa (Roche Diagnostics, United States).

Liver Triglyceride Content Assay

The triglyceride (TG) content in the liver was measured using a TG colorimetric assay kit (Applygen Technologies, Beijing, China) according to the manufacturer's instructions. Fifty milligrams of liver tissue were grounded in liquid nitrogen, and then TG was extracted. TG concentration was measured using a BioTek Epoch full-wavelength microplate reader (Epoch, United States) at a 550 nm wavelength.

Hematoxylin and Eosin Staining

Fat and liver tissues were fixed in 4% paraformaldehyde (PFA) overnight at 4°. The samples were embedded in paraffin and cut into 5 μm thick sections according to routine procedures. Hematoxylin and Eosin (H&E) staining was performed according to a standard procedure. Images were captured under a light microscope (Nikon, Eclipse 50i).

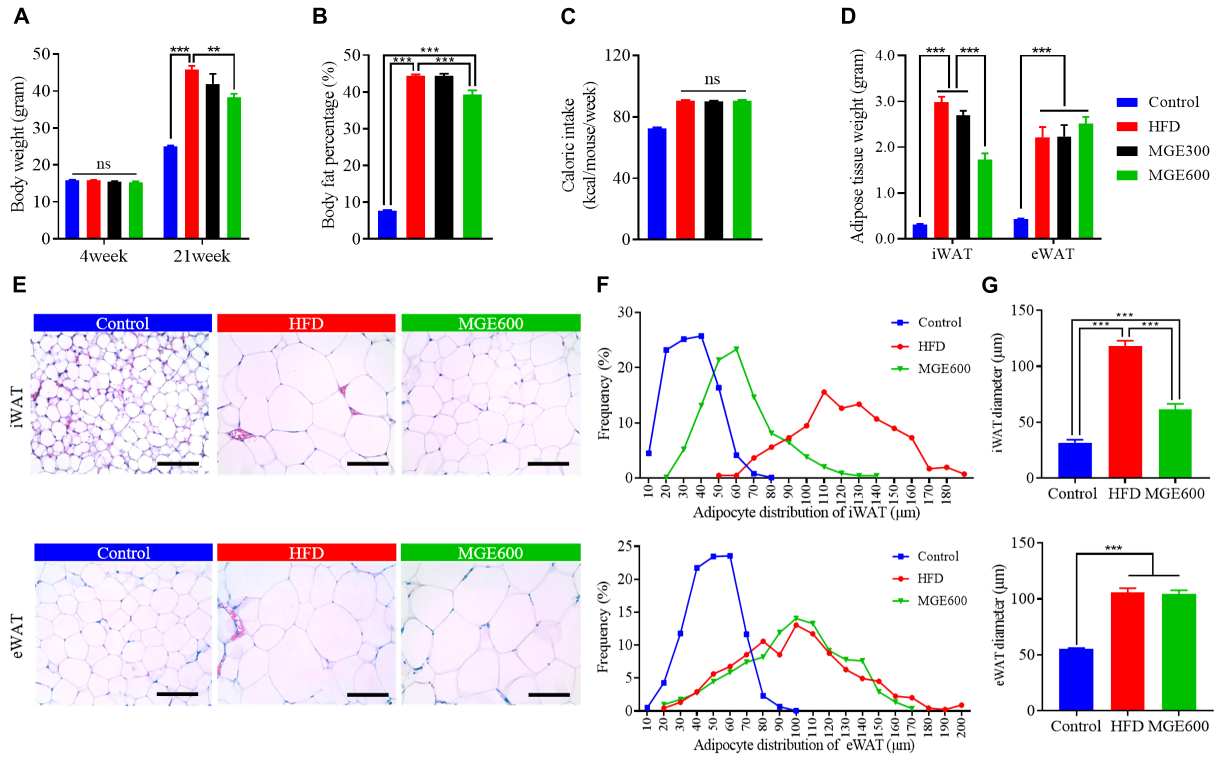

FIGURE 1 | MGE attenuates body weight gain and reduces fat mass in DIO mice. Diet-induced obese (DIO) mice were orally administered 300 and 600 mg body weight MGE from 4 to 21 weeks of age. **(A)** Body weight at the beginning and end of the experiment (n = 12). **(B)** Body fat percentage at the end of the experiment (n = 8). **(C)** Weekly average calorie intake per mice. **(D)** Inguinal adipose tissue (iWAT) and epididymal adipose tissue (eWAT) weight (n = 6). **(E–G)** Representative images of H&E staining, adipocyte distribution, and average adipocyte diameter of iWAT and eWAT (n = 6). Scale bar = 100 μm; magnification 20×. $^{**}P < 0.01$, $^{***}P < 0.001$.

Colonic Microbiota Analyses

The structures of the colonic microbiota were assessed by 16S rRNA amplicon gene sequencing, which was performed by Biomarker Technologies (Beijing, China). Samples were collected for the colons and total genomic DNA was extracted by using the TIANamp Stool DNA Kit (TIANGEN Biotech, Beijing, China), and the V3-V4 regions of the 16S rRNA gene were amplified by using the forward primer 338F (5′-ACTCCTACGGGAGGCAGCA-3′) and reverse primer 806R (5′-GGACTACHVGGGTWTCTAAT-3′). The operational taxonomic unit (OTU) table and taxonomic analysis were obtained from Qiime2 (2019.10) software (31).

Statistical Analyses

Post hoc analyses were performed using Prism 7 software (GraphPad, San Diego, CA, United States) when significance was achieved in the main or simple effects model. Multiple comparisons were corrected using Tukey–Kramer or Dunnett–Hsu adjustment in mixed model procedures. Data are presented as means ± SEM. $P < 0.05$ was considered statistically significant for a null hypothesis of no difference between study test meals. Bioinformatics analyses were carried out at the Multifunction Computer Center of Guangxi University and the R platform (version 4.0.3).

RESULTS

Mogroside-Rich Extract Attenuates Body Weight Gain and Fat Accumulation in Diet-Induced Obese Mice

After challenge with a HFD for eighteen weeks, the mice had vastly higher body weights (Con vs. HFD; 25.1 ± 0.15 vs. 45.9 ± 0.95 g; $P < 0.0001$) and body fat percentage (Con vs. HFD; 7.7 ± 0.25 vs. 44.4 ± 0.41%; $P < 0.0001$) than the mice fed the control diet. There were no significant differences in body weight or body fat content between mice in the HFD and HFD + MGE300 groups, indicating that 300 mg/kg MGE does not attenuate obesity. However, when the mice were treated with 600 mg/kg MGE, the body weight and body fat content were significantly reduced compared with those of the HFD group (**Figures 1A,B**), indicating that 600 mg/kg MGE can attenuate HFD-induced obesity. In addition, compared with the control group, the high-fat diet increased the average weekly calorie intake of mice. However, there was no difference in calorie intake between MGE treated group (MGE300, MGE600) and the HFD group (**Figure 1C**). For individual adipose tissue, when mice were fed an HFD, the inguinal white adipose tissue (iWAT) and epididymal white adipose tissue (eWAT) weights were notably increased compared with those of the mice fed a control diet.

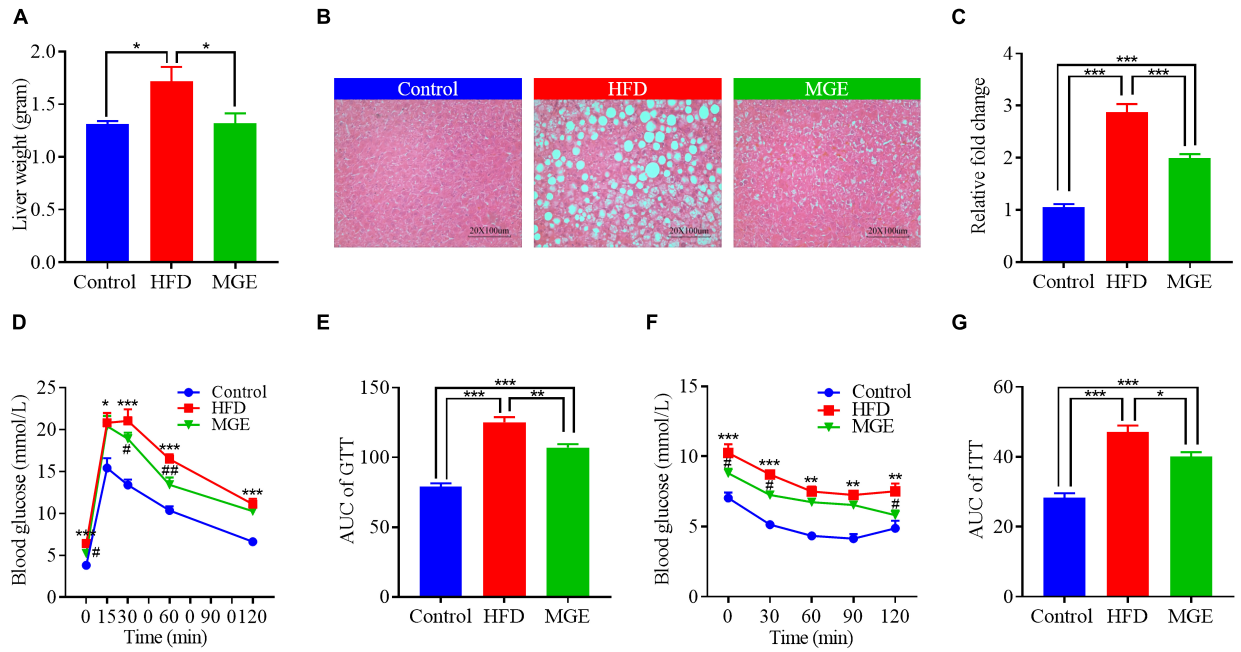

FIGURE 2 | MGE reduces liver fat accumulation and improves glucose and insulin sensitivity in DIO mice. **(A)** Liver weight of mice (n = 7). **(B)** Representative images of liver tissue H&E staining. Scale bar = 100 μm. **(C)** Liver triglyceride concentration relative to the control (n = 7). **(D,E)** Glucose tolerance test (GTT; n = 6). **(F,G)** Insulin tolerance test (ITT; n = 5). AUC, area under curve. $^{*}P < 0.05$, $^{**}P < 0.01$, $^{***}P < 0.001$; $^{\#}P < 0.05$, $^{\#\#}P < 0.01$ vs. HFD group.

A 300 mg/kg MGE did not decrease the iWAT or eWAT weight in the mice fed an HFD. However, 600 mg/kg MGE significantly reduced iWAT weight but had no impact on eWAT weight in the mice fed a HFD (**Figure 1D**). Consistently, the HFD challenge obviously increased the adipocyte size of iWAT and eWAT in the mice. Interestingly, 600 mg/kg MGE treatment reduced the adipocyte size of iWAT but did not change the adipocyte size of eWAT in DIO mice (**Figures 1E–G**). Considering the effects of 600 mg/kg MGE on alleviating obesity, this dose was used in the subsequent analyses.

Mogroside-Rich Extract Reduces Liver Fat Accumulation and Improves Glucose and Insulin Sensitivity in Diet-Induced Obese Mice

We next determined whether MGE treatment might ameliorate fatty liver in DIO mice. As shown in **Figure 2A**, the mice in the HFD group had higher liver weights than those in the control group (Con vs HFD; 1.3 ± 0.03 vs 1.7 ± 0.13 g; $P < 0.05$). H&E staining showed that there were many lipid droplets distributed in the liver of HFD-challenged mice (**Figure 2B**), suggesting that HFD feeding results in fatty liver. We further assayed TG content in the liver and found that the mice in the HFD group had significantly higher TG content than the mice in the control group (**Figure 2C**). This further confirmed that the HFD challenge leads to fatty liver in mice. As expected, MGE treatment markedly reduced the liver weight and TG content in the livers of mice challenged with an HFD, indicating that MGE can alleviate fatty liver in DIO mice (**Figures 2A–C**).

Compared with the control group, the HFD group had significantly higher AUCs of GTT and ITT (**Figures 2D–G**), indicating that the HFD challenge reduces glucose and insulin sensitivity in mice. However, MGE treatment notably reduced the AUCs of the GTT and ITT in the mice challenged with a HFD (**Figures 2D–G**). Taken together, MGE supplementation alleviated fatty liver and improved global metabolic capacities in DIO mice.

Effects of Treatment on Intestinal Microbiota α-Diversity and β-Diversity

High-throughput sequencing generated 1,919,310 raw reads. After removing the low-quality sequences, there were 1,787,645 clean tags, and each sample produced an average of 74,485 clean tags. Based on a 97% similarity cutoff value, all the effective reads were clustered into operational taxonomic units (OTUs).

To identify the differences in intestinal microbiota structure among groups, the α-diversity and β-diversity were compared. As shown in **Figures 3A–D**, the α-diversity indexes (ACE, Shannon, and phylogenetic diversity) in the HFD group were significantly increased compared with those in the control group, but there were no differences between the HFD and MGE groups. On the other hand, non-metric multidimensional scaling (NMDS) and principal coordinates analysis (PCoA) of the unweighted UniFrac distance matrix were used to identify β-diversity. As shown in **Figures 3E,F**, NMDS and PCoA showed that the clusters of the HFD group were significantly different from those in the control group, but MGE treatment significantly ameliorated these alters. Taken together, the above results indicate that MGE can restore

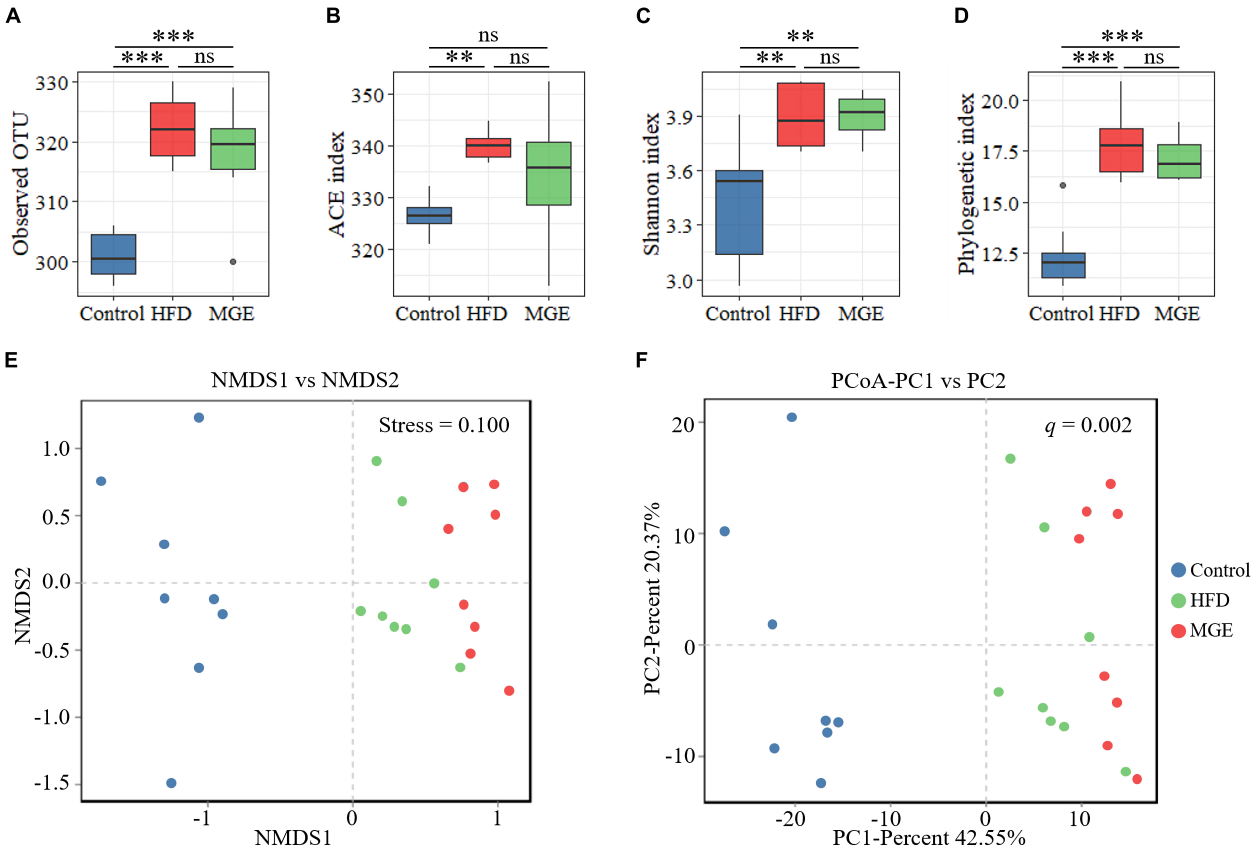

FIGURE 3 | Effects of MGE treatment on intestinal microbiota α-diversity and β-diversity. **(A)** Observed OTU in each group. **(B)** Abundance-based coverage estimator (ACE) index. **(C)** Shannon index. **(D)** Phylogenetic diversity (PD). **(E,F)** Beta diversity analysis: **(E)** non-metric multidimensional scaling (NMDS), **(F)** principal coordinates analysis (PCoA) of the unweighted UniFrac distance matrix. Group significance was statistically analyzed by using the PERMANOVA method. $^{**}P < 0.01$, $^{***}P < 0.001$.

the changes of community structure in microbiota but not species types in DIO mice.

Mogroside-Rich Extract Restores the Relative Abundance of *Firmicutes* and *Bacteroidetes* in Diet-Induced Obese Mice

Combining the unweighted pair-group method with arithmetic mean (UPGMA), the relative abundance of the gut microbiota at the phylum level was identified by QIIME2 taxonomic analysis. As shown in **Figure 4A**, the HFD group had an apparent difference in taxonomic composition compared with the control group, but there was an apparent similarity between the MGE group and the control group. For individual phyla, the relative abundance of *Firmicutes* was significantly increased, but that of *Bacteroidetes* was significantly decreased due to HFD feeding, resulting in an increase in the ratio of *Firmicutes* to *Bacteroidetes* (F/B) in DIO mice (**Figure 4B**). However, MGE treatment restored the relative abundance of *Firmicutes* and *Bacteroidetes,* as well as the ratio of F/B to control levels, in DIO mice (**Figure 4B**). In addition, the linear discriminant analysis effect size (LEfSe) method was used to further determine differences in microbiota abundances (**Figure 4C**). There was 67 differentially abundant microbiota, and 49 out of 67 (73.1%) belonged to *Bacteroidetes* and *Firmicutes*, which further confirmed that MGE can restore the abundance of *Firmicutes* and *Bacteroidetes* in DIO mice.

Mogroside-Rich Extract Restores the Abundance of Intestinal Microbiota at the Genus Level in Diet-Induced Obese Mice

To further explore the effect of MGE on bacterial taxonomic composition at the genus level, a clustering heatmap was constructed. **Figure 5A** displays the top 72 OTUs with significant differences ($P < 0.01$) selected for clustering analysis. Fifty-eight out of 72 OTUs were significantly less abundant in the control group and MGE group than in the HFD group. Interestingly, *Lactococcus*, *Blautia*, *Lactobacillus*, *Ruminiclostridium_9*, *Oscillibacter,* and *Ruminiclostridium* belong to *Firmicutes* and are obesogenic microbiota (**Figure 5B**). In contrast, 14 out of 72 OTUs, including *Bacteroides*, were significantly more abundant

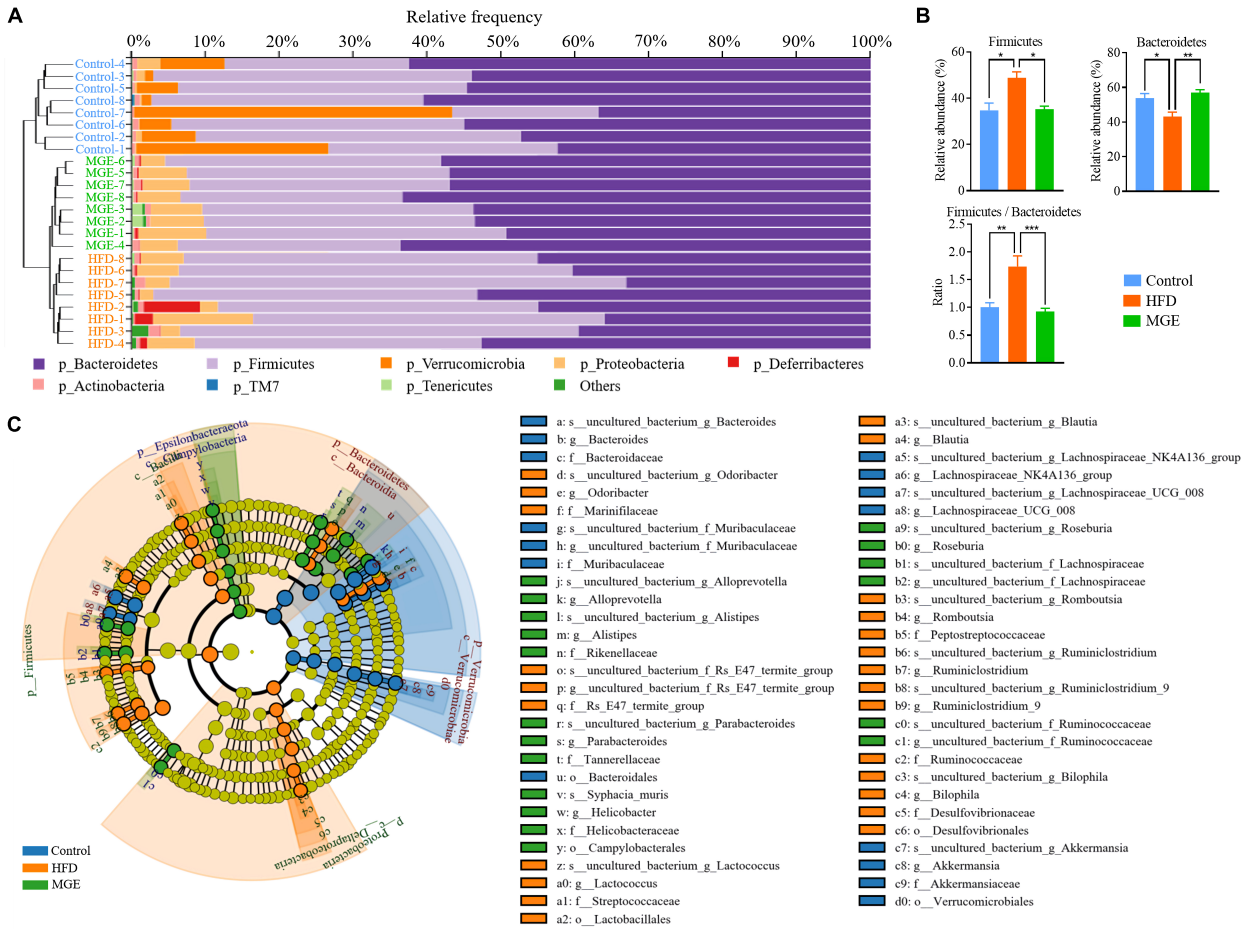

FIGURE 4 | MGE restores the relative abundance of *Firmicutes* and *Bacteroidetes* in DIO mice. **(A)** Microbiota taxonomic composition clustering histogram at the phylum level; left: unweighted pair-group method with arithmetic mean (UPGMA) tree; right: histogram of microbiota abundance. **(B)** Relative abundance of *Firmicutes* and *Bacteroidetes* and the ratio of *Firmicutes* to *Bacteroidetes*. **(C)** Taxonomic cladogram obtained from linear discriminant analysis effect size (LEfSe) sequence analysis. Species taxonomy from phyla to genus (inside-outside). The diameter of each circle represents the relative abundance of the taxon, and the color corresponds to the grouping. Undifferentiated microbiota components (yellow). The predominant microbiota component at each taxonomic level is represented by different colors. $^{*}P < 0.05$, $^{**}P < 0.01$, $^{***}P < 0.001$.

in the control group and MGE group than in the HFD group (**Figure 5B**). Taken together, MGE can restore the intestinal microbiota at the genus level in DIO mice.

Correlation Analyses of Gut Microbiota Structures and Obese Phenotypes

We further performed a correlation analysis between the gut microbiota structures and obese phenotypes. Based on the Spearman index, we found that the abundances of *Firmicutes*, *Lactobacillus,* and *Lactococcus* were positively correlated with obese phenotypes, such as body weight, iWAT weight, body fat content, liver TG concentration, and AUC of GTT and ITT. However, the abundances of *Bacteroidetes* and *Bacteroides* were negatively correlated with the above obesity parameters (**Figure 6A**). The results of correlation analysis show that MGs alleviate obesity and maybe associated with the gut microbiota modulation (**Figure 6B**).

DISCUSSION

Previous studies have demonstrated that MGs can attenuate obesity, but their effect on modulating gut microbiota in this condition remains unknown. In this study, we first observed that MGE treatment can alleviate obesity by inhibiting body weight gain and fat accumulation in adipose tissues and liver, improving insulin and glucose sensibilities in DIO mice. Importantly, we further found that MGE treatment modulates gut microbiota, particularly restores the ratio of *Firmicutes* to *Bacteroidetes* and reduces the relative abundance of obesogenic microbiota. Our findings depict that MGE attenuates obesity at least in part by gut microbiota modulation.

First, we used a DIO mouse model to determine the beneficial effects of MGs on obese animals. When the mice were fed an HFD from 4 to 21 weeks of age, the body weight, global fat mass, and adipose tissue weight were vastly increased. In addition, the increased adipocyte size and accumulated fat content in the

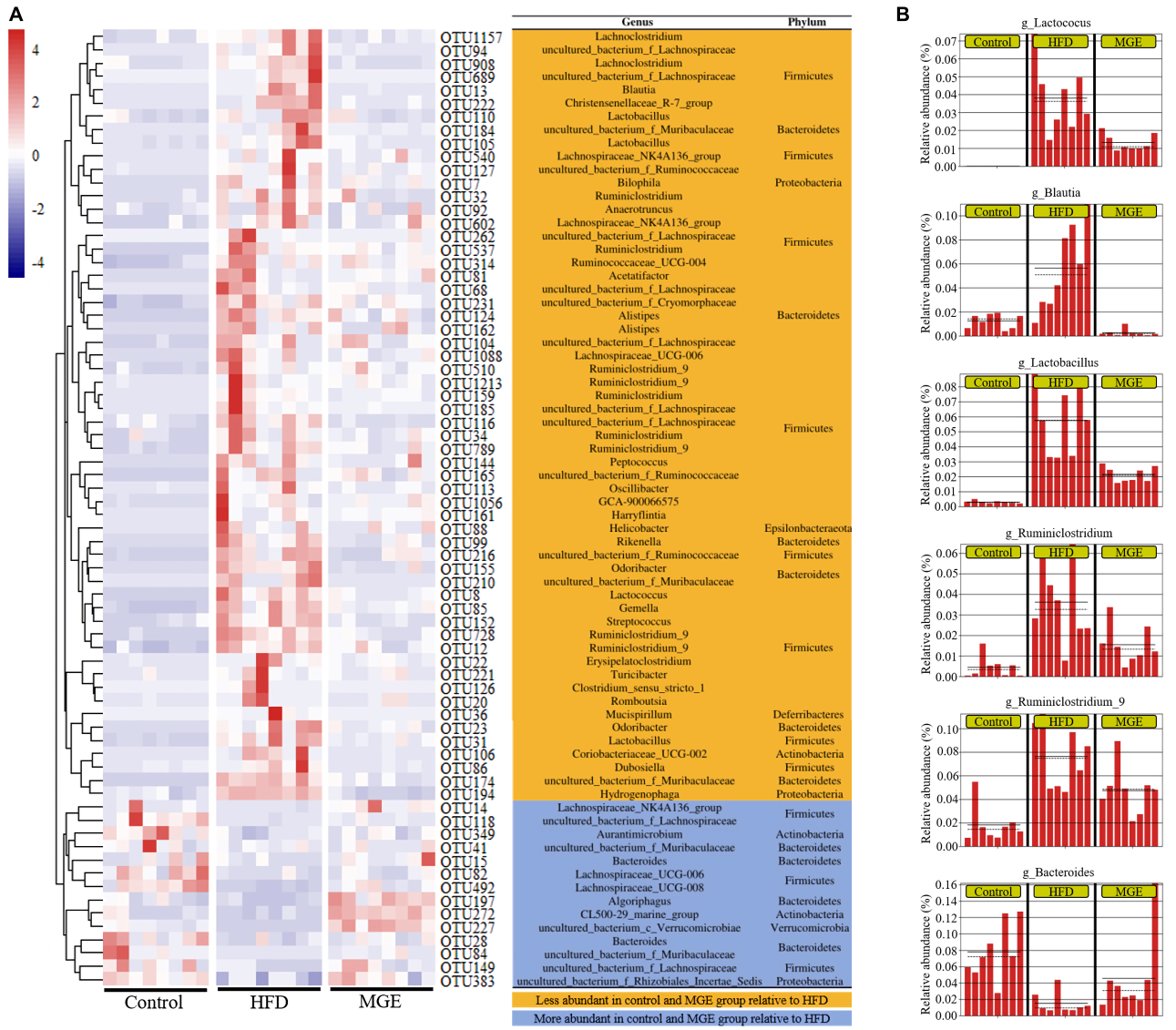

FIGURE 5 | MGE restores the abundance of intestinal microbiota at the genus level in DIO mice. **(A)** OTU differential clustering heatmap with representative bacterial taxon information (genus and phylum). **(B)** The relative abundance of bacterial genera significantly recovered by MGE treatment ($P < 0.01$); solid and dashed lines indicate the mean and median, respectively.

liver indicated that the HFD challenge induced hypertrophic adipose tissues and NAFLD, respectively. Moreover, HFD feeding also impairs global metabolic capacities by reducing glucose and insulin sensibilities. Combined with previous reports (32–35), all the above defective parameters demonstrated that a DIO animal model was successfully established in this study. As expected, when DIO mice were orally administered MGE, body weight gain and fat accumulation were attenuated, and global metabolic capacities were also improved. Our findings reconfirmed that MGs can alleviate obesity (21, 22, 36, 37); therefore, this model can be used to explore the modulation of gut microbiota by MGE.

We next used 16S sequencing to investigate how MGE affects gut microbial compositions and diversities in DIO mice. α-Diversity and β-diversity are two key indicators that reflect the differences in gut microbial communities (38, 39). We found that the α-diversity of the gut microbiota was increased in DIO mice but was not altered by MGE treatment. Similarly, the β-diversity of the gut microbiota was vastly different between the control and HFD groups. Interestingly, MGE treatment could partly restore this alteration in DIO mice. Consistently, a previous study showed that MG can alleviate metabolic disorders by regulating the gut microbiota in T2DM rats (40). This study and a previous report (40) show that MGs can regulate gut microbiota communities, which is a potential mechanism by which MGs attenuate metabolic disorders.

We further found that the abundance of *Firmicutes* was increased while the abundance of *Bacteroidetes* was decreased in DIO mice, whereas these changes were recovered by

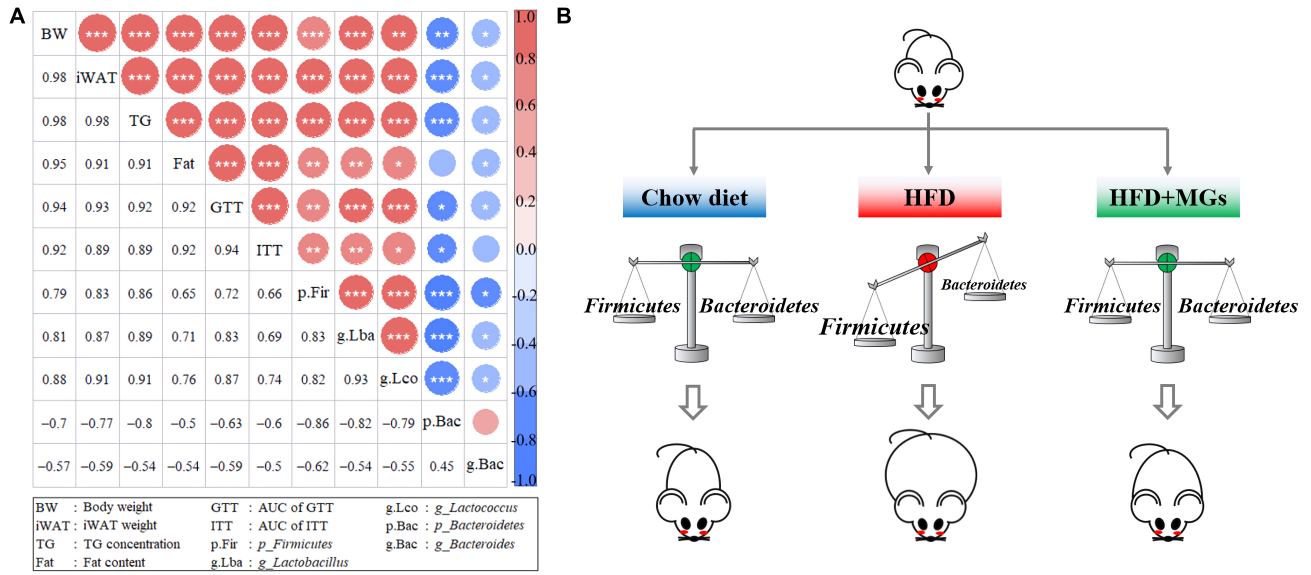

FIGURE 6 | Correlation analyses of gut microbiota structures and obese phenotypes. **(A)** The diagonals represent the indicator; positive correlation (red), negative correlation (blue); the circle diameters correspond to the absolute value of correlation coefficients; the asterisk corresponds to significance: $^{*}P < 0.05$, $^{**}P < 0.01$, $^{***}P < 0.001$. **(B)** The cartoon represents how MGs attenuate obesity by shaping gut microbiota.

MGE treatment. It has been revealed that *Firmicutes* are positively associated with the pathogenesis of obesity; in contrast, *Bacteroidetes* exhibit anti-obesity activity (41). Moreover, the abundance of *Firmicutes* is increased and that of *Bacteroidetes* is reduced in obese individuals (42). Thus, on the one hand, the reduction of *Firmicutes* abundance by antibiotics (vancomycin and bacitracin) can improve insulin resistance in DIO mice (43). On the other hand, *Bacteroidetes* abundance is significantly decreased in leptin-deficient obese mice compared with lean mice (44) because *Bacteroidetes* can obtain energy from indigestible polysaccharides and produce SCFAs to regulate energy metabolism (45). Therefore, MGs attenuate obesity was associated with the intestinal microbiota of specific *Firmicutes* and *Bacteroidetes* at the phylum level.

We next deeply explored the effects of MGE on the intestinal microbiota at the genus level in DIO mice. We observed decreased abundances of *Bacteroides* and increased abundances of *Lactobacillus*, *Lactococcus*, *Ruminiclostridium*, *Ruminiclostridium_9*, *Oscillibacter*, and *Blautia* in DIO mice. Interestingly, these changes were effectively restored by MGE treatment. Consistently, germ-free mice colonized with gut microbiota from DIO mice showed NAFLD, suggesting that certain gut microbiota, such as the genus *Bacteroides*, are responsible for hepatic lipid accumulation (46–48). In addition, *Lactobacillus* was positively correlated with insulin resistance and body weight gain. Furthermore, studies have revealed that *Lactococcus*, *Ruminiclostridium*, *Ruminiclostridium_9*, *Oscillibacter* and *Blautia* are associated with obesity in animal models and humans (49–51). Furthermore, our correlation analyses show that HFD-mediated gut microbiota abundance changes are significantly related to obesity phenotypes, e.g., body weight gain, fat mass, and insulin sensitivity.

CONCLUSION

Siraitia grosvenorii is a kind of medicinal food plant, and its fruit extracts have anti-obesity effects. Our findings reveal that MGE can alleviate intestinal dysbacteriosis in obese mice. Of note, fecal microbiota transplantation (FMT) or co-housing experiments should further strengthen the conclusion that MGE alleviates obesity by gut microbiota modulation.

DATA AVAILABILITY STATEMENT

The datasets presented in this study can be found in online repositories. The name of the repository and accession number can be found below: National Center for Biotechnology Information (NCBI) BioProject, https://www.ncbi.nlm.nih.gov/bioproject/, PRJNA811511.

ETHICS STATEMENT

The animal study was reviewed and approved by Institutional Animal Care and Use Committee (IACUC) of Guangxi University.

AUTHOR CONTRIBUTIONS

SW, KC, and XL conceived the study. SW, KC, JL, JH, KY, and PX performed the experiments. SW, XY, YL, and XL analyzed the data and wrote the manuscript. All authors reviewed the manuscript and approved the final version of the manuscript.

FUNDING

This work was supported by the National Natural Science Foundation of China (No. 82160287), the Scientific Research Foundation of Guangxi University (XTZ170099), the Guangxi Natural Science Foundation Program (2018GXNSFAA138125 and 2020GXNSFAA159099), and the One-hundred Talent Program of Guangxi and the Funding from State Key Laboratory for Conservation and Utilization of Subtropical Agro-bioresources (SKLCUSA-b201913).

REFERENCES

1. Bluher M. Obesity: global epidemiology and pathogenesis. *Nat Rev Endocrinol.* (2019) 15:288–98. doi: 10.1038/s41574-019-0176-8
2. Wright SM, Aronne LJ. Obesity in 2010: the future of obesity medicine: where do we go from here? *Nat Rev Endocrinol.* (2011) 7:69–70. doi: 10.1038/nrendo.2010.231
3. Msika S, Castel B. Present indications for surgical treatment of morbid obesity: how to choose the best operation?. *J Visc Surg.* (2010) 147:e47–51. doi: 10.1016/j.jviscsurg.2010.08.015
4. Gong S, Ye T, Wang M, Wang M, Li Y, Ma L, et al. Traditional Chinese medicine formula Kang Shuai lao pian improves obesity, gut dysbiosis, and fecal metabolic disorders in high-fat diet-fed mice. *Front Pharmacol.* (2020) 11:297. doi: 10.3389/fphar.2020.00297
5. Abdi H, Zhao B, Darbandi M, Ghayour-Mobarhan M, Tavallaie S, Rahsepar AA, et al. The effects of body acupuncture on obesity: anthropometric parameters, lipid profile, and inflammatory and immunologic markers. *ScientificWorldJournal.* (2012) 2012:603539. doi: 10.1100/2012/603539
6. Chen Y, Ma G, Hu Y, Yang Q, Deavila JM, Zhu MJ, et al. Effects of maternal exercise during pregnancy on perinatal growth and childhood obesity outcomes: a meta-analysis and meta-regression. *Sports Med.* (2021) 51:2329–47. doi: 10.1007/s40279-021-01499-6
7. Trigueros L, Pena S, Ugidos AV, Sayas-Barbera E, Perez-Alvarez JA, Sendra E. Food ingredients as anti-obesity agents: a review. *Crit Rev Food Sci Nutr.* (2013) 53:929–42. doi: 10.1080/10408398.2011.574215
8. Wang HN, Xiang JZ, Qi Z, Du M. Plant extracts in prevention of obesity. *Crit Rev Food Sci Nutr.* (2020) 62:2221–34. doi: 10.1080/10408398.2020.1852171
9. Liu C, Dai L, Liu Y, Dou D, Sun Y, Ma L. Pharmacological activities of mogrosides. *Future Med Chem.* (2018) 10:845–50. doi: 10.4155/fmc-2017-0255
10. Gong X, Chen N, Ren K, Jia J, Wei K, Zhang L, et al. The fruits of *Siraitia grosvenorii*: a review of a chinese food-medicine. *Front Pharmacol.* (2019) 10:1400. doi: 10.3389/fphar.2019.01400
11. Qi X, Chen W, Liu L, Yao P, Xie B. Effect of a *Siraitia grosvenori* extract containing mogrosides on the cellular immune system of type 1 diabetes mellitus mice. *Mol Nutr Food Res.* (2006) 50:732–8. doi: 10.1002/mnfr.200500252
12. Sung YY, Kim SH, Yuk HJ, Yang WK, Lee YM, Son E, et al. *Siraitia grosvenorii* residual extract attenuates ovalbumin-induced lung inflammation by down-regulating Il-4, Il-5, Il-13, Il-17, and MUC5AC expression in mice. *Phytomedicine.* (2019) 61:152835. doi: 10.1016/j.phymed.2019.152835
13. Li Y, Zou L, Li T, Lai D, Wu Y, Qin S. Mogroside V inhibits LPS-Induced COX-2 expression/ROS production and overexpression of HO-1 by blocking phosphorylation of AKT1 in RAW264.7 Cells. *Acta Biochim Biophys Sin.* (2019) 51:365–74. doi: 10.1093/abbs/gmz014
14. Du Y, Liu J, Liu S, Hu J, Wang S, Cui K, et al. Mogroside-rich extract from *Siraitia grosvenorii* fruits protects against the depletion of ovarian reserves in aging mice by ameliorating inflammatory stress. *Food Funct.* (2022) 13:121–30. doi: 10.1039/d1fo03194e
15. Liu C, Dai L, Liu Y, Rong L, Dou D, Sun Y, et al. Antiproliferative activity of triterpene glycoside nutrient from monk fruit in colorectal cancer and throat cancer. *Nutrients.* (2016) 8:360. doi: 10.3390/nu8060360
16. Ju P, Ding W, Chen J, Cheng Y, Yang B, Huang L, et al. The protective effects of mogroside V and its metabolite 11-oxo-mogrol of intestinal microbiota against MK801-induced neuronal damages. *Psychopharmacology.* (2020) 237:1011–26. doi: 10.1007/s00213-019-05431-9
17. Nie J, Yan K, Sui L, Zhang H, Zhang H, Yang X, et al. Mogroside V improves porcine oocyte in vitro maturation and subsequent embryonic development. *Theriogenology.* (2019) 141:35–40. doi: 10.1016/j.theriogenology.2019.09.010
18. Yan K, Cui K, Nie J, Zhang H, Sui L, Zhang H, et al. Mogroside V protects porcine oocytes from lipopolysaccharide-induced meiotic defects. *Front Cell Dev Biol.* (2021) 9:639691. doi: 10.3389/fcell.2021.639691
19. Sui L, Yan K, Zhang H, Nie J, Yang X, Xu CL, et al. Mogroside V alleviates oocyte meiotic defects and quality deterioration in benzo(a)pyrene-exposed mice. *Front Pharmacol.* (2021) 12:722779. doi: 10.3389/fphar.2021.722779
20. Harada N, Ishihara M, Horiuchi H, Ito Y, Tabata H, Suzuki YA, et al. Mogrol derived from *Siraitia grosvenorii* mogrosides suppresses 3T3-L1 adipocyte differentiation by reducing camp-response element-binding protein phosphorylation and increasing amp-activated protein kinase phosphorylation. *PLoS One.* (2016) 11:e0162252. doi: 10.1371/journal.pone.0162252
21. Zhang X, Song Y, Ding Y, Wang W, Liao L, Zhong J, et al. Effects of mogrosides on high-fat-diet-induced obesity and nonalcoholic fatty liver disease in mice. *Molecules.* (2018) 23:1894. doi: 10.3390/molecules23081894
22. Liu H, Qi X, Yu K, Lu A, Lin K, Zhu J, et al. AMPK activation is involved in hypoglycemic and hypolipidemic activities of mogroside-rich extract from *Siraitia grosvenorii* (Swingle) fruits on high-fat diet/streptozotocin-induced diabetic mice. *Food Funct.* (2018) 10:151–62. doi: 10.1039/c8fo01486h
23. Ley RE, Turnbaugh PJ, Klein S, Gordon JI. Microbial ecology: human gut microbes associated with obesity. *Nature.* (2006) 444:1022–3. doi: 10.1038/4441022a
24. Turnbaugh PJ, Ley RE, Mahowald MA, Magrini V, Mardis ER, Gordon JI. An obesity-associated gut microbiome with increased capacity for energy harvest. *Nature.* (2006) 444:1027–31. doi: 10.1038/nature05414
25. Yin J, Li Y, Han H, Chen S, Gao J, Liu G, et al. Melatonin reprogramming of gut microbiota improves lipid dysmetabolism in high-fat diet-fed mice. *J Pineal Res.* (2018) 65:e12524. doi: 10.1111/jpi.12524
26. Cotillard A, Kennedy SP, Kong LC, Prifti E, Pons N, Le Chatelier E, et al. Dietary intervention impact on gut microbial gene richness. *Nature.* (2013) 500:585–8. doi: 10.1038/nature12480
27. Mardinoglu A, Wu H, Bjornson E, Zhang C, Hakkarainen A, Rasanen SM, et al. An integrated understanding of the rapid metabolic benefits of a carbohydrate-restricted diet on hepatic steatosis in humans. *Cell Metab.* (2018) 27:559–71.e5. doi: 10.1016/j.cmet.2018.01.005
28. Liu D, Huang J, Luo Y, Wen B, Wu W, Zeng H, et al. Fuzhuan brick tea attenuates high-fat diet-induced obesity and associated metabolic disorders by shaping gut microbiota. *J Agric Food Chem.* (2019) 67:13589–604. doi: 10.1021/acs.jafc.9b05833
29. Chang CJ, Lin CS, Lu CC, Martel J, Ko YF, Ojcius DM, et al. Ganoderma lucidum reduces obesity in mice by modulating the composition of the gut microbiota. *Nat Commun.* (2015) 6:7489. doi: 10.1038/ncomms8489
30. Liang X, Yang Q, Fu X, Rogers CJ, Wang B, Pan H, et al. Maternal obesity epigenetically alters visceral fat progenitor cell properties in male offspring mice. *J Physiol.* (2016) 594:4453–66. doi: 10.1113/JP272123
31. Bolyen E, Rideout JR, Dillon MR, Bokulich NA, Abnet CC, Al-Ghalith GA, et al. Reproducible, interactive, scalable and extensible microbiome data science using QIIME 2. *Nat Biotechnol.* (2019) 37:852–7. doi: 10.1038/s41587-019-0209-9
32. Liang X, Yang Q, Zhang L, Maricelli JW, Rodgers BD, Zhu MJ, et al. Maternal high-fat diet during lactation impairs thermogenic function of brown adipose tissue in offspring mice. *Sci Rep.* (2016) 6:34345. doi: 10.1038/srep34345
33. Tian Q, Zhao J, Yang Q, Wang B, Deavila JM, Zhu MJ, et al. Dietary alpha-ketoglutarate promotes beige adipogenesis and prevents obesity in middle-aged mice. *Aging Cell.* (2020) 19:e13059. doi: 10.1111/acel.13059
34. Zhang F, Ai W, Hu X, Meng Y, Yuan C, Su H, et al. Phytol stimulates the browning of white adipocytes through the activation of amp-activated protein kinase (AMPK) alpha in mice fed high-fat diet. *Food Funct.* (2018) 9:2043–50. doi: 10.1039/C7FO01817G

35. Zhang F, Su H, Song M, Zheng J, Liu F, Yuan C, et al. Calcium supplementation alleviates high-fat diet-induced estrous cycle irregularity and subfertility associated with concomitantly enhanced thermogenesis of brown adipose tissue and browning of white adipose tissue. *J Agric Food Chem.* (2019) 67:7073–81. doi: 10.1021/acs.jafc.9b02663
36. Lin GP, Jiang T, Hu XB, Qiao XH, Tuo QH. Effect of *Siraitia grosvenorii* polysaccharide on glucose and lipid of diabetic rabbits induced by feeding high fat/high sucrose chow. *Exp Diabetes Res.* (2007) 2007:67435. doi: 10.1155/2007/67435
37. Zhang Y, Zhou G, Peng Y, Wang M, Li X. Anti-hyperglycemic and anti-hyperlipidemic effects of a special fraction of luohanguo extract on obese T2DM rats. *J Ethnopharmacol.* (2020) 247:112273. doi: 10.1016/j.jep.2019.112273
38. Li J, Deng Q, Zhang Y, Wu D, Li G, Liu J, et al. Three novel dietary phenolic compounds from pickled *Raphanus sativus* L. Inhibit lipid accumulation in obese mice by modulating the gut microbiota composition. *Mol Nutr Food Res.* (2021) 65:e2000780. doi: 10.1002/mnfr.202000780
39. Zhang XY, Chen J, Yi K, Peng L, Xie J, Gou X, et al. Phlorizin ameliorates obesity-associated endotoxemia and insulin resistance in high-fat diet-fed mice by targeting the gut microbiota and intestinal barrier integrity. *Gut Microbes.* (2020) 12:1–18. doi: 10.1080/19490976.2020.1842990
40. Zhang Y, Peng Y, Zhao L, Zhou G, Li X. Regulating the gut microbiota and scfas in the faeces of T2DM rats should be one of antidiabetic mechanisms of mogrosides in the fruits of *Siraitia grosvenorii*. *J Ethnopharmacol.* (2021) 274:114033. doi: 10.1016/j.jep.2021.114033
41. Cao S-Y, Zhao C-N, Xu X-Y, Tang G-Y, Corke H, Gan R-Y, et al. Dietary plants, gut microbiota, and obesity: effects and mechanisms. *Trends Food Sci Technol.* (2019) 92:194–204. doi: 10.1016/j.tifs.2019.08.004
42. Jumpertz R, Le DS, Turnbaugh PJ, Trinidad C, Bogardus C, Gordon JI, et al. Energy-balance studies reveal associations between gut microbes, caloric load, and nutrient absorption in humans. *Am J Clin Nutr.* (2011) 94:58–65. doi: 10.3945/ajcn.110.010132
43. Hwang I, Park YJ, Kim YR, Kim YN, Ka S, Lee HY, et al. Alteration of gut microbiota by vancomycin and bacitracin improves insulin resistance via glucagon-like peptide 1 in diet-induced obesity. *FASEB J.* (2015) 29:2397–411. doi: 10.1096/fj.14-265983
44. Ley RE, Backhed F, Turnbaugh P, Lozupone CA, Knight RD, Gordon JI. Obesity alters gut microbial ecology. *Proc Natl Acad Sci USA.* (2005) 102:11070–5. doi: 10.1073/pnas.0504978102
45. Johnson EL, Heaver SL, Walters WA, Ley RE. Microbiome and metabolic disease: revisiting the bacterial phylum bacteroidetes. *J Mol Med.* (2017) 95:1–8. doi: 10.1007/s00109-016-1492-2
46. Le Roy T, Llopis M, Lepage P, Bruneau A, Rabot S, Bevilacqua C, et al. Intestinal microbiota determines development of non-alcoholic fatty liver disease in mice. *Gut.* (2013) 62:1787–94. doi: 10.1136/gutjnl-2012-303816
47. Qiao S, Bao L, Wang K, Sun S, Liao M, Liu C, et al. Activation of a specific gut bacteroides-folate-liver axis benefits for the alleviation of nonalcoholic hepatic steatosis. *Cell Rep.* (2020) 32:108005. doi: 10.1016/j.celrep.2020.108005
48. Turnbaugh PJ, Hamady M, Yatsunenko T, Cantarel BL, Duncan A, Ley RE, et al. A core gut microbiome in obese and lean twins. *Nature.* (2009) 457:480–4. doi: 10.1038/nature07540
49. Hippe B, Remely M, Aumueller E, Pointner A, Magnet U, Haslberger AG. *Faecalibacterium prausnitzii* phylotypes in type two diabetic, obese, and lean control subjects. *Benef Microbes.* (2016) 7:511–7. doi: 10.3920/BM2015.0075
50. Pekkala S, Munukka E, Kong L, Pollanen E, Autio R, Roos C, et al. Toll-like receptor 5 in obesity: the role of gut microbiota and adipose tissue inflammation. *Obesity.* (2015) 23:581–90. doi: 10.1002/oby.20993
51. Ottosson F, Brunkwall L, Ericson U, Nilsson PM, Almgren P, Fernandez C, et al. Connection between BMI-related plasma metabolite profile and gut microbiota. *J Clin Endocrinol Metab.* (2018) 103:1491–501. doi: 10.1210/jc.2017-02114

Conflict of Interest: The authors declare that the research was conducted in the absence of any commercial or financial relationships that could be construed as a potential conflict of interest.

Publisher's Note: All claims expressed in this article are solely those of the authors and do not necessarily represent those of their affiliated organizations, or those of the publisher, the editors and the reviewers. Any product that may be evaluated in this article, or claim that may be made by its manufacturer, is not guaranteed or endorsed by the publisher.

frontiers | Frontiers in Nutrition

TYPE Original Research
PUBLISHED 06 October 2022
DOI 10.3389/fnut.2022.984695

OPEN ACCESS

EDITED BY
Ren-You Gan,
Technology and Research, Singapore

REVIEWED BY
Lu Cheng,
Rutgers, The State University of New Jersey, United States
Guijie Chen,
Nanjing Agricultural University, China

*CORRESPONDENCE
Liang Wang
wangliang@dmu.edu.cn

SPECIALTY SECTION
This article was submitted to Nutrition and Microbes, a section of the journal Frontiers in Nutrition

RECEIVED 02 July 2022
ACCEPTED 15 September 2022
PUBLISHED 06 October 2022

CITATION
Rehman AU, Siddiqui NZ, Farooqui NA, Alam G, Gul A, Ahmad B, Asim M, Khan AI, Xin Y, Zexu W, Song Ju H, Xin W, Lei S and Wang L (2022) *Morchella esculenta* mushroom polysaccharide attenuates diabetes and modulates intestinal permeability and gut microbiota in a type 2 diabetic mice model.
Front. Nutr. 9:984695.
doi: 10.3389/fnut.2022.984695

Morchella esculenta mushroom polysaccharide attenuates diabetes and modulates intestinal permeability and gut microbiota in a type 2 diabetic mice model

Ata Ur Rehman[1], Nimra Zafar Siddiqui[1], Nabeel Ahmed Farooqui[1], Gulzar Alam[2], Aneesa Gul[2], Bashir Ahmad[3], Muhammad Asim[3], Asif Iqbal Khan[1], Yi Xin[1], Wang Zexu[1], Hyo Song Ju[1], Wang Xin[1], Sun Lei[1] and Liang Wang[4]*

[1]Department of Biotechnology, College of Basic Medical Science, Dalian Medical University, Dalian, China, [2]Advanced Institute for Medical Sciences, Dalian Medical University, Dalian, China, [3]Department of Biology, University of Haripur, Haripur, Pakistan, [4]Stem Cell Clinical Research Center, National Joint Engineering Laboratory, Regenerative Medicine Center, The First Affiliated Hospital of Dalian Medical University, Dalian, Liaoning, China

Type 2 diabetes mellitus (T2DM) is a health issue that causes serious worldwide economic problems. It has previously been reported that natural polysaccharides have been studied with regard to regulating the gut microbiota, which plays an important role in T2DM. Here, we investigate the effects of *Morchella esculenta* polysaccharide (MEP) on a high-fat diet (HFD) and streptozotocin (STZ)-induced T2DM in BALB/c mice. The administration of MEP effectively regulated hyperglycemia and hyperlipidemia and improved insulin sensitivity. We also determined an improvement in gut microbiota composition by 16sRNA pyrosequencing. Treatment with MEP showed an increase in beneficial bacteria, i.e., *Lactobacillus* and *Firmicutes*, while the proportion of the opportunistic bacteria *Actinobacteria, Corynebacterium,* and *Facklamia* decreased. Furthermore, the treatment of T2DM mice with MEP resulted in reduced endotoxemia and insulin resistance-related pro-inflammatory cytokines interleukin 1β (IL-1β), tumor necrosis factor-alpha (TNF-α), and interleukin 6 (IL-6). Moreover, MEP treatment improved intestinal permeability by modulating the expression of the colon tight-junction proteins zonula occludens-1 (ZO-1), occludin, claudin-1, and mucin-2

protein (MUC2). Additionally, MEP administration affects the metagenome of microbial communities in T2DM mice by altering the functional metabolic pathways. All these findings suggested that MEP is a beneficial prebiotic associated with ameliorating the gut microbiota and its metabolites in T2DM.

KEYWORDS

***Morchella esculenta*, polysaccharide, streptozotocin, type 2 diabetes mellitus, gut microbiota**

Introduction

Type 2 diabetes mellitus (T2DM) is a chronic metabolic syndrome associated with hyperglycemia, impaired insulin sensitivity, low-grade inflammation, beta-cell failure, and impaired metabolism of glucose, proteins, and lipids (1). Disorders of the kidney, gut, liver, blood vessels, heart, and nerves, are frequently the result of uncontrolled hyperglycemia (2). The etiology of T2DM has genetic and environmental factors (e.g., unhealthy lifestyle, obesity, smoking, and lack of exercise) (3). Several oral anti-diabetic drugs alpha-glucosidase inhibitors, thiazolidinediones, and biguanides reduce hyperglycemia, but have adverse side effects such as flatulence, hypoglycemia, and islet cell damage (4).

Recently, polysaccharides derived from natural resources showed the potential to control glucose and lipid metabolism (5). Some have been investigated for their anti-diabetic effects through insulin enhancement and targeting beta-cell dysfunction, alpha-glucosidase, and inhibition of alpha-amylase (6). Polysaccharides from natural resources have been investigated for regulating gut microbiota through fermentation, resulting in the beneficial metabolites such as short-chain fatty acids (SCFAs). Consequently, the perturbation of gut microbiota regulation and their metabolites by the administration of polysaccharides is considered a potential target for treating diabetes (7).

Morchella esculenta is an edible mushroom known for its delicious taste and high nutritional value (8). Consumption of the *Morchella* species as a remedy for various diseases, has been part of traditional Chinese medicine in Malaysia and Japan for over 2,000 years (9). *Morchella esculenta* consists of a variety of bioactive ingredients: proteins, polysaccharides, vitamins and dietary fiber (10), and its polysaccharides have been reported for their anti-proliferation potential against human colon cancer (HT-29 cells) (11). *Morchella esculenta* has also been evaluated for its hepatoprotective potential in mice because of its antioxidation and anti-hyperlipidemic properties (12). *Morchella esculenta* exopolysaccharides have shown an excellent tumor-suppressive effect *in vitro* (13) and immunostimulatory activity by activating T-cells and proliferating splenocytes (14). Moreover, its heteropolysaccharides have strong antioxidant activity and protect zebrafish embryos from oxidative stress (15).

The anti-diabetic activities of *M. esculenta* polysaccharide (MEP) through modulation of gut microbiota, reversal of insulin resistance, and improved intestinal permeability are still unexplored. Therefore, the biological role of *M. esculenta* polysaccharides needs to be explored for its improvement in gut microbiota and protective effect on gut permeability for T2DM.

Materials and methods

Chemicals and reagents

The mushroom *M. esculenta* fruiting body was bought from Shandong Tai'an Yinsheng Food Co., Ltd., Shandong, China. Streptozotocin (STZ) was purchased from Sigma Chemical Co. (St. Louis, MO). High-fat diet (HFD) (45% fat Kcal%) was purchased from MediScience Ltd. (Yangzhou, China). The stool DNA isolation kit (FORGENE) was provided by Chengdu, China, and the gel purification kit (Agencourt AMPure XP 60 mL Kit) was obtained from Beckman Coulter (Brea, CA, USA). The bicinchoninic acid (BCA) protein assay kits from TransGen Biotech Co., Ltd., Beijing, China. All ELISA (enzyme-linked immunosorbent assay) kits were purchased from Shanghai Longton Biotechnology Co., Ltd., in Shanghai. The primary antibodies [goat anti-rabbit, β-actin, claudin-1, zonula occludens-1 (ZO-1), occludin and mucin-2 (MUC2)] secondary antibodies, and the Radioimmunoprecipitation assay (RIPA) buffer were purchased from Proteintech (Wuhan, China). All other chemicals were of analytical grade and obtained from standard commercial sources.

Crude polysaccharides *Morchella esculenta* polysaccharide extraction from mushroom *Morchella esculenta*

The crude polysaccharide from *M. esculenta* mushroom fruiting bodies was extracted according to the protocol

previously reported (16). Briefly, the dried fruiting bodies were crushed into a fine powder and mixed with distilled water at a ratio of 1:50 g/ml, then boiled at 80°C for 3 h. The mixture was deproteinized with trichloroacetic acid at 1.5% (v/v), and the pH was adjusted to 7.0 by 2 M (NaOH) followed by centrifugation for 10 min at 10,000 × g. The supernatant was collected and concentrated by rotary evaporation at 65°C. The concentration of protein was measured by BCA quantification. The concentrated solution was precipitated by 3 volumes of ethanol at 4°C for 12 h and then freeze-dried under freeze-drying vacuum systems.

Monosaccharide composition, protein, and sugar content of *Morchella esculenta* polysaccharide crude polysaccharides

The carbohydrate content of MEP was determined through the phenol-H_2SO_4 method (17), and to determine monosaccharide composition, high-performance liquid chromatography (HPLC) was used (18). In brief, 50 mg of purified polysaccharide powder was hydrolyzed at 120°C for 6 h with 2 mol/L of trifluoroacetic aqueous solution. After hydrolysis, the excess acid was removed by co-distillation with methanol to yield a dry hydrolysate, which was dissolved in NaOH and methanol solutions and then incubated for 1 h at 70°C. After pH normalization, distilled water was added and the mixture was extracted three times with chloroform and filtered through a 0.22 μm nylon membrane (Westborough, MA, USA).

Animals and study design

Fifty-six, four-week-old inbred male BALB/c mice (14 ± 2 g) were obtained from the specific-pathogen-free (SPF) animal care center at Dalian Medical University. The experiment was approved by the Animal Care and Research Ethics Committee, Dalian, China (approval number: ARYX 2019–2021). All mice were acclimatized for 1 week at 22 ± 2°C and 50 ± 10% relative humidity under a 12/12 h light/dark cycle. After acclamation, 16 mice were fed a normal chow diet while the other 40 were fed an HFD (45% fat Kcal%) for 4 weeks. The HFD diet mice were randomly divided into five groups (n = 8 in each group) (**Figure 1**) and injected intraperitoneally with STZ prepared in citrate buffer (pH4.5) at a dose of 60 mg/kg in a fasting condition every fifth day for 4 weeks. The mice on the normal chow diet were injected with an equivalent volume of citrate buffer (19). Fasting blood glucose (FBG) was measured weekly with a glucometer, and mice that had blood glucose levels above 11.1 mmol/L were considered to have T2DM.

After the induction of T2DM, the different groups were made as previously studied (20) and treated as follows: non-MEP treated group (DM); 200 mg/kg metformin (MET); 200 mg/kg MEP low dose (MEPL); 400 mg/kg MEP medium dose (MEPM) and 600 mg/kg MEP high dose (MEPH). Control mice were kept in two groups (n = 8 in each). One was given PBS, and the other was given MEP 200 mg/kg (MEP). The study design and schematic presentation are shown in **Figure 1**. The body weights of all mice were weighed daily to adjust the MEP dosage, while food and water intake were also measured. After 4 weeks of MEP administration, stool samples were collected in sterile eppendorf (EP) tubes and stored immediately at –80°C.

Determination of fasting blood glucose, oral glucose tolerance test, serum insulin level, and homeostasis model of assessment of insulin resistance

FBG was checked by glucometer weekly throughout the experiment by puncturing the tail vein of overnight fasted mice. An OGTT was performed at the end of the experiment. Briefly, a dosage of 0.2 g/kg of glucose was given by gavage to overnight-fasted mice and blood glucose levels were measured at different intervals: 0, 30, 60, 90, and 120 min by a blood glucometer (Bayer, Leverkusen, Germany) as instructed by the manufacturer. After 4 weeks, the mice were sacrificed by cervical dislocation. Blood was collected through the extirpating eyeball, and serum was obtained by centrifuging at 1,000 × g for 10 min. The fasting serum insulin concentration was determined by a commercially available ELISA kit, according to the manufacturer's guidelines. Furthermore, the homeostasis model of assessment of insulin resistance (HOMA-IR) was calculated to measure the insulin sensitivity of T2DM mice by using the following formula: HOMA-IR = fasting plasma insulin mIU/L × fasting serum glucose mmol/L/22.5.

Gut microbiome genomic DNA extraction and 16S rDNA amplicon pyrosequencing analysis

Bacterial genomic DNA samples were isolated using the Power Max (stool/soil) DNA isolation kit (MoBio Laboratories, Carlsbad, CA, USA) and stored at –20°C before further analysis. The isolated genomic DNA was measured using a NanoDropND-1000 (Thermo Fisher Scientific, Waltham, MA, USA), and the quality was evaluated using agarose gel electrophoresis and a spectrophotometer. The 16srRNA gene V4 region was amplified by PCR using the forward primer 515F (5′-GTGCCAGCMGCCGCGGTAA-3′) and the

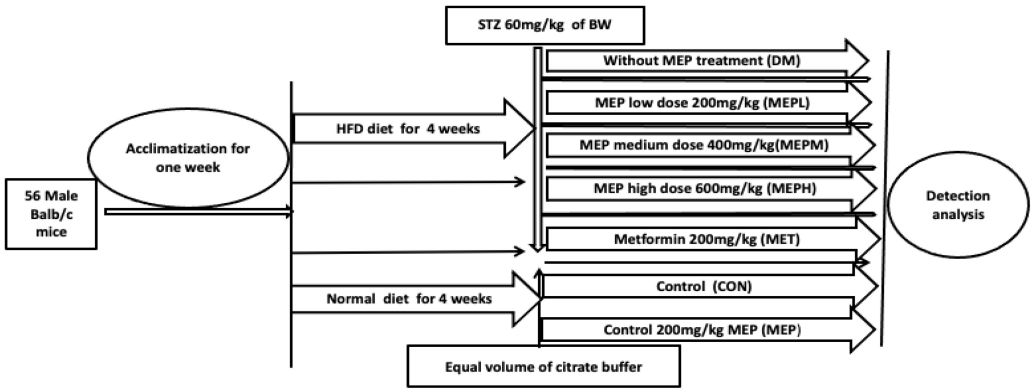

FIGURE 1
Experimental plan and design. The TD2M mouse model was developed by giving a HFD for 4 weeks, followed by intraperitoneal injections of STZ at 60 mg/kg on an overnight fast every fifth day for 8 weeks. The T2DM mice were divided into five groups (n = 8 in each group): no MEP treatment: 200 mg/kg metformin (MET); 200 mg/kg MEP low dose (MEPL); 400 mg/kg MEP medium dose (MEPM); and 600 mg/kg MEP high dose (MEPH). The 16 control mice were divided into two groups (n = 8). One was given PBS as control (CON), and the other was given 200 mg/kg MEP.

reverse primer 806R (5′-GGACTACHVGGGTWTCTAAT-3′) with the following protocol: Thermal cycling of 30 s of initial denaturation at 98°C, followed by 25 cycles of 15 s of denaturation at 98°C, 15 s of annealing at 58°C, and 15 s of extension at 72°C, with a final extension of 1 min at 72°C.

PCR amplicons were purified with Agencourt AMPure XP beads kit (Beckman Coulter, Indianapolis, IN) and quantified using the Pico Green dsDNA Assay Kit (Invitrogen, Carlsbad, CA, USA). The amplicons were then pooled in a normalized manner and sent for sequencing with a pair-end of 2 × 150 bp by using the IllluminaNovoSeq6000 platform GUHE Info Technology Co., Ltd. (Hangzhou, China). The Quantitative Insights of Microbial Ecology (QIIME, v1.9.0) pipeline was used to analyze the sequence data (21), and valid sequences were identified by removing low-quality reads. An operational taxonomic unit (OTU) was chosen, which included dereplication, clustering, and chimera detection using V search V2.4.4. Subsequently, OTU taxonomy classification was performed with the representative sequence by the Green Gene Database. Moreover, OTU-level alpha, Shannon and Simpson diversities, evenness, and richness index were performed by using QIIME and R packages (v3.2.0), e.g., "vegan." The beta diversity was performed through UniFrac distance metrics and visualized via principal coordinate analysis (PCoA), non-metric multidimensional scaling (NMDS), and principal component analysis (PCA) (21).

Metagenomic functional profiling analysis

The analysis of the metagenomic functional profile was assessed using the Phylogenetic Investigation of Communities by Reconstruction of Unobserved States tool (PICRUSt) against the Green Genes database, Kyoto Encyclopedia of Genes and Genomes (KEGG) genes and clusters of orthologous (COG) pathways. The statistical analysis of metagenomic profiles (STAMP) software package version, 2.1.3 was used for functional evaluation. Moreover, to make a figure ligand of ecologically related metabolites and functions in prokaryotic clades (e.g., genera or species), the FAPROTAX database was used (22).

Determination of pro-inflammatory cytokine concentration in serum

The serum concentration of the pro-inflammatory cytokines interleukin 1β (IL-1β), tumor necrosis factor-alpha (TNF-α), and interleukin 6 (IL-6) were determined by using a mouse ELISA kit (Shanghai Longton Biotechnology Co., Ltd., Shanghai, China), following the manufacturer's guidelines.

Western blot analysis

Total protein was extracted from colonic tissue using RIPA lysis buffer containing a protease inhibitor and centrifuged at 12,000 × g for 5 min at 4°C. The protein was quantified by the BCA protein assay kit. Thirty micrograms was fractionated by SDS-PAGE at 8–12% and electroblotted onto polyvinylidene difluoride (PVDF) membranes, which were then blocked for 1.5 h at room temperature in Tris Buffered Saline (TBS) and incubated overnight at 4°C with their respective primary antibodies (1:500–1,000) while β-actin (1:5,000) was loaded as a control. Membranes were washed three times with TBS and incubated with HRP-conjugated secondary antibodies (1:5,000)

at room temperature for 1.5 h. The protein bands were exposed to the enhanced ECL chemiluminescent substrate and visualized using an automated imaging system.

Histopathological and immunohistochemical analysis

Distal colonic tissue (4 μm thick) were fixed in 4% paraformaldehyde at room temperature for 24 h, dehydrated with gradient alcohol, and embedded in paraffin after xylene vitrification. The sections were prepared by microtome (Thermo Fisher Scientific, Waltham, MA, USA), then deparaffinized, rehydrated, and stained with H and E (hematoxylin and eosin) for histological examination. To perform immunohistochemistry (IHC), the deparaffinized and rehydrated section of tissue was incubated for 10 min with 3% H_2O_2. In addition, the tissue slide was heated in antigen retrieval buffer (Na^{+2} EDTA, pH 8.0) for antigen retrieval. Then, it was incubated overnight with MUC2-specific primary antibody at 4°C followed by horseradish peroxidase (HRP)-conjugated secondary antibody at room temperature for 1 h. 3,3 diaminobenzidine (DAB) was used as a substrate and hematoxylin was applied as counterstain. Then the slides were mounted and examined under the light microscope at 20 × magnification.

Statistical analysis

GraphPad Prism (6.01) (La Jolla, CA, USA) was used to analyze all the statistical data. One-way analysis of variance (ANOVA) was performed with Tukey's multiple comparison test to determine the significance of differences, and a *p*-value of 0.05 was considered statistically significant. LEfSe analysis was performed by Kruskal–Wallis, and Wilcoxon tests. Statistical analysis of the OTUs and phenotype was carried out by a Mann–Whitney test.

Results

Characterization and chemical analysis of *Morchella esculenta* polysaccharide

The concentration of polysaccharide (MEP) was found to be 11.96 mg/mL using the phenol-sulfuric acid method and D-glucose as a standard. The yield was 13.5% with total polysaccharide and protein concentrations of 96 and 2.26%, respectively. In comparison to previously analyzed polysaccharides from mushrooms, the yield was 13.2%, with total polysaccharides accounting for 96.66% and protein 2.38% (16). For monosaccharide analysis, the HPLC spectrum indicated that MEP was composed of mannose, ribose, rhamnose, glucuronic acid, galacturonic acid, glucose, galactose, arabinose, and fucose as presented in **Figure 2** and **Table 1**.

Effects of *Morchella esculenta* polysaccharide on body weight, glucose tolerance, and insulin resistance

We found that the STZ-induced T2DM mice exhibited gradual emaciation and decreased body weight, while the control mice showed a gradual increase in body weight. The MEP and metformin administration for 4 weeks significantly reduced the loss of body weight compared to the DM group. Interestingly, the body weight of the MEP group was lower than that of the control, indicating that MEP administration might have had an impact on normal body weight control (**Figure 3A**). T2DM is characterized by impaired glucose tolerance, elevated FBG, and increased insulin levels and resistance. An oral glucose tolerance test (OGTT) was performed after 4 weeks of treatment with MEP. FBG and serum fasting insulin levels were measured in each group. The DM group exhibited the highest FBG (23.1 mmol/L), while the MEPM group had the lowest (13.6 mmol/L). FBG levels in the MET, MEPL, MEPM, and MEPH groups were lower compared to that in the DM group (**Figure 3B**).

The oral glucose tolerance ability of the T2DM mice was severely impaired in the DM group. The blood glucose level at different time intervals remained higher than that of the control group and in the MEP-treated group. The area under the curve (AUC) of OGTT in the DM group was significantly greater, but the AUCs of the control and MEP-treated groups were significantly lower. The MEP effect on OGTT is shown in **Figures 3C,D**. Fasting serum insulin levels increased significantly in the DM group, representing insulin resistance. However, fasting serum insulin levels decreased significantly in T2DM mice treated with metformin and low, medium, and high doses of MEP compared to the DM group (**Figure 3E**). The DM group's homeostasis model assessment-insulin resistance (HOMA-IR) index was significantly higher than that of the control group. However, the metformin and MEP-treated groups MEPL, MEPM, and MEPH HOMA-IR indices were significantly reduced compared to those of the DM group (**Figure 3F**).

Morchella esculenta polysaccharide effects on bacterial alpha and beta diversity indices in type 2 diabetes mellitus

An amplicon pyrosequencing platform was employed to explain the overall composition of the gut microbial community

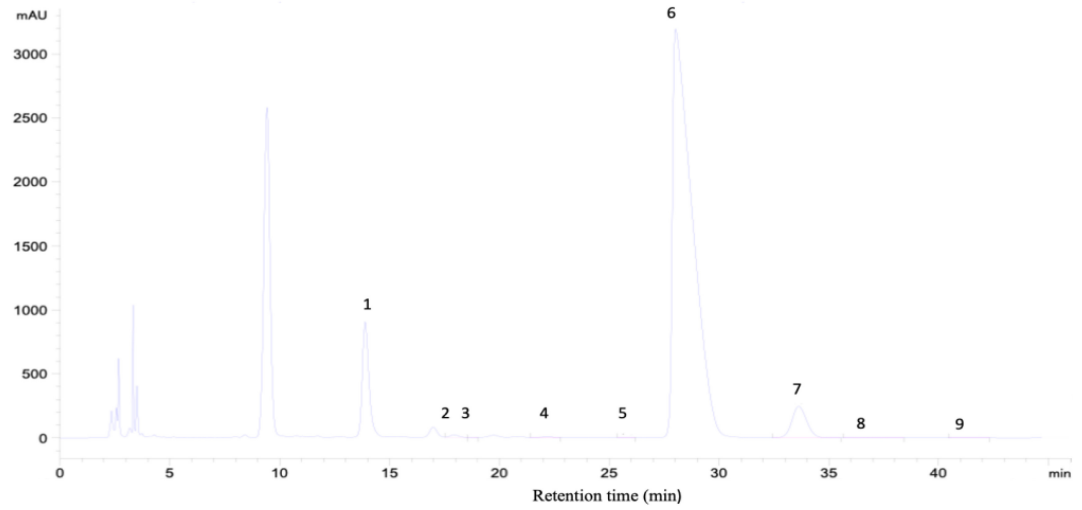

FIGURE 2
Characterization of MEP and monosaccharide composition analysis by HPLC, chromatogram of standard monosaccharide, 1-mannose, 2-ribose, 3-rhamnose, 4-glucuronic acid, 5-galacturonic acid, 6-glucose, 7-galactose, 8-arabinose, and 9-fucose.

in T2DM and control mice after MEP treatment (16S rRNA gene). The alpha and beta diversity of each group was analyzed to evaluate bacterial diversity, abundance, richness, and structural differences. The alpha diversity pattern was analyzed using a rank abundance curve, observed species, and Shannon index to assess the changes. The relative abundance of alpha diversity indices was found to be altered in the DM group compared to the control (Figure 4A). Moreover, the differences among all groups were confirmed by a box plot (Supplementary Figure 1). However, the treatment of MEP altered the alpha diversity in all treated groups of MEP and metformin, as shown in Figure 4A. Other alpha diversity parameters are summarized in Supplementary Table 1. Our results demonstrated that MEP treatment partially improved the altered alpha diversity indices.

To reveal the structural variation of the bacterial community among different groups, the beta diversity pattern was analyzed by using PCA, PCoA, and a NMDS plot (Figure 4B). Our results showed that DM group subjects were clustered separately from the control group. However, the MEP, metformin, and control groups were all relatively closer than the DM group. Significant differences among the groups were observed for PCA in PC1 (p = 0.018), PC2 (p = 0.015), and for PCoA in PC1 (p = 0.015) and PC2 (p = 0.011). These findings strongly suggest that the control and MEP-treated groups had many similarities.

TABLE 1 Monosaccharide composition of *M. esculenta* crude polysaccharide (MEP).

Components	Concentration mg/kg	Percent
Mannose	2334.69	5.77
Ribose	1924.99	0.263
Rhamnose	86.36	0.018
Glucuronic acid	261.74	0.036
Galacuronic acid	42.91	0.006
Glucose	596,658.04	81.35
Galactose	25,981.32	3.543
Xylose	ND	ND
Arabinose sugar	65,966.00	8.99
Fucose	113.73	0.016

Bacterial taxonomic composition in *Morchella esculenta* polysaccharide-treated type 2 diabetes mellitus mice

To reveal whether the MEP administration improved gut microbial composition and structure, OTUs within the range of 592–1289 were analyzed from 21 samples by IllluminaNovoSeq6000. OTU sequencing data are summarized in Supplementary Table 2. At the phylum level, alteration occurred in three major phyla: *Firmicutes, Proteobacteria,* and *Actinobacteria* in the DM group (Figure 5A). *Firmicutes* were reduced (DM, 49.3% vs. control, 64.07%), while *Bacteroidetes* increased (DM, 33.17% vs. control, 31.05%). However, the proportion of *Actinobacteria* showed a dramatic rise (DM, 16.46% vs. control, 0.67%). MEP treatment effectively reversed the altered pattern in the MEP- and MET-treated groups compared to the DM group as presented in Supplementary Table 3. The increased abundance of *Firmicutes* and lower abundance of *Actinobacteria* in the DM group were statistically

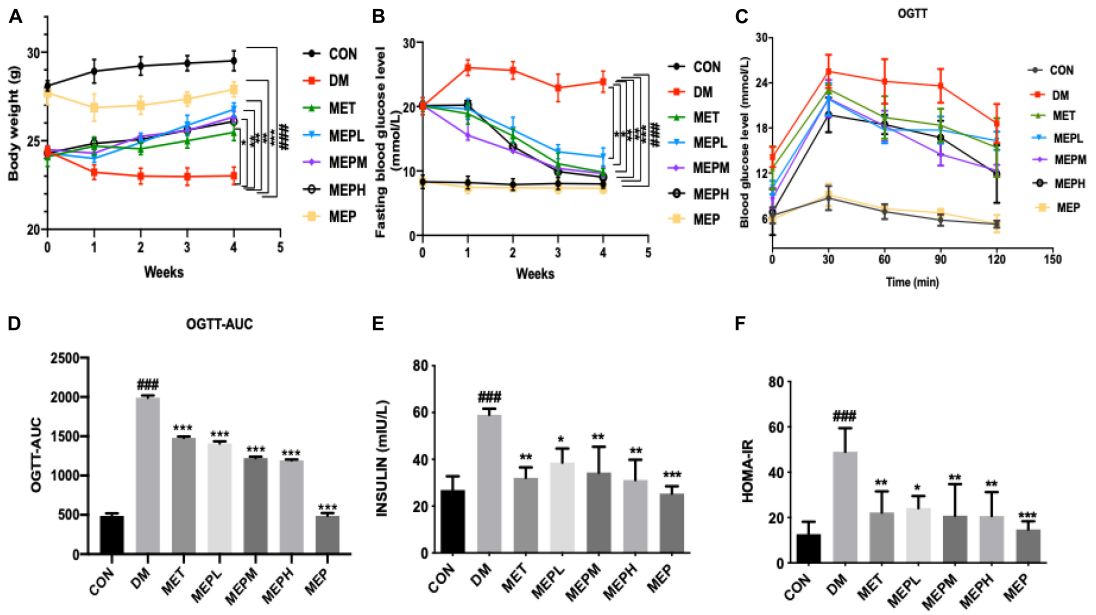

FIGURE 3
(A) The bodyweight of mice was measured daily during MEP treatment **(B)** FBG level, **(C)** OGTT, **(D)** The trapezoidal rule was used to calculate the AUC of OGTT, **(E)** serum insulin level, and **(F)** HOMA-IR was measured after T2DM treatment with MEP in different groups. # indicates a significant difference compared with the control group. $^{###}p < 0.001$ vs. control. *indicates significant difference compared with DM group. $^{*}p < 0.05$, $^{**}p < 0.01$ and $^{***}p < 0.001$ vs. DM. Data were presented as mean ± standard error of mean (SEM).

significant when compared to the control, MEPH, MEP, and MET groups (Figure 5B).

Furthermore, the bacterial composition of T2DM mice showed variation in the family, genus, order, class and species levels of the DM group (Figures 5C–L). At the genus level, *Lactobacillus, Odoribacter, Oscillospira, Corynebacterium, Bacteroides, Facklamia,* and *Prevotella* were found to be abundant flora. Nonetheless, the MEP administration ameliorated the bacterial flora, which had been disturbed to various degrees. *Lactobacillus* decreased drastically (DM, 32.09% vs. control, 69.12%). After MEP and MET treatment, the *Lactobacillus* levels were enhanced: MET (47.41%), MEPL (67.64%), MEPM (64.13%), MEPH (59.12%), and MEP (61.62%) vs. the DM group (32.09%). On the other hand, *Bacteriodes, Corynebacterium,* and *Facklamia* were observed to be higher in the DM group compared to the other groups (Figure 5C and Supplementary Table 4). The DM group showed significantly lower abundance of *Lactobacillus* and higher abundance of *Corynebacterium* and *Facklamia* compared to control and MEP-treated groups (Figure 5D).

Moreover, at the family level, the alteration of the bacterial communities of *Lactobacillaceae, Lachnospiraceae,* and *Enterobacteriaceae* were less abundant and *Corynebacteriaceae* was more abundant in the DM group (Figure 5E and Supplementary Table 5). At the class and order level, *Actinobacteriace* and *Actinomyceletes* increased markedly in the DM group (Figures 5G,I). The statistically significant taxa were observed at the family level *Corynebacteriaceae*, at the class level *Actinomyceletes*, and at the order level *Clostridia* (Figures 5F,H,J). It is noteworthy that after MEP treatment, the bacterial taxonomy was reversed at the species level. As compared to the control, MEP-, and MET-treated groups, the DM groups had an increased abundance of *Staphylococcaceae* and a lower abundance of *Lactobacilliaceae* (Figures 5K,L).

The heat map of microbiome composition with taxonomic-level analysis was clustered following a degree of similarity among all groups (Supplementary Figure 2). Conversely, the relative abundance of perturbed bacterial communities showed amelioration following MEP treatment. In conclusion, our findings revealed that, at the taxonomic level, the bacterial communities of T2DM mice were altered. However, the MET and MEP treatments in all groups improved the composition of the gut microbiota of T2DM mice, and the majority of the flora reverted to normal.

Morchella esculenta polysaccharide effect on the functional profile of gut metabolites in *Morchella esculenta* polysaccharide-treated type 2 diabetes mellitus mice

We further determined the effect of the MEP on the metagenome of microbial communities. We found that

the DM group showed significant differences in KEGG pathways compared to the control and MEP groups. Our findings demonstrated that amino acid and lipid metabolism, biosynthesis of other secondary metabolites, the immune and endocrine systems, and signaling pathways were found to be downregulated in the DM group, while these pathways were significantly upregulated in the MEP treatment groups (Figure 6A). Furthermore, a metagenomic profile analysis revealed that the DM group had higher levels of gene expression in cardiovascular disease, transport and catabolism, xenobiotic biodegradation and metabolism, cell growth and death, and the digestive system (Figure 6B). Furthermore, the gene expression of indole biosynthesis and secondary bile acid biosynthesis were found to be lower in the DM group, while these genes were found significantly highly expressed in the control, MET-, and MEP-treated groups (Figures 6C,D). These results demonstrated an altered functional metagenome among the DM and control groups.

Effect of *Morchella esculenta* polysaccharide on pro-Inflammatory cytokine levels in type 2 diabetes mellitus mice

Serum concentrations of IL-6, IL-1β, and TNF-α were measured in different groups after 4 weeks to determine the immunoregulatory effect of MEP treatment. The DM group showed marked fluctuations compared to the control. Nevertheless, IL-6 decreased significantly in MET or MEPL, MEPM, MEPH, and MEP groups (Figure 7A). Meanwhile, TNF-α also significantly decreased in the MET, MEPL, MEPM, MEPH, and MEP groups (Figure 7B). Furthermore, IL-1β in MET- and MEP-treated groups (MEPL, MEPM, and MEPH) are significantly lower than in the DM group (Figure 7C). These results indicated that MEP treatment has a potential role in reducing T2DM-induced inflammation.

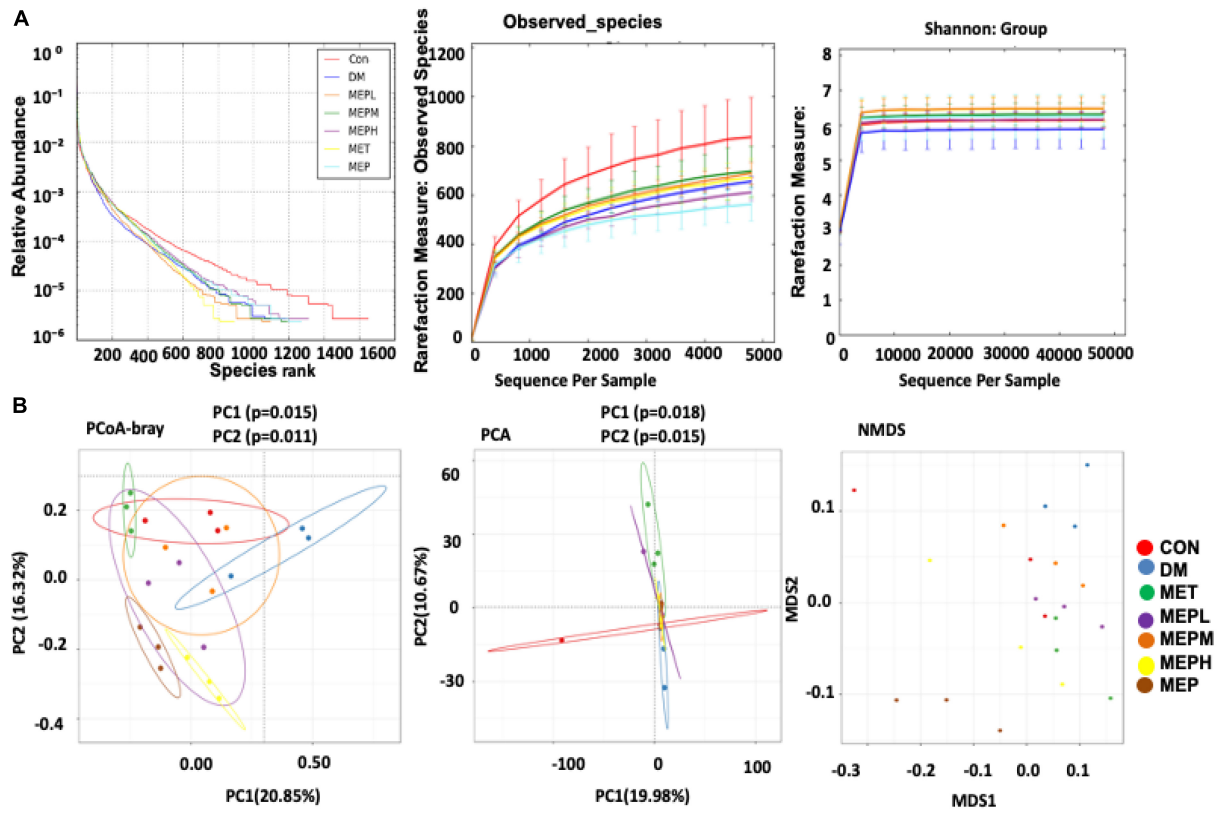

FIGURE 4
Effect of MEP on bacterial diversity indices (alpha and beta) in T2DM mice. **(A)** The rank abundance curve, observed species, and Shannon show alpha diversity. The rank abundance curve represents bacterial abundance and richness, respectively, while the rarefaction measure of the observed species and Shannon index show species diversity, evenness, and abundance. **(B)** The beta diversity indices were analyzed by the PCoA, PCA, and NMDS plot. Every point represents each sample individually. Points with different colors indicate different treatment groups. The distance between the different points represents the differences and similarities within the bacterial community structure.

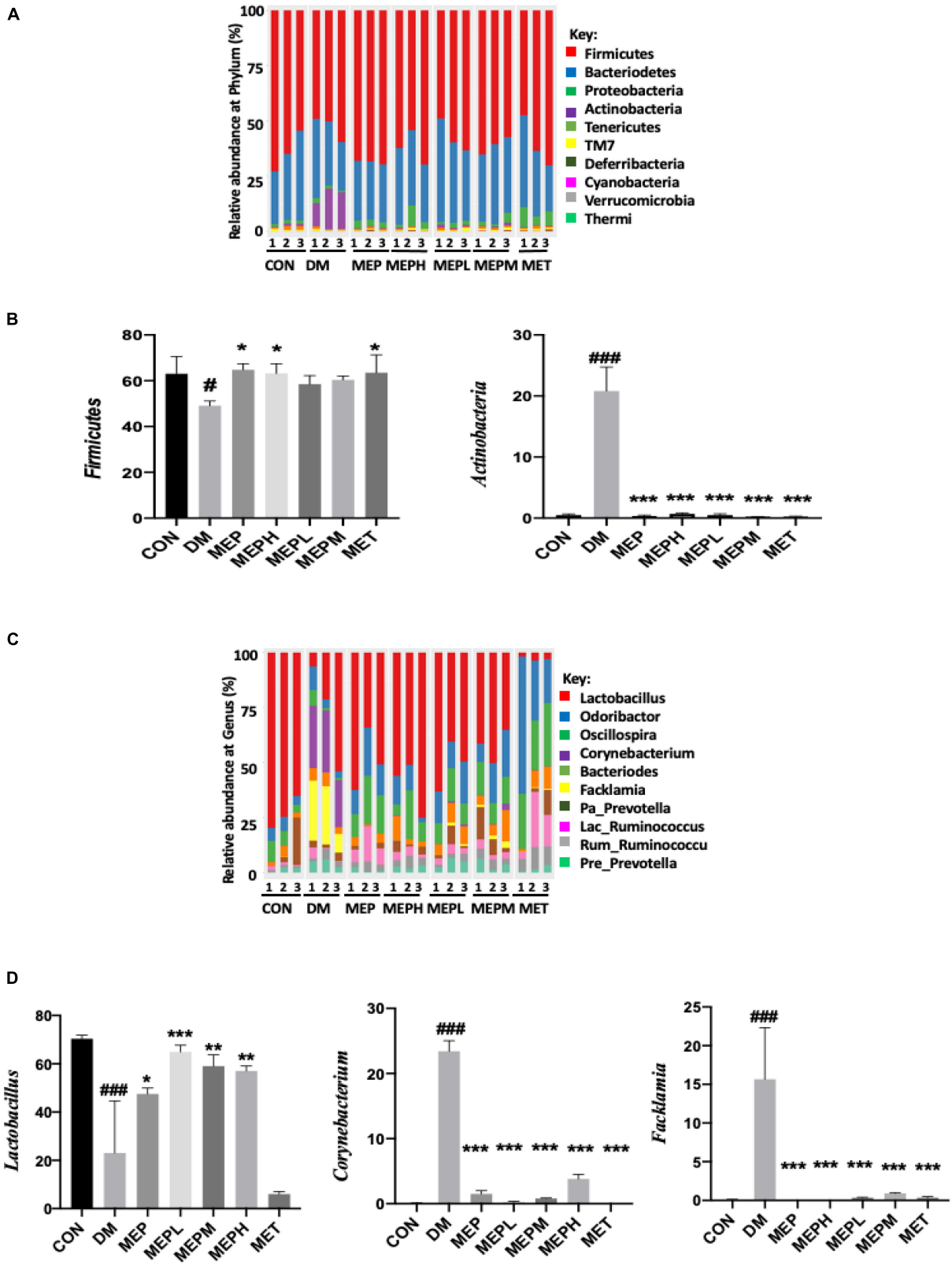

FIGURE 5
(Continued)

Morchella esculenta polysaccharide reduced type 2 diabetes mellitus-induced metabolic endotoxemia and improved intestinal permeability in type 2 diabetes mellitus mice

In previous studies, HFD mice showed higher levels of pro-inflammatory dysbiosis of gut microbiota, leading to impaired intestinal permeability, elevated serum LPS, and metabolic endotoxemia, which eventually resulted in the expression of colon tight junction proteins (ZO-1, occludin, and claudin-1). Therefore, we evaluated the effect of MEP on serum LPS levels and colon tight junction protein expression in T2DM mice. In the DM group, we observed increased LPS levels, which had decreased significantly in the MEP-treated and control groups (Figure 8A). On the other hand, the colon tight junction proteins (ZO-1, occludin, and claudin-1) showed lower expression in the DM group but significantly higher expression in the MEP-treated and control groups (Figures 8B,C–E). These results demonstrated that MEP restores intestinal permeability and reduces endotoxemia in T2DM mice.

Morchella esculenta polysaccharide improved colonic histological changes and modulated the expression of mucin-2 protein

Distal colon tissue histopathological assessment by H and E staining is shown in Figure 9A. The histological observation of colonic tissue in the DM group showed substantial loss and atrophy of crypts; irregular, short villi; a damaged epithelial barrier; and inflammatory cell infiltration. In contrast to the

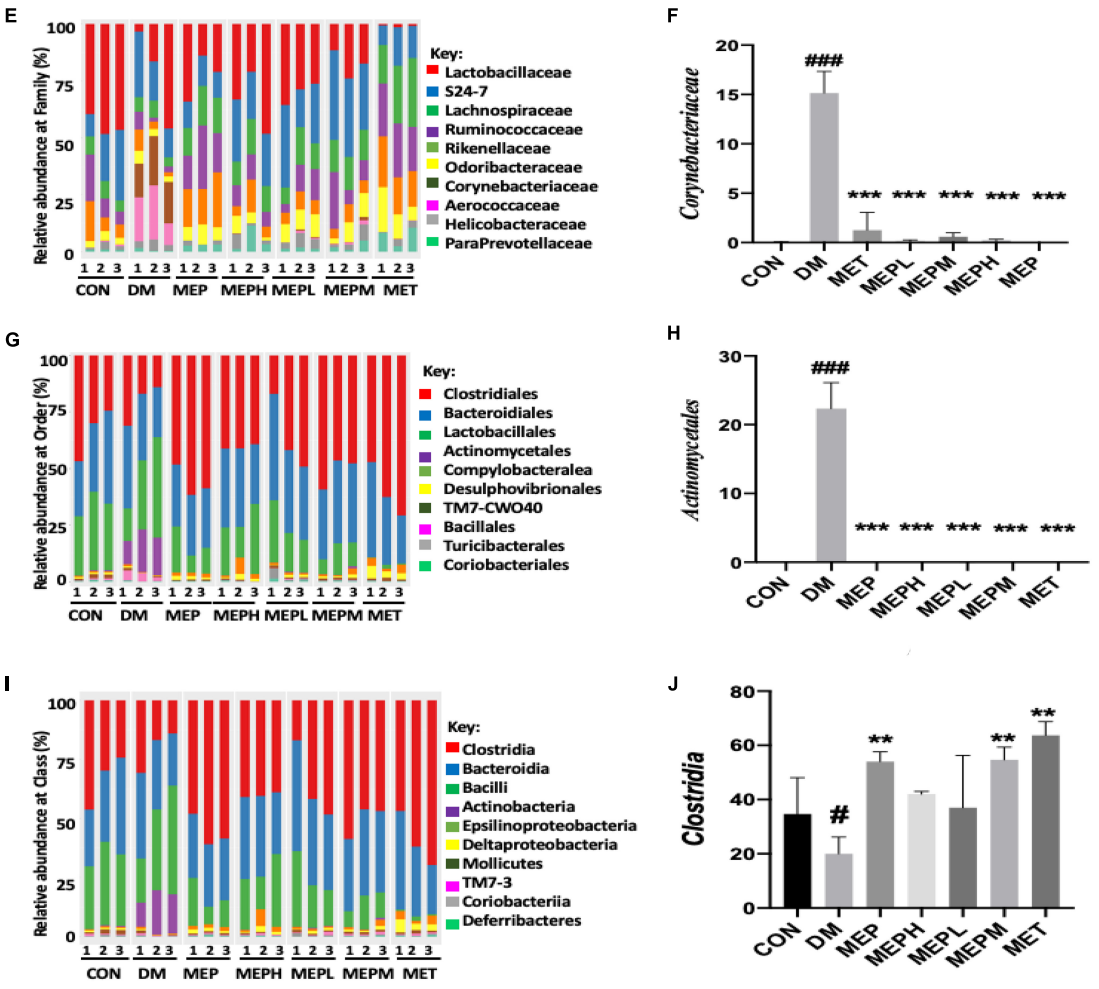

FIGURE 5
(Continued)

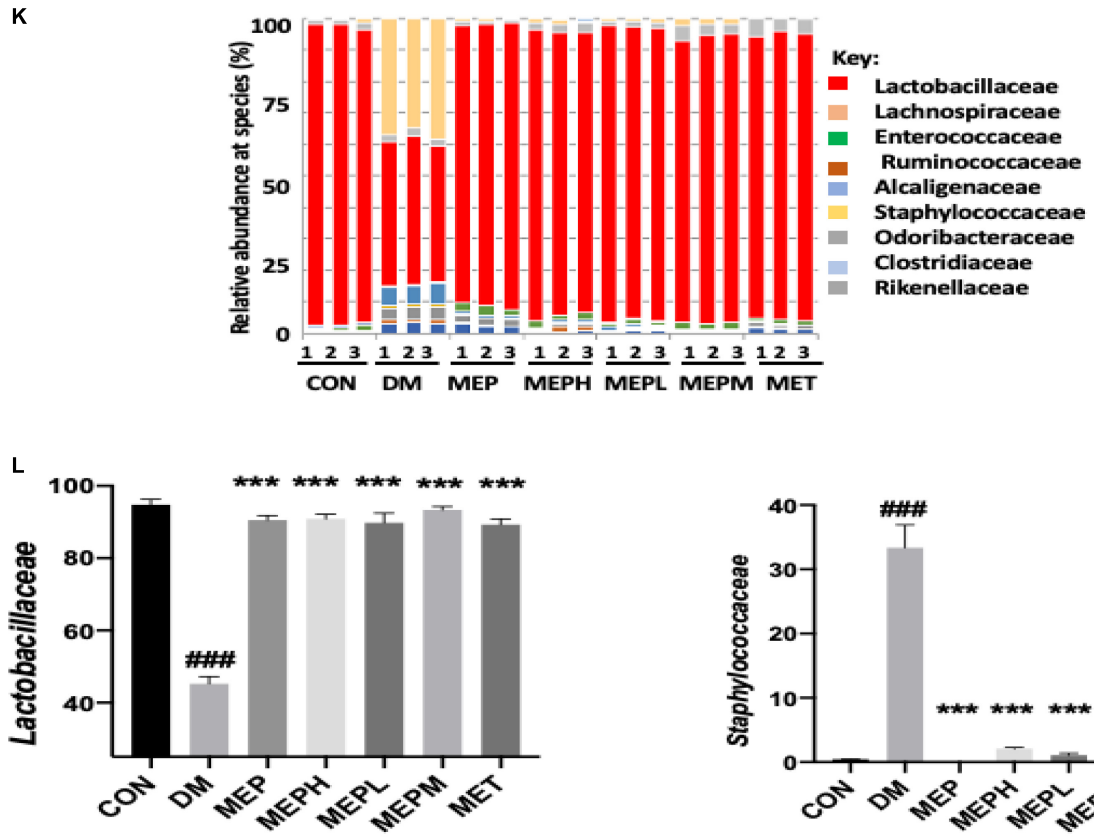

FIGURE 5
Different taxonomic levels of microbial composition in T2DM mice. **(A)** Relative abundance at the phylum level, **(B)** Abundant flora at the phylum level (%), **(C)** Relative abundance at the genus level, **(D)** Abundant flora at the genus level (%), **(E)** Relative abundance at the family level, **(F)** Abundant flora at the family level (%), **(G)** Relative abundance at the order level, **(H)** Abundant flora at the order level (%), **(I)** Relative abundance at the class level, **(J)** Abundant flora at the class level (%), **(K)** Relative abundance at the species level, and **(L)** Abundant flora at the species level (%). # indicates a significant difference compared with control (CON) group. $^{\#}p < 0.05$, and $^{\#\#\#}p < 0.001$ vs. Control. * indicates a significant difference compared with the DM group. $^{*}p < 0.05$, $^{**}p < 0.01$, and $^{***}p < 0.001$ vs. DM.

MEP- and MET-treated groups, these changes were reversed: the villi became well-demarcated regular and elongated with well-defined crypts and goblet cells, and the infiltration of inflammatory cells was alleviated. Moreover, to assess the mucus layer thickness of the epithelial gut barrier, we expressed mucin2 (MUC2) by IHC (**Figure 9B**). Notably, the expression of MUC2 decreased in the DM group compared to the others. These findings demonstrated that MEP may have the potential to ameliorate histological changes and alleviate MUC2 expression in colonic tissue.

Discussion

Several clinical implications of mushroom polysaccharide have been investigated (23), including polysaccharide from *Morchella esculenta* (MEP) mushroom (13). However, the beneficial effect of MEP in particular on gut microbiota has not been studied. We demonstrated that MEP could affect hyperglycemia, insulin sensitivity, dyslipidemia, immunomodulation, and modulate gut microbiota.

We established a T2DM mouse model induced by HFD and STZ, based on a previously published strategy (24). The importance of the HFD- and STZ-induced T2DM model for drug effects has been studied thoroughly (25, 26). This method was widely used by researchers to create animal diabetic models for experimental purposes with clinical features similar to human diabetes (20, 27). Initially, T2DM mice show gradual emaciation, increased food and water intake, and decreased body weight (28). T2DM has been characterized by hyperglycemia, hyperinsulinemia, insulin resistance (HOMA-IR), and impaired glucose tolerance (29). In contrast to these studies, our findings demonstrated that MEP treatment in T2DM mice reduced the FBG level and improved glucose tolerance because OGTT is the most sensitive and common test for measuring the abnormality in glucose homeostasis (30). Previously, polysaccharides were revealed to reduce the rate of glucose diffusion because

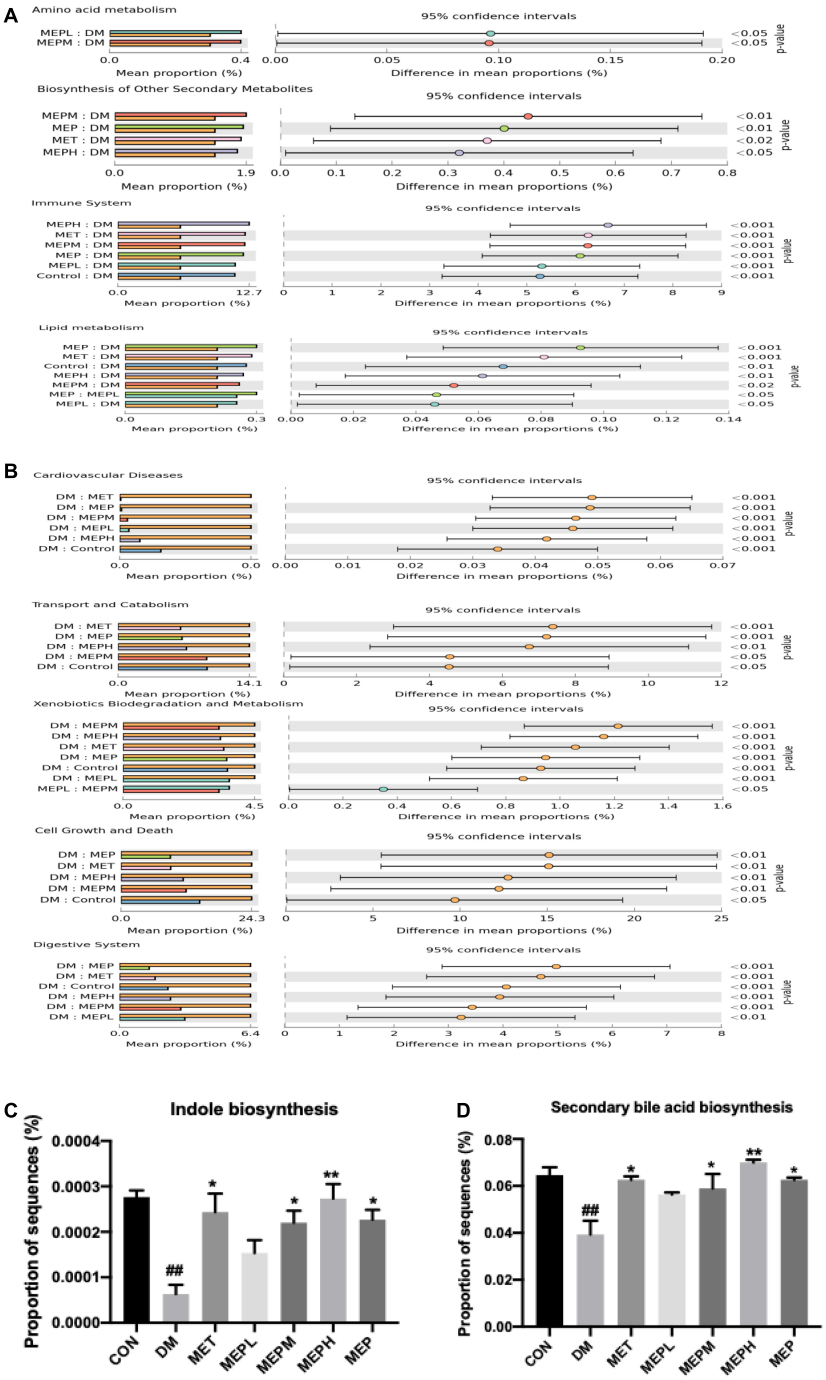

FIGURE 6

Functional profile analysis of gut metabolites in T2DM mice. **(A,B)** COG (Clusters of Orthologous Groups) shows the metabolic pathways functional predictions and KEGG database level 3 indicated with their confidence interval ratio of differences, while *p*-value shows on the right side among different groups. **(C)** Expression of genes involved in indole biosynthesis and **(D)** Secondary bile acid biosynthesis. $^{\#}$ indicates a significant difference compared with control (CON) group. $^{\#\#}p < 0.01$ vs. Control. * indicates a significant difference compared with the DM group. $^{*}p < 0.05$, $^{**}p < 0.01$ vs. DM.

of their viscosity, which may absorb glucose (31). It is known that T2DM is associated with insulin resistance and increased serum insulin levels, which are required to control the glucose burden (28), and insulin resistance is responsible for the pathogenicity of T2DM and beta-cell failure (32). We observed that MEP administration could improve

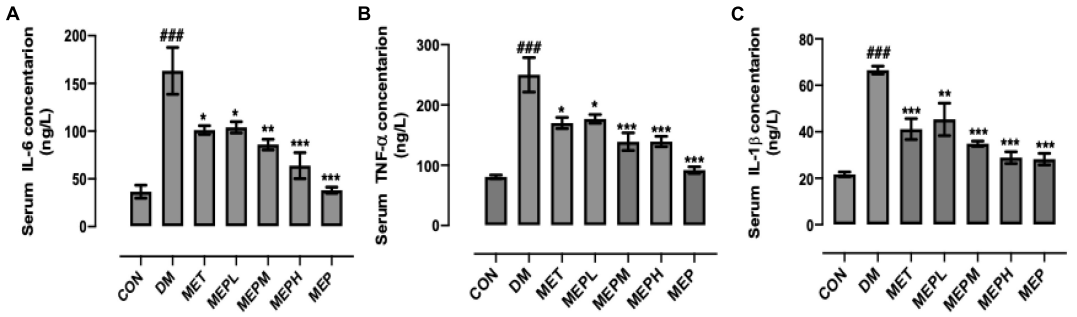

FIGURE 7
Measurement of pro-inflammatory cytokines **(A)** IL-6, **(B)** TNF-α and **(C)** IL-1β by ELISA in T2DM mice. The data are shown with means ± SEM. # indicates a significant difference compared with the control (CON) group. ###$p < 0.001$ vs. control. * indicates a significant difference compared with the DM group. *$p < 0.05$, **$p < 0.01$, and ***$p < 0.001$ vs. DM.

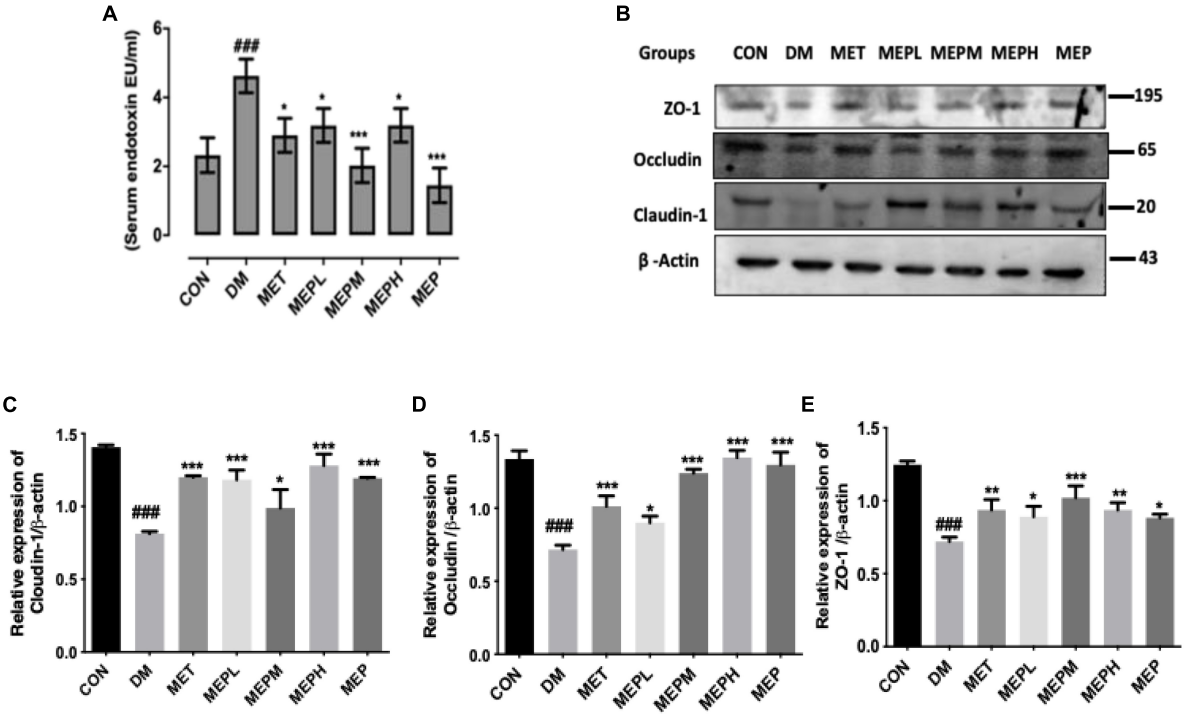

FIGURE 8
Effect of MEP treatment on serum endotoxin LPS (lipopolysaccharide) levels and colon tight junction proteins in T2DM mice. **(A)** Effect of MEP on T2DM induced endotoxemia. Serum LPS Level was measured by serum endotoxin (EU mL) Limulus amoebocyte lysate assay. **(B)** Effect of MEP on colon tight junction proteins (ZO-1, occludin, and slaudin-1) in T2DM mice. **(C–E)** Bar graph showing quantification of the western blot of the respective protein against β-actin as an internal control by Image J software. The data was obtained by three independent experiments and is expressed as mean SEM ($n = 3$). # indicates a significant difference compared with control (CON) group. ###$p < 0.001$ vs. control. * indicates a significant difference compared with the DM group. *$p < 0.05$, **$p < 0.01$ and ***$p < 0.001$ vs. DM. Data were presented as mean ± SEM.

hyperinsulinemia and HOMA-IR, which is consistent with previous research findings.

The serum concentration of IL-6, IL-1β, and TNF-α were measured after 4 weeks of treatment with MEP in different groups to determine the immunoregulatory effect of MEP. Our results demonstrated that MEP administration regulated the abnormal secretion of pro-inflammatory cytokines, mainly IL-1β, IL-6, and TNF-α. Previously, the overproduction of IL-6 and TNF-α in T2DM patients led to the development of vascular inflammation and insulin resistance (33, 34). TNF-α is mostly expressed in adipose cells and is associated with insulin resistance (34), while highly expressed IL-6 causes

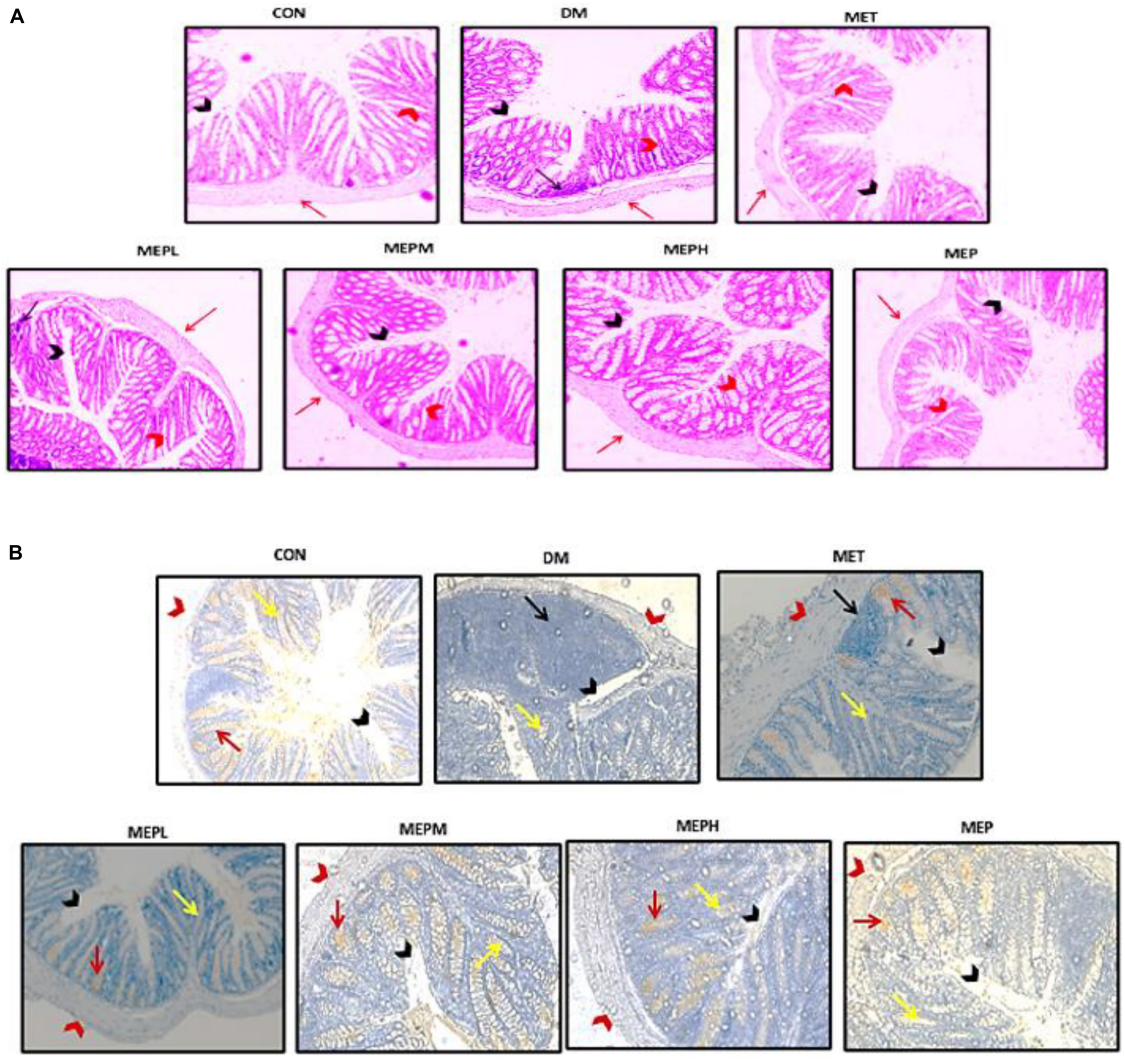

FIGURE 9
Effect of MEP on colonic histological changes by H&E (haematoxylin and eosin) staining and (MUC2) expression by IHC (immunohistochemistry) staining in T2DM mice. **(A)** Photomicrographs of distal colonic tissue, the (black arrows) indicate inflammatory cells, (black arrowhead) indicate mucosal space, (red arrow) epithelium surface and (red arrowhead) epithelial and goblet cells at magnification 20×. **(B)** Photomicrographs of the immunohistochemistry (red arrow) indicate MUC2 expression, (black arrows) indicated inflammatory cells, (black arrowhead) indicates mucosal space, (red arrows head) epithelium surface, and (yellow arrow) shows epithelial and goblet cells by the magnification of 20×.

cytotoxicity in pancreatic β cells (35). These findings indicated that MEP could regulate hyperglycemia and dyslipidemia in HFD- and STZ-induced T2DM mice by lowering the insulin resistance-related pro-inflammatory cytokines. Nevertheless, their molecular mechanisms remained unknown and needed further mechanistic studies to find out how MEP regulates glucose and lipid metabolism.

Moreover, gut microbiota dysbiosis is responsible for ulcerative colitis, inflammatory bowel diseases (IBD), and obesity (36), and is also associated with low-grade inflammation in T2DM (37). The dysbiosis of certain bacterial species that cause insulin resistance and metabolic syndromes have been reported (38, 39). In our findings, we found perturbations of bacterial abundance and richness in the DM group compared to the control group. However, when treated with MEP, bacterial abundance and diversity were augmented. The most abundant phyla of the gut microbial community were *Firmicutes, Actinobacteria, Proteobacteria,* and *Bacteroides.* Previously, many studies revealed that *Actinobacteria* increased (40, 41) while *Firmicutes* decreased in T2DM (42). Consistent with this result, our findings demonstrated an increased proportion of *Actinobacteria* and a decreased proportion of *Firmicutes* in the DM group. However, treatment with MEP potentially restored dysbiosis at the phylum level and showed similarity with the control and all MEP- and MET-treated groups. We further demonstrated the microbial community at the genus level.

The probiotic *Lactobacillus* and *Prevotella* were found to be higher in the control, MEP-, and MET-treated groups. The growth of *Lactobacillus* and *Prevotella* was positively regulated by the MEP. These findings are consistent with previous studies because metformin increases the growth of *Lactobacillus* (43). Its enhancement has a hypolipidemic effect (44), whereas an increase in *Prevotella* abundance is associated with SCFA metabolites, which improve glucose metabolism (45).

The gut microbiota has a key role in digestion, which affects the state of diabetes, as is well documented. *Bacteroides vulgatus* and *Lactobacillus fermentum* were previously identified as cholesterol-lowering bacteria (44, 46). *Prevotella* is associated with improvement in glucose metabolism and the production of essential metabolites (45). *Prevotella* was used as a probiotic to reduce inflammation in adipose tissues (47). Increased *Actinobacteria* levels have been linked to elevated LPS levels, metabolic syndrome, insulin resistance, and obesity (40). *Clostridium bolteae* was found in high abundance as an opportunistic pathogen in diabetes, and *Clostridium* spp. are commensal bacteria in the colon that are harmful in large quantities (48). *Bifidobacterium* spp. (probiotic) has previously been shown to lower obesity (49).

The function of the organs, including the colon, were affected by hyperglycemia due to damaged blood vessels (50), so we examined the histopathological changes in colonic tissue in T2DM mice. Interestingly, our findings demonstrated that those treated with MEP showed amelioration in the histological alteration of colonic tissue. Previously, it was reported that T2DM and dysbiosis of gut microbiota led to impaired intestinal permeability (51), increased LPS levels and caused endotoxemia and metabolic disorders (52), which eventually affected the expression of colon tight junction proteins (ZO-1, occludin, and claudin-1) (51). Gut microbiota dysbiosis also led to decreased expression of the MUC2 protein, an important component of the gut barrier epithelium (53). Consistent with these findings, our results demonstrated that MEP treatment restored intestinal permeability by enhancing tight junctions (ZO-1, occludin, and claudin-1), regulating MUC2 protein expression, and reducing endotoxemia through lowering LPS levels in the T2DM mice.

Undoubtedly, diabetes mellitus is a systemic metabolic disorder that affects various tissues and organs in the body (54). The alteration of glucose metabolism in diabetic mice causes severe alterations in amino acid, lipid, and energy metabolism. This metabolic instability has been linked to a higher risk of vascular complications (55). Therefore, as diabetes progresses, it becomes increasingly important to identify metabolic changes all over the body (56). Moreover, the diverse functions played by altered microbial flora indicate that their dysbiosis would negatively impact metabolic pathways. Gut microbial activity have a direct or indirect impact on the host's gastrointestinal function, as well as some influence on the auto-immune and metabolic systems.

Additionally, considering the significance of MEP in alleviating T2DM symptoms and modulating gut microbiota, we investigated these altered microbial flora to determine their unfavorable effects on functional metabolic pathways since T2DM is associated with altered metabolic pathways and metabolites (57). Amino acid and lipid metabolism, biosynthesis of other secondary metabolites, the immune and endocrine system, and signaling pathways were downregulated, while cardiovascular diseases, transport and catabolism, cell growth and death, and the digestive system were upregulated by MEP treatment. Recent findings connect dysregulation of bile acid biosynthesis to insulin resistance, dyslipidemia, and diabetes (58). However, natural indole alkaloids are on target for their anti-diabetic potential (59). In our study, the gene expression of indole biosynthesis and secondary bile acid biosynthesis was modulated by MEP treatment. These results demonstrated an altered functional metagenome among DM, control and MEP-treated groups.

Conclusion

Altogether, polysaccharides extracted from MEP have the potential to reduce hyperglycemia and hyperlipidemia in T2DM mice. Treatment with MEP slowed the loss of body weight and improved polyphagia and polydipsia, glucose tolerance, and insulin resistance in T2DM mice. T2DM-induced inflammation was reduced by decreasing the production of pro-inflammatory cytokines. More importantly, MEP modulated the gut microbiota composition by reducing harmful bacterial taxa (*Actinobacteria, Corynebacterium, Facklamia,* and *Bacteroides*) while enhancing beneficial bacterial taxa (*Firmicutes*, and *Lactobacillus*). In addition, MEP has the potential to reduce endotoxemia, improve intestinal permeability, and ameliorate the metagenome of microbial communities by altering the functional metabolic pathways. We expect that the use of such bioactive polysaccharides for their prebiotic effects could be made feasible in the immediate future.

Data availability statement

The original contributions presented in this study are included in the article/**Supplementary material**, further inquiries can be directed to the corresponding author/s.

Ethics statement

The animal study was reviewed and approved by the Dalian Medical University Committee for animal experiments.

Author contributions

YX and AR: conceptualization. AR, NS, and NF: methodology. AR, GA, and AK: software. AR and AK: formal analysis. AR, WZ, HS, WX, and SL: investigation. YX: resources, supervision and project administration. AR: manuscript writing. AR, GA, AG, BA, MA, and LW: review and editing. YX and LW: validation, visualization, and funding acquisition. All authors contributed to the article and approved the submitted version.

Funding

This study was funded and supported by the National Natural Science Foundation of China (Grant Nos. 31600614 and 82072953), Top Young Talents of Liaoning Provincial Government (Grant No. XLYC1907009), Dalian Outstanding Young Scientific and Technological Talents (Grant No. 2021RJ12), and the Chinese Scholarship Council (CSC) (Grant No. 2018SLJO19077).

Acknowledgments

We would like to express gratitude to YX for his supervision during the study. We also thank LW and the funding body for their technical skills and assistance in completing this research.

Conflict of interest

The authors declare that the research was conducted in the absence of any commercial or financial relationships that could be construed as a potential conflict of interest.

Publisher's note

All claims expressed in this article are solely those of the authors and do not necessarily represent those of their affiliated organizations, or those of the publisher, the editors and the reviewers. Any product that may be evaluated in this article, or claim that may be made by its manufacturer, is not guaranteed or endorsed by the publisher.

Supplementary material

The Supplementary Material for this article can be found online at: https://www.frontiersin.org/articles/10.3389/fnut.2022.984695/full#supplementary-material

References

1. Farzaei M, Rahimi R, Farzaei F, Abdollahi M. Traditional medicinal herbs for the management of diabetes and its complications: an evidence-based review. *Int J Pharmacol.* (2015) 11:874–87. doi: 10.3923/ijp.2015.874.887

2. Zhao C, Yang C, Wai STC, Zhang Y, Paoli P. Regulation of glucose metabolism by bioactive phytochemicals for the management of type 2 diabetes mellitus. *Crit Rev Food Sci Nutr.* (2019) 59:830–47. doi: 10.1080/10408398.2018.1501658

3. Gillani SW, Abdul MIM, Ansari IA, Zaghloul HA, Ata-ur-Rehman S, Baig MR. Predicting relationship of eating behavior, physical activity and smoking with type II diabetes and related comorbidities among *Saudi citizens*: cross-sectional observational study. *Int J Diab Dev Countr.* (2019) 39:115–22. doi: 10.1007/s13410-018-0645-y

4. Smushkin G, Vella A. What is type 2 diabetes? *Medicine (Abingdon).* (2010) 38:597–601. doi: 10.1016/j.mpmed.2010.08.008

5. Yang CF, Lai SS, Chen YH, Liu D, Liu B, Ai C, et al. Anti-diabetic effect of oligosaccharides from seaweed *Sargassum confusum* via JNK-IRS1/PI3K signalling pathways and regulation of gut microbiota. *Food Chem Toxicol.* (2019) 131:110562. doi: 10.1016/j.fct.2019.110562

6. Wu J, Shi S, Wang H, Wang S. Mechanisms underlying the effect of polysaccharides in the treatment of type 2 diabetes: a review. *Carbohydr Polym.* (2016) 144:474–94. doi: 10.1016/j.carbpol.2016.02.040

7. Cani PD. Human gut microbiome: hopes, threats and promises. *Gut.* (2018) 67:1716–25. doi: 10.1136/gutjnl-2018-316723

8. Tietel Z, Masaphy S. True morels (*Morchella*)-nutritional and phytochemical composition, health benefits and flavor: a review. *Crit Rev Food Sci Nutr.* (2018) 58:1888–901. doi: 10.1080/10408398.2017.1285269

9. Hobbs C. *Kombucha: Tea Mushroom: The Essential Guide*. Santa Cruz, CA: Botanical Press (1995).

10. Gursoy N, Sarikurkcu C, Cengiz M, Solak MHJF, Toxicology C. Antioxidant activities, metal contents, total phenolics and flavonoids of seven *Morchella* species. *Food Chem Toxicol.* (2009) 47:2381–8. doi: 10.1016/j.fct.2009.06.032

11. Liu C, Sun Y, Mao Q, Guo X, Li P, Liu Y, et al. Characteristics and antitumor activity of *Morchella esculenta* polysaccharide extracted by pulsed electric field. *Int J Mol Sci.* (2016) 17:986. doi: 10.3390/ijms17060986

12. Dong Y, Qi Y, Liu M, Song X, Zhang C, Jiao X, et al. Antioxidant, anti-hyperlipidemia and hepatic protection of enzyme-assisted *Morehella esculenta* polysaccharide. *Int J Biol Macromol.* (2018) 120:1490–9. doi: 10.1016/j.ijbiomac.2018.09.134

13. Hu M, Chen Y, Wang C, Cui H, Duan P, Zhai T, et al. Induction of apoptosis in HepG2 cells by polysaccharide MEP-II from the fermentation broth of *Morchella esculenta*. *Biotechnol Lett.* (2013) 35:1–10. doi: 10.1007/s10529-012-0917-4

14. Cui HL, Chen Y, Wang SS, Kai GQ, Fang YM. Isolation, partial characterisation and immunomodulatory activities of polysaccharide from *Morchella esculenta*. *J Sci Food Agric.* (2011) 91:2180–5. doi: 10.1002/jsfa.4436

15. Cai Z-N, Li W, Mehmood S, Pan W-J, Wang Y, Meng F-J, et al. Structural characterization, in vitro and in vivo antioxidant activities of a heteropolysaccharide from the fruiting bodies of *Morchella esculenta*. *Carbohydr Polym.* (2018) 195:29–38. doi: 10.1016/j.carbpol.2018.04.069

16. Kanwal S, Joseph TP, Owusu L, Xiaomeng R, Meiqi L, Yi XA. Polysaccharide isolated from *Dictyophora indusiata* promotes recovery from antibiotic-driven intestinal dysbiosis and improves gut epithelial barrier function in a mouse model. *Nutrients.* (2018) 10:8. doi: 10.3390/nu10081003

17. Dubois M, Gilles KA, Hamilton JK, Rebers PT, Smith F. Colorimetric method for determination of sugars and related substances. *Analy Chem.* (1956) 28:350–6. doi: 10.1021/ac60111a017

18. Hao L, Sheng Z, Lu J, Tao R, Jia S. Characterization and antioxidant activities of extracellular and intracellular polysaccharides from *Fomitopsis pinicola*. *Carbohydr Polym.* (2016) 141:54–9. doi: 10.1016/j.carbpol.2015.11.048

19. Zhu K, Nie S, Li C, Lin S, Xing M, Li W, et al. A newly identified polysaccharide from *Ganoderma atrum* attenuates hyperglycemia and hyperlipidemia. *Int J Biol Macromol.* (2013) 57:142–50. doi: 10.1016/j.ijbiomac.2013.03.009

20. Nie Q, Hu J, Gao H, Fan L, Chen H, Nie S. Polysaccharide from *Plantago asiatica* L. attenuates hyperglycemia, hyperlipidemia and affects colon microbiota in type 2 diabetic rats. *Food Hydrocolloids.* (2019) 86:34–42. doi: 10.1016/j.foodhyd.2017.12.026

21. Caporaso JG, Kuczynski J, Stombaugh J, Bittinger K, Bushman FD, Costello EK, et al. QIIME allows analysis of high-throughput community sequencing data. *Nat Methods.* (2010) 7:335–6. doi: 10.1038/nmeth.f.303

22. Langille MG, Zaneveld J, Caporaso JG, McDonald D, Knights D, Reyes JA, et al. Predictive functional profiling of microbial communities using 16S rRNA marker gene sequences. *Nat Biotechnol.* (2013) 31:814–21. doi: 10.1038/nbt.2676

23. Jayachandran M, Xiao J, Xu B. A critical review on health promoting benefits of edible mushrooms through gut microbiota. *Int J Mol Sci.* (2017) 18:9. doi: 10.3390/ijms18091934

24. Zhang M, Lv X-Y, Li J, Xu Z-G, Chen L. The characterization of high-fat diet and multiple low-dose streptozotocin induced type 2 diabetes rat model. *Exp Diab Res.* (2008) 2008:704045. doi: 10.1155/2008/704045

25. Reed M, Meszaros K, Entes L, Claypool M, Pinkett J, Gadbois T, et al. A new rat model of type 2 diabetes: the fat-fed, streptozotocin-treated rat. *Metab Clin Exp.* (2000) 49:1390–4. doi: 10.1053/meta.2000.17721

26. Srinivasan K, Viswanad B, Asrat L, Kaul C, Ramarao P. Combination of high-fat diet-fed and low-dose streptozotocin-treated rat: a model for type 2 diabetes and pharmacological screening. *Pharmacol Res.* (2005) 52:313–20. doi: 10.1016/j.phrs.2005.05.004

27. Goyal SN, Reddy NM, Patil KR, Nakhate KT, Ojha S, Patil CR, et al. Challenges and issues with streptozotocin-induced diabetes - a clinically relevant animal model to understand the diabetes pathogenesis and evaluate therapeutics. *Chem Biol Int.* (2016) 244:49–63. doi: 10.1016/j.cbi.2015.11.032

28. Pan Y, Wang C, Chen Z, Li W, Yuan G, Chen H. Physicochemical properties and antidiabetic effects of a polysaccharide from corn silk in high-fat diet and streptozotocin-induced diabetic mice. *Carbohydr Polym.* (2017) 164:370–8. doi: 10.1016/j.carbpol.2017.01.092

29. Li S, Chen H, Wang J, Wang X, Hu B, Lv F. Involvement of the PI3K/Akt signal pathway in the hypoglycemic effects of tea polysaccharides on diabetic mice. *Int J Biol Macromol.* (2015) 81:967–74. doi: 10.1016/j.ijbiomac.2015.09.037

30. Ceriello A. Postprandial hyperglycemia and diabetes complications: is it time to treat? *Diabetes.* (2005) 54:1–7. doi: 10.2337/diabetes.54.1.1

31. Ou S, Kwok K, Li Y, Fu L. In vitro study of possible role of dietary fiber in lowering postprandial serum glucose. *J Agric Food Chem.* (2001) 49:1026–9. doi: 10.1021/jf000574n

32. Abdul-Ghani MA, Tripathy D, DeFronzo RA. Contributions of beta-cell dysfunction and insulin resistance to the pathogenesis of impaired glucose tolerance and impaired fasting glucose. *Diabetes Care.* (2006) 29:1130–9. doi: 10.2337/dc05-2179

33. Sandler S, Bendtzen K, Eizirik DL, Welsh M. Interleukin-6 affects insulin secretion and glucose metabolism of rat pancreatic islets in vitro. *Endocrinology.* (1990) 126:1288–94. doi: 10.1210/endo-126-2-1288

34. Maedler K, Sergeev P, Ris F, Oberholzer J, Joller-Jemelka HI, Spinas GA, et al. Glucose-induced beta cell production of IL-1beta contributes to glucotoxicity in human pancreatic islets. *J Clin Invest.* (2002) 110:851–60. doi: 10.1172/JCI200215318

35. Esposito K, Nappo F, Marfella R, Giugliano G, Giugliano F, Ciotola M, et al. Inflammatory cytokine concentrations are acutely increased by hyperglycemia in humans: role of oxidative stress. *Circulation.* (2002) 106:2067–72. doi: 10.1161/01.CIR.0000034509.14906.AE

36. Patterson E, Ryan PM, Cryan JF, Dinan TG, Ross RP, Fitzgerald GF, et al. Gut microbiota, obesity and diabetes. *Postgrad Med J.* (2016) 92:286–300. doi: 10.1136/postgradmedj-2015-133285

37. Hur KY, Lee MS. Gut microbiota and metabolic disorders. *Diab Metab J.* (2015) 39:198–203. doi: 10.4093/dmj.2015.39.3.198

38. Caparros-Martin JA, Lareu RR, Ramsay JP, Peplies J, Reen FJ, Headlam HA, et al. Statin therapy causes gut dysbiosis in mice through a PXR-dependent mechanism. *Microbiome.* (2017) 5:95. doi: 10.1186/s40168-017-0312-4

39. Xu P, Wang J, Hong F, Wang S, Jin X, Xue T, et al. Melatonin prevents obesity through modulation of gut microbiota in mice. *J Pineal Res.* (2017) 62:4. doi: 10.1111/jpi.12399

40. Caricilli AM, Saad MJ. The role of gut microbiota on insulin resistance. *Nutrients.* (2013) 5:829–51. doi: 10.3390/nu5030829

41. Kong LC, Wuillemin PH, Bastard JP, Sokolovska N, Gougis S, Fellahi S, et al. Insulin resistance and inflammation predict kinetic body weight changes in response to dietary weight loss and maintenance in overweight and obese subjects by using a bayesian network approach. *Am J Clin Nutr.* (2013) 98:1385–94. doi: 10.3945/ajcn.113.058099

42. Larsen N, Vogensen FK, van den Berg FW, Nielsen DS, Andreasen AS, Pedersen BK, et al. Gut microbiota in human adults with type 2 diabetes differs from non-diabetic adults. *PLoS One.* (2010) 5:e9085. doi: 10.1371/journal.pone.0009085

43. Rodriguez J, Hiel S, Delzenne NM. Metformin: old friend, new ways of action-implication of the gut microbiome? *Curr Opin Clin Nutr Metab Care.* (2018) 21:294–301. doi: 10.1097/MCO.0000000000000468

44. Bhathena J, Martoni C, Kulamarva A, Urbanska AM, Malhotra M, Prakash S. Orally delivered microencapsulated live probiotic formulation lowers serum lipids in hypercholesterolemic hamsters. *J Med Food.* (2009) 12:310–9. doi: 10.1089/jmf.2008.0166

45. Kovatcheva-Datchary P, Nilsson A, Akrami R, Lee YS, De Vadder F, Arora T, et al. Dietary fiber-induced improvement in glucose metabolism is associated with increased abundance of prevotella. *Cell Metab.* (2015) 22:971–82. doi: 10.1016/j.cmet.2015.10.001

46. Gérard P, Lepercq P, Leclerc M, Gavini F, Raibaud P, Juste C. *Bacteroides* sp. strain D8, the first cholesterol-reducing bacterium isolated from human feces. *Appl Environ Microbiol.* (2007) 73:5742–9. doi: 10.1128/AEM.02806-06

47. Roselli M, Pieper R, Rogel-Gaillard C, de Vries H, Bailey M, Smidt H, et al. Immunomodulating effects of probiotics for microbiota modulation, gut health and disease resistance in pigs. *Animal Feed Sci Technol.* (2017) 233:104–19. doi: 10.1016/j.anifeedsci.2017.07.011

48. Qin J, Li Y, Cai Z, Li S, Zhu J, Zhang F, et al. A metagenome-wide association study of gut microbiota in type 2 diabetes. *Nature.* (2012) 490:55–60. doi: 10.1038/nature11450

49. Wen L, Duffy A. Factors influencing the gut microbiota, inflammation, and type 2 diabetes. *J Nutr.* (2017) 147:1468S–75S. doi: 10.3945/jn.116.240754

50. Li C, Ding Q, Nie SP, Zhang YS, Xiong T, Xie MY. Carrot juice fermented with *Lactobacillus plantarum* NCU116 ameliorates type 2 diabetes in rats. *J Agric Food Chem.* (2014) 62:11884–91. doi: 10.1021/jf503681r

51. Cani PD, Possemiers S, Van de Wiele T, Guiot Y, Everard A, Rottier O, et al. Changes in gut microbiota control inflammation in obese mice through a mechanism involving GLP-2-driven improvement of gut permeability. *Gut.* (2009) 58:1091–103. doi: 10.1136/gut.2008.165886

52. Kim KA, Gu W, Lee IA, Joh EH, Kim DH. High fat diet-induced gut microbiota exacerbates inflammation and obesity in mice via the TLR4 signaling pathway. *PLoS One.* (2012) 7:e47713. doi: 10.1371/journal.pone.0047713

53. Van der Sluis M, De Koning BA, De Bruijn AC, Velcich A, Meijerink JP, Van Goudoever JB, et al. Muc2-deficient mice spontaneously develop colitis, indicating that MUC2 is critical for colonic protection. *Gastroenterology.* (2006) 131:117–29. doi: 10.1053/j.gastro.2006.04.020

54. Chen P, Liu J. Metabonomics and diabetes mellitus. *Adv Ther.* (2007) 24:1036–45. doi: 10.1007/BF02877709

55. Nair K, Halliday D, Garrow J. Increased energy expenditure in poorly controlled type 1 (insulin-dependent) diabetic patients. *Diabetologia.* (1984) 27:13–6. doi: 10.1007/BF00253494

56. Griffin JL, Vidal-Puig A. Current challenges in metabolomics for diabetes research: a vital functional genomic tool or just a ploy for gaining funding? *Physiol Geno.* (2008) 34:1–5. doi: 10.1152/physiolgenomics.00009.2008

57. Wu H, Esteve E, Tremaroli V, Khan MT, Caesar R, Mannerås-Holm L, et al. Metformin alters the gut microbiome of individuals with treatment-naive type 2 diabetes, contributing to the therapeutic effects of the drug. *Nat Med.* (2017) 23:850–8. doi: 10.1038/nm.4345

58. Tomkin GH, Owens D. Obesity diabetes and the role of bile acids in metabolism. *J Trans Int Med.* (2016) 2:73. doi: 10.1515/jtim-2016-0018

59. Zhu Y, Zhao J, Luo L, Gao Y, Bao H, Li P, et al. Research progress of indole compounds with potential antidiabetic activity. *Eur J Med Chem.* (2021) 223:113665. doi: 10.1016/j.ejmech.2021.113665

frontiers | Frontiers in Nutrition

TYPE Review
PUBLISHED 09 November 2022
DOI 10.3389/fnut.2022.1030063

OPEN ACCESS

EDITED BY
Ding-Tao Wu,
Chengdu University, China

REVIEWED BY
Xin Wu,
Chinese Academy of Sciences (CAS), China
Tünde Pusztahelyi,
University of Debrecen, Hungary

*CORRESPONDENCE
Jinrong Wang
wangjr@haut.edu.cn

SPECIALTY SECTION
This article was submitted to Nutrition and Microbes, a section of the journal Frontiers in Nutrition

RECEIVED 28 August 2022
ACCEPTED 20 October 2022
PUBLISHED 09 November 2022

CITATION
Gan L, Wang J and Guo Y (2022) Polysaccharides influence human health *via* microbiota-dependent and -independent pathways. *Front. Nutr.* 9:1030063. doi: 10.3389/fnut.2022.1030063

Polysaccharides influence human health *via* microbiota-dependent and -independent pathways

Liping Gan[1], Jinrong Wang[1]* and Yuming Guo[2]

[1]School of Bioengineering, Henan University of Technology, Zhengzhou, China, [2]State Key Laboratory of Animal Nutrition, College of Animal Science and Technology, China Agricultural University, Beijing, China

Polysaccharides are the most diverse molecules and can be extracted from abundant edible materials. Increasing research has been conducted to clarify the structure and composition of polysaccharides obtained from different materials and their effects on human health. Humans can only directly assimilate very limited polysaccharides, most of which are conveyed to the distal gut and fermented by intestinal microbiota. Therefore, the main mechanism underlying the bioactive effects of polysaccharides on human health involves the interaction between polysaccharides and microbiota. Recently, interest in the role of polysaccharides in gut health, obesity, and related disorders has increased due to the wide range of valuable biological activities of polysaccharides. The known roles include mechanisms that are microbiota-dependent and involve microbiota-derived metabolites and mechanisms that are microbiota-independent. In this review, we discuss the role of polysaccharides in gut health and metabolic diseases and the underlying mechanisms. The findings in this review provide information on functional polysaccharides in edible materials and facilitate dietary recommendations for people with health issues. To uncover the effects of polysaccharides on human health, more clinical trials should be conducted to confirm the therapeutic effects on gut and metabolic disease. Greater attention should be directed toward polysaccharide extraction from by-products or metabolites derived from food processing that are unsuitable for direct consumption, rather than extracting them from edible materials. In this review, we advanced the understanding of the structure and composition of polysaccharides, the mutualistic role of gut microbes, the metabolites from microbiota-fermenting polysaccharides, and the subsequent outcomes in human health and disease. The findings provide insight into the proper application of polysaccharides in improving human health.

KEYWORDS

polysaccharide, microbiota, gut health, metabolic disease, biological activity

Introduction

Polysaccharides, which are composed of more than 10 monosaccharide units connected by glycosidic linkages, are the most abundant types of carbohydrates and are present in various living organisms, including plants, fungi, and marine algae. Depending on their composition of monosaccharides, polysaccharides are classified as either homopolysaccharides, which comprise only one type of monosaccharide (e.g., starch), or heteropolysaccharides, which are composed of two or more different monomeric units (e.g., pectin). Polysaccharides can serve as reserve carbohydrates and/or structural components that contribute to complex physiological processes in plants and other organisms (1). The reserve polysaccharides primally exist in the cytoplasm, whereas the structural polysaccharides are mainly stored in the primary and secondary cell walls. Both serve as carbohydrate sources, provide fibers in human and animal diets, and affect physical function and health (**Figure 1**) (2).

Polysaccharides are primarily consumed by oral administration and pass through the intestines for further utilization; therefore, polysaccharides have great biological benefits for bowel health (3). Humans and animals can directly process only simple sugars and a certain type of starch; thus, a large portion of polysaccharides (e.g., fiber) reaches the hindgut intact and is fermented by the intestinal microbiota. The microbiota and their derived metabolites have a great impact on human health and physiology (4). Therefore, considerable research has focused on the interaction between polysaccharides and intestinal microbiota as well as on shaping the structure of gut microbiota to determine polysaccharides' effects on human health (5). Dietary fiber deficiency changes the gut microbiota and leads to gut dysbiosis, which occurs in various diseases, especially metabolic diseases (6). The increased incidence of insulin resistance, obesity, and other metabolic disease is partly due to increased systemic and tissue inflammation caused by increased systemic levels of bacterial endotoxins and DNA (7). Therefore, improving gut health through polysaccharide intervention, which can manipulate gut microbiota, can influence metabolic disease (8).

Furthermore, the influence of polysaccharides on gut health and metabolic diseases is not limited to mechanisms linked to the intestinal microbiota. Some *in vitro* studies have shown that polysaccharides can directly modulate the health of humans. Astragalus polysaccharides protected bladder epithelial cells against *Escherichia coli* infection by upregulating TLR4 expression and subsequently increased the secretion of IL-6 and IL-8 (9). Polysaccharides can activate the B-cell TLR4/TLR2-p38 MAPK signaling pathway to enhance immune response (10). In addition, some polysaccharides, such as the pectin-type polysaccharides from *Smilax china* L., can be absorbed in the small intestine and are distributed in the liver and kidney (11). Oral absorption constitutes the basis of the direct effect of polysaccharides on human health. The widespread distribution and fundamental function of polysaccharides in plants as well as the extraction of different polysaccharides from various organisms and their positive effects on the health of humans and animals have been reported (12). However, it is unclear whether polysaccharides from different organisms have similar effects on animals and humans or if it is necessary to extract polysaccharides from various plants or other organisms even when their polysaccharide concentration is low. Therefore, this review focuses on how polysaccharides from terrestrial plants, fungi, and marine algae influence human health, especially gut health and metabolic disease. Additionally, it aims to identify the underlying mechanisms of bioactive polysaccharides in gut health and metabolic disease to provide insight for further research and application of polysaccharides in human and animal health.

Statistical review of the effects of polysaccharides on health

Research on the influence of polysaccharides on human and animal health published during 2013–2022 was ascertained using VOSViewer, and the terms "polysaccharides" and "health or gut health or microbiota or obesity or type 2 diabetes or non-alcoholic fatty liver disease" were searched in the Web of Science. A total of 7,497 records, including 1,590 review articles, 5,799 articles, and 459 other types of documents, were downloaded from the SSCI database of Web of Science. The yearly publication of related topics has been continually increasing (**Figure 2**), depicting the increased interest in research on the effects of polysaccharides on health. Of note, the number of publications in 2022 (**Figure 2**) represents those published in the first three quarters of the year, as the search in Web of Science was conducted on 10 September 2022. Therefore, the number of publications on "polysaccharides" and "health" will likely to exceed 1,500 in 2022. Among the countries that have published more than 130 related articles, both China and the USA have the most publications (3,239 and 1,210, respectively; **Figure 2A**). Furthermore, the number of publications from China has increased dramatically since 2017 (**Figure 2B**). The increased number of publications on polysaccharides and its effects on human and animal health may be attributable to the Chinese medicinal processing activities as water extraction is the main method that is used to prepare Chinese medicines, and this method is similar to the procedure for the extraction of polysaccharides. The major keywords that were associated with the search terms which appeared more than 100 times were summarized (**Figure 2C**), and the top 15 keywords are listed in **Table 1**. Unsurprisingly, except for "polysaccharides," "intestinal microbiota" was the most frequently identified keyword in the publications. Intestinal microbiotas play a vital role in the digestion of polysaccharides and exert functions on the health

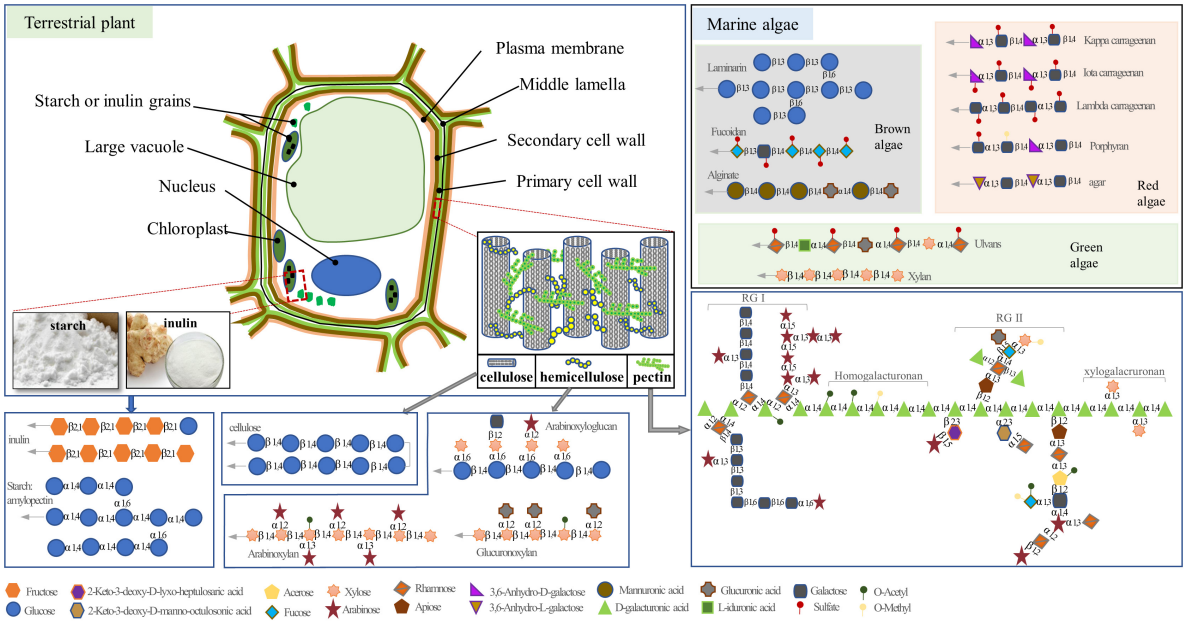

FIGURE 1
The structure of polysaccharides in plant and marine algae. The gray arrows indicate the possibility of extended polymer length.

of humans and animals. Furthermore, "antioxidant ability" appeared frequently in the downloaded publications, thereby indicating the biofunctions of polysaccharides as antioxidants. The "sulfated polysaccharides" and "fucoidan" that were found in various species of brown algae have increasingly received attention for their marked antioxidant ability. Moreover, from the occurrences of "extraction," "structural characterization," and "purification," we can infer that, with the development of sequencing and other technologies, scientists have become more interested in obtaining pure polysaccharides to clarify their structural characteristics and functions.

Interaction between polysaccharides and microbiota

The gastrointestinal tract houses several trillion microbial cells which are strongly associated with human health. Carbohydrates are the main source of energy and nutrients for intestinal microbiota and thus influence microbial composition through the modulation of specific species and their derived metabolites (13). Moreover, the microbiota possesses a larger repertoire of degradative enzymes and is adept at foraging glycans and polysaccharides that are derived from plants, animals, and other sources (14). The mutual dependence between polysaccharides and gut microbiota constitutes an important basis for the participation of polysaccharides in a diverse array of physiological processes in humans.

Polysaccharides degradation by microbiota

The huge diversity of polysaccharides has partly resulted from the various component sugar substituents and their linkage patterns, which can be branched at different positions on a single substituent by α- or β-glycosides (15). In addition, polysaccharides can be covalently coupled to other molecules, such as protein, lipids, and even RNA (16), and thereby adopt a secondary structure. At the same time, some studies have revealed the three-dimensional molecular conformation of polysaccharides, such as polysaccharides from *Laminaria japonica* (17), which inevitably adds complexity to the polysaccharides.

In general, the more complex the polysaccharides are, the greater the number of enzymes that are required in the breakdown process. However, for humans, only 17 enzymes are encoded for the digestion of food glycans, specifically for a certain type of starch (18), whereas gut bacteria can produce hundreds of enzymes with catalytic specificities that range well beyond that of starch (15, 19). The carbohydrate-active enzymes (CAZymes), which are encoded by intestinal microbiota, are required to break down the glycoconjugates and polysaccharides to release fermentable monosaccharides that can be used as an energy source by intestinal cells and/or bacteria. Glycoside hydrolases (GHs) and polysaccharide lyases (PLs) are two main types of CAZymes that cleave glycosidic bonds between carbohydrates and between a carbohydrate and a non-carbohydrate moiety (18). The animal gut harbors

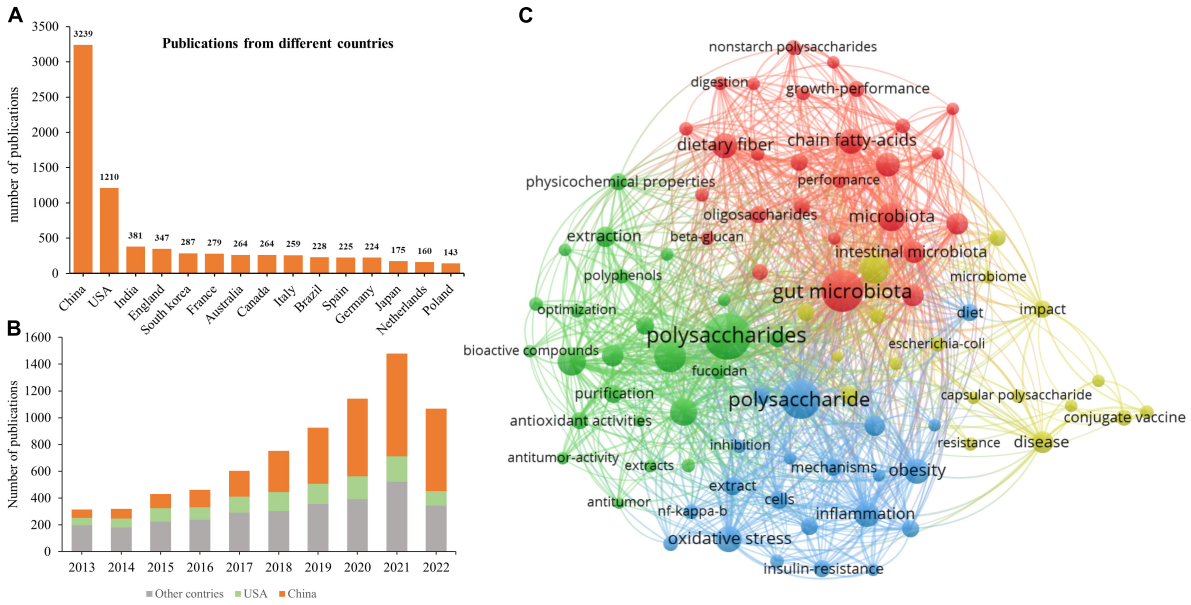

FIGURE 2
Publication analysis of polysaccharides in the last 10 years. **(A)** Total publications related to polysaccharides and human health from 2013 to 2022. **(B)** The yearly output from different countries. **(C)** Network visualization of terms associated with polysaccharides and human health.

TABLE 1 The top 15 highest occurrences of keywords.

Items	Occurrences	Total link strength		Occurrences	Total link strength
Keywords					
Polysaccharides	3748	11964	Inflammation	415	1602
Gut microbiota	2526	9027	Fermentation	378	1650
Antioxidant activity	1278	4151	Metabolism	336	1246
In vitro	673	2102	Disease	314	845
Health	580	1948	Structural characterization	313	1082
Extraction	527	1759	Expression	306	917
Chain fatty-acids	418	1800	Purification	247	899
Obesity	416	1529			

trillions of microbes, of which Firmicutes and Bacteroidetes are the most commonly represented phyla. The Bacteroidetes encode more CAZymes than other phyla (18). *Bacteroides thetaiotaomicron*, a dominant member of human distal gut microbiota, contains more than 261 GHs and PLs (20). Furthermore, the comparative genomic analysis revealed that fully sequenced intestinal Bacteroidetes contain genes that encode sulfatases and the related active enzymes, which are crucial for fermenting sulfated polysaccharides, such as mucin and glycosaminoglycans in mucus, as well as fucoidans in brown seaweeds and carrageenan in red seaweeds (21, 22). With the capacity to utilize an extensive array of dietary and host-derived polysaccharides, the Bacteroidetes are considered glycan-degrading generalists. However, Firmicutes and Actinobacteria appear more specialized with a preference for the reserve polysaccharides of plants (23).

Different phyla have different fermentation mechanisms for processing polysaccharides. The gram-negative Bacteroidetes pack their diverse array of CAZymes into discrete polysaccharides utilization loci (PUL) gene clusters, which have been identified in all intestinal Bacteroidetes and encode substantial numbers of surface proteins that are required for the utilization of polysaccharides. Therefore, the polysaccharides targeted by Bacteroidetes require extracellular hydrolysis before being transported into the cell. The well-studied starch utilization system (Sus) is the first PUL that was described for starch processing in *B. thetaiotaomicron* (24). However, in contrast to the Bacteroidetes, the gram-positive Firmicutes and Actinobacteria depend more on a diverse array of transporters, such as ABC-transport systems, to import smaller sugars for intracellular processing, which provides an important competitive advantage against the predominant Bacteroidetes

(25). The mechanisms of polysaccharide degradation that use either the PUL or Sus system by Bacteroidetes and the ABC system by Firmicutes and Actinobacteria have been described previously (26) and are not covered in depth here. Overall, the microbiota plays a critical role in the host's digestion of polysaccharides.

Influence of polysaccharides on microbiota

The exceptional diversity of dietary polysaccharides has a profound influence on the composition and structure of intestinal microbiota (27). Different microbial species have different preferences for glycans, which determine the structure and monosaccharide composition of polysaccharides and have a great impact on intestinal microbiota. Wu et al. (28) reported that okra pectic-polysaccharides with different structures selectively changed the composition of intestinal microbiota (27). *Enteromorpha* polysaccharide enriched the abundance of *Bacteroides*, which helps to break down the polysaccharides (29). At the same time, several studies that focused on the capacity of gut bacteria to catabolize marine algal polysaccharides, such as porphyran and agarose, have revealed the geographic distribution of intestinal microbiota (30–32). *B. plebeius*, which contains genes that encode porphyranases and agaroses, has been isolated from Japanese individuals whose diet typically includes seaweed. However, the gut metagenome analyses from North American individuals showed the absence of porphyranases and agaroses (31). Furthermore, a study of *Desulfobulbus* and *Methanosarcina* indicated that the spatial distribution of microbial communities significantly correlated with geographic distance (32). The abovementioned studies indicated that the sources of polysaccharides directly influence the composition of intestinal microbiota. Moreover, the inclusion of pea fiber in the diet of gnotobiotic mice that were cloned with a defined consortium of human-gut-derived bacteria significantly increased the abundance of *B. thetaiotaomicron*. In addition, the richness of *B. cacccae* in the model revealed the pronounced effects of high-molecular weight inulin on the composition of the microbiota (33). Polysaccharides can directly encourage the expansion of certain bacterial species by serving as nutrient sources for their growth. Another study that involved the incubation of different human gut-derived bacteria with different glycans *in vitro* showed that some species and strains from *Bacteroides* and *Parabacteroides* exhibited the ability to bind one or more specific glycans, thereby indicating that different glycans are responsible for the expansion of different bacterial species or strains (34). Furthermore, microbiota that has limited metabolic capacities for processing complex polysaccharides must rely on other organisms that are capable of fermenting polysaccharides through microbe–microbe interactions, such as commensalism, mutualism, and competition (26, 33, 35, 36). Therefore, many types of complex polysaccharides help to confer additional diversity to the gut microbiota partly through the interactions among microbes.

Different types of polysaccharides enable rational manipulation of the microbiota based on the species' metabolic capacity. The CAZymes (e.g., extracellular β-2,6 endo-fructanase) that are encoded by intestinal bacteria enable the metabolic processing of β-2,6-linked fructan levan. Therefore, dietary involvement of β-2,6-linked fructan levan enriches the abundance of *B. thetaiotaomicron* (37). Genome analysis coupled with efforts to culture human gut microorganisms is constantly aiding the elucidation of the mechanisms underlying mutualistic behavior, which has long been attributed to human gut microbes in the processing of dietary fiber polysaccharides (15, 23, 34, 38). The interaction between microbiota, polysaccharides, and their subsequent metabolites are highly correlated with human health and physiological process.

Polysaccharides play vital roles in the physiological status of humans

Dietary polysaccharides have diverse, crucial influences on human health. Interactions with microbiota partly explain the underlying mechanisms as polysaccharides are predominantly administered *via* the oral route, and therefore, exert functions for improving human health through their absorption. Due to the lack of methods and technologies to detect polysaccharides, some researchers consider that polysaccharides have poor intestinal absorption after oral administration. However, with improved detection technology, studies have found that after oral administration, polysaccharides can be absorbed into the circulatory system even if they have high molecular weight and complicated structures (11, 39, 40). Moreover, the oral absorption mechanisms of polysaccharides and the factors influencing them are well-reviewed by Zheng et al. (41) and are accordingly not covered in depth here. Overall, direct gut absorption and the interaction with intestinal microbiota are key aspects for understanding the mechanisms of polysaccharide function in human intestinal and metabolic health.

Polysaccharides influence intestinal health

A functional intestine and an intact intestinal barrier, which permit nutrient transport from the lumen into the blood and simultaneously restrict the passage of potentially harmful microorganisms and toxins, constitute an integral regulator of human health (7, 42). Observational findings that have been accumulated during the last 10 years suggest

that polysaccharides have profound biological benefits for bowel health, including anti-inflammation, gut epithelial barrier protection, and immune modulation through both microbiota-dependent and -independent mechanisms (3, 12). Most polysaccharides pass through the small intestine intact and can successfully reach the large bowel, where they can be either fermented by the microbiota or excreted in the stool. Due to their capacity for water retention, polysaccharides in the large bowel could attract water and add bulk to the digesta which increases intestinal peristalsis and softens the stool, thus diluting toxin concentrations, increasing the frequency of defecation, and preventing constipation and its associated problems, such as hemorrhoids (3, 43, 44). Moreover, dietary ingestion of high concentrations of non-starch polysaccharides (NSP) is associated with increased stool weight and a decreased risk of bowel cancer (45). In addition, polysaccharides enhance bowel health by promoting the immune system and reducing inflammation. Polysaccharides from astragalus that mainly contained rhamnose, glucose, galactose, and arabinose ameliorated dextran sulfate sodium (DSS)-induced colitis and increased the colon length by inhibiting NF-κB activation, and thus downregulating TNF-α, IL-1β, and IL-6 expression and subsequently reducing proinflammatory responses (46). Similarly, *Scutellaria baicalensis* Georgi polysaccharides, which are mainly composed of mannose, ribose, glucuronic acid, glucose, xylose, and arabinose, suppressed DSS-induced colitis through inhibition of NF-κB and NLRP3 inflammasome activation, and thereby decreasing pro-inflammatory cytokines secretion in mice and macrophages (47). There is increasing evidence that Peyer's patches hold the key to how polysaccharides enhance intestinal immune status. Polysaccharides from molokhia (*Corchorus olitorius* L.) leaves could increase bone marrow cell proliferation as well as immunoglobulin A and cytokine production *via* Peyer's patches (48), which is consistent with the hypothesis of Han (49) who states that polysaccharides could enter Peyer's patches to trigger immune responses even without entering the blood circulation. Moreover, polysaccharides from *Coptis chinensis* Franch. (50), *Atractylodes lancea* (51), and *Lavandula angustifolia* Mill. (52) could be taken up by Peyer's patches and stimulate the immune cells inside it to regulate cytokine secretion. Therefore, polysaccharides can exert immune-enhancing functions without absorption into the bloodstream, which benefits gut health by improving the immune status of the gut. Furthermore, polysaccharides, such as α-D-glucan, could enhance the intestinal barrier function by increasing the expression of tight junction proteins (53, 54).

Additionally, the interaction of polysaccharides and intestinal microbiota plays a crucial role in gut health. A deficiency of dietary polysaccharides leads to gut dysbiosis. As the microbiota mostly relies on polysaccharides as a nutrient source, the absence of these nutrients in the diet forces the microbiota to transition toward the use of indigenous host glycans, which causes the expansion of pathogenic organisms and decreased abundance of probiotics and the linked metabolites. Evidence has revealed that the microbiota can erode the colonic mucus layer in the absence of dietary polysaccharides, thus accelerating enteric pathogen invasion and intestinal disease progression when challenged with the pathogen *Citrobacter rodentium* (15, 55). Low concentrations of dietary polysaccharides induced inflammation and increased intestinal permeability that led to increased pathogen invasion into other tissues, which is highly associated with the onset of obesity and other metabolic diseases (56) (**Figure 3**). Comparatively, the dietary inclusion of polysaccharides is important for supporting the function and stability of gut microbiota and, eventually, for maintaining gut health. Polysaccharides derived from *Lentinula edodes* encouraged the expansion of *B. acidifaciens* (57). In addition, polysaccharides from *Flammulina velutipes* improved colitis by shaping the structure of the colonic microbiota and inflammatory responses. Bacteria-derived polysaccharides, including glucorhamnan, which are synthesized and secreted by *Ruminococcus gnavus*, influence intestinal health *via* the regulation of intestinal inflammatory states (58). Furthermore, the microbiota-derived metabolites, such as short-chain fatty acids (SCFAs) (59), enhanced the intestinal fermentation of diverse polysaccharides and have profound effects on bowel health. SCFAs can be used directly as energy sources by colonic epithelial cells, support their proliferation, and enhance the epithelial barrier function (60). Polysaccharides from *Cistanche* (61), *Vigna radiata* L. skin (62), enriched probiotic bacteria and SCFA in the intestine of mice. In addition, both *in vivo* and *in vitro* studies indicated that polysaccharides from soybean or marine algae could enhance the abundance of probiotic bacteria whereas inhibiting pathogens in the intestine (19, 63, 64). Thus, polysaccharides are crucial for intestinal health, which further benefits the health of the body.

The relationship between polysaccharides and obesity

The prevalence of obesity has been increasing dramatically worldwide, and the progression and maintenance of obesity include genetic and environmental factors, diet (e.g., high availability of high-energy foods with less dietary fiber), and lifestyle (e.g., sedentary ways of life) that leads to excess peripheral and visceral lipid accumulation (65). Moreover, dysbiosis of intestinal microbiota acts both as a cause and a consequence of obesity (66–68). Notably, obesity is associated with systemic low-grade inflammation and various health issues, such as type 2 diabetes (due to insulin resistance), fatty liver disease, short life expectancy, and so on (69). Therefore, identifying efficient strategies to prevent or ameliorate obesity is important for the health of people who are overweight

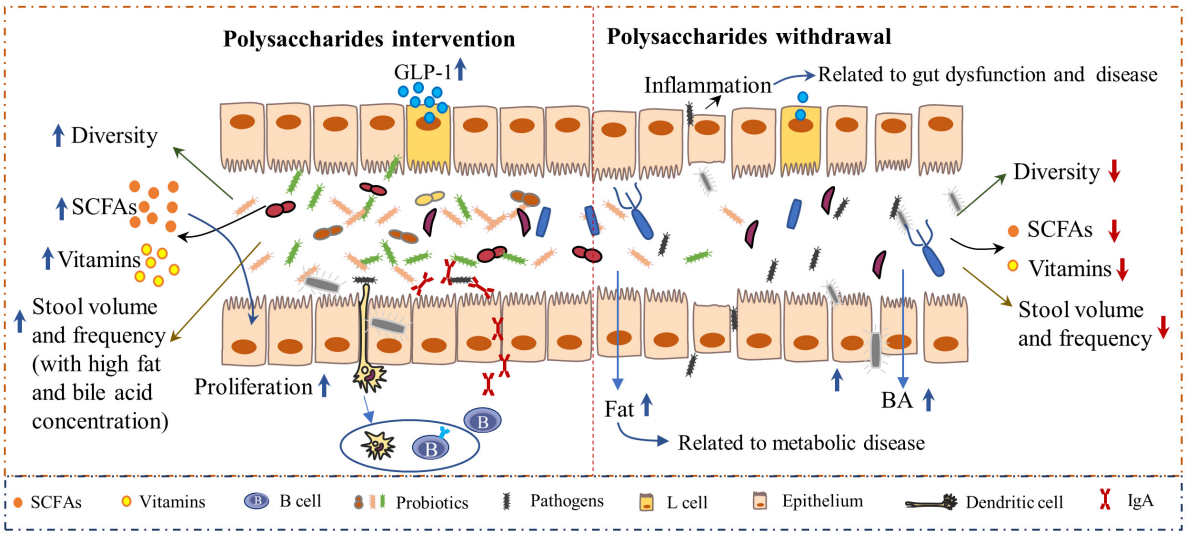

FIGURE 3
The inclusion of polysaccharides has a profound impact on gut health. Polysaccharide-based interventions increased microbiota-derived metabolites, such as short-chain fatty acids (SCFA) and vitamins **(Left)**. SCFAs can bind to receptors on L cells and subsequently induce the secretion of glucagon-like peptide 1 (GLP-1), which can affect energy expenditure (132). Polysaccharides are highly associated with increased stool volume, frequency, and fat and bile acid concentrations (45, 46, 133), which reinforce gut health. Moreover, the intestinal immune system is enhanced by polysaccharides, as indicated by the increased secretion of immunoglobulin A (sIgA) levels. However, when the diet contains very low concentrations of polysaccharides, the balance between the gut microbiota and immunity will be disrupted **(Right)**, resulting in decreased diversity of microbiota with an increased abundance of pathogens, which elicit gut inflammation and subsequent bowel disease.

or obese. Recently, interest in the role of polysaccharides in preventing obesity has increased, and the anti-obesity properties and mechanisms of polysaccharides have been reported by several studies (70–72) (**Figure 4**).

Most polysaccharides cannot be digested to directly provide energy to animals. Therefore, the dietary inclusion of polysaccharides could reduce calorie intake. Moreover, due to their complex special structure, polysaccharides are characterized by great fat-binding capacities, which leads to the increased excretion of dietary or endogenous fatty acids (73). Polysaccharides can bind bile acids in the intestine to enhance its excretion, thus enabling new bile acid synthesis in the liver and consuming more cholesterol (74). Consistent results were obtained in research on xyloglucan and inulin supplementation, which increased the fecal total bile acid concentration (75). Decreasing the energy intake as well as increasing fatty acids and cholesterol excretion is of great importance for decreasing lipid accumulation, and thus could benefit overweight individuals. Besides this, enhancing energy expenditure is another mode of action that actualizes the anti-obesity property of polysaccharides. *Lyophyllum decastes* polysaccharides enhance energy expenditure in diet-induced obese mice, which might be due to the upregulation of the secondary bile acids-activated TGR5 pathway (74). Furthermore, the enhanced brown tissue activity by polysaccharides (74, 76) could explain the energy expenditure property of polysaccharides to some extent.

Inhibition of lipogenesis and promotion of lipolysis/fatty acid oxidation are very important to restrict fat accumulation. Peroxisome proliferator-activated receptor gamma (PPARγ) is a transcriptional factor that directs the differentiation of adipocytes, whereas PPARα is a key transcriptional factor for fatty acid oxidation (77). In addition to dietary sources, endogenous fatty acid production from *de novo* lipogenesis in mammalian tissues, including liver, white adipose tissue, and brown adipose tissue, has been identified in both healthy and obese individuals. Polysaccharides inhibit hepatic lipogenesis and lipogenesis in white adipose tissues, (78, 79), mainly through the inhibition of core enzymes, such as acetyl-CoA carboxylase (ACC) and fatty acid synthase (FAS), in the lipogenic process (80). Moreover, PPARγ expression could be inhibited by dietary polysaccharides in the liver and adipose tissues of diet-induced obese mice (81). *In vitro* experiments using 3T3-L1 cells demonstrated the direct inhibition of adipocyte differentiation by quinoa polysaccharide through PPARγ inhibition (79, 82, 83), and activation of the AMPK/PPARα pathway by polysaccharides was observed in obese mice, which implies increased fatty acids oxidation and energy expenditure. Therefore, polysaccharides could prevent obesity and/or ameliorate obesity by inhibiting lipogenesis while enhancing lipolysis. Although polysaccharides with anti-obesity properties have different sources, structure, and composition, they have similar modes of actions in ameliorating diet-induced obesity.

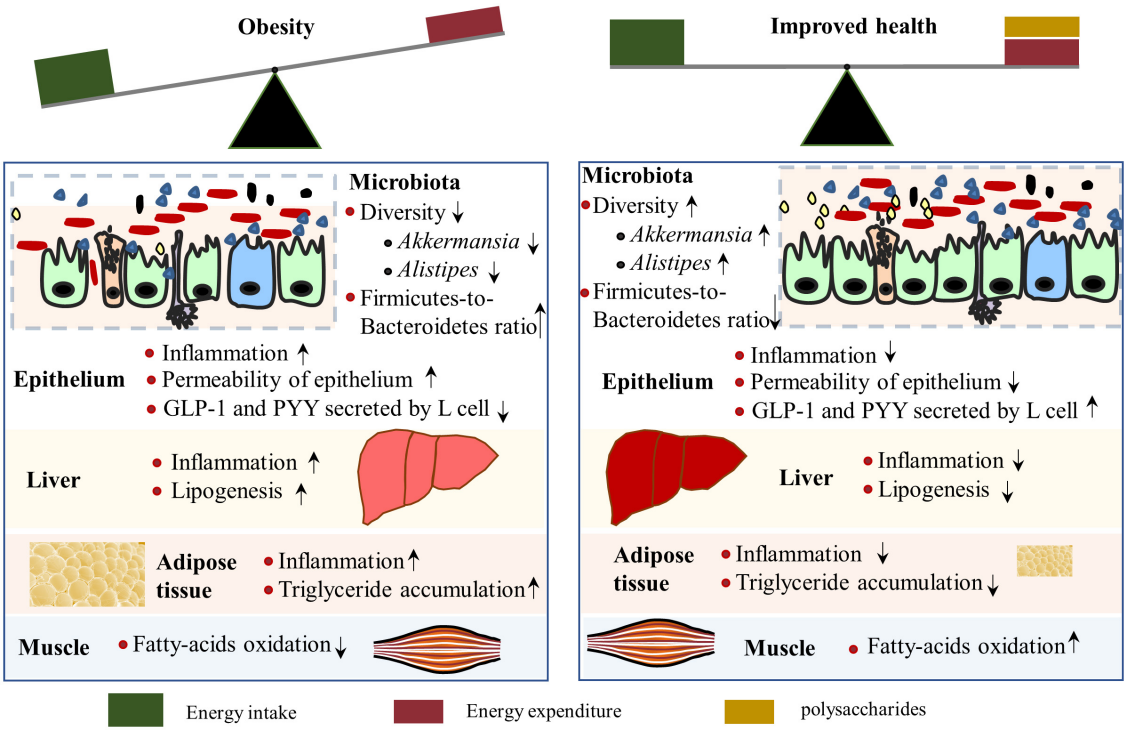

FIGURE 4
Mechanisms by which polysaccharides alleviate obesity. A polysaccharide-rich diet contributes to the maintenance of a healthy gut and reduces inflammation of the liver and adipose tissue **(Right)**. Intestinal microbiota composition is associated with obesity, of which low diversity, reduced abundance of *Akkermansia* and *Alistipes*, and enhanced Firmicutes-to-Bacteroidetes ratio were observed in obese individuals. However, polysaccharide supplementation can reverse the microbiota changes in obese situations, along with increased glucagon-like peptide 1 (GLP-1) levels, which is positively related to energy expenditure.

The fundamental influence of polysaccharides on intestinal microbiota explains its primary mechanism in reducing obesity, which has been studied in many research articles (70, 71, 84, 85) and reviews (86, 87). High-weight molecular polysaccharides isolated from *Ganoderma lucidum* reduced body weight and fat accumulation in obese mice by altering the intestinal microbiota composition, as indicated by the decreased Firmicutes-to-Bacteroidetes ratios and improved gut barrier function. Research on HG-type pectin, derived from *Ficus pumila* L. fruits, increased the abundance of *Akkermansia* and *Alistipes* in obese mice. The subsequent metabolites, myristoleic acid, and pentadecanoic acid, are negatively associated with serum lipid concentration and contribute to decreased fat concentration (88). A fucoidan from Sargassum fusiform has similar effects, which restored *Alistipes* abundance (89). The microbiota species enriched by polysaccharides in obese animals correlated with a reduction of obesity, thus providing insights to guide the development of probiotics and functional prebiotics to prevent obesity in clinical practice.

Interestingly, xyloglucan compounded with arabinoxylan or inulin supplementation activated intestinal or hepatic G protein-coupled 5 (TGR5) of mice that were fed a high-fat diet (75). TGR5 signals in enteroendocrine L-cells induce glucagon-like peptide 1 (GLP-1) and peptide YY (PYY) excretion, thereby attenuating food consumption rate, improving liver and pancreatic function, and promoting glucose metabolism, as well as activating TGR5 in adipose and muscle tissues to increase energy expenditure (90). TGR5 activation by polysaccharides prevents diet-induced obesity through attenuation of energy intake and increased energy expenditure. Therefore, dietary inclusion of more of the abovementioned polysaccharides is considered a good strategy to alleviate obesity.

Polysaccharides and control of type 2 diabetes

Diabetes mellitus comprises a group of metabolic diseases characterized by chronic hyperglycemia, along with many complications, such as diabetic nephropathy and cardiovascular disease. Usually, diabetes can be divided into two main broad categories: type 1 diabetes and type 2 diabetes mellitus (T2DM), which account for the majority (~90%) of total diabetes prevalence (91, 92). Known as non-insulin-dependent diabetes mellitus, T2DM is largely induced by insulin resistance and

dysfunction of insulin-producing β cells, which decreases the tissue sensitivity to insulin and has insufficient biological effects, thereby leading to hyperglycemia (91). However, unlike type 1 diabetes, which is not preventable with the current knowledge, effective approaches are available to prevent T2DM and its complications (93). Increasing evidence has shown that polysaccharides exhibit antidiabetic effects. Considering the growing reports on polysaccharides as therapy for T2DM and their popularity as dietary supplements, this subsection is designed to clarify the various mechanisms of such therapeutic applications.

The application of polysaccharides in the diet- and/or drug-induced T2DM animal models ameliorated glucose tolerance (94), inhibited insulin resistance (95), protected damaged pancreatic islets (96), improved β cell function (95), enhanced lipid metabolism thus increasing insulin sensitivity in the liver (97), and reduced oxidative stress and inflammatory response (98) to relieve T2DM. Polysaccharides from *Anoectochilus roxburghii* could inhibit the key gluconeogenesis enzymes, thereby increasing glucose absorption (99), which explains the function of polysaccharides in decreasing fasting blood glucose levels. *Echinops* spp. polysaccharide B could increase muscle and liver glycogen content (100), which lowers the blood glucose level in T2DM. Polysaccharides from *Sphacelotheca sorghi* (Link) Clint (101) and *Auricularia auricula-judae* (102) enhanced the hepatic health of T2DM by activating the PI3K/Akt signaling pathway. *Echinops* spp. polysaccharide B increased the number of insulin receptors in the liver and muscles, thus decreasing insulin resistance in T2MD (100). Besides their use as a dietary source, polysaccharides can be used to protect insulin that is administered orally. The ability to improve the permeability *via* transcellular and/or paracellular pathways and even selectivity for targeted delivery of insulin through nano- and microencapsulation of polysaccharides is considered an important technological strategy to protect insulin against the harsh conditions of the gastrointestinal tract (103).

In addition to the abovementioned functions, polysaccharides can affect T2DM by influencing the structure of intestinal microbiota and their derived metabolites, the composition of which plays pivotal roles in the pathogenetic process of T2DM (104). Patients with T2DM have increased relative abundances of the phyla Firmicutes and Actinobacteria and decreased relative abundances of Bacteroidetes. Consistently, Lactobacillus and Eubacteria were significantly enriched (104), whereas abundances of Bifidobacterium were decreased in T2DM patients (105). Inulin supplementation increased the abundance of *Bifidobacterium* and increased the integrity of the gut barrier, which was negatively correlated with T2DM (75, 105). *Apocynum venetum* polysaccharides reversed the gut microbiota dysbiosis in diabetic mice by increasing probiotic abundances, such as *Odoribacter*, *Parasutterella*, *Lactobacillus*, and *Akkermansia*, whereas decreasing *Enterococcus* and *Aerococcus* levels, which are correlated with improved liver glycogen contents and reduced insulin resistance (95, 106, 107). Dietary polysaccharides enriched the SCFA-producing strains in the intestine, including *Bifidobacterium* and *Romboutsia*, thus enhancing SCFAs concentrations, inhibiting the growth of other detrimental bacteria, and benefiting T2DM patients (104, 108). The bacteria-derived SCFAs have been shown to decrease proinflammatory cytokines and inhibit lipolysis in adipose, which is responsible for glucose disposal of T2DM patients by regulating free fatty acids in blood (109). Butyrate was reported to improve hepatic fatty acid oxidation and activate the AMPK-acetyl-CoA carboxylase pathway, thereby regulating glucose metabolism and inhibiting insulin resistance in the liver (95, 110). Meanwhile, acetate intervention in obese mice improved the expression of genes involved in oxidative and glucose metabolism and glucose transporter in skeletal muscle, enhancing glucose disposal for which skeletal muscle accounts for 85% of postabsorptive blood glucose (111). Collectively, considering the high price as well as the indistinct safety property of the drug used in T2DM patients currently, polysaccharides with anti-diabetes features can be used as promising ingredients for T2DM patients.

The role of polysaccharides in non-alcoholic fatty liver disease

Non-alcoholic fatty liver disease (NAFLD) is a chronic liver disease characterized by excess triglyceride accumulation in hepatocytes due to both increased inflow of free fatty acids and *de novo* hepatic lipogenesis, which affects a high proportion of the world's population (112). Mechanistic insights into fat accumulation, subsequent hepatocyte injury, and the roles of the immune system and gut microbiome are unfolding (113). The inflow of lipids accumulated in livers mainly originates from three processes namely, *de novo* lipogenesis (DNL), dietary sources, and circulating esterified-fatty acids. Moreover, approximately 40% of the lipids derive from DNL and dietary sugars and fats, whereas the remaining 60% arise from lipolysis of dysfunctional adipose tissues (114, 115). Furthermore, the diacylglycerol intermediates, accumulated during the above-described process, impair hepatic insulin signaling by activating protein kinase Cε (PKCε) (116). Hepatocyte insulin resistance promotes hyperglycemia and enhances more compensatory insulin production, which prompts DNL by activation of carbohydrate-response element binding protein (ChREBP) and sterol regulatory element binding protein-1c (SREBP-1c) (113). ChREBP and SREBP-1c synergistically induce FAS and ACC expression, which catalyzes fatty acid synthesis, and are complexly regulated by various nuclear receptors, such as PPARα and farnesoid X receptor (FXR) (117–119) (**Figure 5**). Reduced hepatic fatty acid oxidation was reported

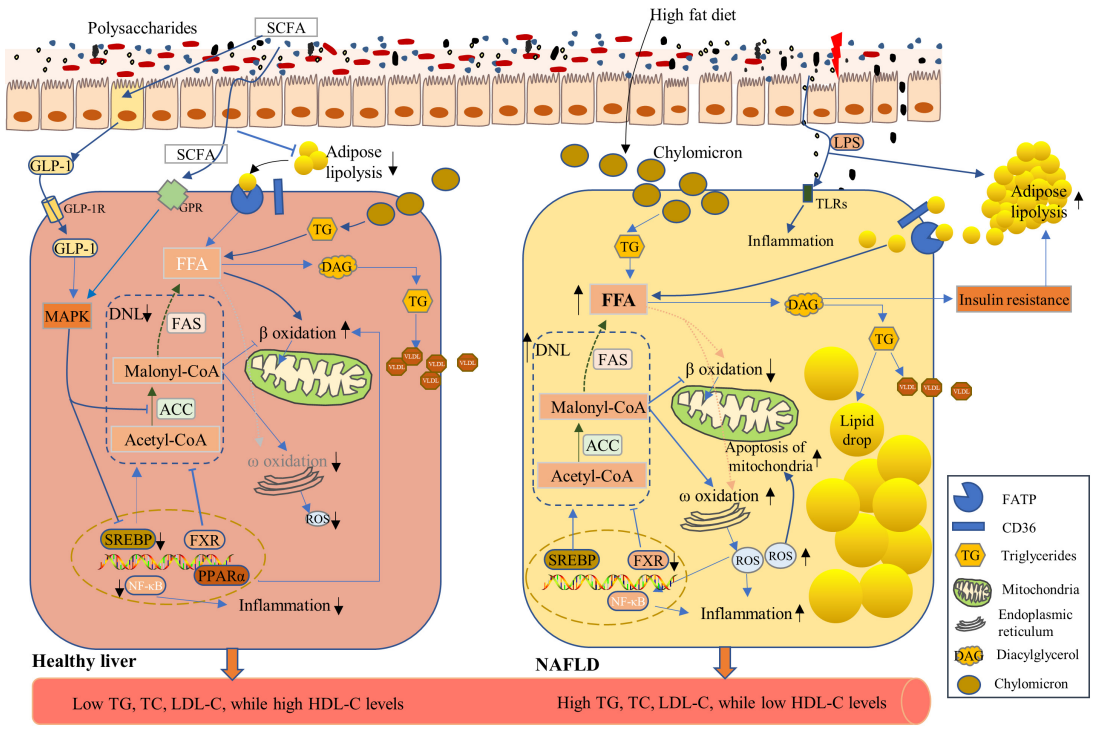

FIGURE 5
Effects of polysaccharides on the non-alcoholic fatty liver disease (NAFLD). NAFLD is characterized by increased lipid accumulation within hepatocytes, mainly through the uptake of chylomicron processed from dietary fat, circulating free fatty acids (FFA) from lipolysis of adipose tissues, and elevated *de novo* lipogenesis (DNL) (119, 123) **(Right Panel)**, leading to high levels of triglycerides (TG), total cholesterol (TC), and low-density lipoprotein-cholesterol (LDL-C), as well as low levels of high-density lipoprotein-cholesterol (HDL-C) in the serum. High-fat diet induces high levels of chylomicron storage in the hepatocytes, which contributed to high FFA levels in hepatocytes. An intermediate metabolite in triglyceride synthesis, diacylglycerol (DAG), induces insulin resistance, which further enhances the lipolysis of adipose tissues and the subsequent high FFA concentrations. FA synthesis is catalyzed by acetyl-CoA carboxylase (ACC) and fatty acid synthase (FAS), and their expression can be induced by sterol-response-binding-protein-1c (SREBP-1c) and be inhibited by farnesoid X receptor (FXR). Under NAFLD conditions, SREBP-1c expression was enhanced with enhanced DNL **(Right Panel)**. Polysaccharide application enhanced the expression of FXR and reduced DNL. Lipid accumulation within hepatocyte was limited, and FA oxidation was enhanced via improved β-oxidation and GLP-1 function to ensure healthy hepatic lipid metabolism **(Left Panel)**.

among the pathophysiological changes of NAFLD (120). Accumulated fatty acids inside hepatocytes impose a strain on mitochondria, leading to the dysfunction of mitochondria and the production of ROS. The ROS and subsequent activation of Jun N-terminal kinase (JNK) in turn result in mitochondrial damage, which adds to the stress on the endoplasmic reticulum and further inhibits β oxidation of fatty acids. Moreover, hepatic inflammation, which is triggered by fatty acids, bacterial endotoxins, and ROS, exacerbates hepatocyte damage (113, 119, 121).

To date, there are no effective medical interventions to completely reverse NAFLD other than diet/lifestyle modification. However, polysaccharides that target the hepatocytic DNL, inflammation of the liver, and intestinal microbiota currently have been under investigation to develop promising pharmacological therapies for the treatment of NAFLD. *Ginkgo biloba* leaf polysaccharides (GBLP) are mainly composed of galactose (32.21%), mannose (20.82%), glucose (9.39%), arabinose (6.71%), rhamnose (14.76%), and galacturonic acid (16.11%), which markedly reduced the serum levels of TC, triglycerides, LDL-C, and free fatty acids and significantly increased HDL-C concentrations in NAFLD rats induced by a high-fat diet. Levels of hepatic triglycerides and lipids decreased after GBLP administration in NAFLD rats (122). As increased DNL is a distinct characteristic of NAFLD (123), it is important to impede the process by using functional ingredients. Guar gum supplementation in chicken diet markedly increased SCFA concentrations, leading to increased GLP-1 levels, activation of mitogen-activated protein kinase (MAPK) pathways in hepatocytes, and subsequent suppression of lipid accumulation in hepatocytes by inhibiting SREBP1 and ACC activities (124). Chicory polysaccharides inhibited DNL through the inhibition of genes related to DNL in hepatocytes, whereas the β-oxidation and anti-inflammatory factors were enhanced in NAFLD rats (125). Based on the serum metabolomic analysis, chicory polysaccharides inhibited fatty acid biosynthesis and enhanced β oxidation of very long-chain fatty acids, which implies the

probable mechanisms for alleviating NAFLD (126). *Ganoderma amboinense* polysaccharides enhance hepatic fat transport and mitochondrial function in NAFLD mice. MDG-1, an insulin-like β-fructan polysaccharide extracted from Ophiopogon japonicus, decreased the activity of PPARγ and upregulated the expression and phosphorylation of AMPK, SREBP-1c, and ACC-1, thus improving lipid metabolism in high-fat diet mice and reducing the pathogenesis of NAFLD (127). Targeting intestinal microbiota is another strategy to prevent NAFLD. MDG significantly increased the diversity of microbiota, of which *Akkermansia muciniphila* was highly abundant following MDG intervention in NAFLD mice (128). However, most trials evaluating the function of polysaccharides were conducted in animal or cell models and further research is needed to identify whether polysaccharides have therapeutic effects on NAFLD patients, and more clinical trials should be conducted.

Limitations and perspectives

Due to the natural source and low toxicity of polysaccharides, considerable efforts have been focused on discovering polysaccharides that can be used as novel therapeutics in various diseases (129). Polysaccharides can be used as carriers to protect some labile drugs and facilitate their survival in hostile gastrointestinal tract environment (103). Interestingly, most polysaccharides exhibit positive effects on human health although they have different compositions and structures. Moreover, publications on polysaccharides are steadily increasing for various reasons. First, as polysaccharides exist in almost all living systems, it is reasonable to infer that thousands of different polysaccharides can be extracted. Furthermore, the extracted polysaccharides usually are not composed of one pure substrate but comprise a mixture of a series or different kinds of polysaccharides with diverse chain lengths and dissimilar branches or linkages. Therefore, the extraction conditions will highly influence the composition and the structure of the polysaccharides, which might induce different consequences when applied under different conditions. However, as the functional ingredients can be directly obtained from the diet, the extraction of polysaccharides from edible plant or organisms that needs considerable energy expenditure is not recommended. Furthermore, Han et al. (130) reported that the functional ingredients of N-methylserotonin from orange fibers by-products were released by intestinal microbiota, which might be disposed of in the extraction process. Therefore, additional efforts are needed to identify functional polysaccharides from non-edible dietary by-products.

Additionally, the polysaccharide-interaction-based approach to promote health is unlikely to elicit consistent effects across individuals (131). The large molecular weight and complex structure of polysaccharides limit their usage in tissues other than the intestine, as the majority of polysaccharides cannot be digested in the small intestine or absorbed by the intestinal epithelium. Most of the functions of polysaccharides in other tissues are mediated through metabolites obtained *via* fermentation by microbiota. However, the gut microbes varied among different individuals, which explains why the interindividual variation in the gut microbiome is usually linked to differential effects of polysaccharides on the host metabolic phenotypes. Experiments for detecting the function of polysaccharides in different health conditions are warranted, and more clinical trials should be conducted to enable the application of polysaccharides as therapeutic drugs. However, the development of more efficient and economic approaches for the preparation and modification of polysaccharides and elucidation of the structure-activity relationship remain as significant challenges.

Author contributions

LG, JW, and YG wrote the manuscript. JW had primary responsibility for final content. All authors read and approved the final manuscript.

Funding

This work was supported by the National Key Research and Development Program of China (grant number 2021YFD1300300), the National Natural Science Foundation of China (grant number 32202696), the Scientific Research Startup Project of Henan University of Technology (grant number 31401405), and the Innovative Funds Plan of Henan University of Technology (grant number 2020ZKCJ25).

Conflict of interest

The authors declare that the research was conducted in the absence of any commercial or financial relationships that could be construed as a potential conflict of interest.

Publisher's note

References

1. Voragen AGJ, Coenen GJ, Verhoef RP, Schols HA. Pectin, a versatile polysaccharide present in plant cell walls. *Struct Chem.* (2009) 20:263–75.

2. Jarvis MC. Plant cell walls: supramolecular assemblies. *Food Hydrocoll.* (2011) 25:257–62.

3. Ho Do M, Seo YS, Park HY. Polysaccharides: bowel health and gut microbiota. *Crit Rev Food Sci Nutr.* (2021) 61:1212–24.

4. Krautkramer KA, Fan J, Backhed F. Gut microbial metabolites as multi-kingdom intermediates. *Nat Rev Microbiol.* (2020) 19:77–94. doi: 10.1038/s41579-020-0438-4

5. Zhang P, Jia J, Jiang P, Zheng W, Li X, Song S, et al. Polysaccharides from edible brown seaweed *Undaria pinnatifida* are effective against high-fat diet-induced obesity in mice through the modulation of intestinal microecology. *Food Funct.* (2022) 13:2581–93. doi: 10.1039/d1fo04012j

6. Agus A, Clément K, Sokol H. Gut microbiota-derived metabolites as central regulators in metabolic disorders. *Gut.* (2020) 70:1174–82.

7. Massier L, Bluher M, Kovacs P, Chakaroun RM. Impaired intestinal barrier and tissue bacteria: pathomechanisms for metabolic diseases. *Front Endocrinol.* (2021) 12:616506. doi: 10.3389/fendo.2021.616506

8. Chakaroun RM, Massier L, Kovacs P. Gut microbiome, intestinal permeability, and tissue bacteria in metabolic disease: perpetrators or bystanders? *Nutrients.* (2020) 12:1082.

9. Yin X, Chen L, Liu Y, Yang J, Ma C, Yao Z, et al. Enhancement of the innate immune response of bladder epithelial cells by *Astragalus* polysaccharides through upregulation of TLR4 expression. *Biochem Biophys Res Commun.* (2010) 397:232–8. doi: 10.1016/j.bbrc.2010.05.090

10. Lin KI, Kao YY, Kuo HK, Yang WB, Chou A, Lin HH, et al. Reishi polysaccharides induce immunoglobulin production through the TLR4/TLR2-mediated induction of transcription factor blimp-1. *J Biol Chem.* (2006) 281:24111–23. doi: 10.1074/jbc.M601106200

11. Zhang Y, Liu J, Dou P, Wu Z, Zheng Z, Pan X, et al. Oral absorption characteristics and mechanisms of a pectin-type polysaccharide from *Smilax* china L. across the intestinal epithelium. *Carbohydr Polym.* (2021) 270:118383. doi: 10.1016/j.carbpol.2021.118383

12. Feng, Y, Wassie T, Gan R, Wu X. Structural characteristics and immunomodulatory effects of sulfated polysaccharides derived from marine algae. *Crit Rev Food Sci Nutr.* (2022):1–17. doi: 10.1080/10408398.2022.2043823

13. Kolodziejczyk AA, Zheng D, Elinav E. Diet-microbiota interactions and personalized nutrition. *Nat Rev Microbiol.* (2019) 17:742–53.

14. Flint HJ, Scott KP, Duncan SH, Louis P, Forano E. Microbial degradation of complex carbohydrates in the gut. *Gut Microbes.* (2012) 3:289–306.

15. Porter NT, Martens EC. The critical roles of polysaccharides in gut microbial ecology and physiology. *Annu Rev Microbiol.* (2017) 71:349–69.

16. Flynn RA, Pedram K, Malaker SA, Batista PJ, Smith BAH, Johnson AG, et al. Small RNAs are modified with N-glycans and displayed on the surface of living cells. *Cell.* (2021) 184:3109.e–24.e. doi: 10.1016/j.cell.2021.04.023

17. Cui J, Wang Y, Kim E, Zhang C, Zhang G, Lee Y. Structural characteristics and immunomodulatory effects of a long-chain polysaccharide from *Laminaria japonica*. *Front Nutr.* (2022) 9:762595. doi: 10.3389/fnut.2022.762595

18. Kaoutari AE, Armougom F, Gordon JI, Raoult D, Henrissat B. The abundance and variety of carbohydrate-active enzymes in the human gut microbiota. *Nat Rev Microbiol.* (2013) 11:497–504. doi: 10.1038/nrmicro3050

19. Wu DT, An LY, Liu W, Hu YC, Wang SP, Zou L. In vitro fecal fermentation properties of polysaccharides from Tremella fuciformis and related modulation effects on gut microbiota. *Food Res Int.* (2022) 156:111185. doi: 10.1016/j.foodres.2022.111185

20. Xu J, Bjursell MK, Himrod J, Deng S, Carmichael LK, Chiang HC, et al. A genomic view of the human-*Bacteroides* thetaiotaomicron symbiosis. *Science.* (2003) 299:2074–6. doi: 10.1126/science.1080029

21. Shannon E, Conlon M, Hayes M. Seaweed components as potential modulators of the gut microbiota. *Mar Drugs.* (2021) 19:358.

22. Benjdia A, Martens EC, Gordon JI, Berteau O. Sulfatases and a radical S-adenosyl-L-methionine (AdoMet) enzyme are key for mucosal foraging and fitness of the prominent human gut symbiont, *Bacteroides thetaiotaomicron*. *J Biol Chem.* (2011) 286:25973–82. doi: 10.1074/jbc.M111.228841

23. Rogowski A, Briggs JA, Mortimer JC, Tryfona T, Terrapon N, Lowe EC, et al. Glycan complexity dictates microbial resource allocation in the large intestine. *Nat Commun.* (2015) 6:7481.

24. Martens EC, Koropatkin NM, Smith TJ, Gordon JI. Complex glycan catabolism by the human gut microbiota: the bacteroidetes sus-like paradigm. *J Biol Chem.* (2009) 284:24673–7.

25. Ejby M, Fredslund F, Andersen JM, Vujicic Zagar A, Henriksen JR, Andersen TL, et al. An ATP binding cassette transporter mediates the uptake of alpha-(1,6)-linked dietary oligosaccharides in bifidobacterium and correlates with competitive growth on these substrates. *J Biol Chem.* (2016) 291:20220–31. doi: 10.1074/jbc.M116.746529

26. Cockburn DW, Koropatkin NM. Polysaccharide degradation by the intestinal microbiota and its influence on human health and disease. *J Mol Biol.* (2016) 428:3230–52.

27. Koropatkin NM, Cameron EA, Martens EC. How glycan metabolism shapes the human gut microbiota. *Nat Rev Microbiol.* (2012) 10:323–35.

28. Wu DT, He Y, Yuan Q, Wang SP, Gan RY, Hu YC, et al. Effects of molecular weight and degree of branching on microbial fermentation characteristics of okra pectic-polysaccharide and its selective impact on gut microbial composition. *Food Hydrocoll.* (2022) 132:107897.

29. Wassie T, Lu Z, Duan X, Xie C, Gebeyew K, Yumei Z, et al. Dietary *Enteromorpha* polysaccharide enhances intestinal immune response, integrity, and caecal microbial activity of broiler chickens. *Front Nutr.* (2021) 8:783819. doi: 10.3389/fnut.2021.783819

30. Thomas F, Barbeyron T, Tonon T, Génicot S, Czjzek M, Michel G. Characterization of the first alginolytic operons in a marine bacterium: from their emergence in marine Flavobacteriia to their independent transfers to marine *Proteobacteria* and human gut *Bacteroides*. *Environ Microbiol.* (2012) 14:2379–94. doi: 10.1111/j.1462-2920.2012.02751.x

31. Hehemann JH, Correc G, Barbeyron T, Helbert W, Czjzek M, Michel G. Transfer of carbohydrate-active enzymes from marine bacteria to Japanese gut microbiota. *Nature.* (2010) 464:908–12. doi: 10.1038/nature08937

32. Carbonero F, Oakley BB, Purdy KJ. Metabolic flexibility as a major predictor of spatial distribution in microbial communities. *PLoS One.* (2014) 9:e85105. doi: 10.1371/journal.pone.0085105

33. Patnode ML, Beller ZW, Han ND, Cheng J, Peters SL, Terrapon N, et al. Interspecies competition impacts targeted manipulation of human gut bacteria by fiber-derived glycans. *Cell.* (2019) 179:59–73e13. doi: 10.1016/j.cell.2019.08.011

34. Patnode ML, Guruge JL, Castillo JJ, Couture GA, Lombard V, Terrapon N, et al. Strain-level functional variation in the human gut microbiota based on bacterial binding to artificial food particles. *Cell Host Microbe.* (2021) 29:664–673e5. doi: 10.1016/j.chom.2021.01.007

35. Heinken A, Thiele I. Anoxic conditions promote species-specific mutualism between gut microbes in silico. *Appl Environ Microbiol.* (2015) 81:4049–61. doi: 10.1128/AEM.00101-15

36. Blasche S, Kim Y, Mars RAT, Machado D, Maansson M, Kafkia E, et al. Metabolic cooperation and spatiotemporal niche partitioning in a kefir microbial community. *Nat Microbiol.* (2021) 6:196–208. doi: 10.1038/s41564-020-00816-5

37. Sonnenburg ED, Zheng H, Joglekar P, Higginbottom SK, Firbank SJ, Bolam DN, et al. Specificity of polysaccharide use in intestinal *bacteroides* species determines diet-induced microbiota alterations. *Cell.* (2010) 141:1241–52. doi: 10.1016/j.cell.2010.05.005

38. Chen RY, Mostafa I, Hibberd MC, Das S, Mahfuz M, Naila NN, et al. A microbiota-directed food intervention for undernourished children. *N Engl J Med.* (2021) 384:1517–28.

39. Yang B, Li Y, Shi W, Liu Y, Kan Y, Chen J, et al. Use of fluorescent 2-AB to explore the bidirectional transport mechanism of *Pseudostellaria heterophylla* polysaccharides across caco-2 cells. *Molecules.* (2022) 27:3192. doi: 10.3390/molecules27103192

40. Zheng Z, Pan X, Wang H, Wu Z, Sullivan MA, Liu Y, et al. Mechanism of lentinan intestinal absorption: clathrin-mediated endocytosis and macropinocytosis. *J Agric Food Chem.* (2021) 69:7344–52. doi: 10.1021/acs.jafc.1c00349

41. Zheng Z, Pan X, Luo L, Zhang Q, Huang X, Liu Y, et al. Advances in oral absorption of polysaccharides: mechanism, affecting factors, and improvement strategies. *Carbohydr Polym.* (2022) 282:119110. doi: 10.1016/j.carbpol.2022.119110

42. Manresa MC, Taylor CT. Hypoxia Inducible Factor (HIF) Hydroxylases as Regulators of Intestinal Epithelial Barrier Function. *Cell Mol Gastroenterol Hepatol.* (2017) 3:303–15.

43. Jeddou KB, Chaari F, Maktouf S, Nouri-Ellouz O, Helbert CB, Ghorbel RE. Structural, functional, and antioxidant properties of water-soluble polysaccharides from potatoes peels. *Food Chem.* (2016) 205:97–105. doi: 10.1016/j.foodchem.2016.02.108

44. McClements DJ, Decker EA. *Designing Functional Foods*. Oxford: Woodhead Publishing (2009).

45. Cummings JH, Bingham SA, Heaton KW, Eastwood MA. Fecal weight, colon cancer risk, and dietary intake of nonstarch polysaccharides (dietary fiber). *Gastroenterology.* (1992) 103:1783–9.

46. Lv J, Zhang Y, Tian Z, Liu F, Shi Y, Liu Y, et al. Astragalus polysaccharides protect against dextran sulfate sodium-induced colitis by inhibiting NF-kappacapital VE, Cyrillic activation. *Int J Biol Macromol.* (2017) 98:723–9. doi: 10.1016/j.ijbiomac.2017.02.024

47. Cui L, Wang W, Luo Y, Ning Q, Xia Z, Chen J, et al. Polysaccharide from *Scutellaria baicalensis* Georgi ameliorates colitis via suppressing NF-kappaB signaling and NLRP3 inflammasome activation. *Int J Biol Macromol.* (2019) 132:393–405. doi: 10.1016/j.ijbiomac.2019.03.230

48. Lee HB, Son SU, Lee JE, Lee SH, Kang CH, Kim YS, et al. Characterization, prebiotic and immune-enhancing activities of rhamnogalacturonan-I-rich polysaccharide fraction from molokhia leaves. *Int J Biol Macromol.* (2021) 175:443–50. doi: 10.1016/j.ijbiomac.2021.02.019

49. Han QB. Critical problems stalling progress in natural bioactive polysaccharide research and development. *J Agric Food Chem.* (2018) 66:4581–3. doi: 10.1021/acs.jafc.8b00493

50. Chen Q, Ren R, Zhang Q, Wu J, Zhang Y, Xue M, et al. Coptis chinensis Franch polysaccharides provide a dynamically regulation on intestinal microenvironment, based on the intestinal flora and mucosal immunity. *J Ethnopharmacol.* (2021) 267:113542. doi: 10.1016/j.jep.2020.113542

51. Zhang YY, Zhuang D, Wang HY, Liu CY, Lv GP, Meng LJ. Preparation, characterization, and bioactivity evaluation of oligosaccharides from *Atractylodes lancea* (Thunb.) DC. *Carbohydr Polym.* (2022) 277:118854. doi: 10.1016/j.carbpol.2021.118854

52. Georgiev YN, Paulsen BS, Kiyohara H, Ciz M, Ognyanov MH, Vasicek O, et al. The common lavender (*Lavandula angustifolia* Mill.) pectic polysaccharides modulate phagocytic leukocytes and intestinal Peyer's patch cells. *Carbohydr Polym.* (2017) 174:948–59. doi: 10.1016/j.carbpol.2017.07.011

53. Jin M, Wang Y, Yang X, Yin H, Nie S, Wu X. Structure characterization of a polysaccharide extracted from noni (*Morinda citrifolia* L.) and its protective effect against DSS-induced bowel disease in mice. *Food Hydrocoll.* (2019) 90:189–97.

54. Liu W, Tang S, Zhao Q, Zhang W, Li K, Yao W, et al. The alpha-D-glucan from marine fungus *Phoma herbarum* YS4108 ameliorated mice colitis by repairing mucosal barrier and maintaining intestinal homeostasis. *Int J Biol Macromol.* (2020) 149:1180–8. doi: 10.1016/j.ijbiomac.2020.01.303

55. Desai MS, Seekatz AM, Koropatkin NM, Kamada N, Hickey CA, Wolter M, et al. A dietary fiber-deprived gut microbiota degrades the colonic mucus barrier and enhances pathogen susceptibility. *Cell.* (2016) 167:1339–53.

56. Araujo JR, Tomas J, Brenner C, Sansonetti PJ. Impact of high-fat diet on the intestinal microbiota and small intestinal physiology before and after the onset of obesity. *Biochimie.* (2017) 141:97–106. doi: 10.1016/j.biochi.2017.05.019

57. Xu X, Zhang X. Lentinula edodes-derived polysaccharide alters the spatial structure of gut microbiota in mice. *PLoS One.* (2015) 10:e0115037. doi: 10.1371/journal.pone.0115037

58. Henke MT, Kenny DJ, Cassilly CD, Vlamakis H, Xavier RJ, Clardy J. Ruminococcus gnavus, a member of the human gut microbiome associated with Crohn's disease, produces an inflammatory polysaccharide. *Proc Natl Acad Sci U.S.A.* (2019) 116:12672–7. doi: 10.1073/pnas.1904099116

59. Sonnenburg JL, Backhed F. Diet-microbiota interactions as moderators of human metabolism. *Nature.* (2016) 535:56–64. doi: 10.1038/nature18846

60. Parada Venegas D, De la Fuente MK, Landskron G, Gonzalez MJ, Quera R, Dijkstra G, et al. Short chain fatty acids (SCFAs)-mediated gut epithelial and immune regulation and its relevance for inflammatory bowel diseases. *Front Immunol.* (2019) 10:277. doi: 10.3389/fimmu.2019.00277

61. Fu Z, Han L, Zhang P, Mao H, Zhang H, Wang Y, et al. Cistanche polysaccharides enhance echinacoside absorption in vivo and affect the gut microbiota. *Int J Biol Macromol.* (2020) 149:732–40. doi: 10.1016/j.ijbiomac.2020.01.216

62. Xie J, Song Q, Yu Q, Chen Y, Hong Y, Shen M. Dietary polysaccharide from Mung bean [*Vigna radiate* (Linn.) Wilczek] skin modulates gut microbiota and short-chain fatty acids in mice. *Int J Food Sci Technol.* (2021) 57:2581–9.

63. Chen P, Chen X, Hao L, Du P, Li C, Han H, et al. The bioavailability of soybean polysaccharides and their metabolites on gut microbiota in the simulator of the human intestinal microbial ecosystem (SHIME). *Food Chem.* (2021) 362:130233. doi: 10.1016/j.foodchem.2021.130233

64. Pratap K, Majzoub ME, Taki AC, Hernandez SM, Magnusson M, Glasson CRK, et al. The algal polysaccharide ulvan and carotenoid astaxanthin both positively modulate gut microbiota in mice. *Foods.* (2022) 11:565. doi: 10.3390/foods11040565

65. Cecchini M, Sassi F, Lauer JA, Lee YY, Guajardo-Barron V, Chisholm D. Tackling of unhealthy diets, physical inactivity, and obesity: health effects and cost-effectiveness. *Lancet.* (2010) 376:1775–84. doi: 10.1016/S0140-6736(10)61514-0

66. Zhao LP. The gut microbiota and obesity: from correlation to causality. *Nat Rev Microbiol.* (2013) 11:639–47.

67. Zhu L, Fu J, Xiao X, Wang F, Jin M, Fang W, et al. Faecal microbiota transplantation-mediated jejunal microbiota changes halt high-fat diet-induced obesity in mice via retarding intestinal fat absorption. *Microb Biotechnol.* (2022) 15:337–52. doi: 10.1111/1751-7915.13951

68. Boscaini S, Leigh SJ, Lavelle A, Garcia-Cabrerizo R, Lipuma T, Clarke G, et al. Microbiota and body weight control: Weight watchers within? *Mol Metab.* (2022) 57:101427.

69. Kopelman PG. Obesity as a medical problem. *Nature.* (2000) 404:635–43.

70. Huang R, Zhu Z, Wu S, Wang J, Chen M, Liu W, et al. Polysaccharides from *Cordyceps militaris* prevent obesity in association with modulating gut microbiota and metabolites in high-fat diet-fed mice. *Food Res Int.* (2022) 157:111197. doi: 10.1016/j.foodres.2022.111197

71. Wei B, Zhang B, Du AQ, Zhou ZY, Lu DZ, Zhu ZH, et al. Saccharina japonica fucan suppresses high fat diet-induced obesity and enriches fucoidan-degrading gut bacteria. *Carbohydr Polym.* (2022) 290:119411. doi: 10.1016/j.carbpol.2022.119411

72. Yu M, Yue J, Hui N, Zhi Y, Hayat K, Yang X, et al. anti-hyperlipidemia and gut microbiota community regulation effects of selenium-rich *Cordyceps militaris* polysaccharides on the high-fat diet-fed mice model. *Foods.* (2021) 10:2252. doi: 10.3390/foods10102252

73. Mfopa A, Mediesse FK, Mvongo C, Nkoubatchoundjwen S, Lum AA, Sobngwi E, et al. Antidyslipidemic potential of water-soluble polysaccharides of *Ganoderma applanatum* in MACAPOS-2-induced obese rats. *Evid Based Complement Alternat Med.* (2021) 2021:2452057. doi: 10.1155/2021/2452057

74. Wang T, Han J, Dai H, Sun J, Ren J, Wang W, et al. Polysaccharides from *Lyophyllum decastes* reduce obesity by altering gut microbiota and increasing energy expenditure. *Carbohydr Polym.* (2022) 295:119862. doi: 10.1016/j.carbpol.2022.119862

75. Chen H, Zhou S, Li J, Huang X, Cheng J, Jiang X, et al. Xyloglucan compounded inulin or arabinoxylan against glycometabolism disorder via different metabolic pathways: gut microbiota and bile acid receptor effects. *J Funct Foods.* (2020) 74:104162.

76. Sharma PP, Baskaran V. Polysaccharide (laminaran and fucoidan), fucoxanthin and lipids as functional components from brown algae (*Padina tetrastromatica*) modulates adipogenesis and thermogenesis in diet-induced obesity in C57BL6 mice. *Algal Res.* (2021) 54:102187.

77. Ristow M, Wieland DM, Pfeiffer A, Krone W, Kahn CR. Obesity associated with a mutation in a genetic regulator of adipocyte differentiation. *N Engl J Med.* (1998) 339:953–9. doi: 10.1056/NEJM199810013391403

78. Lan Y, Sun Q, Ma Z, Peng J, Zhang M, Wang C, et al. Seabuckthorn polysaccharide ameliorates high-fat diet-induced obesity by gut microbiota-SCFAs-liver axis. *Food Funct.* (2022) 13:2925–37. doi: 10.1039/d1fo03147c

79. Li R, Xue Z, Li S, Zhou J, Liu J, Zhang M, et al. Mulberry leaf polysaccharides ameliorate obesity through activation of brown adipose tissue and modulation of the gut microbiota in high-fat diet fed mice. *Food Funct.* (2022) 13:561–73. doi: 10.1039/d1fo02324a

80. Liu Q, Ma R, Li S, Fei Y, Lei J, Li R, et al. Dietary supplementation of *Auricularia auricula*-judae polysaccharides alleviate nutritional obesity in mice via regulating inflammatory response and lipid metabolism. *Foods.* (2022) 11:942. doi: 10.3390/foods11070942

81. Xie F, Zou T, Chen J, Liang P, Wang Z, You J. Polysaccharides from *Enteromorpha prolifera* improves insulin sensitivity and promotes adipose thermogenesis in diet-induced obese mice associated with activation of PGC-1α-FNDC5/irisin pathway. *J Funct Foods.* (2022) 90:104994.

82. Tian D, Zhong X, Fu L, Zhu W, Liu X, Wu Z, et al. Therapeutic effect and mechanism of polysaccharides from *Anoectochilus roxburghii* (Wall.) Lindl. in diet-induced obesity. *Phytomedicine.* (2022) 99:154031. doi: 10.1016/j.phymed.2022.154031

83. Teng C, Shi Z, Yao Y, Ren G. Structural characterization of quinoa polysaccharide and its inhibitory effects on 3T3-L1 adipocyte differentiation. *Foods* (2020) 9:1511. doi: 10.3390/foods9101511

84. Wang Y, Fei Y, Liu L, Xiao Y, Pang Y, Kang J, et al. *Polygonatum odoratum* polysaccharides modulate gut microbiota and mitigate experimentally induced obesity in rats. *Int J Mol Sci.* (2018) 19:3587. doi: 10.3390/ijms19113587

85. Pung HC, Lin WS, Lo YC, Hsu CC, Ho CT, Pan MH. Ulva prolifera polysaccharide exerts anti-obesity effects via upregulation of adiponectin expression and gut microbiota modulation in high-fat diet-fed C57BL/6 mice. *J Food Drug Anal.* (2022) 30:46–61. doi: 10.38212/2224-6614.3395

86. Lee HB, Kim YS, Park HY. Pectic polysaccharides: targeting gut microbiota in obesity and intestinal health. *Carbohydr Polym.* (2022) 287:119363. doi: 10.1016/j.carbpol.2022.119363

87. Sun CY, Zheng ZL, Chen CW, Lu BW, Liu D. Targeting gut microbiota with natural polysaccharides: effective interventions against high-fat diet-induced metabolic diseases. *Front Microbiol.* (2022) 13:859206. doi: 10.3389/fmicb.2022.8592

88. Wu J, Xu Y, Su J, Zhu B, Wang S, Liu K, et al. Roles of gut microbiota and metabolites in a homogalacturonan-type pectic polysaccharide from Ficus pumila Linn. fruits mediated amelioration of obesity. *Carbohydr Polym.* (2020) 248:116780. doi: 10.1016/j.carbpol.2020.116780

89. Liu X, Xi X, Jia A, Zhang M, Cui T, Bai X, et al. A fucoidan from Sargassum fusiforme with novel structure and its regulatory effects on intestinal microbiota in high-fat diet-fed mice. *Food Chem.* (2021) 358:129908. doi: 10.1016/j.foodchem.2021.129908

90. Tremaroli V, Backhed F. Functional interactions between the gut microbiota and host metabolism. *Nature.* (2012) 489:242–9.

91. Lin X. Research progress in the mechanism of polysaccharide in relieving type 2 diabetes. *AIP Conf Proc.* (2019) 2058:020010.

92. Forouhi NG, Wareham NJ. Epidemiology of diabetes. *Medicine.* (2010) 38:602–6.

93. World Health Organization. *Global Report on Diabetes*. Geneva: World Health Organization (2016).

94. Wang HY, Guo LX, Hu WH, Peng ZT, Wang C, Chen ZC, et al. Polysaccharide from tuberous roots of *Ophiopogon japonicus* regulates gut microbiota and its metabolites during alleviation of high-fat diet-induced type-2 diabetes in mice. *J Funct Foods.* (2019) 63:103593.

95. Fang J, Lin Y, Xie H, Farag MA, Feng S, Li J, et al. Dendrobium officinale leaf polysaccharides ameliorated hyperglycemia and promoted gut bacterial associated SCFAs to alleviate type 2 diabetes in adult mice. *Food Chem X.* (2022) 13:100207. doi: 10.1016/j.fochx.2022.100207

96. Yang S, Yan J, Yang L, Meng Y, Wang N, He C, et al. Alkali-soluble polysaccharides from mushroom fruiting bodies improve insulin resistance. *Int J Biol Macromol.* (2019) 126:466–74. doi: 10.1016/j.ijbiomac.2018.12.251

97. Chen M, Xu J, Wang Y, Wang Z, Guo L, Li X, et al. *Arctium lappa* L. polysaccharide can regulate lipid metabolism in type 2 diabetic rats through the SREBP-1/SCD-1 axis. *Carbohydr Res.* (2020) 494:108055. doi: 10.1016/j.carres.2020.108055

98. Sun W, Zhang Y, Jia L. Polysaccharides from *Agrocybe cylindracea* residue alleviate type 2-diabetes-induced liver and colon injuries by p38 MAPK signaling pathway. *Food Bioscience.* (2022) 47:101690.

99. Gao H, Ding L, Liu R, Zheng X, Xia X, Wang F, et al. Characterization of *Anoectochilus roxburghii* polysaccharide and its therapeutic effect on type 2 diabetic mice. *Int J Biol Macromol.* (2021) 179:259–69. doi: 10.1016/j.ijbiomac.2021.02.217

100. Hao G, Ma X, Jiang M, Gao Z, Yang Y. *Echinops* Spp. polysaccharide B ameliorates metabolic abnormalities in a rat model of type 2 diabetes mellitus. *Curr Top Nutr Res.* (2020) 19:106–14.

101. Fu X, Song M, Lu M, Xie M, Shi L. Hypoglycemic and hypolipidemic effects of polysaccharide isolated from *Sphacelotheca sorghi* in diet-streptozotocin-induced T2D mice. *J Food Sci.* (2022) 87:1882–94. doi: 10.1111/1750-3841.16091

102. Xu N, Zhou Y, Lu X, Chang Y. *Auricularia auricula*-judae (Bull.) polysaccharides improve type 2 diabetes in HFD/STZ-induced mice by regulating the AKT/AMPK signaling pathways and the gut microbiota. *J Food Sci.* (2021) 86:5479–94. doi: 10.1111/1750-3841.15963

103. Meneguin AB, Silvestre ALP, Sposito L, de Souza MPC, Sabio RM, Araujo VHS, et al. The role of polysaccharides from natural resources to design oral insulin micro- and nanoparticles intended for the treatment of diabetes mellitus: a review. *Carbohydr Polym.* (2021) 256:117504. doi: 10.1016/j.carbpol.2020.117504

104. Que Y, Cao M, He J, Zhang Q, Chen Q, Yan C, et al. Gut bacterial characteristics of patients with type 2 diabetes mellitus and the application potential. *Front Immunol.* (2021) 12:722206. doi: 10.3389/fimmu.2021.722206

105. Fang Q, Hu J, Nie Q, Nie S. Effects of polysaccharides on glycometabolism based on gut microbiota alteration. *Trends Food Sci Technol.* (2019) 92:65–70. doi: 10.3389/fimmu.2020.588079

106. Yuan Y, Zhou J, Zheng Y, Xu Z, Li Y, Zhou S, et al. Beneficial effects of polysaccharide-rich extracts from Apocynum venetum leaves on hypoglycemic and gut microbiota in type 2 diabetic mice. *Biomed Pharmacother.* (2020) 127:110182. doi: 10.1016/j.biopha.2020.110182

107. Li H, Fang Q, Nie Q, Hu J, Yang C, Huang T, et al. Hypoglycemic and hypolipidemic mechanism of tea polysaccharides on type 2 diabetic rats via gut microbiota and metabolism alteration. *J Agric Food Chem.* (2020) 68:10015–28. doi: 10.1021/acs.jafc.0c01968

108. Zhao L, Zhang F, Ding X, Wu G, Lam YY, Wang X, et al. Gut bacteria selectively promoted by dietary fibers alleviate type 2 diabetes. *Science.* (2018) 359:1151–6. doi: 10.1126/science.aao5774

109. Wu J, Shi S, Wang H, Wang S. Mechanisms underlying the effect of polysaccharides in the treatment of type 2 diabetes: a review. *Carbohydr Polym.* (2016) 144:474–94.

110. Mollica MP, Mattace Raso G, Cavaliere G, Trinchese G, De Filippo C, Aceto S, et al. Butyrate regulates liver mitochondrial function, efficiency, and dynamics in insulin-resistant obese mice. *Diabetes.* (2017) 66:1405–18. doi: 10.2337/db16-0924

111. Canfora EE, Jocken JW, Blaak EE. Short-chain fatty acids in control of body weight and insulin sensitivity. *Nat Rev Endocrinol.* (2015) 11:577–91.

112. Angulo P, Lindor KD. Non-alcoholic fatty liver disease. *J Gastroenterol Hepatol.* (2002) 17:S186–90.

113. Brunt EM, Wong VW, Nobili V, Day CP, Sookoian S, Maher JJ, et al. Nonalcoholic fatty liver disease. *Nat Rev Dis Primers.* (2015) 1:15080.

114. Donnelly KL, Smith CI, Schwarzenberg SJ, Jessurun J, Boldt MD, Parks EJ. Sources of fatty acids stored in liver and secreted via lipoproteins in patients with nonalcoholic fatty liver disease. *J Clin Invest.* (2005) 115:1343–51. doi: 10.1172/JCI23621

115. Engin A. Non-alcoholic fatty liver disease. In: Engin AB, Engin A editors. *Obesity and Lipotoxicity. Advances in Experimental Medicine and Biology*. Cham: Springer (2017).

116. Samuel VT, Liu ZX, Wang A, Beddow SA, Geisler JG, Kahn M, et al. Inhibition of protein kinase Cepsilon prevents hepatic insulin resistance in nonalcoholic fatty liver disease. *J Clin Invest.* (2007) 117:739–45.

117. Shen LL, Liu H, Peng J, Gan L, Lu L, Zhang Q, et al. Effects of farnesoid X receptor on the expression of the fatty acid synthetase and hepatic lipase. *Mol Biol Rep.* (2011) 38:553–9.

118. Knight BL, Hebbachi A, Hauton D, Brown AM, Wiggins D, Patel DD, et al. A role for PPARα in the control of SREBP activity and lipid synthesis in the liver. *Biochem J.* (2005) 389:413–21.

119. Bechmann LP, Hannivoort RA, Gerken G, Hotamisligil GS, Trauner M, Canbay A. The interaction of hepatic lipid and glucose metabolism in liver diseases. *J Hepatol.* (2012) 56:952–64.

120. Cariou B, Byrne CD, Loomba R, Sanyal AJ. Nonalcoholic fatty liver disease as a metabolic disease in humans: a literature review. *Diabetes Obes Metab.* (2021) 23:1069–83.

121. Dallio M, Sangineto M, Romeo M, Villani R, Romano AD, Loguercio C, et al. Immunity as cornerstone of non-alcoholic fatty liver disease: the contribution of oxidative stress in the disease progression. *Int J Mol Sci* (2021) 22:436. doi: 10.3390/ijms22010436

122. Yan Z, Fan R, Yin S, Zhao X, Liu J, Li L, et al. Protective effects of *Ginkgo biloba* leaf polysaccharide on nonalcoholic fatty liver disease and its mechanisms. *Int J Biol Macromol.* (2015) 80:573–80. doi: 10.1016/j.ijbiomac.2015.05.054

123. Lambert JE, Ramos-Roman MA, Browning JD, Parks EJ. Increased de novo lipogenesis is a distinct characteristic of individuals with nonalcoholic fatty liver disease. *Gastroenterology.* (2014) 146:726–35. doi: 10.1053/j.gastro.2013.11.049

124. Zhang JM, Sun YS, Zhao LQ, Chen TT, Fan MN, Jiao HC, et al. SCFAs-induced GLP-1 secretion links the regulation of gut microbiome on hepatic lipogenesis in chickens. *Front Microbiol.* (2019) 10:2176. doi: 10.3389/fmicb.2019.02176

125. Li S, Wu Y, Jiang H, Zhou F, Ben A, Wang R, et al. Chicory polysaccharides alleviate high-fat diet-induced non-alcoholic fatty liver disease via alteration of lipid metabolism- and inflammation-related gene expression. *Food Sci Hum Wellness.* (2022) 11:954–64.

126. Zhu H, Wang Z, Wu Y, Jiang H, Zhou F, Xie X, et al. Untargeted metabonomics reveals intervention effects of chicory polysaccharide in a rat model of non-alcoholic fatty liver disease. *Int J Biol Macromol.* (2019) 128:363–75. doi: 10.1016/j.ijbiomac.2019.01.141

127. Wang X, Shi L, Wang X, Feng Y, Wang Y. MDG-1, an *Ophiopogon* polysaccharide, restrains process of non-alcoholic fatty liver disease via modulating the gut-liver axis. *Int J Biol Macromol.* (2019) 141:1013–21. doi: 10.1016/j.ijbiomac.2019.09.007

128. Zhang L, Wang Y, Wu F, Wang X, Feng Y, Wang Y. MDG, an *Ophiopogon japonicus* polysaccharide, inhibits non-alcoholic fatty liver disease by regulating the abundance of *Akkermansia muciniphila*. *Int J Biol Macromol.* (2022) 196:23–34. doi: 10.1016/j.ijbiomac.2021.12.036

129. Yao W, Qiu H, Cheong K, Zhong S. Advances in anti-cancer effects and underlying mechanisms of marine algae polysaccharides. *Int J Biol Macromol.* (2022) 221:472–85. doi: 10.1016/j.ijbiomac.2022.09.055

130. Han ND, Cheng J, Delannoy-Bruno O, Webber D, Terrapon N, Henrissat B, et al. Microbial liberation of N-methylserotonin from orange fiber in gnotobiotic mice and humans. *Cell.* (2022) 185:2495.e–509.e.

131. Murga-Garrido SM, Hong Q, Cross TL, Hutchison ER, Han J, Thomas SP, et al. Gut microbiome variation modulates the effects of dietary fiber on host metabolism. *Microbiome.* (2021) 9:117.

132. Fan Y, Pedersen O. Gut microbiota in human metabolic health and disease. *Nat Rev Microbiol.* (2020) 19:55–71.

133. Tang C, Sun J, Liu J, Jin C, Wu X, Zhang X, et al. Immune-enhancing effects of polysaccharides from purple sweet potato. *Int J Biol Macromol.* (2019) 123:923–30.

Frontiers in Nutrition

Explores what and how we eat in the context of health, sustainability and 21st century food science

A multidisciplinary journal that integrates research on dietary behavior, agronomy and 21st century food science with a focus on human health.

Discover the latest Research Topics

See more →

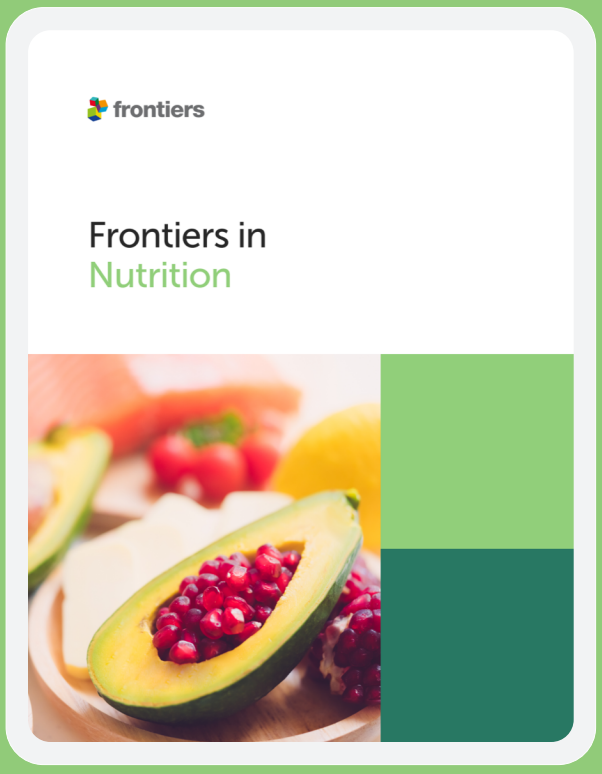

Frontiers

Avenue du Tribunal-Fédéral 34
1005 Lausanne, Switzerland
frontiersin.org

Contact us

+41 (0)21 510 17 00
frontiersin.org/about/contact